



**National Library
of Canada**

**Bibliothèque nationale
du Canada**

Canadian Theses Service Service des thèses canadiennes

Ottawa, Canada
K1A 0N4

NOTICE

The quality of this microform is heavily dependent upon the quality of the original thesis submitted for microfilming. Every effort has been made to ensure the highest quality of reproduction possible.

If pages are missing, contact the university which granted the degree.

Some pages may have indistinct print especially if the original pages were typed with a poor typewriter ribbon or if the university sent us an inferior photocopy.

Reproduction in full or in part of this microform is governed by the Canadian Copyright Act, R.S.C. 1970, c. C-30, and subsequent amendments.

AVIS

La qualité de cette microforme dépend grandement de la qualité de la thèse soumise au microfilmage. Nous avons tout fait pour assurer une qualité supérieure de reproduction.

S'il manque des pages, veuillez communiquer avec l'université qui a conféré le grade.

La qualité d'impression de certaines pages peut laisser à désirer, surtout si les pages originales ont été dactylographiées à l'aide d'un ruban usé ou si l'université nous a fait parvenir une photocopie de qualité inférieure.

La reproduction, même partielle, de cette microforme est soumise à la Loi canadienne sur le droit d'auteur, SRC 1970, c. C-30, et ses amendements subséquents.

UNIVERSITY OF ALBERTA

THE REACTIVITY OF SOLVATED ELECTRONS WITH IONIC SOLUTES IN
1-PROPANOL/WATER, 2-PROPANOL/WATER AND 2-BUTANOL/WATER
MIXTURES

by



SEDIGALLAGE LEETUS ANNESLEY PEIRIS

A THESIS

SUBMITTED TO THE FACULTY OF GRADUATE STUDIES AND RESEARCH
IN PARTIAL FULFILMENT OF THE REQUIREMENTS FOR THE DEGREE
OF DOCTOR OF PHILOSOPHY

DEPARTMENT OF CHEMISTRY

EDMONTON, ALBERTA

FALL 1990



**National Library
of Canada**

**Bibliothèque nationale
du Canada**

Canadian Theses Service Service des thèses canadiennes

**Ottawa, Canada
K1A 0N4**

The author has granted an irrevocable non-exclusive licence allowing the National Library of Canada to reproduce, loan, distribute or sell copies of his/her thesis by any means and in any form or format, making this thesis available to interested persons.

The author retains ownership of the copyright in his/her thesis. Neither the thesis nor substantial extracts from it may be printed or otherwise reproduced without his/her permission.

L'auteur a accordé une licence irrévocable et non exclusive permettant à la Bibliothèque nationale du Canada de reproduire, prêter, distribuer ou vendre des copies de sa thèse de quelque manière et sous quelque forme que ce soit pour mettre des exemplaires de cette thèse à la disposition des personnes intéressées.

L'auteur conserve la propriété du droit d'auteur qui protège sa thèse. Ni la thèse ni des extraits substantiels de celle-ci ne doivent être imprimés ou autrement reproduits sans son autorisation.

ISBN 0-315-64858-9

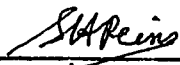
UNIVERSITY OF ALBERTA

RELEASE FORM

NAME OF AUTHOR: SEDIGALLAGE LEETUS ANNESLEY PEIRIS
TITLE OF THESIS: THE REACTIVITY OF SOLVATED ELECTRONS WITH
IONIC SOLUTES IN 1-PROPANOL/WATER, 2-PROPANOL/
WATER AND 2-BUTANOL/WATER MIXTURES
DEGREE: DOCTOR OF PHILOSOPHY
YEAR THIS DEGREE GRANTED: 1990

Permission is hereby granted to THE UNIVERSITY OF ALBERTA LIBRARY to reproduce single copies of this thesis and to lend or sell such copies for private, scholarly or scientific research purposes only.

The author reserves other publication rights, and neither the thesis nor extensive extracts from it may be printed or otherwise reproduced without the author's written permission.



(signed)

PERMANENT ADDRESS:

Mahawatta
Kuda Arukgoda
Alubomulla
Sri Lanka

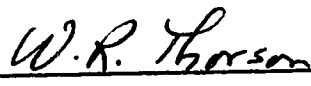
DATE: 4th July, 90

THE UNIVERSITY OF ALBERTA
FACULTY OF GRADUATE STUDIES AND RESEARCH


The undersigned certify that they have read, and recommend to the Faculty of Graduate Studies and Research, for acceptance, a thesis entitled THE REACTIVITY OF SOLVATED ELECTRONS WITH IONIC SOLUTES IN 1-PROPANOL/WATER, 2-PROPANOL/WATER AND 2-BUTANOL/WATER MIXTURES submitted by SEDIGALLAGE LEETUS ANNESLEY PEIRIS in partial fulfilment of the requirements for the degree of DOCTOR OF PHILOSOPHY.



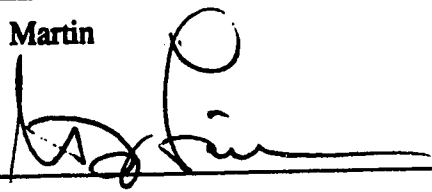
G.R. Freeman, Supervisor



W.R. Thorson



J.S. Martin



H.J. Liu



G. Rostoker



M.A. Rodgers, External Examiner

DATE: 3rd July, 90

TO MY PARENTS

ABSTRACT

We have studied the effects of solvent structure on solvated electron reaction rates with ions in 1-propanol/water, 2-propanol/water and 2-butanol/water mixed solvents. Both negative ions (NO_3^- and CrO_4^{2-}) and positive ions (H_3^+ , Ag_s^+ , Tl_s^+ , Cu_s^{2+} , and Al_s^{3+}) were studied.

Alcohol/water mixtures are good systems to study the effects of solvent structure on solvated electron reactivity because varying the composition of the mixture results in strong variations in the structure as reflected in physical properties such as viscosity.

The observed rate constants of the nearly diffusion controlled reactions were compared to the Smoluchowski-Debye-Stokes-Einstein equation for the rate constant k_2 of a bimolecular reaction between charged or polar species:

$$k_2 = \kappa RTf r_r/1.5 \eta r_d$$

where κ = probability that a reactant encounter pair will react, R = gas constant, T = temperature, f = Debye electrostatic interaction factor, r_r = effective radius for reaction, η = solvent viscosity, and r_d = effective radius for mutual diffusion of reactants. This equation is useful in evaluating the effects of bulk solvent properties on reaction rates. Residual effects are attributed to the nonhomogeneous structure of the solvent.

The value of $k_2\eta/fT$ was predicted theoretically to be proportional to the ratio of reaction parameters $\kappa r_r/r_d$. However our observations demonstrate that alcohol-water mixtures behave in a fashion which deviates significantly from this theoretical prediction. More clearly for positive ions, the value of $k_2\eta/fT$ increases when about 10 mol% alcohol is added to water, passes through a maximum near 80 mol% water and decreases again towards the alcohol side of the plot. Plots of r_d estimated from measured molar conductivities Λ_0 of the reactant perchloric acid and the various salts display a minimum in the vicinity of 90 mol% water; the decrease of r_d as small amounts of alcohol are added to

water indicates that the microscopic viscosity around the ions is lower than the shear viscosity of the bulk solvent. This phenomenon is confirmed from the behavior of $zk_2/f\Lambda_0T$ plots, which indicate the variation of κr_f with solvent composition; the values of $zk_2/f\Lambda_0T$ are much less dependent on solvent composition than are the values of $k_2\eta/fT$; the values of r_d are solvent dependent.

Rate constants, activation energies E_2 , and pre-exponential factors A_2 vary with the composition of the mixed solvents. The liquid structure influences both the rate of diffusion of the reactants and the probability of reaction of a reactant encounter pair.

ACKNOWLEDGEMENTS

The author expresses appreciation to the many persons associated with him during the time this thesis was researched and written.

Thanks are due to the staff of the Radiation Research Centre, the non-academic staff of the Chemistry Department and Miss Annabelle Wiseman who typed this thesis.

The author wishes to express his sincerest thanks to Professor G.R. Freeman for his guidance during the time this thesis was researched and written.

Appreciation is extended to the Natural Sciences and Engineering Research Council of Canada for financial assistance.

TABLE OF CONTENTS

CHAPTER ONE: INTRODUCTION	1
I. The Solvated Electron.....	1
II. Properties of Solvated Electrons.....	3
A. Mobility	3
B. Optical Absorption Spectrum	3
1. Absorption Band Width.....	4
2. Bound and Continuum Transitions.....	4
3. Models.....	5
4. Optical Absorption Spectrum in Hydroxylic Solvents	6
III. Structure and Properties of Hydroxylic Solvents.....	6
A. Structure of Water.....	7
B. Structure of Alcohols.....	7
C. Water/Alcohol Mixtures	8
1. Static Dielectric Properties.....	8
2. Thermodynamic Properties.....	9
3. Viscosity.....	9
IV. Reactivity of Solvated Electrons	10
V. Present Work.....	14
CHAPTER TWO: EXPERIMENTAL.....	15
I. Materials	15
II. Apparatus for Kinetic Measurements.....	15
A. Sample Cells.....	15
B. Bubbling System.....	16
C. Irradiation, Detection and Control Systems.....	16
1. The Van de Graaff Accelerator.....	16

2.	Secondary Emission Monitor	18
3.	Optical Detection System	18
(a)	The light source	18
(b)	Monochromator grating and filters.....	21
(c)	Digital voltmeter, oscilloscope and plotter	21
4.	Temperature Control System.....	21
(a)	Cooling and heating	21
(b)	Cell holder box.....	22
III.	Conductivity Measurements.....	23
A.	Impedance Bridge.....	23
B.	Conductance Cells	23
C.	Constant Temperature Bath	24
IV.	Techniques	24
A.	Sample Preparations	24
B.	Kinetic Measurements	26
C.	Conductivity Measurements	28
CHAPTER THREE: RESULTS.....		31
I.	Reactions of Solvated Electrons with Ionic Electron Acceptors.....	31
II.	Reactions of Solvated Electrons in 1-Propanol/Water Mixtures	31
A.	Reaction of Solvated Electrons with Nitrate Ions	31
B.	Reaction of Solvated Electrons with Chromate Ions.....	40
C.	Reaction of Solvated Electrons with Hydrogen Ions	48
D.	Reaction of Solvated Electrons with Silver Ions	57
E.	Reaction of Solvated Electrons with Copper(II) Ions.....	66
F.	Reaction of Solvated Electrons with Aluminum Ions.....	75
III.	Reactions of Solvated Electrons in 2-Propanol/Water Mixtures	85
A.	Reaction of Solvated Electrons with Nitrate Ions	85

B. Reaction of Solvated Electrons with Chromate Ions.....	93
C. Reaction of Solvated Electrons with Hydrogen Ions	100
D. Reaction of Solvated Electrons with Silver Ions	108
E. Reaction of Solvated Electrons with Copper(II) Ions.....	116
F. Reaction of Solvated Electrons with Aluminum Ions.....	124
IV. Reactions of Solvated Electrons in 2-Butanol/Water Mixtures.....	132
A. Reaction of Solvated Electrons with Nitrate Ions	132
B. Reaction of Solvated Electrons with Hydrogen Ions	139
C. Reaction of Solvated Electrons with Thallium Ions.....	146
D. Reaction of Solvated Electrons with Copper(II) Ions.....	153
E. Reaction of Solvated Electrons with Aluminum Ions.....	160
V. Conductivities of Inorganic Electrolytes in Alcohol/Water Mixtures	167
A. 1-Propanol/Water Mixtures	167
B. 2-Propanol/Water Mixtures	206
C. 2-Butanol/Water Mixtures.....	243
CHAPTER FOUR: DISCUSSION	274
I. Solvated Electron Reactions with Negative Ions.....	274
A. Effect of Solvent Viscosity.....	284
B. Comparison with Ionic Conductivities (Diffusion Coefficients)	286
II. Solvated Electron Reactions with Positive Ions.....	291
A. Effect of Solvent Viscosity.....	301
B. Comparison with Ionic Conductivities	310
III. Conclusion	320

REFERENCES.....	323

LIST OF TABLES

TABLE		PAGE
1.	Dielectric constants, f values and second-order rate constants for the reaction of solvated electrons with lithium nitrate in 1-propanol/water mixtures.....	37
2.	Rate parameters for the reaction of solvated electrons with lithium nitrate in 1-propanol/water mixtures.....	38
3.	Dielectric constants, f values and second-order rate constants for the reaction of solvated electrons with lithium chromate in 1-propanol/water mixtures.....	45
4.	Rate parameters for the reaction of solvated electrons with lithium chromate in 1-propanol/water mixtures	46
5.	Dielectric constants, f values and second-order rate constants for the reaction of solvated electrons with perchloric acid in 1-propanol/water mixtures.....	54
6.	Rate parameters for the reaction of solvated electrons with perchloric acid in 1-propanol/water mixtures.....	55
7.	Dielectric constants, f values and second-order rate constants for the reaction of solvated electrons with silver perchlorate in 1-propanol/water mixtures.....	63
8.	Rate parameters for the reaction of solvated electrons with silver perchlorate in 1-propanol/water mixtures.....	64
9.	Dielectric constants, f values and second-order rate constants for the reaction of solvated electrons with copper(II) perchlorate in 1-propanol/water mixtures.....	72

TABLE	PAGE
10. Rate parameters for the reaction of solvated electrons with copper(II) perchlorate in 1-propanol/water mixtures.....	73
11. Dielectric constants, f values and second-order rate constants for the reaction of solvated electrons with aluminum perchlorate in 1-propanol/water mixtures.....	82
12. Rate parameters for the reaction of solvated electrons with aluminum perchlorate in 1-propanol/water mixtures.....	83
13. Dielectric constants, f values and second-order rate constants for the reaction of solvated electrons with lithium nitrate in 2-propanol/water mixtures.....	90
14. Rate parameters for the reaction of solvated electrons with lithium nitrate in 2-propanol/water mixtures.....	91
15. Dielectric constants, f values and second-order rate constants for the reaction of solvated electrons with lithium chromate in 2-propanol/water mixtures.....	97
16. Rate parameters for the reaction of solvated electrons with lithium chromate in 2-propanol/water mixtures.....	98
17. Dielectric constants, f values and second-order rate constants for the reaction of solvated electrons with perchloric acid in 2-propanol/water mixtures.....	105
18. Rate parameters for the reaction of solvated electrons with perchloric acid in 2-propanol/water mixtures.....	106
19. Dielectric constants, f values and second-order rate constants for the reaction of solvated electrons with silver perchlorate in 2-propanol/water mixtures.....	113

TABLE	PAGE
20. Rate parameters for the reaction of solvated electrons with silver perchlorate in 2-propanol/water mixtures	114
21. Dielectric constants, f values and second-order rate constants for the reaction of solvated electrons with copper(II) perchlorate in 2-propanol/water mixtures.....	121
22. Rate parameters for the reaction of solvated electrons with copper(II) perchlorate in 2-propanol/water mixtures.....	122
23. Dielectric constants, f values and second-order rate constants for the reaction of solvated electrons with aluminum perchlorate in 2-propanol/water mixtures.....	129
24. Rate parameters for the reaction of solvated electrons with aluminum perchlorate in 2-propanol/water mixtures	130
25. Dielectric constants, f values and second-order rate constants for the reaction of solvated electrons with lithium nitrate in 2-butanol/water mixtures.....	136
26. Rate parameters for the reaction of solvated electrons with lithium nitrate in 2-butanol/water mixtures.....	137
27. Dielectric constants, f values and second-order rate constants for the reaction of solvated electrons with perchloric acid in 2-butanol/water mixtures.....	143
28. Rate parameters for the reaction of solvated electrons with perchloric acid in 2-butanol/water mixtures	144
29. Dielectric constants, f values and second-order rate constants for the reaction of solvated electrons with thallium acetate in 2-butanol/water mixtures.....	150

TABLE	PAGE
30. Rate parameters for the reaction of solvated electrons with thallium acetate in 2-butanol/water mixtures	151
31. Dielectric constants, f values and second-order rate constants for the reaction of solvated electrons with copper(II) perchlorate in 2-butanol/water mixtures.....	157
32. Rate parameters for the reaction of solvated electrons with copper(II) perchlorate in 2-butanol/water mixtures	158
33. Dielectric constants, f values and second-order rate constants for the reaction of solvated electrons with aluminum perchlorate in 2-butanol/water mixtures.....	164
34. Rate parameters for the reaction of solvated electrons with aluminum perchlorate in 2-butanol/water mixtures.....	165
35. Temperature and composition dependence of molar conductance of lithium nitrate in 1-propanol/water mixtures.....	200
36. Temperature and composition dependence of molar conductance of lithium chromate in 1-propanol/water mixtures	201
37. Temperature and composition dependence of molar conductance of perchloric acid in 1-propanol/water mixtures.....	202
38. Temperature and composition dependence of molar conductance of silver perchlorate in 1-propanol/water mixtures.....	203
39. Temperature and composition dependence of molar conductance of copper(II) perchlorate in 1-propanol/water mixtures	204
40. Temperature and composition dependence of molar conductance of aluminum perchlorate in 1-propanol/water mixtures.....	205
41. Temperature and composition dependence of molar conductance of lithium nitrate in 2-propanol/water mixtures.....	238

TABLE	PAGE
42. Temperature and composition dependence of molar conductance of lithium chromate in 2-propanol/water mixtures	239
43. Temperature and composition dependence of molar conductance of perchloric acid in 2-propanol/water mixtures.....	240
44. Temperature and composition dependence of molar conductance of silver perchlorate in 2-propanol/water mixtures.....	241
45. Temperature and composition dependence of molar conductance of copper(II) perchlorate in 2-propanol/water mixtures	242
46. Temperature and composition dependence of molar conductance of aluminum perchlorate in 2-propanol/water mixtures.....	243
47. Temperature and composition dependence of molar conductance of lithium nitrate in 2-butanol/water mixtures.....	269
48. Temperature and composition dependence of molar conductance of perchloric acid in 2-butanol/water mixtures.....	270
49. Temperature and composition dependence of molar conductance of thallium acetate in 2-butanol/water mixtures.....	271
50. Temperature and composition dependence of molar conductance of copper(II) perchlorate in 2-butanol/water mixtures	272
51. Temperature and composition dependence of molar conductance of aluminum perchlorate in 2-butanol/water amixtures	273

LIST OF FIGURES

FIGURE		PAGE
1.	The bubbling system	17
2.	The secondary emission monitor.....	19
3.	The path of the analyzing light	20
4.	Temperature control of the water bath.....	25
5.	Temperature regulating system.....	25
6.	The sample sealing procedure	27
7.	Typical solvated electron kinetic trace	29
8.	(A-J) Temperature and concentration dependence of the first order rate constants for the reaction of solvated electrons with lithium nitrate in 1-propanol/water mixtures.....	32
9.	Arrhenius plots for the reaction of solvated electrons with lithium nitrate in 1-propanol/water mixtures.....	39
10.	(A-H) Temperature and concentration dependence of the first-order rate constant for the reaction of solvated electrons with lithium chromate in 1-propanol/water mixtures	40
11.	Arrhenius plots for the reaction of solvated electrons with lithium chromate in 1-propanol/water mixtures	47
12.	(A-J) Temperature and concentration dependence of the first-order rate constant for the reaction of solvated electrons with perchloric acid in 1-propanol/water mixtures	48
13.	Arrhenius plots for the reaction of solvated electrons with perchloric acid in 1-propanol/water mixtures.....	56

FIGURE	PAGE
14. (A-J) Temperature and concentration dependence of the first-order rate constant for the reaction of solvated electrons with silver perchlorate in 1-propanol/water mixtures.....	57
15. Arrhenius plots for the reaction of solvated electrons with silver perchlorate in 1-propanol/water mixtures	65
16. (A-J) Temperature and concentration dependence of the first-order rate constant for the reaction of solvated electrons with copper(II) perchlorate in 1-propanol/water mixtures	66
17. Arrhenius plots for the reaction of solvated electrons with copper(II) perchlorate in 1-propanol/water mixtures.....	74
18. (A-K) Temperature and concentration dependence of the first-order rate constant for the reaction of solvated electrons with aluminum perchlorate in 1-propanol/water mixtures	75
19. Arrhenius plots for the reaction of solvated electrons with aluminum perchlorate in 1-propanol/water mixtures	84
20. (A-I) Temperature and concentration dependence of the first-order rate constant for the reaction of solvated electrons with lithium nitrate in 2-propanol/water mixtures	85
21. Arrhenius plots for the reaction of solvated electrons with lithium nitrate in 2-propanol/water mixtures.....	92
22. (A-G) Temperature and concentration dependence of the first-order rate constant for the reaction of solvated electrons with lithium chromate in 2-propanol/water mixtures	93
23. Arrhenius plots for the reaction of solvated electrons with lithium chromate in 2-propanol/water mixtures	99

FIGURE	PAGE
24. (A-I) Temperature and concentration dependence of the first-order rate constant for the reaction of solvated electrons with perchloric acid in 2-propanol/water mixtures	100
25. Arrhenius plots for the reaction of solvated electrons with perchloric acid in 2-propanol/water mixtures.....	107
26. (A-H) Temperature and concentration dependence of the first-order rate constant for the reaction of solvated electrons with silver perchlorate in 2-propanol/water mixtures	108
27. Arrhenius plots for the reaction of solvated electrons with silver perchlorate in 2-propanol/water mixtures	115
28. (A-I) Temperature and concentration dependence of the first-order rate constant for the reaction of solvated electrons with copper(II) perchlorate in 2-propanol/water mixtures	116
29. Arrhenius plots for the reaction of solvated electrons with copper(II) perchlorate in 2-propanol/water mixtures.....	123
30. (A-I) Temperature and concentration dependence of the first-order rate constant for the reaction of solvated electrons with aluminum perchlorate in 2-propanol/water mixtures	124
31. Arrhenius plots for the reaction of solvated electrons with aluminum perchlorate in 2-propanol/water mixtures	131
32. (A-G) Temperature and concentration dependence of the first-order rate constant for the reaction of solvated electrons with lithium nitrate in 2-butanol/water mixtures.....	132
33. Arrhenius plots for the reaction of solvated electrons with lithium nitrate in 2-butanol/water mixtures.....	138

FIGURE	PAGE
34. (A-G) Temperature and concentration dependence of the first-order rate constant for the reaction of solvated electrons with perchloric acid in 2-butanol/water mixtures	139
35. Arrhenius plots for the reaction of solvated electrons with perchloric acid in 2-butanol/water mixtures	145
36. (A-G) Temperature and concentration dependence of the first-order rate constant for the reaction of solvated electrons with thallium acetate in 2-butanol/water mixtures.....	146
37. Arrhenius plots for the reaction of solvated electrons with thallium acetate in 2-butanol/water mixtures	152
38. (A-G) Temperature and concentration dependence of the first-order rate constant for the reaction of solvated electrons with copper(II) perchlorate in 2-butanol/water mixtures	153
39. Arrhenius plots for the reaction of solvated electrons with copper(II) perchlorate in 2-butanol/water mixtures	159
40. (A-G) Temperature and concentration dependence of the first-order rate constant for the reaction of solvated electrons with aluminum perchlorate in 2-butanol/water mixtures.....	160
41. Arrhenius plots for the reaction of solvated electrons with aluminum perchlorate in 2-butanol/water mixtures.....	166
42. (A-H) Temperature and concentration dependence of the conductance of lithium nitrate in 1-propanol/water mixtures.....	168
43. (A-F) Temperature and concentration dependence of the conductance of lithium chromate in 1-propanol/water mixtures	172
44. (A-H) Temperature and concentration dependence of the conductance of perchloric acid in 1-propanol/water mixtures.....	175

FIGURE	PAGE
45. (A-I) Temperature and concentration dependence of the conductance of silver perchlorate in 1-propanol/water mixtures.....	179
46. (A-J) Temperature and concentration dependence of the conductance of copper(II) perchlorate in 1-propanol/water mixtures	184
47. (A-H) Temperature and concentration dependence of the conductance of aluminum perchlorate in 1-propanol/water mixtures.....	189
48. Arrhenius plots of molar conductance of lithium nitrate in 1-propanol/water mixtures.....	193
49. Arrhenius plots of molar conductance of lithium chromate in 1-propanol/water mixtures.....	194
50. Arrhenius plots of molar conductance of perchloric acid in 1-propanol/water mixtures.....	195
51. Arrhenius plots of molar conductance of silver perchlorate in 1-propanol/water mixtures.....	196
52. Arrhenius plots of molar conductance of copper(II) perchlorate in 1-propanol/water mixtures.....	197
53. Arrhenius plots of molar conductance of aluminum perchlorate in 1-propanol/water mixtures.....	198
54. Composition dependence of the activation energy of conductance of some inorganic electrolytes in 1-propanol/water mixtures.....	199
55. (A-H) Temperature and concentration dependence of the conductance of lithium nitrate in 2-propanol/water mixtures.....	207
56. (A-D) Temperature and concentration dependence of the conductance of lithium chromate in 2-propanol/water mixtures	211
57. (A-G) Temperature and concentration dependence of the conductance of perchloric acid in 2-propanol/water mixtures.....	213

FIGURE	PAGE
58. (A-I) Temperature and concentration dependence of the conductance of silver perchlorate in 2-propanol/water mixtures.....	217
59. (A-H) Temperature and concentration dependence of the conductance of copper(II) perchlorate in 2-propanol/water mixtures	222
60. (A-H) Temperature and concentration dependence of the conductance of aluminum perchlorate in 2-propanol/water mixtures.....	226
61. Arrhenius plots of molar conductance of lithium nitrate in 2-propanol/water mixtures.....	230
62. Arrhenius plots of molar conductance of lithium chromate in 2-propanol/water mixtures.....	231
63. Arrhenius plots of molar conductance of perchloric acid in 2-propanol/water mixtures.....	232
64. Arrhenius plots of molar conductance of silver perchlorate in 2-propanol/water mixtures.....	233
65. Arrhenius plots of molar conductance of copper(II) perchlorate in 2-propanol/water mixtures.....	234
66. Arrhenius plots of molar conductance of aluminum perchlorate in 2-propanol/water mixtures.....	235
67. Composition dependence of the activation energy of conductance of some inorganic electrolytes in 2-propanol/water mixtures.....	236
68. (A-G) Temperature and concentration dependence of the conductance of lithium nitrate in 2-butanol/water mixtures.....	245
69. (A-F) Temperature and concentration dependence of the conductance of perchloric acid in 2-butanol/water mixtures.....	249
70. (A-G) Temperature and concentration dependence of the conductance of thallium acetate in 2-butanol/water mixtures.....	252

FIGURE	PAGE
71. (A-G) Temperature and concentration dependence of the conductance of copper(II) perchlorate in 2-butanol/water amixtures.....	256
72. (A-F) Temperature and concentration dependence of the conductance of aluminum perchlorate in 2-butanol/water mixtures	260
73. Arrhenius plots of molar conductance of lithium nitrate in 2-butanol/water mixtures.....	263
74. Arrhenius plots of molar conductance of perchloric acid in 2-butanol/water mixtures.....	264
75. Arrhenius plots of molar conductance of thallium acetate in 2-butanol/water mixtures.....	265
76. Arrhenius plots of molar conductance of copper(II) perchlorate in 2-butanol/water mixtures.....	266
77. Arrhenius plots of molar conductance of aluminum perchlorate in 2-butanol/water mixtures.....	267
78. Composition dependence of the activation energy of conductance of some inorganic electrolytes in 2-butanol/water mixtures.....	268
79. Temperature dependence of the Debye factor f at different values of Dielectric permittivity ϵ for CrO_4^{2-} , NO_3^- , and nitrobenzene.....	275
80. Solvent dependence of the activation energy near 298K for NO_3^- , CrO_4^{2-} and nitrobenzene	277
81. Solvent dependence of $\log A_2$ near 298K for NO_3^- , CrO_4^{2-} and nitrobenzene.....	278
82. Arrhenius plots for the reaction of solvated electrons with nitrobenzene in 1-propanol/water (A) and 2-propanol/water (B) mixtures.....	280

FIGURE	PAGE
83. Arrhenius plots for the reaction of solvated electrons with nitrobenzene in 2-butanol/water mixtures	281
84. Solvent dependence of $k_2(A)$ and k_2/f (B) at 298K for NO_3^- , CrO_4^{2-} and nitrobenzene in 1-propanol/water, 2-propanol/water and 2-butanol/water mixtures.....	283
85. Solvent dependence of $k_2\eta/fT$ at 298K for NO_3^- , CrO_4^{2-} and nitrobenzene in 1-propanol/water, 2-propanol/water and 2-butanol/water mixtures.....	285
86. Solvent dependence of molar conductivities of lithium nitrate and lithium chromate at 298K in 1-propanol/water, 2-propanol/water and 2-butanol/water mixtures.....	287
87. Arrhenius plots of the association constants of LiNO_3 and Li_2CrO_4 in alcohol-rich solvents of 1-propanol/water, 2-propanol/water and 2-butanol/water.....	289
88. Solvent composition dependence of $z_ik_2/f\Lambda_0T$ at 298K for some inorganic electrolytes in 1-propanol/water, 2-propanol/water and 2-butanol/water mixtures.....	290
89. Solvent composition dependence of r_d of $\text{Li}_s^+ + \text{NO}_3^-$ and $\text{Li}_s^+ + \text{CrO}_4^{2-}$ at 298K in 1-propanol/water, 2-propanol/water and 2-butanol/water.....	292
90. Temperature dependence of the Debye factor f at different values of dielectric permittivity. (A) for $z = +1$ using $r_f = 1.0$ nm; (B) for $z = +2$ using $r_f = 0.5$ nm; and (C) for $z = +3$ using $r_f = 0.35$ nm...	294
91. The composition dependence of k_2/f for positive ions in 1-propanol/water mixtures at 298K.....	295

FIGURE	PAGE
92. The composition dependence of k_2/f for positive ions in 2-propanol/water mixtures at 298K.....	296
93. The composition dependence of k_2/f for positive ions in 2-butanol/water mixtures at 298K	297
94. The composition dependence of k_2 for positive ions in 1-propanol/water mixtures at 298K.....	298
95. The composition dependence of k_2 for positive ions in 2-propanol/water mixtures at 298K.....	299
96. The composition dependence of k_2 for positive ions in 2-butanol/water mixtures at 298K	300
97. The composition dependence of the activation energies for the reaction of solvated electrons with positive ions in 1-propanol/water mixtures.....	302
98. The composition dependence of the activation energies for the reaction of solvated electrons with positive ions in 2-propanol/water mixtures.....	303
99. The composition dependence of the activation energies for the reaction of solvated electrons with positive ions in 2-butanol/water mixtures.....	304
100. The composition dependence of $\log A_2$ for the reaction of solvated electrons with positive ions in 1-propanol/water mixtures.....	305
101. The composition dependence of $\log A_2$ for the reaction of solvated electrons with positive ions in 2-propanol/water mixtures.....	306
102. The composition dependence of $\log A_2$ for the reaction of solvated electrons with positive ions in 2-butanol/water mixtures.....	307

FIGURE	PAGE
103. The composition dependence of $k_2\eta/rT$ for positive ions in 1-propanol/water (A) and 2-propanol/water (B) mixtures at 298K.	308
104. The composition dependence of $k_2\eta/rT$ for positive ions in 2-butanol/water mixtures at 298K	309
105. The composition dependence of molar conductivity of some inorganic electrolytes in 1-propanol/water mixtures at 298K.....	311
106. The composition dependence of molar conductivity of some inorganic electrolytes in 2-propanol/water mixtures at 298K.....	312
107. The composition dependence of molar conductivity of some inorganic electrolytes in 2-butanol/water mixtures at 298K	313
108. Arrhenius plots of the association constants of $AgClO_4$ and $TlOAc$ in alcohol-rich solvents of 2-propanol/water and 2-butanol/water. (A) $AgClO_4$ in 2-propanol/water; (B) $TlOAc$ in 2-butanol/water....	315
109. The composition dependence of $z_ik_2/f\Lambda_0T$ for some inorganic electrolytes in 1-propanol/water (A) and 2-propanol/water (B) mixtures at 298K.....	317
110. The composition dependence of $z_ik_2/f\Lambda_0T$ for some inorganic electrolytes in 2-butanol/water mixtures at 298K	318
111. The composition dependence of the mutual radius for diffusion of some inorganic electrolytes in 1-propanol/water (A), 2-propanol/water (B) and 2-butanol/water (C) mixtures at 298K...	320

CHAPTER ONE

INTRODUCTION

This thesis is concerned with reaction rates of solvated electrons with solutes in alcohol-water mixed solvents. By way of introduction we summarize the properties of injected electrons in liquids, the relevant properties of alcohol/water mixed solvents, and the general features of reaction rates for solvated electrons in solvents of this type.

I. The Solvated Electron

The history of solvated electrons began early in the 19th century. In November 1808 Humphry Davy observed a blue color when he heated potassium metal in dry ammonia gas (1). A paragraph from Davy's laboratory notebook, quoted in ref. 1, was "When 8 grains of potassium were heated in ammonical gas - it assumed a beautiful metallic appearance and gradually became of a fine blue color." Fifty years later, in 1864, W. Weyl observed a blue color when sodium or potassium was dissolved in liquid ammonia (2). C.A. Kraus in 1922 provided the final proof that the blue color was due to solvated electrons, by comparing transference and conductance properties in solutions of alkali metals dissolved in liquid ammonia (3). Solvated electrons were similarly obtained in other solvents such as methylamine and ethylenediamine (4) by dissolving sodium or potassium in them. Later, solvated electrons were obtained by pulse radiolysis in water (5), alcohols (methanol, ethanol (6)), hydrocarbons (methylcyclohexane, hexene-1 (7)), ethers (diethyl ether, di-n-propyl ether (8)), *etc.*

Solvated electrons have been used to convert a wide range of chemical substances to their reduced forms (*e.g.* to convert benzene to 1,4-dihydrobenzene (9)).

Radiolysis (10) is the most convenient method to form solvated electrons. In radiolysis, the liquid is usually irradiated with a pulse of high energy electrons. When these electrons penetrate the liquid medium, they lose energy by ionization and excitation

of the liquid molecules. Small local volumes of ions and electrons, excited and dissociated molecules are formed along the path of the high energy electrons. The reactive intermediates in these local volumes, called microzones, dissipate in a few nanoseconds by reacting together or diffusing into the bulk of the liquid (11).

The lower energy secondary electrons produced by the high energy primaries also lose their excess energy by ionization and excitation of molecules in the medium. The de-energized electrons ultimately enter one of several types of states, depending on the solvent properties.

(a) In an electrophilic solvent, the slowed-down electrons attach to solvent molecules to form negative ions.

(b) If the electrons are not attached to specific molecules they reach a state of thermal equilibration with the solvent medium, resulting in *solvated electrons*. As discussed in the next section, these solvated electrons can be detected by distinctive properties such as electrical mobility and optical absorption spectra.

Two broad types of solvated electron species can be formed, depending on the solvent involved. A thermalized electron can be localized in a coulombic (electrostatic) potential well in a solvent whose molecules are polar or strongly and anisotropically polarizable; the potential well is created by several suitably oriented solvent molecules (12). On the other hand if a solvent molecule is isotropically polarizable, the potential well is very shallow and the electron is not then localized to any large extent. Such electrons, which are very mobile, are called "quasifree" electrons (12).

An electron polarizes the electron clouds of nearby molecules in about 10^{-15} seconds. Thus the trapped electron immediately finds itself in an electronically polarized potential well (13). The electric field of the electron causes the medium molecules to reorient along the axis of permanent dipole or that of the maximum polarizability. The trap becomes deeper. It takes about a picosecond for the trapped electron to relax into the solvated state (12,13).

II. Properties of Solvated Electrons

As suggested above the properties of solvated electrons depend on the nature of the solvent. Geometry and polarity of the solvent molecules affect the electron-solvent interaction, and therefore the energy of solvation.

Electron spin resonance (ESR) studies have shown the paramagnetic nature of the solvated electron states (14).

The thermodynamic properties of solvated electrons such as the standard potential (15) and the solvation energy and entropy (16) are still not accurately known (15) because the energetics of solvent ionization and of solvent relaxation about the newly separated charges have not yet been completely resolved.

A. Mobility

Solvated electrons are different from quasifree electrons. They are much less mobile. The mobility of a delocalized electron could be $\sim 10^{-2} \text{ m}^2/\text{V}\cdot\text{s}$ in comparison to $10^{-6} \text{ m}^2/\text{V}\cdot\text{s}$ of a localized electron. Conductivity studies provide data on the mobility of solvated electrons. Their mobility is several times higher than that of normal ions. In water for example, the mobility of solvated electrons is equal to that of hydroxide ions and smaller than that of protons (17). In nonpolar liquids the mobilities depend strongly on the structure of the solvent molecules, and are usually several orders of magnitude greater than those of ordinary ions (11,18).

B. Optical Absorption Spectrum

Photo-absorption of solvated electrons occurs in the ultraviolet to infrared region. The absorption band is broad and asymmetric with a long tail extending to higher energies. The energy at the absorption maximum, $E_{A\text{max}}$, and the width of the band depend on the polarity of the solvent.

In protic solvents such as water, alcohols (19) and ammonia (20), the energy of maximum absorption E_{Amax} lies in the visible to near-infrared regions since the interaction of the solvated electron with these strongly polar molecules is very large. In nonpolar aliphatic hydrocarbons (7) on the other hand, where solvation energy arises from interaction with induced dipole moments, absorption maxima occur further to the infrared. Values of E_{Amax} for polar but aprotic solvents such as ethers (8) lie between these extremes.

Values of E_{Amax} are temperature dependent. Thermal agitation of the solvent makes the traps shallower. Therefore, values of E_{Amax} decrease with increasing temperature (19).

1. Absorption Band Width

The solvated electron absorption band has a similar form in a wide range of solvents: it is always broad and asymmetric, skewed to higher energies. This can be interpreted as the result of both homogeneous and heterogeneous broadening effects. Homogeneous broadening assumes that a single species is responsible for the absorption (all traps in the medium are the same) but attributes broadening to the coupling between solvated electron levels in the trap and molecular motions of the surrounding dipolar molecules (21,22). Heterogeneous broadening on the other hand attributes the band width to a wide variation of solvated electron trap depths, each trapped electron state having a different absorption spectrum. Since both factors must play a part, we say that the band is nonhomogeneously broadened.

2. Bound and Continuum Transitions

The absorption bands of solvated electrons have also been interpreted as arising from two types of electronic transitions (24-28):

- (i) Bound-bound transitions (from ground state level of a trap to an excited discrete level of the trap);

- (ii) Bound-continuum transitions (from ground level to continuum levels associated with the liquid as a whole).

The strong skewing of the absorption band toward higher energies has been interpreted as evidence for strong contributions of bound-continuum transitions, since it is argued that a more symmetric shape would result from bound-bound transitions alone. Evidence for this is given by studies of photoconductivity spectra, assuming that higher mobilities generated in photoconductive processes result from excitation of the electron to a continuum level of the liquid. By estimating the threshold or minimum energy E_{th} for photoconductivity and comparing it with the characteristics of the optical absorption spectrum as a whole an idea of the extent of bound-continuum transitions in the absorption spectrum can be obtained (29-34). Results show that both bound-bound and bound-continuum transitions contribute to the spectrum; typically E_{th} is less than E_{Amax} and therefore a major portion of the spectrum is due to bound-continuum transitions. In studies of photoconductivity in mixtures of polar/nonpolar solvents (31-34), it has been concluded that bound-bound transitions play an increasing role as the fraction of polar component increases, perhaps due to deepening of the traps.

3. Models

Several early theoretical models have been used to explain the optical absorption spectra of solvated electrons. These were all based on the localization of the electron in a cavity.

(a) In the simplest model (35), the electron is localized in a physical cavity, with positive ends of the dipolar solvent molecules oriented around it.

(b) In the continuum model (36), the electron is considered to be located in a cavity inside a polarized continuous dielectric medium.

(c) In the semi-continuum models (37,38), the electron is assumed to be in a spherical cavity which is surrounded by a solvation shell containing a fixed number of

solvent molecules, and the solvent outside this shell is assumed to be a continuous dielectric medium.

E_{Amax} values have been calculated using these models, but the line shape is always much narrower and more symmetrical than observed. Statistical mechanical models that consider the molecular properties of the solvent in greater detail are being developed (39-42).

According to an ESR study of solvated electrons in aqueous glasses (43) the electron is solvated at the centre of an octahedron made up of six water molecules.

4. Optical Absorption Spectrum in Hydroxylic Solvents

The absorption energies of electrons in water, alcohol and their mixtures are greater than those in other polar solvents such as ammonia and amines (44) because of the stronger electron-solvent interactions in the hydroxylic solvents.

The E_{Amax} values of solvated electrons in alcohols are in the order of primary > secondary > tertiary (19,45). E_{Amax} values are, in general, independent of chain length for primary alcohols (46) because the alkyl group beyond the α -carbon has apparently not much effect on the interaction between the electron and the solvent (46,47).

The weaker orientational alignment of solvent dipoles around the electron is probably the reason for lower E_{Amax} values in secondary and tertiary alcohols.

The widths of the solvated electron absorption band at half height ($W_{1/2}$) in alcohols are about twice that in water (48). The $W_{1/2}$ values in amines are also about twice that in ammonia (49). In alcohols, bound to continuum transition mode has been considered as the major contributor in the absorption spectra of solvated electrons. The extent of bound to bound transition depends on the type of alcohol (30,48).

III. Structure and Properties of Hydroxylic Solvents

As is shown in the present work, reactivities of solvated electrons in hydroxylic solvents depend not only on the nature of the solvated electron state itself but also on the

structural features of the solvent and resulting properties such as diffusion coefficients, viscosity, dielectric relaxation times, *etc.* An introduction to these topics is therefore also useful.

A. Structure of Water

According to earliest models of the structure of water, based on radial distribution functions, water was considered to have a "broken down" ice structure (50). In ice, each water molecule is hydrogen bonded tetrahedrally to four other molecules. The distribution functions of water (51,52) indicate slightly more than four nearest neighbors. There are different kinds of models proposed for the structure of water, they fall into two broad categories: (a) uniformist models (53-57) and (b) mixture models (58-62).

According to the uniformist models, water consists of a single type of three-dimensional random hydrogen bond network. There are no significant amounts of monomer water. There is an equilibrium between free and bonded hydroxyl groups. The structure is regarded as a network of cavities with structural order that is approximately tetrahedral.

According to the mixture models, water consists of a mixture of two or more species. These are water molecules with no hydrogen bonds or with up to four hydrogen bonds. The hydrogen bonded water molecules form an open network full of cavities or clusters of water molecules. These exist in equilibrium with monomer water which makes the medium denser than ice.

No single model can explain all the properties of water, but experimental results are usually explainable with one or the other of these models. Simulations of water structure are being done in order to develop a better model for water (63,64).

B. Structure of Alcohols

The liquid structures of alcohols are simpler than those of water because there is only one hydroxyl group per molecule. Some alcohols can form up to three hydrogen bonds

per molecule, while water can form four hydrogen bonds. Various spectroscopic studies have shown that monomers, dimers and polymers all exist (65-67). There are linear or ring polymers where approximately two hydrogen bonds per alcohol molecule are formed. Alcohols with larger alkyl groups tend to exist mainly as monomers and ring-like polymers because of the steric hindrance (68). Lower alcohols can make a third hydrogen bond which leads to a three-dimensional linkage of polymer chains (69,70).

C. Water/Alcohol Mixtures

1. Static Dielectric Properties

Information about the short range order in a liquid can be obtained from dielectric properties. The Kirkwood structure factor, g_k , which is calculated from the dielectric constant, dipole moment and density, is a measure of the short-range order (71). When the molecular dipoles are oriented in series the value of g_k is greater than one. For head-to-tail interaction between molecular dipoles, g_k is less than one. Random orientation gives $g_k = 1$.

As a result of the existence of short-range order in water and primary alcohols the g_k values are greater than unity (49,72,73). The value of g_k increases with increasing chain length for primary alcohols because the alcohols with longer chains are better aligned. Small alcohols can form a third hydrogen bond cross-linking the polymer chains. This must be the reason for its lower g_k value which arises because of the difficulty of alignment.

The g_k values increase slightly when water is added to methanol or tertiary alcohols (73,74). Water can make hydrogen bonds with these alcohol molecules resulting in a better linear arrangement of dipoles. Thus water has a structure building effect in these cases. On the other hand the g_k values decrease when water is added to other alcohols (73), and water acts as a structure breaker on these alcohols.

2. Thermodynamic Properties

The thermodynamic functions of mixing of alcohol and water have been useful in the study of the structure of alcohol/water mixtures (75-77). The extent of change depends on the alkyl group. Hydrogen bond formation gives rise to a negative enthalpy of mixing and a positive value implies hydrogen bond rupture. When a small amount of alcohol is dissolved in water a decrease in enthalpy and entropy results. The interpretation is that (a) the alcohol molecule promotes water-water hydrogen bonding (78,79) or (b) water molecules order around the alcohol molecule and form clathrate-like structures (80). Therefore, the structure of water is strengthened by alcohol molecules (77,79).

The enthalpy of mixing of higher alcohols with water is positive; water acts as a structure breaker (75,76).

3. Viscosity

The viscosity of a liquid is related to the rate of diffusion in a liquid. The viscosity is higher in alcohols with longer and branched alkyl groups. The bulkiness of the alkyl group makes it difficult to flow. Viscosities are strongly composition dependent in mixtures in alcohol and water. The following are the important qualitative features of viscosity of alcohol/water mixtures (62,81): (a) A maximum in viscosity occurs at a composition around 75 mole percent water, (b) a sharp increase in viscosity occurs when a few mole percent of alcohol is added to water, and (c) only small changes in viscosity occur when a few mole percent of water is added to alcohol.

Viscosity is increased when some alcohol is added to water. This is perhaps due to the clathrate-like structure formation (80). In the lower alcohols, water acts as a structure maker, indicated by an increase in viscosity. Viscosity decreases when water is added to larger alcohols which can be explained by the formation of water nucleated alcohol complexes (19,76) or by the breakdown of alcohol structure by water (82).

IV. Reactivity of Solvated Electrons

Another possible source of information about solvated electrons is to study their reactivities with different types of solute. Rates of solvated electron reactions have been measured in water (83), alcohols (84-90), alcohol mixtures (91-94), and alcohol/water mixtures (95-108). The present work continues and extends this work to the particular case of ionic solutes.

As stated earlier, variations in composition of alcohol/water mixtures strongly affect the details of packing and structural order of molecules in the liquid. These variations affect not only bulk properties of the liquid but also the detailed environment and stability of the solvated electron state, its mobility, and other properties relevant to reactivity. Hence rates of reaction of solvated electrons with various solutes vary strongly when composition is varied in these liquid mixtures.

One way of understanding some of these effects is to study the correlation of solvated electron reaction rates with those bulk physical properties of the solvent mixtures which also depend strongly on composition. Three useful examples of such properties are:

(a) Excess enthalpy of mixing (60,77,109). It is negative in the water-rich region but in the alcohol-rich region, it is negative for lower alcohols and positive for higher alcohols.

(b) Viscosity. A maximum always occurs near 75 mole percent water (82). The specific composition at which the maximum occurs depends on the type of alcohol. Larger alcohol molecules will give a maximum with a smaller amount of alcohol added.

(c) Dielectric relaxation. Dielectric relaxation time of water (or alcohol) increases with the addition of a small amount of alcohol (or water) (110-112).

Solvated electron reactions have been studied in alcohol/water mixtures such as methanol/water (95-97,108), ethanol/water (95-99,108), 1-propanol/water (101),

2-propanol/water (106), 1-butanol/water (102), 2-butanol/water (105), isobutanol/water (105), and t-butanol/water (104,105,107) systems. The composition dependence of the nearly diffusion controlled rate constants has been analyzed using the Stokes-Smoluchowski (113) and Debye (114) models, assuming that in these cases the rate variation is directly attributable to variation in diffusion coefficients with solvent composition. The rate constants for the reactions with inefficient electron-acceptors are explained in terms of the energy of solvation of electrons in the different solvents, rather than in terms of solvent transport properties (104,105).

In the Stokes-Smoluchowski model, the rate constant k_2 of a diffusion controlled reaction between species i and j is given by

$$k_2 = 4\pi N_A(D_i + D_j)(r_{ri} + r_{rj}) \quad [1]$$

where 4π is steradians (all directions of approach of i to j lead to reaction), N_A is Avogadro's constant, D_i and D_j are the diffusion coefficients of i and j , and $(r_{ri} + r_{rj}) = r_r$ is the reaction radius of the reacting pair.

The Debye modification of the Stokes-Smoluchowski relation has been used to analyze the solvent effects on the reaction kinetics of solvated electrons with charged and polar electron acceptors in alcohol/water mixtures (106-108). In the Debye model a factor f , which considers the coulombic interaction potential $U(R)$ between the electron and a dipolar or ionic solute, is applied.

$$k_2 = 4\pi N_A(D_i + D_j)(r_{ri} + r_{rj})f \quad [2]$$

where

$$f = (U(R)/k_B T)[\exp(U(R)/k_B T) - 1]^{-1} \quad [3]$$

For the reaction of a solvated electron e_s^- with a molecule S



the potential energy when S is an ion of charge $z\xi$ is given by

$$U(r_f) = -z\xi^2/4\pi\epsilon_0\epsilon r_f, \quad [5]$$

where $-\xi$ is the charge on the electron, z is the elementary charge on S, ϵ_0 is the permittivity of vacuum and ϵ is the relative permittivity (dielectric constant) of the solvent between the electron and the ion.

For the electron-dipole interaction,

$$U(r_f) = -M\xi\cos\theta/4\pi\epsilon_0\epsilon r_f^2, \quad [6]$$

where M is the dipole moment of the molecular reaction, and θ is the angle of approach of e_s to the dipole axis of S.

The diffusion coefficients in equation [2] are related to the molar electrical conductivities λ_i ($C\cdot m^2/V\cdot s\cdot mol$) of ions i :

$$\begin{aligned} D_i(m^2/s) &= \lambda_i k_B T / z_i^2 N_A \xi^2 \\ &= 8.95 \times 10^{-10} \lambda_i T / z_i^2 \end{aligned} \quad [7]$$

Equations [2] and [7] can be rearranged to give the effective reaction radius r_f for a diffusion controlled reaction:

$$r_f = \frac{k_2}{\left(\left[\lambda_i / z_i^2 + \lambda_e \right] \right) f} \cdot \frac{\xi^2}{4\pi k_B T} \quad [8]$$

$$= 1.48 \times 10^{-16} k_2 / ([\lambda_i / z_i^2] + \lambda_e) fT$$

Here λ_i and λ_e are the molar conductivities of the reactant ion and e_3 respectively.

For reactions that do not occur at every diffusive encounter of the reactant pair an encounter efficiency κ (<1) is introduced.

$$\kappa r_f = 1.48 \times 10^{-16} k_2 / ([\lambda_i / z_i^2] + \lambda_e) fT \quad [9]$$

Values of the molar conductivities of the individual reactant ions and e_3 are not known for most of the solvents, so as an approximation the molar conductivities of salts such as $\Lambda(\text{Li}^+, \text{NO}_3^-)$ and $\Lambda(2\text{Li}^+, \text{CrO}_4^{2-})$ have been used. $z_i k_2 / \Lambda fT$ gives an idea of the variation of κr_f in different solvents.

Diffusion coefficients can also be expressed in terms of solvent viscosity if the solute molecules are larger than or similar in size to the solvent molecules, using the Stokes-Einstein relation (115),

$$D_i \approx k_B T / 6\pi\eta r_{di}, \quad [10]$$

where r_{di} is the effective radius of the molecule i for diffusion. Equations [2] and [10] can be rearranged to

$$k_2 \approx R T r_f / 1.5\eta r_d, \quad [11]$$

where $R = N_A k_B = 8.3 \text{ J/mol}\cdot\text{K}$ is the gas constant, $r_d^{-1} = (r_{di}^{-1} + r_{dj}^{-1})$, and r_d is the effective radius for mutual diffusion of i and j .

Introduction of the reaction encounter efficiency κ into equation [11] and rearrangement gives

$$k_2 \eta / fT \approx 5.5 \kappa (r_f / r_d) \quad [12]$$

To the extent that this crude model is satisfactory, the solvent dependence of the measurable quantity $k_2 \eta / fT$ indicates the solvent dependence of $\kappa(r_f / r_d)$.

Although these models ignore effects that solvent structure (molecular packing and relative orientation) exerts on reactant diffusion and reaction probabilities, the equations are useful in evaluating effects of bulk fluid properties such as viscosity and dielectric constant. Once the effects of bulk fluid properties are accounted for, unexplained features remaining can be attributed to effects of nonhomogeneous structure in the solvent.

The effects of temperature on reaction kinetics can also provide valuable data for postulating mechanisms. Changes in reaction rates due to temperature change are generally expressed in terms of the activation energy (E_a) and the frequency factor (A) of the modified Arrhenius equation [13]:

$$k_2/f = A_2 e^{-E_2/RT} \quad [13]$$

V. Present Work

At the time we started this work few data were available regarding the solvent structure effects on solvated electron reactions with ionic electron acceptors in alcohol/water mixtures. The objective of this study is to learn more about the behavior of solvated electrons in 1-propanol/water, 2-propanol/water and 2-butanol/water mixtures and the effects of solvent structure on the reactions of e_s^- with ions in these mixtures. Rate measurements were carried out as a function of temperature in order to obtain information about the temperature effects on these reactions. Electrical conductivity measurements were also carried out in order to obtain information about the diffusion coefficients since the diffusion coefficients of the reacting species are related to molar electrical conductivities. The activation energies of nearly diffusion-controlled reactions are similar to those of diffusion of the corresponding ions in solution, so the temperature dependence of the molar conductivities ⁴⁵ were also investigated.

CHAPTER TWO

EXPERIMENTAL

I. Materials

1-Propanol, 2-propanol and 2-butanol were obtained from Aldrich Chemical Co. (99+%, spectroscopic grade, gold label). They were dried for two weeks on Davison Molecular Sieves 3Å and then treated for one day under UHP argon (Liquid Carbonic Canada Ltd.) with sodium borohydride (~2g/L) at ~330K. The alcohol was then fractionally distilled under argon through an 80 × 2.3 cm column packed with glass helices, discarding the first 20% and last 40%. The water content of the collected 40%, measured by Karl-Fisher titration, was 0.1 mol% in 1-propanol, 0.2 mol% in 2-propanol and 0.1 mol% in 2-butanol. The solvated electron half life after a 100 ns pulse of 1.9 MeV electrons (~3 J/kg, 2×10^{16} eV/g) at 298K was about 8 μs in 1-propanol and 2-propanol, and 4 μs in 2-butanol.

Water was purified in a Barnstead Nanopure II ion exchange system. The solvated electron half life after a 100 ns pulse of radiation was 20 μs.

Lithium nitrate (99.999% Aldrich, gold label), lithium chromate (K and K reagent grade), silver perchlorate (Strem, reagent grade), thallium acetate (96%, BDH Chemicals Ltd.), copper(II) perchlorate (Aldrich, reagent grade), aluminum(III) perchlorate (98%, Aldrich Chemical Co.), and perchloric acid (70%, Fisher Scientific Co.) were used as received.

II Apparatus for Kinetic Measurements

A. Sample Cells

Cells of Suprasil Quartz obtained from Terochem Laboratories were used at atmospheric pressure for temperatures varying from 276K to 372K. The cells had an

optical path length of 1 cm. Inside dimensions were $1 \times 1 \times 4.5$ cm. The cell was topped by a grade seal so that it could be attached to a Pyrex tube.

B. Bubbling System

The kinetic samples in quartz cells were bubbled with argon and sealed before the irradiation. The bubbling system shown in Figure 1 was made by connecting 1 cm^3 syringes to a long Pyrex tube. The gas flow was controlled by Pyrex/Teflon stopcocks (No. 7282, Canadian Laboratory Supplies Ltd.). The rate of bubbling through the stainless steel needles (30 cm long, 0.625 mm i.d.), which were attached to the syringes was about $20 \text{ cm}^3/\text{minute}$.

C. Irradiation, Detection and Control Systems

1. The Van de Graaff Accelerator

A Van de Graaff accelerator (type AK-60 2 MeV) manufactured by High Voltage Engineering Corporation was used as the source of high energy electrons. The maximum peak current delivered during a pulsed operation was 150 mA. Pulse widths of 3, 10, 30, and 100 nanoseconds (ns), and 1 microsecond (μs) were available. Of these only 100 ns pulse width was used to obtain an appropriate pulse dose.

A concrete maze shielded the entrance from the control room to the accelerator and the target room. Closing and locking the iron-gate at the control room end of the maze sounded a warning buzzer for 15 seconds. It was not possible to operate the accelerator until the cessation of the buzzer. Opening of the iron gate resulted in immediate shut down of the accelerator.

Steering and focussing of the electron beam was normally done by fixing a piece of phosphorescent paper to the end of the accelerator beam pipe. The paper could be viewed by a closed circuit television. Each pulse of electrons caused a visible glow where it struck the phosphor. Thus accurate steering and focussing were done by adjusting the

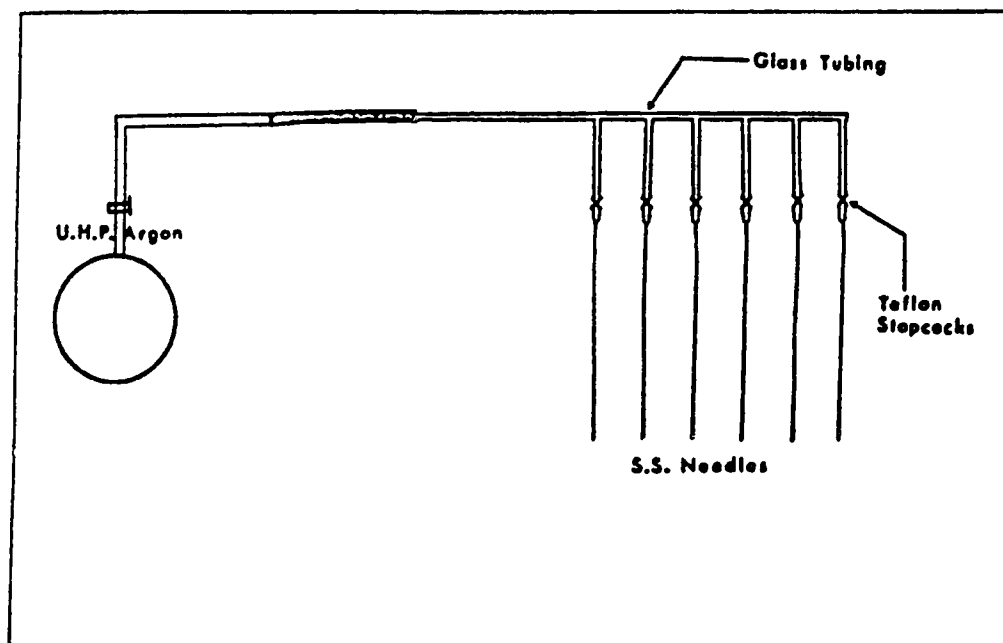


Fig. 1 The Bubbling System

current in the electromagnets. When equipment blocked visual observation the steering of the beam was done by maximizing either the secondary emission monitor's (SEM) dose or the optical absorption of solvated electrons in a water sample.

2. Secondary Emission Monitor

The secondary emission monitor (SEM) indicated the relative dose for each electron pulse. It consisted of three thin metal foils placed inside the accelerator beam pipe perpendicular to the path of high energy electrons (Figure 2). These foils were positioned near the electron window and they were made of cobalt-based, high strength alloy (Havar) obtained from the Hamilton Watch Company, Precision Metal Division. This material (average atomic number 27) was better than gold (atomic number 79) because of less beam attenuation by electron scattering.

The diameter of these foils were 5 cm and they were kept 0.5 cm apart from each other. The outer two were mounted at a potential of 50 V. Passage of an electron pulse generated secondary electrons at the foils. The electrons ejected from the center foil were collected by outer foils, the net result being a current flow from the center foil. Current flow occurred only during a high energy electron pulse and was measured by a gated integrator, digitized and displayed on a digital readout.

3. Optical Detection System

(a) *The light source.* Figure 3 shows a schematic diagram of the path of the analyzing light.

A high pressure Xenon arc lamp (Optical Radiation Corporation, model XLN 1000 W) contained in a lamp housing (Photochemical Research Associates, model PRA ALH 220) was used as the source of light. A rhodium-coated, off-axis paraboloid mirror (Melles Griot-02 POH 015) placed in the beam path absorbed the UV light with wavelength shorter than 320 nm. Formation of excess ozone was prevented by this. The

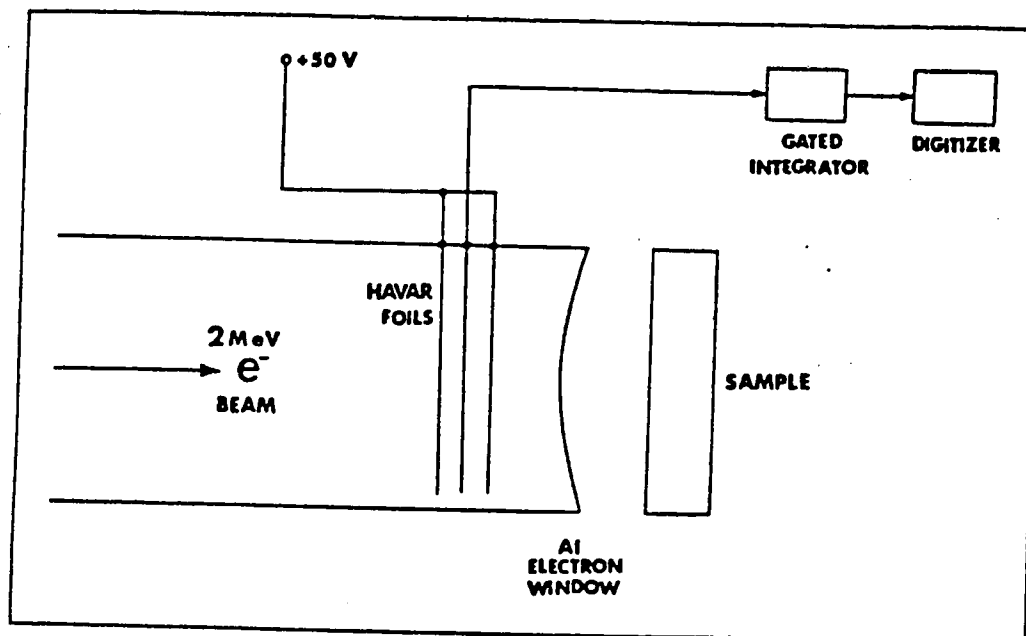


Fig. 2 The Secondary Emission Monitor

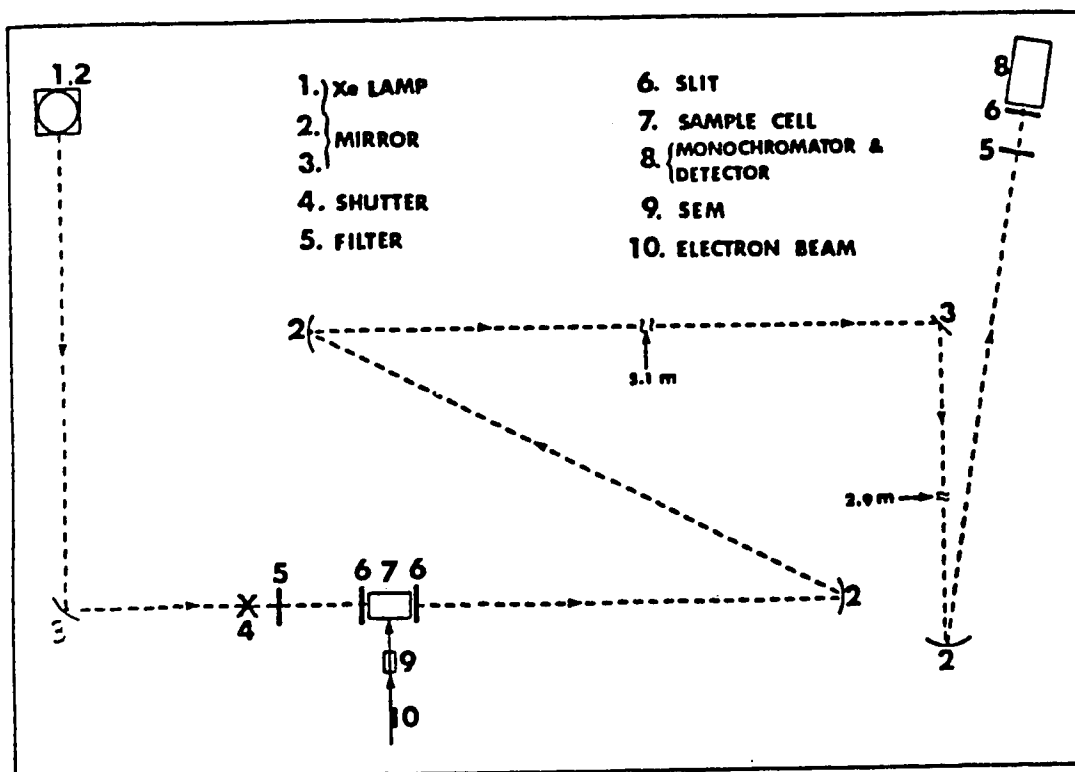


Fig. 3 The Path of the Analyzing Light

lamp was usually run at 1 kW and pulsed to 9.75 kW for 500 μ s when a decay signal was desired.

The light shutter was used to protect the sample from unnecessary exposure. It was opened for only 55 ms. The light beam was focussed at the center of the irradiation cell by using the above mentioned mirror. The light beam was brought from the irradiation room to the control room through a hole in the 1.2 m thick wall by reflecting on-front surface aluminized mirrors coated with silicon monoxide. Finally, the light was focussed into the monochromator housing by a concave mirror.

(b) Monochromator grating and filters. The monochromator was a Bauch and Lomb type 33-86-25. For light from 350 nm to 800 nm the type 33-86-02 grating was used and for light from 700 to 1000 nm the type 33-86-03 grating was used. The two Corning filters used were type CS-2-64 for light from 700 to 1000 nm, and CS-3-73 for light from 480 to 700 nm. The front and back slit widths of the monochromator were 2.5 mm and 1.4 mm respectively.

(c) Digital voltmeter, oscilloscope and plotter. The incident light intensity at the detector, recorded as a voltage on a digital multimeter (Fluke 8810 A), was displayed on an oscilloscope (Tektronix R 7623). The signals were displayed as plots of voltage against time on a digital plotter (Zeta 1200). All information related to the particular signal such as total light, dose, temperature, sensitivity, time scale, half-life curve, and cell holder number were also printed on the chart.

4. Temperature Control System

(a) Cooling and heating. Temperatures from 277 K to 298 K were achieved by boiling liquid nitrogen. The temperature of the resulting nitrogen gas was regulated by using another heater. Liquid nitrogen was boiled at a controlled rate from a 50 L, narrow-necked aluminum Dewar vessel (Lakeshore Cryotonics Inc.). A stainless steel pipe (5 cm diameter) which was fixed to a lid, fitted snugly into the neck of the Dewar. This pipe

extended to the bottom of the Dewar. A nichrome heating coil (600 W) was attached to the inside of the steel pipe to about 7 cm from the bottom.

A Rubatex foam-rubber pipe (1 meter long) was used to transport the cold nitrogen to the sample box. Both ends of the pipe had glass inserts to which a leather seal was connected. Before entering the cell box, the cold gas that came through this pipe flowed through another stainless steel pipe (2.5 cm diameter) that had another nichrome heating wire (0.00024 m diameter, 4 m long) inserted inside it. The temperature of the nitrogen gas was regulated by this heating wire.

A laboratory heat gun (Master Appliance Corporation, model AH 0751) was used to achieve temperatures from 296 K to 372 K. The nichrome wire heated the air to the required temperature.

(b) *Cell holder box.* A box insulated with foam glass (Pittsburgh Corning Corporation) contained eight cell holders which were mounted on a circular (7 cm diameter) aluminum base. The base was connected to a motor so that the cell holder could make clockwise and counterclockwise full cycle rotations when the cells were not being irradiated. Just before irradiation the pre-selected cell stopped in front of the electron window. The gas that flowed through the holes in the aluminum base was stirred by the rotating cell holder before leaving *via* a hole (2.5 cm diameter) in the lid.

A thermocouple mounted in a cell (thermocouple cell) filled with solvent monitored the temperature of the system. The temperature controller (Taylor Microscan 1300) utilized a temperature sensor which was fixed to one of the cell holders. A Fluke Digital thermometer (model 2100 A) displayed the temperature of the thermocouple. The temperature of the thermocouple cell and the difference between the temperatures of the thermocouple cell and the air were plotted on a chart recorder (Clevite Corporation, model 15 6327 57). When the chart recorder displayed a steady temperature for a period of 15 minutes the thermal equilibrium in the system was deemed to be established. At this time, the variation of the temperature of the thermocouple cell was only ± 0.1 K.

III. Conductivity Measurements

A. Impedance Bridge

Conductivity measurements were done with an impedance bridge (type 1608-A, General Radio Co.). It was a self-contained system which included six bridges for the measurement of conductance, capacitance, resistance, and inductance, as well as the internal generators and detectors for AC and DC measurements. To obtain the conductance reading the variable resistor and capacitor were adjusted until the null balance was achieved. Most of the time the conductance mode (G_p mode) was used. For the values of conductance less than about 0.60 microsiemen, the bridge was set to one of the capacitance modes (C_p mode). Then the values of conductance were calculated from the capacitance data. The oscillator frequency was 1 kHz for AC measurements.

B. Conductance Cells

Pyrex conductivity cells (YSI 3403) were obtained from Yellow Springs Instrument Co., Inc. The temperature range of the measurements was 277 K to 353 K. The cell chamber was 5 cm deep. The overall length was 20 cm and the outer diameter was 1.2 cm.

Graduated cylinders, 25 cm³ (16 cm long, 1.4 cm i.d.), were used to contain the electrolyte solutions. In order to have a tight seal between the container and the cell, a rubber adapter made from no. 2 stopper was fixed to the cell. Two layers of Parafilm (American Can Company) were wrapped around the adapter-container junction to provide a tight seal, especially at high temperatures.

A secondary standard solution (YSI 3161, specific conductance of $1000 \pm 5 \mu\text{S}/\text{cm}$) available from Yellow Springs Instrument Co., Inc. was used to calibrate the cells. This solution contained water, 0.002%, iodone (an anti-microbial) and potassium chloride (ACS reagent grade).

The electrodes of the cells were coated with platinum black which was very important for cell operation. When the electrodes looked grey the cells were replatinized using a replatinizing solution (YSI 3140) on a platinizing instrument (YSI 3139). The current was kept at about 50 milliamp during the platinization. When a strong cleaning of the cells was required they were treated with a solution of equal parts of isopropyl alcohol and 10 M HCl before the replatinization.

C. Constant Temperature Bath

A 10 L glass Dewar filled with water was used to measure conductances at various temperatures. Inserted in this water were a motor controlled stirrer, a refrigeration unit (Tecumseh model AE 1343 AA), a heating coil, and a knife-heater (Cenco, 53 ohm, 350 W). The heating coil was controlled by a variac (Ohmite, model VT). The knife-heater was controlled by a temperature regulating system (Figures 4 and 5). The temperature was measured with a platinum resistance digital thermometer (Fluke, model 2189 A) to 0.01 K. A chart recorder (Sargent, model SR) was used to record the temperature variation in the bath.

IV. Techniques

A. Sample Preparations

Glassware, including the quartz cells, was cleaned according to the following procedure. First they were rinsed with ethanol and then some concentrated nitric acid was added to them. The acid was rinsed off by washing them many times with distilled water. Then they were washed with potassium hydroxide. Finally they were rinsed many times with distilled water and dried at 383 K in an oven.

Solvent mixtures were prepared in 1000 cm³ flasks by volume measurements. Stock solutions of solutes were prepared in 25 or 50 cm³ volumetric flasks. Solid solutes were weighed in volumetric flasks on an analytical balance (August Sauter, model Monopan).

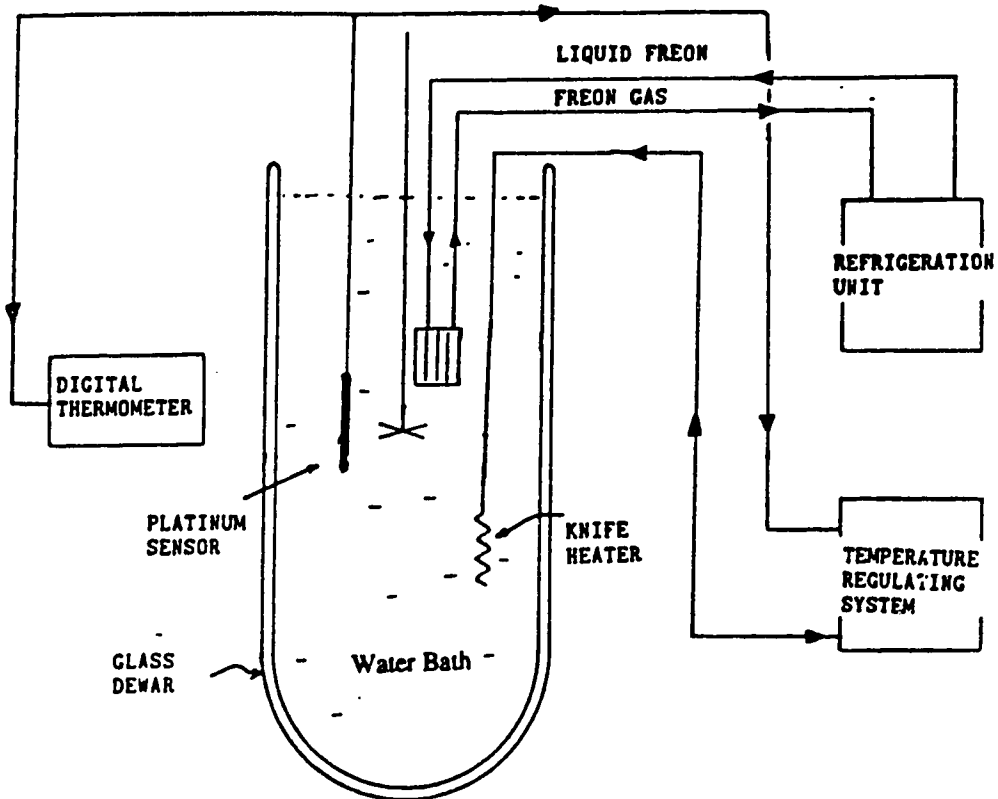


Fig 4 Temperature Control of the Water Bath

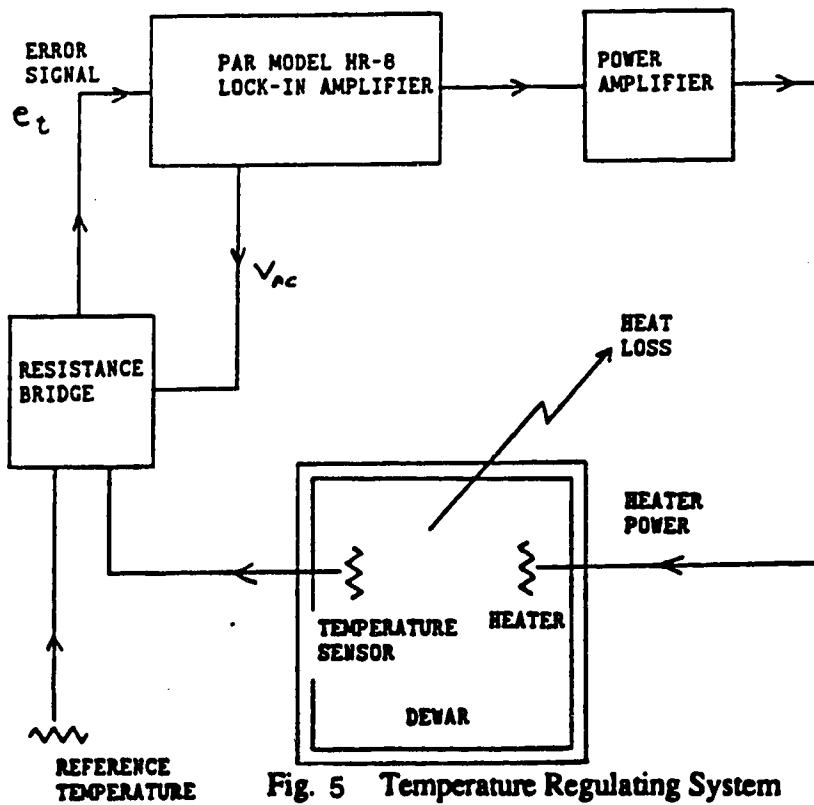


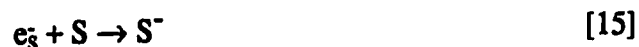
Fig. 5 Temperature Regulating System

The balance was readable to 0.0001 g and the precision was 0.0001 g. Perchloric acid samples were made by measuring 70% perchloric acid solution with a glass pipet. Sample solutions were made by transferring aliquots of stock solutions using syringes or volumetric pipets. Four to six sample solutions with different concentrations were prepared.

Figure 6 shows the procedure for sealing cells that contain the sample solutions for kinetic measurements, after they were deaerated by bubbling with argon for 30 minutes. At the end of the 30 minute period (Step 1), the needle was withdrawn just above the liquid level and the argon flow rate was increased (Step 2). The sealing area was heated with a low flame in order to vaporize volatile substances from the wall of the tube. Then the needle was further withdrawn (Step 3) and the seal was made as soon as possible.

B. Kinetic Measurements

Solvated electrons can react with the solvent or the solute according to the following equations:



Both reactions are first-order because the concentrations of the solvent and the solute are much greater than that of the solvated electron. Therefore, the observed first-order rate constant (k_{obs}) is given by

$$k_{obs} = k_1 + k_2[S] \quad [16]$$

where k_1 is the first-order rate constant of reaction [14] and k_2 is the second-order rate constant of reaction [15].

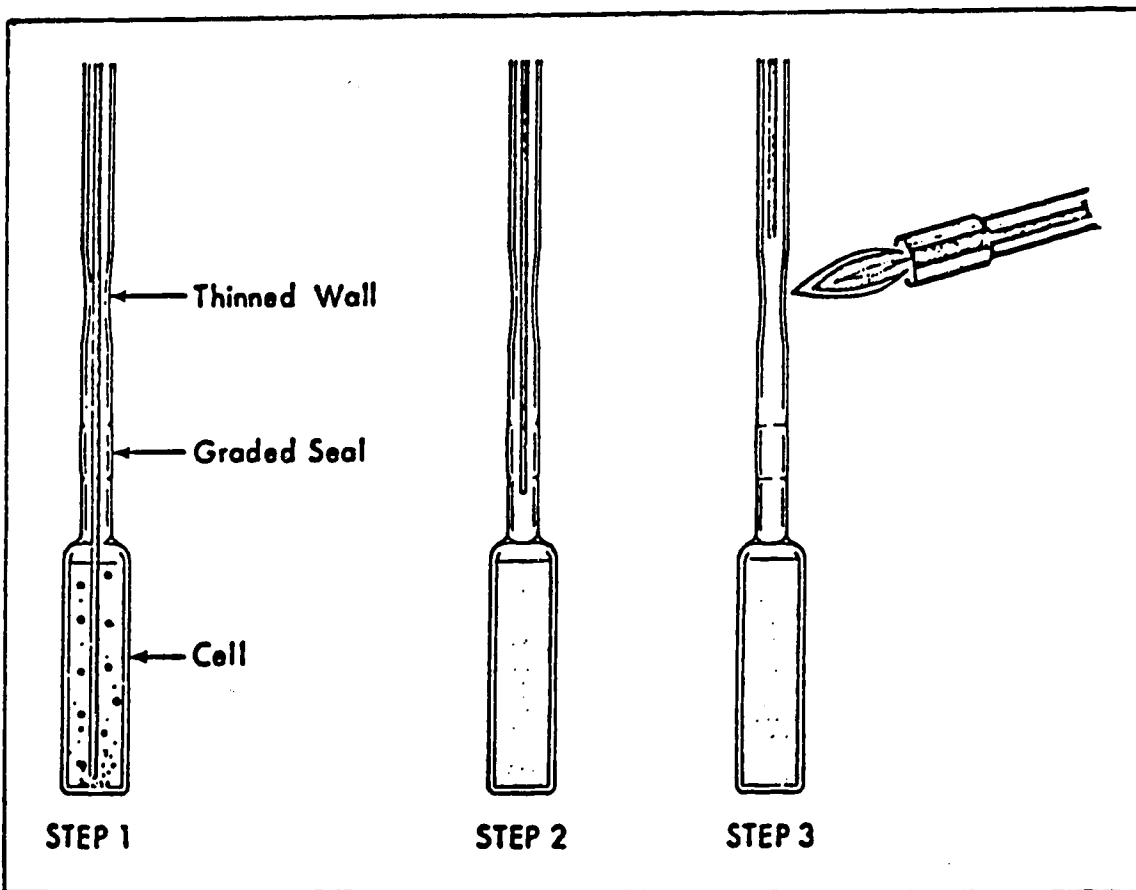


Fig. 6 The Sample Sealing Procedure

The decay curve in each solvent was measured at the wavelength of maximum absorption (λ_{max}) of the solvated electrons. Figure 7 shows an example of the decay curve of the solvated electrons. It was for 3.2×10^{-3} mol/m³ of aluminum perchlorate in 10 mol% water in 1-propanol at 312 K ($\lambda_{\text{max}} = 740$ nm).

From the half-life of the first-order decay k_{obs} can be calculated.

$$k_{\text{obs}} = \frac{\ln 2}{t_{1/2}} \quad [17]$$

The decay curve at the beginning of the decay was sometimes not first-order. This could be due to the reaction of solvated electrons inside microzones (geminate reaction) or delayed response of the detector. Therefore, when the half-lives were measured from the decay curve, the beginning of the trace was ignored. In another method, the half-lives were measured from a half-life trace generated by the computer, as a result of calculating a large set of half-lives along the trace. The half-life was then obtained by measuring the vertical distance between the reference point (the lower + mark in Figure 7) and the half-life trace. A horizontal half-life trace corresponds to a first-order decay.

Second-order rate constants k_2 were obtained from the plots of k_{obs} against solute concentration (equation [16]). The values of k_2 obtained at different temperatures allowed the determination of reaction parameters such as activation energy (E_2) and Arrhenius factor (A_2). They were derived from the plots of log of the k_2/f against the reciprocal of the absolute temperature (equation [18]).

$$\ln(k_2/f) = \ln A_2 - E_2/RT \quad [18]$$

C. Conductivity Measurements

The specific conductance (κ) was calculated from the following equation,

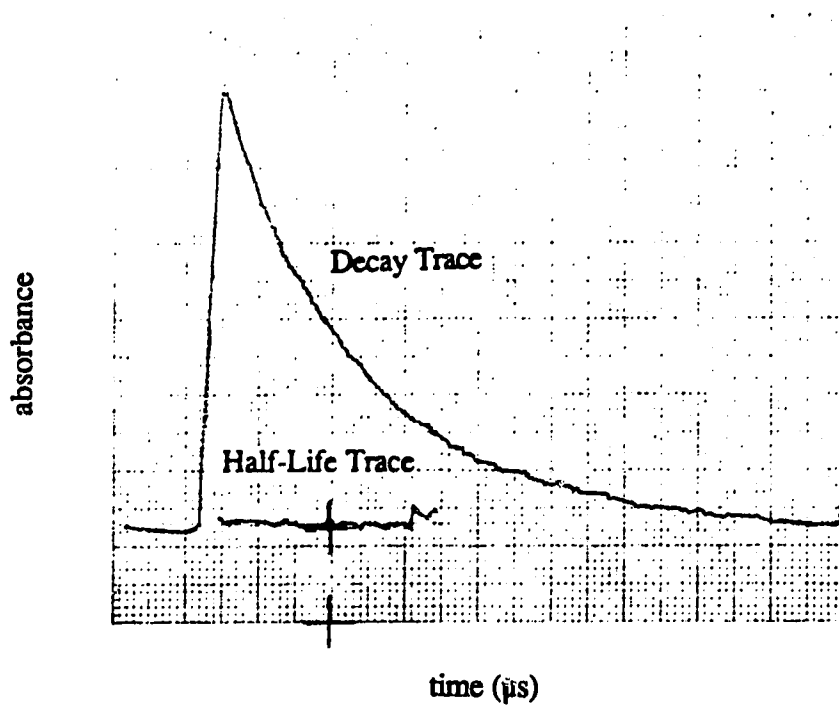


Fig. 7 Typical Solvated Electron Kinetic Trace

$$\kappa = C \times L \quad [19]$$

where L is the conductance (in Siemen) and C is the cell constant (m^{-1}). When the values of conductance were less than about $0.60 \text{ } \leq S$ it was not possible to get a good null in the conductance mode. Then the bridge was set to one of the capacitance modes (C_p mode) and the value of conductance was calculated from the following equation,

$$L = \omega C_p D \quad [20]$$

where ω is the angular speed (rad/s) of the AC voltage, C_p is the capacitance (picofarad) and D is the dissipation factor.

The values of molar conductance (Λ) were obtained from the plots of specific conductance against solute concentration. The activation energies of the conducting process (E_A) were obtained from the plots of the log of the molar conductance against the reciprocal of the absolute temperature.

CHAPTER THREE

RESULTS

I. Reactions of Solvated Electrons with Ionic Electron Acceptors

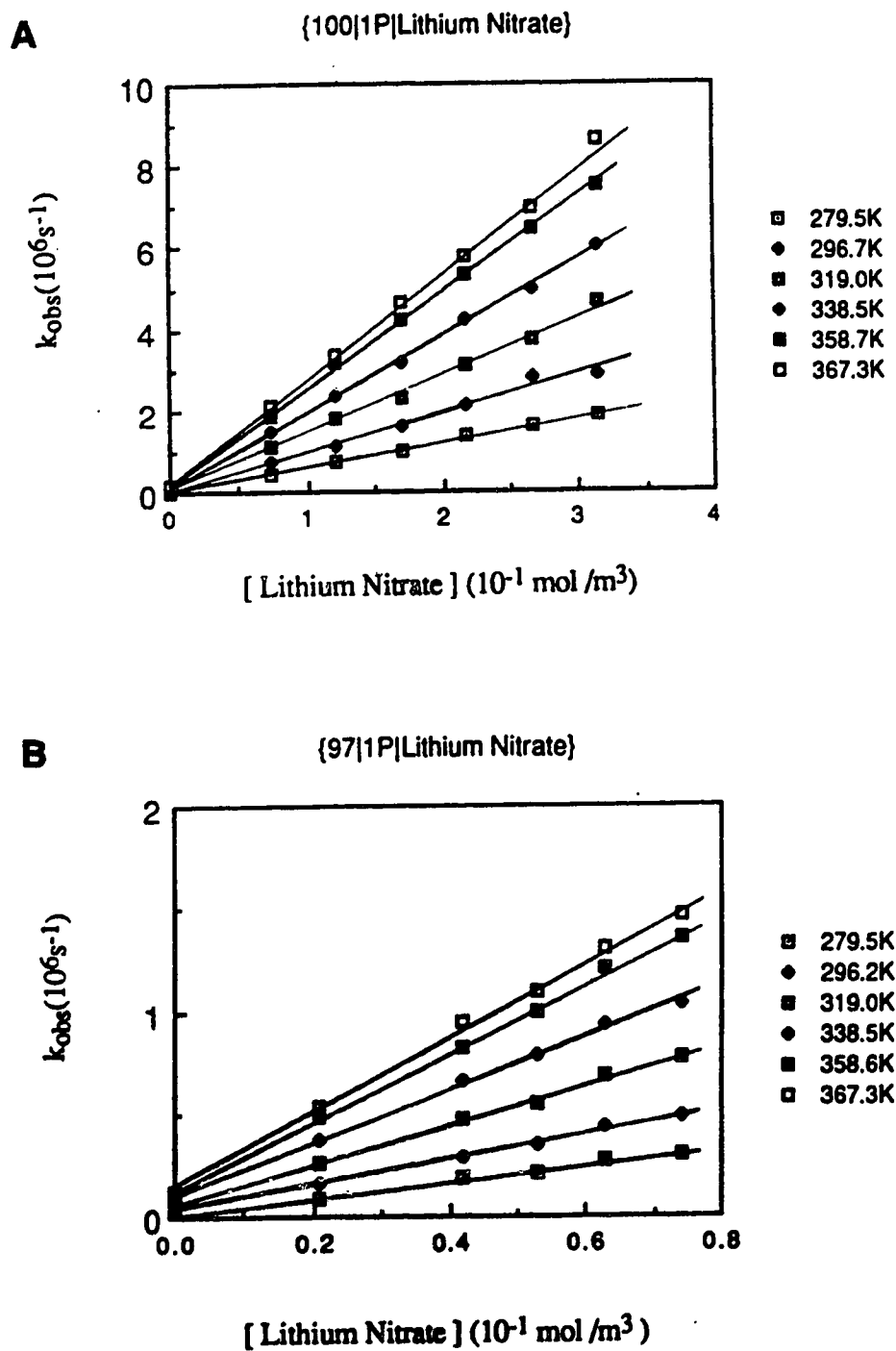
In this study, the reactions of solvated electrons with nitrate (NO_3^-), chromate (CrO_4^{2-}), hydrogen ion (H^+), silver ion (Ag^+), thallium ion (Tl^+), copper ion (Cu^{2+}), and aluminum ion (Al^{3+}) were investigated in alcohol/water mixtures. The alcohols were 1-propanol, 2-propanol and 2-butanol. Reaction rates with the counter ions Li^+ , ClO_4^- and CH_3COO^- are negligible (83).

II. Reactions of Solvated Electrons in 1-Propanol/Water Mixtures

A. Reaction of Solvated Electrons with Nitrate Ions

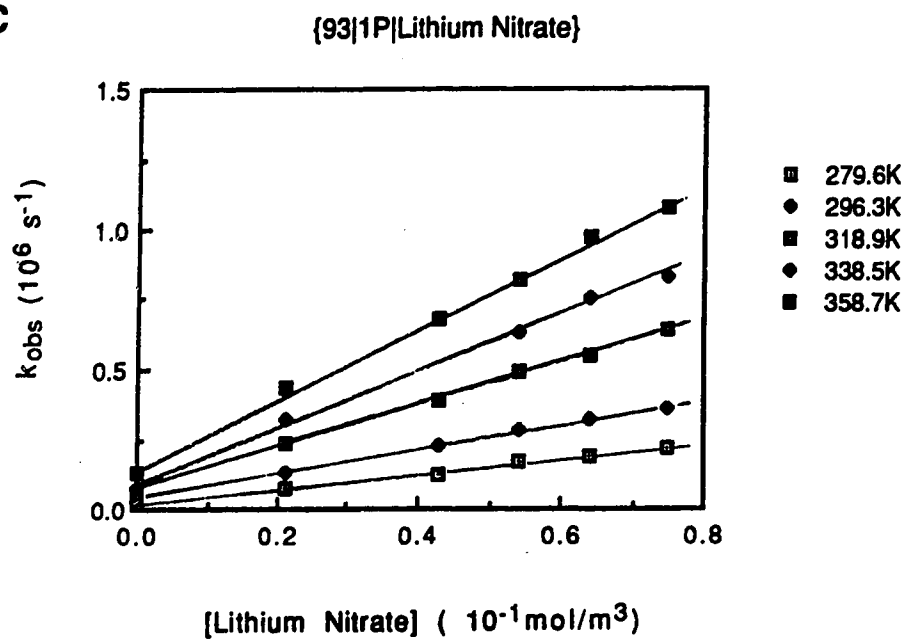
The temperature and concentration dependence of the first-order rate constant (first-order with respect to time) for the reaction of solvated electrons with lithium nitrate is shown in Figure 8 (A-J). The concentration range was 0.03-0.5 mol/m³. Table 1 shows the second-order rate constants (second-order with respect to initial concentration), dielectric constants and the coulombic factors f at various temperatures in different alcohol/water mixtures. The rate constant in water at 298 K is 9.4×10^6 m³/mol·s. The values reported in the literature are 9.4×10^6 m³/mol·s (104) and 8.5×10^6 m³/mol·s (116). Table 2 shows the rate parameters obtained from the modified Arrhenius plots k_2/f vs $1/T$, shown in Figure 9.

Fig. 8 (A-J) Temperature and concentration dependence of the first order rate constants for the reaction of solvated electrons with lithium nitrate in 1-propanol / water mixtures.

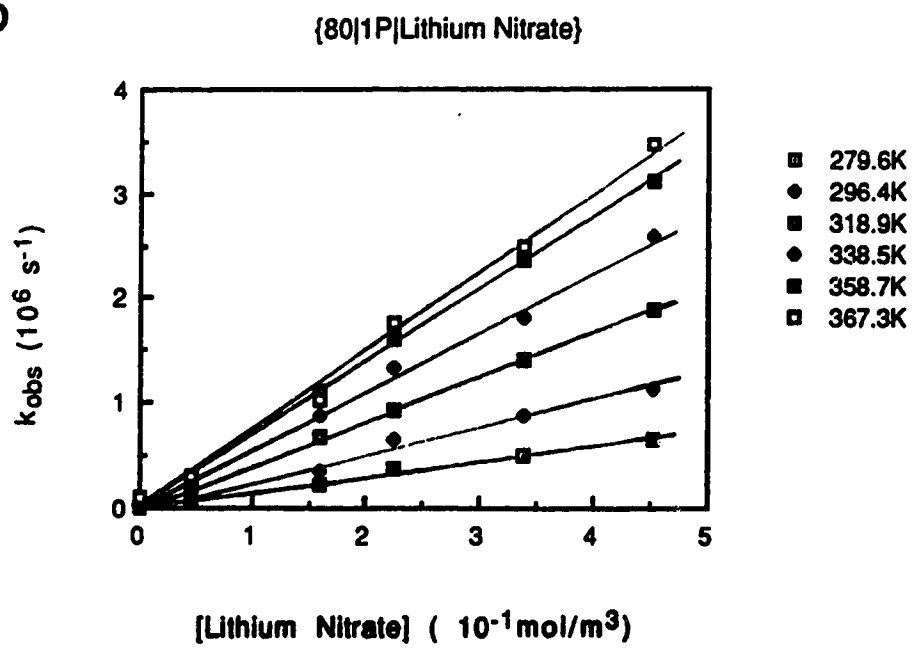


In the graph code {A|B|C} , A stands for the mol % of water in the solvent mixture, B represents the alcohol and C represents the electron acceptor. 1P is 1-propanol, 2P is 2-propanol and 2B is 2-butanol.

C

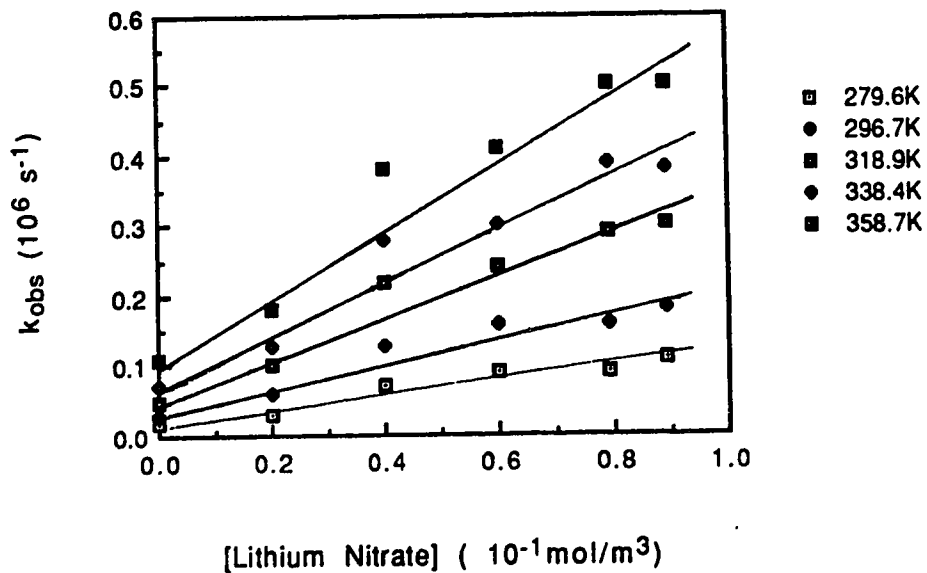


D



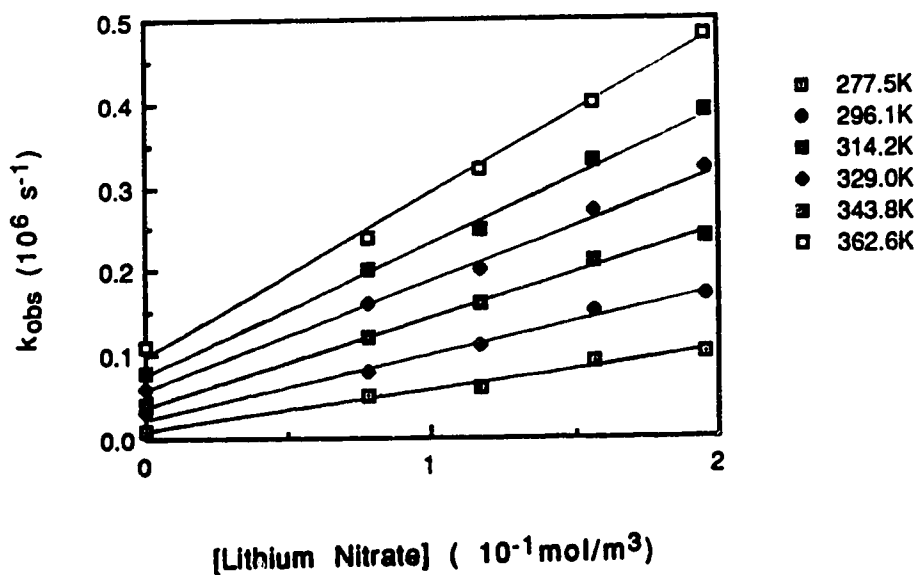
II

{70}P[Lithium Nitrate]

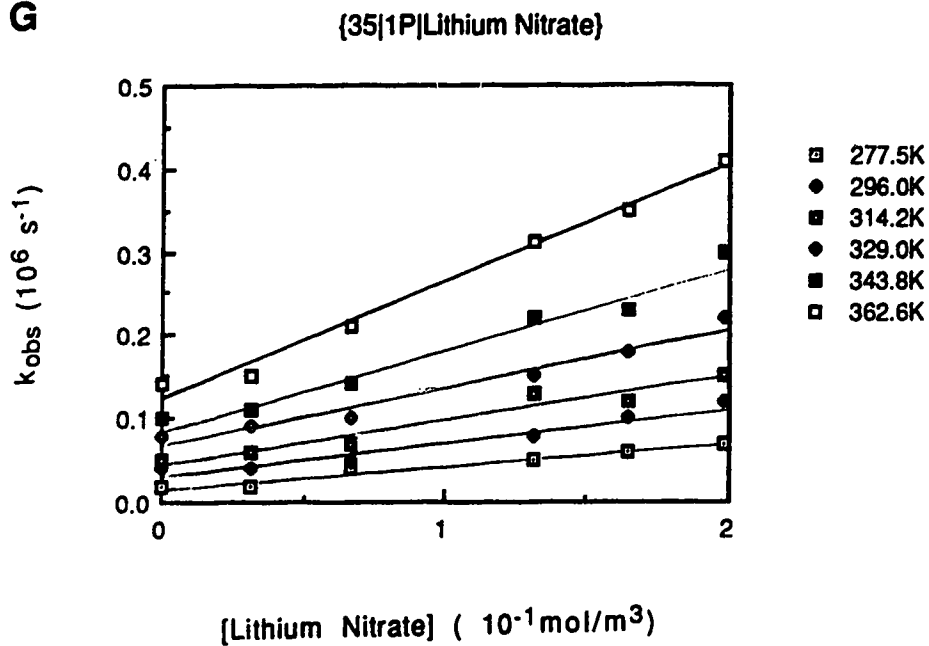


III

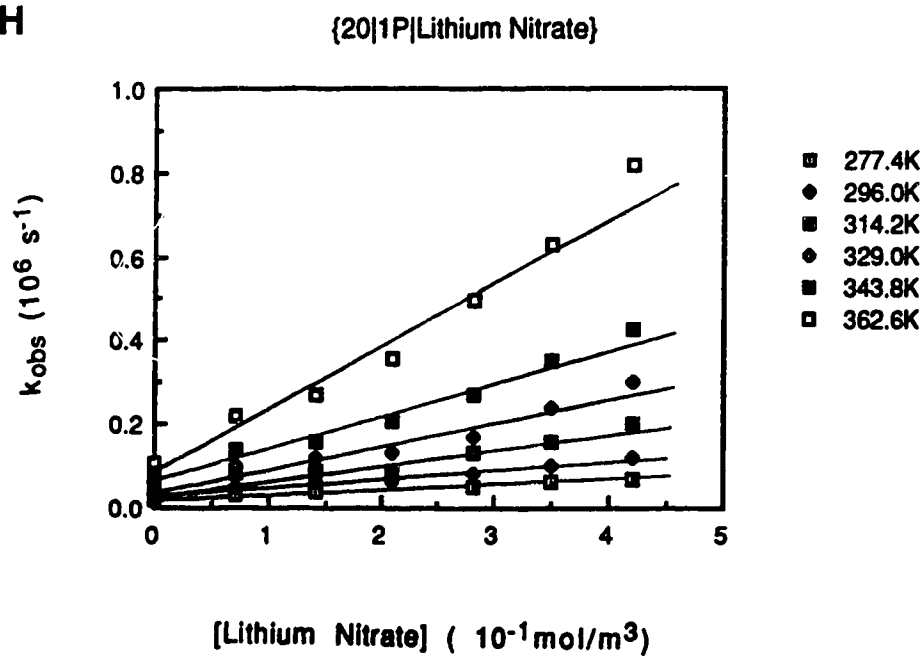
{51}P[Lithium Nitrate]



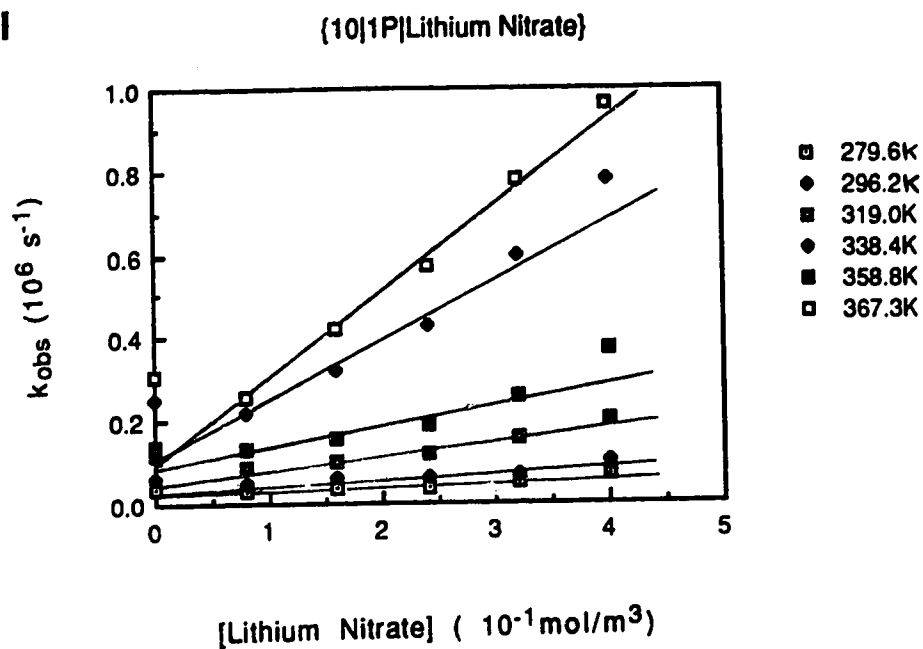
G



H



I



J

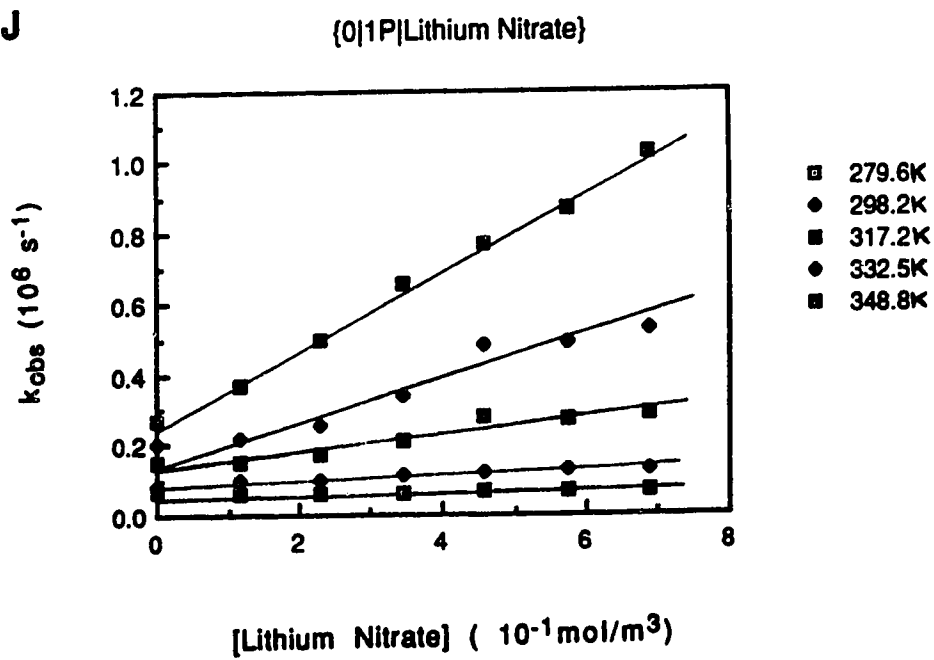


Table 1. Dielectric constants, f values and second-order rate constants for the reaction of solvated electrons with lithium nitrate in 1-propanol/water mixtures at various temperatures.

X_w	Temp (K)	ϵ	f	k_2 ($10^6 \text{ m}^3/\text{mol}\cdot\text{s}$)	X_w	Temp (K)	ϵ	f	k_2 ($10^6 \text{ m}^3/\text{mol}\cdot\text{s}$)
1.00	279.5	86.6	0.79	5.8	0.51	277.5	31.0	0.49	0.46
	296.7	78.9	0.78	9.3		296.1	27.6	0.47	0.75
	319.0	71.3	0.77	14		314.2	24.5	0.45	1.0
	338.5	64.6	0.77	19		329.0	22.7	0.44	1.3
	358.7	59.0	0.76	23		343.8	17.7	0.35	1.7
	367.3	56.0	0.75	25		362.6	15.6	0.32	1.9
0.97	279.5	79.5	0.77	3.9	0.35	277.5	26.7	0.43	0.25
	296.2	72.0	0.76	6.2		296.0	24.0	0.42	0.43
	319.0	65.2	0.76	9.7		314.2	21.0	0.39	0.54
	338.5	58.8	0.75	13		329.0	19.5	0.37	0.71
	358.6	53.4	0.74	17		343.8	17.7	0.35	1.0
	367.3	50.6	0.73	18		362.6	15.6	0.32	1.4
0.93	279.6	71.9	0.75	2.6	0.20	277.4	24.7	0.40	0.093
	296.3	65.2	0.74	4.5		296.0	22.7	0.39	0.17
	318.9	58.8	0.73	7.8		314.2	19.2	0.35	0.29
	338.5	52.7	0.72	9.8		329.0	17.7	0.33	0.46
	358.7	47.7	0.71	13		343.8	16.0	0.31	0.71
						362.6	14.5	0.29	1.2
0.80	279.6	51.6	0.66	1.4	0.10	279.6	23.5	0.38	0.06
	296.4	46.5	0.65	2.5		296.2	21.0	0.36	0.11
	318.9	41.5	0.64	4.1		319.2	18.2	0.33	0.28
	338.5	36.9	0.62	5.4		338.4	15.8	0.30	0.59
	358.7	33.0	0.60	6.8		358.8	13.7	0.26	1.3
	367.3	31.0	0.59	7.4		367.3	12.7	0.24	1.9
0.70	279.6	41.8	0.60	0.96	0.00	279.6	22.8	0.37	0.033
	296.7	37.5	0.58	1.7		298.2	20.2	0.34	0.091
	318.9	33.2	0.56	2.8		317.2	17.5	0.31	0.32
	338.4	29.3	0.54	3.5		332.5	15.8	0.29	0.67
	358.7	25.3	0.51	4.5		348.8	14.2	0.26	1.1

Table 2. Rate parameters for the reaction of solvated electrons with lithium nitrate in 1-propanol/water mixtures.

X_w	$\eta^{(a)}$ (10^{-3} Pa·s)	$k_2^{(a)}$ (10^6 m ³ /mol·s)	$k_2/f^{(a)}$ (10^6 m ³ /mol·s)	$E_2^{(b,c)}$ (kJ/mol)	$\log A_2^{(c)}$ (A_2 in m ³ /mol·s)	$E_\eta^{(d)}$ (kJ/mol)
1.00	0.89	9.4	12	17	9.96	16
0.97	1.34	6.3	8.3	17	9.95	26
0.93	1.84	4.7	6.4	22	10.61	
0.80	2.64	2.6	4.0	20	10.10	
0.70	2.72	1.68	2.9	20	9.95	27
0.51	2.50	0.74	1.6	19	9.49	24
0.35	2.32	0.41	0.95	20	9.43	
0.20	2.16	0.18	0.47	29	10.78	
0.10	2.06	0.13	0.36	36	11.90	19
0.00	1.96	0.09	0.26	46	13.50	18

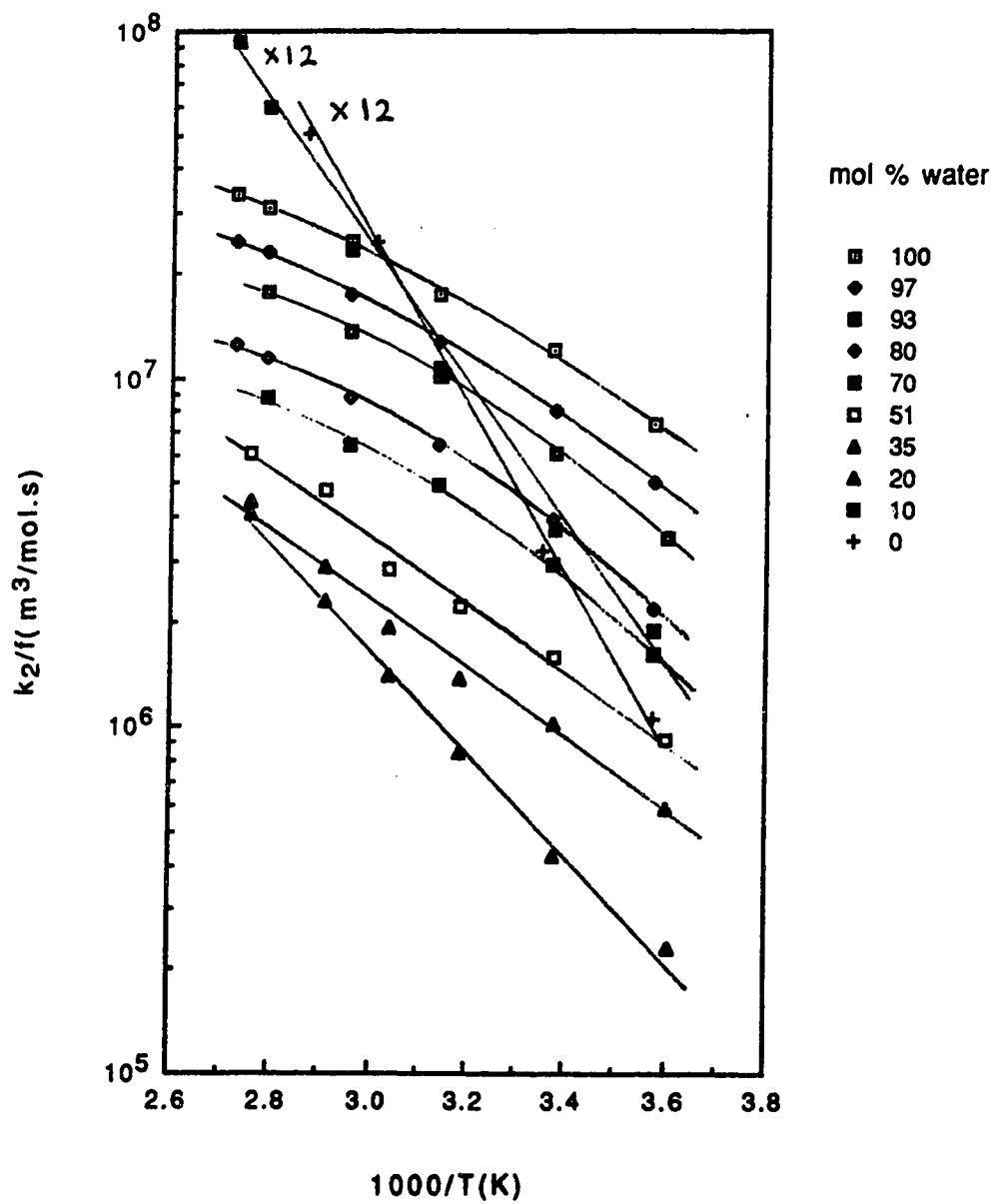
(a) At 298K.

(b) Near 298K.

(c) From Arrhenius plots of k_2/f .

(d) From ref. 106.

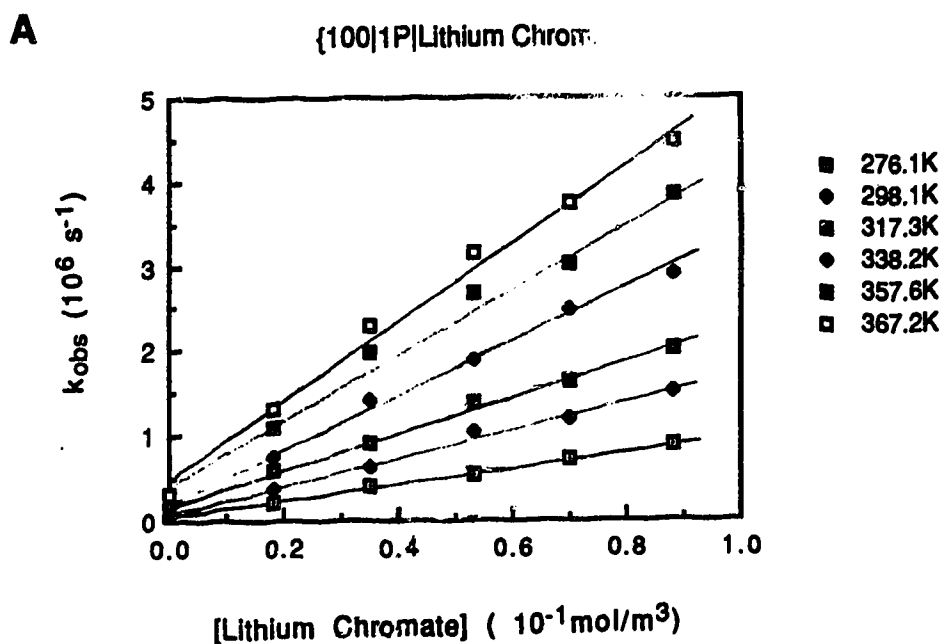
Fig. 9 Arrhenius plots for the reactions of solvated electrons with lithium nitrate in 1-propanol/water mixtures.

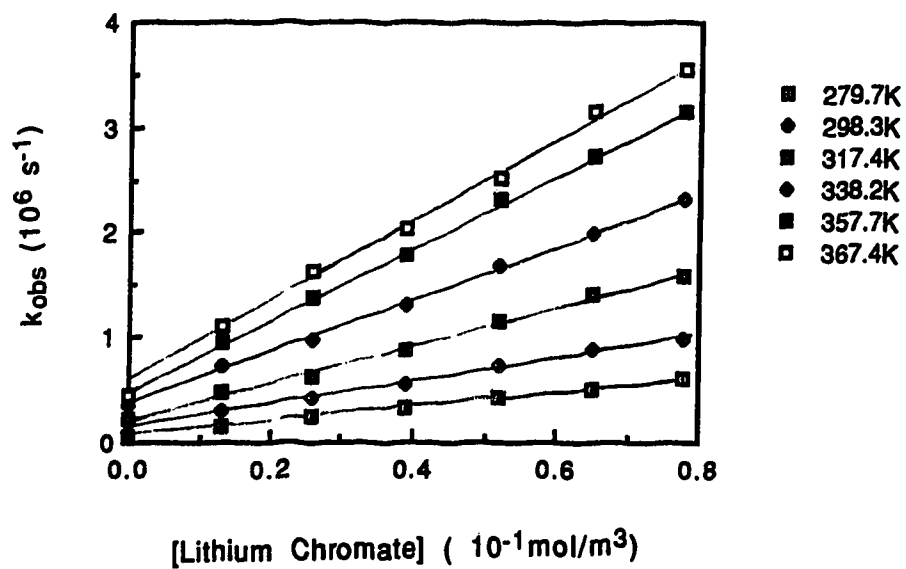
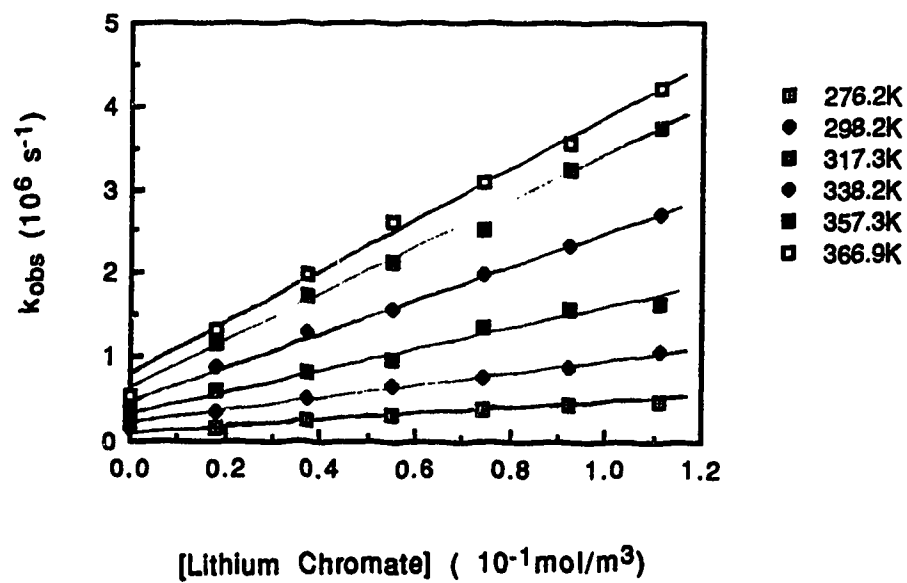


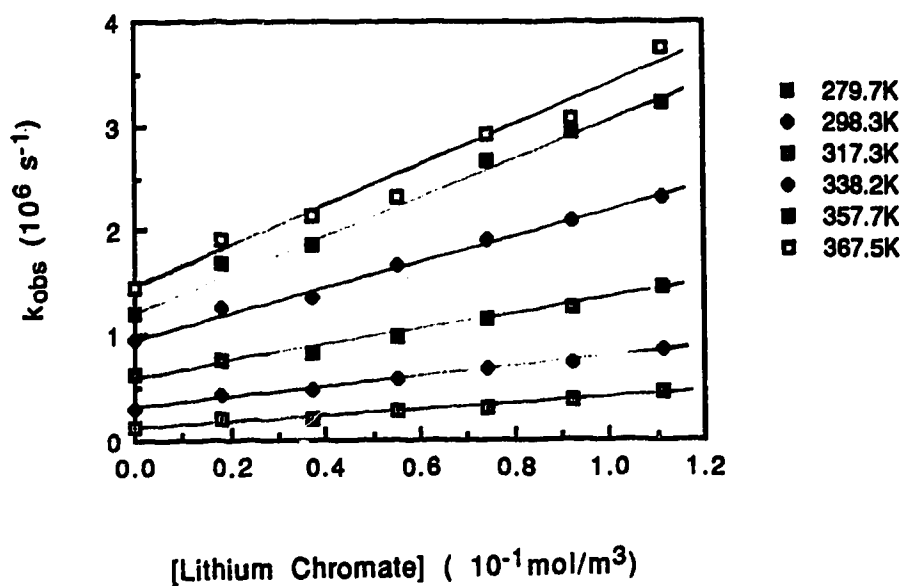
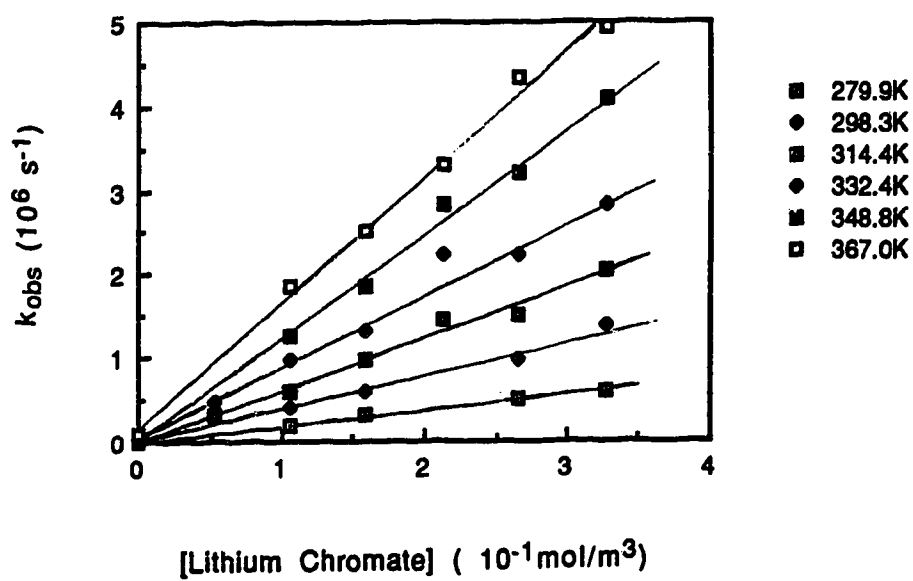
B. Reaction of Solvated Electrons with Chromate Ions

The temperature and concentration dependence of the first-order rate constant for the reaction of solvated electrons with lithium chromate are shown in Figure 10 (A-H). The concentration range of CrO_4^{2-} was 0.09-0.18 mol/m³. Table 3 shows the second-order rate constants, dielectric constants and the coulombic factors f at various temperatures in different alcohol/water mixtures. The rate constant in water at 298 K is 1.6×10^6 m³/mol·s. The values reported in the literature are 1.7×10^7 m³/mol·s (104) and 1.8×10^7 m³/mol·s (117). Table 4 shows the rate parameters obtained from the modified Arrhenius plots shown in Figure 11.

Fig. 10 Temperature and concentration dependence of the first-order rate constant for the reaction of solvated electrons with lithium chromate in 1-propanol/water mixtures

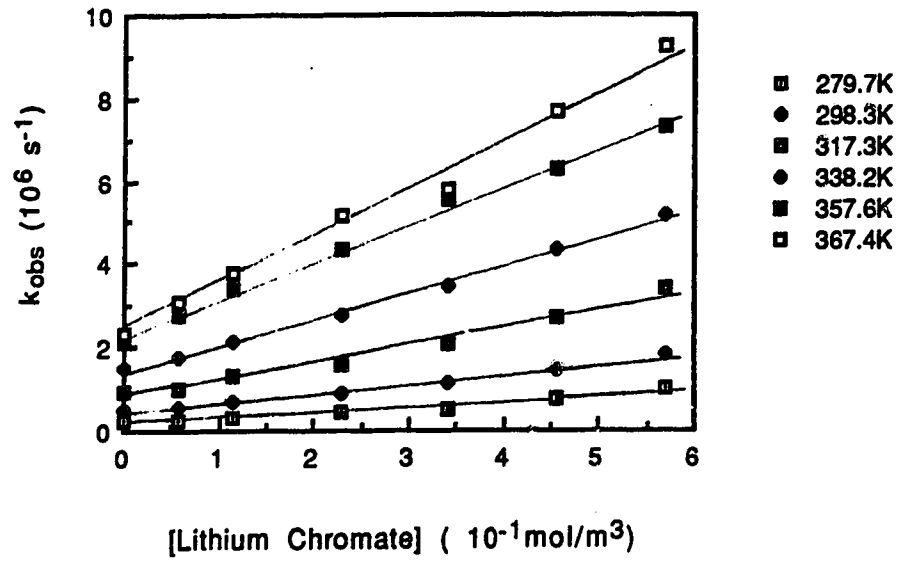


B**{97|1P|Lithium Chromate}****C****{94|1P|Lithium Chromate}**

D**{81|1P|Lithium Chromate}****E****{68|1P|Lithium Chromate}**

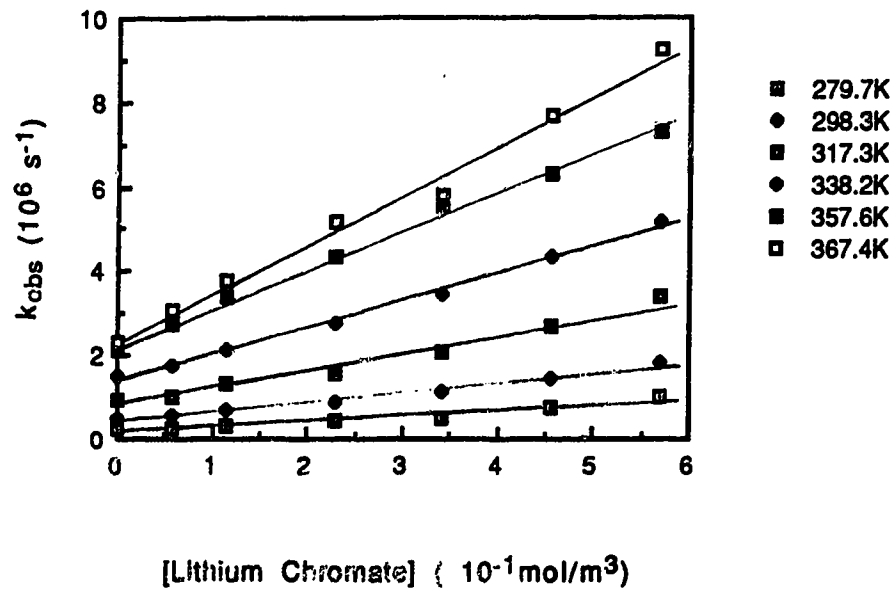
F

{51|1P|Lithium Chromate}



G

{35|1P|Lithium Chromate}



H

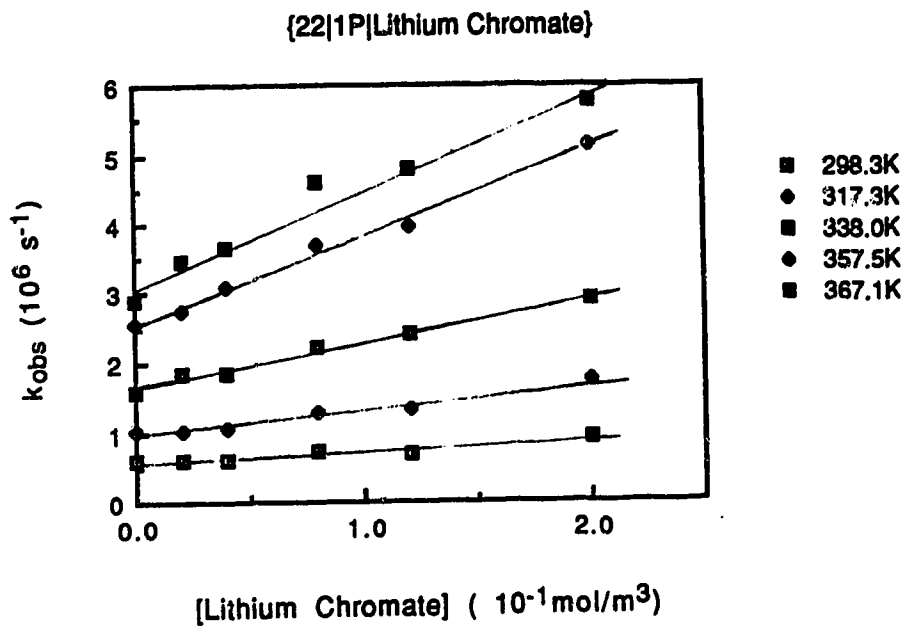


Table 3. Dielectric constants, f values and second-order rate constants for the reaction of solvated electrons with lithium chromate in 1-propanol/water mixtures at various temperatures.

X_w	Temp (K)	ϵ	f	$k_2^{(a)}$ ($10^7 \text{ m}^3/\text{mol}\cdot\text{s}$)	X_w	Temp (K)	ϵ	f	k_2 ($10^7 \text{ m}^3/\text{mol}\cdot\text{s}$)
1.00	276.1	87.5	0.69	0.93	0.68	279.9	39.3	0.43	0.20
	298.1	78.2	0.69	1.6		298.3	35.1	0.41	0.38
	317.3	71.3	0.68	2.1		314.4	32.2	0.39	0.60
	338.2	64.7	0.68	3.1		332.4	29.0	0.37	0.84
	357.6	58.9	0.66	4.0		348.8	26.1	0.35	1.2
	367.2	55.9	0.65	4.7		367.0	23.1	0.32	1.5
0.97	279.7	78.6	0.67	0.70	0.51	279.7	30.5	0.32	0.14
	298.3	71.4	0.66	1.1		298.3	27.4	0.31	0.23
	317.4	65.2	0.65	1.8		317.3	24.5	0.29	0.39
	338.2	58.8	0.64	2.5		338.2	21.5	0.26	0.63
	357.7	53.4	0.63	3.5		357.6	18.8	0.23	0.89
	367.4	50.6	0.62	3.9		367.4	17.6	0.21	1.1
0.94	276.2	74.3	0.65	0.40	0.35	279.6	26.5	0.27	0.10
	298.2	66.1	0.64	0.79		298.1	23.7	0.25	0.17
	317.3	60.1	0.63	1.3		317.2	21.0	0.22	0.27
	338.2	54.9	0.62	2.0		337.9	18.4	0.20	0.45
	357.3	48.7	0.60	2.8		357.3	16.0	0.17	0.69
	366.9	46.2	0.59	2.9		367.0	14.9	0.15	0.83
0.81	279.7	51.7	0.53	0.25	0.22	298.3	21.7	0.21	0.13
	298.3	46.5	0.52	0.48		317.3	19.2	0.19	0.36
	317.3	42.0	0.50	0.79		338.0	16.6	0.16	0.65
	338.2	37.3	0.48	1.2		357.5	14.5	0.14	1.2
	357.7	33.4	0.46	1.8		367.1	13.4	0.12	1.3
	367.5	31.4	0.45	2.0					

Table 4. Rate parameters for the reaction of solvated electrons with lithium chromate in 1-propanol/water mixtures.

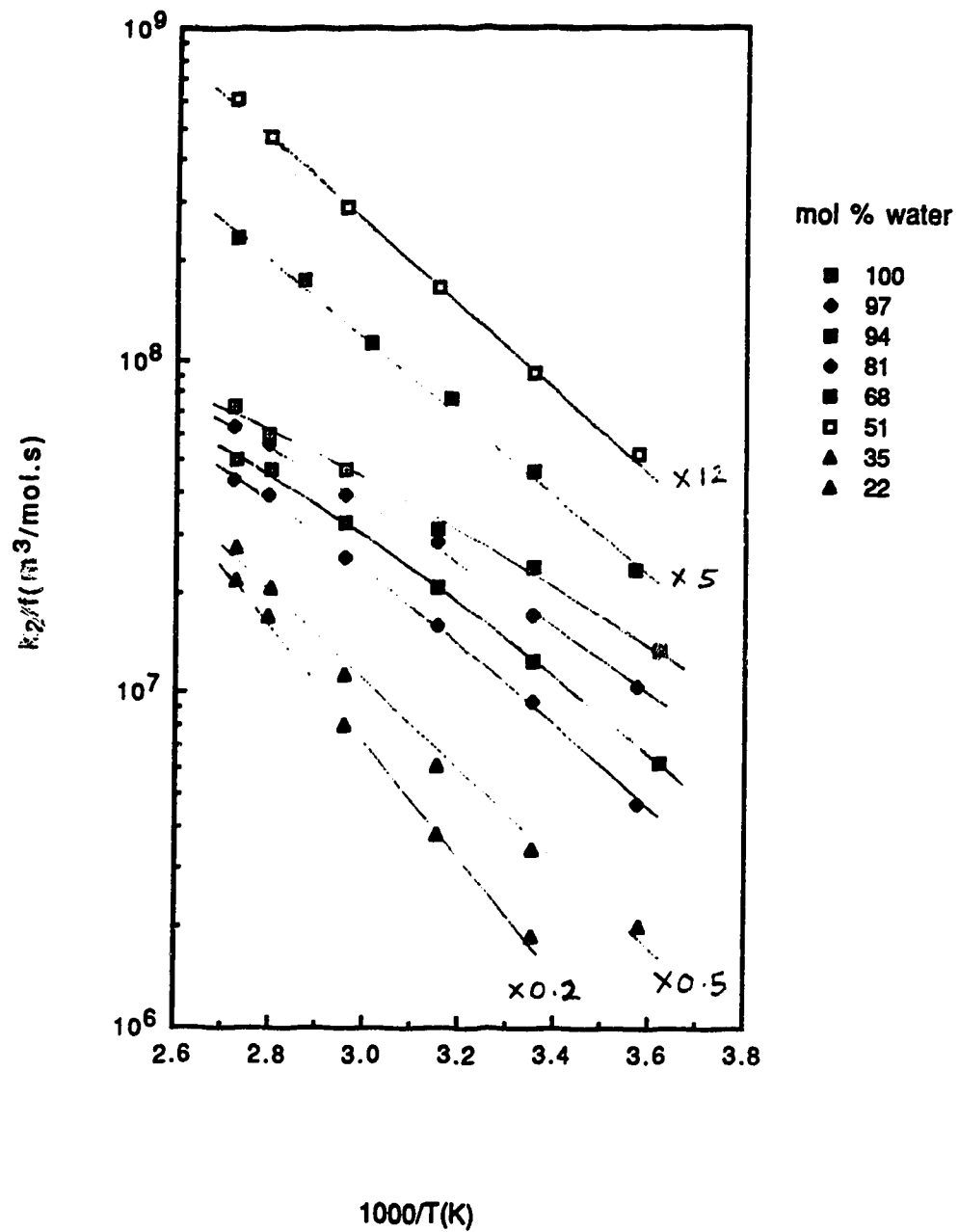
X_w	$\eta^{(a)}$ (10^{-3} Pa·s)	$k_2^{(a)}$ (10^7 m ³ /mol·s)	$k_2/f^{(a)}$ (10^7 m ³ /mol·s)	$E_2^{(b,c)}$ (kJ/mol)	$\log A_2^{(c)}$ (A_2 in m ³ /mol·s)
1.00	0.89	1.6	2.3	16	10.10
0.97	1.34	1.2	1.8	19	10.54
0.94	1.65	0.79	1.2	21	10.80
0.81	2.63	0.48	0.92	23	10.90
0.73	2.72	0.38	0.93	22	10.86
0.51	2.51	0.2	0.77	24	11.10
0.35	2.32	0.17	0.65	26	11.36
0.22	2.18	0.19	0.90	33	11.96

(a) At 298K.

(b) Near 298K

(c) From Arrhenius plots of k_2/f .

Fig. 11 Arrhenius plots for the reactions of solvated electrons with lithium chromate in 1-propanol/water mixtures.



C. Reaction of Solvated Electrons with Hydrogen Ions

The temperature and concentration dependence of the first-order rate constant for the reaction of solvated electrons with hydrogen ions are shown in Figure 12 (A-J). The concentration range was 0.01-0.13 mol/m³. Table 5 shows the second-order rate constants, dielectric constants and the coulombic factor *f* at various temperatures in different alcohol/water mixtures. The rate constant at 298 K is 2.6×10^7 m³/mol·s in water. The values reported in the literature are $(2.0-2.8) \times 10^7$ m³/mol·s (83). Table 6 shows the rate parameters obtained from the modified Arrhenius plots shown in Figure 13. In some of the k_{obs} versus [H⁺] plots, the best fit lines are below the points corresponding to the pure solvent sample. This was observed in the cases of copper(II) and aluminum(III). This has also been observed in the t-butyl/water (118), methanol/water (119) and ethanol/water (119) mixed solvents for copper(II). It has been explained in terms of the presence of a small amount of chelating or precipitating agent. Similar behavior for hydrogen ion has been observed in water, methanol and ethanol (120). It has been explained in terms of the adsorption of some acid on the cell walls. Since only the intercept is affected there is no effect on the second-order rate constants.

A

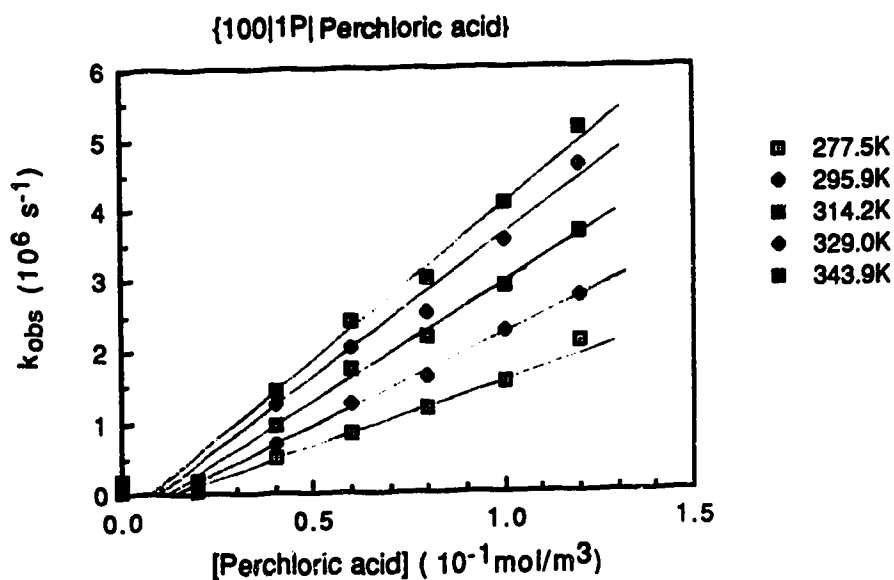
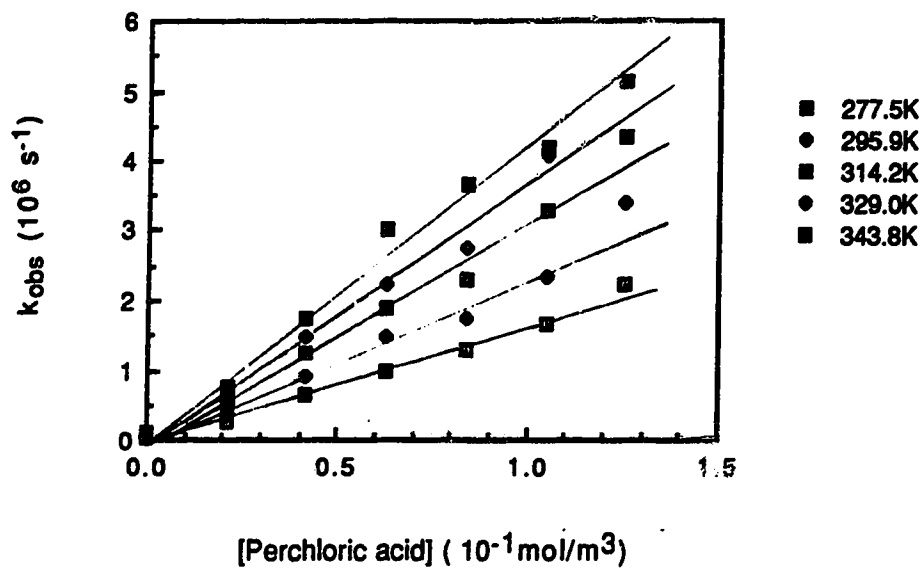
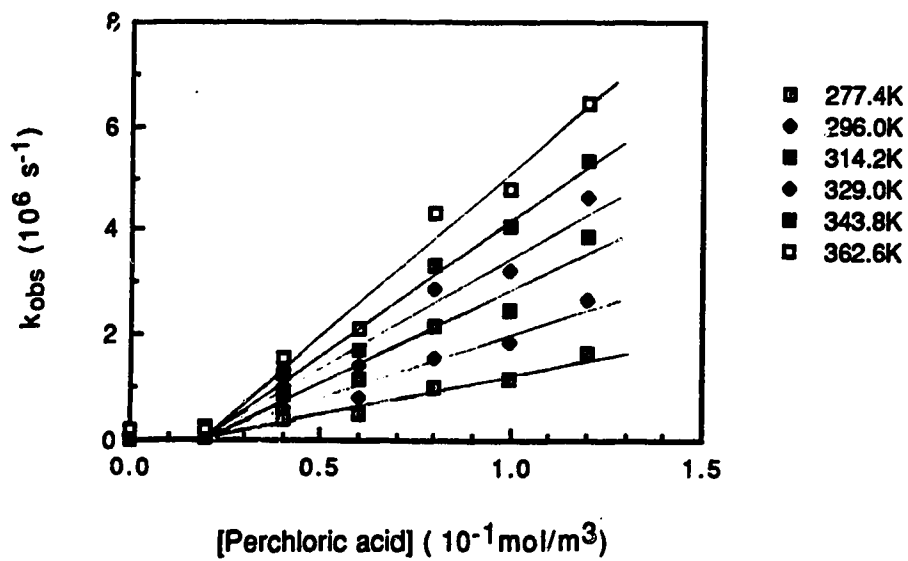
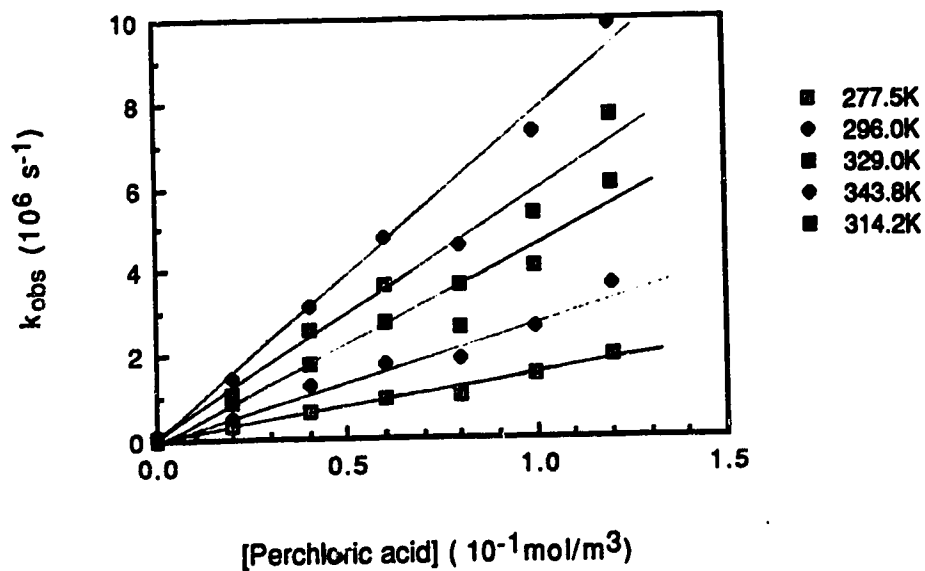
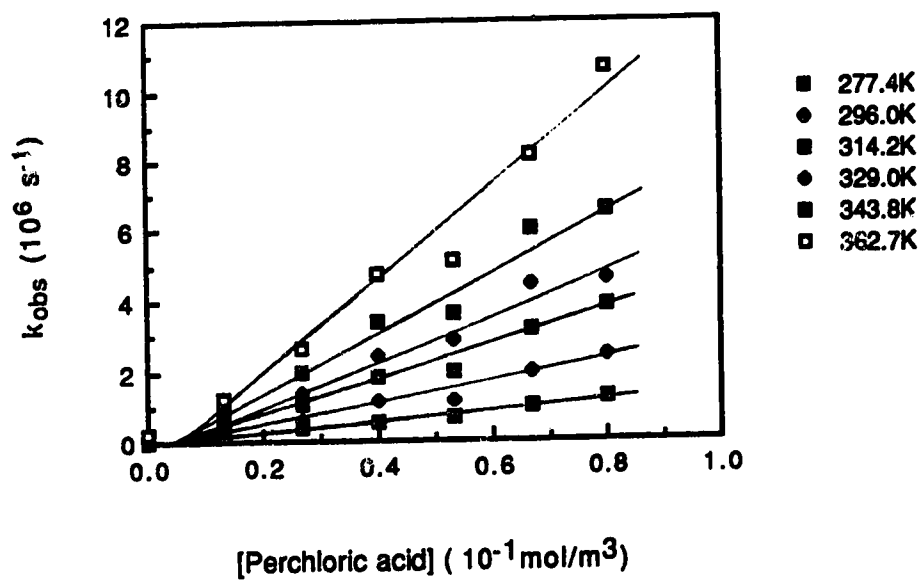
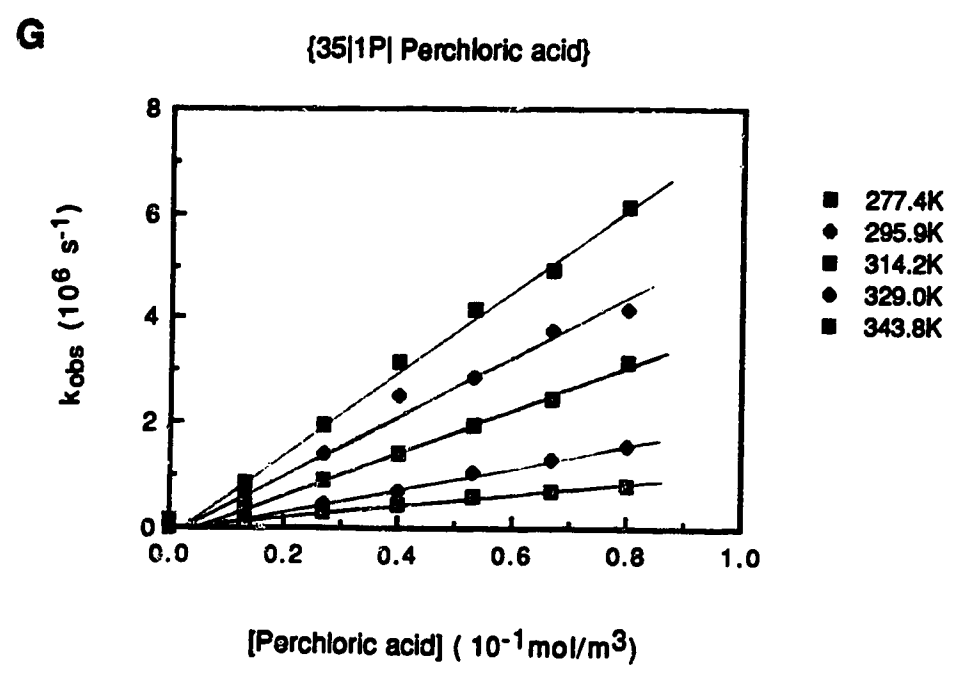
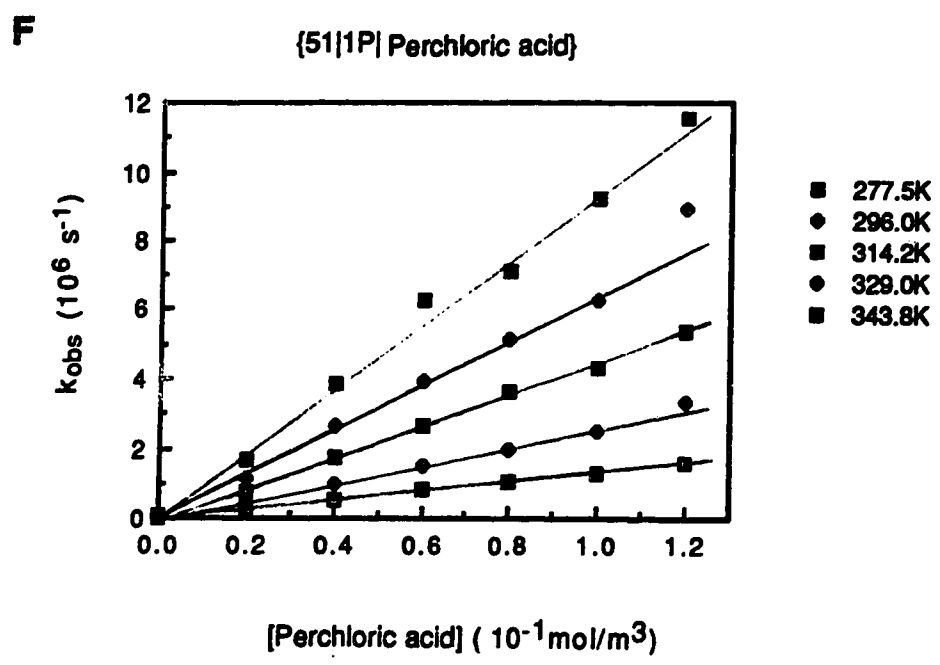
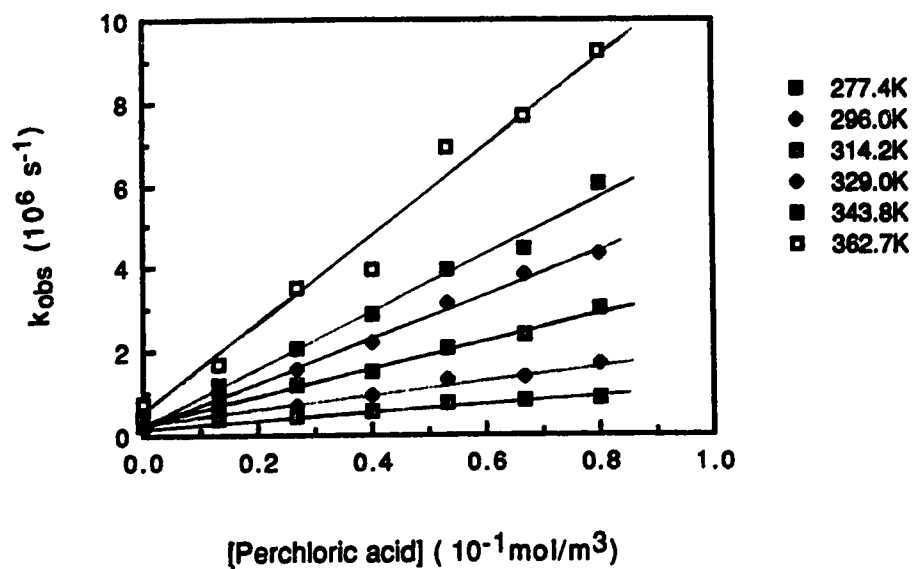
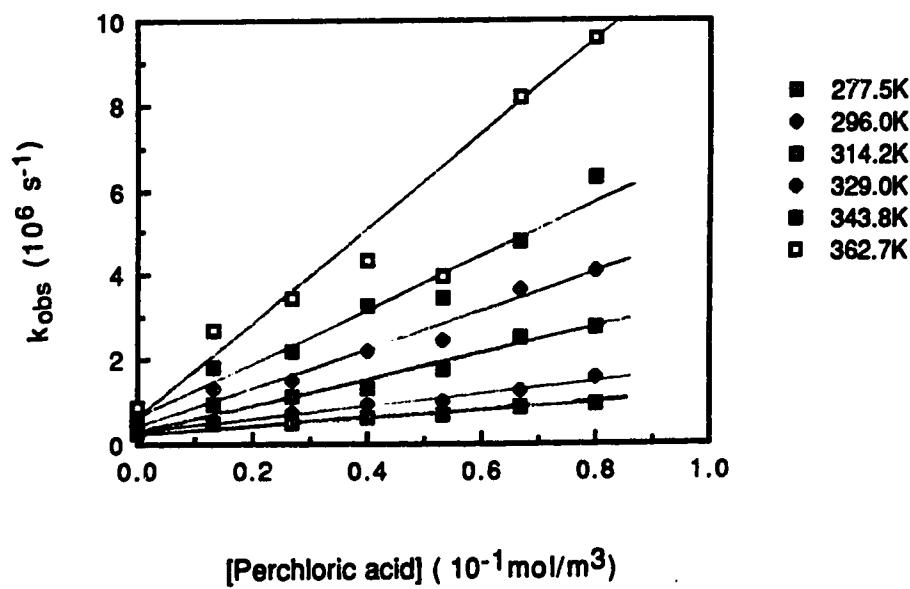


Fig.12 (A-J) Temperature and concentration dependence of the first order rate constants for the reaction of solvated electrons with perchloric acid in 1-propanol/water mixtures.

B**{97|1P|Perchloric acid}****C****{93|1P|Perchloric acid}**

D**{81|1P| Perchloric acid}****E****{68|1P| Perchloric acid}**



H**{20|1P| Perchloric acid}****I****{10|1P| Perchloric acid}**

J

{01P| Perchloric acid}

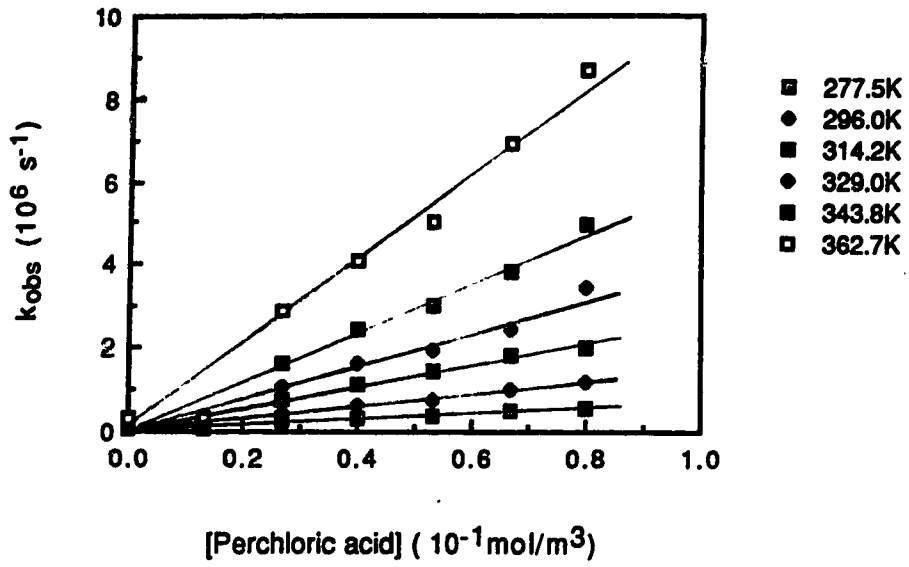


Table 5. Dielectric constants, f values and second-order rate constants for the reaction of solvated electrons with perchloric acid in 1-propanol/water mixtures at various temperatures.

X_w	Temp (K)	ϵ	f	k_2 ($10^7 \text{ m}^3/\text{mol}\cdot\text{s}$)	X_w	Temp (K)	ϵ	f	k_2 ($10^7 \text{ m}^3/\text{mol}\cdot\text{s}$)
1.00	277.5	86.8	1.39	1.8	0.51	277.5	31.0	2.27	1.3
	295.9	79.3	1.40	2.6		296.0	27.6	2.35	2.5
	314.2	72.5	1.41	3.2		314.2	24.5	2.45	4.4
	329.0	67.7	1.42	4.1		329.0	22.7	2.50	6.3
	343.9	63.0	1.43	4.6		343.8	17.7	2.93	9.5
0.97	277.5	79.6	1.42	1.6	0.35	277.4	26.7	2.52	1.1
	295.9	72.4	1.44	2.3		295.9	24.0	2.60	2.0
	314.2	66.4	1.45	3.0		314.2	21.0	2.75	3.8
	329.0	61.7	1.47	3.7		329.0	19.5	2.81	5.6
	343.8	57.4	1.48	4.5		343.8	17.7	2.93	7.9
0.93	277.4	72.0	1.48	1.5	0.20	277.4	24.7	2.67	0.83
	296.0	65.6	1.49	2.4		296.0	22.7	2.71	1.8
	314.2	60.0	1.51	3.3		314.2	19.2	2.95	3.3
	329.0	55.5	1.53	4.2		329.0	17.7	3.0	5.2
	343.8	51.4	1.55	4.9		343.8	16.0	3.2	6.7
	362.6	46.5	1.58	6.1		362.7	14.5	3.3	11
0.81	277.5	52.5	1.68	1.7	0.10	277.5	23.6	2.76	0.77
	296.0	47.2	1.71	3.1		296.0	21.0	2.88	1.4
	314.2	42.8	1.75	5.0		314.2	18.7	3.0	3.0
	329.0	39.5	1.78	6.6		329.0	17.0	3.1	4.5
	343.8	36.4	1.81	8.5		343.8	15.2	3.3	6.7
						362.7	13.2	3.6	11
0.68	277.4	40.0	1.93	1.6	0.00	277.5	22.9	2.83	0.77
	296.0	35.7	1.99	3.3		296.0	21.0	2.88	1.5
	314.2	32.2	2.04	5.2		314.2	18.0	3.1	2.9
	329.0	29.5	2.09	6.9		329.0	16.5	3.2	4.2
	343.8	26.1	2.20	9.6		343.8	14.7	3.4	6.4
	362.7	23.9	2.25	14		362.7	12.7	3.7	11

Table 6. Rate parameters for the reaction of solvated electrons with perchloric acid in 1-propanol/water mixtures.

X_w	$\eta^{(a)}$ (10^{-3} Pa·s)	$k_2^{(a)}$ (10^7 m ³ /mol·s)	$k_2/f^{(a)}$ (10^7 m ³ /mol·s)	$E_2^{(b,c)}$ (kJ/mol)	$\log A_2^{(c)}$ (A_2 in m ³ /mol·s)
1.00	0.89	2.6	1.9	12	9.42
0.97	1.34	2.4	1.7	13	9.57
0.93	1.86	2.5	1.7	15	9.78
0.81	2.63	3.3	1.9	17	10.26
0.68	2.73	3.3	1.7	19	10.60
0.51	2.56	2.7	1.2	22	10.85
0.35	2.32	2.3	0.89	23	10.87
0.20	2.16	1.9	0.68	24	10.95
0.10	2.06	1.6	0.55	24	11.04
0.00	1.96	1.7	0.57	23	10.69

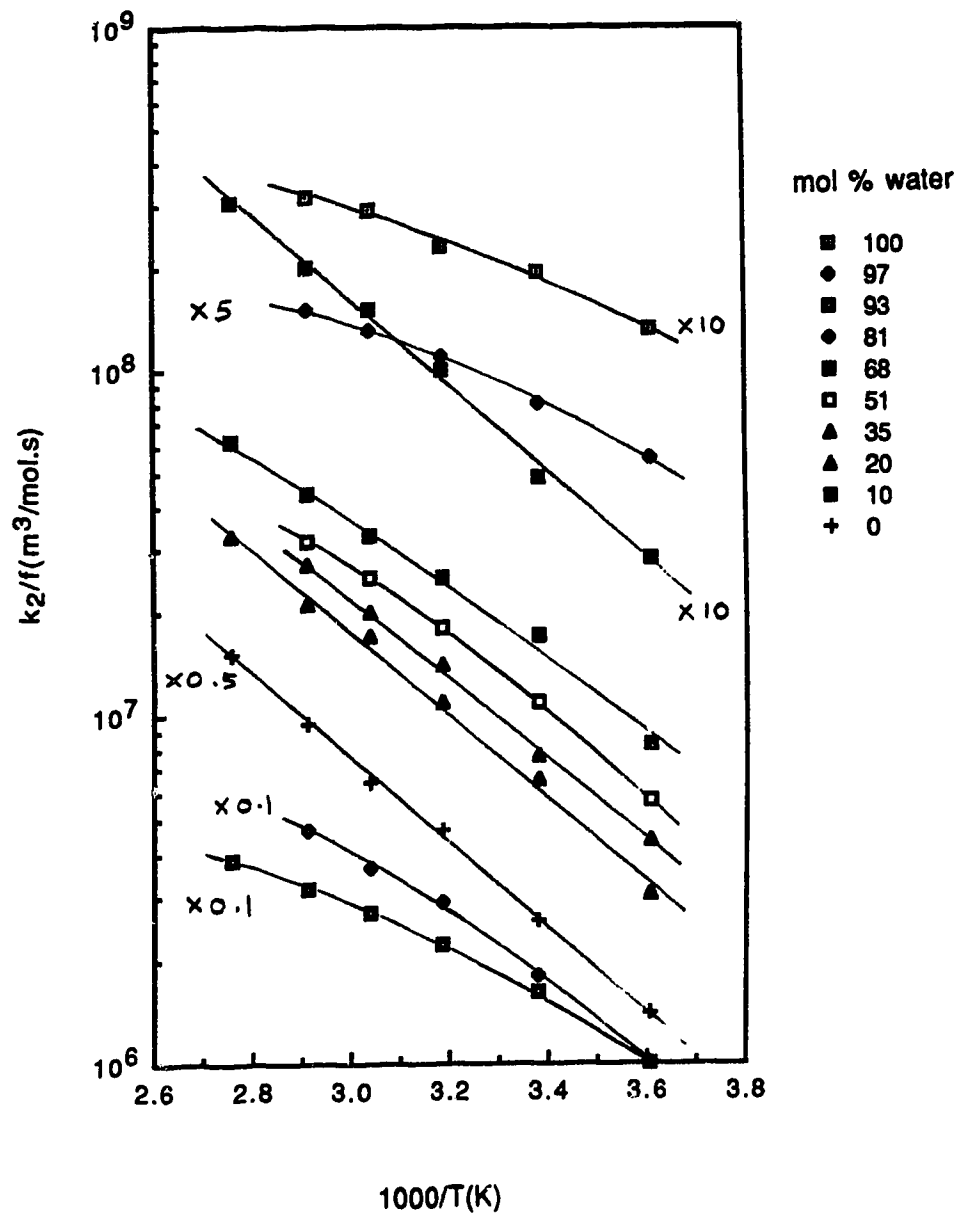
(a) At 298K.

(b) Near 298K.

(c) From Arrhenius plots of k_2/f .

Fig. 13

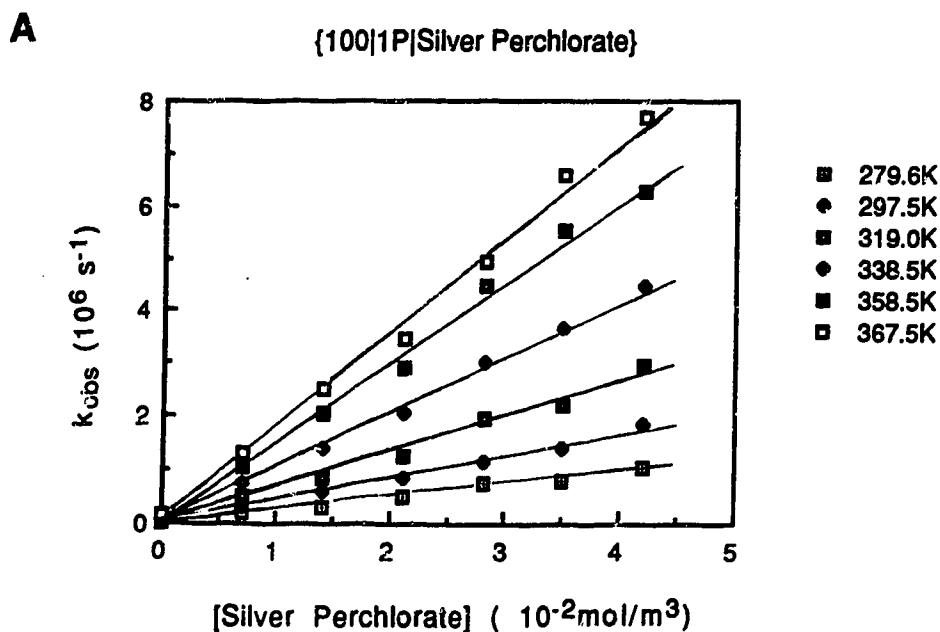
Arrhenius plots for the reaction of solvated electrons with perchloric acid in 1-propanol/water mixtures



D. Reaction of Solvated Electrons with Silver Ions

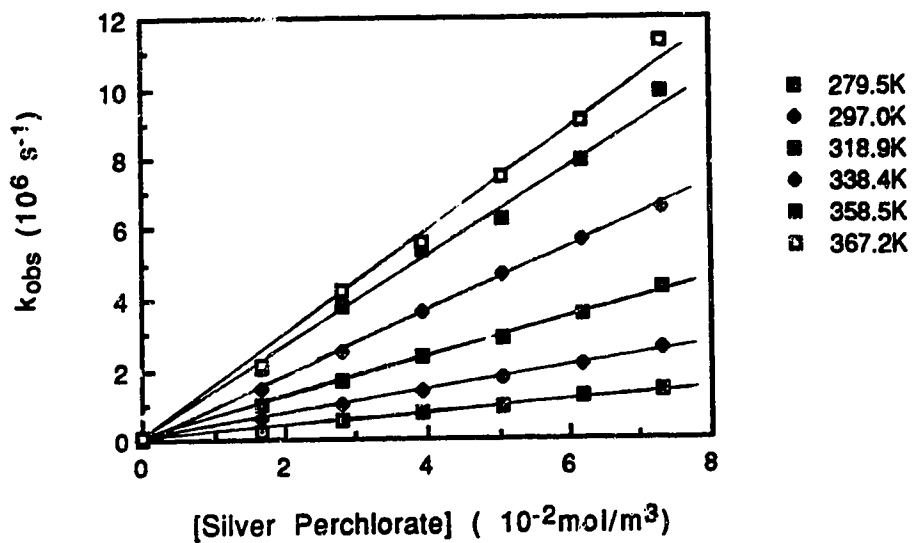
The temperature and concentration dependence of the first-order rate constant for the reaction of solvated electrons with silver ions are shown in Figure 14 (A-J). The concentration range of silver ion was 3-73 mmol/m³. Table 7 shows the second order rate constants, dielectric constants and the coulombic factors *f* at various temperatures in different alcohol/water mixtures. The rate constant at 298 K is 4.2×10^7 m³/mol•s in water and 1.1×10^7 m³/mol•s in 1-propanol. The values reported in the literature are 3.6×10^7 m³/mol•s (118) and 4.2×10^7 m³/mol•s (104) in water, and 0.76×10^7 m³/mol•s in 1-propanol (91). Table 8 shows the rate parameters obtained from the modified Arrhenius plots shown in Figure 15.

Fig. 14 Temperature and concentration dependence of the first-order
(A-J) rate constant for the reaction of solvated electrons with
silver perchlorate in 1-propanol/water mixtures



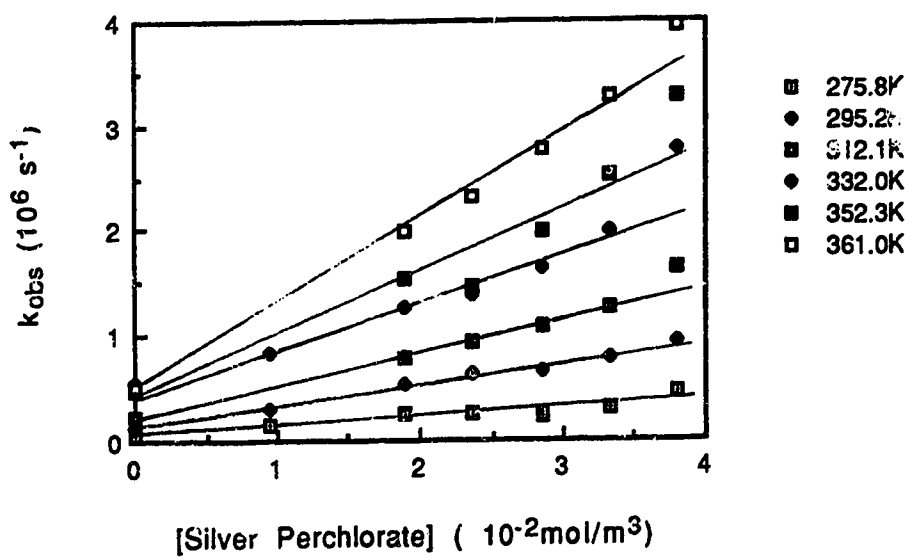
B

{97|1P|Silver Perchlorate}

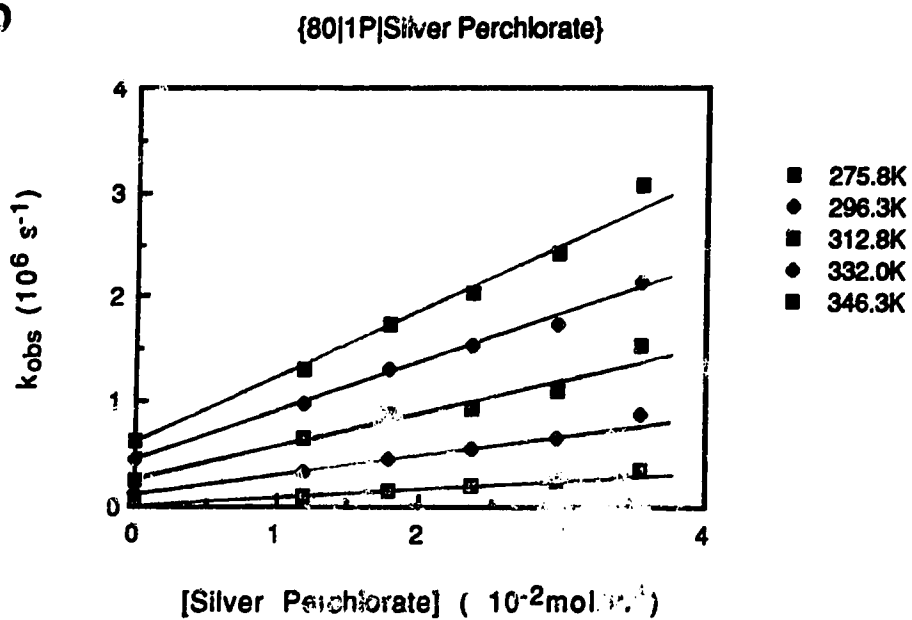


C

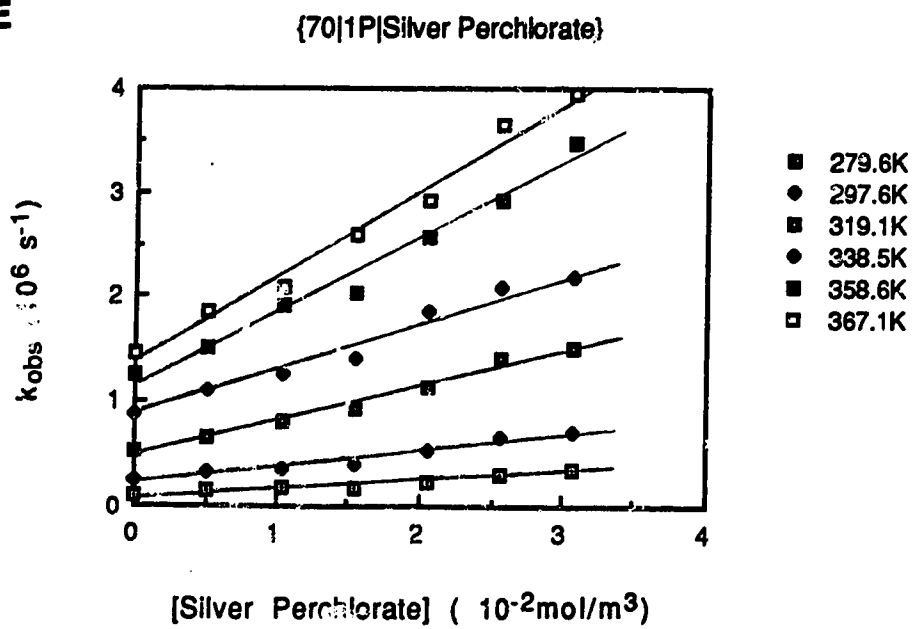
{93|1P|Silver Perchlorate}



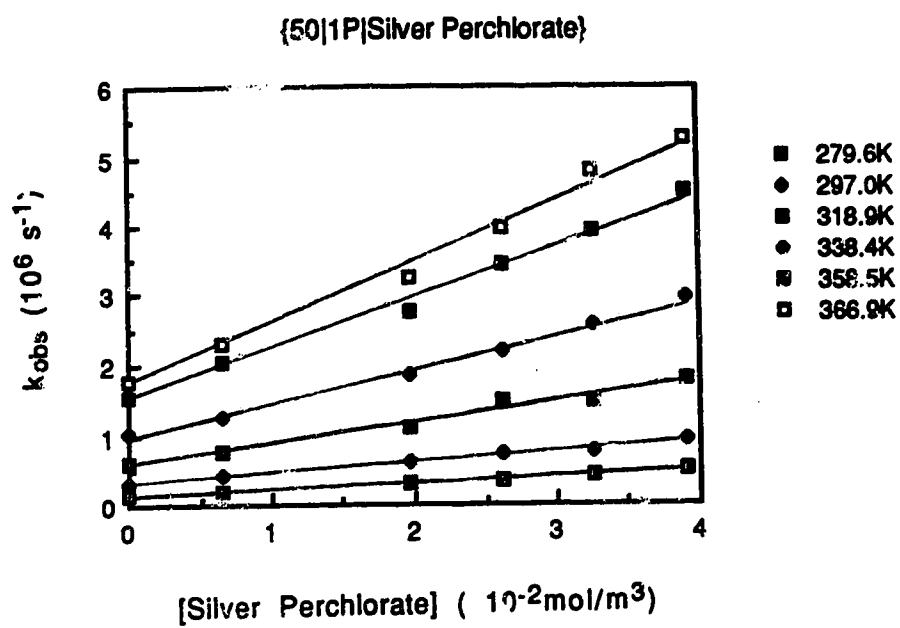
D



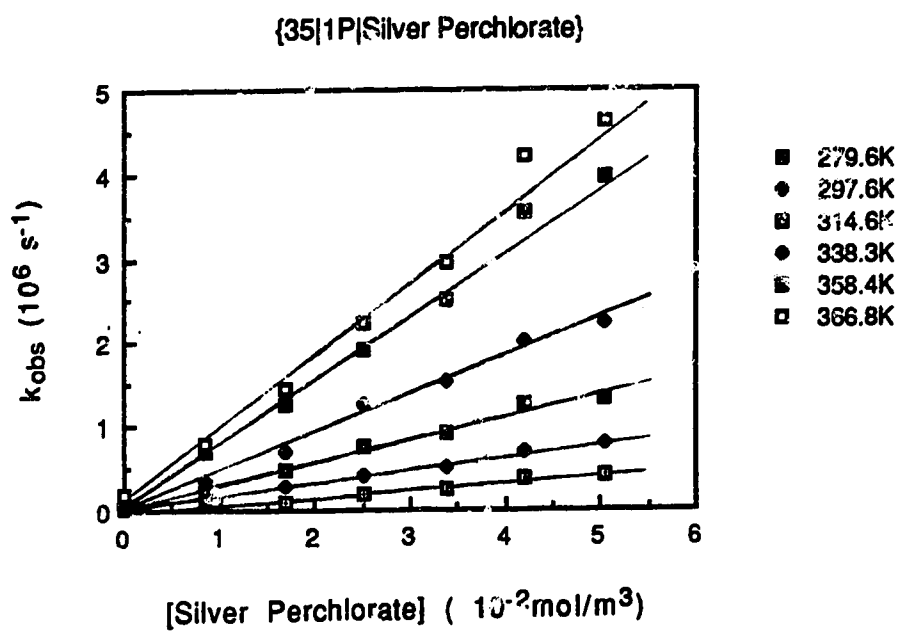
E



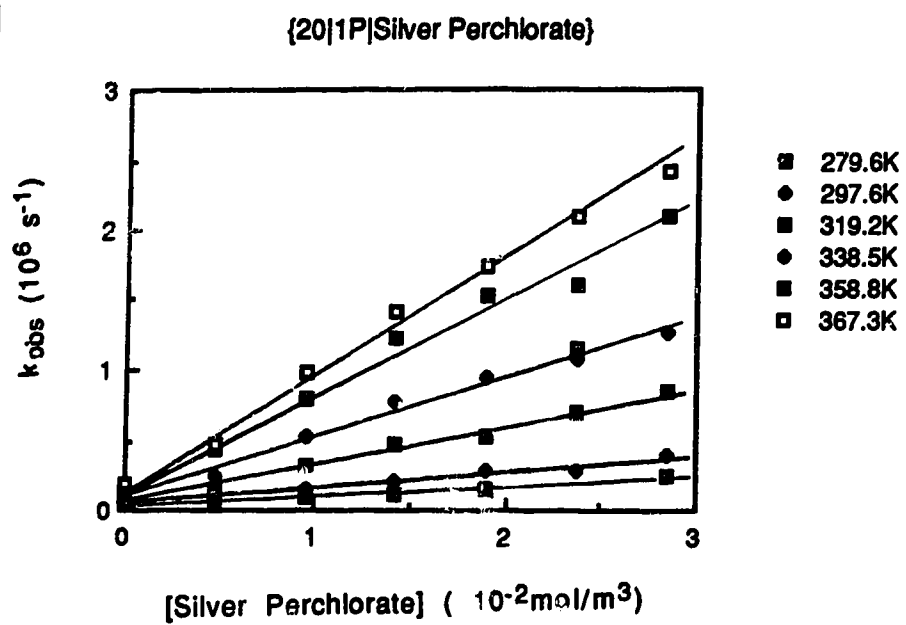
F



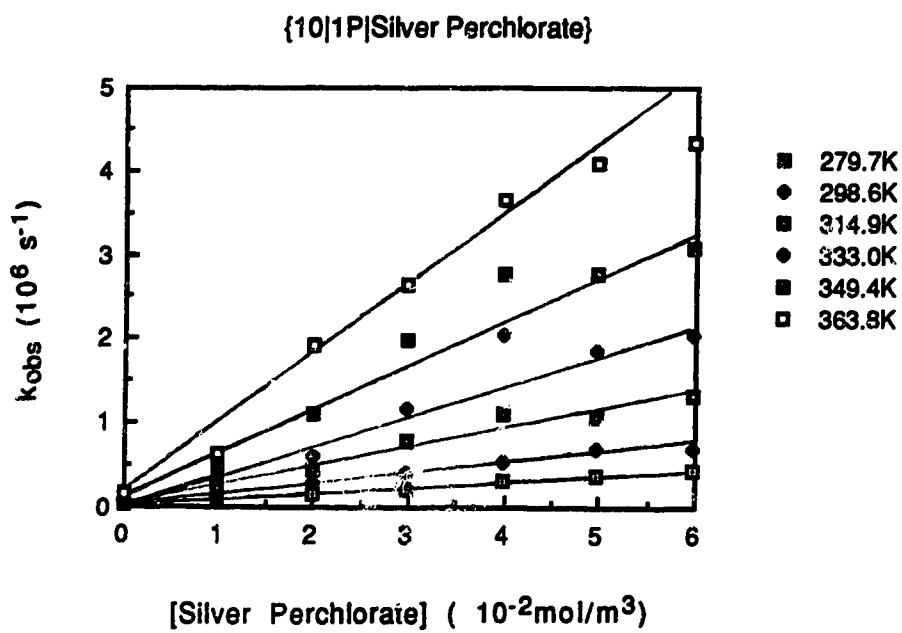
G



H



I



J

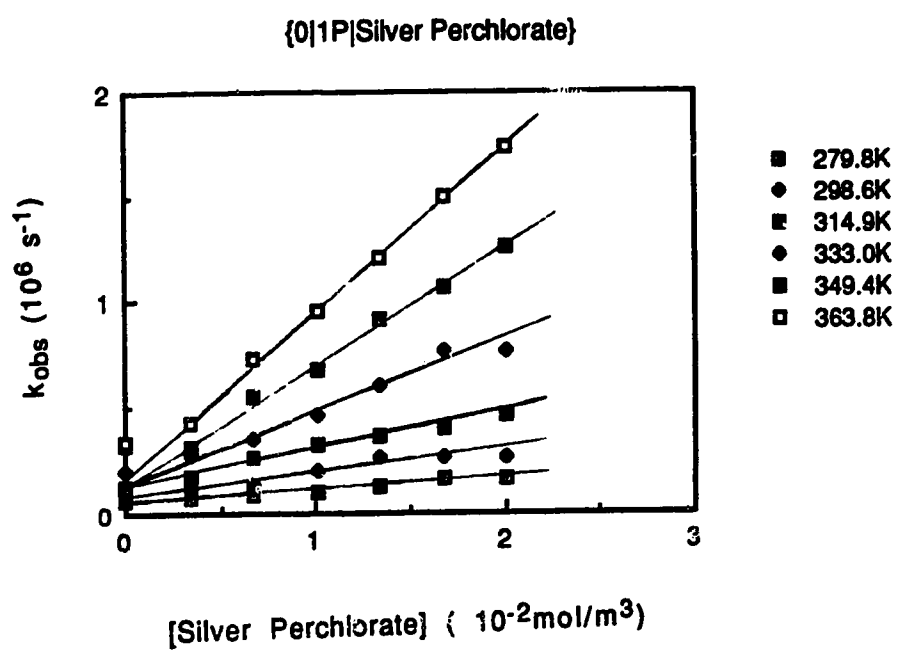


Table 7. Dielectric constants, f values and second-order rate constants for the reaction of solvated electrons with silver perchlorate in 1-propanol/water mixtures at various temperatures.

X_w	Temp (K)	ϵ	f	k_2 ($10^7 \text{ m}^3/\text{mol}\cdot\text{s}$)	X_w	Temp (K)	ϵ	f	k_2 ($10^7 \text{ m}^3/\text{mol}\cdot\text{s}$)
1.00	279.6	86.6	1.38	2.4	0.50	279.6	30.2	2.29	0.90
	297.5	78.7	1.40	4.2		297.0	27.5	2.35	1.4
	319.0	71.3	1.41	6.7		318.9	24.0	2.46	2.9
	338.5	64.6	1.43	10		338.4	21.2	2.58	4.7
	358.8	59.0	1.45	15		358.5	18.5	2.74	7.2
	369.5	56.0	1.46	18		366.9	16.7	2.91	8.4
0.97	279.5	79.5	1.42	1.9	0.35	279.6	26.5	2.52	0.81
	297.0	72.0	1.44	3.5		297.6	23.9	2.59	1.5
	318.9	65.2	1.45	5.8		314.6	21.5	2.70	2.7
	338.4	58.8	1.48	9.1		338.3	18.5	2.87	4.5
	358.5	53.4	1.50	13		358.4	16.0	3.08	7.1
	367.2	50.6	1.52	14		366.8	15.0	3.19	8.3
0.93	275.8	72.6	1.47	1.0	0.20	279.6	24.4	2.68	0.71
	295.2	65.9	1.49	2.0		297.6	21.8	2.78	1.2
	312.1	60.6	1.51	3.1		319.2	19.0	2.94	2.8
	332.0	54.7	1.53	4.4		338.5	16.7	3.11	4.3
	352.3	49.2	1.56	5.8		358.8	14.4	3.4	7.1
	361.0	47.0	1.57	7.9		367.3	13.5	3.5	12
0.80	275.8	52.3	1.69	0.8	0.10	279.7	23.5	2.76	0.74
	296.3	46.5	1.72	1.8		298.6	20.7	2.89	1.4
	312.8	42.5	1.76	2.8		314.9	18.6	3.0	2.2
	332.0	38.4	1.79	4.6		333.0	16.5	3.2	3.6
	346.3	35.3	1.83	6.0		349.4	14.6	3.4	5.5
							363.8	13.2	3.6
0.70	279.6	41.5	1.89	0.97	0.00	279.8	22.5	2.85	0.53
	297.6	37.4	1.93	1.5		298.6	20.0	2.98	1.1
	319.1	33.0	1.99	3.2		314.9	18.0	3.1	2.0
	338.5	29.5	2.06	4.5		333.0	16.0	3.3	3.4
	358.6	26.0	2.15	7.2		349.4	14.0	3.5	5.5
	367.1	24.5	2.20	8.2		363.8	12.7	3.7	7.9

Table 8. Rate parameters for the reaction of solvated electrons with silver perchlorate in 1-propanol/water mixtures.

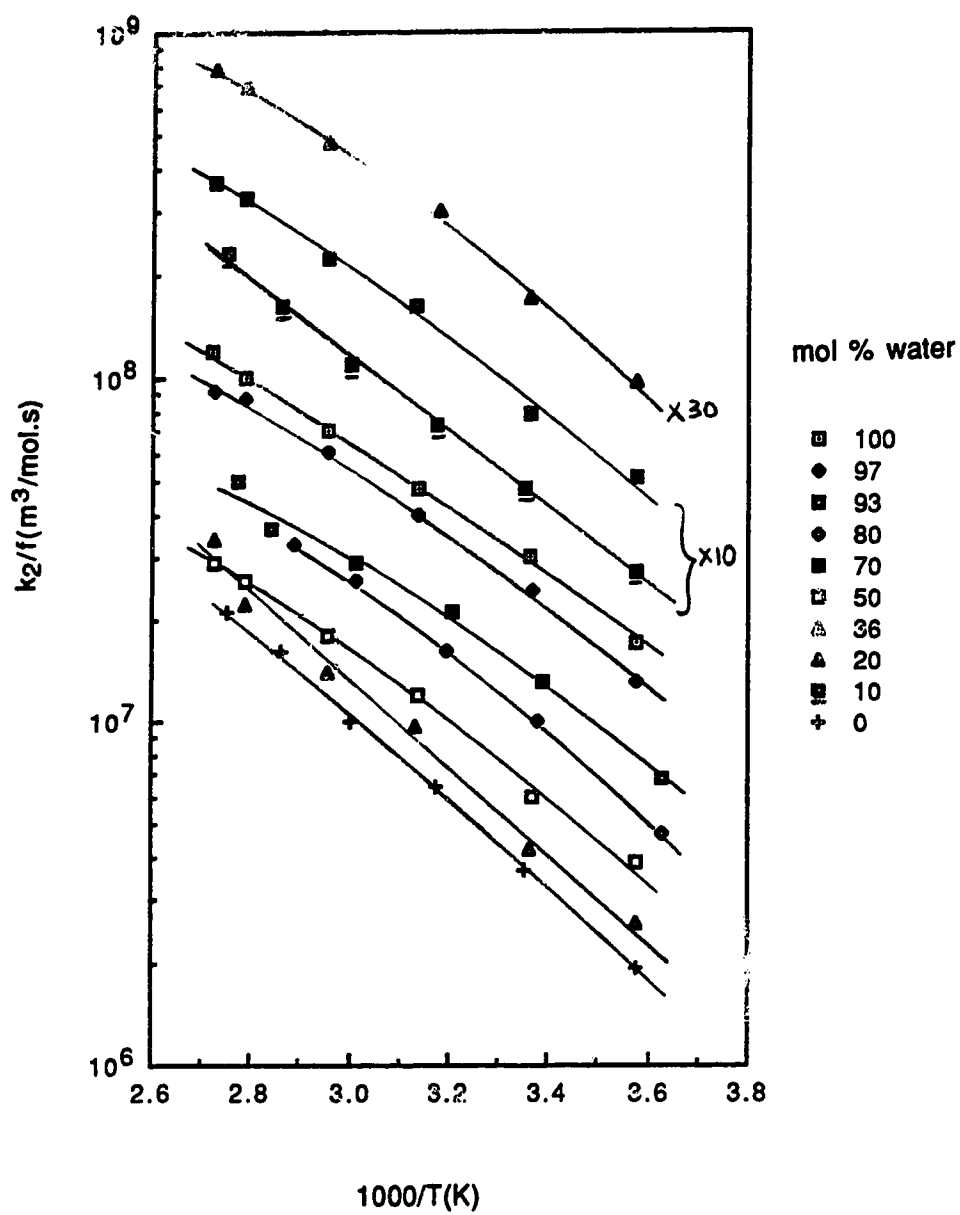
X_w	$\eta^{(a)}$ (10^{-3} Pa·s)	$k_2^{(a)}$ (10^7 m ³ /mol·s)	$k_2/\eta^{(a)}$ (10^7 m ³ /mol·s)	$E_2^{(b,c)}$ (kJ/mol)	$\log A_2^{(c)}$ (A_2 in m ³ /mol·s)
1.00	0.89	4.2	3.0	19	10.83
0.97	1.34	3.5	2.4	20	10.83
0.93	1.86	2.1	1.4	21	10.77
0.80	2.64	1.8	1.0	24	11.21
0.70	2.74	1.7	0.88	22	10.83
0.50	2.50	1.6	0.68	22	10.69
0.36	2.32	1.5	0.58	23	10.80
0.20	2.16	1.3	0.47	23	10.63
0.10	2.06	1.3	0.45	22	10.48
0.00	1.96	1.1	0.37	25	10.88

(a) At 298K.

(b) Near 298K.

(c) From Arrhenius plot.

Fig. 15 Arrhenius plots for the reaction of solvated electrons with silver perchlorate in 1-propanol/water mixtures

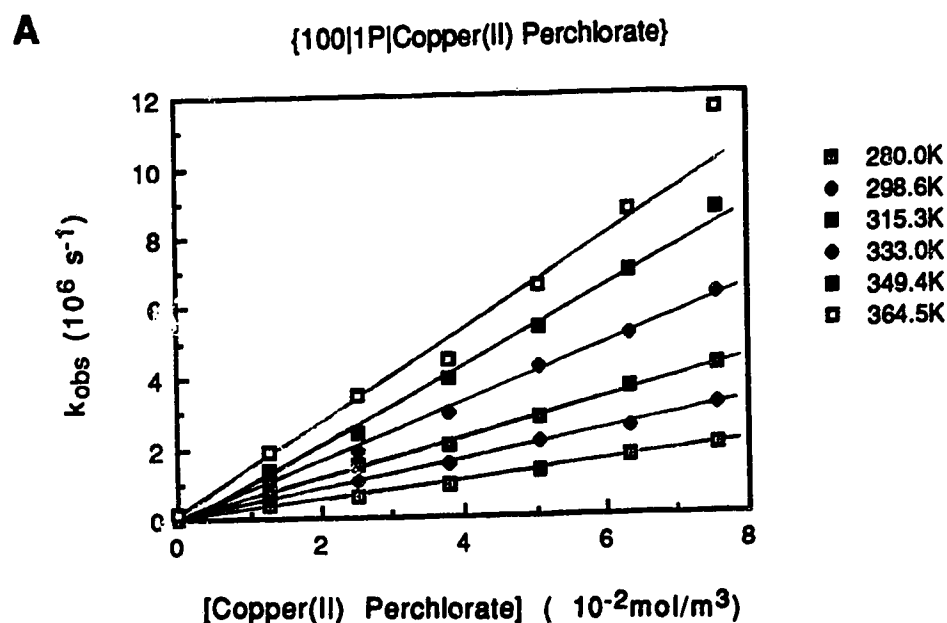


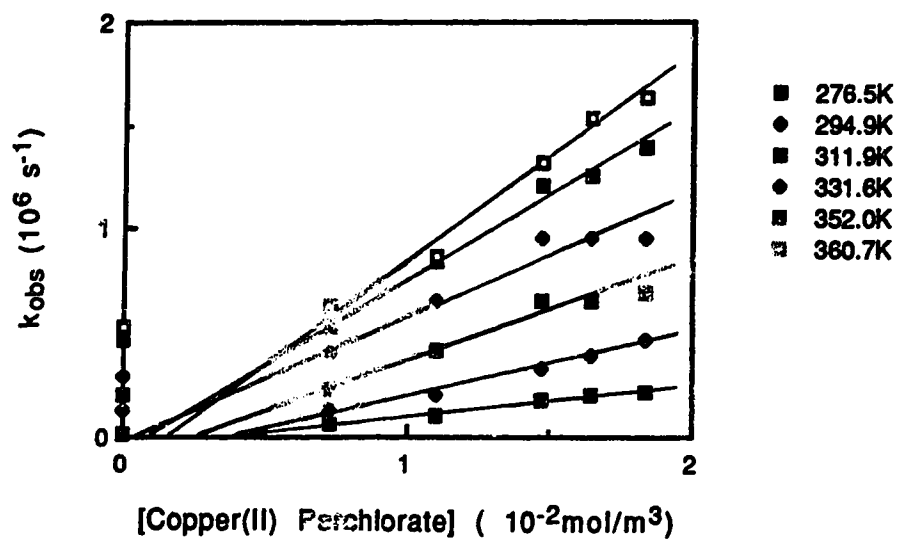
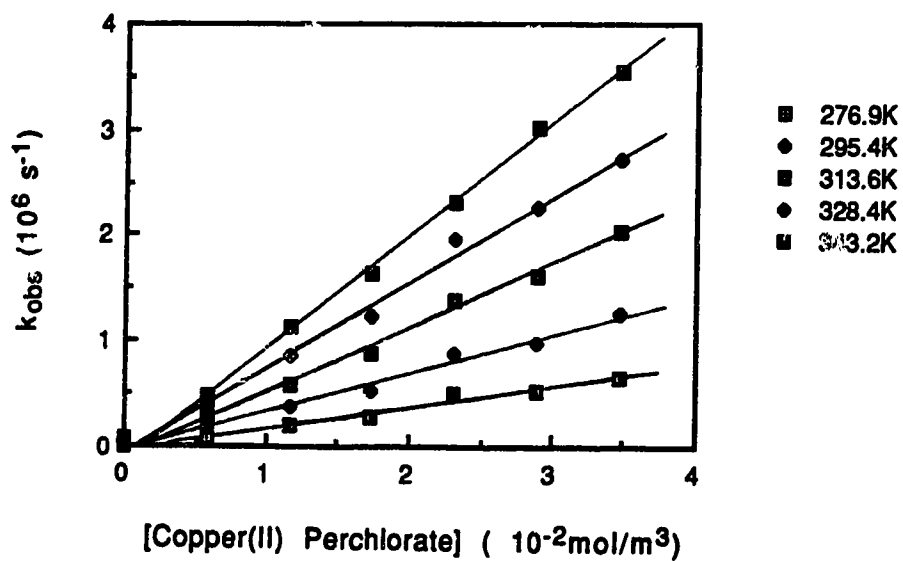
E. Reaction of Solvated Electrons with Copper(II) Ions

The temperature and concentration dependence of the first-order rate constants for the reaction of solvated electrons with copper(II) ion are shown in Figure 16 (A-J). The concentration range of Cu^{2+} was 2-75 mmol/m^3 .

Table 9 shows the second-order rate constants, dielectric constants and the coulombic factors f at various temperatures in different alcohol/water mixtures. The rate constant at 298 K is $3.9 \times 10^7 \text{ m}^3/\text{mol}\cdot\text{s}$ in water. The values reported in the literature are $3.8 \times 10^7 \text{ m}^3/\text{mol}\cdot\text{s}$ (104) and $4.0 \times 10^7 \text{ m}^3/\text{mol}\cdot\text{s}$ (86). Table 10 shows the rate parameters obtained from the modified Arrhenius plots shown in Figure 17.

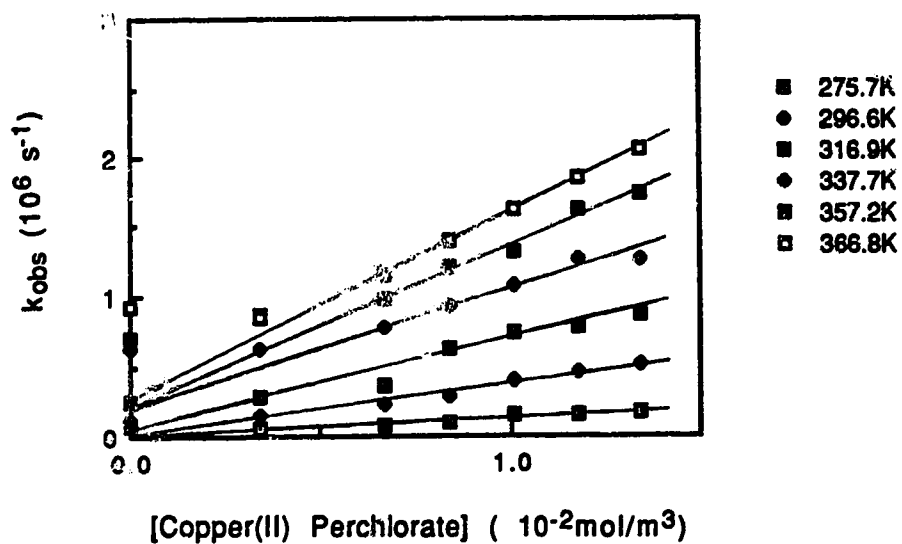
Fig. 16 Temperature and concentration dependence of the first-order rate constant for the reaction of solvated electrons with copper(II) perchlorate in 1-propanol/water mixtures



B**{97|1P|Copper(II) Perchlorate}****C****{93|1P|Copper(II) Perchlorate}**

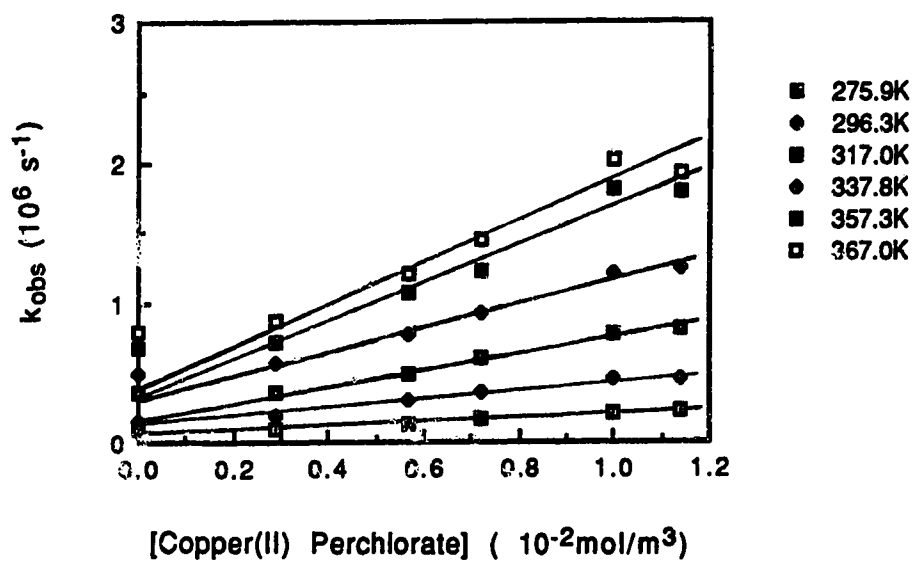
D

{81}1P[Copper(II) Perchlorate]

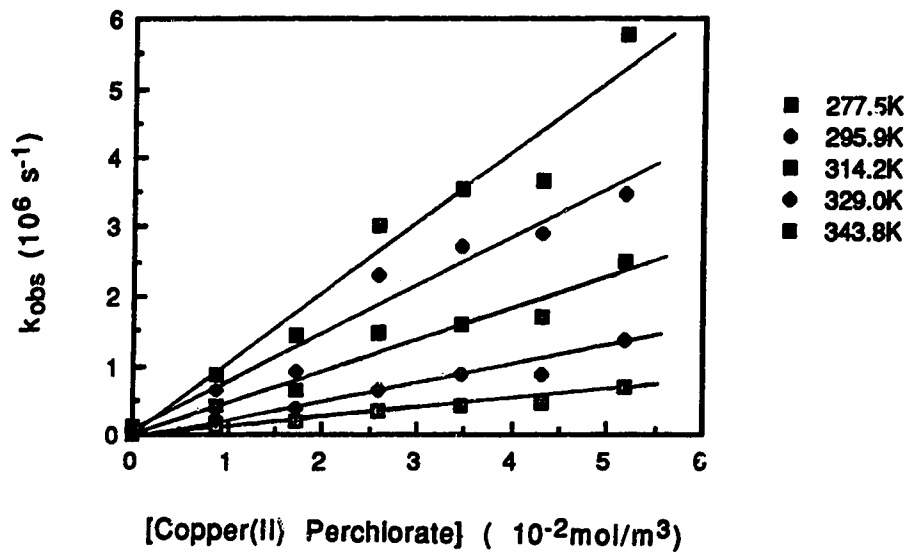


E

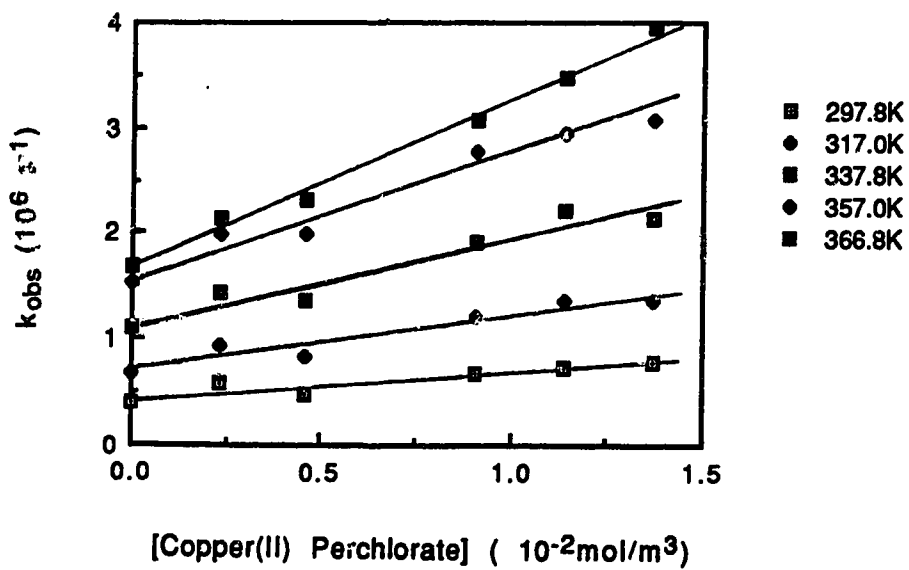
{68}1P[Copper(II) Perchlorate]



F

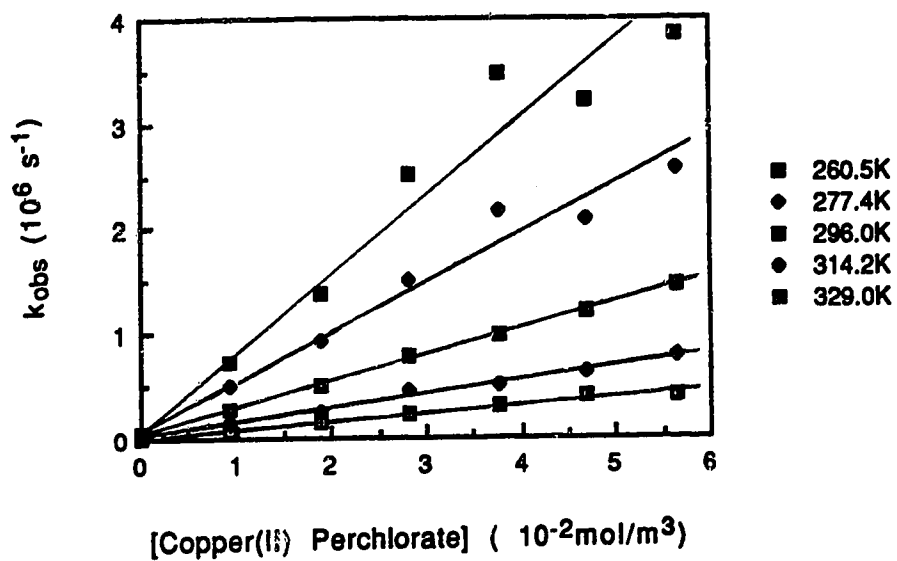
 $\{^{51}\text{P}\}\text{Copper(II) Perchlorate}$ 

G

 $\{^{33}\text{P}\}\text{Copper(II) Perchlorate}$ 

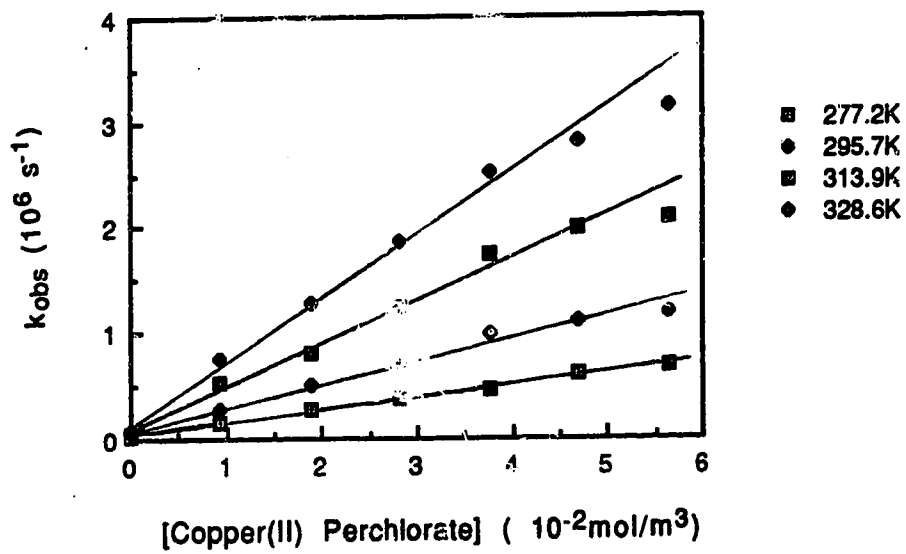
H

{20|1P|Copper(II) Perchlorate}



I

{10|1P|Copper(II) Perchlorate}



J

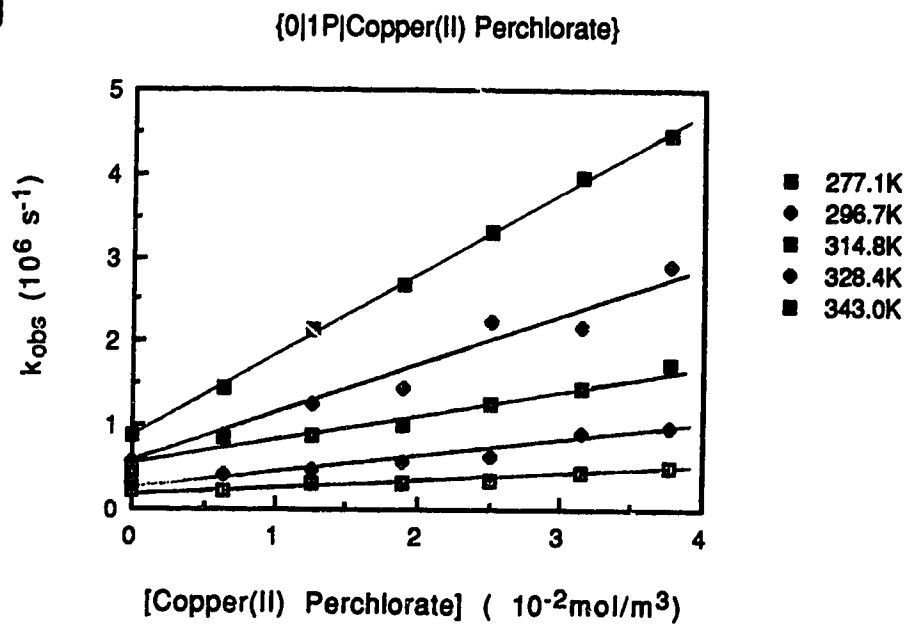


Table 9. Dielectric constants, f values and second-order rate constants for the reaction of solvated electrons with copper(II) perchlorate in 1-propanol/water mixtures at various temperatures.

X_w	Temp (K)	ϵ	f	k_2 ($10^7 \text{ m}^3/\text{mol}\cdot\text{s}$)	X_w	Temp (K)	ϵ	f	k_2 ($10^7 \text{ m}^3/\text{mol}\cdot\text{s}$)
1.00	280.0	85.7	3.0	2.5	0.51	277.5	31.0	7.8	1.4
	298.6	77.8	3.0	4.0		295.9	27.6	8.2	2.8
	315.3	72.2	3.1	5.6		314.2	24.5	8.7	4.7
	333.0	66.5	3.2	8.2		329.0	22.7	8.9	7.3
	349.4	61.5	3.3	11		343.8	17.7	11.0	10
	364.5	57.0	3.3	13					
0.97	276.5	80.0	3.2	1.7	0.33	297.8	23.5	9.5	2.7
	294.9	72.7	3.3	3.2		317.0	21.0	10.0	5.0
	311.9	67.0	3.3	4.8		337.8	18.3	10.8	7.8
	331.6	61.0	3.4	6.7		357.0	16.0	12.0	12
	352.0	55.0	3.6	8.2		366.8	14.8	12.3	16
	360.7	52.5	3.6	10					
0.93	276.9	72.2	3.5	2.0	0.20	260.5	27.5	9.3	0.75
	295.4	65.8	3.5	3.6		277.4	24.7	9.7	1.3
	313.6	60.0	3.7	6.0		296.0	22.7	9.9	2.6
	328.4	55.6	3.8	8.3		314.2	19.2	11.1	4.4
	343.2	51.5	3.9	11		329.0	17.7	11.5	6.7
0.81	295.7	53.0	4.6	1.4	0.10	277.2	23.6	10.2	1.1
	296.6	47.0	4.8	4.0		295.7	21.0	10.7	2.5
	316.9	42.2	5.0	6.0		313.9	18.7	11.4	4.2
	337.7	37.6	5.3	8.0		313.9	18.7	11.4	4.2
	357.2	33.5	5.6	11		328.6	17.0	11.9	6.3
	366.8	31.5	5.8	13					
0.68	275.9	40.3	6.0	1.2	0.00	277.1	23.0	10.5	0.91
	296.3	35.6	6.3	3.0		296.7	20.4	11.0	1.9
	317.0	31.6	6.7	5.8		314.8	18.0	11.8	3.6
	337.8	28.0	7.1	8.7		328.4	16.5	12.3	5.8
	357.3	24.8	7.5	12		343.0	14.7	13.2	9.7
	367.0	23.3	7.8	13					

Table 10. Rate parameters for the reaction of solvated electrons with copper(II) perchlorate in 1-propanol/water mixtures.

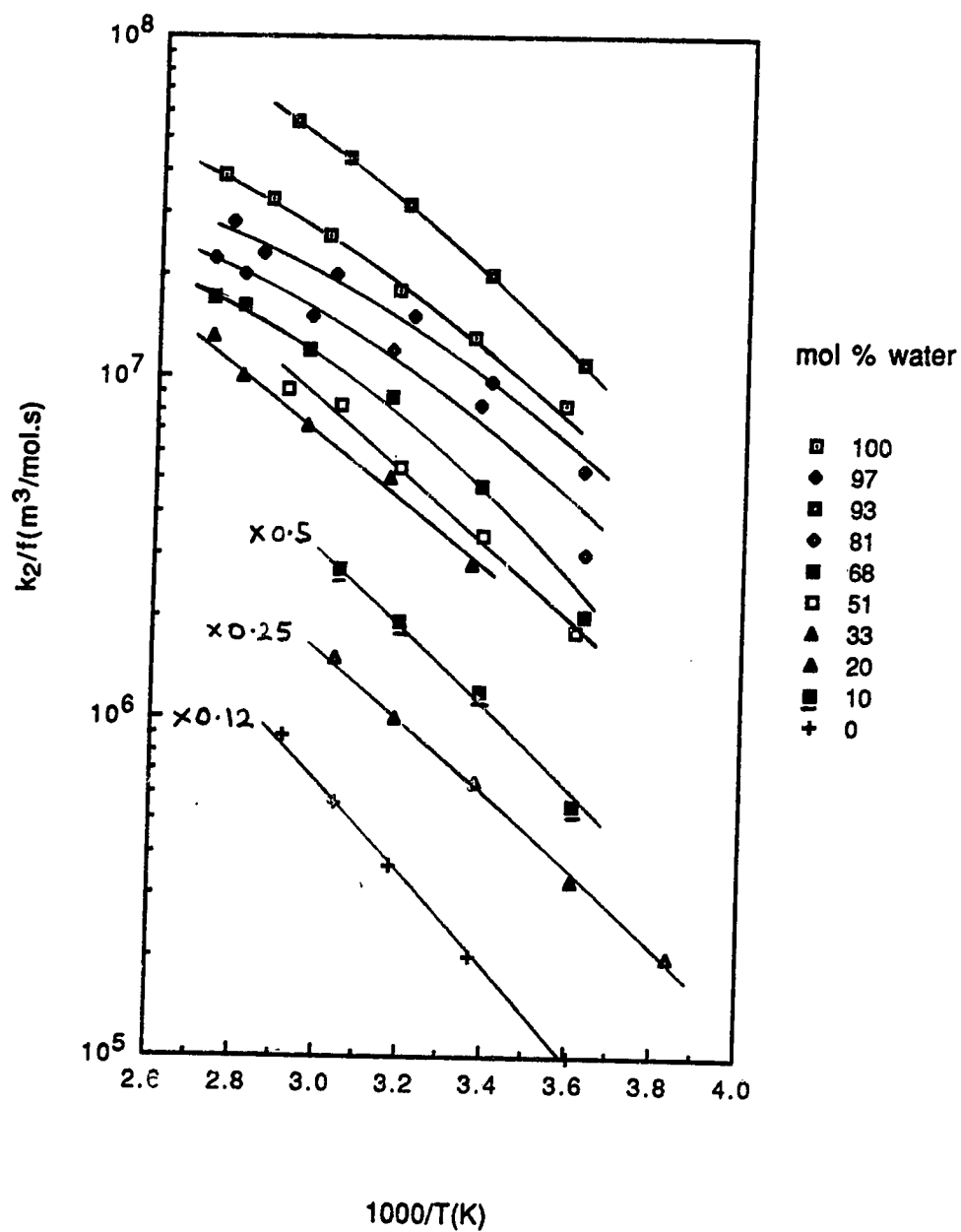
X_w	$\eta^{(a)}$ (10^{-3} Pa·s)	$k_2^{(a)}$ (10^7 m ³ /mol·s)	$k_2/f^{(a)}$ (10^7 m ³ /mol·s)	$E_2^{(b,c)}$ (kJ/mol)	$\log A_2^{(c)}$ (A_2 in m ³ /mol·s)
1.00	0.89	3.9	1.3	18	10.20
0.97	1.34	3.4	1.0	18	10.21
0.93	1.92	3.9	1.1	20	10.60
0.81	2.63	3.5	0.73	23	10.87
0.68	2.72	3.1	0.49	24	10.96
0.51	2.56	2.9	0.36	20	10.00
0.33	2.30	2.9	0.31	20	10.00
0.20	2.16	2.8	0.27	21	10.06
0.10	2.06	2.5	0.23	23	10.16
0.00	1.96	2.1	0.19	25	10.72

(a) At 298K.

(b) Near 298K.

(c) From Arrhenius plots of k_2/f .

Fig. 17 Arrhenius plots for the reaction of solvated electrons with copper(II) perchlorate in 1-propanol/water mixtures

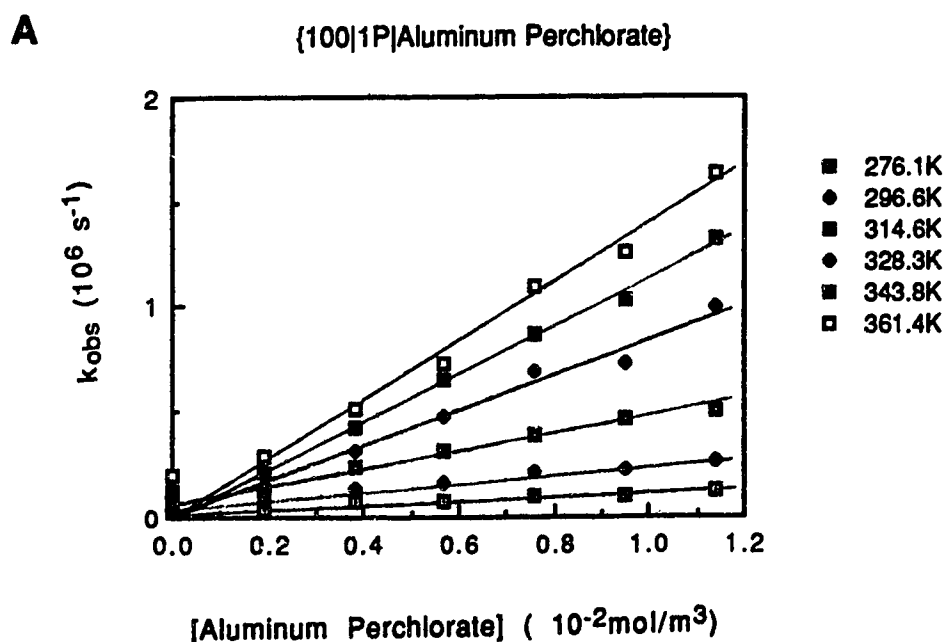


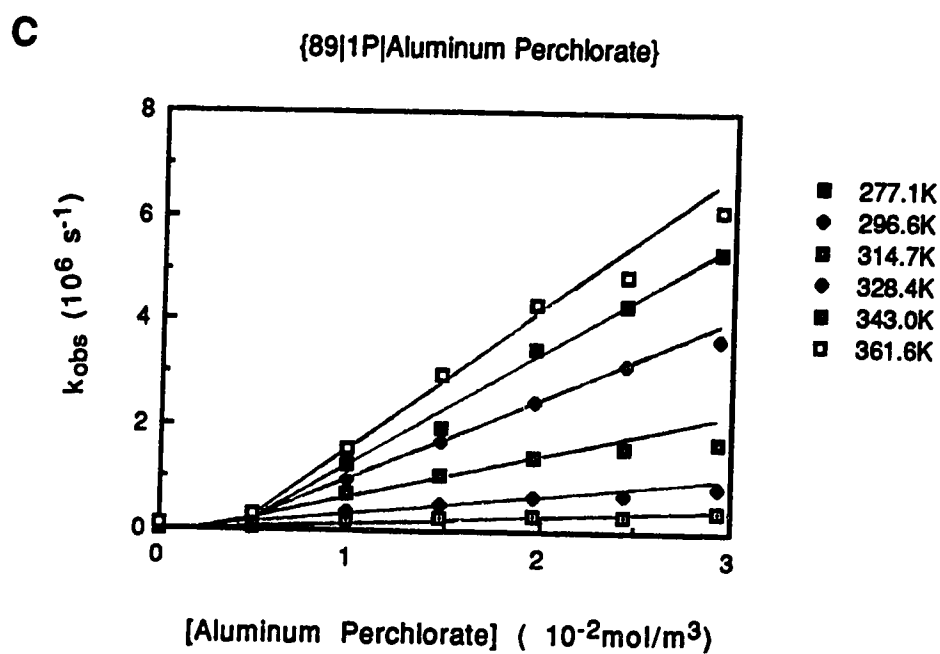
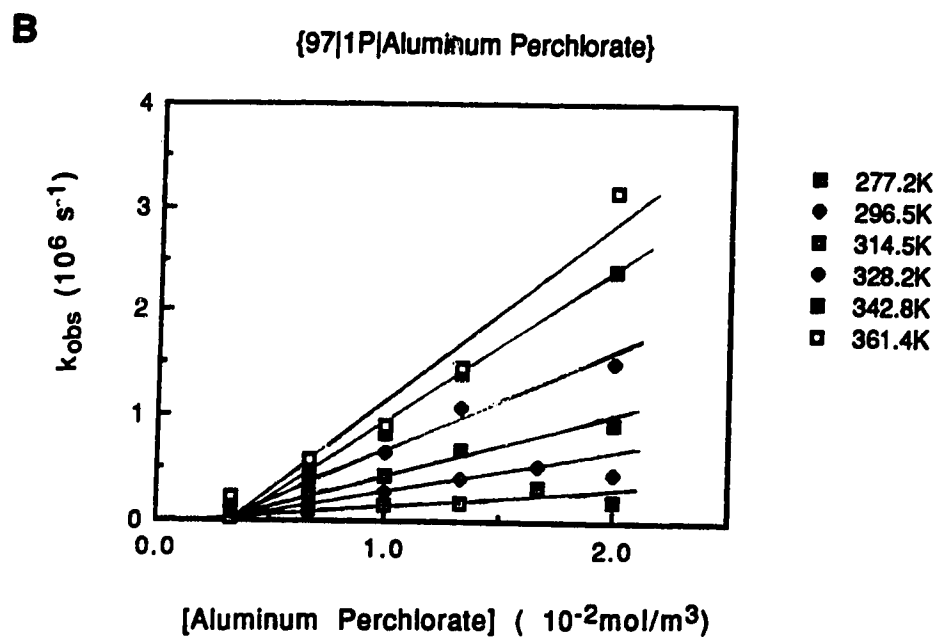
F. Reaction of Solvated Electrons with Aluminum Ions

The temperature and concentration dependence of the first-order rate constants for the reaction of solvated electrons with aluminum(III) are shown in Figure 18 (A-M). The concentration range was 2-32 mmol/m³.

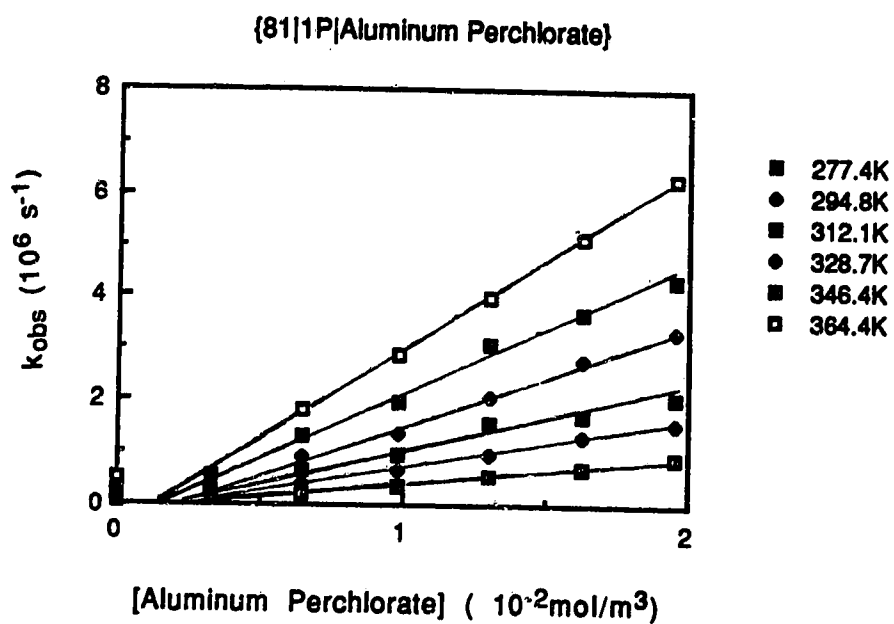
Table 11 shows the second-order rate constants, dielectric constants and the coulombic factors f at various temperatures in different alcohol/water mixtures. The rate constant at 298 K is 2.5×10^7 m³/mol·s in water. The value reported in the literature is 2.0×10^6 m³/mol·s (83). The negative intercept could be the reason for this large difference between the experimental and literature results. (An experiment done in a lower concentration range can give a lower second-order rate constant.) Table 12 shows the rate parameters obtained from the modified Arrhenius plots shown in Figure 19.

Fig. 18 Temperature and concentration dependence of the first-order
(A-M) rate constant for the reaction of solvated electrons with
 aluminum perchlorate in 1-propanol/water mixtures

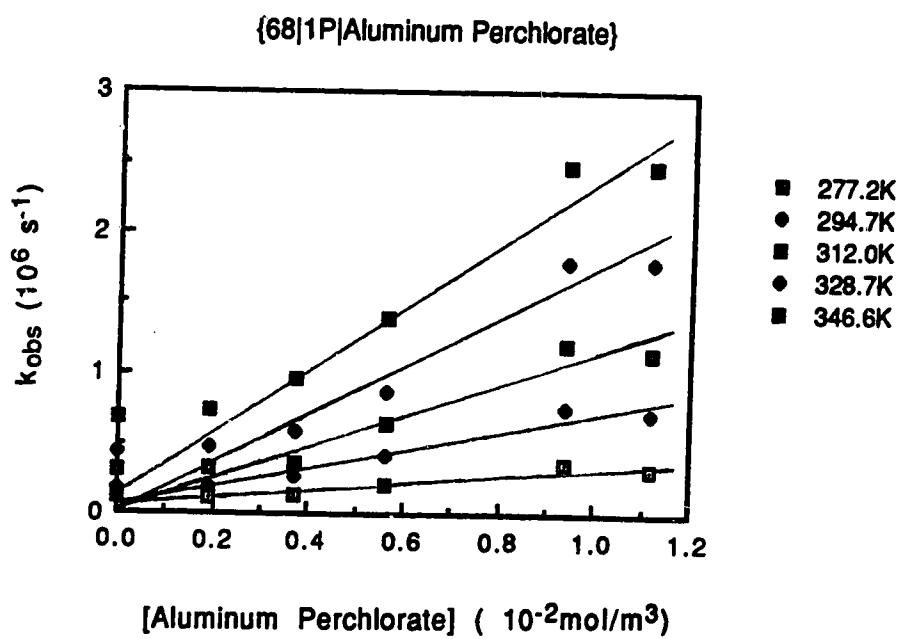




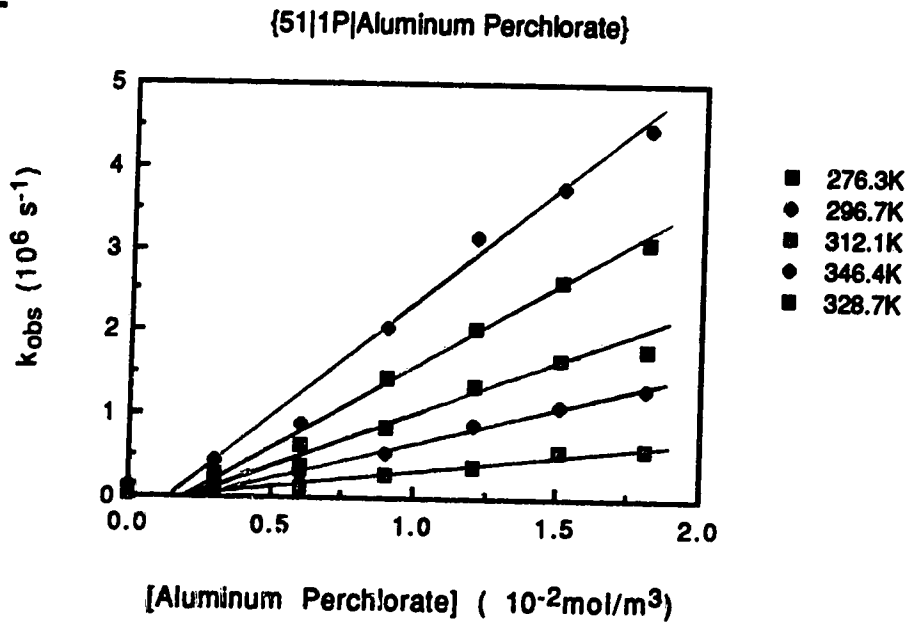
D



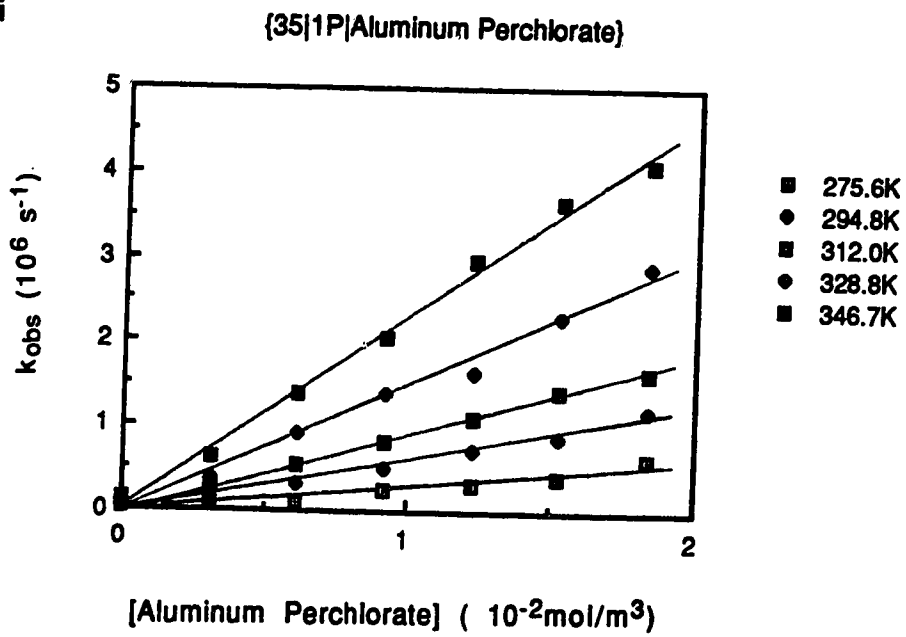
E



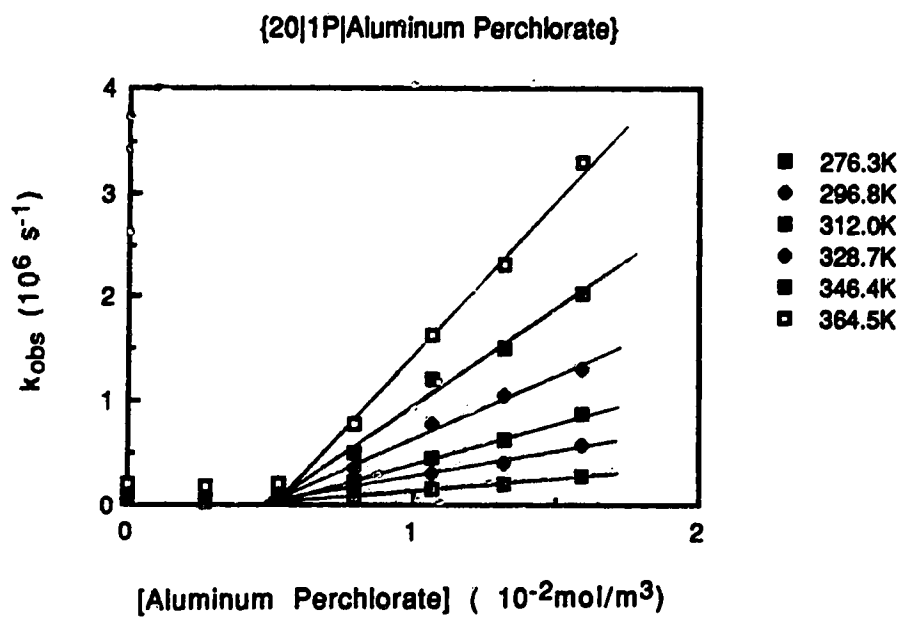
F



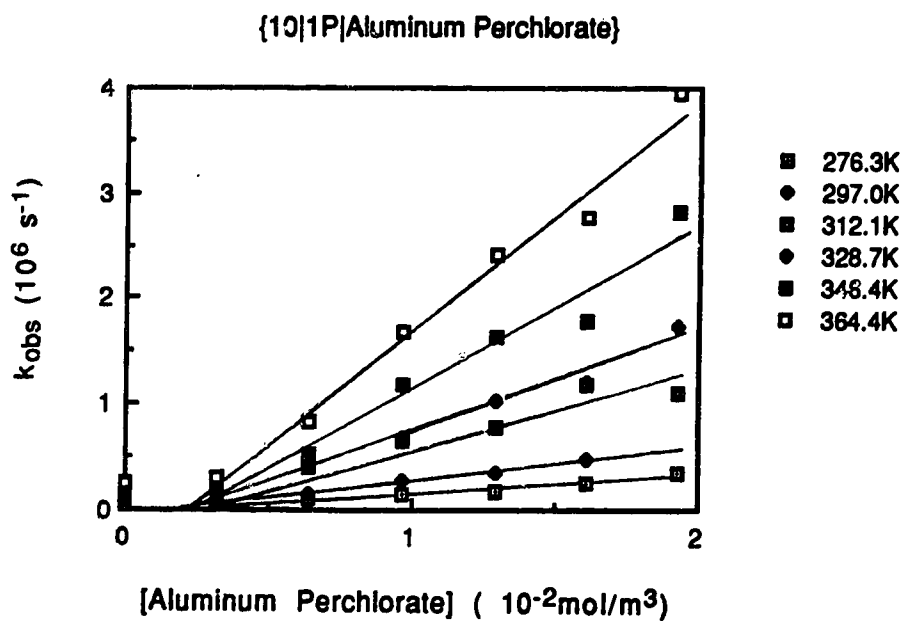
G



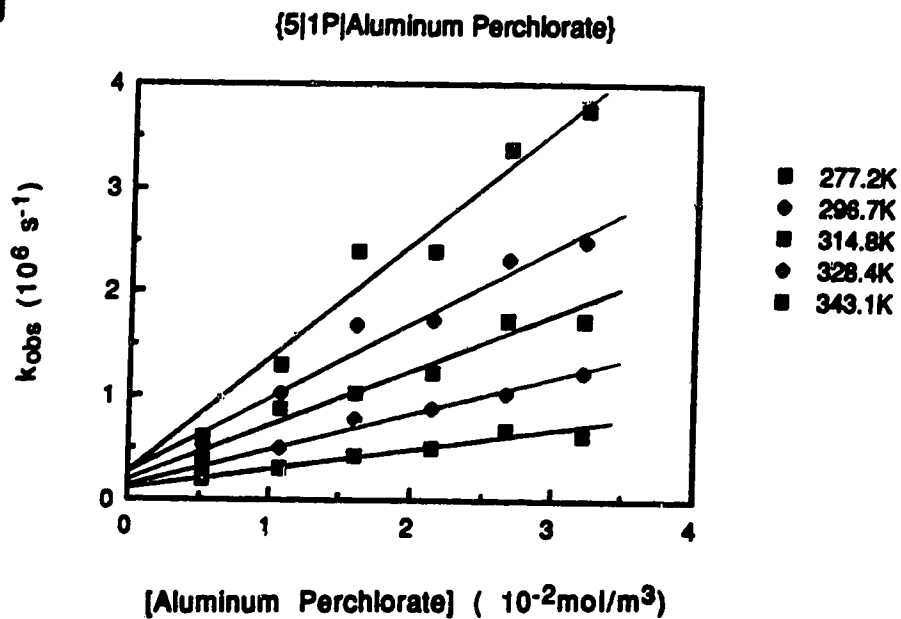
H



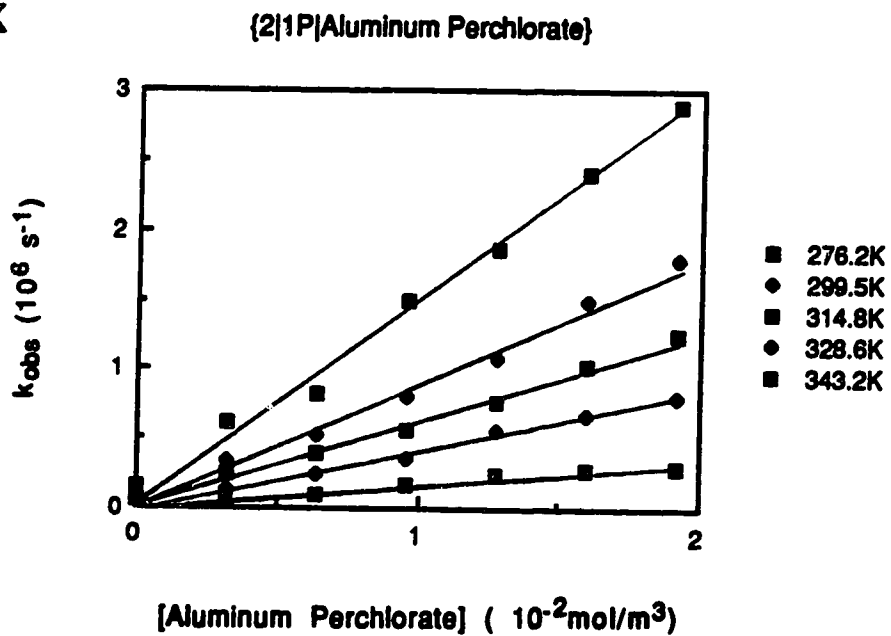
I



J

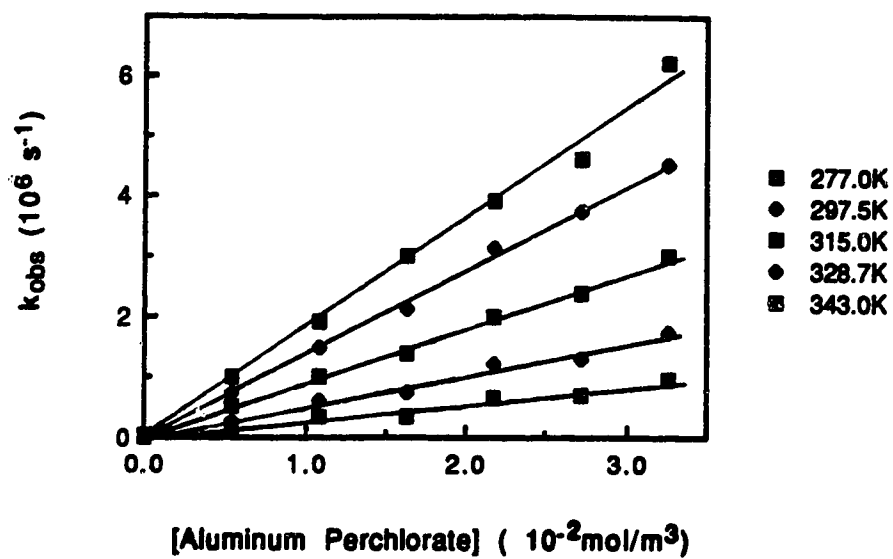


K



L

{11P|Aluminum Perchlorate}



M

{01P|Aluminum Perchlorate}

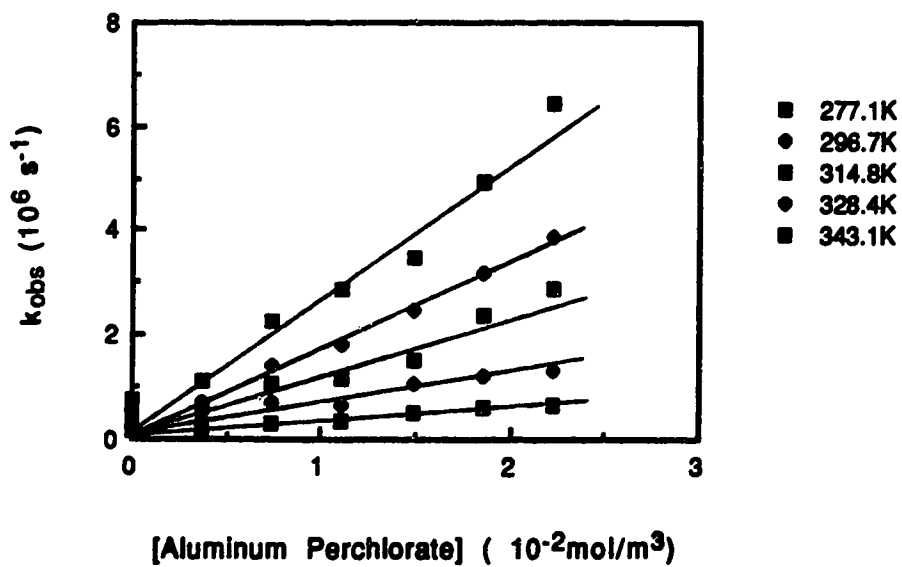


Table 11. Dielectric constants, f values and second-order rate constants for the reaction of solvated electrons with aluminum perchlorate in 1-propanol/water mixtures at various temperatures.

X_w	Temp (K)	ϵ	f	k_2 ($10^7 \text{ m}^3/\text{mol}\cdot\text{s}$)	X_w	Temp (K)	ϵ	f	k_2 ($10^7 \text{ m}^3/\text{mol}\cdot\text{s}$)
1.00	276.1	87.5	5.9	0.91	0.35	275.6	27.2	19.1	2.6
	296.6	79.0	6.1	2.0		294.8	24.2	20.1	5.6
	314.6	72.5	6.3	4.3		312.0	22.0	20.8	8.9
	328.6	68.0	6.4	8.6		328.8	19.6	22.2	15
	343.8	63.0	6.6	11		346.7	17.5	23.6	23
	361.4	57.9	6.8	14					
0.97	277.2	79.7	6.5	1.4	0.20	276.3	25.0	20.7	2.4
	296.5	72.2	6.7	3.6		296.8	22.0	21.9	5.0
	314.5	66.5	6.8	5.5		312.0	20.0	22.9	8.0
	328.2	62.0	7.0	9.0		328.7	17.8	24.4	13
	342.8	57.7	7.2	14		346.4	15.8	26.1	18
	361.4	52.5	7.5	18		364.5	13.7	28.6	29
0.89	277.1	64.5	8.0	1.6	0.10	276.3	23.8	21.8	1.9
	296.6	58.2	8.3	4.2		297.0	21.0	22.9	3.5
	314.7	53.0	8.6	8.3		312.1	19.0	24.1	6.5
	328.4	49.2	8.9	15		328.7	17.0	25.6	10
	343.0	45.5	9.2	21		346.4	15.0	27.5	17
	361.6	41.0	9.6	28		364.4	13.0	30.2	24
0.81	277.4	52.5	9.8	4.7	0.05	277.2	23.3	22.1	1.9
	294.8	47.5	10.2	8.6		296.7	20.7	23.3	3.5
	312.1	43.3	10.6	12		314.8	18.3	24.8	6.3
	328.7	39.5	11.0	19		328.4	16.6	26.2	9.5
	346.4	36.2	11.4	26		343.1	15.0	27.8	14
	364.4	32.0	12.3	34					
0.68	277.2	40.0	12.9	3.6	0.00	277.1	23.0	22.4	3.1
	294.7	36.0	13.5	7.7		296.7	20.4	23.6	6.3
	312.0	32.5	14.1	12		314.8	18.0	25.2	11
	328.7	29.5	14.8	17		328.4	16.5	26.4	16
	346.6	26.5	15.6	23		343.1	14.9	28.0	25
0.51	276.3	31.2	16.6	3.7					
	296.7	27.7	17.4	7.9					
	312.1	25.4	18.0	12					
	328.7	23.0	18.9	19					
	346.4	20.5	20.1	27					

Table 12. Rate parameters for the reaction of solvated electrons with aluminum perchlorate in 1-propanol/water mixtures.

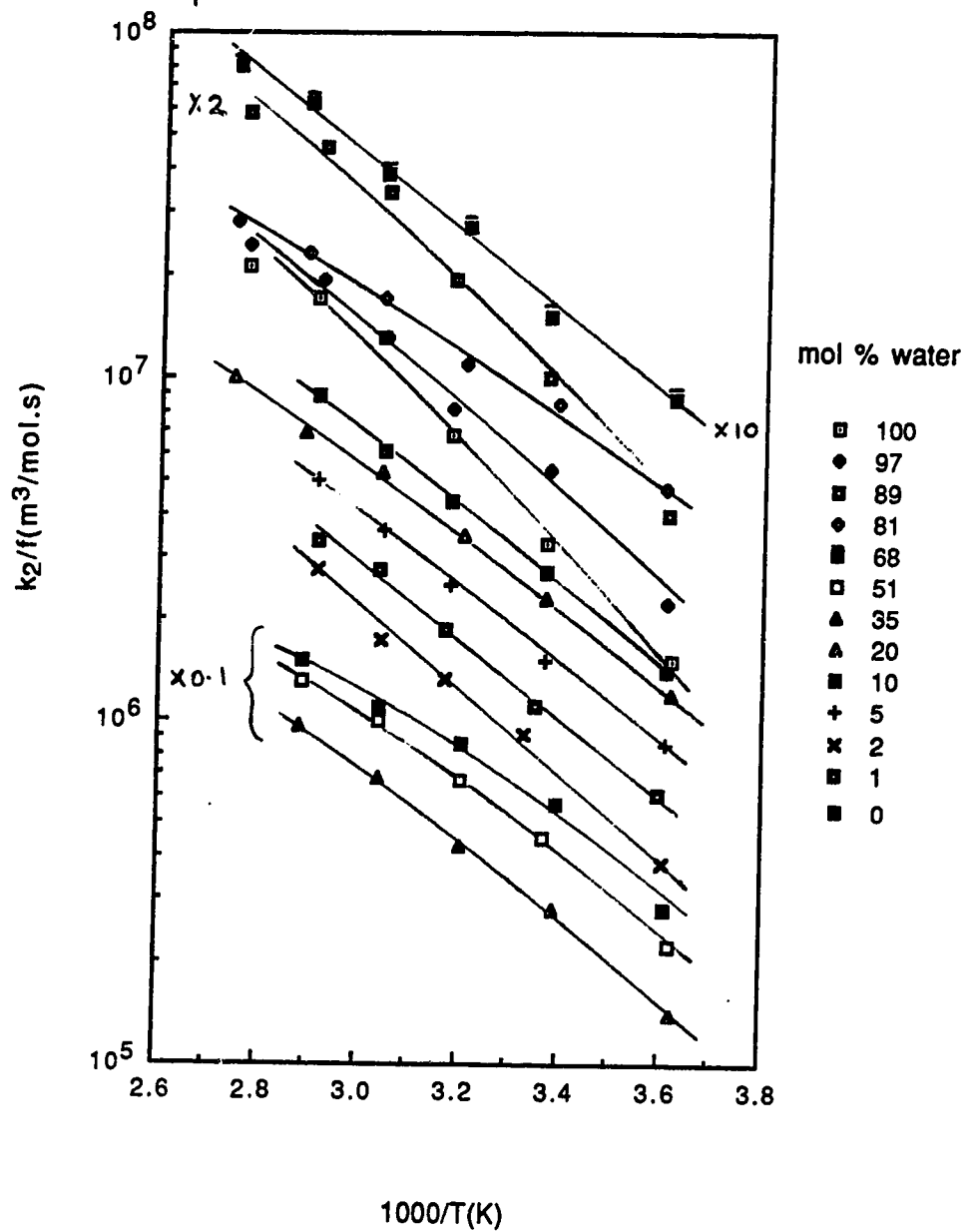
X_w	$\eta^{(a)}$ (10^{-3} Pa·s)	$k_2^{(a)}$ (10^7 m ³ /mol·s)	$k_2/f^{(a)}$ (10^7 m ³ /mol·s)	$E_2^{(b,c)}$ (kJ/mol)	$\log A_2^{(c)}$ (A_2 in m ³ /mol·s)
1.00	0.89	2.5	0.41	34	11.79
0.97	1.34	3.5	0.52	26	11.25
0.89	2.26	4.5	0.54	28	11.54
0.81	2.63	8.8	0.86	19	10.27
0.68	2.73	8.2	0.62	20	10.27
0.51	2.56	8.0	0.47	21	10.33
0.35	2.32	5.9	0.30	20	10.00
0.20	2.16	5.2	0.24	21	10.04
0.10	2.06	4.1	0.18	21	9.98
0.05	2.01	3.8	0.16	22	10.07
0.00	1.96	6.7	0.28	22	10.38

(a) At 298K.

(b) Near 298K.

(c) From Arrhenius plots of k_2/f .

Fig. 19 Arrhenius plots for the reaction of solvated electrons with aluminum perchlorate in 1-propanol/water mixtures

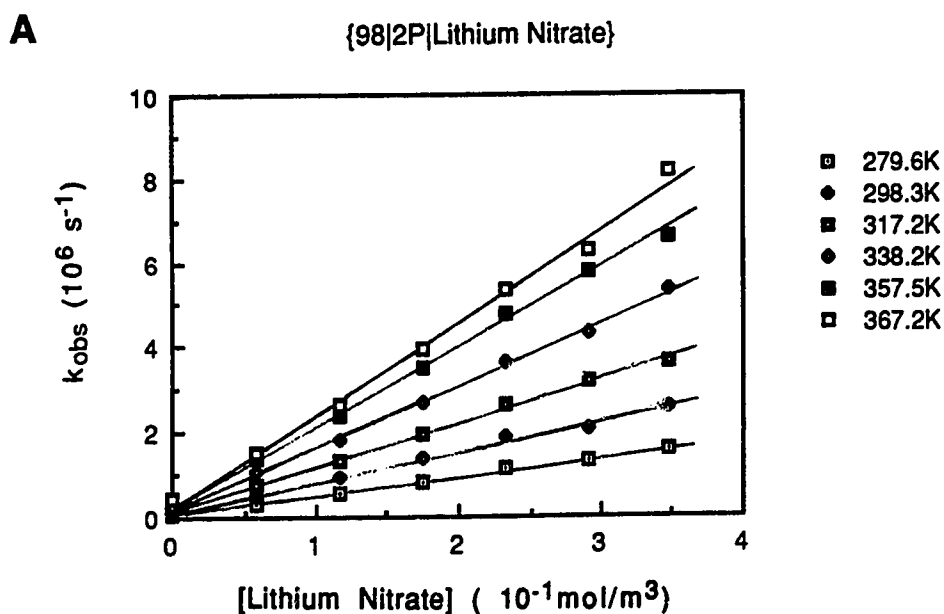


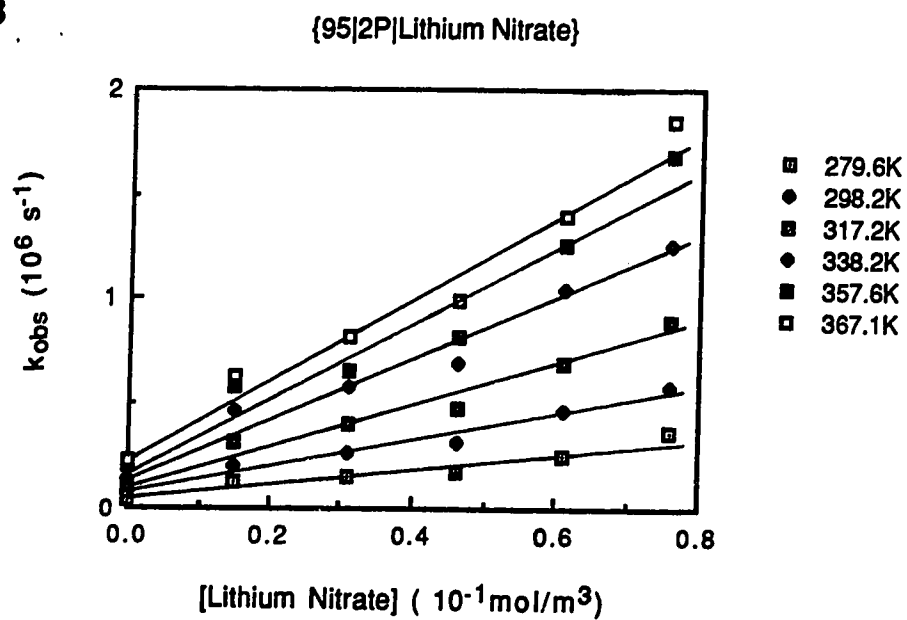
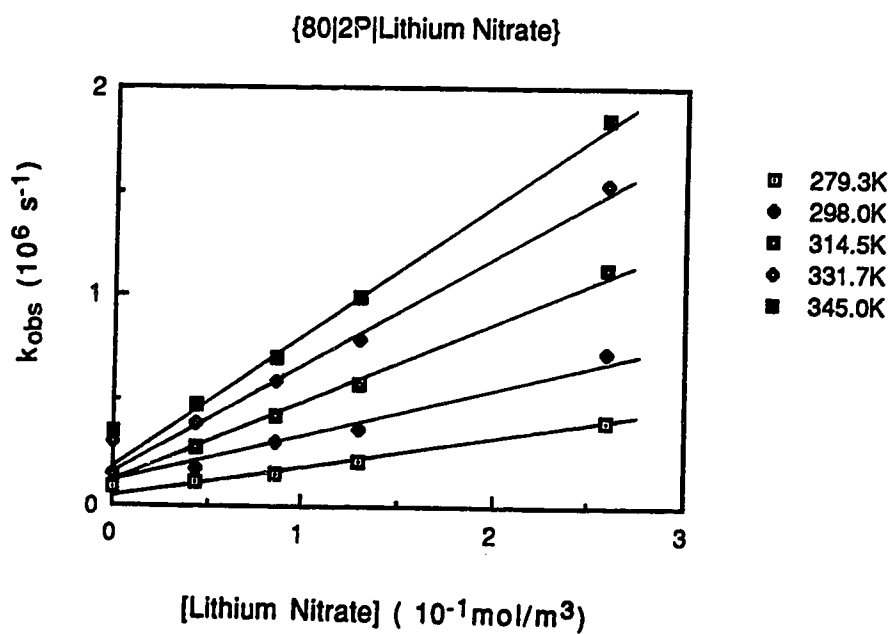
III. Reactions of Solvated Electrons in 2-Propanol/Water Mixtures

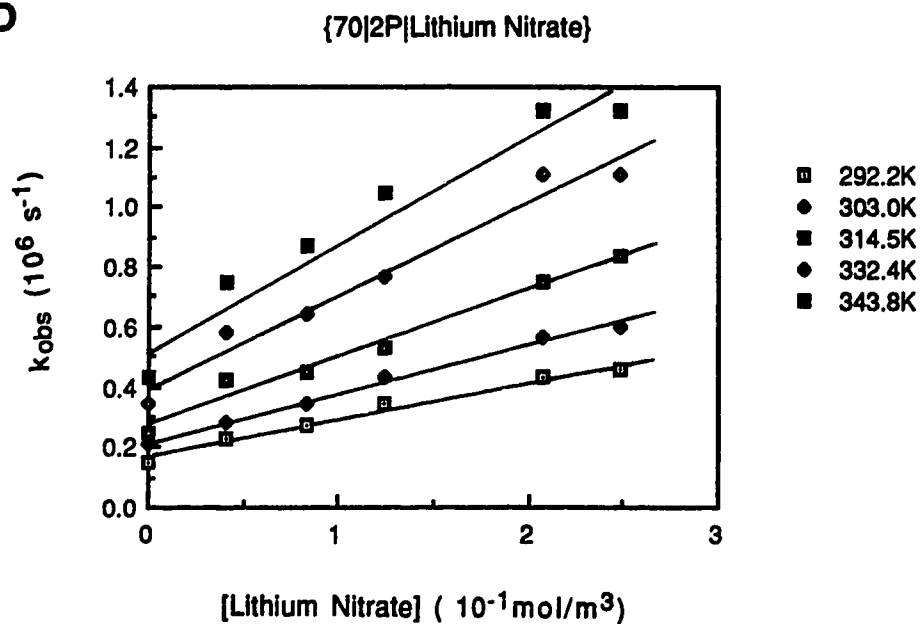
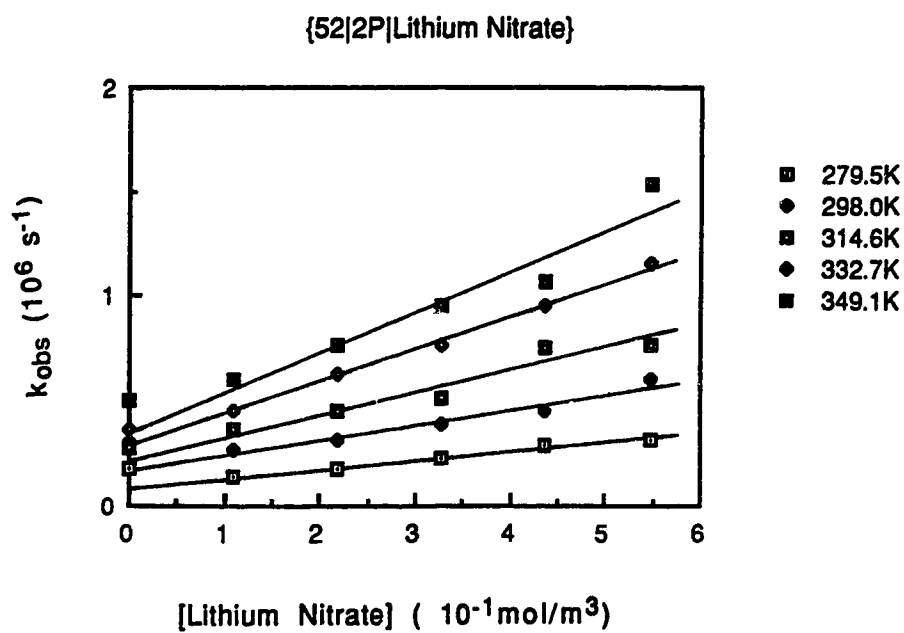
A. Reaction of Solvated Electrons with Nitrate Ions

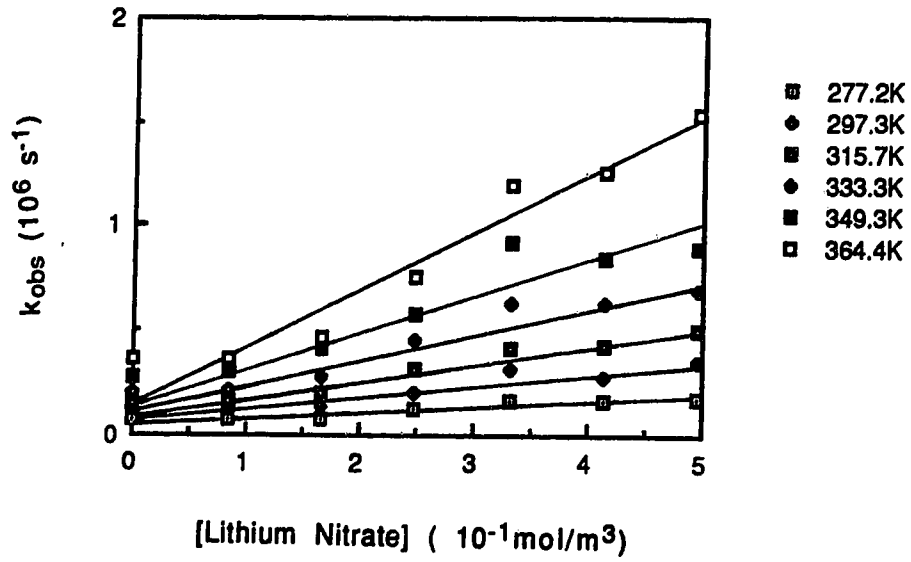
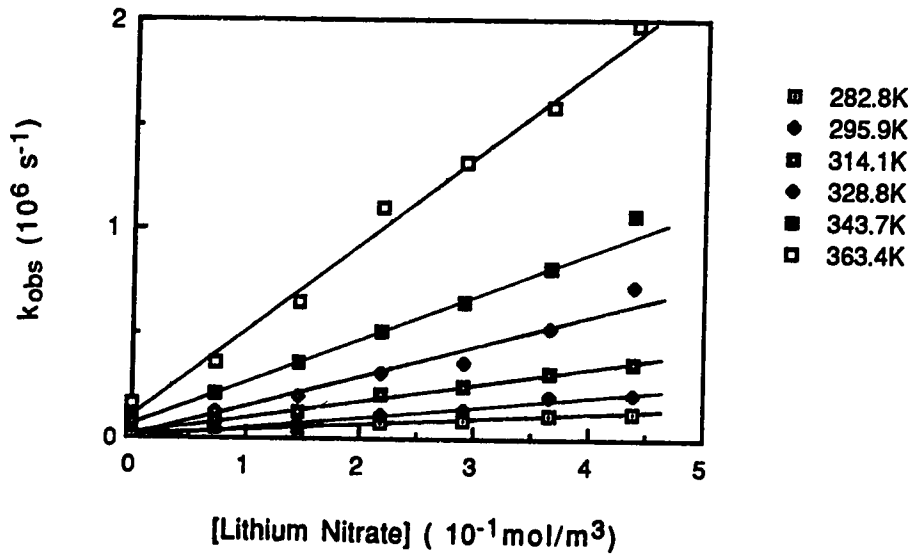
The temperature and concentration dependence of the first-order rate constant for the reaction of solvated electrons with nitrate ion are shown in Figure 20 (A-I). The concentration range was 0.03-0.5 mol/m³. Table 13 shows the second-order rate constants, dielectric constants and the coulombic factors *f* at various temperatures in different alcohol/water mixtures. Table 14 shows the rate parameters obtained from the modified Arrhenius plots shown in Figure 21.

Fig. 20 Temperature and concentration dependence of the first-order rate constant for the reaction of solvated electrons with lithium nitrate in 2-propanol/water mixtures



B**C**

D**E**

F**{36}2P|Lithium Nitrate****G****{20}2P|Lithium Nitrate**

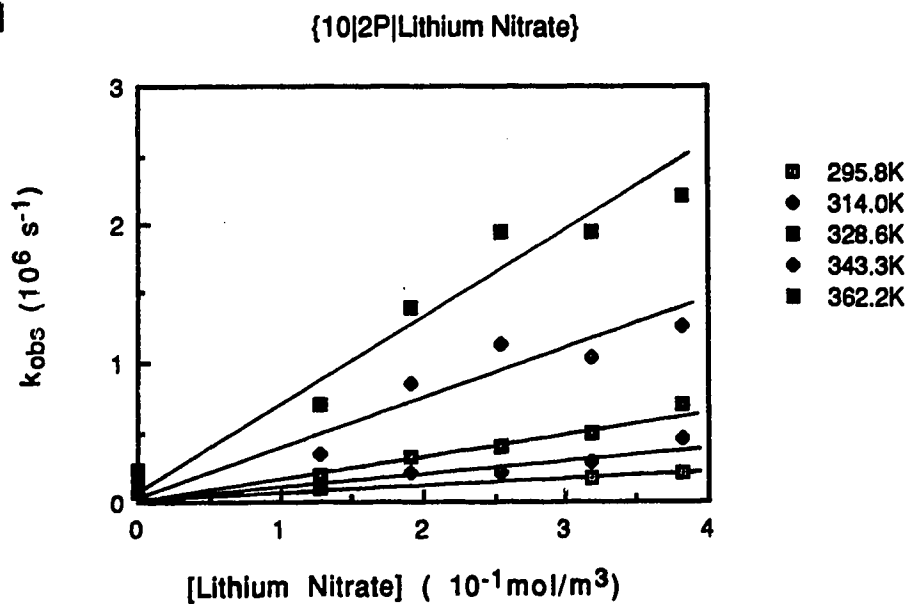
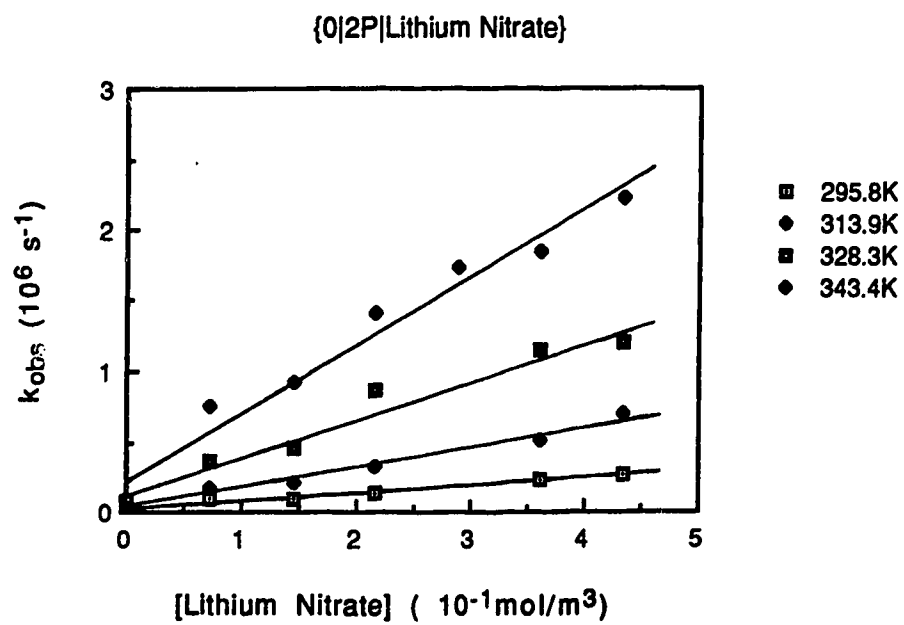
H**I**

Table 14. Rate parameters for the reaction of solvated electrons with lithium nitrate in 2-propanol/water mixtures.

X_w	$\eta^{(a)}$ (10^{-3} Pa·s)	$k_2^{(a)}$ (10^6 m ³ /mol·s)	$k_2/f^{(a)}$ (10^6 m ³ /mol·s)	$E_2^{(b,c)}$ (kJ/mol)	$\log A_2^{(c)}$ (A_2 in m ³ /mol·s)	$E_{\eta}^{(d)}$ (kJ/mol)
1.00	0.89	9.4	12	16	9.91	16
0.98	1.26	7.1	9.2	17	10.00	20
0.95	1.80	6.2	8.3	22	10.70	
0.81	3.01	2.5	3.9	23	10.65	25
0.70	3.06	1.5	2.6	23	10.40	25
0.52	2.72	0.74	1.7	20	9.71	25
0.36	2.39	0.53	1.4	24	10.40	
0.20	2.19	0.51	1.5	33	11.96	
0.10	2.13	0.55	1.8	38	12.94	23
0.00	2.08	0.65	2.2	42	13.69	22

(a) At 298K.

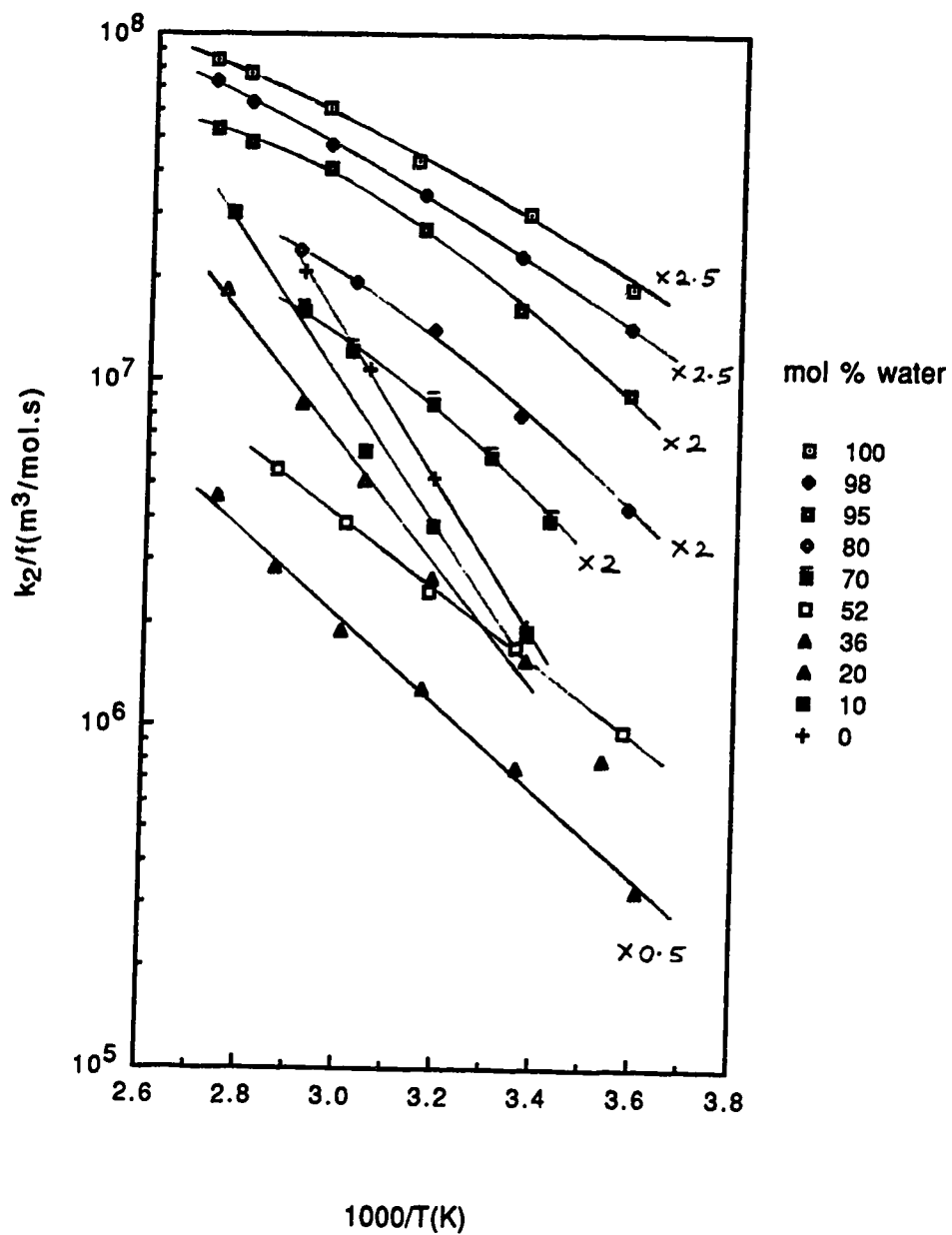
(b) Near 298K.

(c) From Arrhenius plots of k_2/f .

(d) From ref. 106.

Fig. 21

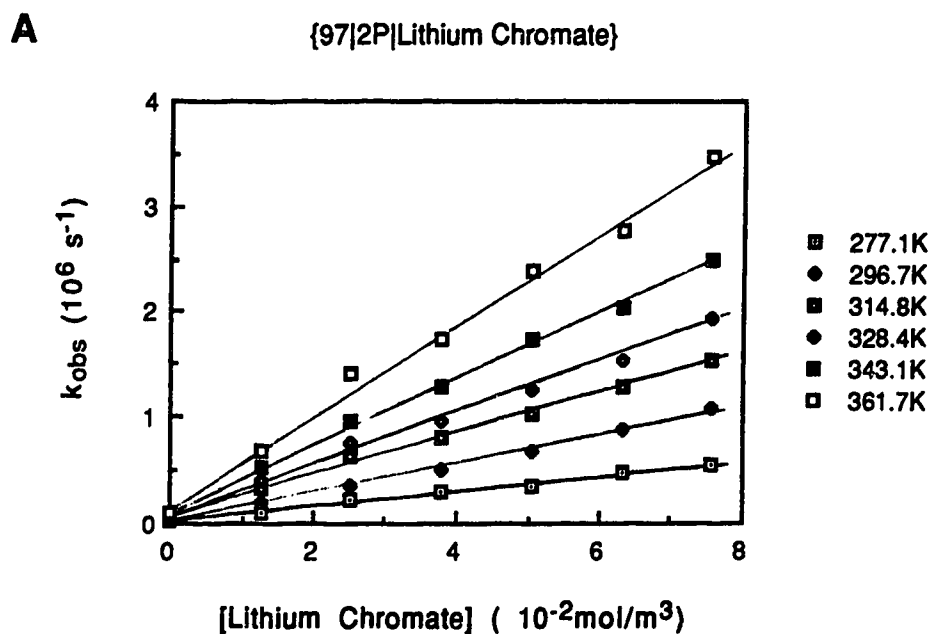
Arrhenius plots for the reaction of solvated electrons with
lithium nitrate in 2-propanol/water mixtures



B. Reaction of Solvated Electrons with Chromate Ions

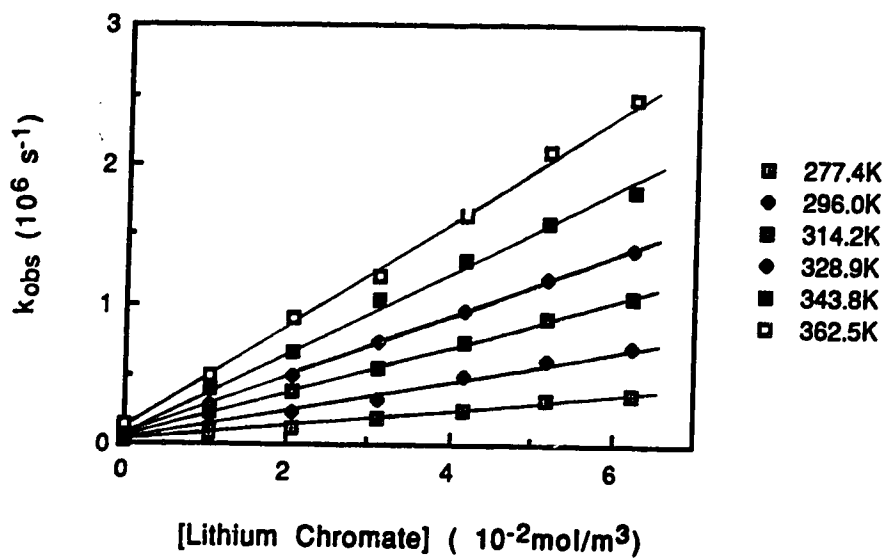
The temperature and concentration dependence of the first-order rate constants for the reaction of solvated electrons with chromate ion are shown in Figure 22 (A-G). The concentration range was 0.09-0.18 mol/m³. Table 15 shows the second-order rate constants, dielectric constants and the coulombic factors *f* at various temperatures in different alcohol/water mixtures. Table 16 shows the rate parameters obtained from the modified Arrhenius plots shown in Figure 23.

Fig. 22 Temperature and concentration dependence of the first-order rate constant for the reaction of solvated electrons with lithium chromate in 2-propanol/water mixtures

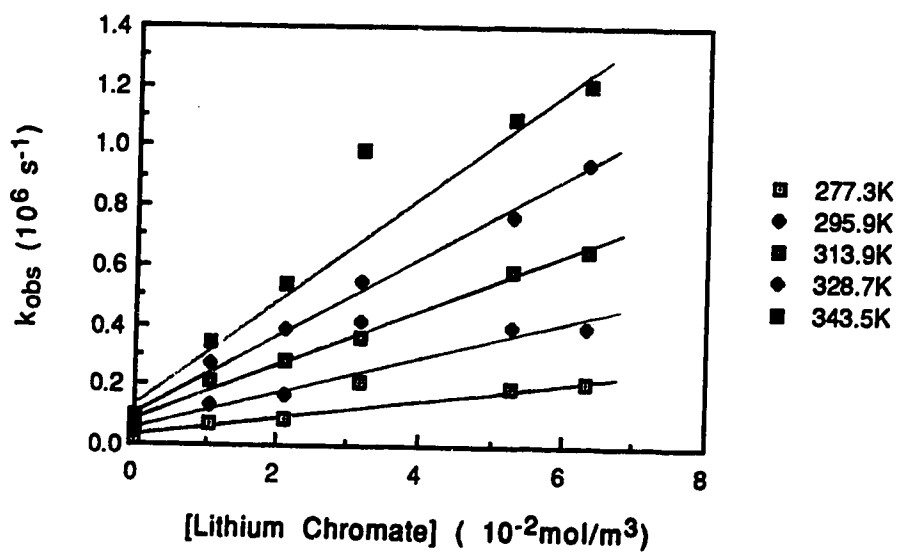


B

{95|2P|Lithium Chromate}

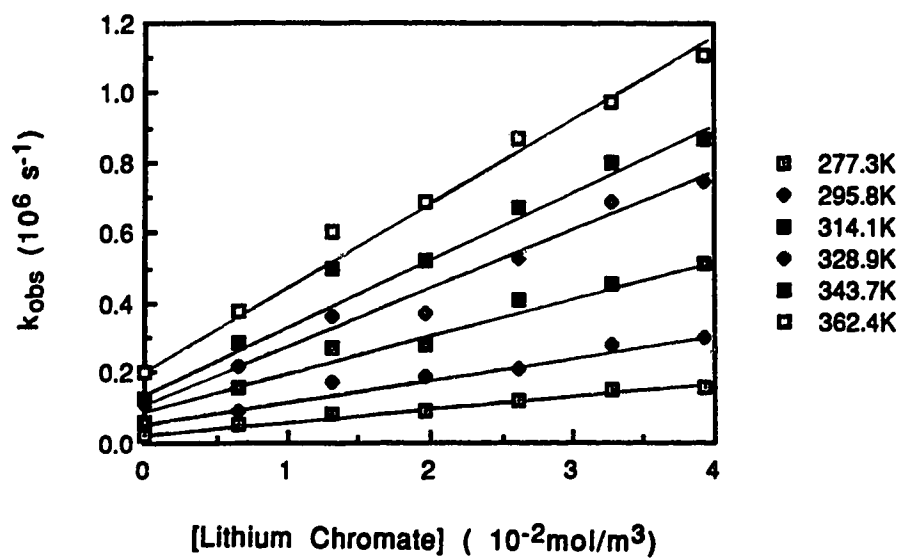
**C**

{81|2P|Lithium Chromate}



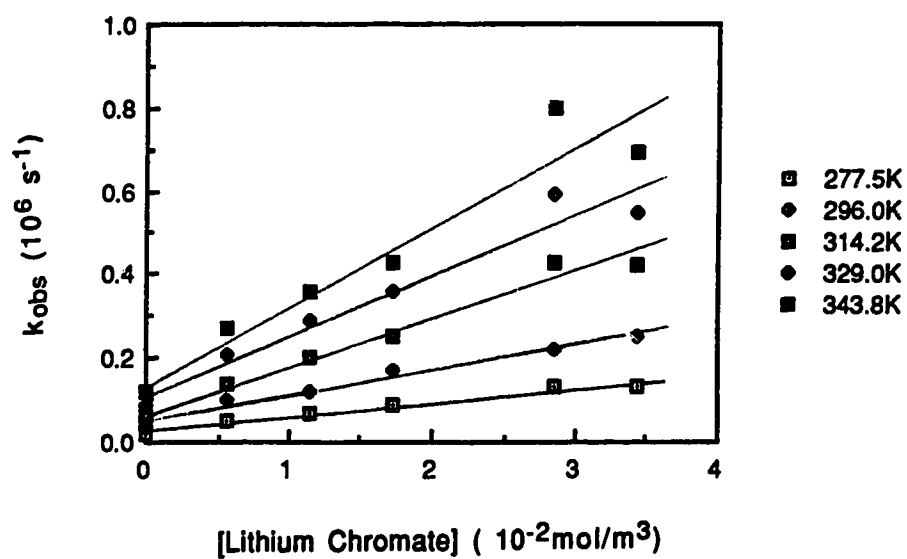
D

{68}2P|Lithium Chromate}



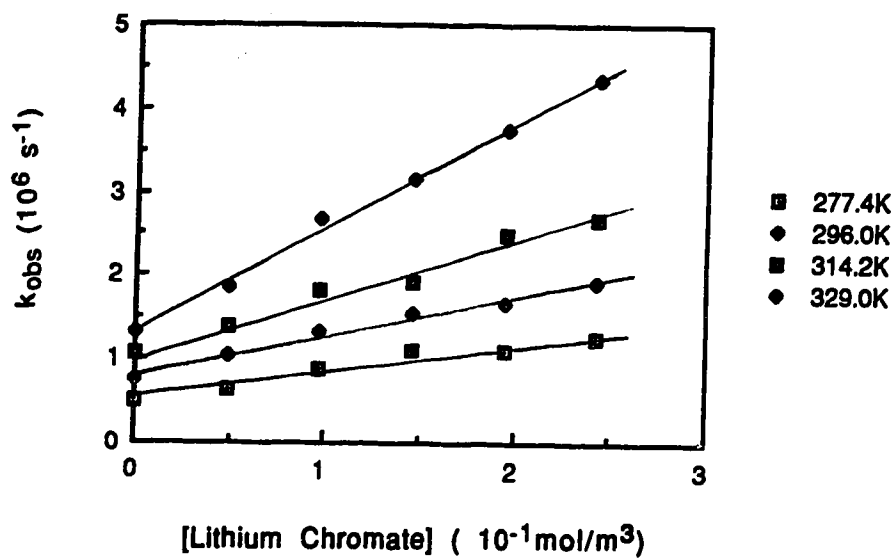
E

{52}2P|Lithium Chromate}



F

{36|2P|Lithium Chromate}



G

{20|2P|Lithium Chromate}

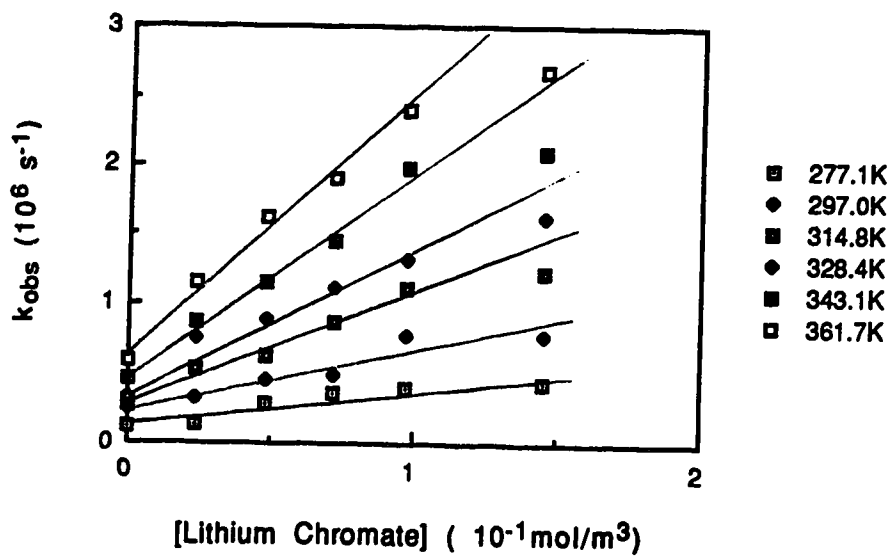


Table 15. Dielectric constants, f values and second-order rate constants for the reaction of solvated electrons with lithium chromate in 2-propanol/water mixtures at various temperatures.

X_w	Temp (K)	ϵ	f	k_2 ($10^7 \text{ m}^3/\text{mol}\cdot\text{s}$)	X_w	Temp (K)	ϵ	f	k_2 ($10^7 \text{ m}^3/\text{mol}\cdot\text{s}$)
1.00	276.1	87.5	0.69	0.93	0.68	277.3	39.2	0.42	0.36
	298.1	78.2	0.69	1.6		295.8	35.0	0.40	0.59
	317.3	71.3	0.68	2.1		314.1	31.5	0.38	1.1
	338.2	64.7	0.67	3.1		328.9	29.0	0.37	1.6
	357.6	58.9	0.66	4.0		343.7	26.5	0.35	1.9
	367.2	55.9	0.65	4.7		362.4	23.7	0.32	2.3
0.97	277.1	78.6	0.67	0.71	0.52	277.5	29.4	0.30	0.31
	296.7	71.8	0.66	1.3		296.0	25.8	0.28	0.59
	314.8	66.0	0.65	2.0		314.2	23.0	0.25	1.0
	328.4	61.4	0.64	2.5		329.0	21.0	0.24	1.5
	343.1	57.0	0.63	3.1		343.8	19.1	0.22	1.8
	361.7	52.0	0.62	4.3					
0.95	277.4	74.8	0.65	0.58	0.36	277.4	24.7	0.23	0.30
	296.0	67.2	0.64	1.1		296.0	21.6	0.21	0.44
	314.2	61.8	0.63	1.7		314.2	19.2	0.19	0.71
	328.9	57.5	0.62	2.2		329.0	17.4	0.17	1.2
	343.8	53.5	0.61	2.9					
	362.5	48.8	0.60	3.7					
0.81	277.3	51.7	0.53	0.31	0.20	277.1	22.8	0.20	0.24
	295.9	46.7	0.52	0.60		297.0	19.8	0.18	0.46
	313.9	42.6	0.50	0.91		314.8	17.5	0.15	0.83
	328.7	39.5	0.49	1.3		328.4	15.8	0.14	1.1
	343.5	36.5	0.48	1.8		343.1	14.2	0.12	1.5
	360.4	33.1	0.46	2.2		361.7	12.6	0.10	2.0

Table 16. Rate parameters for the reaction of solvated electrons with lithium chromate in 2-propanol/water mixtures.

X_w	$\eta^{(a)}$ (10^{-3} Pa·s)	$k_2^{(a)}$ (10^6 m ³ /mol·s)	$k_2/f^{(a)}$ (10^6 m ³ /mol·s)	$E_2^{(b,c)}$ (kJ/mol)	$\log A_2^{(c)}$ (A_2 in m ³ /mol·s)
1.00	0.89	15.5	23	16	10.10
0.97	1.38	13.2	20	19	10.56
0.95	1.80	11.0	17	21	10.89
0.81	3.10	6.6	13	24	11.24
0.68	3.06	7.2	18	25	11.68
0.52	2.72	6.8	24	27	12.07
0.36	2.39	5.2	25	25	11.85
0.22	2.19	4.8	28	30	12.70

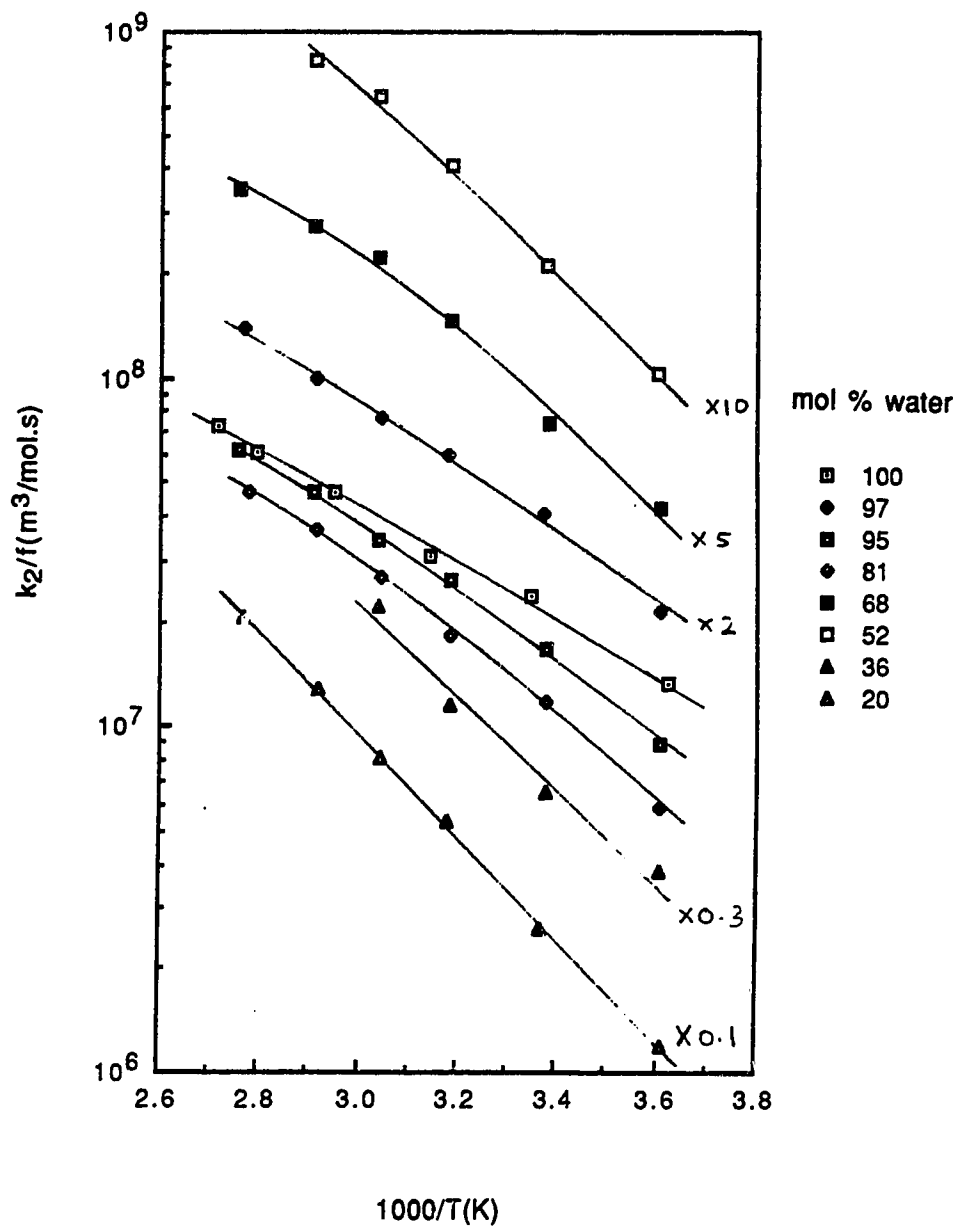
(a) At 298K.

(b) Near 298K.

(c) From Arrhenius plots of k_2/f .

Fig. 23

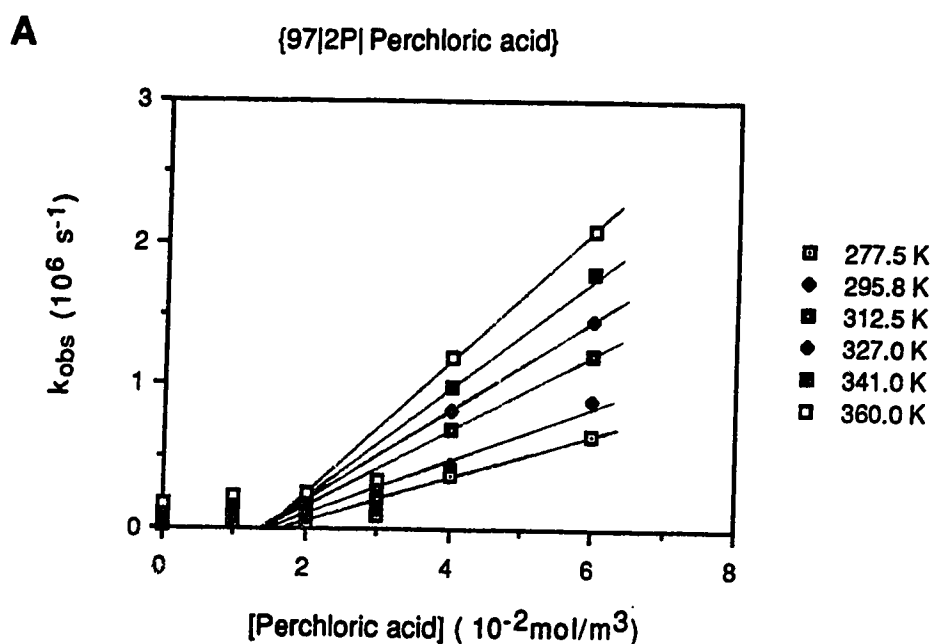
Arrhenius plots for the reaction of solvated electrons with
lithium chromate in 2-propanol/water mixtures

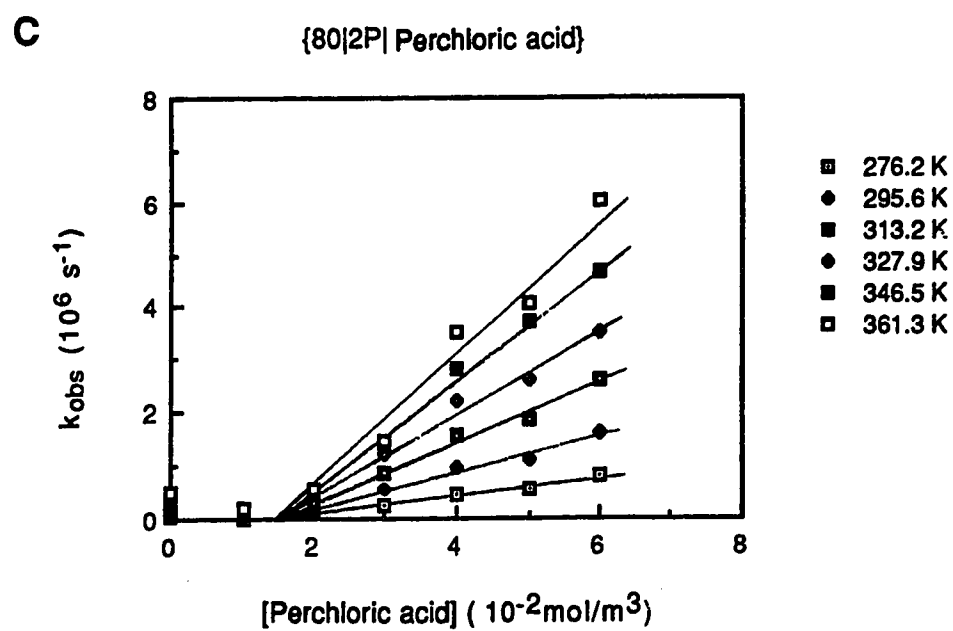
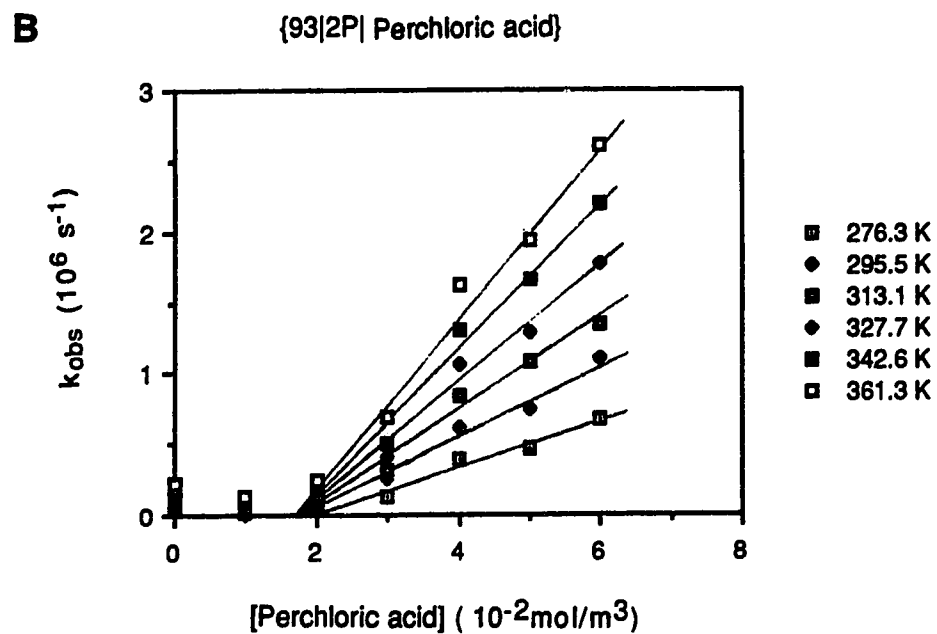


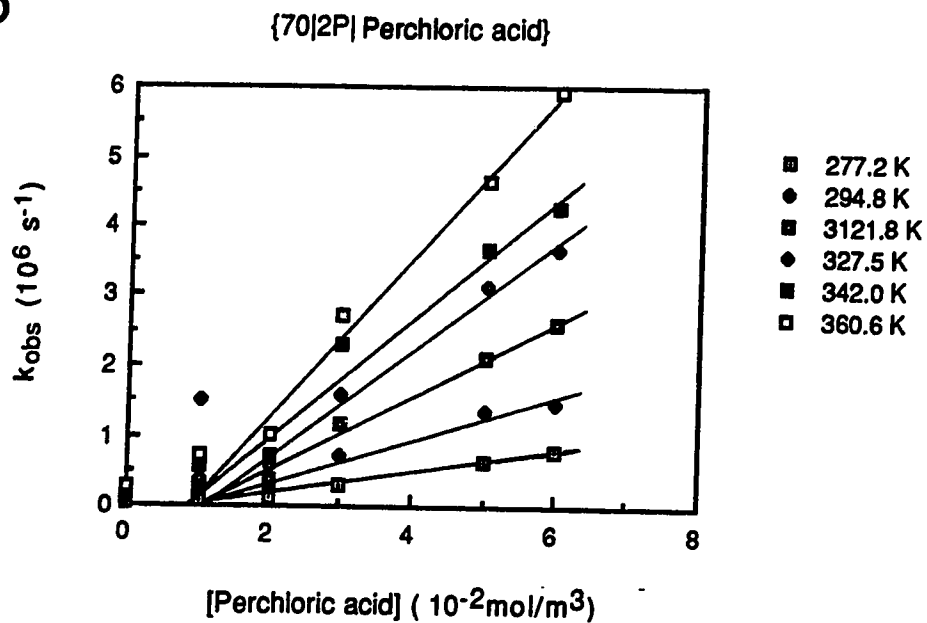
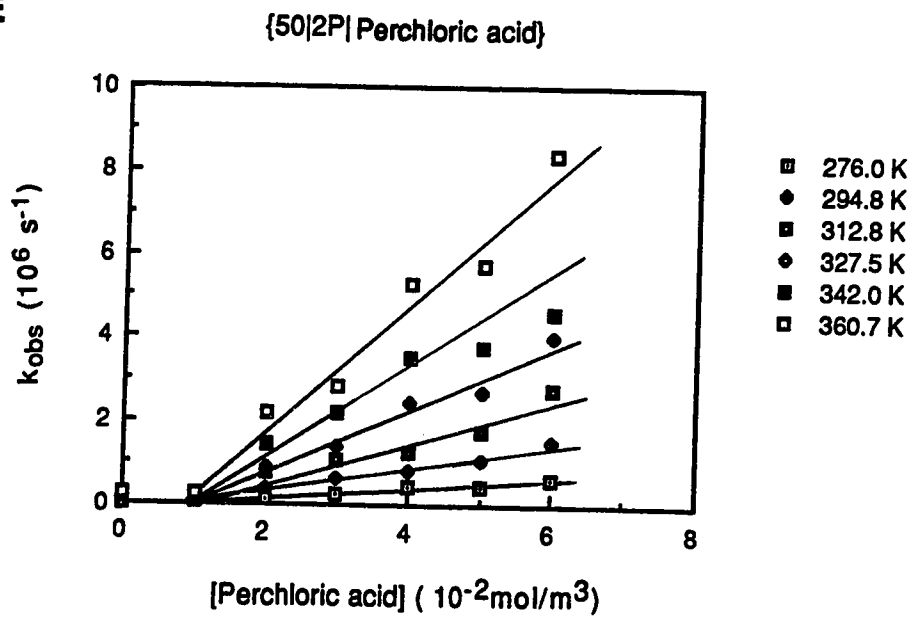
C. Reaction of Solvated Electrons with Hydrogen Ions

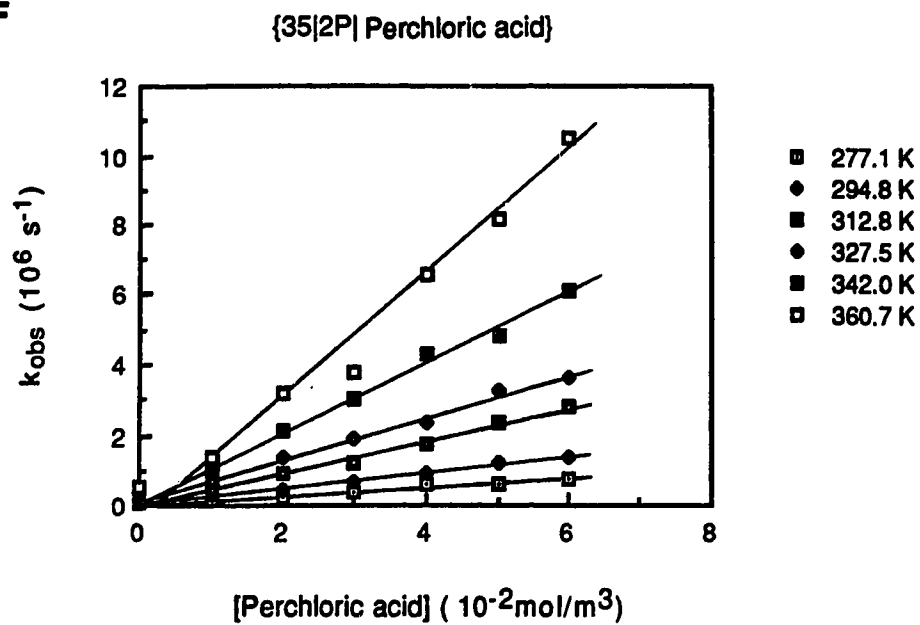
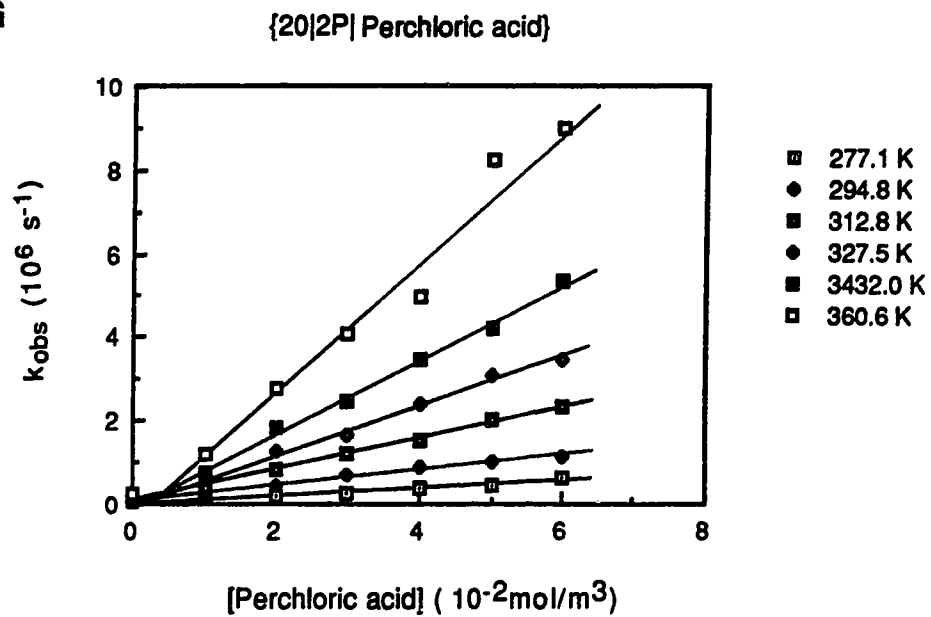
The temperature and concentration dependence of the first-order rate constant for the reaction of solvated electrons with hydrogen ion are shown in Figure 24 (A-I). The concentration range was 0.01-0.06 mol/m³. Table 17 shows the second-order rate constants, dielectric constants and the coulombic factors *f* at various temperatures in different alcohol/water mixtures. Table 18 shows the rate parameters obtained from the modified Arrhenius plots shown in Figure 25.

Fig. 24 Temperature and concentration dependence of the first-order rate constant for the reaction of solvated electrons with perchloric acid in 2-propanol/water mixtures

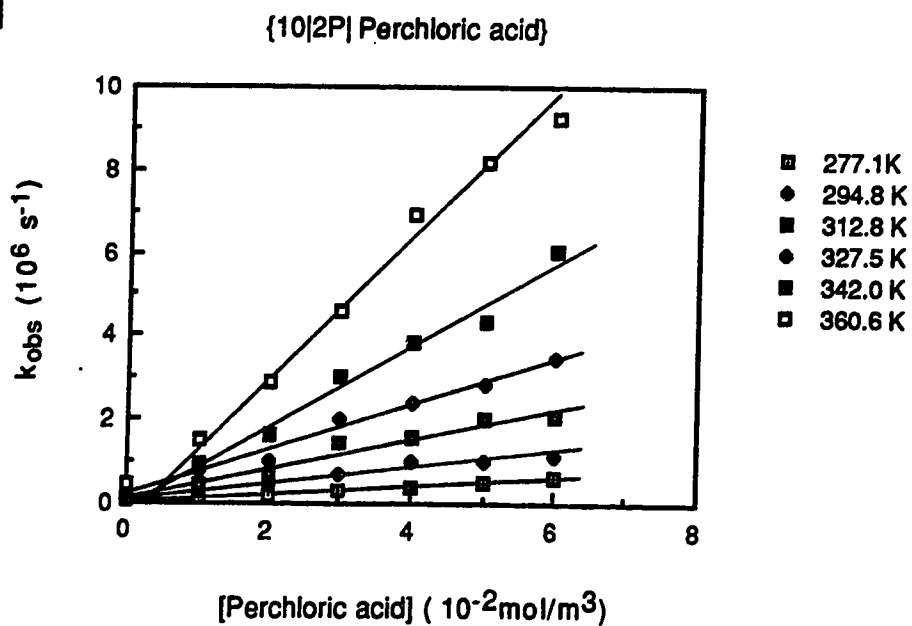




D**E**

F**G**

H



I

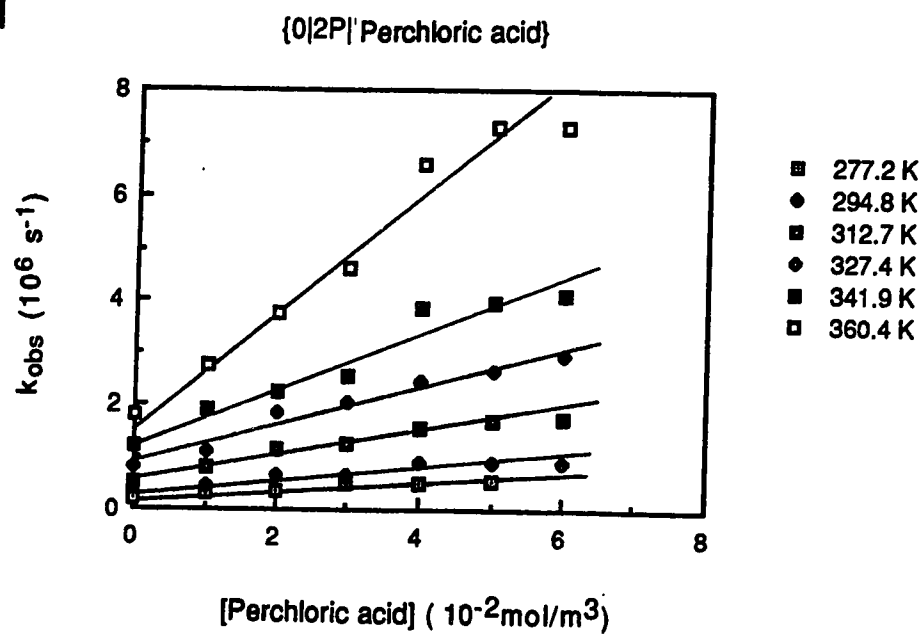


Table 17. Dielectric constants, f values and second-order rate constants for the reaction of solvated electrons with perchloric acid in 2-propanol/water mixtures at various temperatures.

X_w	Temp (K)	ϵ	f	k_2 ($10^7 \text{ m}^3/\text{mol}\cdot\text{s}$)	X_w	Temp (K)	ϵ	f	k_2 ($10^7 \text{ m}^3/\text{mol}\cdot\text{s}$)
1.00	277.5	86.8	1.39	1.8	0.50	276.0	27.4	2.48	1.3
	295.9	79.3	1.40	2.6		294.8	25.2	2.51	2.7
	314.2	72.5	1.41	3.2		312.8	22.6	2.61	5.0
	329.0	67.7	1.42	4.1		327.5	20.7	2.69	7.5
	343.9	63.0	1.43	4.6		342.0	19.0	2.78	10
					360.7	16.7	2.96	15	
0.97	277.5	78.4	1.43	1.5	0.35	277.1	24.6	2.68	1.2
	295.8	71.9	1.44	2.0		294.8	21.8	2.81	2.0
	312.5	66.5	1.45	2.7		312.8	19.4	2.94	4.6
	327.0	62.0	1.47	3.2		327.5	18.5	2.94	6.0
	341.0	57.8	1.48	4.0		342.0	16.0	3.2	10
	360.0	52.5	1.51	4.6		360.7	14.0	3.4	18
0.93	276.3	71.0	1.48	1.8	0.20	277.1	23.0	2.82	1.0
	295.5	64.7	1.50	2.6		294.8	21.8	2.81	2.0
	313.1	59.5	1.51	3.2		312.8	19.4	2.94	3.8
	327.7	55.5	1.53	4.2		327.5	16.0	3.3	6.0
	342.6	51.5	1.55	5.3		342.0	14.5	3.5	9.0
	361.3	46.8	1.57	5.9		360.6	12.7	3.7	13
0.80	277.1	50.7	1.71	1.7	0.10	277.1	22.0	2.92	1.0
	296.5	45.6	1.74	3.2		29.8	20.0	3.0	2.0
	314.6	41.5	1.77	5.4		312.8	16.8	3.3	4.1
	329.2	38.5	1.80	7.1		327.5	15.2	3.5	5.6
	342.9	36.0	1.82	9.3		342.0	13.7	3.7	10
	361.5	32.5	1.87	13		360.6	12.0	3.9	17
0.70	277.2	40.7	1.92	1.7	0.00	276.2	21.3	3.0	0.88
	294.8	36.6	1.97	3.5		296.0	18.4	3.2	1.6
	312.8	33.0	2.02	5.6		314.0	16.0	3.4	3.2
	327.5	30.5	2.06	8.3		329.0	14.5	3.6	4.7
	342.0	28.0	2.11	10		343.0	13.0	3.8	8.2
	360.6	25.0	2.20	12		362.0	11.5	4.1	14

Table 18. Rate parameters for the reaction of solvated electrons with perchloric acid in 2-propanol/water mixtures.

X_w	$\eta^{(a)}$ (10^{-3} Pa·s)	$k_2^{(a)}$ (10^7 m ³ /mol·s)	$k_2/f^{(a)}$ (10^7 m ³ /mol·s)	$E_2^{(b,c)}$ (kJ/mol)	$\log A_2^{(c)}$ (A_2 in m ³ /mol·s)
1.00	0.89	2.6	1.9	12	9.42
0.97	1.38	2.1	1.6	13	9.52
0.93	2.02	2.6	1.7	13	9.43
0.80	3.03	3.4	1.9	20	10.86
0.70	3.09	3.7	1.9	21	10.90
0.50	2.68	3.1	1.2	23	11.21
0.35	2.38	2.6	0.92	25	11.32
0.20	2.20	2.3	0.76	26	11.39
0.10	2.13	2.3	0.72	25	11.24
0.00	2.08	1.9	0.58	24	10.91

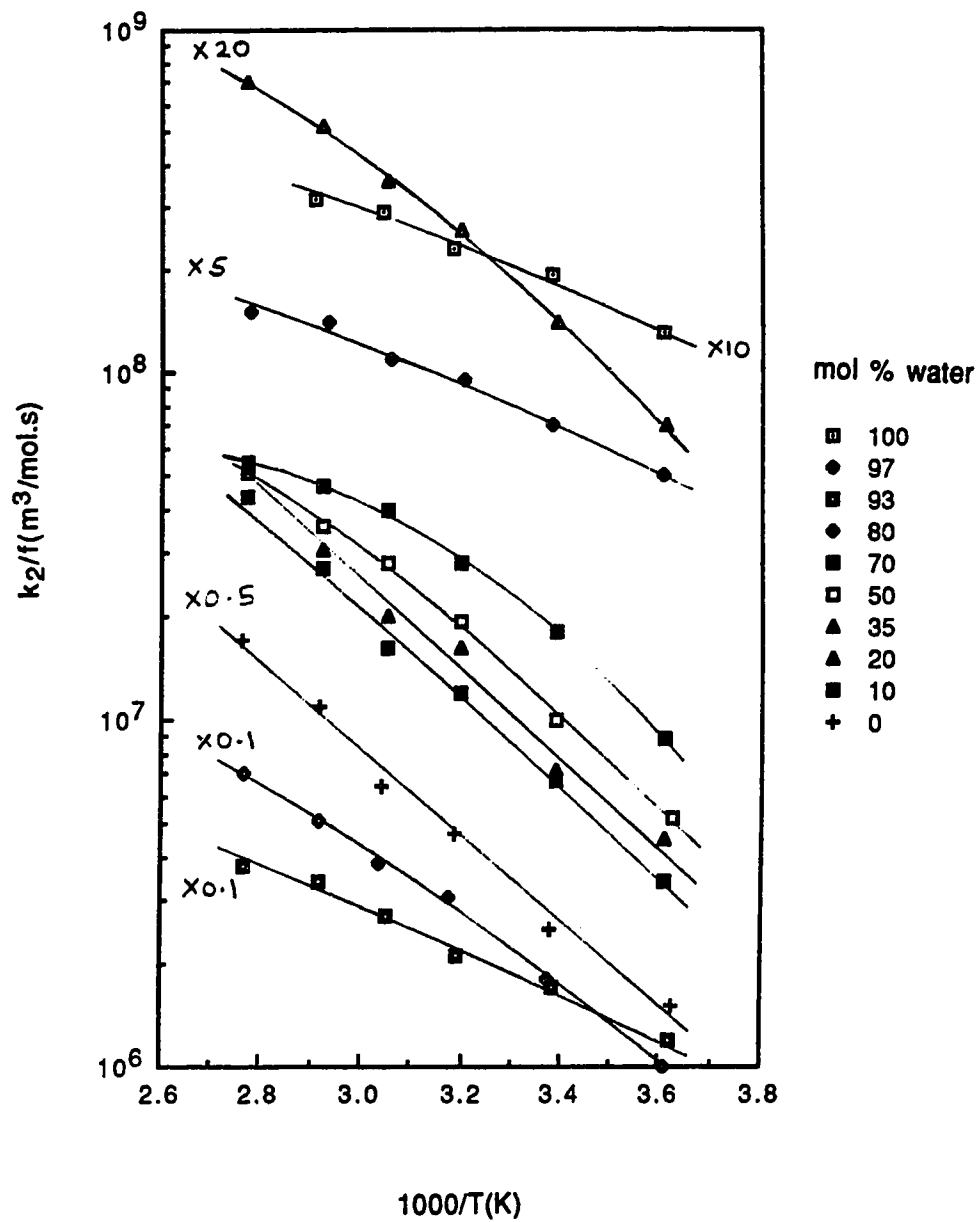
(a) At 298K.

(b) Near 298K.

(c) From Arrhenius plots of k_2/f .

Fig. 25

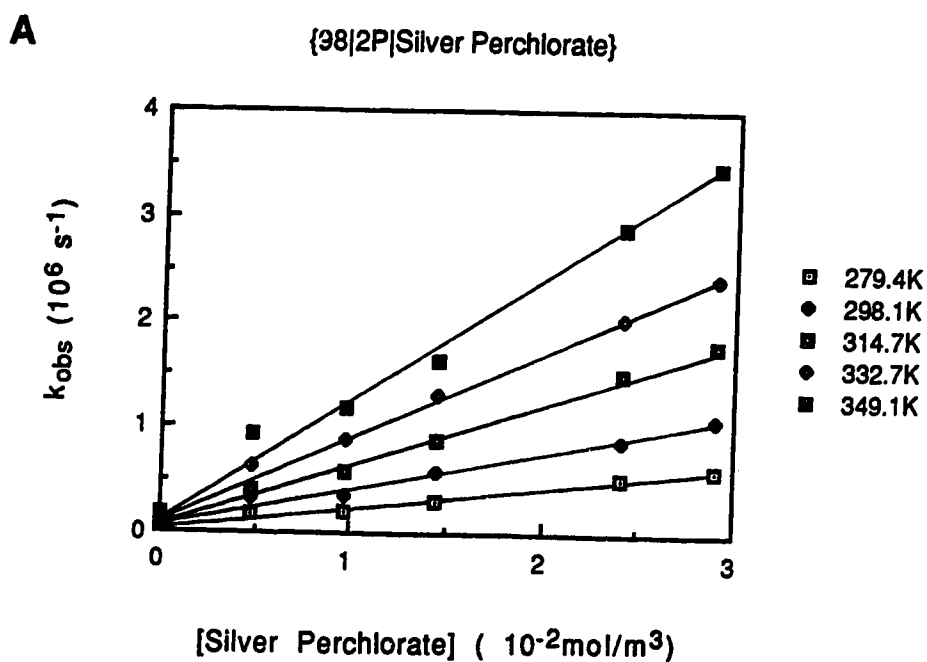
Arrhenius plots for the reaction of solvated electrons with
perchloric acid in 2-propanol/water mixtures

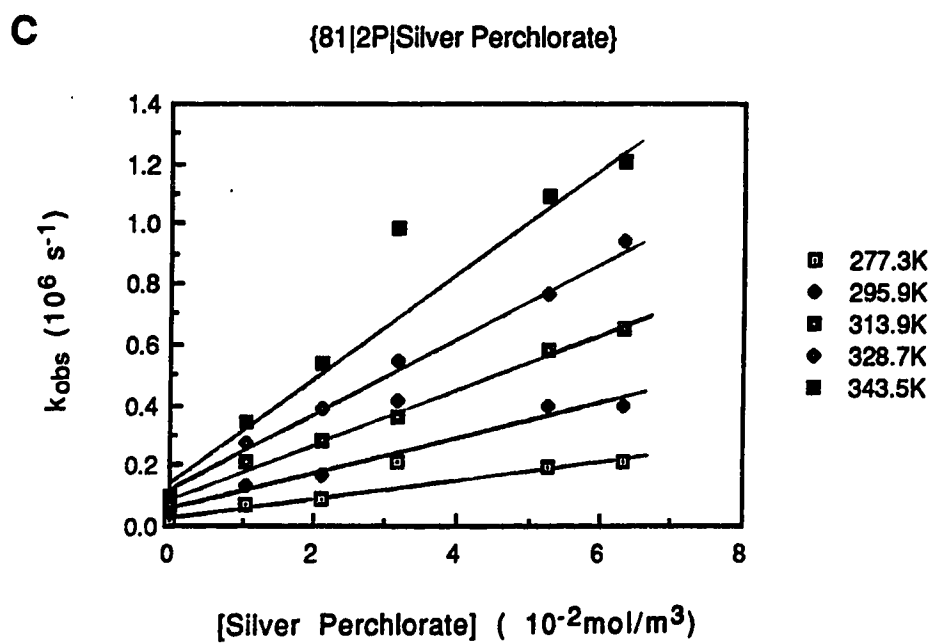
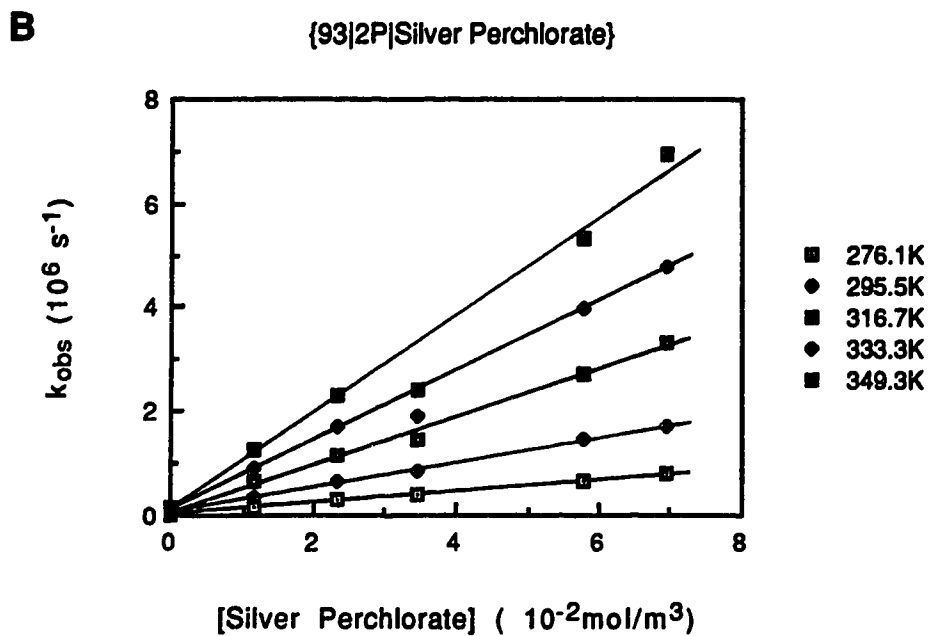


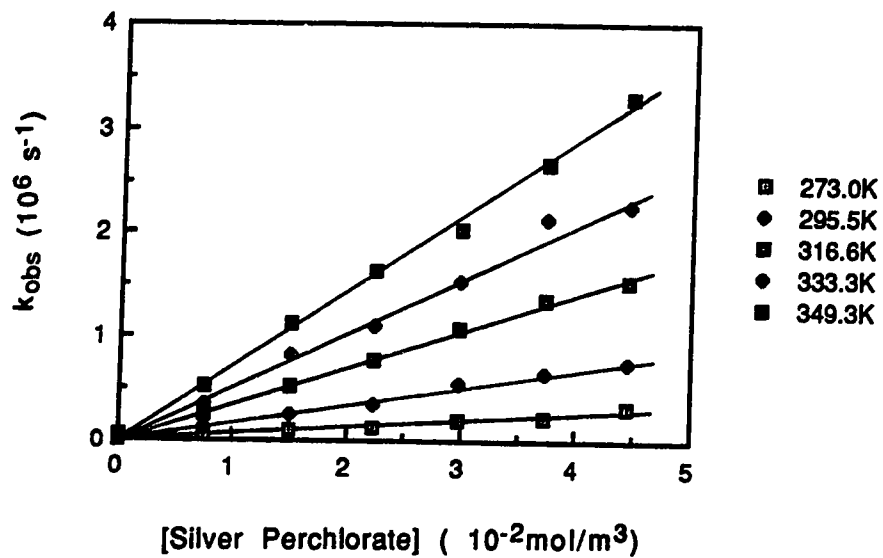
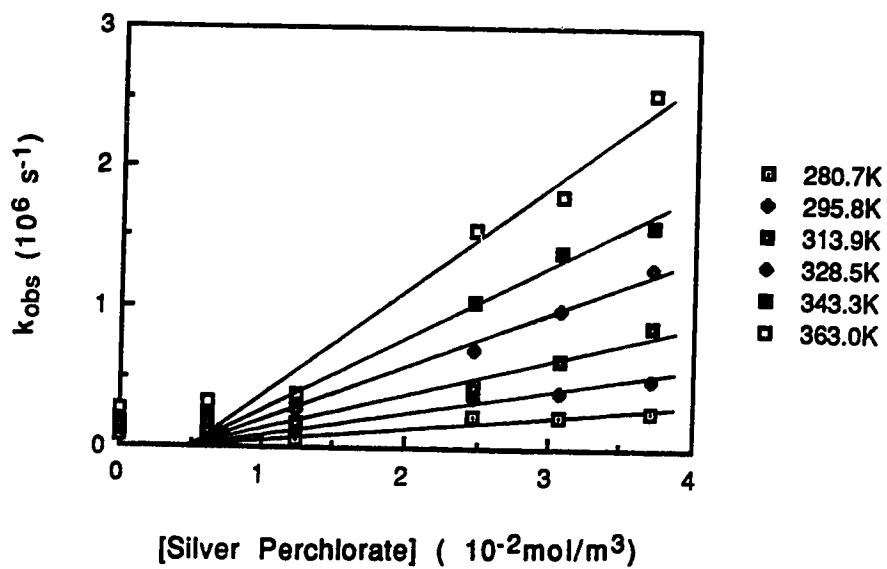
D. Reaction of Solvated Electrons with Silver Ions

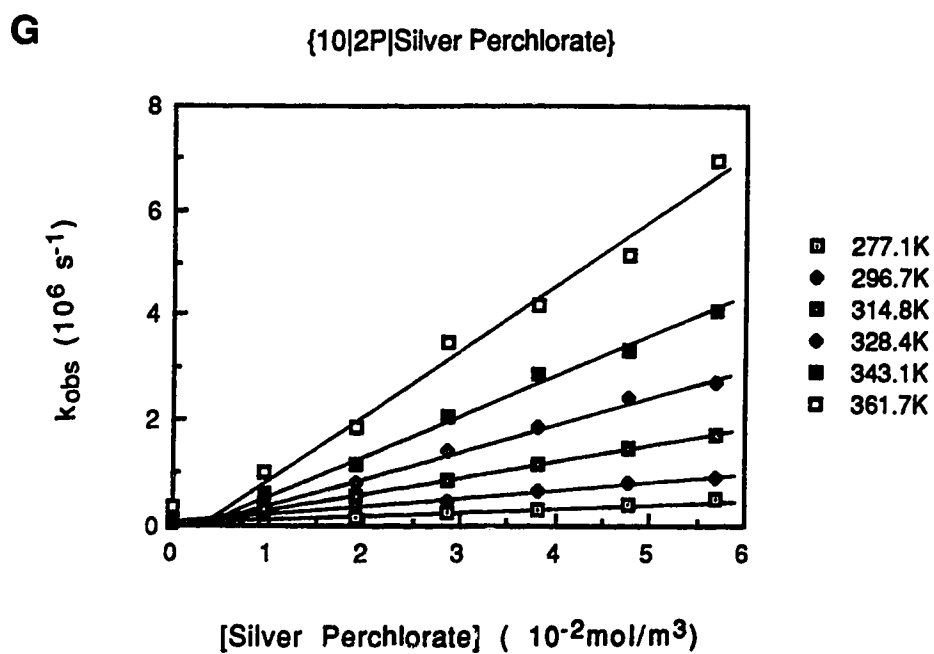
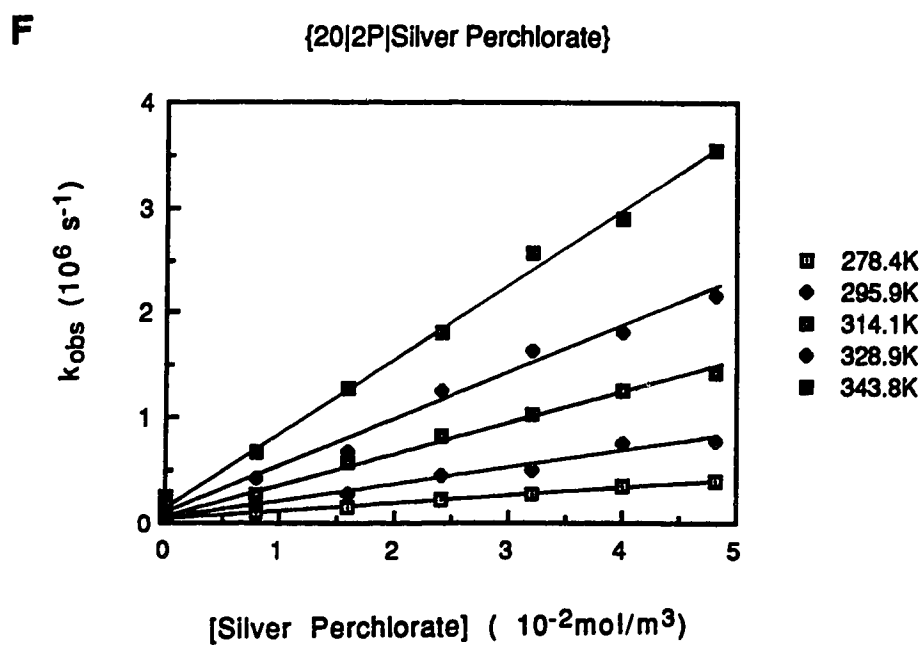
The temperature and concentration dependence of the first-order rate constant for the reaction of solvated electrons with silver ion are shown in Figure 26 (A-H). The concentration range was 5-70 mmol/m³. Table 19 shows the second-order rate constants, dielectric constants and the coulombic factor *f* at various temperatures in different alcohol/water mixtures. Table 20 shows the rate parameters obtained from the modified Arrhenius plots shown in Figure 27.

Fig. 26 Temperature and concentration dependence of the first-order rate constant for the reaction of solvated electrons with silver perchlorate in 2-propanol/water mixtures





D**{71|2P|Silver Perchlorate}****E****{51|2P|Silver Perchlorate}**



H

{0}2P|Silver Perchlorate

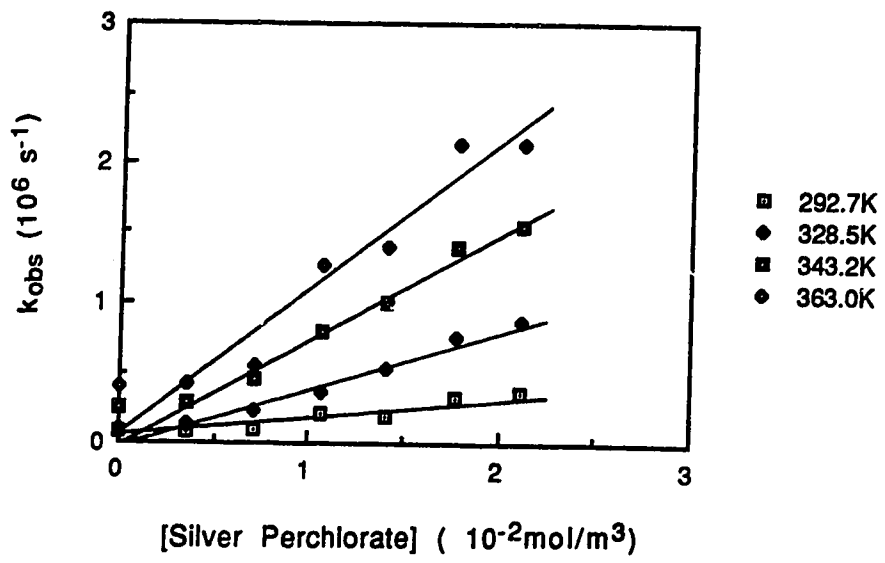


Table 19. Dielectric constants, f values and second-order rate constants for the reaction of solvated electrons with silver perchlorate in 2-propanol/water mixtures at various temperatures.

X_w	Temp (K)	ϵ	f	k_2 ($10^7 \text{ m}^3/\text{mol}\cdot\text{s}$)	X_w	Temp (K)	ϵ	f	k_2 ($10^7 \text{ m}^3/\text{mol}\cdot\text{s}$)
1.00	279.6	86.6	1.38	2.4	0.52	280.7	28.6	2.38	0.83
	297.5	78.7	1.40	4.2		295.8	26.0	2.45	1.5
	319.0	71.3	1.41	6.7		313.9	23.0	2.57	2.4
	338.5	64.6	1.43	10		328.5	21.0	2.66	3.6
	358.8	59.0	1.45	15		343.3	19.4	2.73	4.9
	367.5	56.0	1.46	18		363.3	17.0	2.90	7.2
0.98	279.4	79.5	1.42	2.0	0.20	278.4	22.5	2.86	0.79
	298.1	73.0	1.43	3.4		295.9	19.6	3.0	1.8
	314.7	67.5	1.44	5.7		314.1	17.4	3.2	2.9
	332.7	62.0	1.46	7.9		328.9	15.6	3.4	4.4
	349.1	57.4	1.47	11		343.8	13.5	3.7	6.9
0.93	276.1	71.0	1.49	1.1	0.10	277.1	22.0	2.93	0.79
	295.5	64.6	1.50	2.4		296.7	18.9	3.1	1.7
	316.7	59.0	1.51	4.6		314.8	16.5	3.3	3.2
	333.3	54.0	1.53	6.7		328.4	15.0	3.5	5.0
	349.3	49.8	1.56	9.4		343.1	13.7	3.7	7.7
						361.7	12.0	3.9	12
0.81	295.5	46.8	1.72	1.8	0.00	292.7	18.8	3.2	1.5
	316.5	42.0	1.76	3.6		328.5	14.5	3.6	4.2
	333.3	38.6	1.78	5.4		343.2	13.0	3.8	7.1
	349.3	35.5	1.82	7.1		363.0	11.5	4.1	10
0.71	273.0	43.0	1.87	0.67					
	295.5	37.5	1.94	1.7					
	316.6	32.5	2.02	3.5					
	333.3	30.0	2.06	5.1					
	349.3	27.5	2.11	7.2					

Table 20. Rate parameters for the reaction of solvated electrons with silver perchlorate in 2-propanol/water mixtures.

X_w	$\eta^{(a)}$ (10^{-3} Pa·s)	$k_2^{(a)}$ (10^7 m ³ /mol·s)	$k_2/f^{(a)}$ (10^7 m ³ /mol·s)	$E_2^{(b,c)}$ (kJ/mol)	$\log A_2^{(c)}$ (A_2 in m ³ /mol·s)
1.00	0.89	4.2	3.0	19	10.83
0.98	1.20	3.5	2.4	20	10.85
0.93	2.02	2.6	1.7	22	11.04
0.81	3.02	1.9	1.1	23	11.16
0.71	3.10	1.8	0.92	24	11.19
0.51	2.72	1.6	0.64	22	10.58
0.20	2.20	1.7	0.56	22	10.70
0.10	2.13	1.8	0.56	24	11.04
0.00	2.08	1.7	0.52	24	10.98

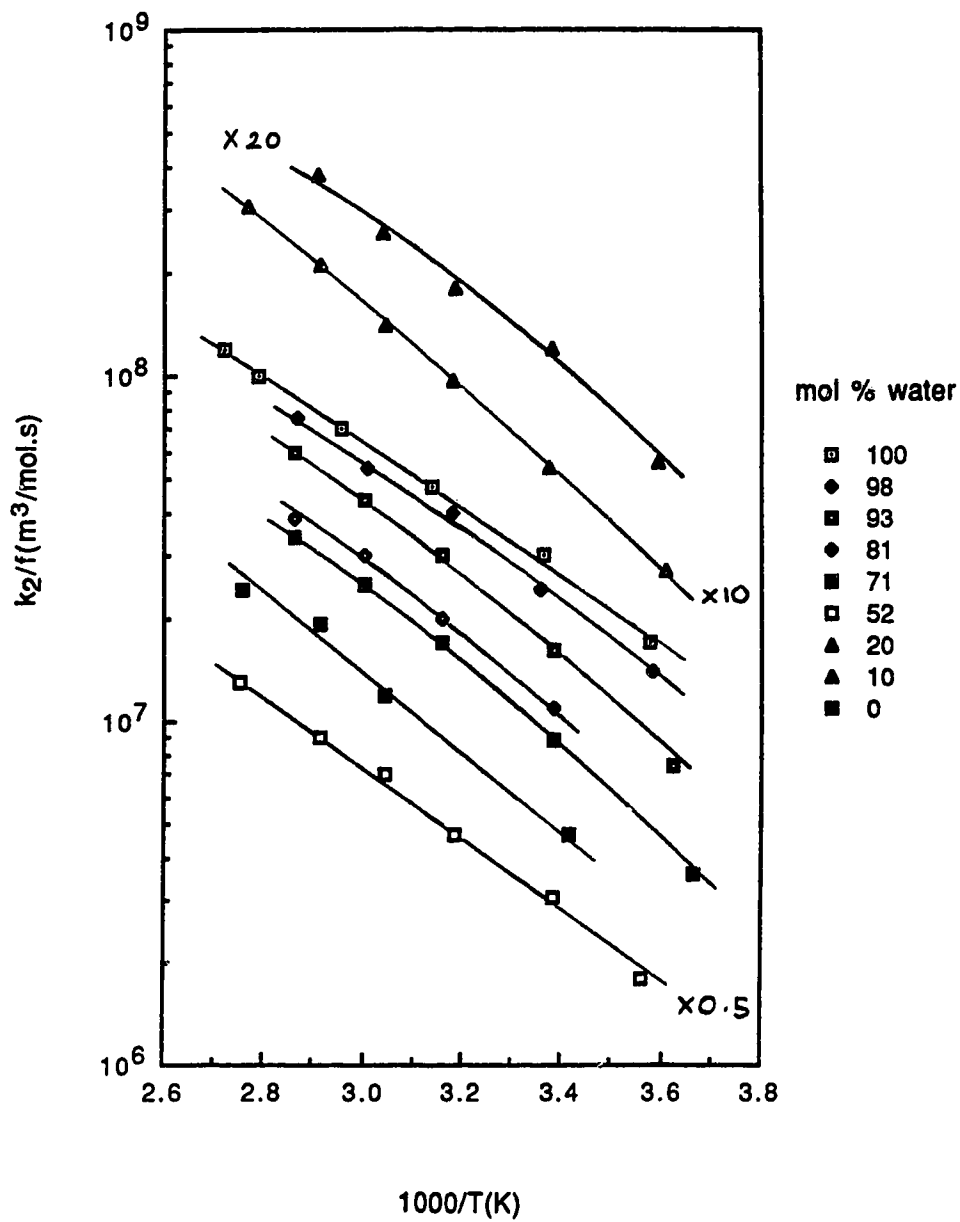
(a) At 298K.

(b) Near 298K.

(c) From Arrhenius plots of k_2/f .

Fig. 27

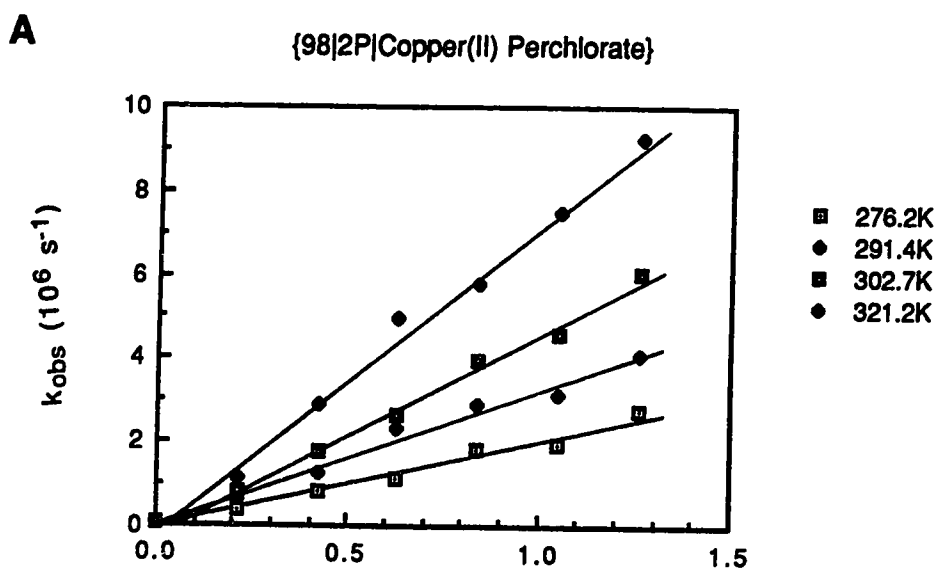
Arrhenius plots for the reaction of solvated electrons with silver perchlorate in 2-propanol/water mixtures

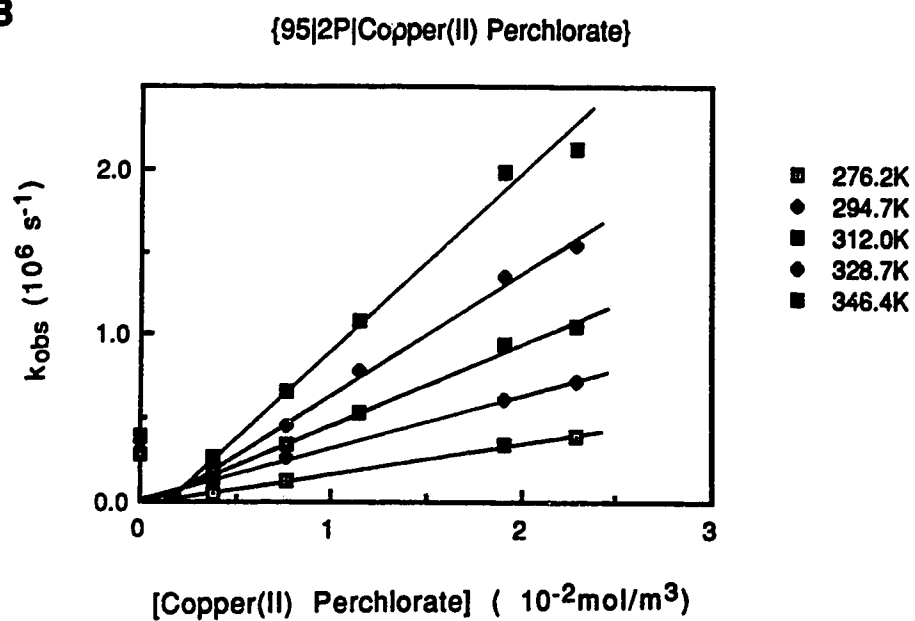
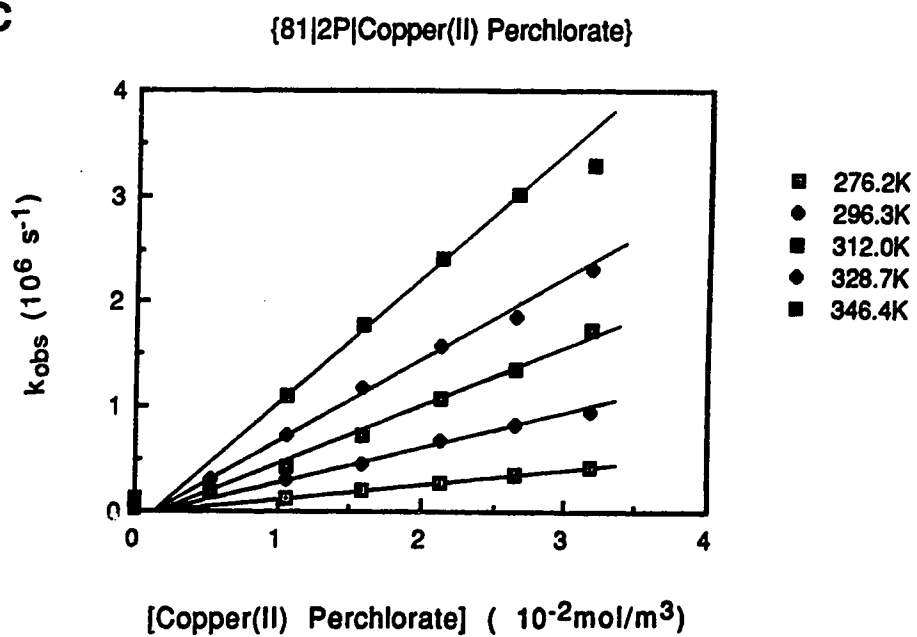


E. Reaction of Solvated Electrons with Copper(II) Ions

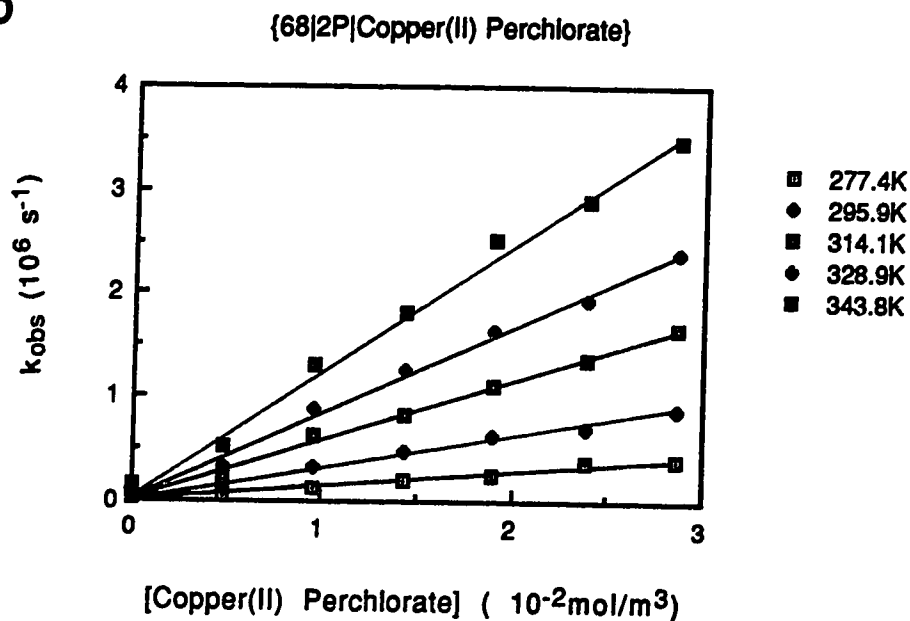
The temperature and concentration dependence of the first-order rate constant for the reaction of solvated electrons with copper(II) ion are shown in Figure 28 (A-I). The concentration range was 4-125 mmol/m³. Table 21 shows the second-order rate constants, dielectric constants and the coulombic factor *f* at various temperatures in different alcohol/water mixtures. Table 22 shows the rate parameters obtained from the modified Arrhenius plots shown in Figure 29.

Fig. 28 (A-I) Temperature and concentration dependence of the first-order rate constant for the reaction of solvated electrons with copper(II) perchlorate in 2-propanol/water mixtures

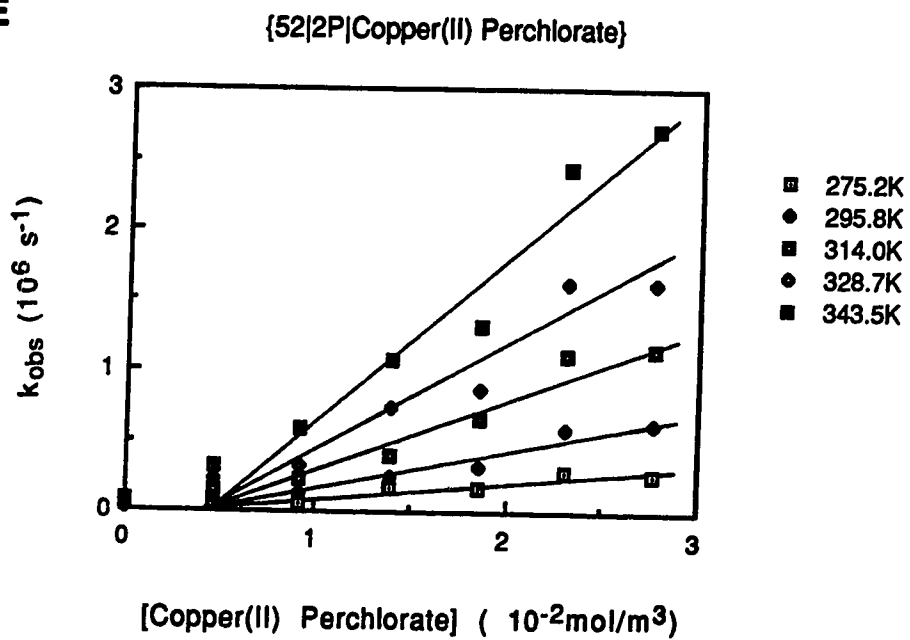


B**C**

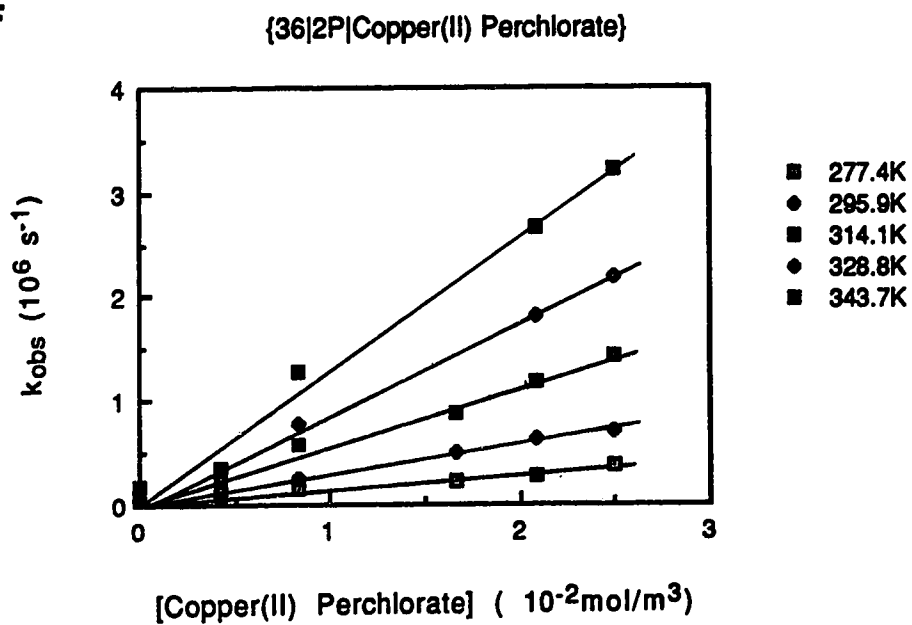
D



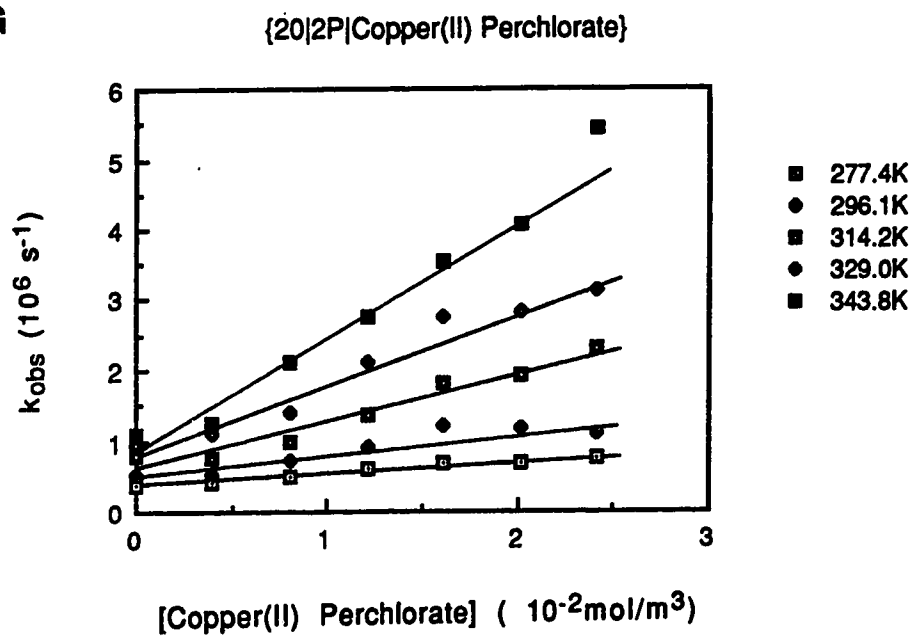
E



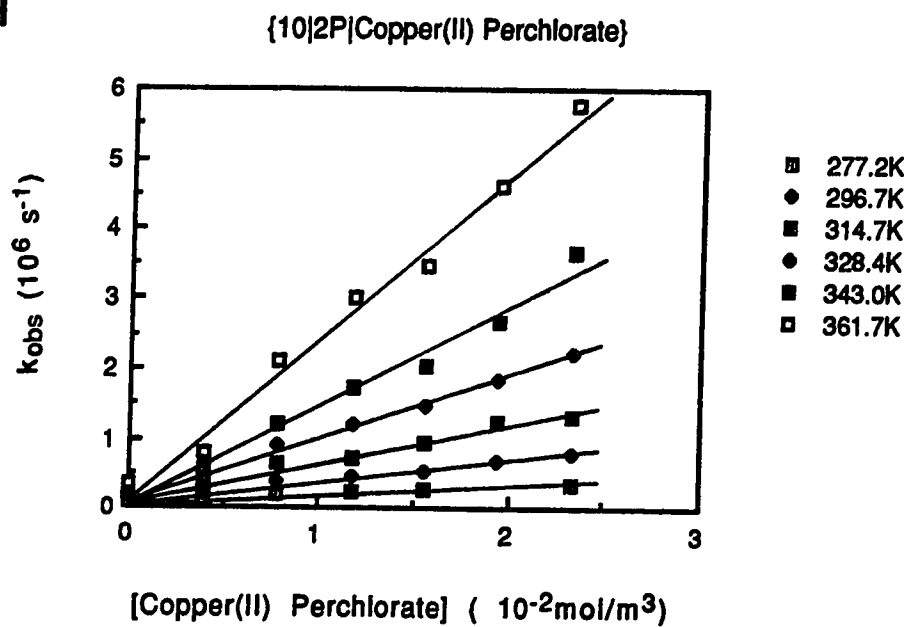
F



G



H



I

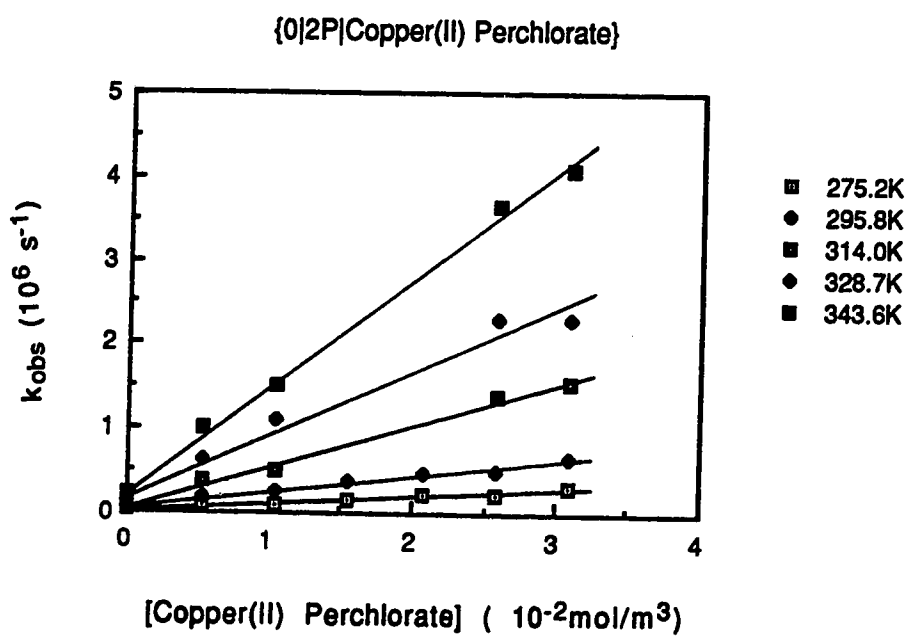


Table 21. Dielectric constants, f values and second-order rate constants for the reaction of solvated electrons with copper(II) perchlorate in 2-propanol/water mixtures at various temperatures.

X_w	Temp (K)	ϵ	f	k_2 ($10^7 \text{ m}^3/\text{mol}\cdot\text{s}$)	X_w	Temp (K)	ϵ	f	k_2 ($10^7 \text{ m}^3/\text{mol}\cdot\text{s}$)
1.00	280.0	85.7	3.0	2.5	0.52	275.2	29.7	8.2	1.2
	298.6	77.8	3.0	4.0		295.8	26.0	8.7	2.6
	315.3	72.2	3.1	5.6		314.0	23.0	9.2	5.0
	333.0	66.5	3.2	8.2		328.7	21.0	9.7	7.3
	364.5	57.0	3.3	13		343.5	19.4	10.0	11
0.98	276.2	80.8	3.1	2.1	0.36	277.4	24.7	9.7	1.5
	291.4	75.0	3.2	3.4		295.9	21.6	10.4	3.0
	302.7	71.5	3.2	4.8		314.1	19.2	11.1	5.6
	321.2	65.4	3.3	7.4		328.8	17.4	11.7	8.7
						343.7	15.8	12.3	13
0.95	276.2	74.0	3.4	1.9	0.20	277.4	21.9	11.0	1.6
	294.7	67.7	3.5	3.2		296.1	19.8	11.4	2.8
	312.0	61.0	3.6	4.8		314.2	17.4	12.2	5.9
	328.7	57.5	3.6	7.6		329.0	15.8	12.8	9.5
	346.4	52.9	3.7	11		343.8	14.4	13.5	15
0.81	276.2	52.0	4.7	1.5	0.10	277.2	22.0	10.9	1.1
	296.3	46.6	4.9	3.4		296.7	18.9	11.9	2.9
	312.0	43.0	5.0	5.5		314.7	16.5	12.9	5.6
	328.7	39.5	5.2	8.2		328.4	15.0	13.6	8.7
	346.4	36.0	5.4	13		343.0	13.7	14.2	13
					361.7	12.0	15.4	23	
0.68	277.4	39.0	6.2	1.5	0.00	275.2	21.5	11.3	0.95
	295.9	35.0	6.5	3.2		295.8	18.4	12.3	2.0
	314.1	31.5	6.8	5.8		314.0	16.0	13.3	5.0
	328.9	29.0	7.0	8.3		328.7	14.5	14.0	7.5
	343.8	26.5	7.3	12		343.6	13.0	14.9	13

Table 22. Rate parameters for the reaction of solvated electrons with copper(II) perchlorate in 2-propanol/water mixtures.

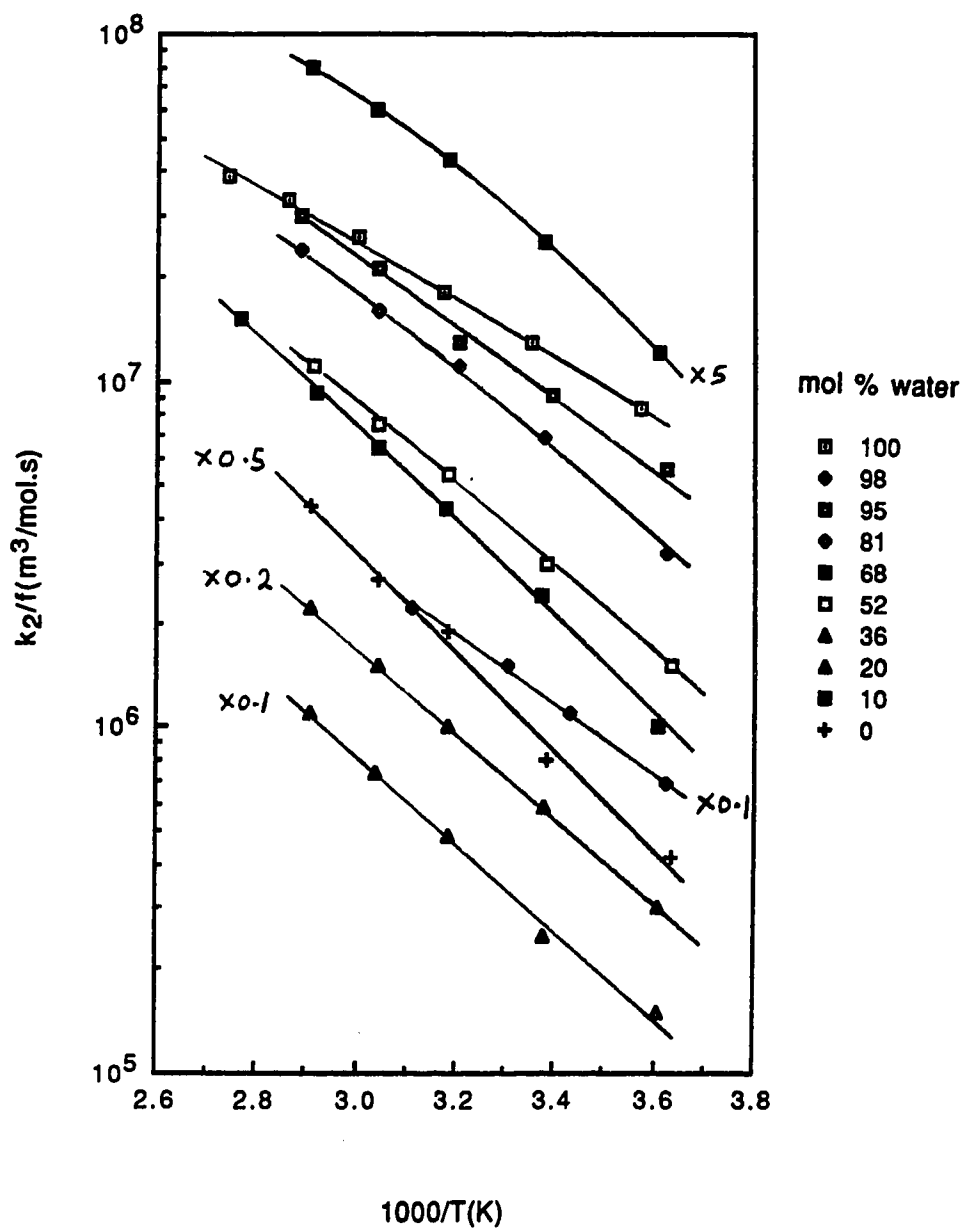
X_w	$\eta^{(a)}$ (10^{-3} Pa·s)	$k_2^{(a)}$ (10^7 m ³ /mol·s)	$k_2/f^{(b)}$ (10^7 m ³ /mol·s)	$E_2^{(b,c)}$ (kJ/mol)	$\log A_2^{(c)}$ (A_2 in m ³ /mol·s)
1.00	0.89	3.9	1.3	18	10.20
0.98	1.20	4.1	1.3	20	10.55
0.95	1.78	3.5	1.0	21	10.64
0.81	3.02	3.5	0.71	23	10.85
0.68	3.07	2.9	0.44	25	11.02
0.52	2.70	2.9	0.33	23	10.49
0.36	2.40	3.3	0.32	24	10.72
0.20	2.20	3.4	0.30	25	10.83
0.10	2.13	2.9	0.24	27	11.05
0.00	2.08	2.5	0.20	29	11.29

(a) At 298K.

(b) Near 298K.

(c) From Arrhenius plots of k_2/f .

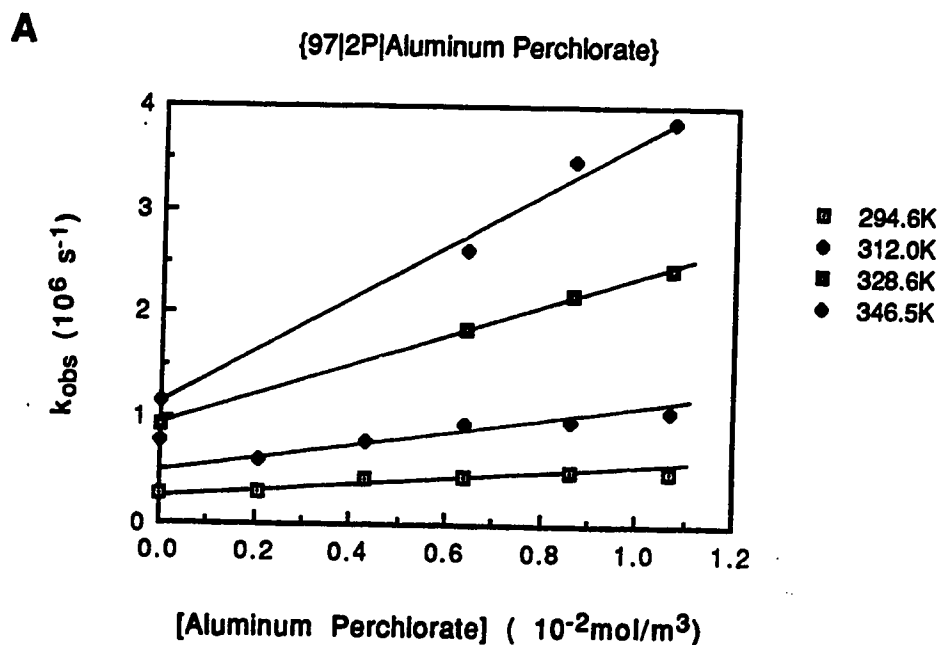
Fig. 29 Arrhenius plots for the reaction of solvated electrons with copper(II) perchlorate in 2-propanol/water mixtures



F. Reaction of Solvated Electrons with Aluminum Ions

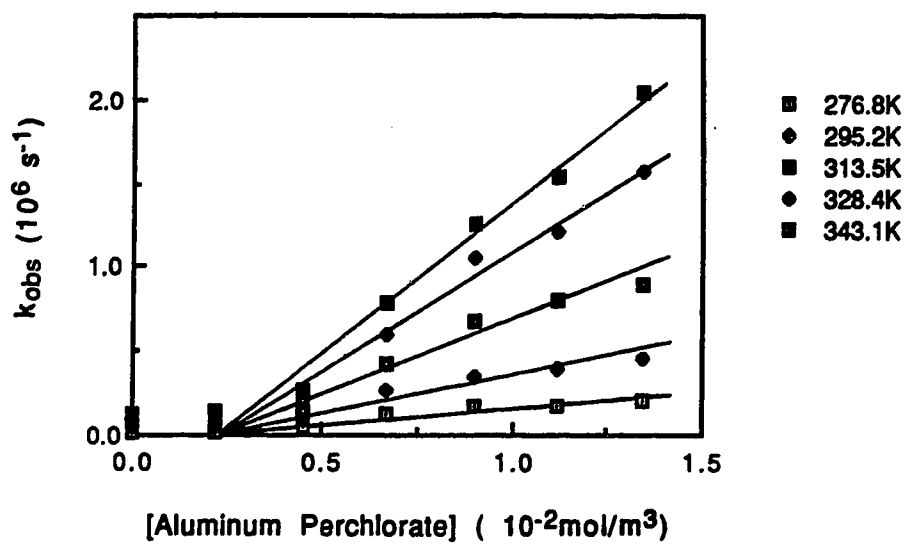
The temperature and concentration dependence of the first-order rate constant for the reaction of solvated electrons with aluminum ion are shown in Figure 30 (A-I). The concentration range was 2-34 mmol/m³. Table 23 shows the second-order rate constants, dielectric constants and the coulombic factor f at various temperatures in different alcohol/water mixtures. Table 24 shows the rate parameters obtained from the modified Arrhenius plots shown in Figure 31.

Fig. 30 Temperature and concentration dependence of the first-order rate constant for the reaction of solvated electrons with aluminum perchlorate in 2-propanol/water mixtures

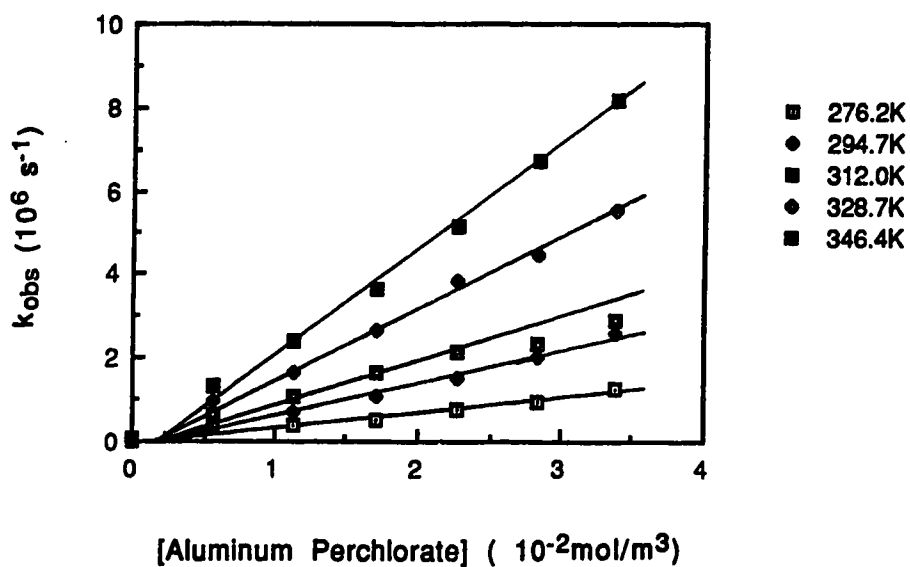


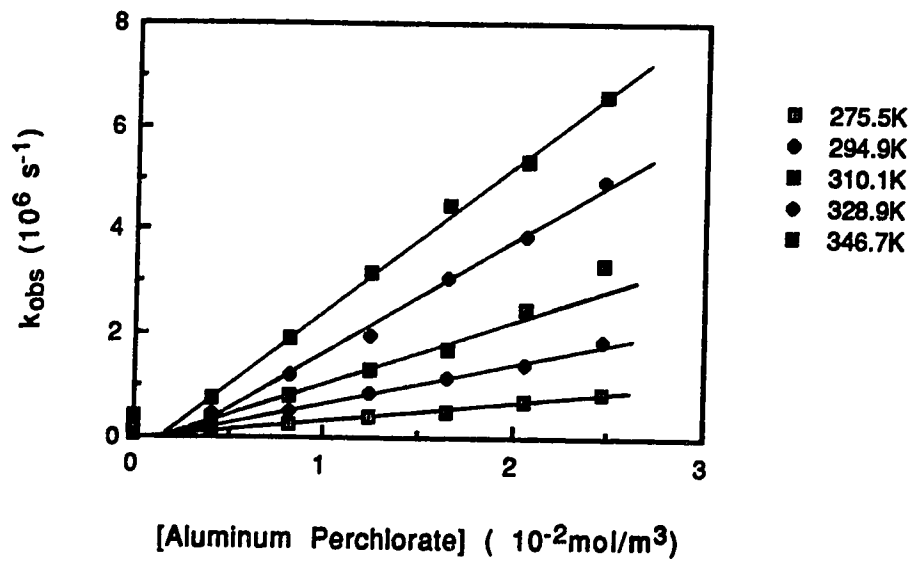
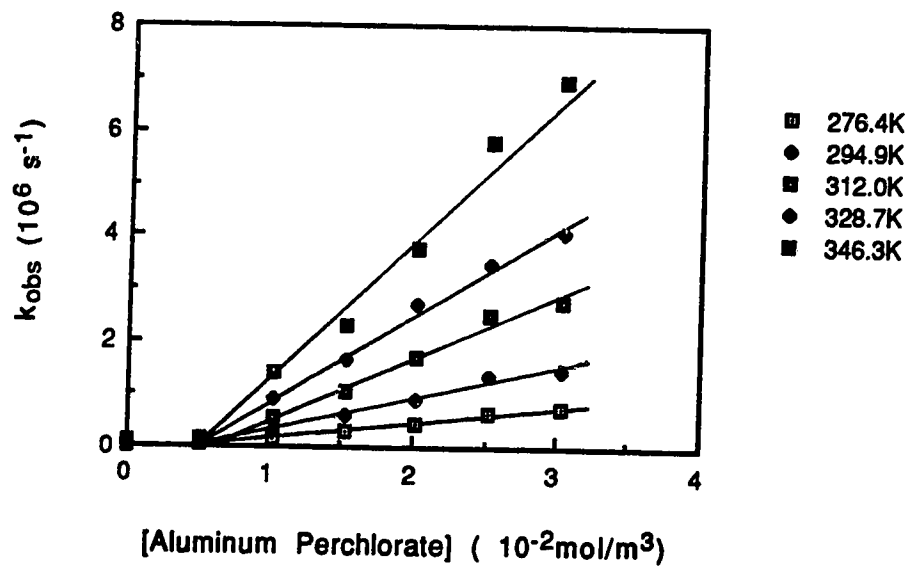
B

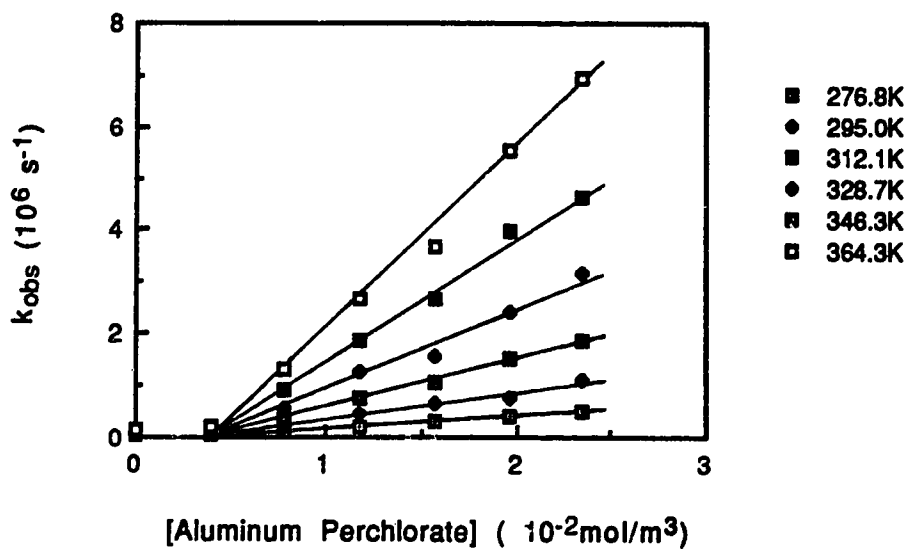
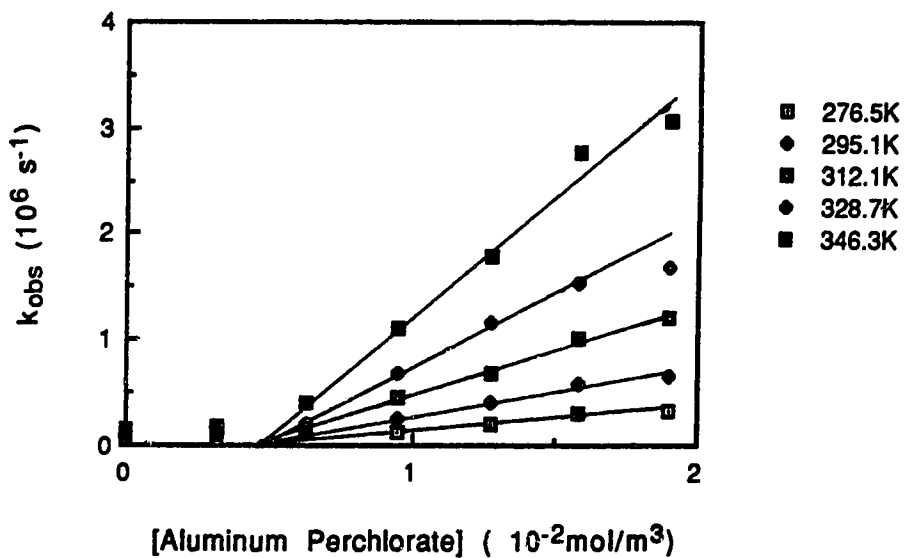
{93|2P|Aluminum Perchlorate}

**C**

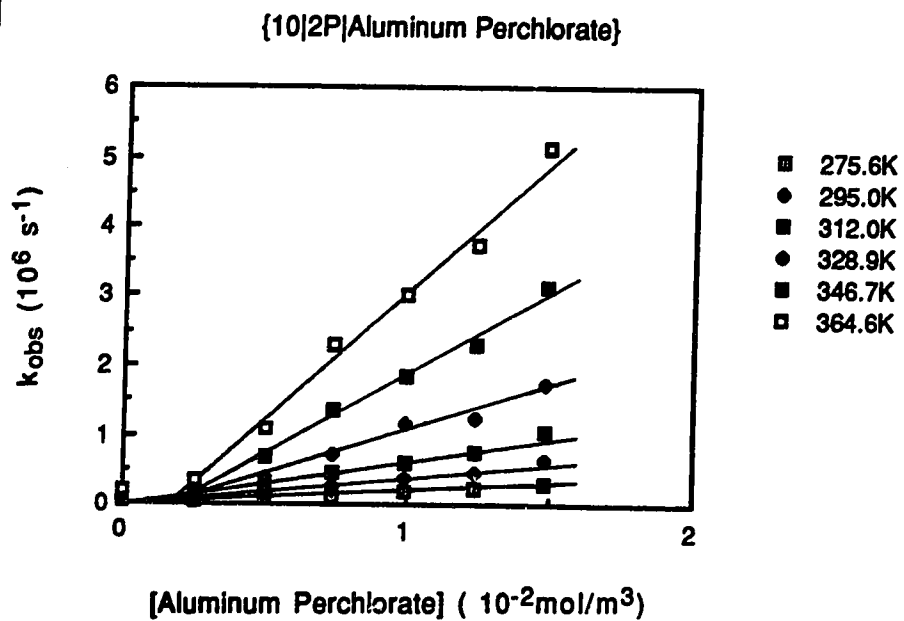
{81|2P|Aluminum Perchlorate}



D**{68[2P]Aluminum Perchlorate}****E****{52[2P]Aluminum Perchlorate}**

F**{36}2P|Aluminum Perchlorate****G****{20}2P|Aluminum Perchlorate**

H



I

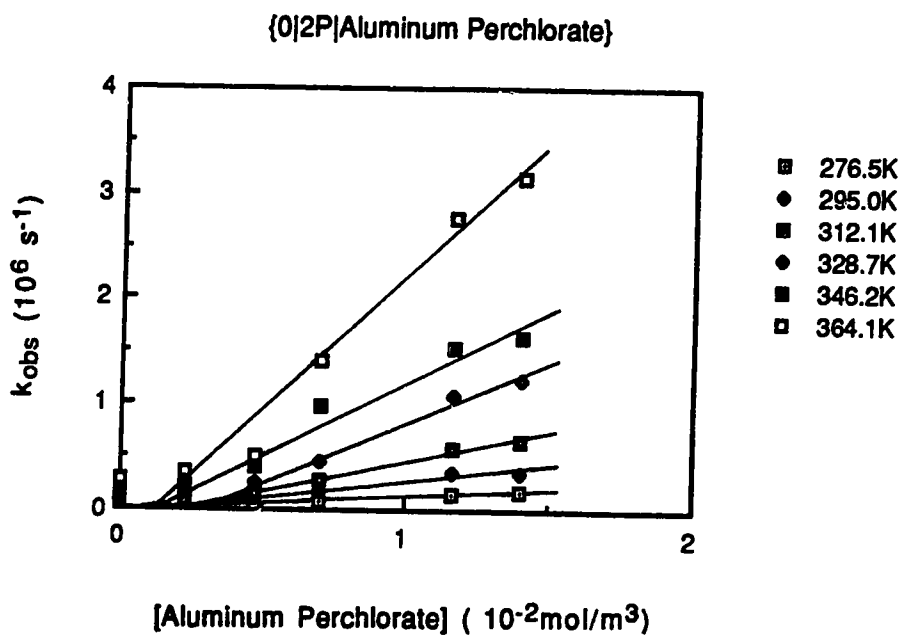


Table 23. Dielectric constants, f values and second-order rate constants for the reaction of solvated electrons with aluminum perchlorate in 2-propanol/water mixtures at various temperatures.

X_w	Temp (K)	ϵ	f	k_2 ($10^7 \text{ m}^3/\text{mol}\cdot\text{s}$)	X_w	Temp (K)	ϵ	f	k_2 ($10^7 \text{ m}^3/\text{mol}\cdot\text{s}$)
1.00	276.1	87.5	5.9	0.91	0.52	276.4	29.5	17.5	3.3
	296.6	79.0	6.1	2.0		294.9	26.0	18.7	6.3
	314.6	72.5	6.3	4.3		312.0	23.4	19.6	11
	328.6	68.0	6.4	8.6		328.7	21.0	20.7	16
	343.8	63.0	6.6	11		346.3	18.8	22.0	25
	361.4	57.9	6.8	14					
0.97	294.6	74.2	6.6	2.7	0.36	276.8	24.8	20.8	2.6
	312.0	68.5	6.7	5.7		295.0	21.7	22.3	5.3
	328.6	63.5	6.9	14		312.1	19.5	23.5	9.4
	346.5	58.0	7.1	24		328.7	17.4	25.0	15
						346.3	15.5	26.6	24
						364.3	13.7	28.7	35
0.93	276.8	70.8	7.3	2.1	0.20	276.5	23.0	22.5	2.6
	295.2	64.7	7.5	4.6		295.1	20.0	24.2	4.9
	313.5	59.5	7.7	8.9		312.1	17.7	25.9	8.3
	328.4	55.2	7.9	14		328.7	15.8	27.5	15
	343.1	51.5	8.1	18		346.3	14.0	29.5	22
0.81	276.2	52.0	10.0	3.8	0.10	275.6	22.2	23.4	2.2
	294.7	47.0	10.3	7.7		295.0	20.0	24.2	4.6
	312.0	43.0	10.7	11		312.0	17.0	27.0	7.7
	328.7	39.5	11.0	18		328.9	15.0	29.0	13
	346.4	36.0	11.5	26		346.7	13.4	30.8	23
						364.6	11.7	33.5	39
0.68	275.5	39.5	13.1	3.6	0.00	276.5	21.2	24.4	1.7
	294.9	35.2	13.8	7.5		295.0	18.5	26.2	3.6
	310.1	32.2	14.3	12		312.1	16.3	28.1	6.3
	328.9	29.0	15.0	21		328.7	14.5	30.0	11
	346.7	26.0	15.9	29		346.2	12.8	32.3	14
						364.1	11.4	34.5	25

Table 24. Rate parameters for the reaction of solvated electrons with aluminum perchlorate in 2-propanol/water mixtures.

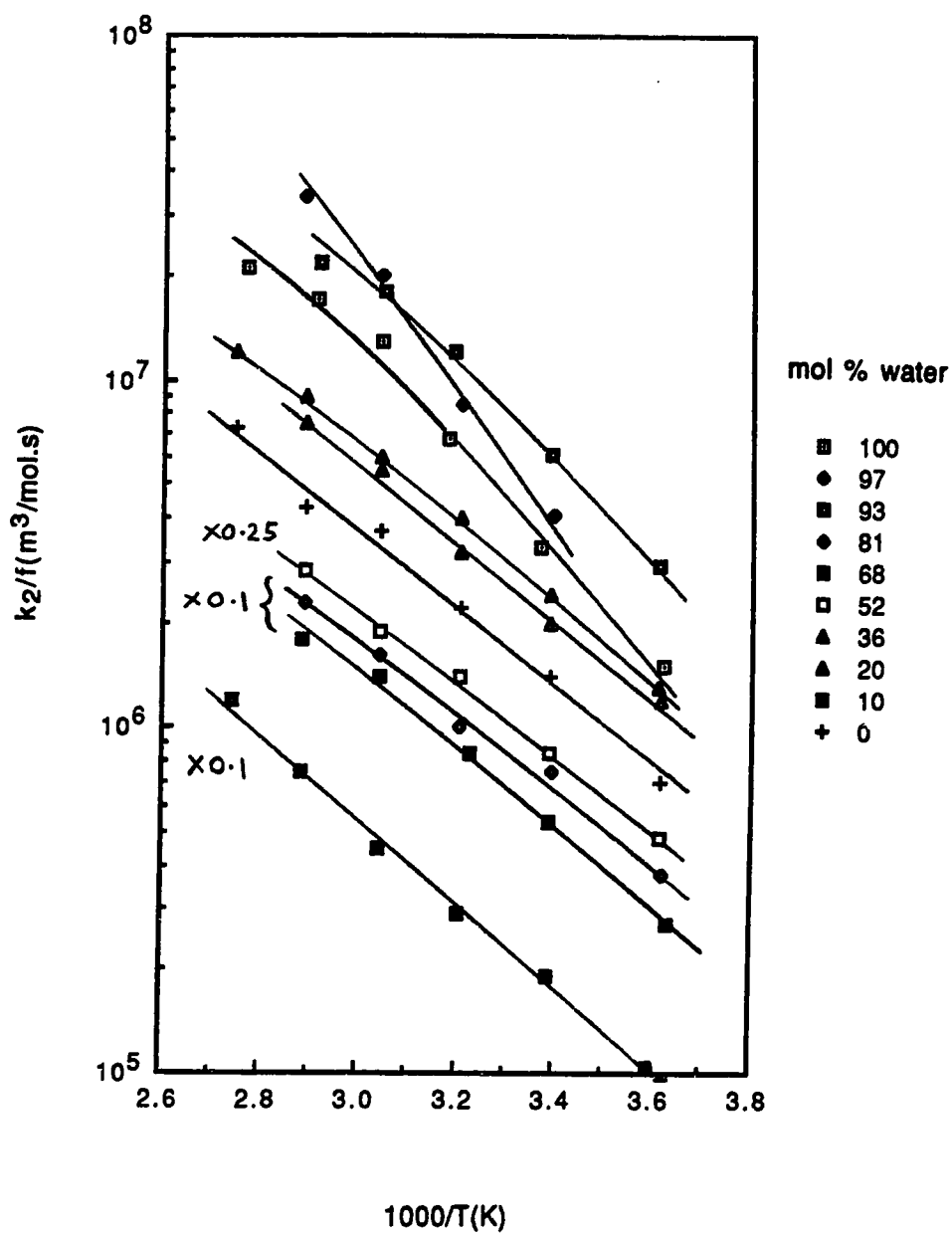
X_w	$\eta^{(a)}$ (10^{-3} Pa·s)	$k_2^{(a)}$ (10^7 m ³ /mol·s)	$k_2/f^{(a)}$ (10^7 m ³ /mol·s)	$E_2^{(b,c)}$ (kJ/mol)	$\log A_2^{(c)}$ (A_2 in m ³ /mol·s)
1.00	0.89	2.5	0.41	34	11.79
0.97	2.02	1.38	0.49	37	13.09
0.93	2.02	4.9	0.64	26	11.36
0.81	3.02	7.8	0.75	21	10.55
0.68	3.07	8.6	0.61	22	10.60
0.52	2.70	7.5	0.39	20	10.14
0.36	2.40	6.0	0.27	24	10.54
0.20	2.20	5.5	0.22	22	10.22
0.10	2.13	5.1	0.20	23	10.41
0.00	2.08	3.9	0.5	22	10.04

(a) At 298K.

(b) Near 298K.

(c) From Arrhenius plots of k_2/f .

Fig. 31 Arrhenius plots for the reaction of solvated electrons with aluminum perchlorate in 2-propanol/water mixtures

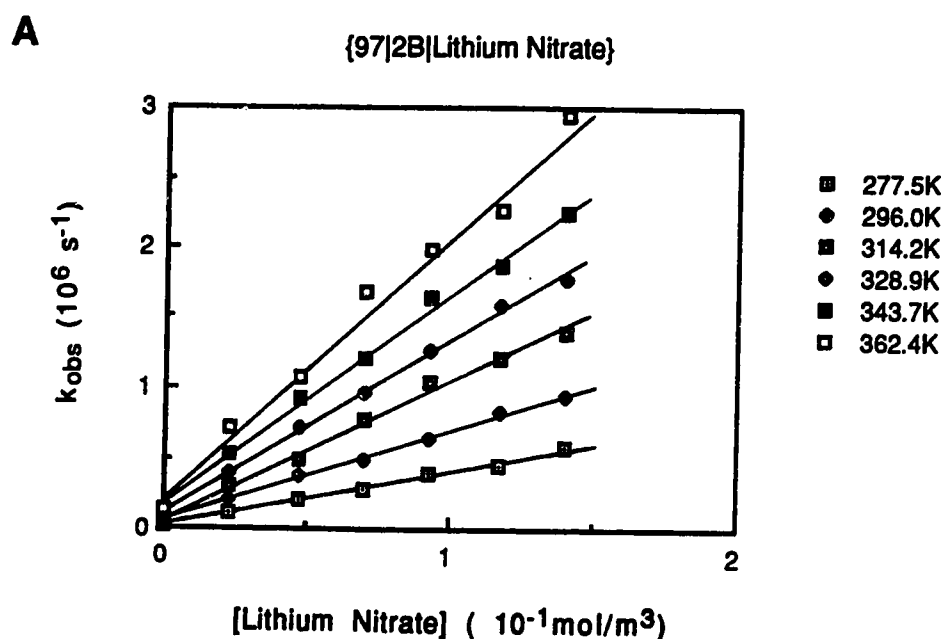


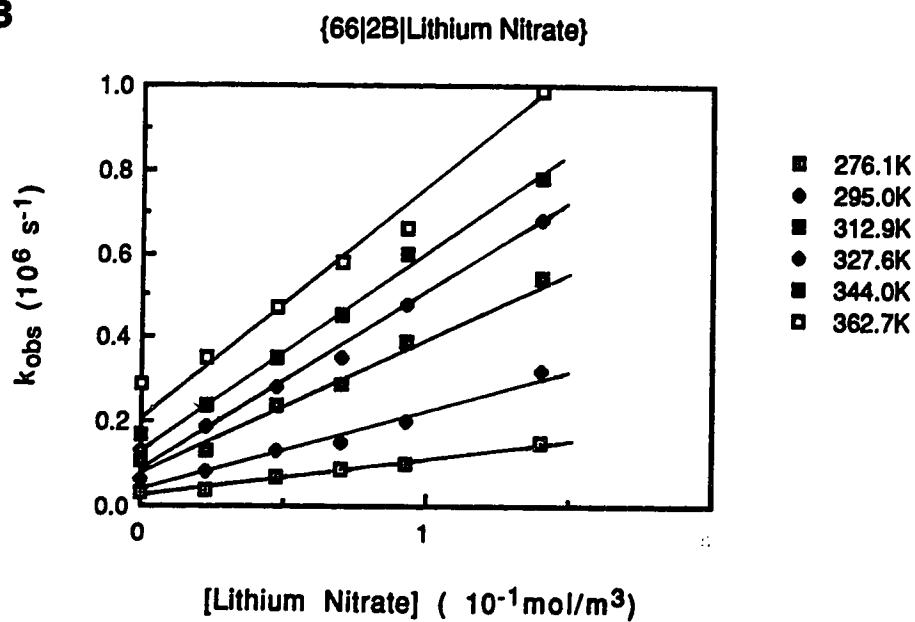
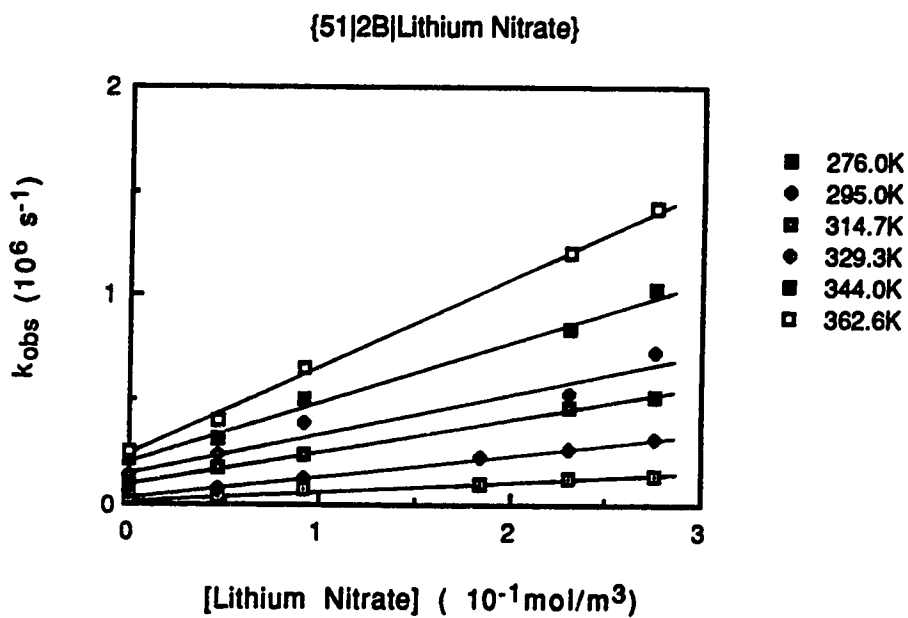
IV. Reactions of Solvated Electrons in 2-Butanol/Water Mixtures

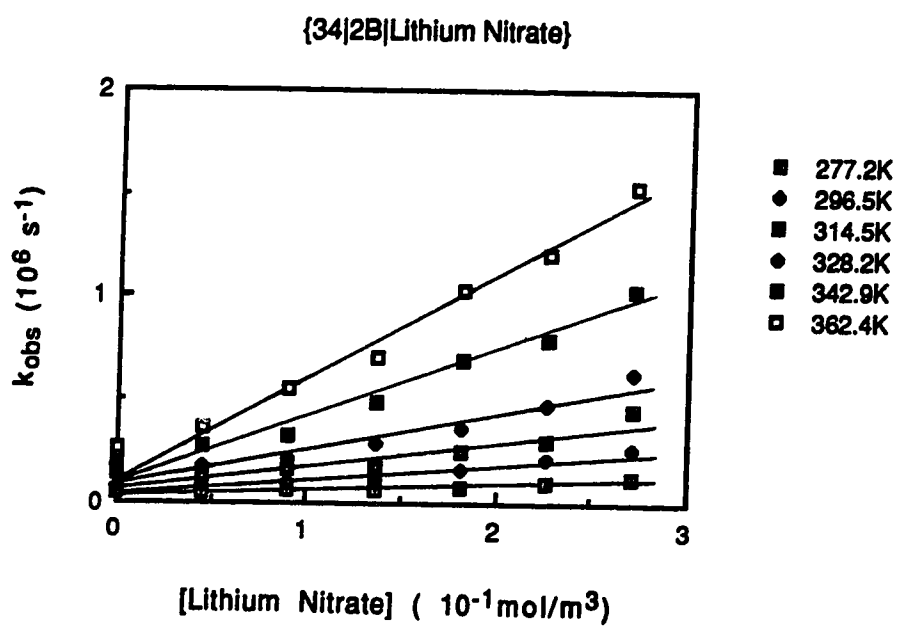
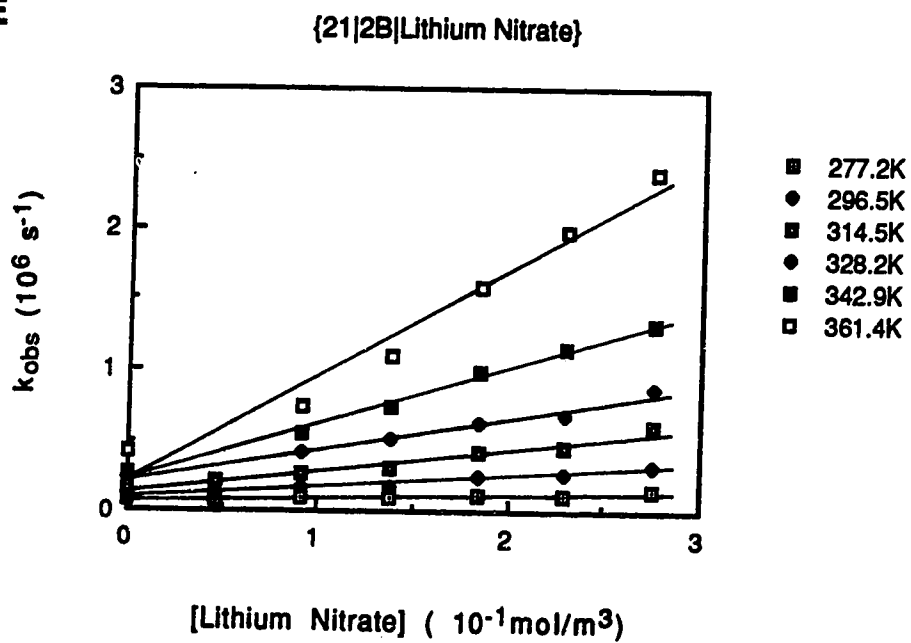
A. Reaction of Solvated Electrons with Nitrate Ions

The temperature and concentration dependence of the first-order rate constant for the reaction of solvated electrons with nitrate ion are shown in Figure 32 (A-G). The concentration range was 0.02-0.28 mol/m³. Table 25 shows the second-order rate constants, dielectric constants and the coulombic factor *f* at various temperatures in different alcohol/water mixtures. Table 26 shows the rate parameters obtained from the modified Arrhenius plots shown in Figure 33.

Fig. 32 Temperature and concentration dependence of the first-order rate constant for the reaction of solvated electrons with lithium nitrate in 2-butanol/water mixtures

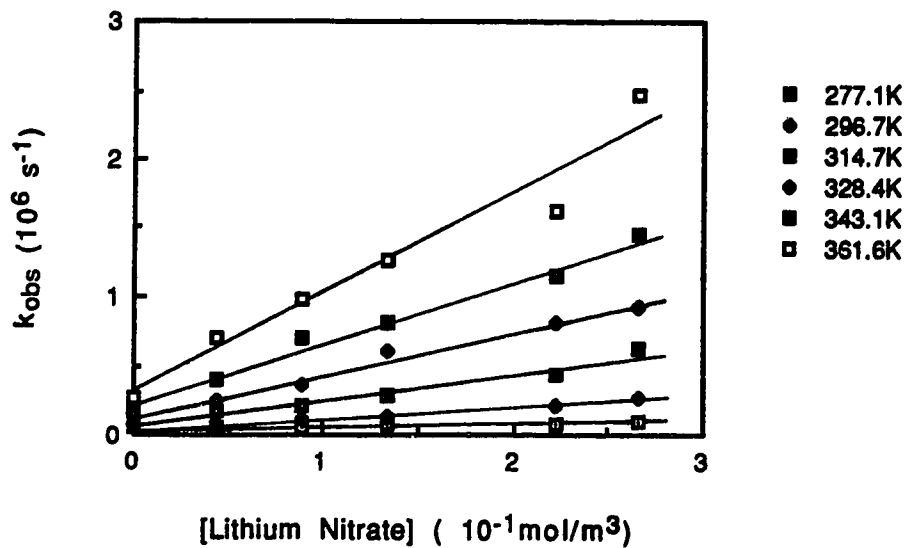


B**C**

D**E**

F

{10|2B|Lithium Nitrate}



G

{0|2B|Lithium Nitrate}

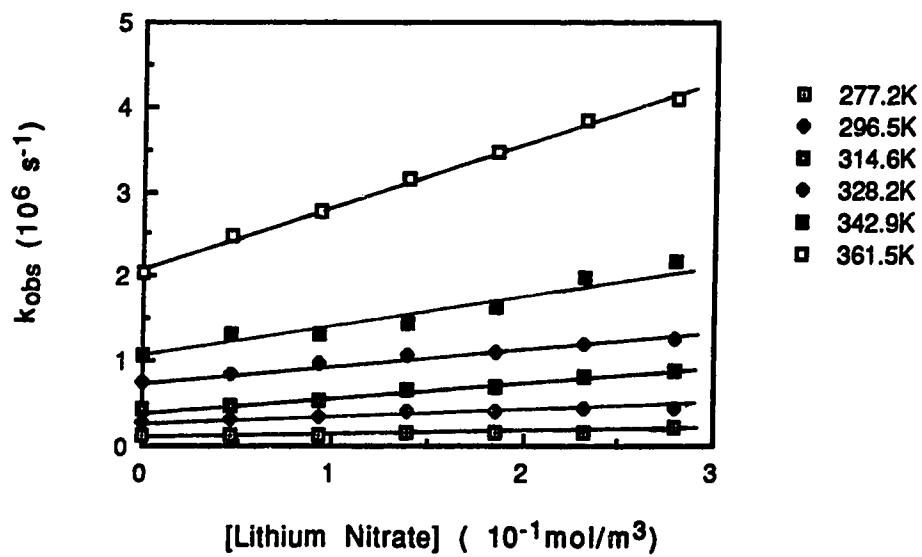


Table 25. Dielectric constants, f values and second-order rate constants for the reaction of solvated electrons with lithium nitrate in 2-butanol/water mixtures at various temperatures.

X_w	Temp (K)	ϵ	f	k_2 ($10^6 \text{ m}^3/\text{mol}\cdot\text{s}$)	X_w	Temp (K)	ϵ	f	k_2 ($10^6 \text{ m}^3/\text{mol}\cdot\text{s}$)
1.00	279.5	86.6	0.79	5.8	0.34	277.2	20.2	0.32	0.42
	296.7	78.9	0.78	9.3		296.5	16.8	0.27	0.71
	319.0	71.3	0.77	14		314.5	14.5	0.23	1.3
	338.5	64.6	0.77	19		328.2	13.0	0.21	1.8
	358.7	59.0	0.76	23		342.9	11.6	0.18	3.2
	367.3	56.0	0.75	25		362.4	10.0	0.15	5.0
0.97	277.5	78.6	0.77	4.0	0.21	277.2	19.2	0.30	0.28
	296.0	70.7	0.76	6.4		296.5	15.8	0.24	0.77
	314.2	64.2	0.75	9.8		314.5	13.5	0.21	1.4
	328.9	59.5	0.74	13		328.2	11.8	0.17	2.1
	343.7	55.7	0.74	15		342.9	10.2	0.14	4.0
	362.4	51.0	0.73	19		361.4	8.6	0.10	7.2
0.66	276.1	30.5	0.48	0.87	0.10	277.1	19.2	0.30	0.24
	295.0	26.6	0.45	1.7		296.7	15.8	0.24	0.78
	312.9	23.6	0.43	2.7		314.7	13.5	0.21	1.5
	327.6	21.6	0.41	3.9		328.4	11.8	0.17	3.0
	344.0	19.6	0.39	5.0		343.1	10.1	0.14	4.4
	362.7	16.0	0.33	5.7		361.6	8.2	0.09	7.4
0.51	276.0	23.6	0.38	0.42	0.00	277.2	20.5	0.32	0.30
	295.0	20.2	0.34	0.95		296.5	16.7	0.27	0.63
	314.7	17.6	0.31	1.5		314.6	14.0	0.22	1.5
	344.0	14.6	0.27	2.9		328.2	12.0	0.18	1.8
	362.6	13.0	0.25	4.2		342.9	10.0	0.13	3.5
							361.5	8.4	0.097

Table 26. Rate parameters for the reaction of solvated electrons with lithium nitrate in 2-butanol/water mixtures.

X_w	$\eta^{(a)}$ (10^{-3} Pa·s)	$k_2^{(a)}$ (10^6 m ³ /mol·s)	$k_2/f^{(a)}$ (10^6 m ³ /mol·s)	$E_2^{(b,c)}$ (kJ/mol)	$\log A_2^{(c)}$ (A_2 in m ³ /mol·s)	$E_\eta^{(d)}$ (kJ/mol)
1.00	0.89	9.6	12	16	9.91	16
0.97	1.45	6.8	9.1	19	10.25	17
0.66	3.32	1.8	4.0	24	10.76	24
0.51	3.06	0.98	2.9	25	10.86	24
0.34	2.85	0.80	3.1	32	12.06	
0.20	2.75	0.78	3.3	36	12.74	23
0.10	2.78	0.77	3.1	45	13.45	24
0.00	3.05	0.75	2.9	44	13.83	26

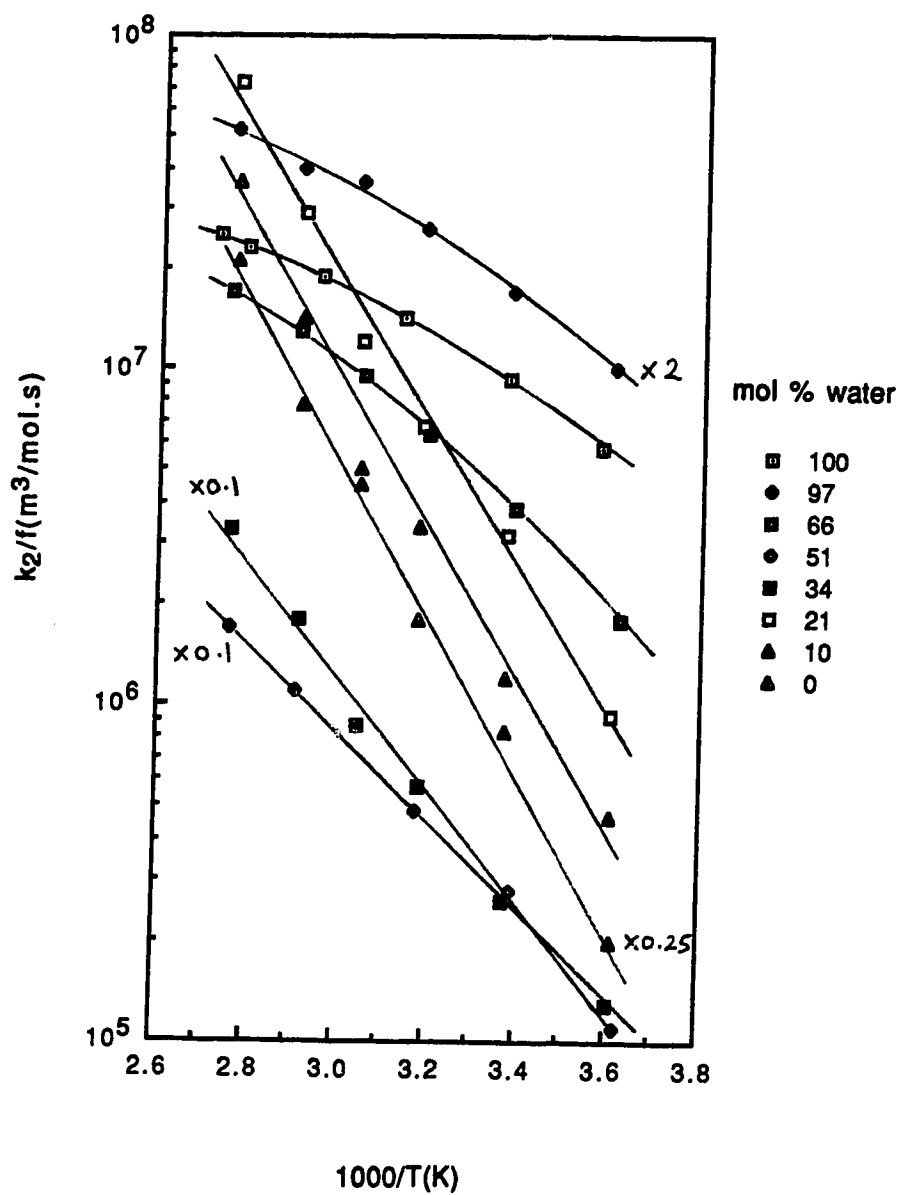
(a) At 298K.

(b) Near 298K.

(c) From Arrhenius plots of k_2/f .

(d) From ref. 105.

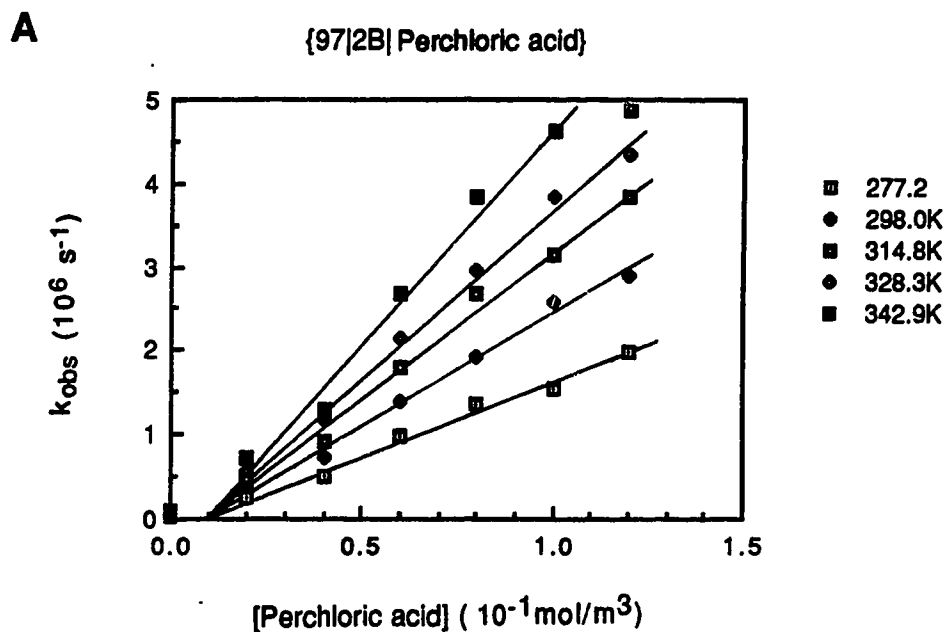
Fig. 33 Arrhenius plots for the reaction of solvated electrons with lithium nitrate in 2-butanol/water mixtures



B. Reaction of Solvated Electrons with Hydrogen Ions

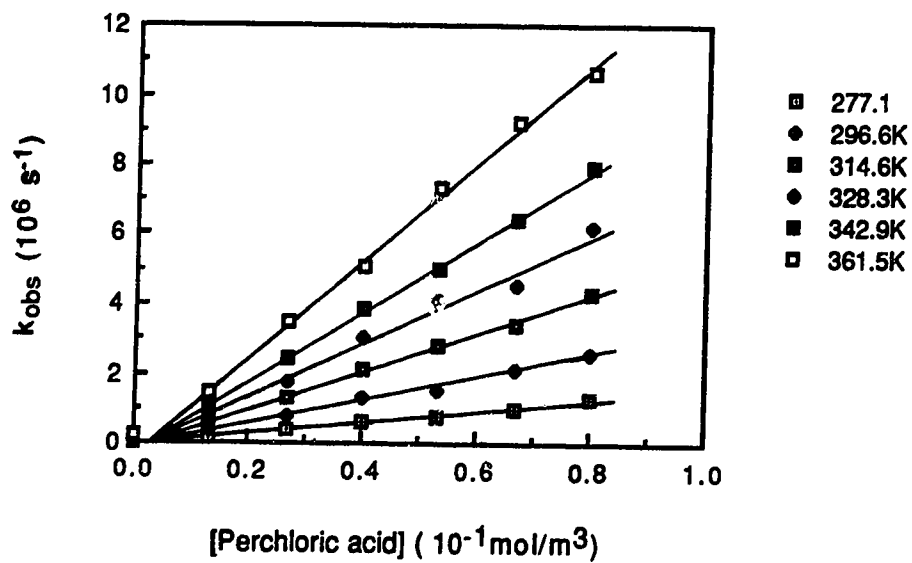
The temperature and concentration dependence of the first-order rate constant for the reaction of solvated electrons with hydrogen ion are shown in Figure 34 (A-G). The concentration range was 0.01-0.12 mol/m³. Table 27 shows the second-order rate constants, dielectric constants and the coulombic factors *f* at various temperatures in different alcohol/water mixtures. Table 28 shows the rate parameters obtained from the modified Arrhenius plots shown in Figure 35.

Fig. 34 Temperature and concentration dependence of the first-order rate constant for the reaction of solvated electrons with perchloric acid in 2-butanol/water mixtures

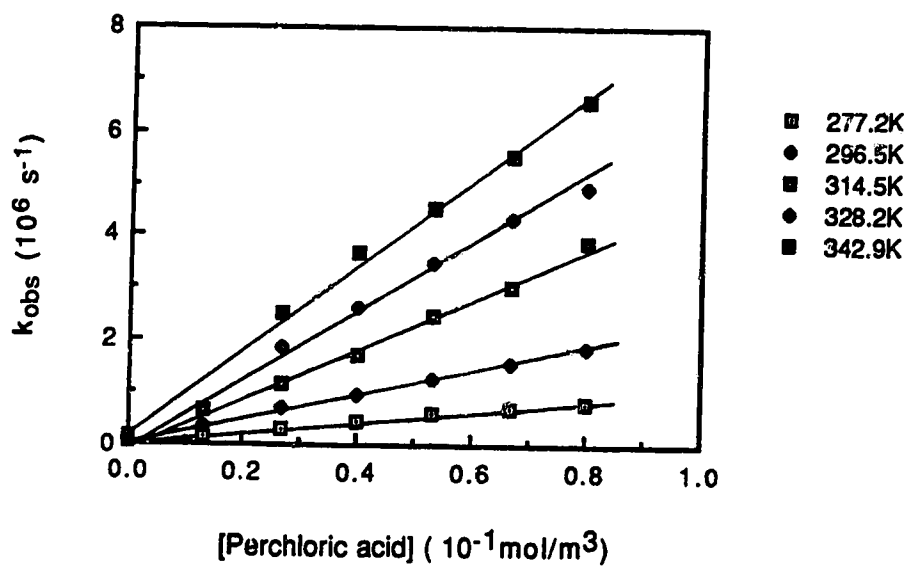


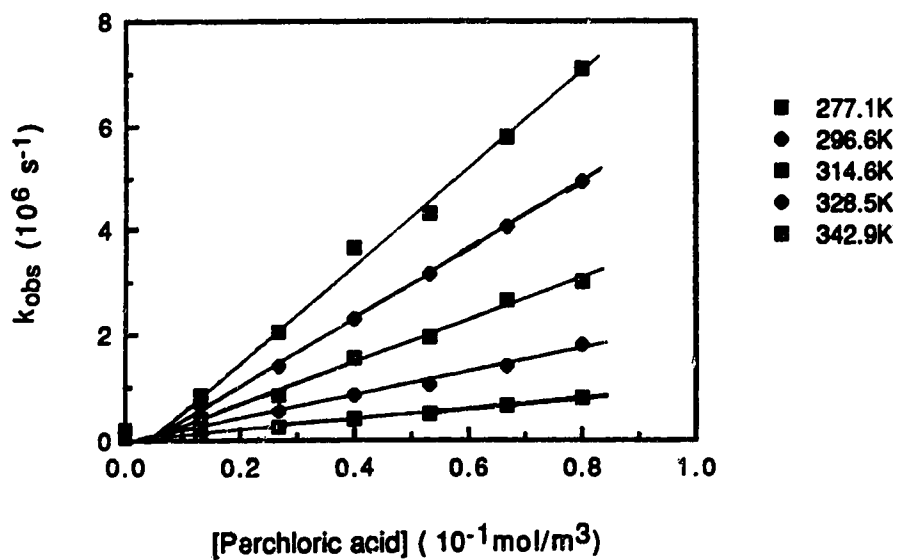
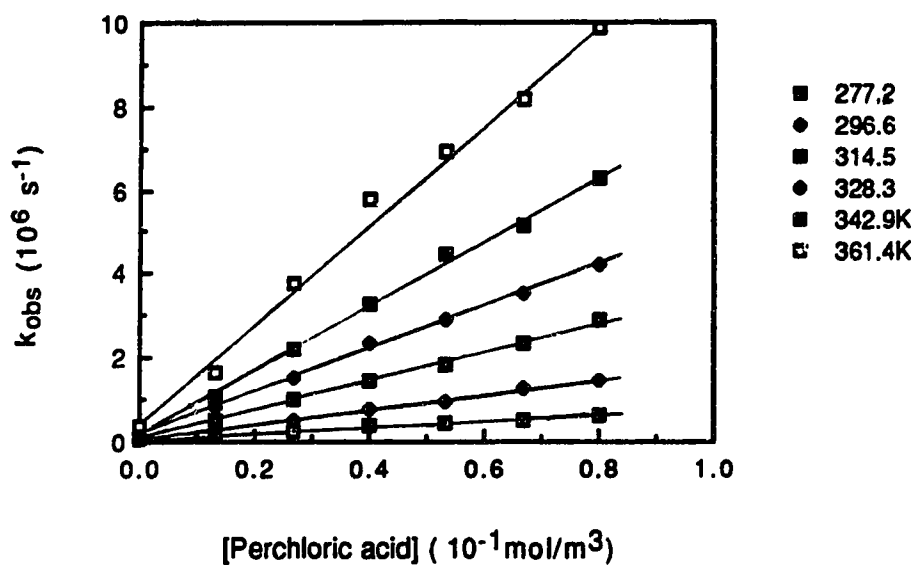
B

{66|2B| Perchloric acid}

**C**

{51|2B| Perchloric acid}



D**{34|2B|Perchloric acid}****E****{20|2B|Perchloric acid}**

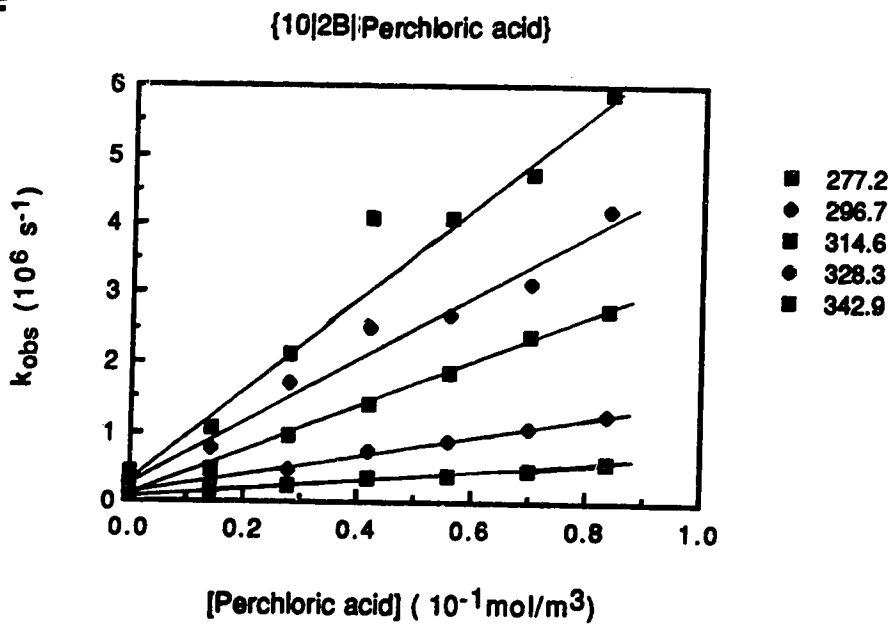
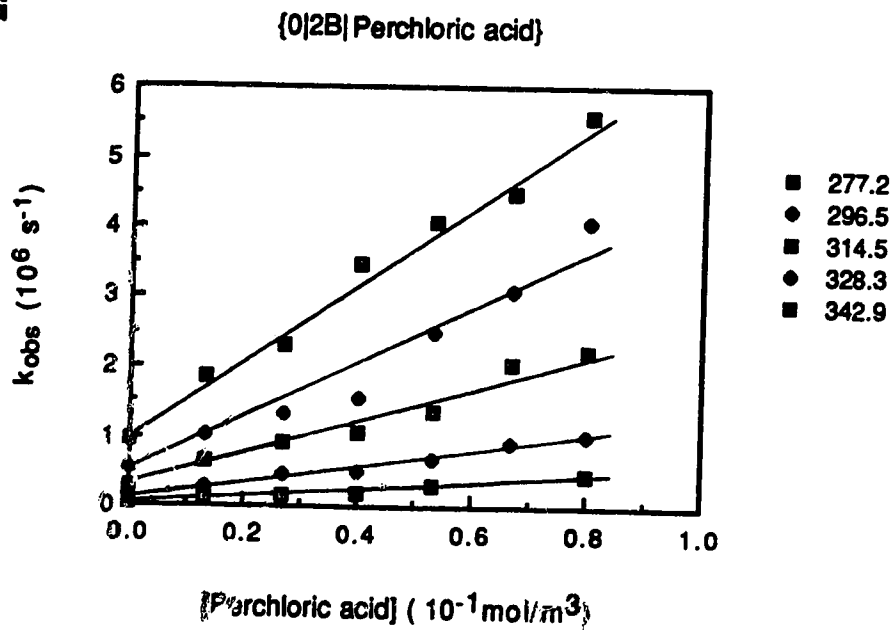
F**G**

Table 27. Dielectric constants, f values and second-order rate constants for the reaction of solvated electrons with perchloric acid in 2-butanol/water mixtures at various temperatures.

X_w	Temp (K)	ϵ	f	k_2 ($10^7 \text{ m}^3/\text{mol}\cdot\text{s}$)	X_w	Temp (K)	ϵ	f	k_2 ($10^7 \text{ m}^3/\text{mol}\cdot\text{s}$)
1.00	277.5	86.8	1.39	1.8	0.34	277.1	20.2	3.14	1.1
	295.9	79.3	1.40	2.6		296.6	16.8	3.5	2.4
	314.2	72.5	1.41	3.2		314.6	14.5	3.8	4.2
	329.0	67.7	1.42	4.1		328.5	13.0	4.0	6.5
	343.9	63.0	1.43	4.6		342.9	11.6	4.3	9.3
0.97	277.2	78.7	1.43	1.8	0.20	277.2	19.2	3.3	0.77
	298.0	70.0	1.45	2.7		296.6	15.8	3.7	1.8
	314.8	64.0	1.47	3.5		314.5	13.5	4.0	3.3
	328.3	59.8	1.48	4.0		328.3	11.8	4.4	5.1
	342.9	56.0	1.50	5.1		342.9	10.2	4.8	7.8
					361.4	8.6	5.4	12	
0.66	277.1	30.3	2.30	1.5	0.10	277.2	19.2	3.3	0.56
	296.6	26.4	2.42	3.3		296.6	15.8	3.7	1.4
	314.6	23.5	2.52	5.5		314.6	13.5	4.0	3.1
	328.3	21.5	2.61	7.5		328.3	11.8	4.4	4.4
	342.9	19.7	2.70	10		342.9	10.1	4.9	6.6
361.5	16.0	3.06	14						
0.51	277.2	23.3	2.79	1.1	0.00	277.2	20.5	3.1	0.48
	296.5	20.0	2.99	2.6		296.5	16.7	3.5	1.1
	314.5	17.6	3.17	5.0		314.5	14.0	3.9	2.2
	328.2	16.0	3.32	6.9		328.3	12.0	4.3	3.8
	342.9	14.6	3.46	8.9		342.9	10.0	4.9	5.6

Table 28. Rate parameters for the reaction of solvated electrons with perchloric acid in 2-butanol/water mixtures.

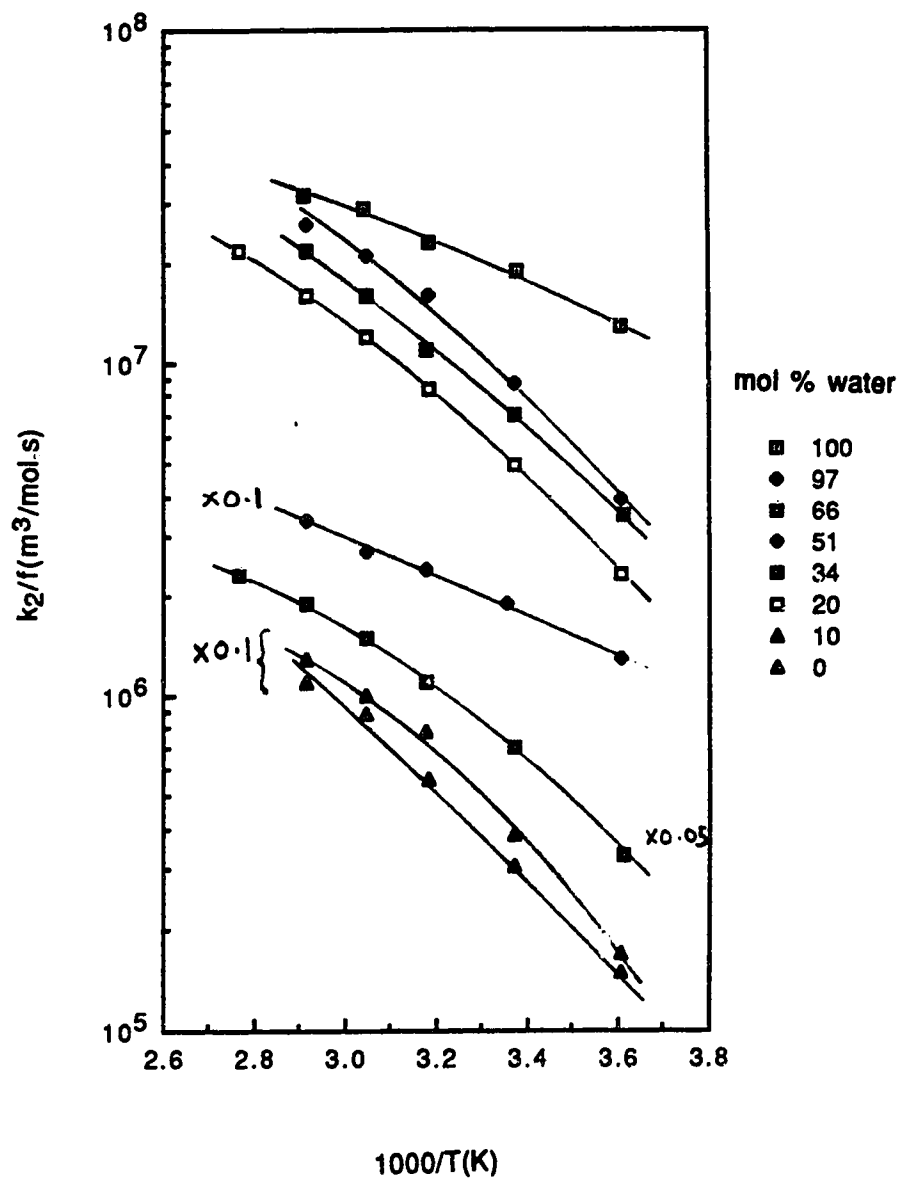
X_w	$\eta^{(a)}$ (10^{-3} Pa·s)	$k_2^{(a)}$ (10^7 m ³ /mol·s)	$k_2/f^{(a)}$ (10^7 m ³ /mol·s)	$E_2^{(b,c)}$ (kJ/mol)	$\log A_2^{(c)}$ (A_2 in m ³ /mol·s)
1.00	0.89	2.6	1.9	12	9.42
0.97	1.45	2.7	1.9	11	8.27
0.66	3.32	3.4	1.4	22	11.00
0.51	3.06	2.9	0.97	24	11.15
0.34	2.85	2.4	0.69	22	10.67
0.20	2.74	1.9	0.51	24	10.95
0.10	2.78	1.6	0.43	27	11.39
0.00	3.05	1.3	0.37	25	10.97

(a) At 298K.

(b) Near 298K.

(c) From Arrhenius plots of k_2/f .

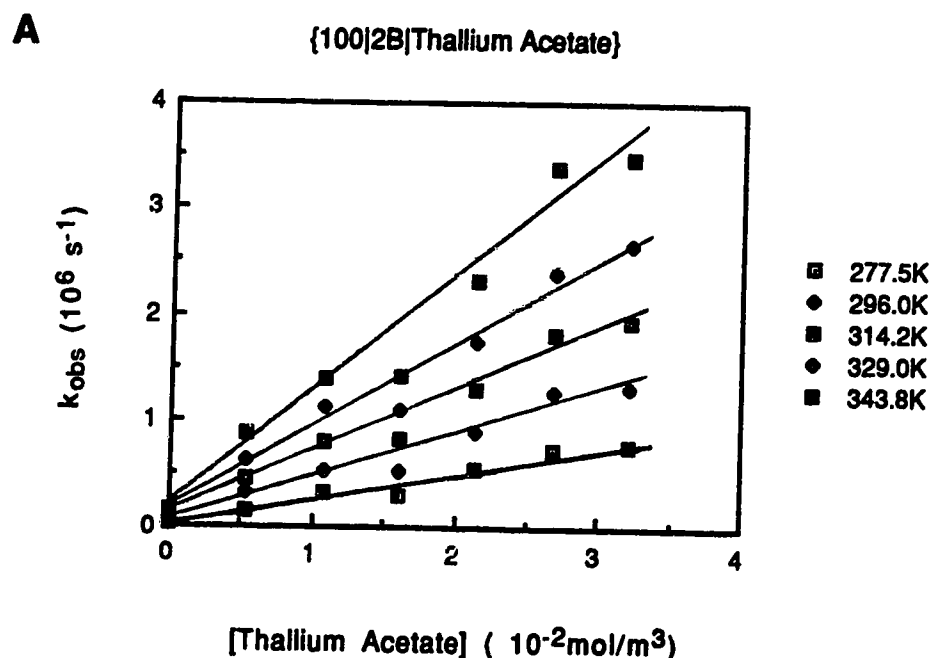
Fig. 35 Arrhenius plots for the reaction of solvated electrons with perchloric acid in 2-butanol/water mixtures

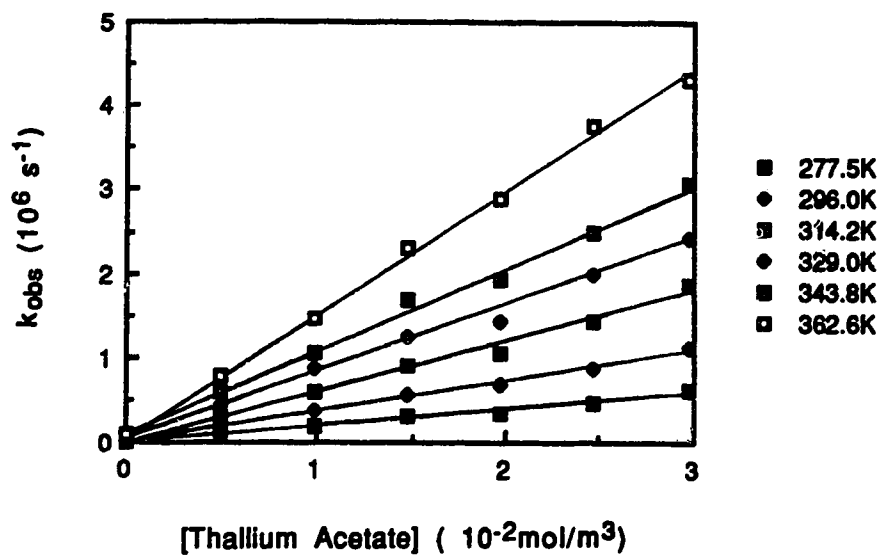
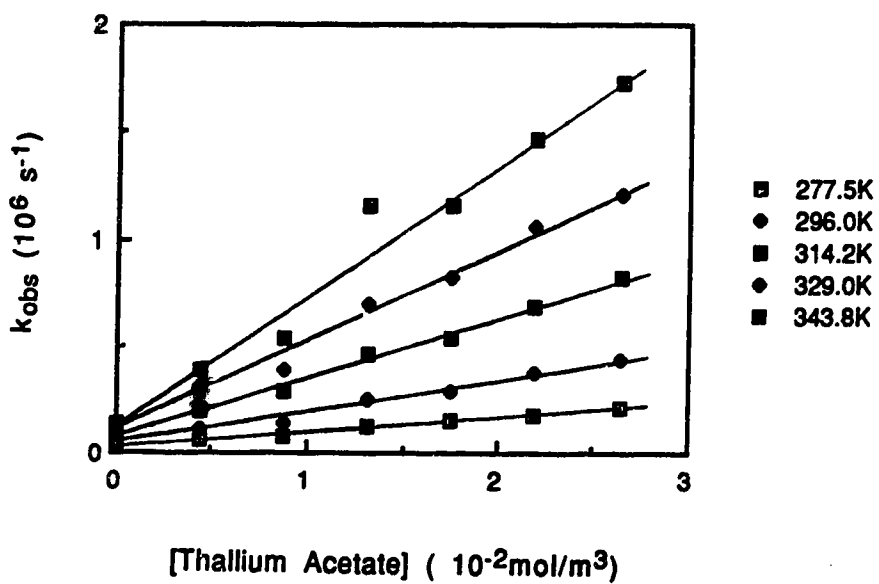


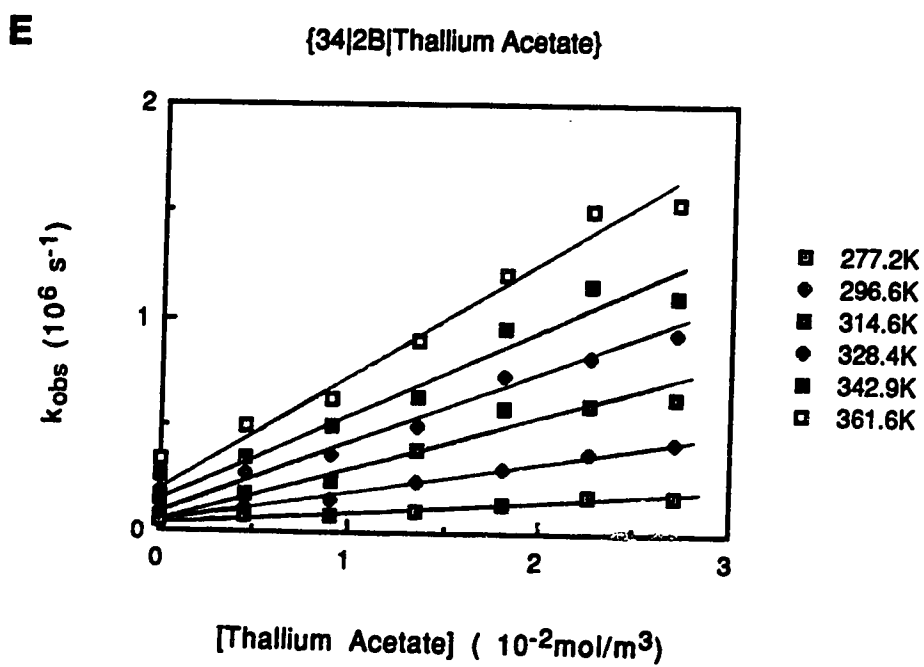
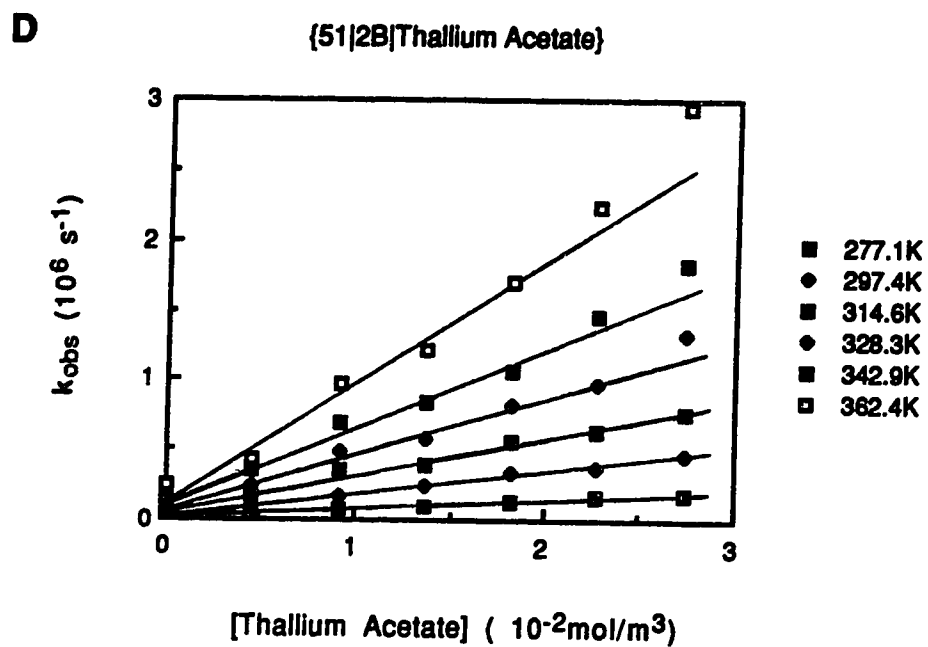
C. Reaction of Solvated Electrons with Thallium Ions

The temperature and concentration dependence of the first-order rate constant for the reaction of solvated electrons with thallium ion are shown in Figure 36 (A-G). The concentration range was 4-54 mmol/m³. Table 29 shows the second-order rate constants, dielectric constants and the coulombic factors *f* at various temperatures in different alcohol/water mixtures. The rate constant in water at 298K is 4.1×10^7 m³/mol·s. The values reported in the literature are 2.8×10^7 , 3.0×10^7 and 4.0×10^7 m³/mol·s (83). Table 30 shows the rate parameters obtained from the modified Arrhenius plots shown in Figure 37.

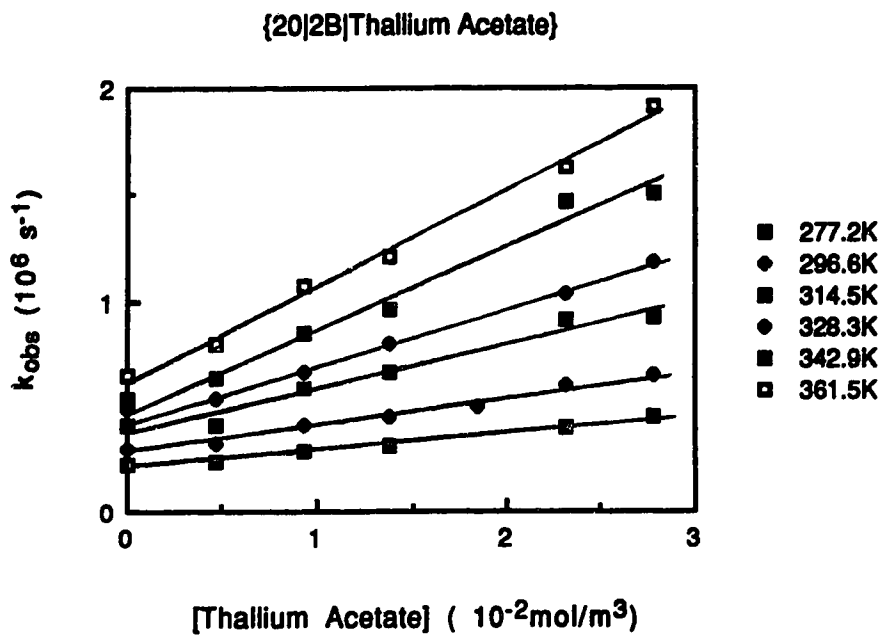
Fig. 36 Temperature and concentration dependence of the first-order rate constant for the reaction of solvated electrons with thallium acetate in 2-butanol/water mixtures



B**{97|2B|Thallium Acetate}****C****{66|2B|Thallium Acetate}**



F



G

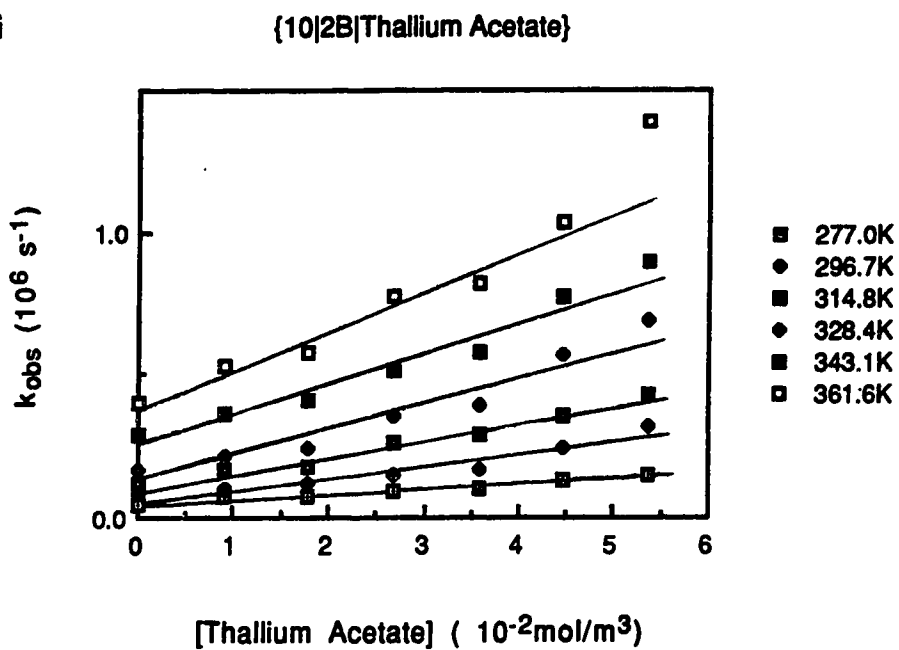


Table 29. Dielectric constants, f values and second-order rate constants for the reaction of solvated electrons with thallium acetate in 2-butanol/water mixtures at various temperatures.

X_w	Temp (K)	ϵ	f	k_2 ($10^7 \text{ m}^3/\text{mol}\cdot\text{s}$)	X_w	Temp (K)	ϵ	f	k_2 ($10^7 \text{ m}^3/\text{mol}\cdot\text{s}$)
1.00	277.5	86.8	1.39	2.2	0.34	277.2	20.2	3.1	0.63
	296.0	79.3	1.40	4.0		296.6	16.8	3.5	1.4
	314.2	72.5	1.41	6.0		314.6	14.5	3.8	2.4
	329.0	67.7	1.42	7.8		328.4	13.0	4.0	3.3
	343.8	63.0	1.43	11		342.9	11.6	4.3	4.0
						361.6	10.2	4.6	5.6
0.97	277.5	78.6	1.43	2.0	0.20	277.2	19.2	3.3	0.77
	296.0	70.7	1.45	3.6		296.6	15.8	3.6	1.2
	314.2	64.2	1.47	6.0		314.5	13.5	4.0	2.0
	329.0	59.5	1.49	7.9		328.3	11.8	4.4	2.5
	343.8	55.7	1.50	10		342.9	10.7	4.8	3.7
	362.6	51.0	1.52	15		361.5	8.6	5.4	4.3
0.66	277.5	30.2	2.31	0.67	0.10	277.0	19.2	3.3	0.20
	296.0	26.5	2.42	1.4		296.7	15.8	3.7	0.44
	314.2	23.5	2.52	2.8		314.8	13.5	4.0	0.62
	329.0	21.5	2.61	4.1		328.4	11.8	4.4	0.93
	343.8	19.6	2.70	5.9		343.1	10.1	4.9	1.1
							361.6	8.2	5.6
0.51	277.2	23.3	2.79	0.71					
	297.4	19.8	3.0	1.7					
	314.6	17.6	3.2	2.5					
	328.3	16.0	3.3	3.8					
	342.9	14.6	3.5	5.6					
	362.4	13.0	3.6	8.7					

Table 30. Rate parameters for the reaction of solvated electrons with thallium acetate in 2-butanol/water mixtures.

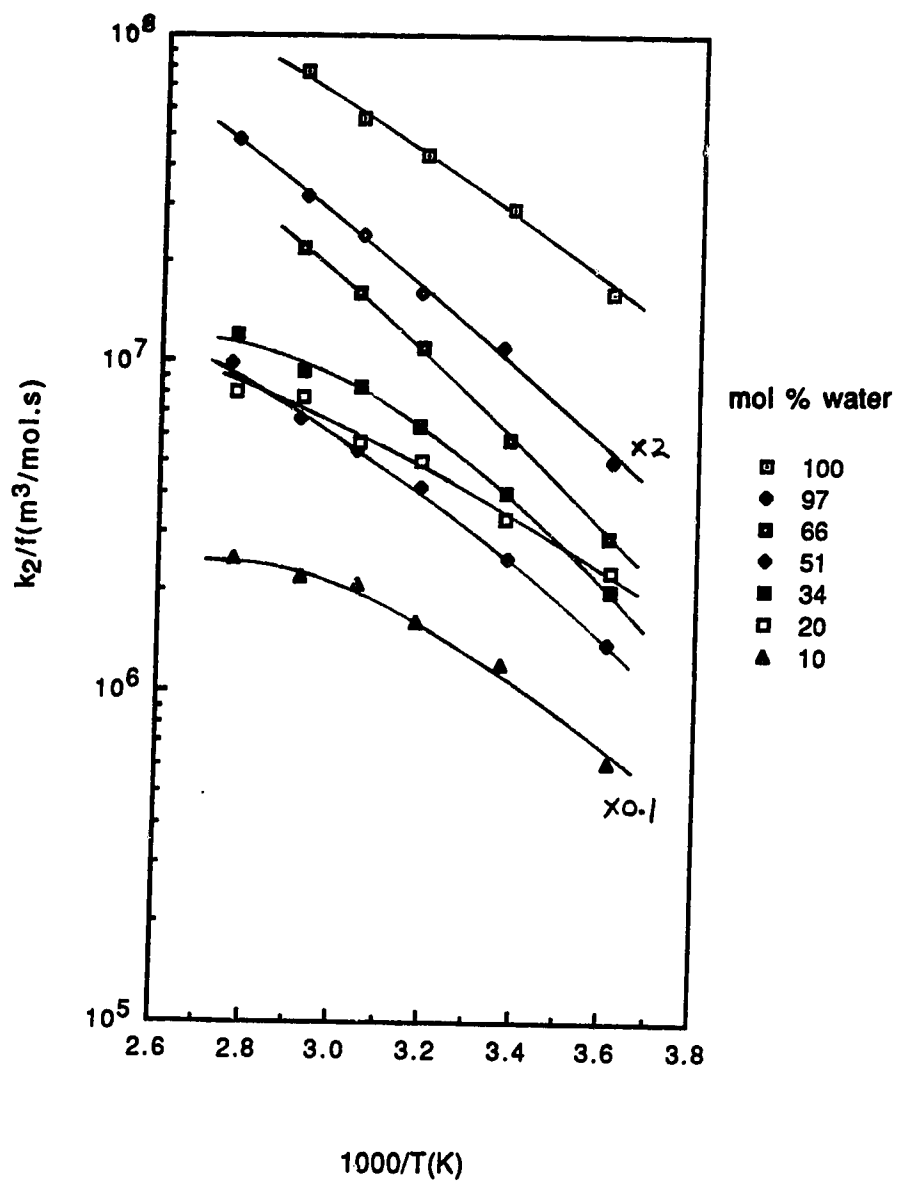
X_w	$\eta^{(a)}$ (10^{-3} Pa·s)	$k_2^{(a)}$ (10^7 m ³ /mol·s)	$k_2/f^{(a)}$ (10^7 m ³ /mol·s)	$E_2^{(b,c)}$ (kJ/mol)	$\log A_2^{(c)}$ (A_2 in m ³ /mol·s)
1.00	0.89	4.1	2.9	19	10.34
0.97	1.45	3.8	2.7	23	10.92
0.66	3.32	1.6	0.65	25	11.24
0.51	3.06	1.6	0.53	22	10.63
0.34	2.85	1.5	0.43	21	10.20
0.20	2.74	1.3	0.35	15	9.19
0.10	2.78	0.43	0.12	16	8.95

(a) At 298K.

(b) Near 298K.

(c) From Arrhenius plots of k_2/f .

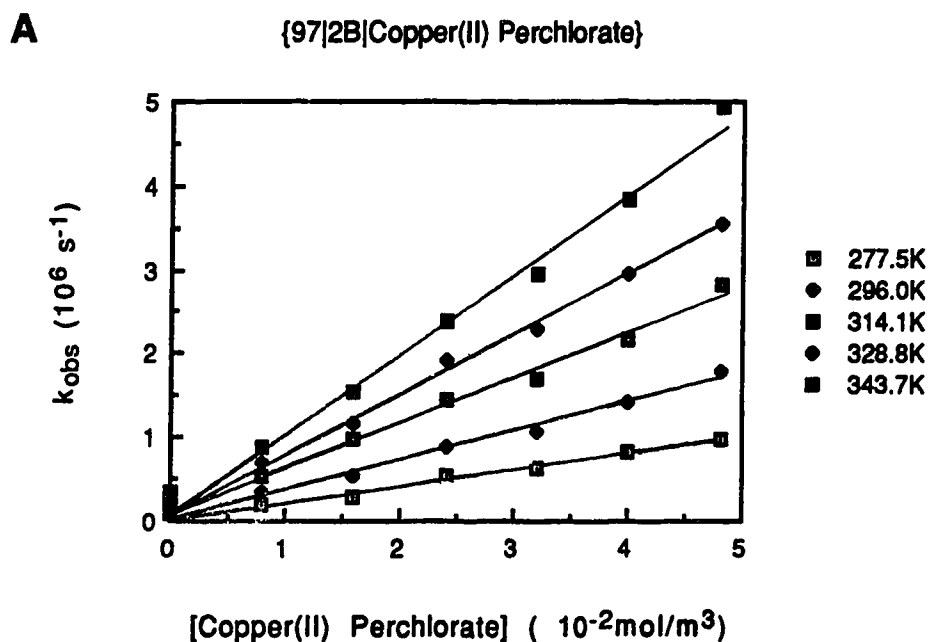
Fig. 37 Arrhenius plots for the reaction of solvated electrons with thallium acetate in 2-butanol/water mixtures

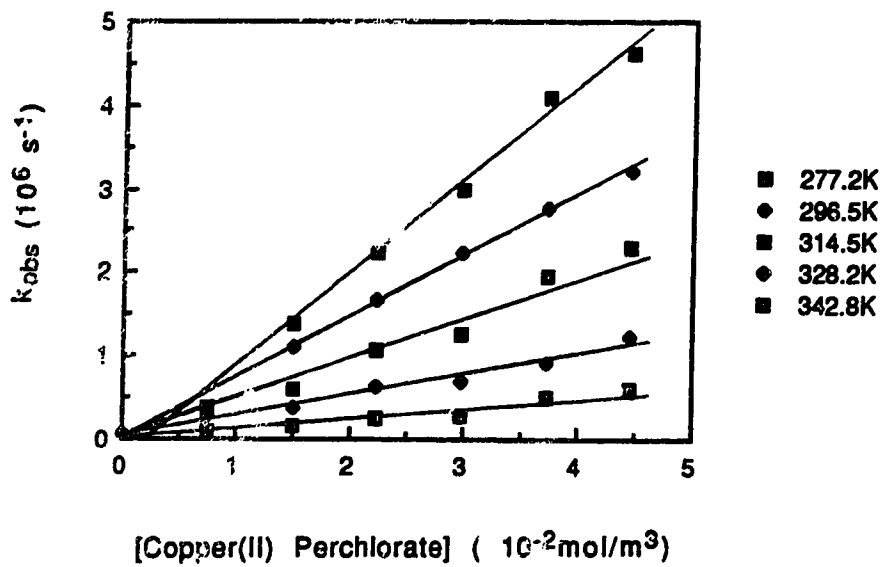
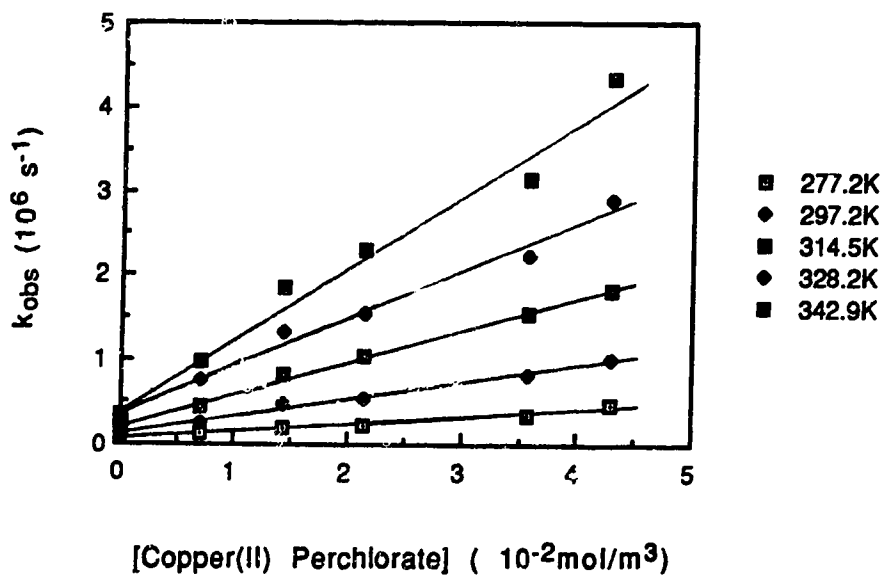


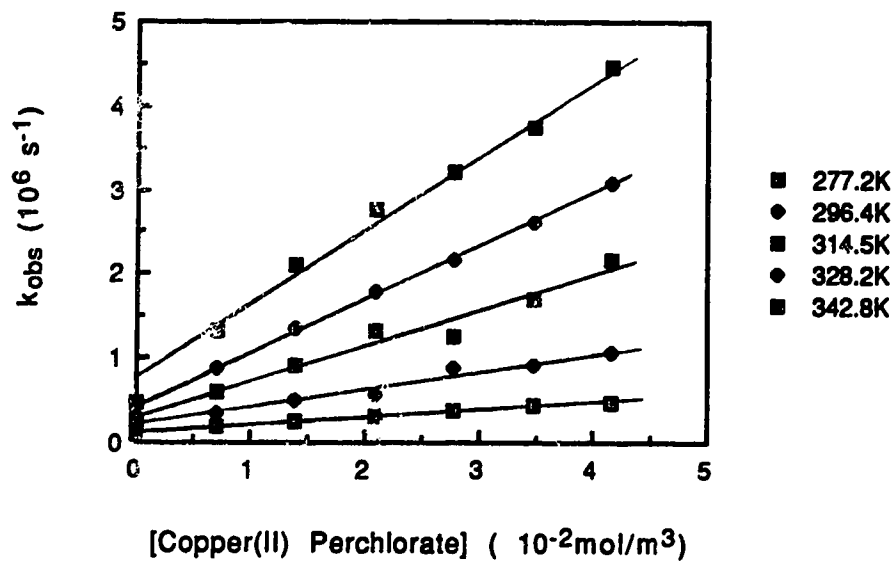
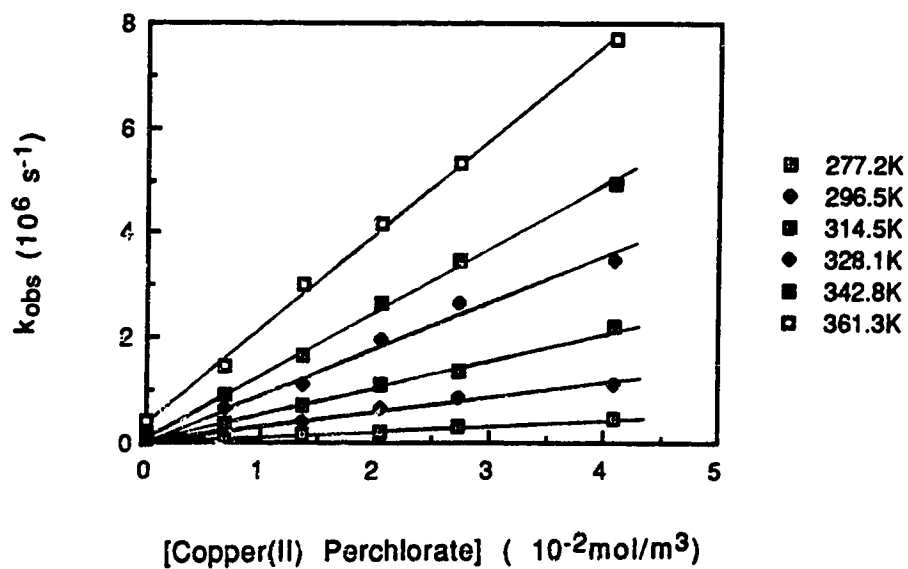
D. Reaction of Solvated Electrons with Copper(II) Ions

The temperature and concentration dependence of the first-order rate constant for the reaction of solvated electrons with copper(II) ion are shown in Figure 38 (A-G). The concentration range was 5-54 mmol/m³. Table 31 shows the second-order rate constants, dielectric constants and the coulombic factor *f* at various temperatures in different alcohol/water mixtures. Table 32 shows the rate parameters obtained from the modified Arrhenius plots shown in Figure 39.

Fig. 38 Temperature and concentration dependence of the first-order rate constant for the reaction of solvated electrons with copper(II) perchlorate in 2-butanol/water mixtures



B**{66|2B|Copper(II) Perchlorate}****C****{52|2B|Copper(II) Perchlorate}**

D**{34|2B|Copper(II) Perchlorate}****E****{20|2B|Copper(II) Perchlorate}**

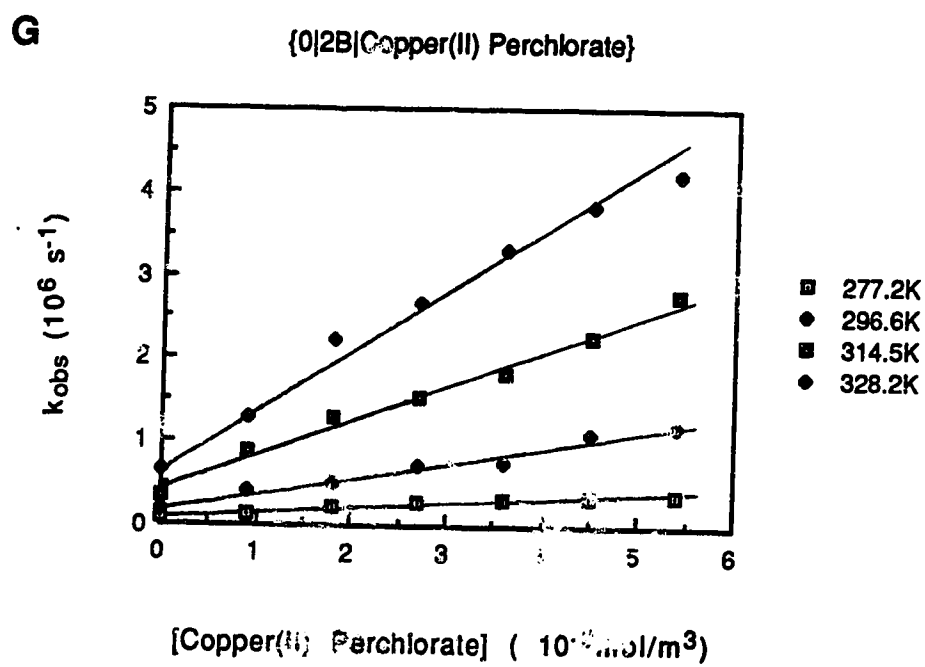
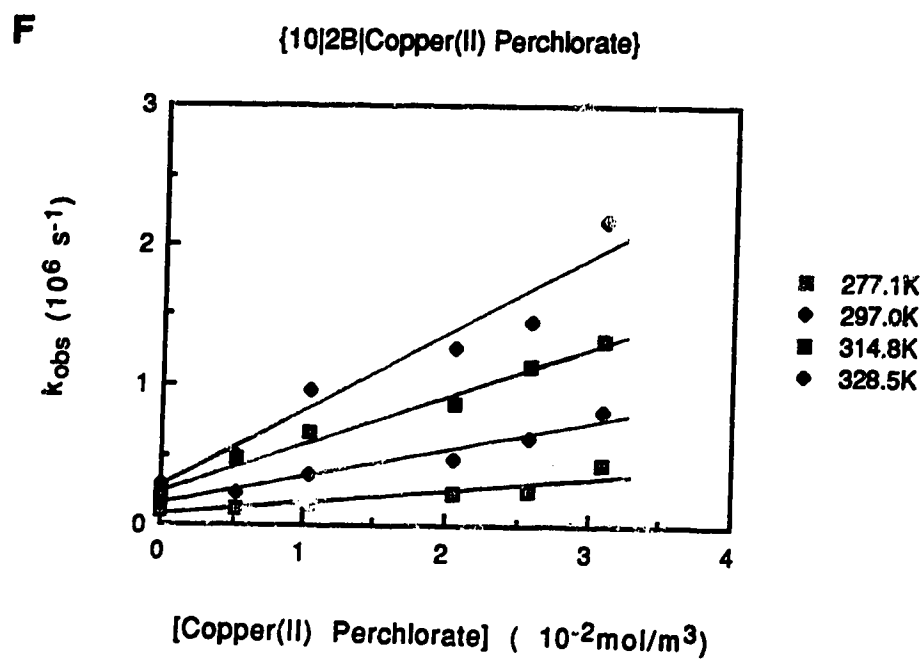


Table 31. Dielectric constants, f values and second-order rate constants for the reaction of solvated electrons with copper(II) perchlorate in 2-butanol/water mixtures at various temperatures.

X_w	Temp (K)	ϵ	f	k_2 ($10^7 \text{ m}^3/\text{mol}\cdot\text{s}$)	X_w	Temp (K)	ϵ	f	k_2 ($10^7 \text{ m}^3/\text{mol}\cdot\text{s}$)
1.00	280.0	85.7	3.0	2.5	0.34	277.2	20.2	11.9	0.95
	298.6	77.8	3.0	4.0		296.4	16.8	13.4	2.1
	315.3	72.2	3.1	5.6		314.5	14.5	14.6	4.3
	333.0	66.5	3.2	8.2		328.2	13.0	15.6	6.2
	349.4	61.5	3.3	11		342.8	11.6	16.8	9.1
	364.5	57.0	3.3	13					
0.97	277.5	78.6	3.2	2.0	0.20	277.2	19.2	12.5	1.1
	296.0	70.7	3.3	3.7		296.5	15.8	14.2	2.6
	314.1	64.2	3.4	5.4		314.5	13.5	15.7	5.0
	328.8	59.5	3.5	7.3		328.1	11.8	17.2	8.8
	343.7	55.7	3.6	9.6		342.8	10.2	19.1	12
						361.3	8.6	21.5	19
0.66	277.2	30.3	8.0	1.1	0.10	277.1	19.2	12.5	0.63
	296.5	26.4	8.5	2.3		297.0	15.7	14.3	1.9
	314.5	23.5	9.0	4.6		314.8	13.5	15.7	3.6
	328.2	21	9.5	7.3		328.5	11.8	17.2	5.3
	342.8	19.5	9.9	11					
0.52	277.2	23.3	10.3	0.88	0.00	277.2	20.5	11.7	0.61
	297.2	19.9	11.3	2.1		296.6	16.7	13.5	1.7
	314.5	17.6	12.1	3.7		314.5	14.0	15.2	4.1
	328.2	16.0	12.7	5.7		328.2	12.0	16.9	7.3
	342.9	14.6	13.3	8.5					

Table 32. Rate parameters for the reaction of solvated electrons with copper(II) perchlorate in 2-butanol/water mixtures.

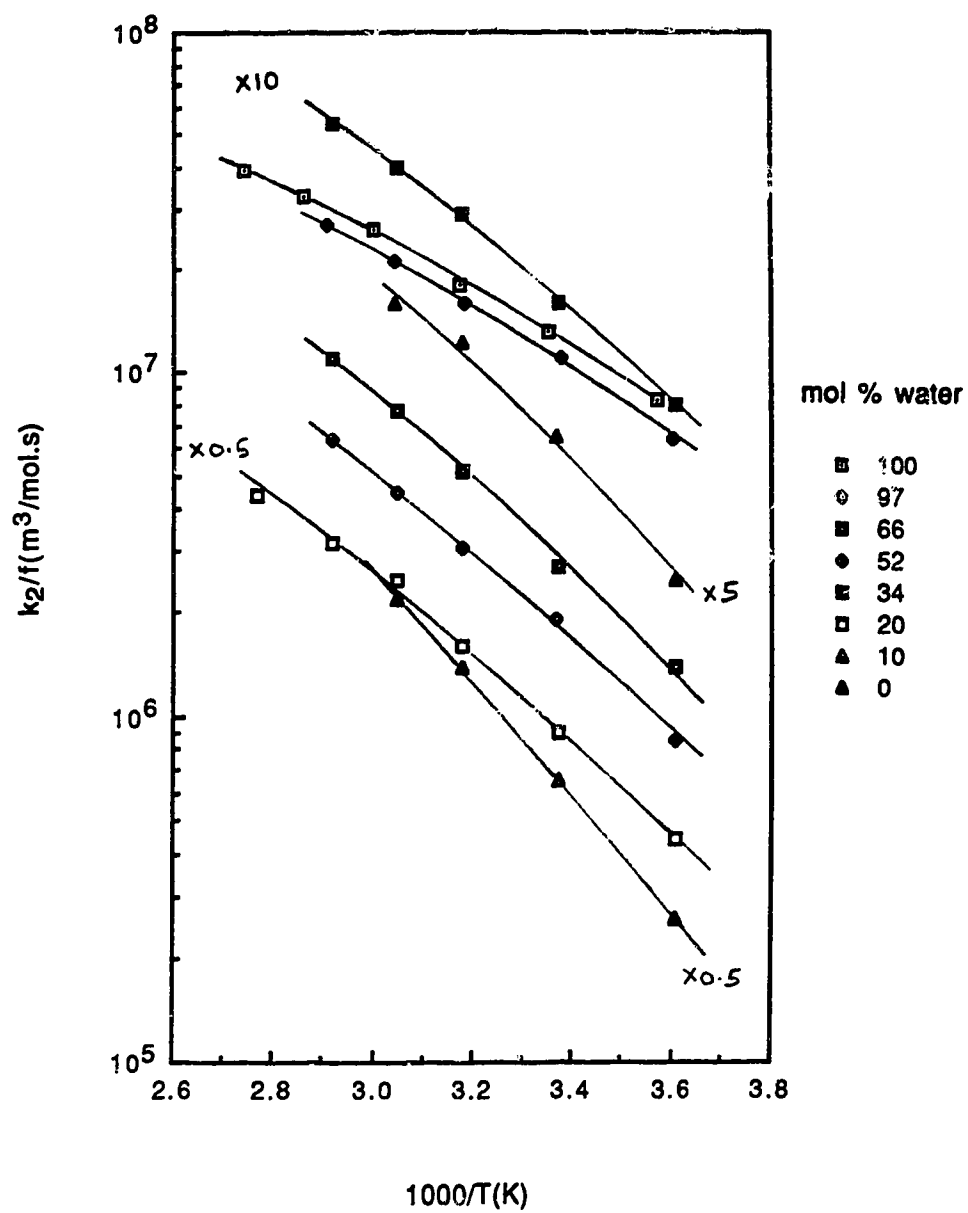
X_w	$\eta^{(a)}$ (10^{-3} Pa·s)	$k_2^{(a)}$ (10^7 m ³ /mol·s)	$k_2/f^{(a)}$ (10^7 m ³ /mol·s)	$E_2^{(b,c)}$ (kJ/mol)	$\log A_2^{(c)}$ (A_2 in m ³ /mol·s)
1.00	0.89	3.9	1.3	18	10.25
0.97	1.45	3.7	1.1	17	10.09
0.66	3.32	2.6	0.30	26	11.00
0.52	3.08	2.1	0.19	24	10.52
0.34	2.85	2.4	0.18	24	10.41
0.20	2.74	2.6	0.18	24	10.50
0.10	2.78	2.0	0.18	27	10.83
0.00	3.05	1.9	0.14	32	11.76

(a) At 298K.

(b) Near 298K.

(c) From Arrhenius plots of k_2/f .

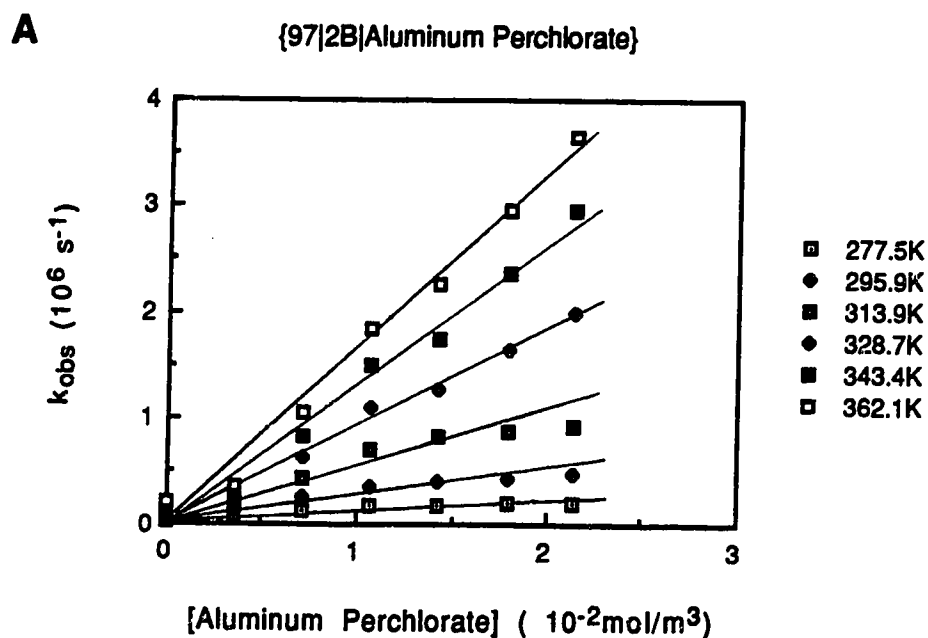
Fig. 39 Arrhenius plots for the reaction of solvated electrons with copper(II) perchlorate in 2-butanol/water mixtures

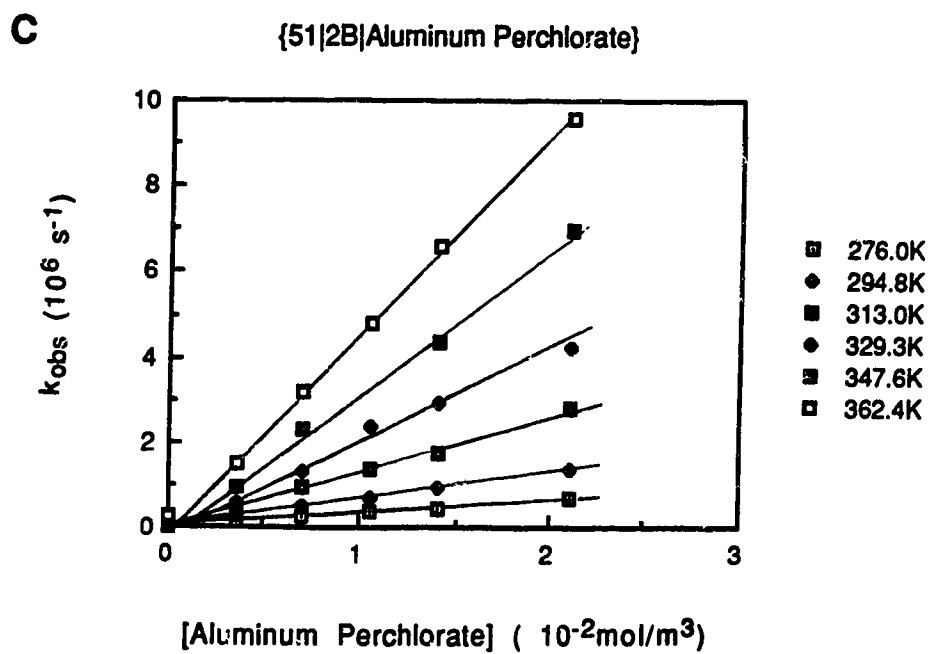
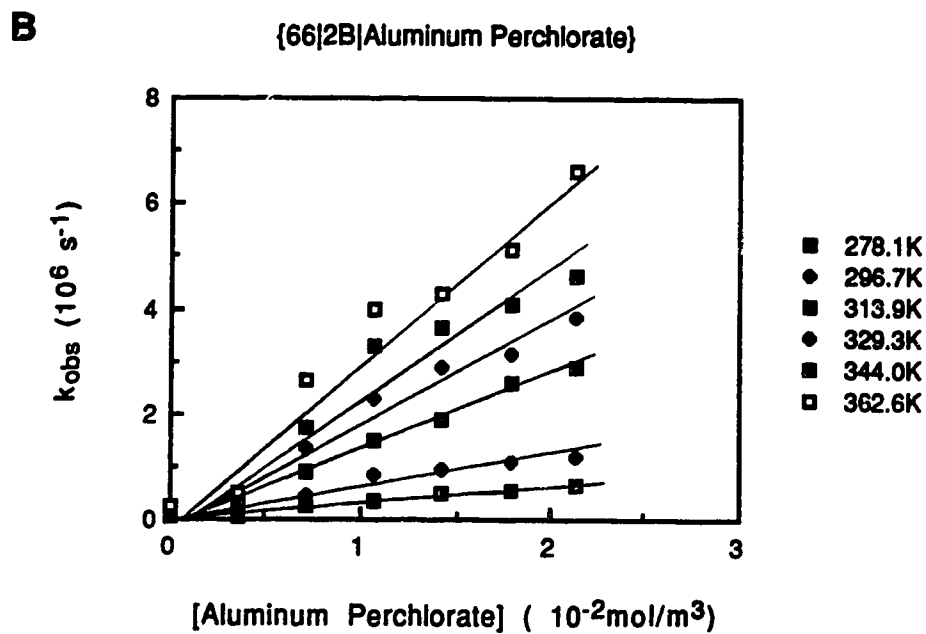


E. Reaction of Solvated Electrons with Aluminum Ions

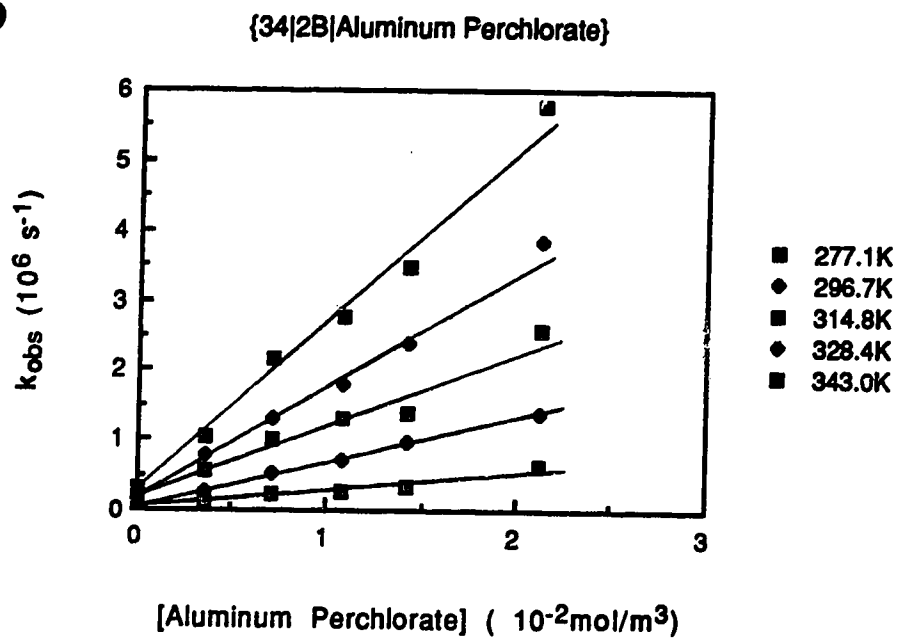
The temperature and concentration dependence of the first-order rate constant for the reaction of solvated electrons with aluminum ion are shown in Figure 40 (A-G). The concentration range was 2-24 mmol/m³. Table 33 shows the second-order rate constants, dielectric constants and the coulombic factor *f* at various temperatures in different alcohol/water mixtures. Table 34 shows the rate parameters obtained for the modified Arrhenius plots shown in Figure 41.

Fig. 40
(A-G) Temperature and concentration dependence of the first-order rate constant for the reaction of solvated electrons with aluminum perchlorate in 2-butanol/water mixtures

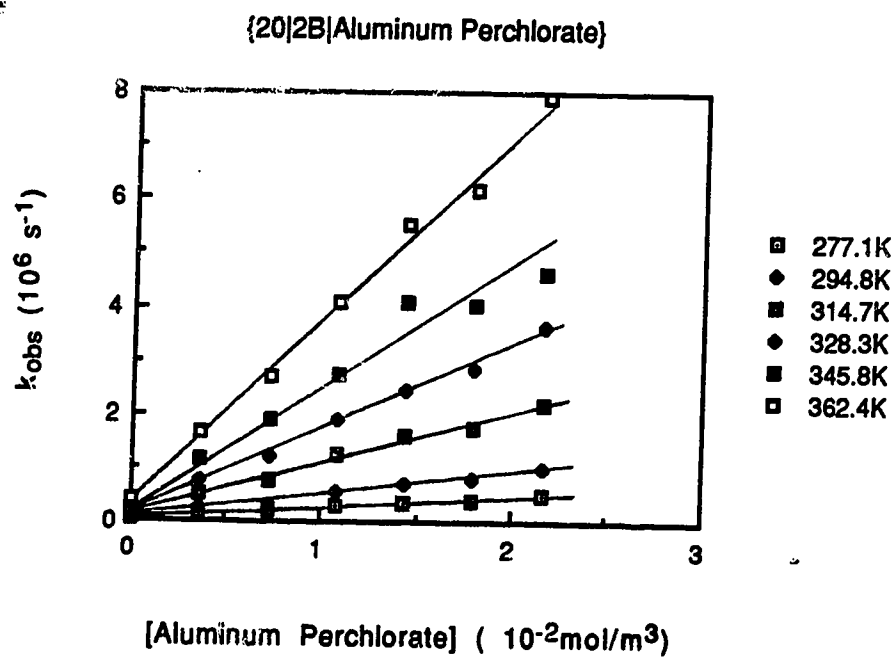




D

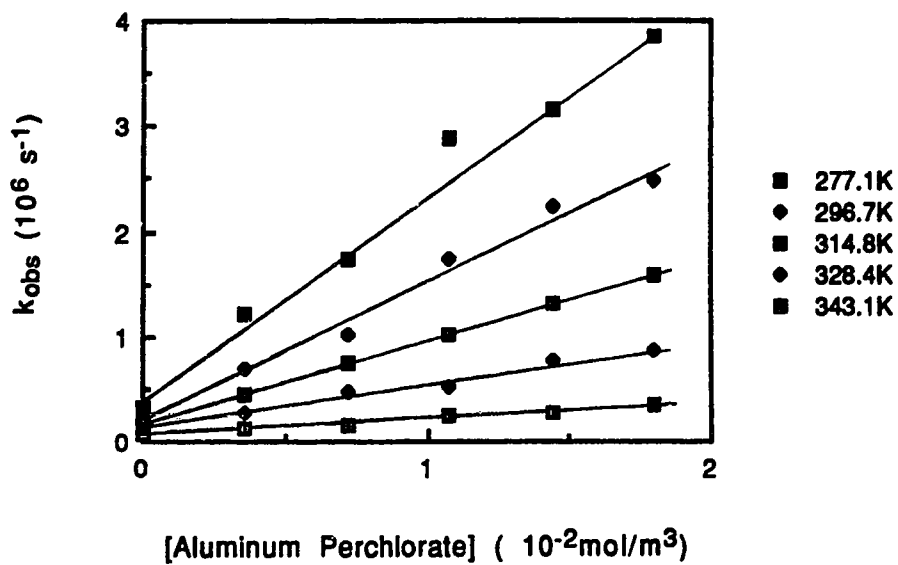


E



F

{10|2B|Aluminum Perchlorate}



G

{0|2B|Aluminum Perchlorate}

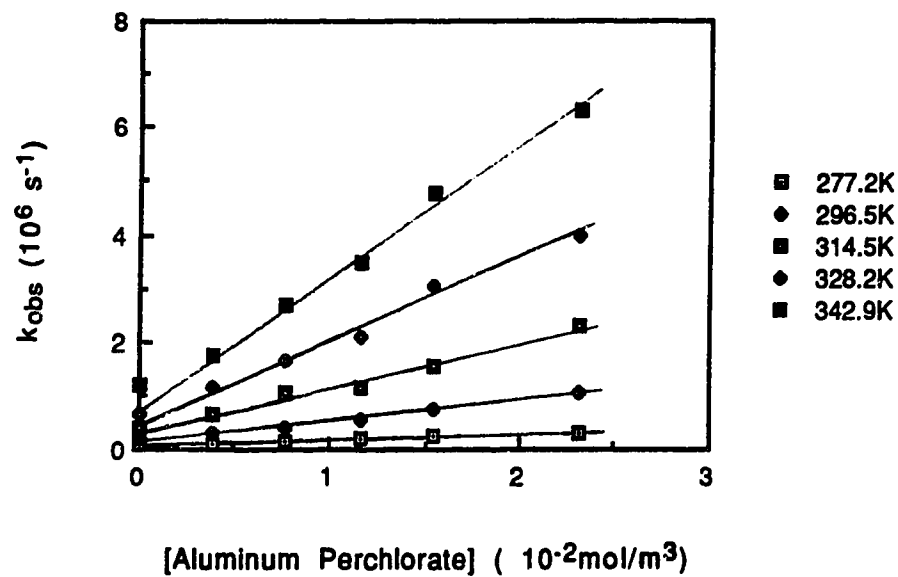


Table 33. Dielectric constants, f values and second-order rate constants for the reaction of solvated electrons with aluminum perchlorate in 2-butanol-water mixtures at various temperatures.

X_w	Temp (K)	ϵ	f	k_2 ($10^7 \text{ m}^3/\text{mol}\cdot\text{s}$)	X_w	Temp (K)	ϵ	f	k_2 ($10^7 \text{ m}^3/\text{mol}\cdot\text{s}$)
1.00	276.1	87.5	5.9	0.91	0.34	277.1	20.2	25.6	2.1
	296.6	79.0	6.1	2.0		296.7	16.8	28.7	5.6
	314.6	72.5	6.3	4.3		314.8	14.5	31.3	9.6
	328.6	68.0	6.4	8.6		328.4	13.0	33.5	15
	343.8	63.0	6.6	11		343.0	11.6	36.0	23
	361.4	57.9	6.8	14					
0.97	277.5	78.6	6.6	1.1	0.20	277.1	19.2	26.9	2.2
	295.9	70.7	6.8	2.6		294.8	16.0	30.3	4.4
	313.9	64.2	7.1	5.6		314.7	13.3	34.2	9.5
	328.7	59.5	7.3	9.1		328.3	11.8	36.9	15
	343.4	55.8	7.5	13		345.8	10.0	41.4	23
	362.1	51.3	7.7	16		362.4	8.5	46.4	35
0.66	278.1	30.0	17.1	3.6	0.10	277.1	19.2	26.9	1.5
	296.7	26.4	18.3	6.6		296.7	15.8	30.5	4.0
	313.9	23.5	19.4	15		314.8	13.5	33.7	7.8
	329.3	21.5	20.2	20		328.4	11.8	36.9	13
	344.0	19.6	21.2	26		343.1	10.1	41.3	19
	362.6	16.0	24.7	31					
0.51	276.0	23.6	22.0	3.1	0.00	277.2	20.5	25.2	1.6
	294.8	20.2	24.0	6.6		296.5	16.7	28.9	4.2
	313.0	17.9	25.5	13		314.5	14.0	32.5	8.3
	329.3	16.1	27.0	22		328.2	12.0	36.3	16
	347.6	14.3	28.8	34		342.9	10.0	41.7	26
	362.4	13.0	30.4	47					

Table 34. Rate parameters for the reaction of solvated electrons with aluminum perchlorate in 2-butanol/water mixtures.

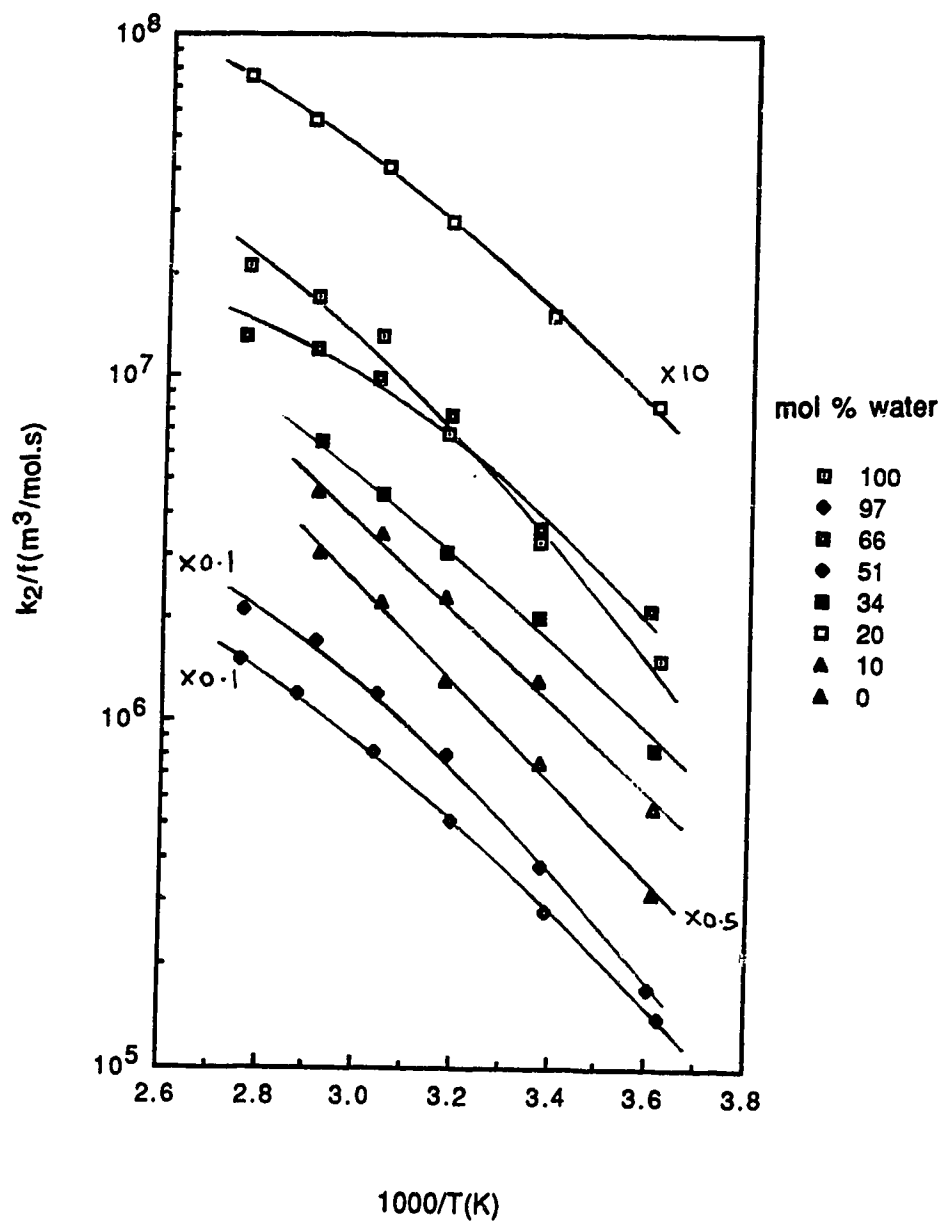
X_w	$\eta^{(a)}$ (10^{-3} Pa·s)	$k_2^{(a)}$ (10^7 m ³ /mol·s)	$k_2/f^{(a)}$ (10^7 m ³ /mol·s)	$E_2^{(b,c)}$ (kJ/mol)	$\log A_2^{(c)}$ (A_2 in m ³ /mol·s)
1.00	0.89	2.5	0.41	34	11.79
0.97	1.45	3.0	0.43	28	11.60
0.66	3.32	8.0	0.44	24	10.76
0.51	3.06	7.8	0.32	25	10.91
0.34	2.85	5.5	0.19	23	10.38
0.20	2.74	5.3	0.17	24	10.36
0.15	2.78	4.2	0.14	26	10.60
0.00	3.05	4.5	0.16	27	10.95

(a) At 298K.

(b) Near 298K.

(c) From Arrhenius plots of k_2/f .

Fig. 41 Arrhenius plots for the reaction of solvated electrons with aluminum perchlorate in 2-butanol/water mixtures



V. Conductivities of Inorganic Electrolytes in Alcohol/Water Mixtures

The conductivities of lithium nitrate, lithium chromate, perchloric acid, silver perchlorate, thallium acetate, copper(II) perchlorate, and aluminum perchlorate were measured at various temperatures ranging from 277K to 353K in 1-propanol/water, 2-propanol/water, and 2-butanol/water mixed solvents.

A. 1-Propanol/Water Mixtures

The molar conductances (Λ) of the electrolytes were obtained from the specific conductance *versus* electrolyte concentration plots: LiNO_3 , (Figure 42 (A-H)); Li_2CrO_4 , Figure 43 (A-F); HClO_4 , Figure 44 (A-H); AgClO_4 , Figure 45 (A-I); $\text{Cu}(\text{ClO}_4)_2$, Figure 46 (A-J); $\text{Al}(\text{ClO}_4)_3$, Figure 47 (A-H). The activation energy (E_A) for the ion migration process was obtained from the plots of molar conductance *versus* $1/\text{Temp}$. The Arrhenius plots of the molar conductance are shown in Figure 48 for LiNO_3 , Figure 49 for Li_2CrO_4 , Figure 50 for HClO_4 , Figure 51 for AgClO_4 , Figure 52 for $\text{Cu}(\text{ClO}_4)_2$, and Figure 53 for $\text{Al}(\text{ClO}_4)_3$. The results are summarized in Figure 54 and Tables 35-40.

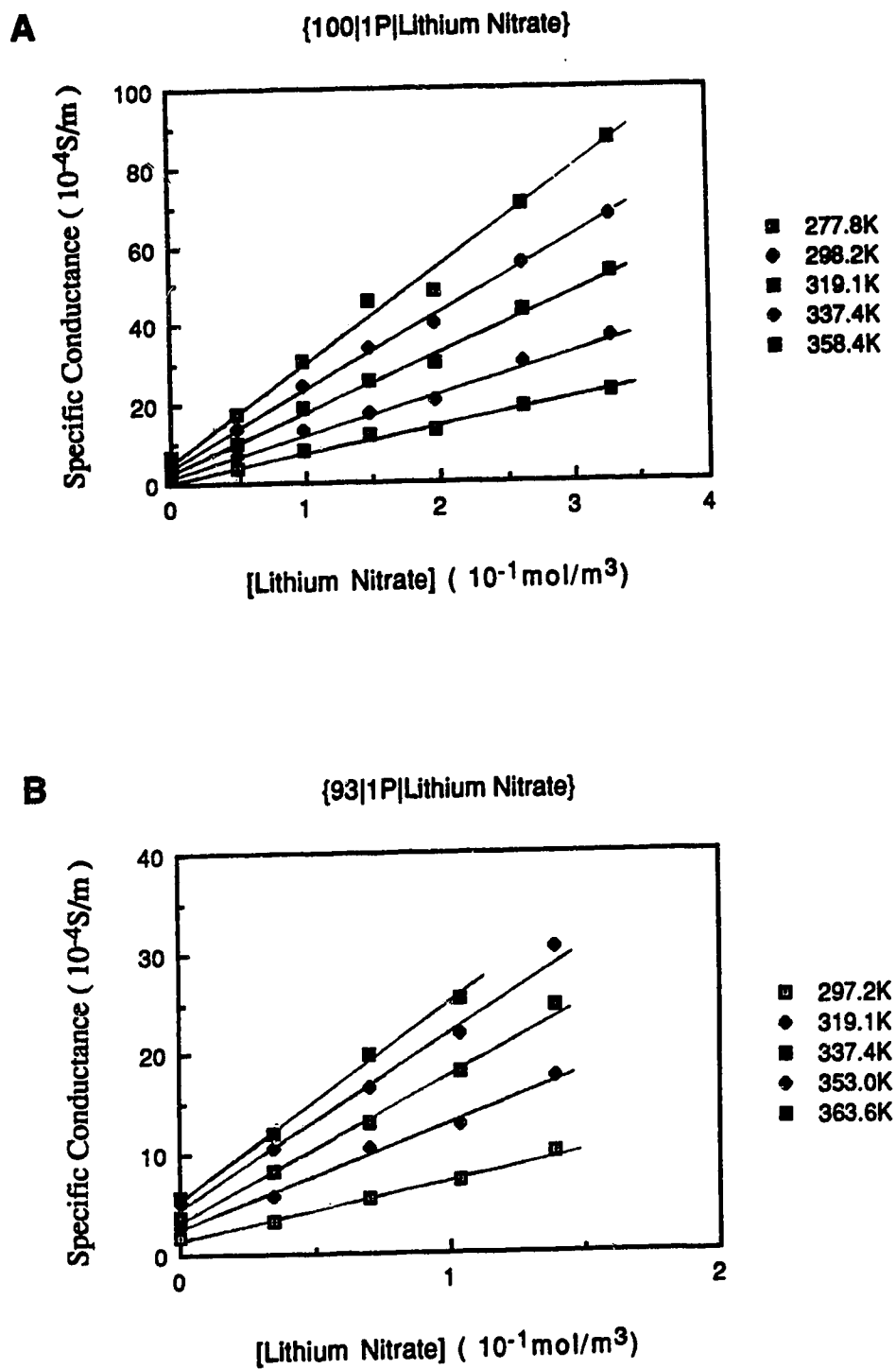
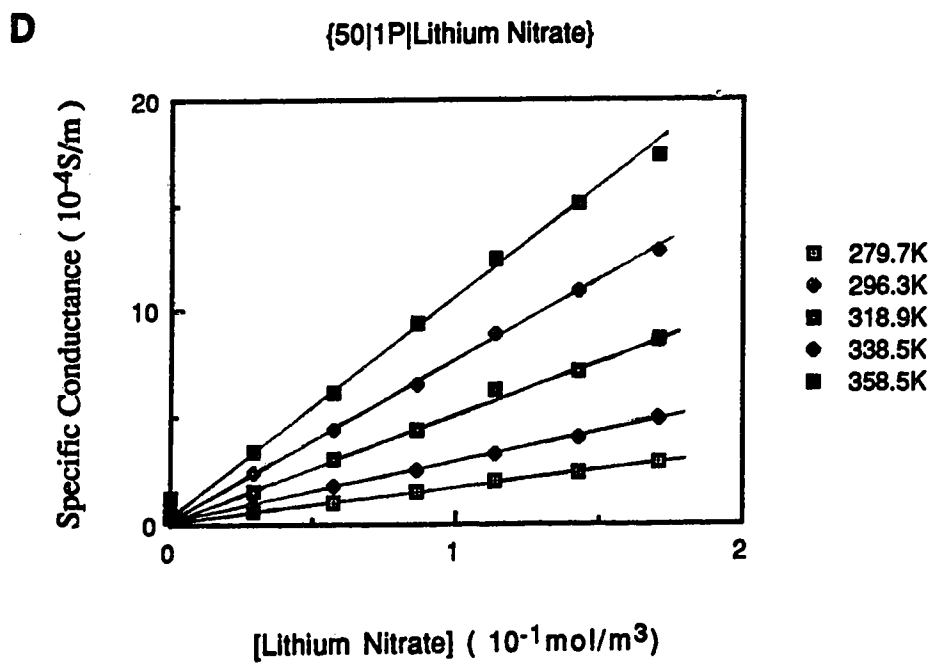
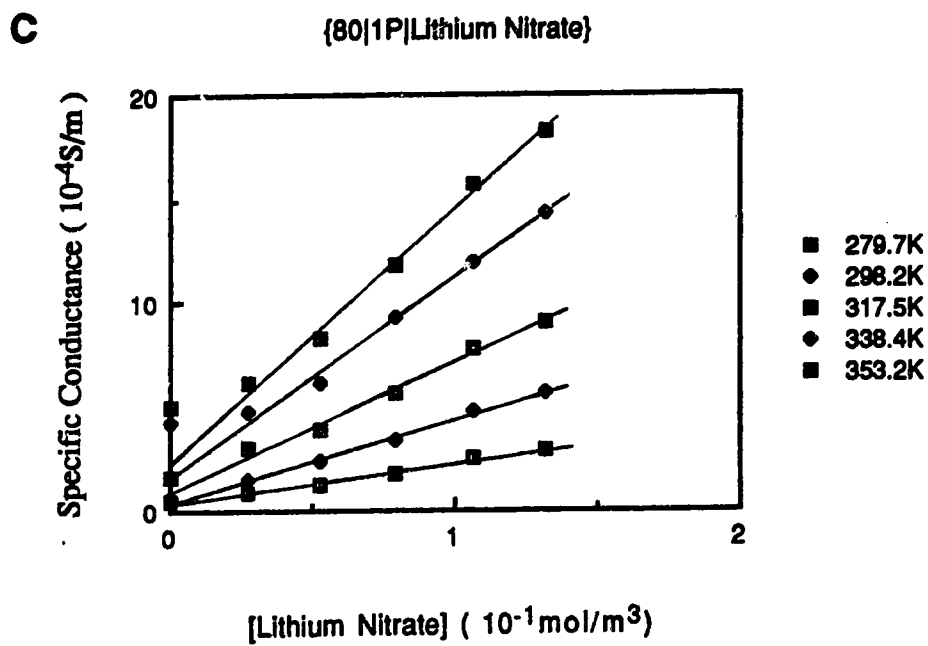
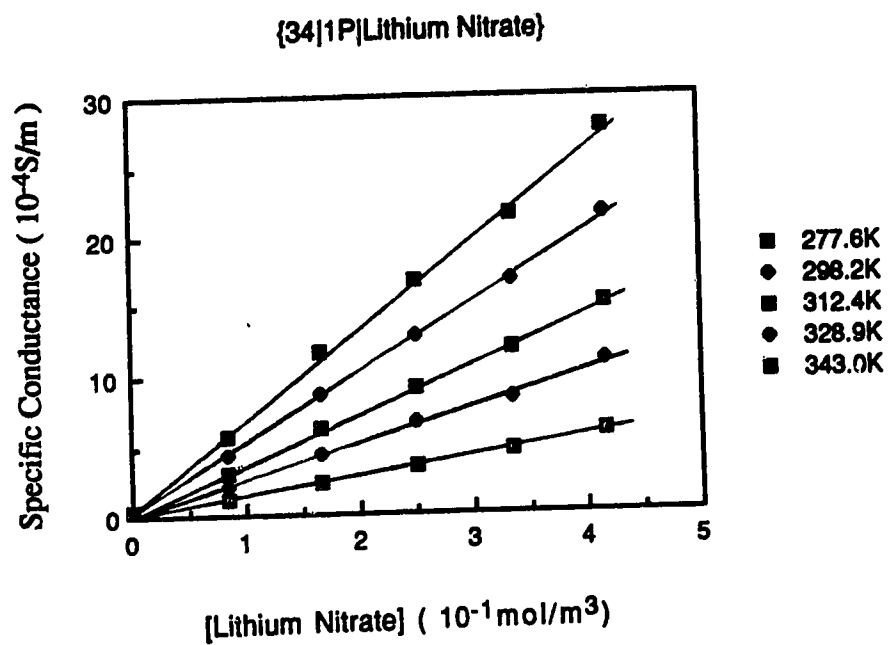
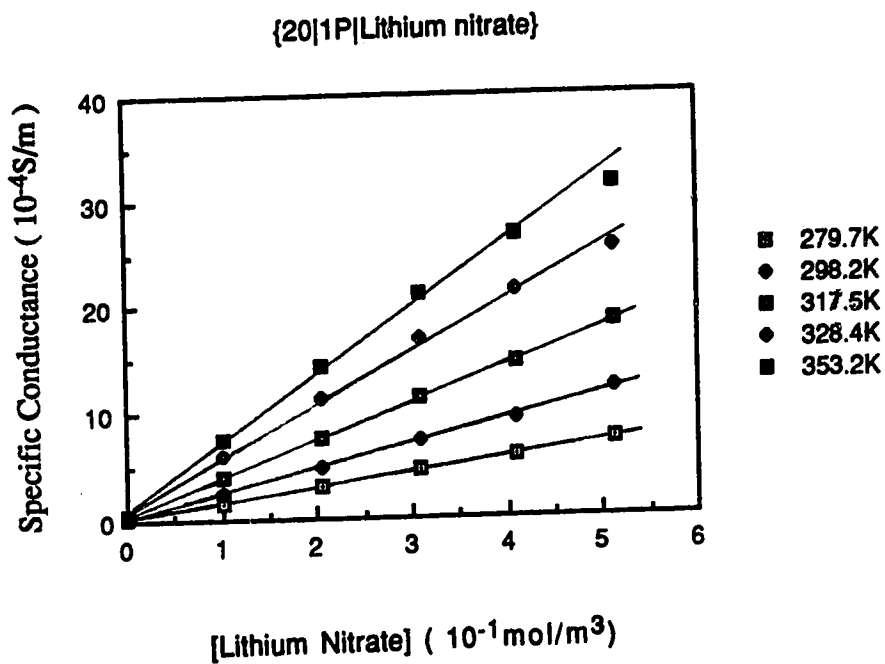


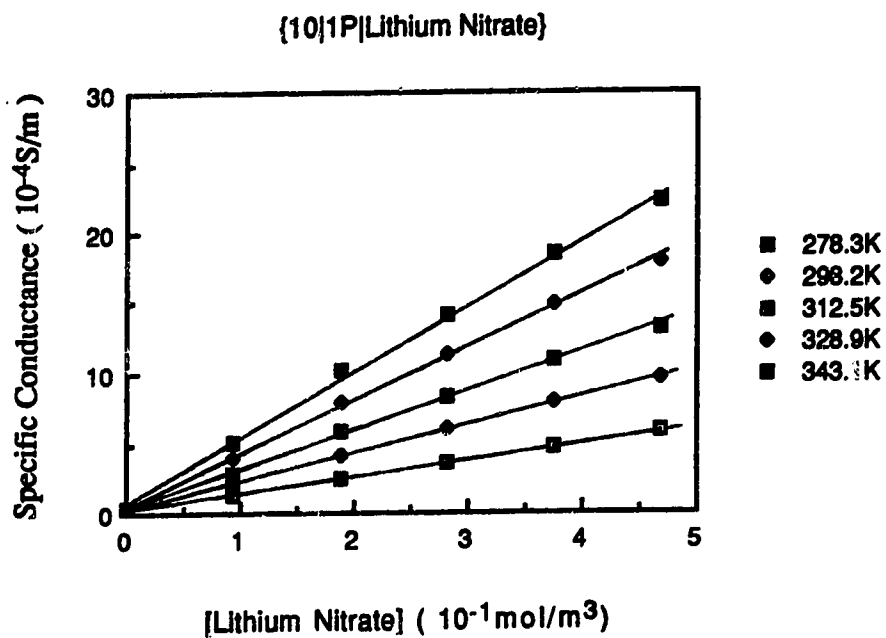
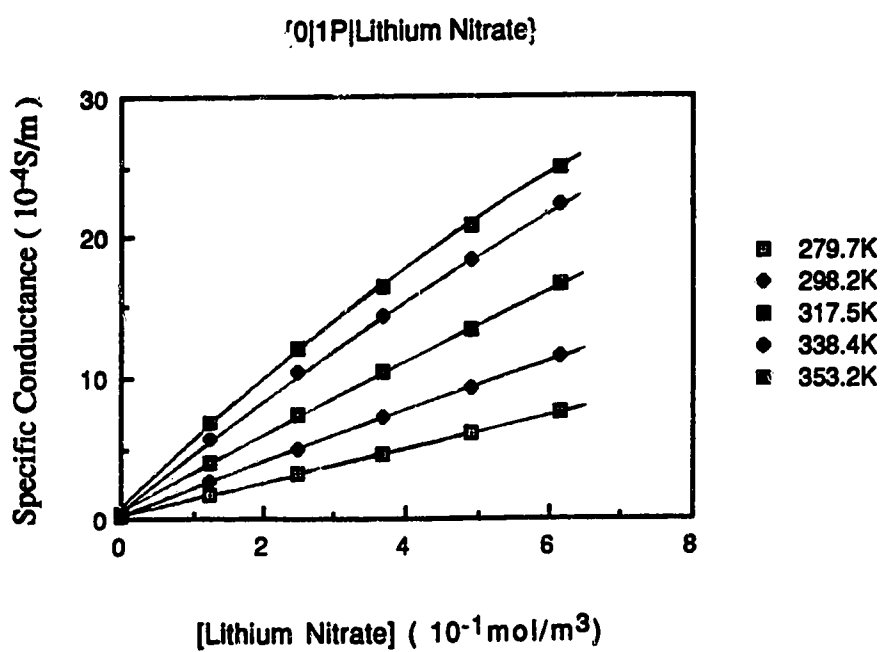
Fig.42

(A-H)

Temperature and concentration dependence of the conductance of lithium nitrate in 1-propanol/water mixtures



E**F**

G**H**

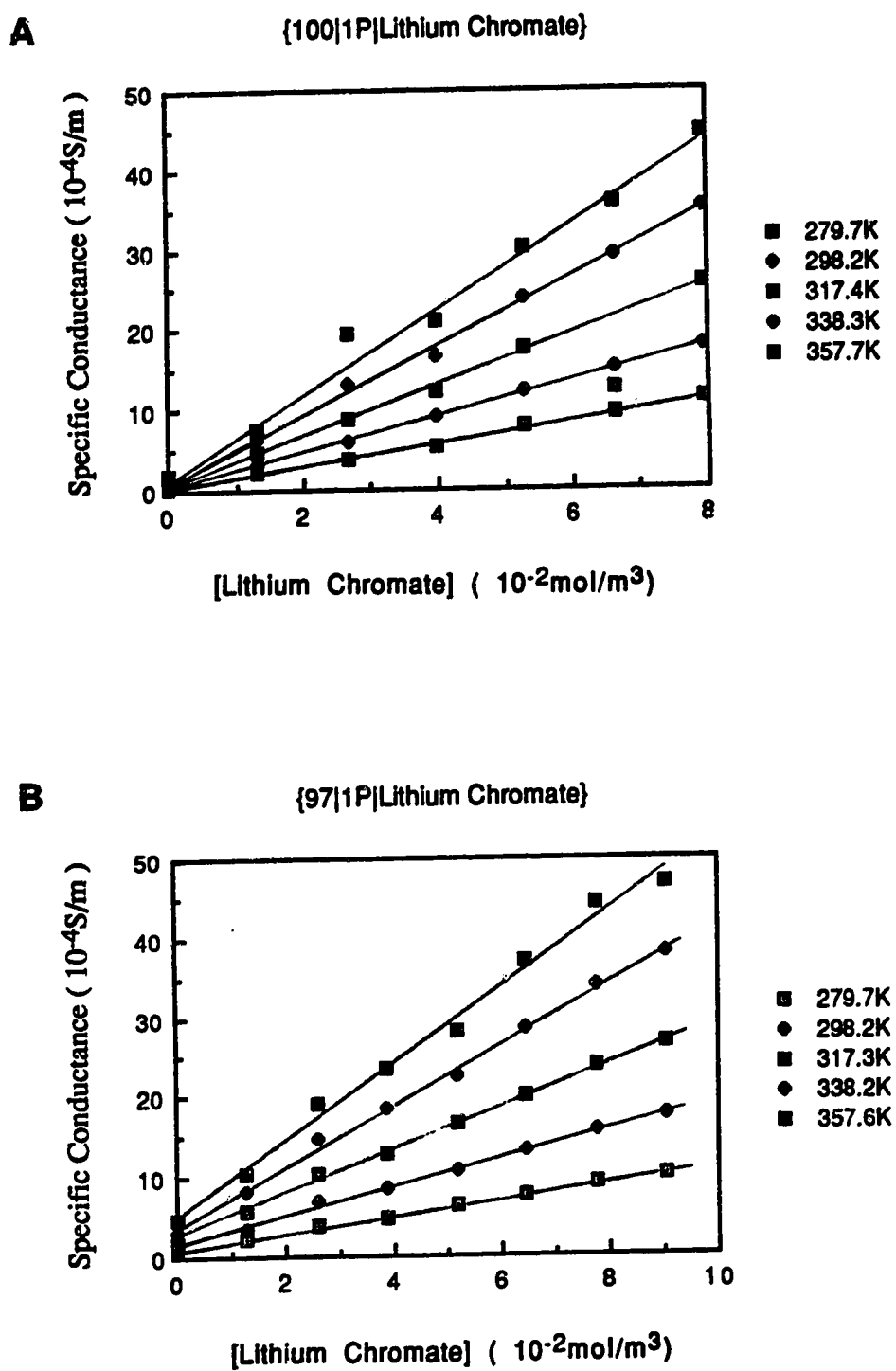
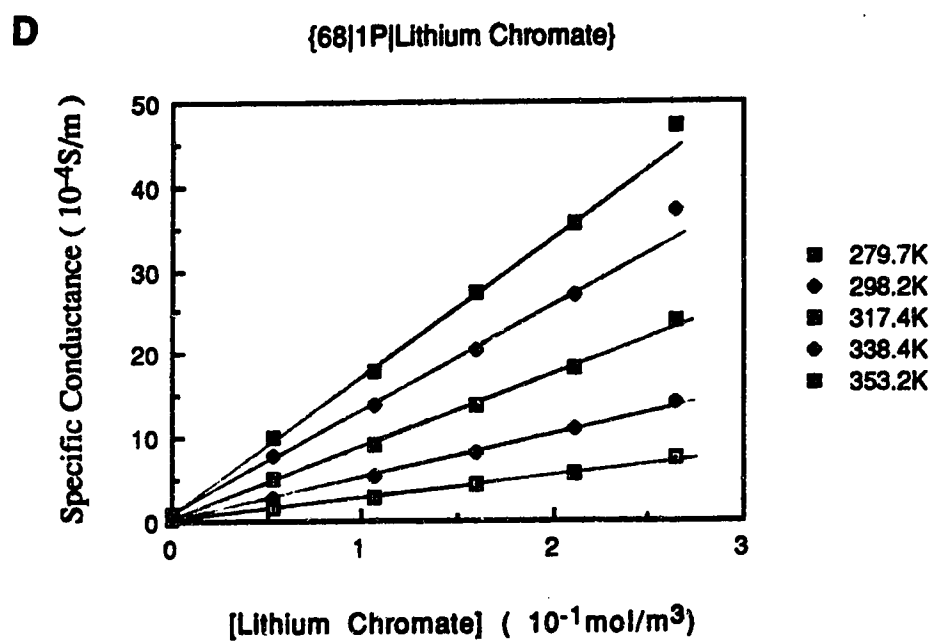
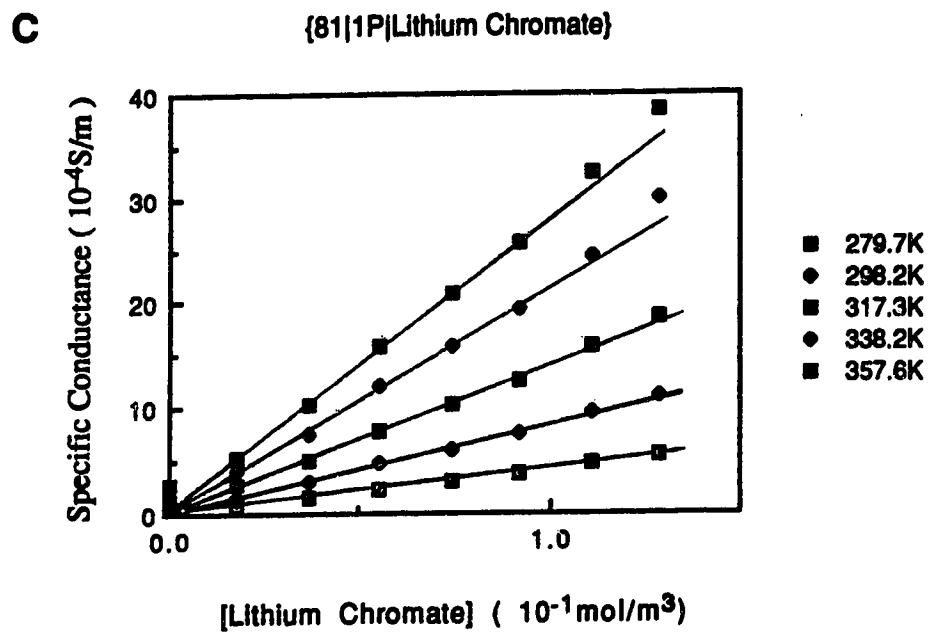
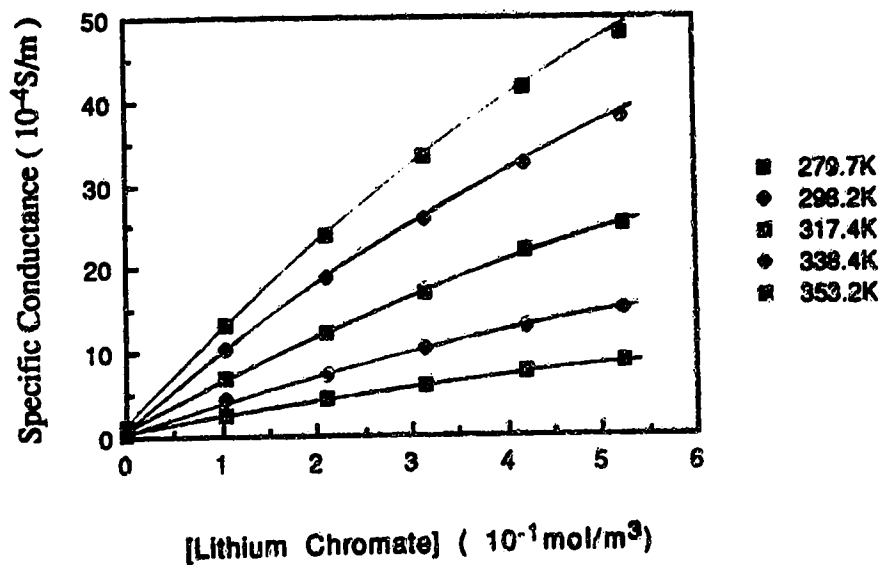


Fig.43 Temperature and concentration dependence of the conductance of
(A-F) lithium chromate in 1-propanol/water mixtures



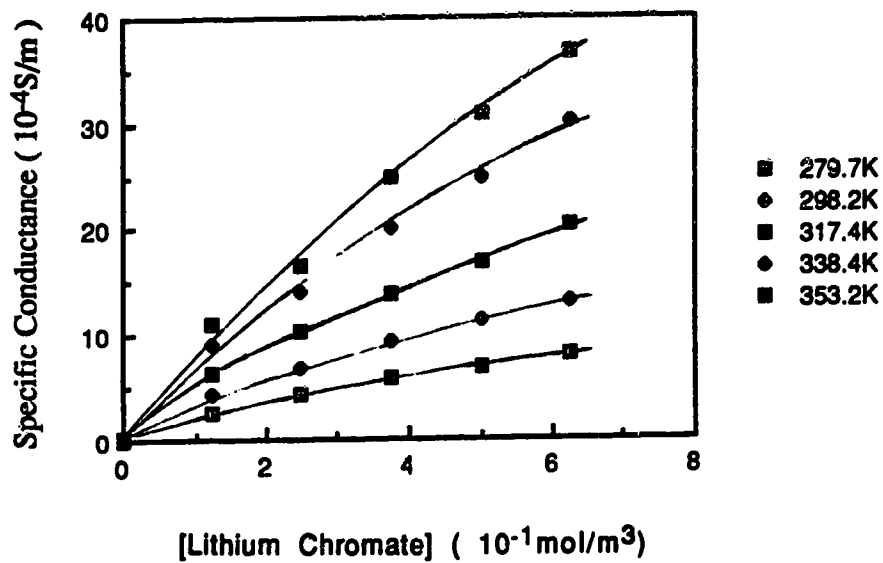
E

{35}1P[Lithium Chromate]



F

{22}1P[Lithium Chromate]



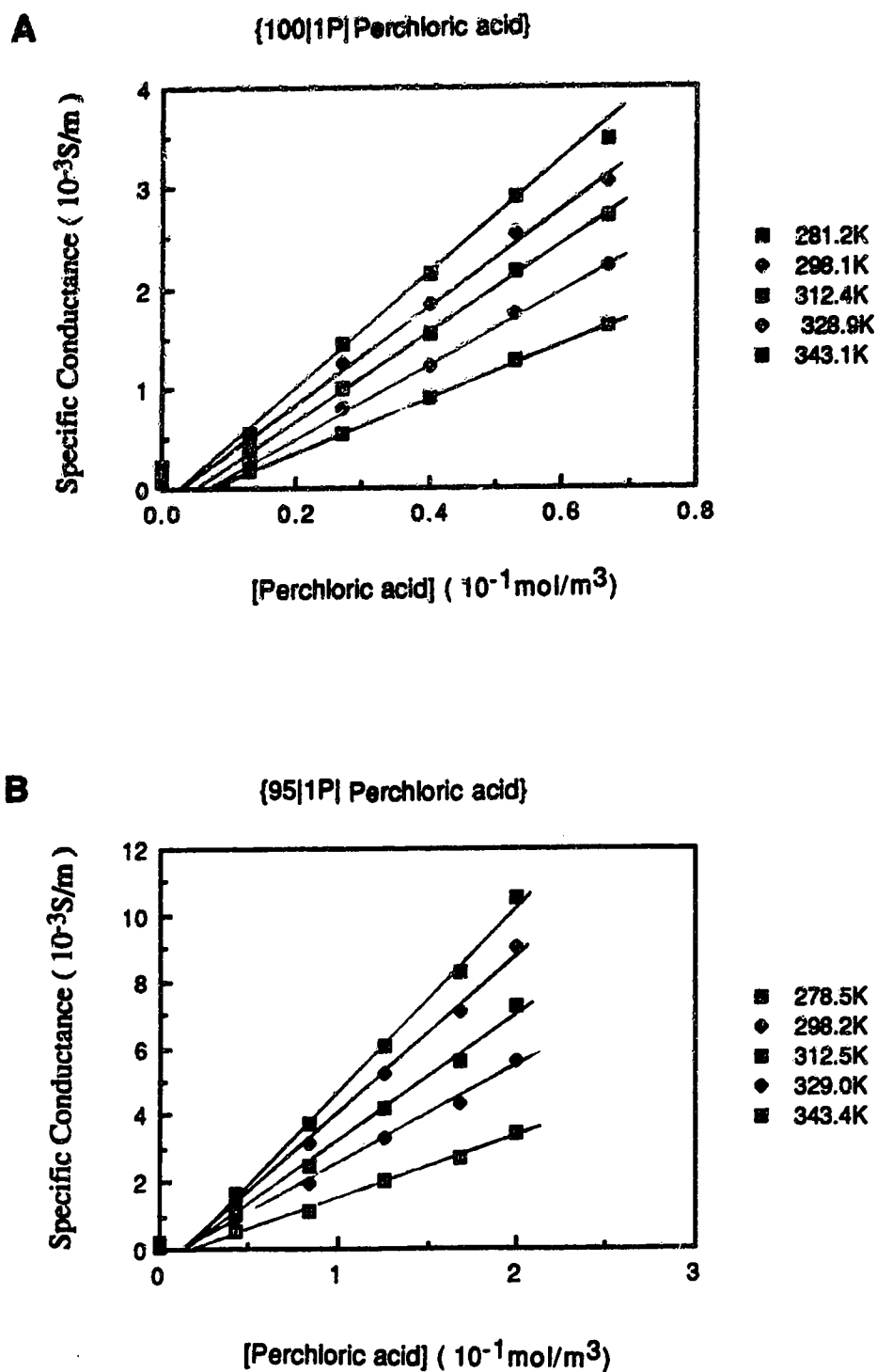
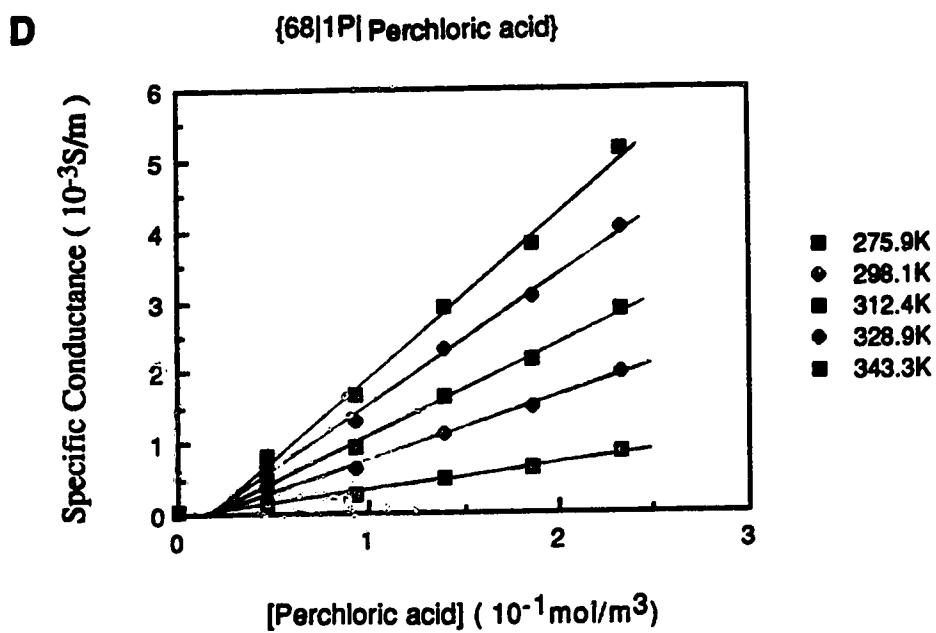
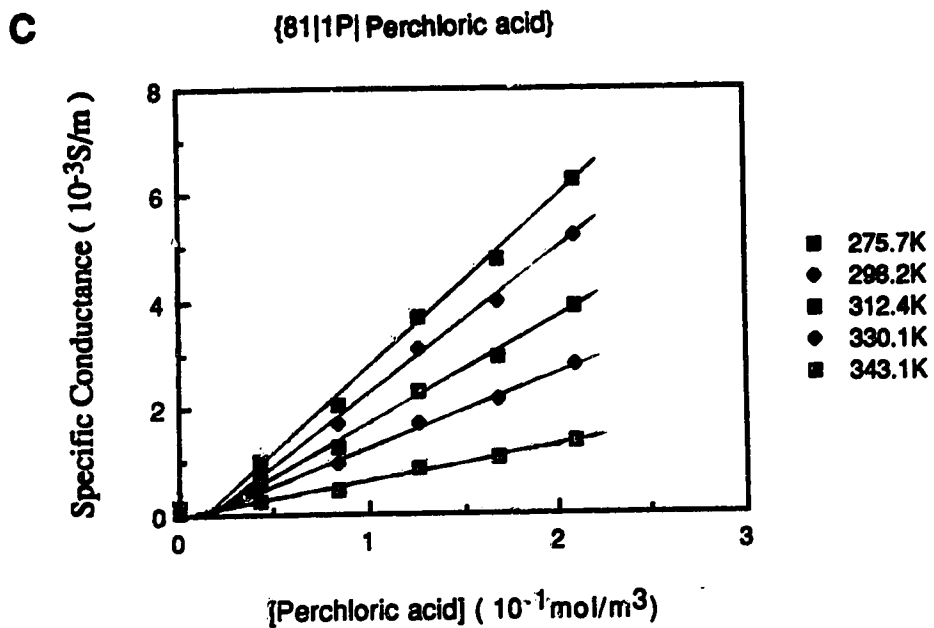
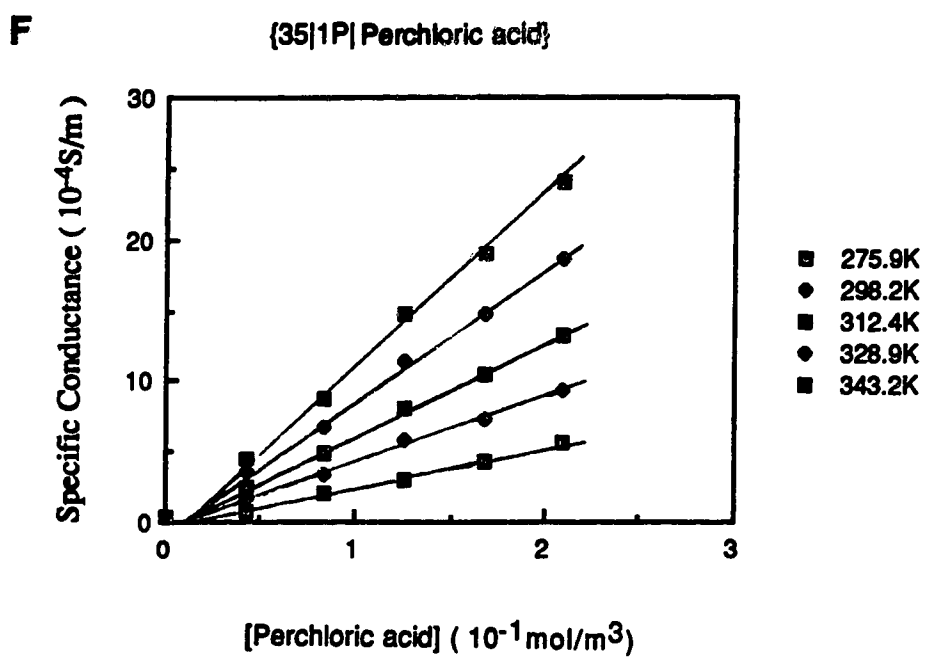
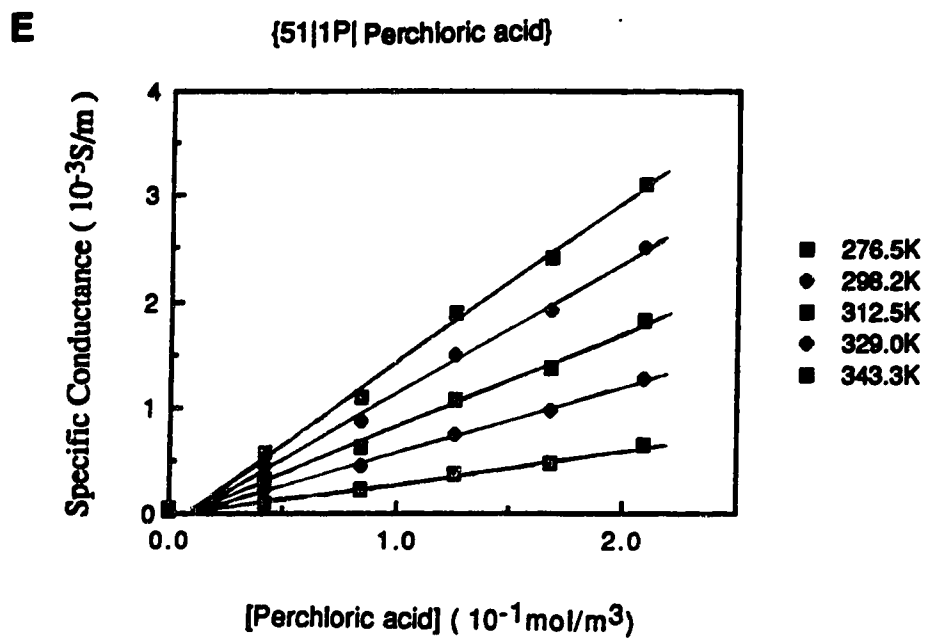
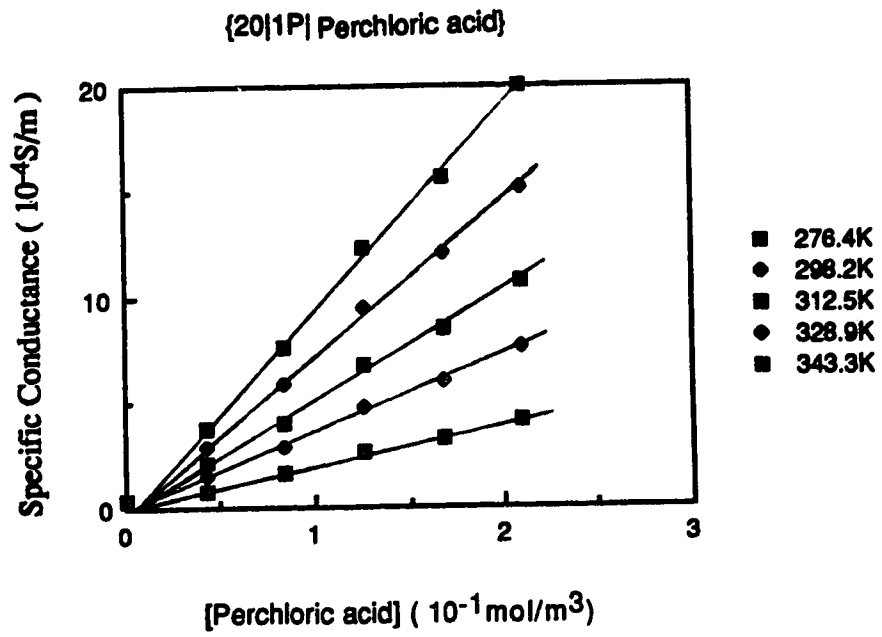
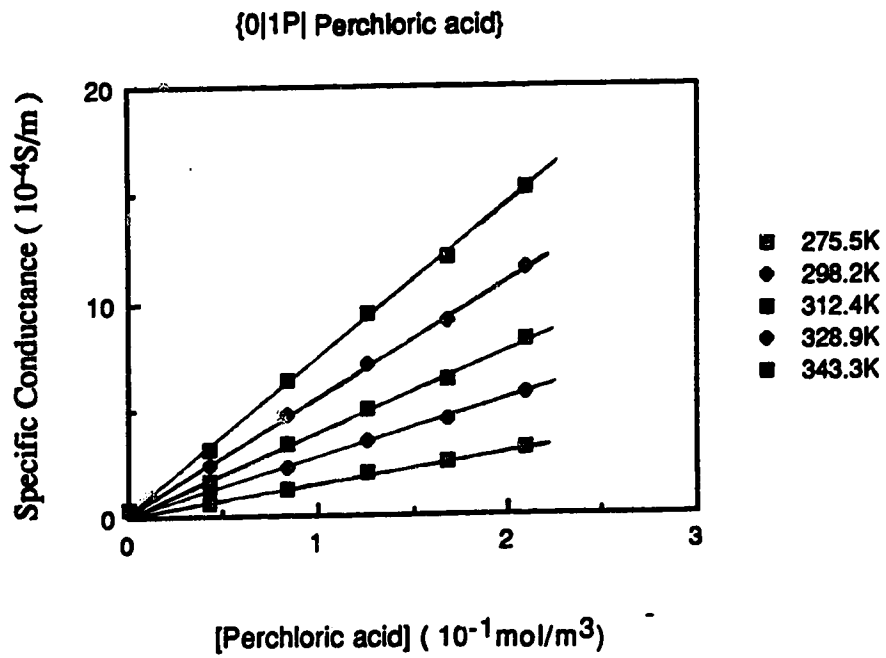


Fig.44
(A-H)

Temperature and concentration dependence of the conductance of
perchloric acid in 1-propanol/water mixtures





G**H**

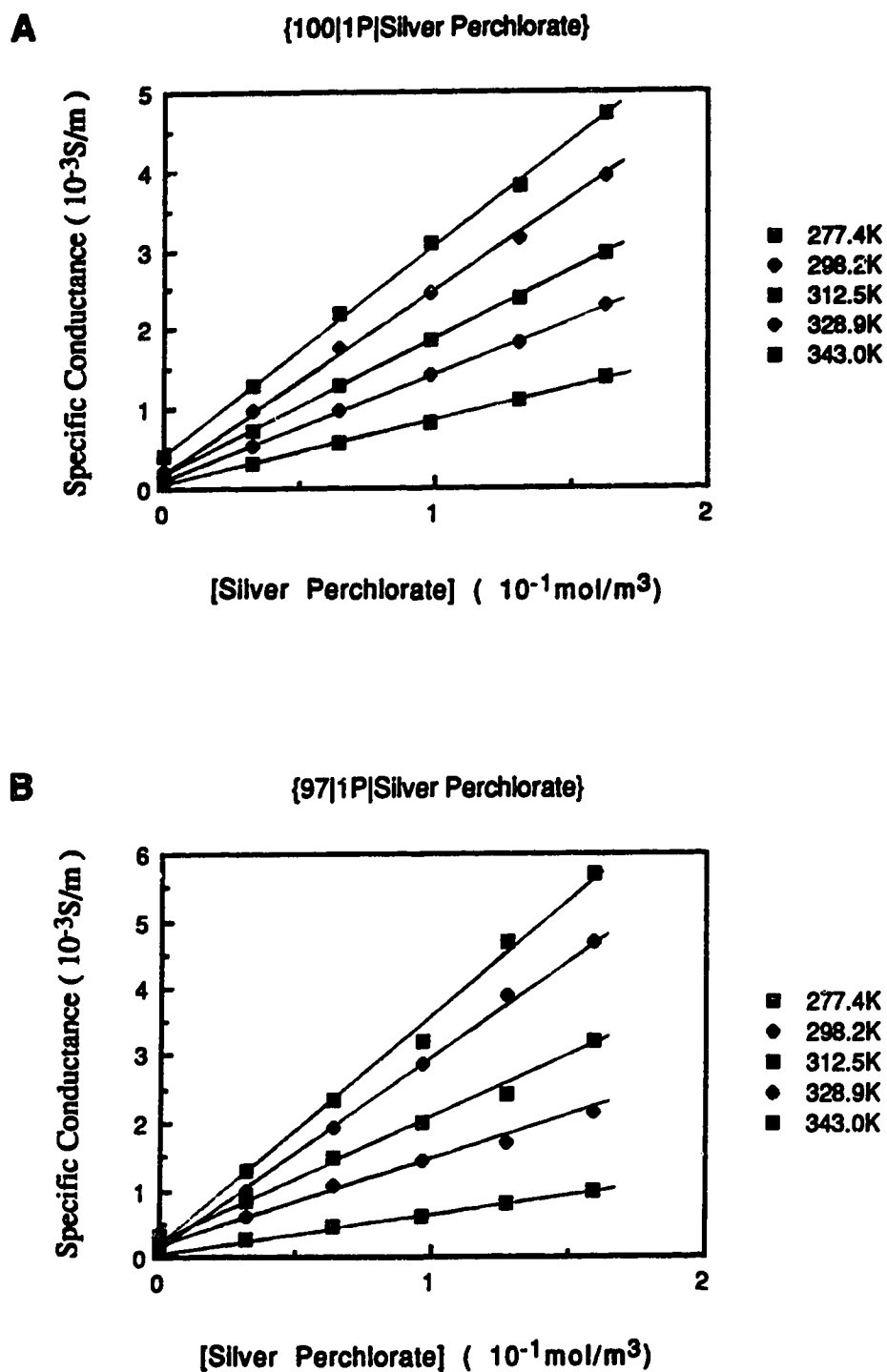
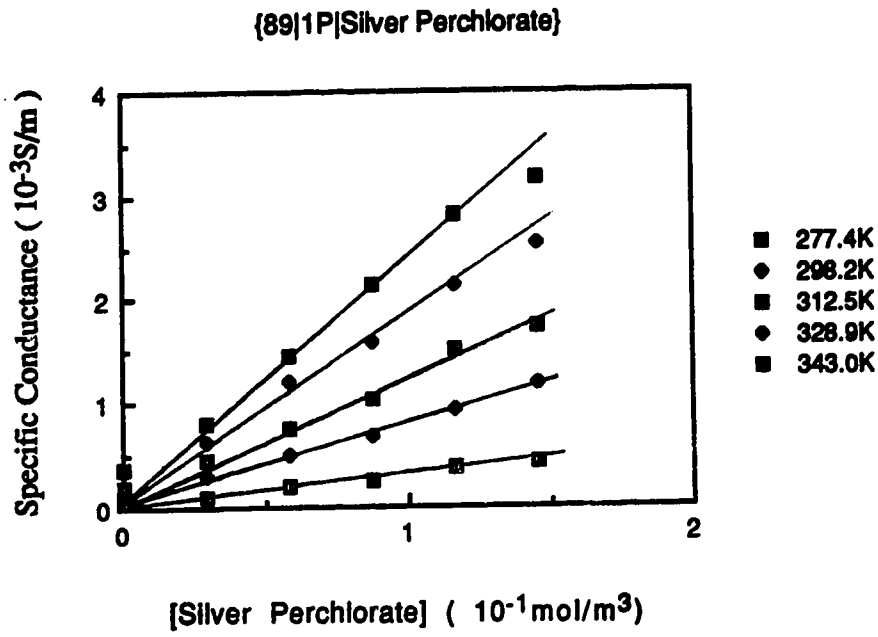
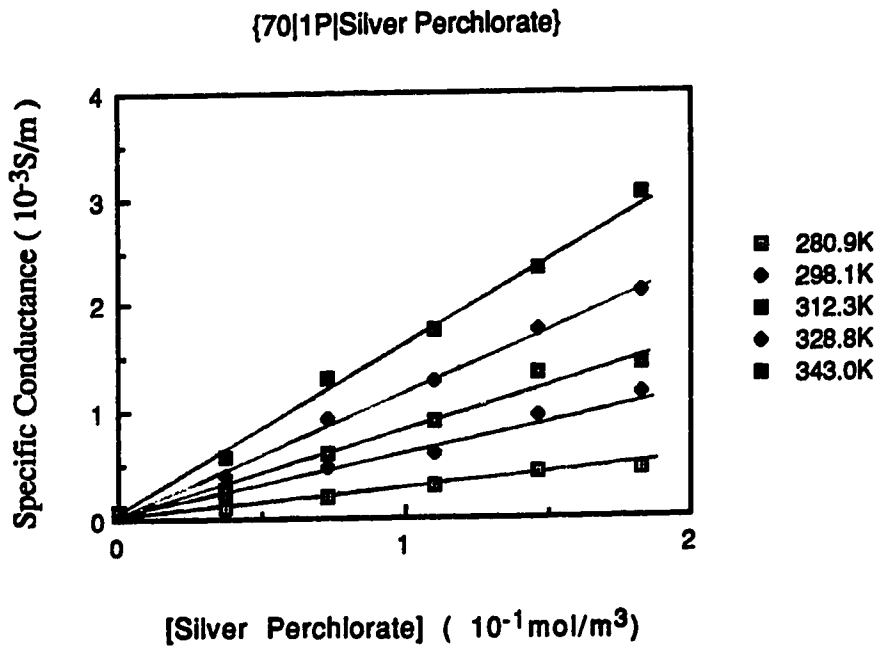


Fig.45

Temperature and concentration dependence of the conductance of

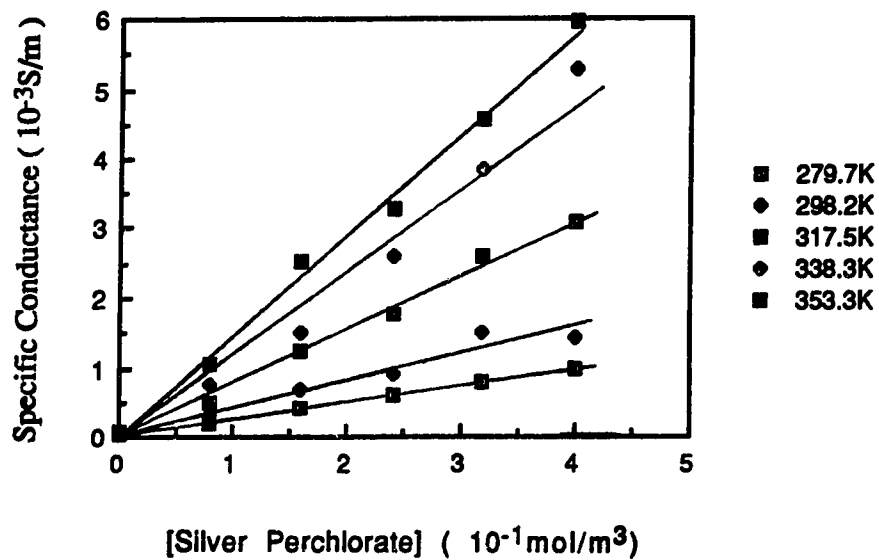
(A-I)

silver perchlorate in 1-propanol/water mixtures

C**D**

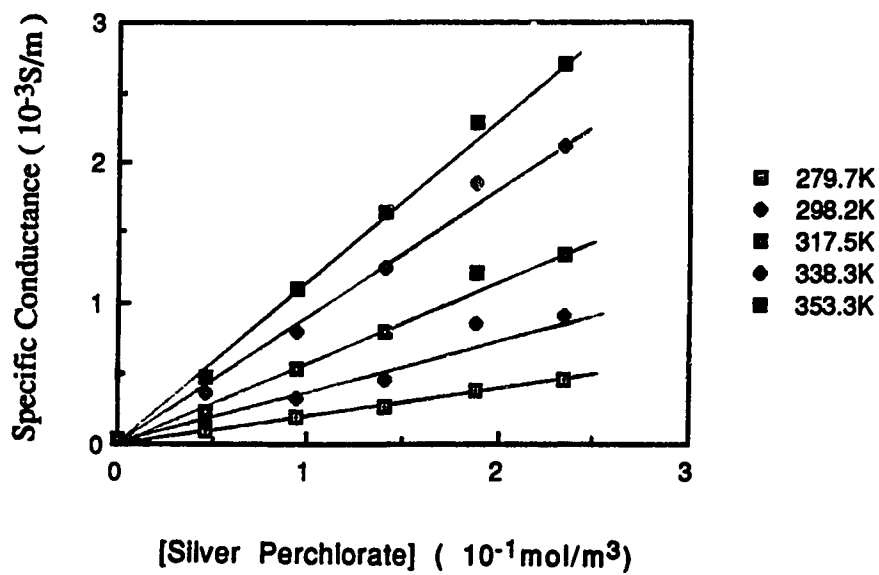
E

{50|1P|Silver Perchlorate}



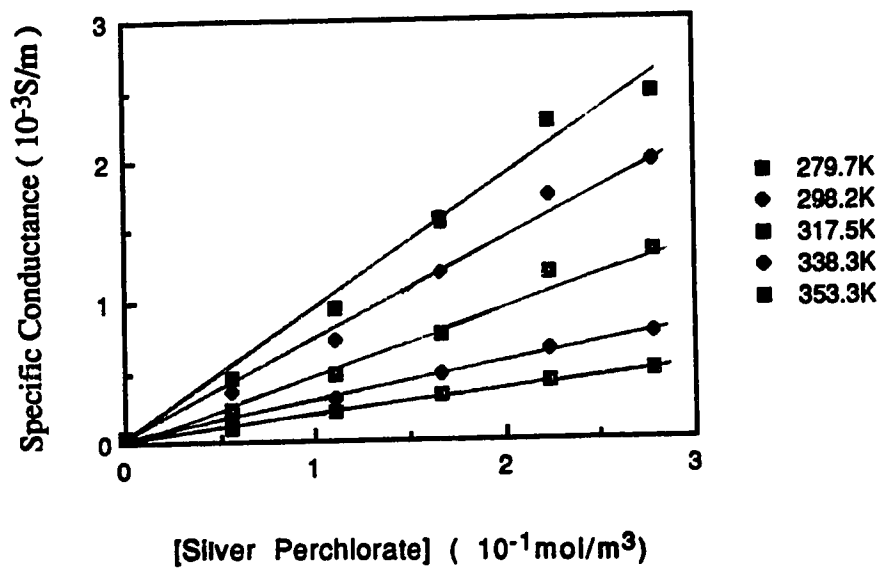
F

{36|1P|Silver Perchlorate}



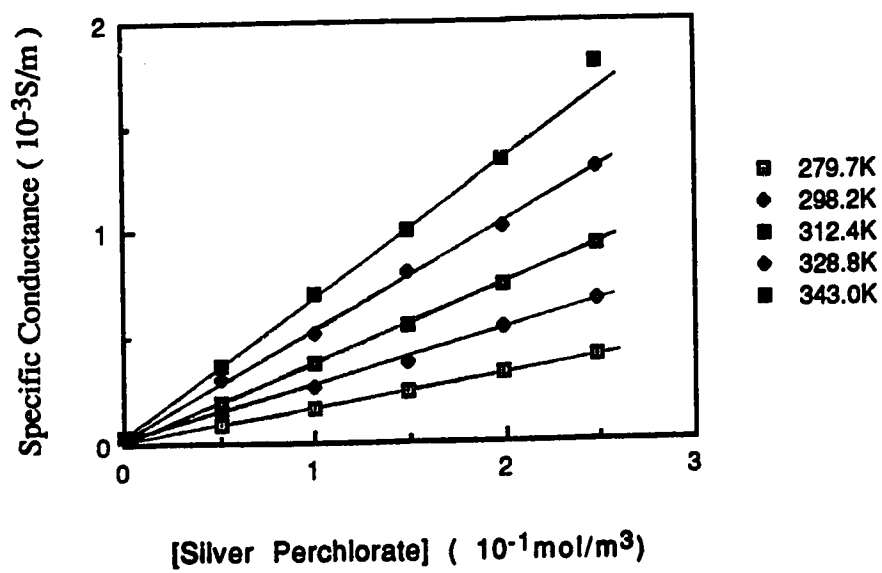
G

{20|1P|Silver Perchlorate}

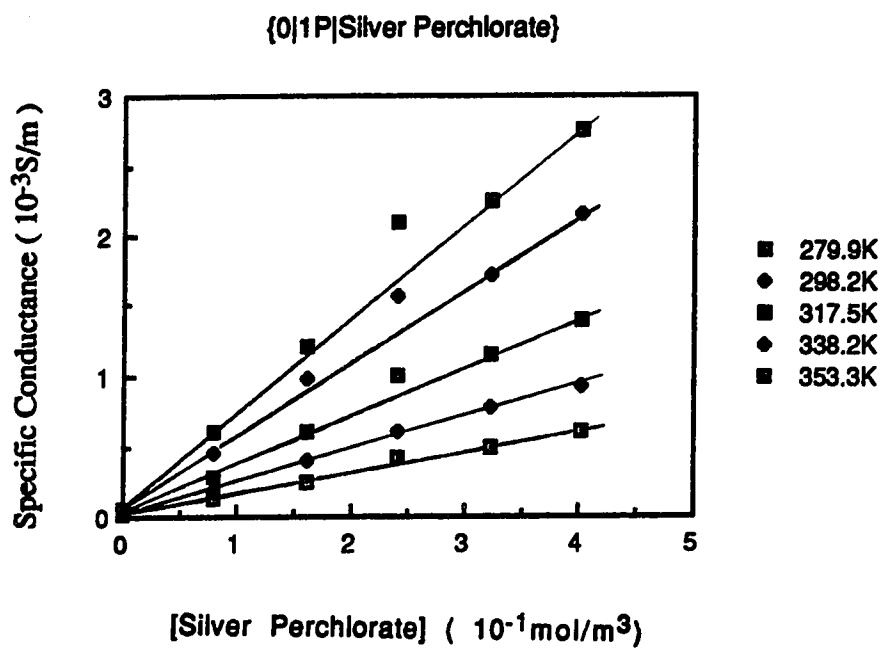


H

{10|1P|Silver Perchlorate}



I



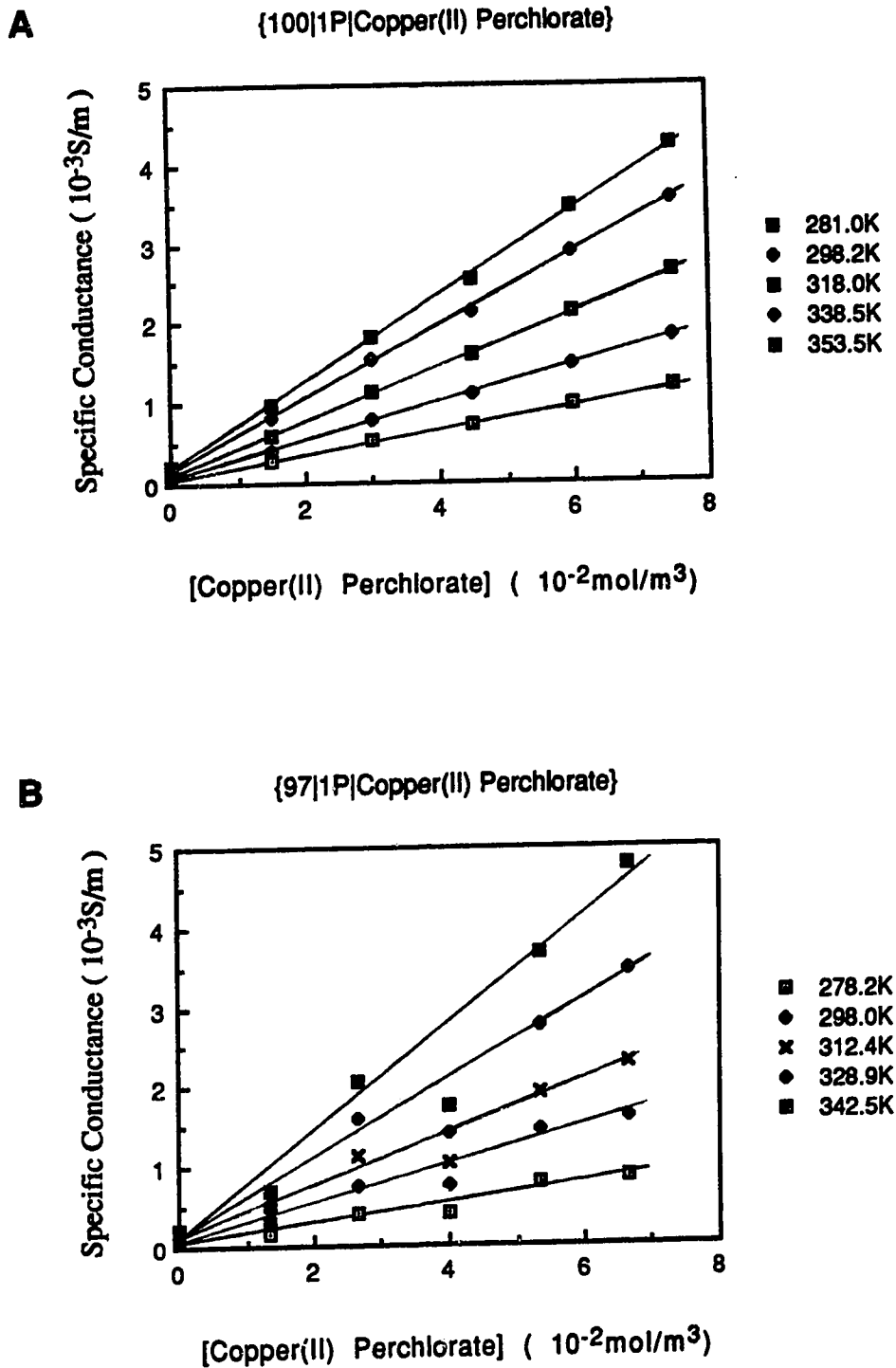


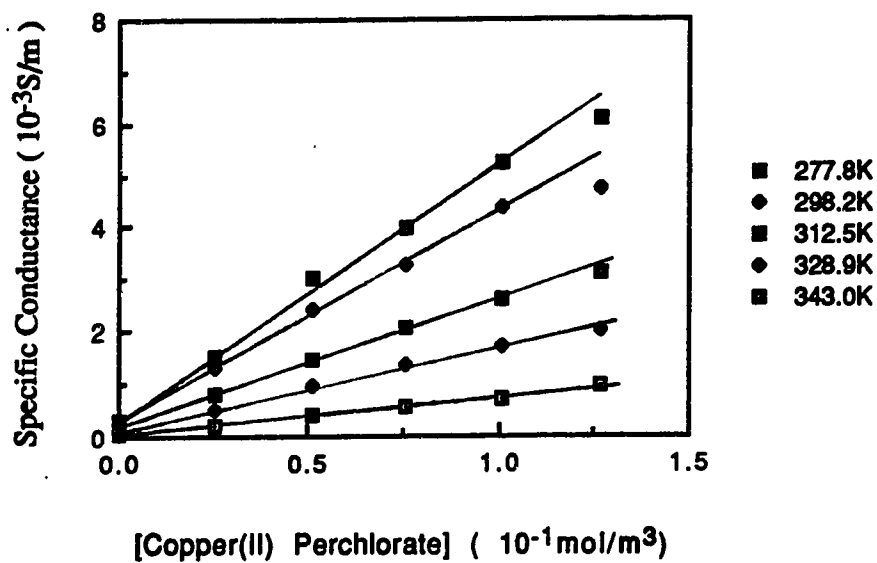
Fig.46

Temperature and concentration dependence of the conductance of
copper(II) perchlorate in 1-propanol/water mixtures

(A-J)

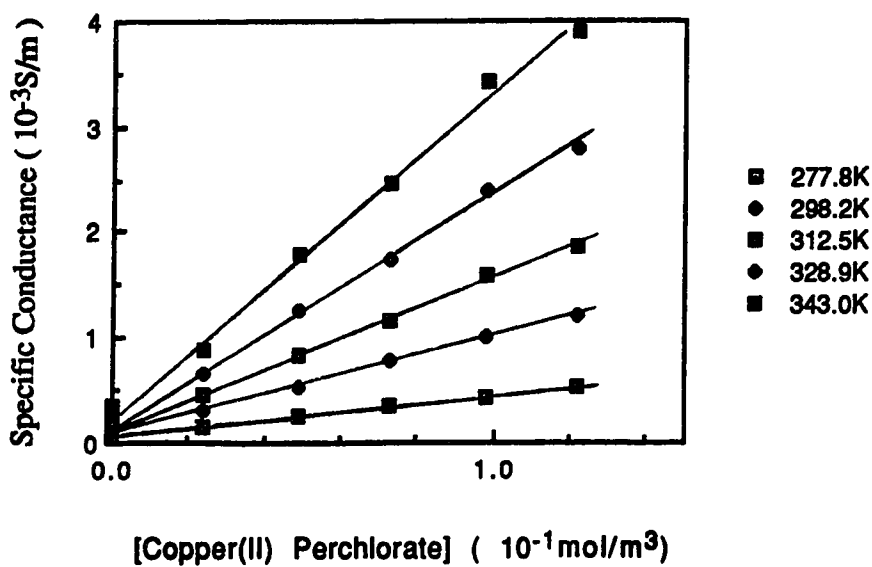
C

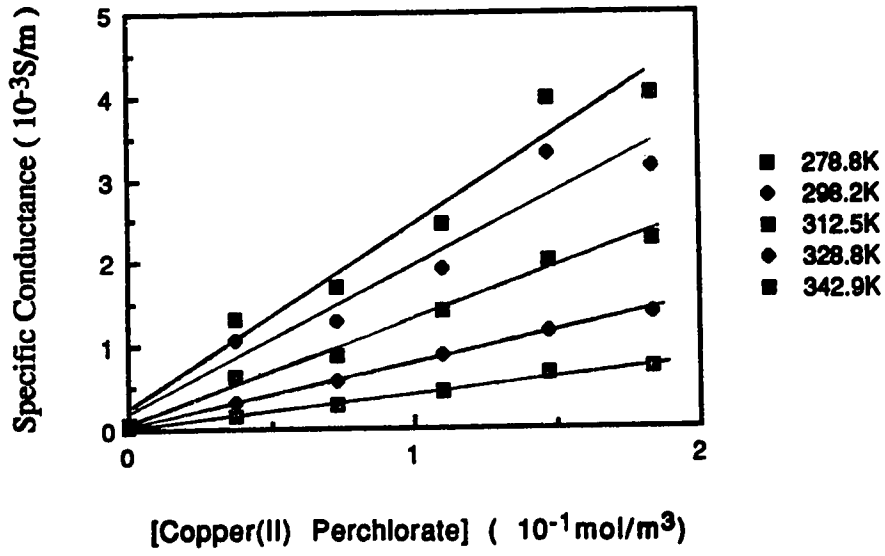
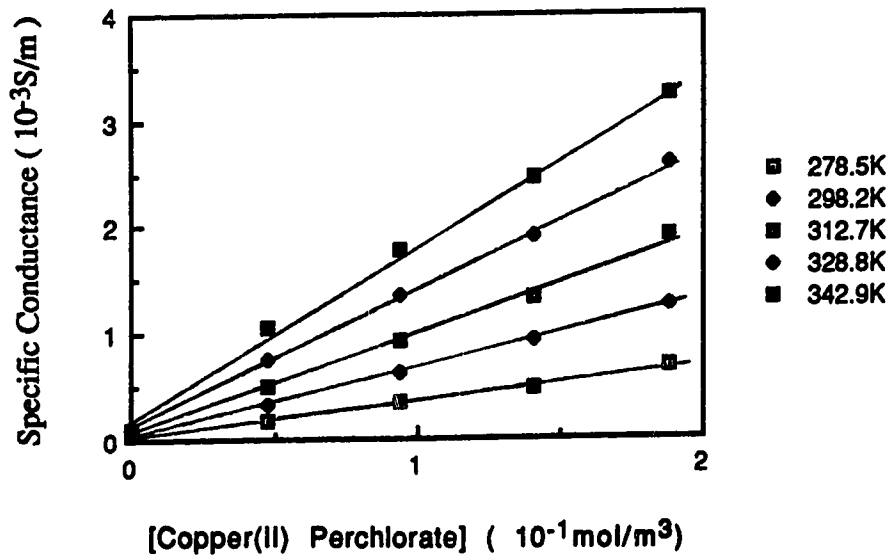
{93}P[Copper(II) Perchlorate]



D

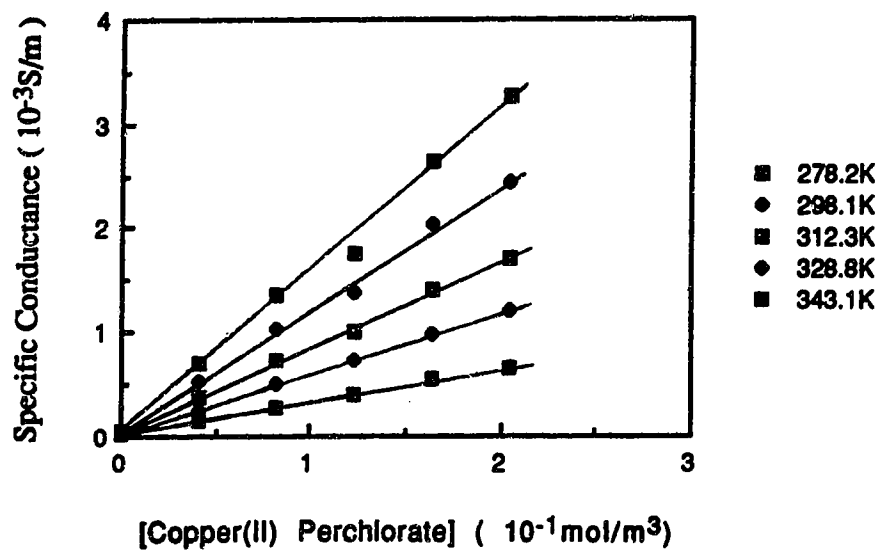
{81}P[Copper(II) Perchlorate]



F**{68|1P|Copper(II) Perchlorate}****F****{51|1P|Copper(II) Perchlorate}**

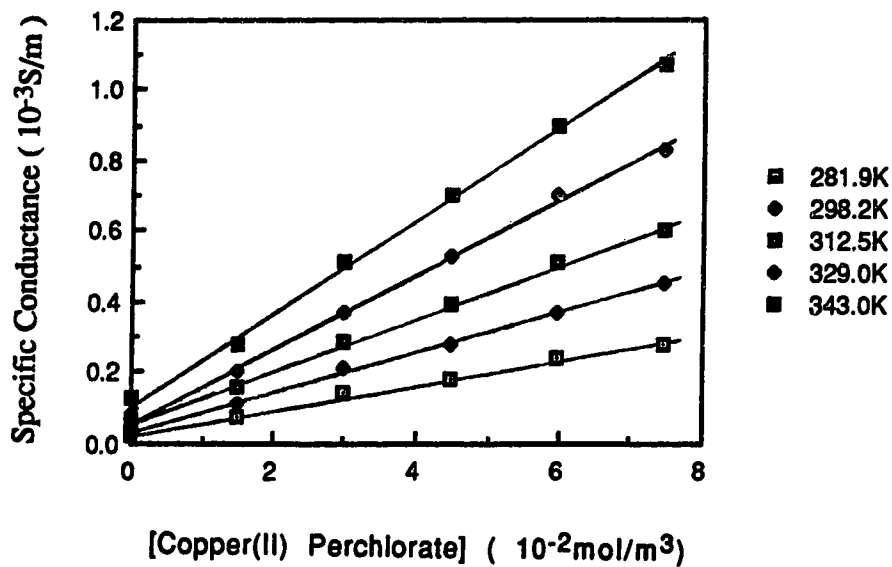
G

{34|1P|Copper(II) Perchlorate}



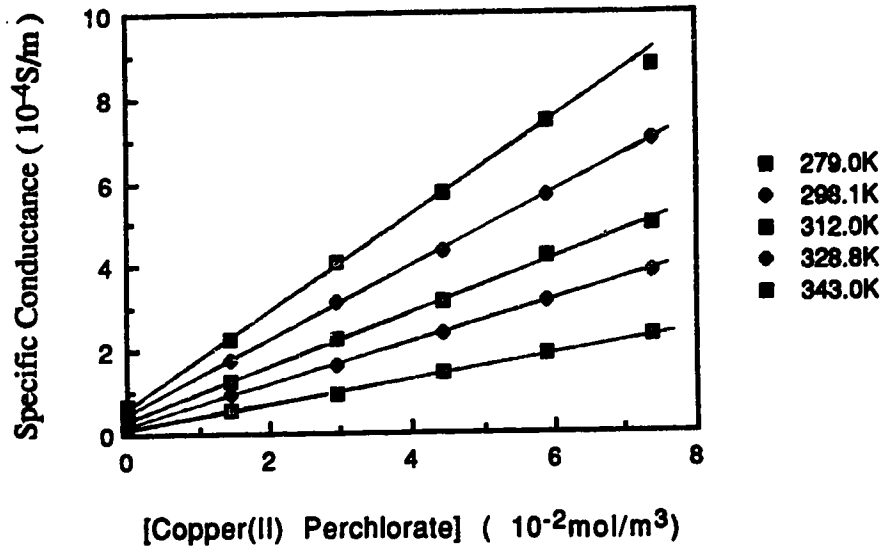
H

{20|1P|Copper(II) Perchlorate}



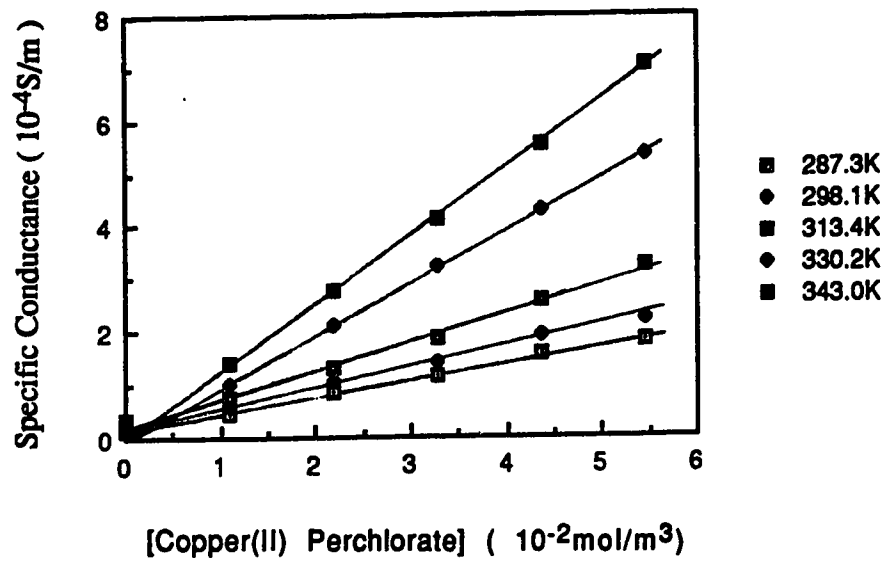
I

{10|1P|Copper(II) Perchlorate}



J

{0|1P|Copper(II) Perchlorate}



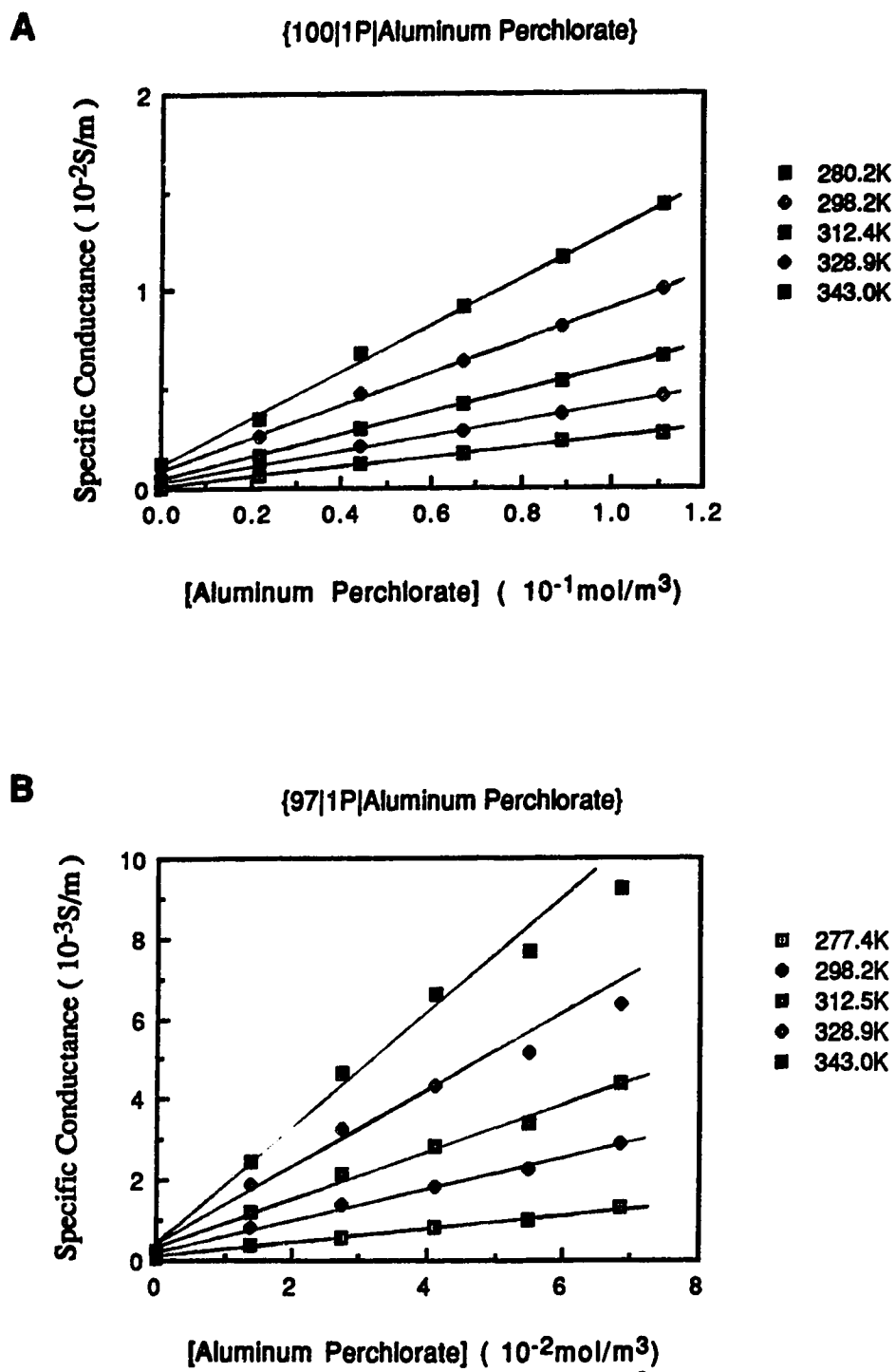
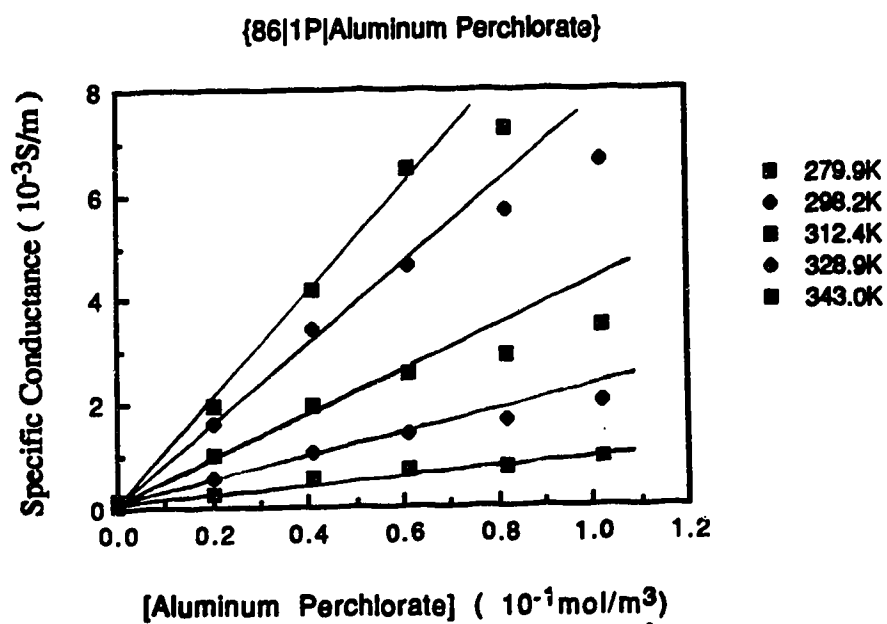
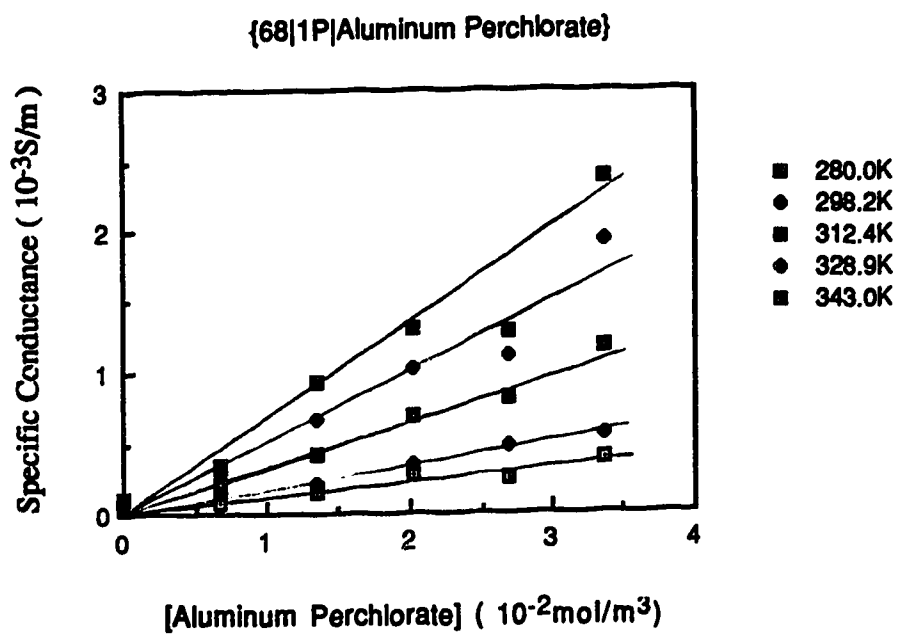


Fig.47 Temperature and concentration dependence of the conductance of
(A-H) aluminum perchlorate in 1-propanol/water mixtures

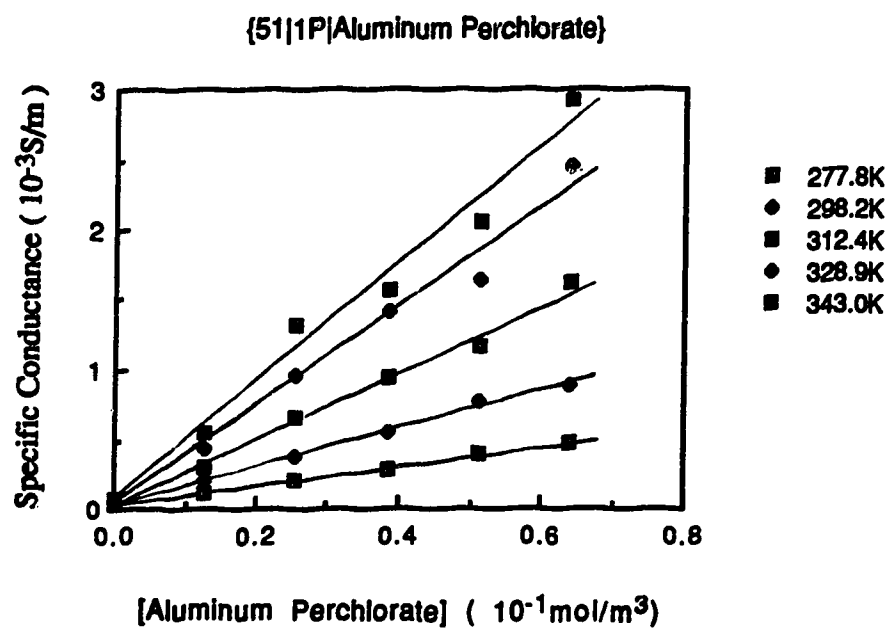
C



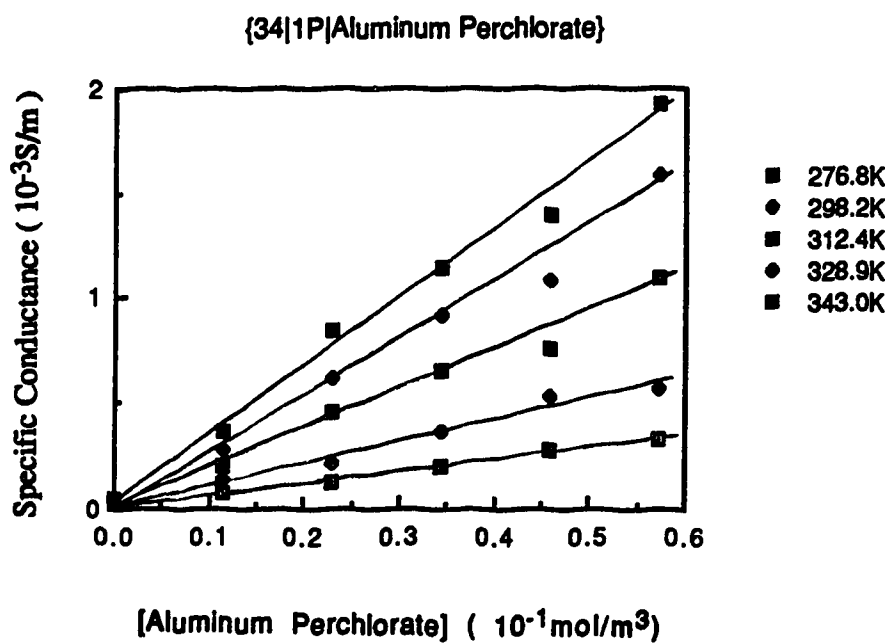
D



E



F



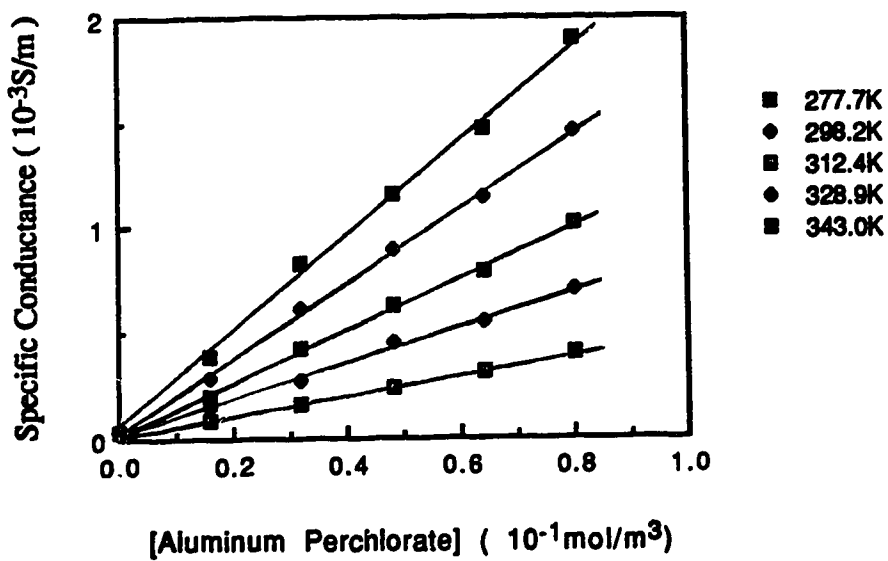
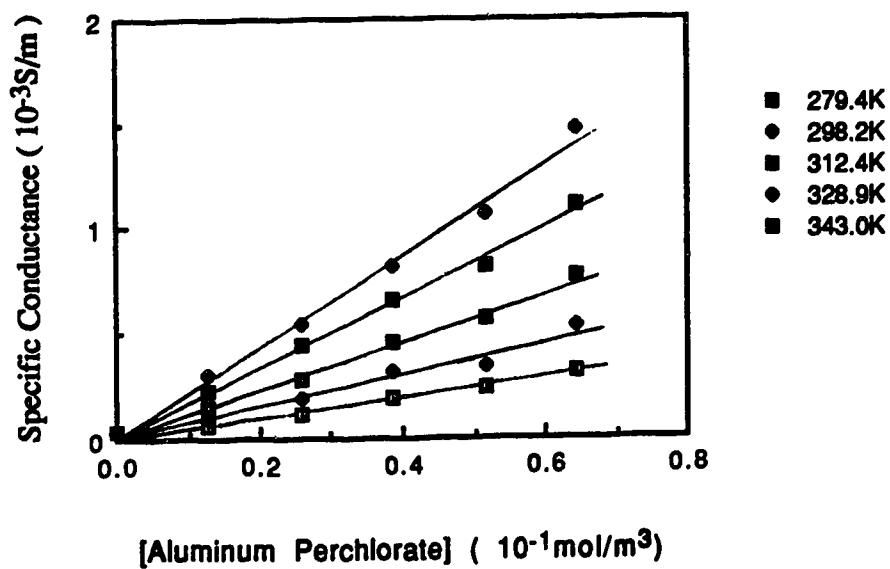
G**{20|1P|Aluminum Perchlorate}****H****{0|1P|Aluminum Perchlorate}**

Fig. 48 Arrhenius plots of molar conductance of lithium nitrate
in 1-propanol/water mixtures

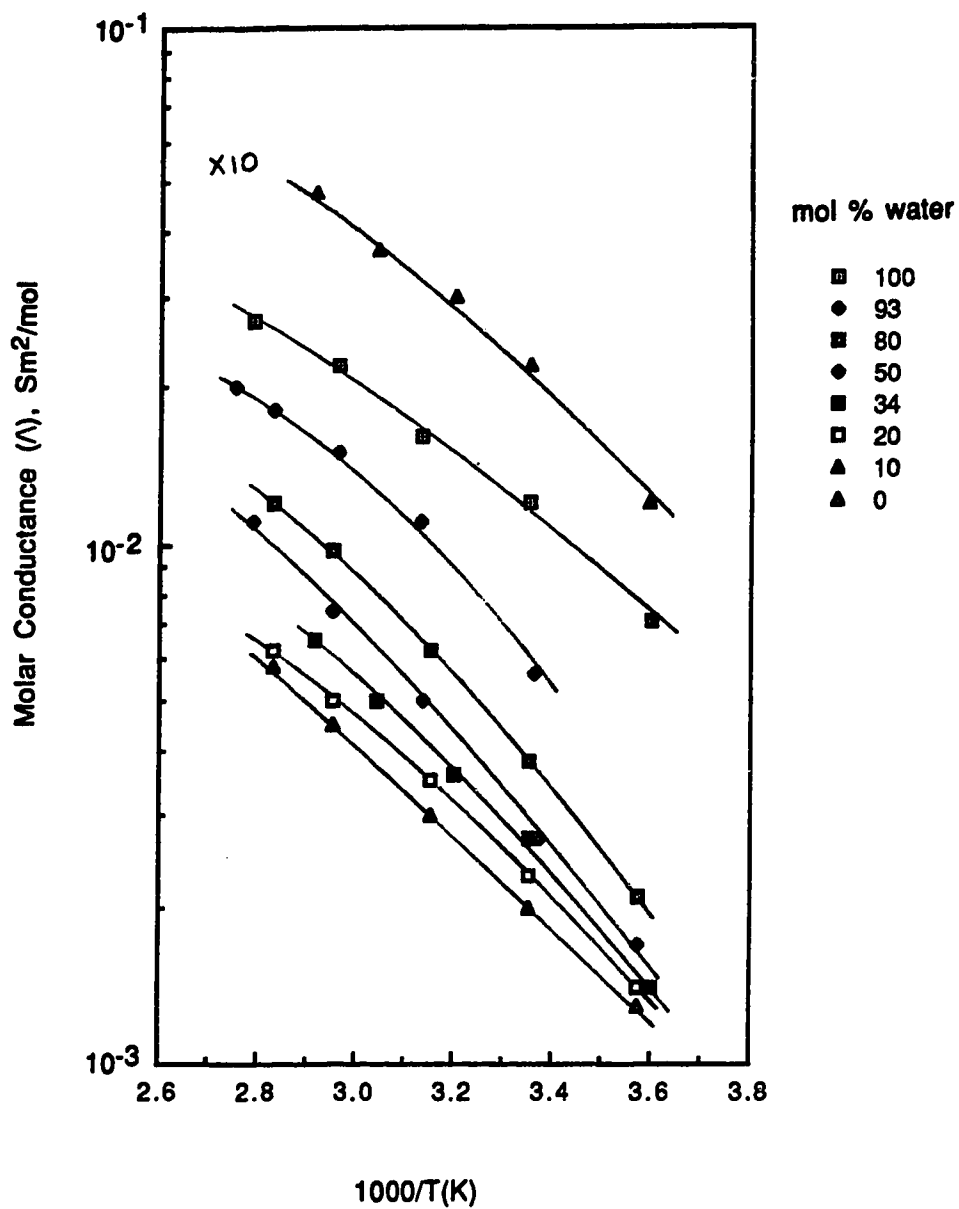


Fig. 49 Arrhenius plots of molar conductance of lithium chromate
in 1-propanol/water mixtures

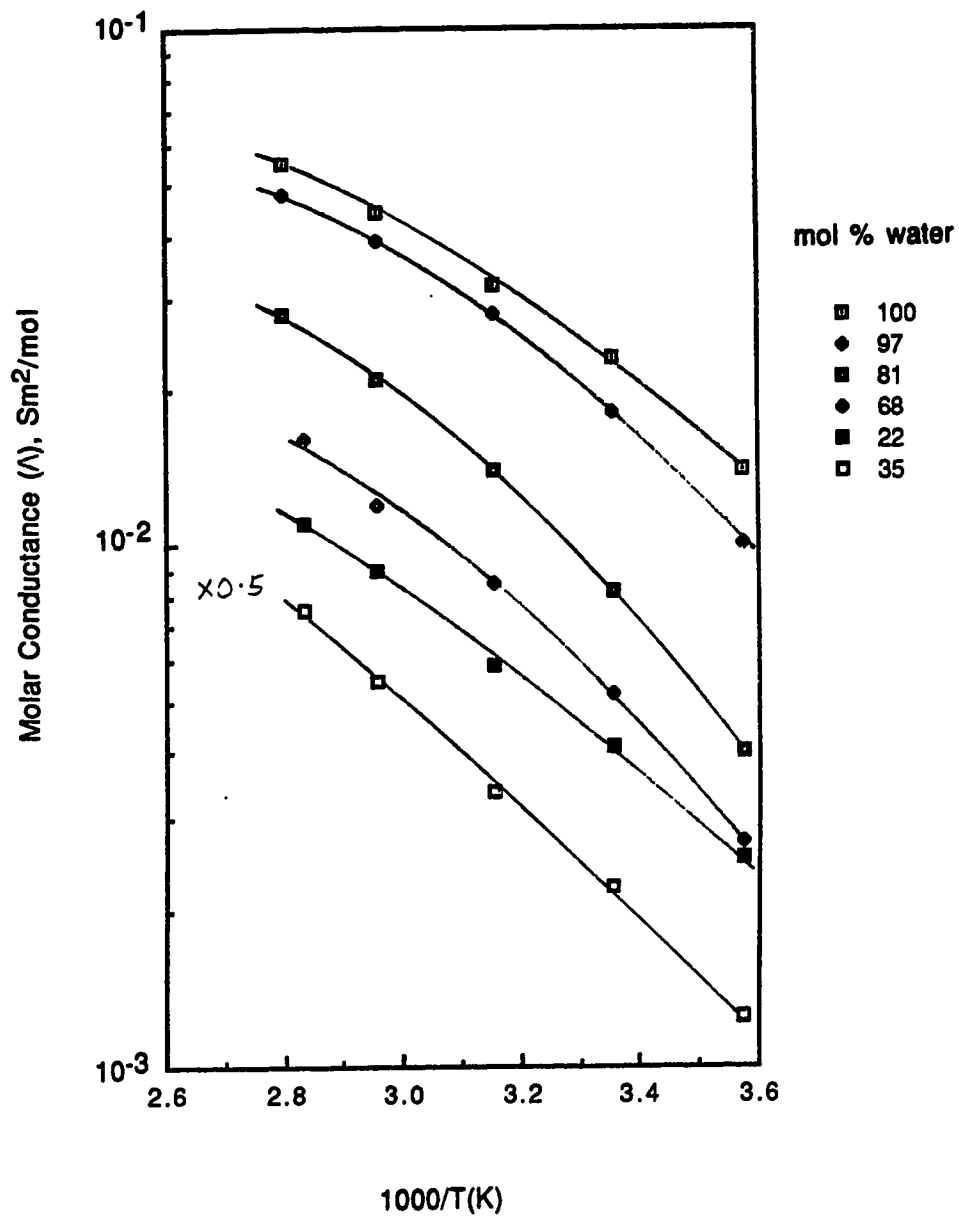


Fig. 50 Arrhenius plots of molar conductance of perchloric acid
in 1-propanol/water mixtures

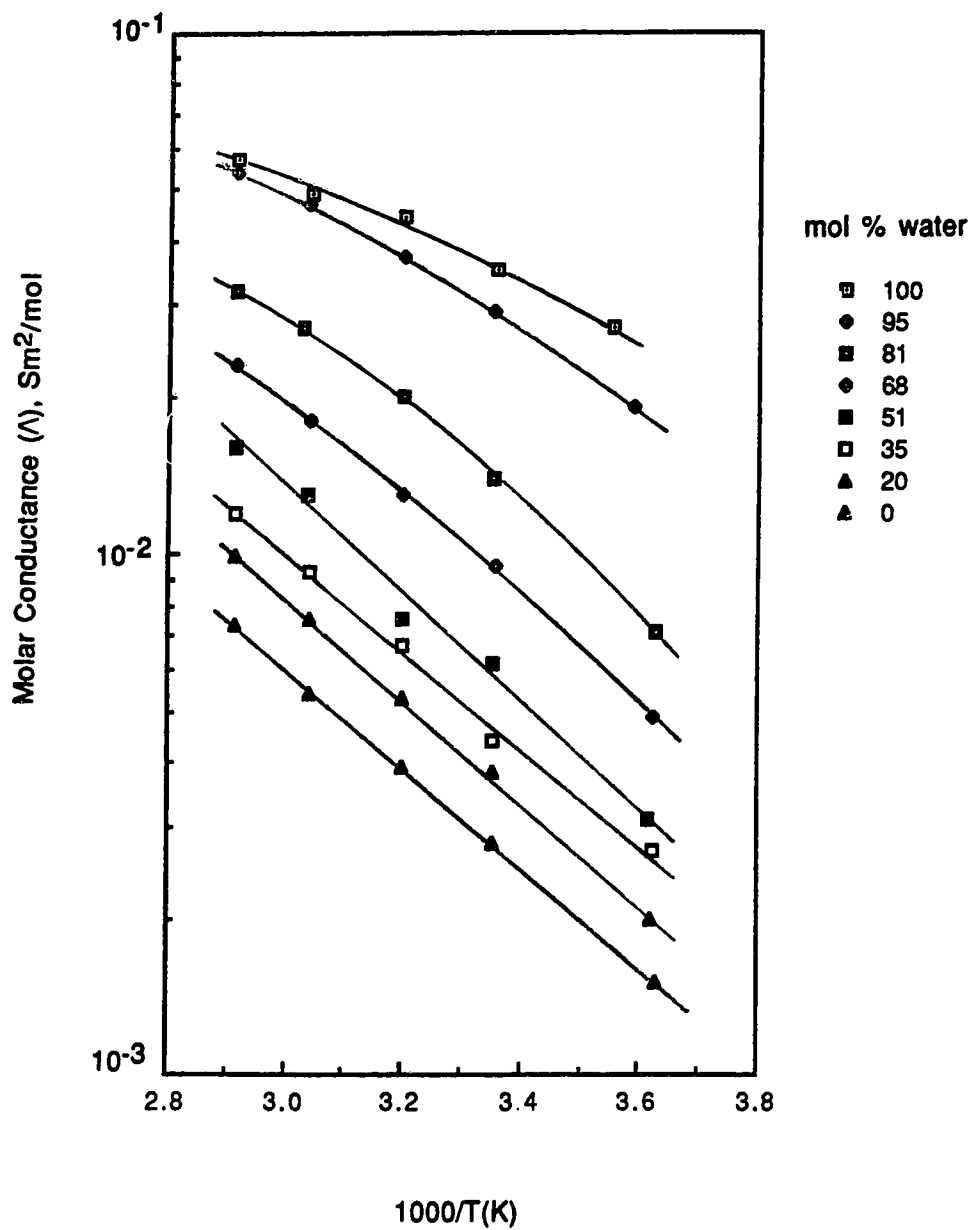


Fig. 51 Arrhenius plots of molar conductance of silver perchlorate
in 1-propanol/water mixtures

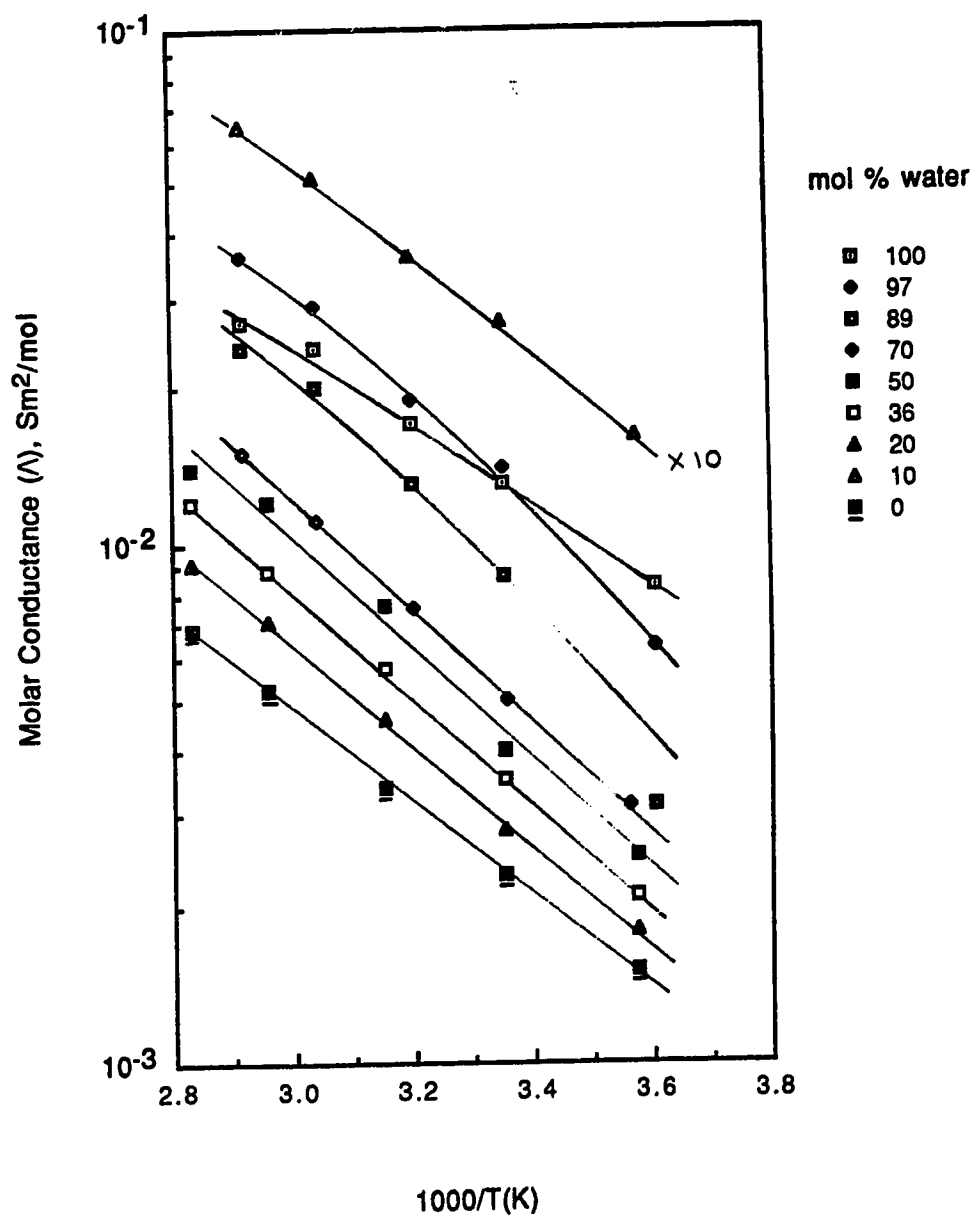


Fig. 52 Arrhenius plots of molar conductance of copper(II) perchlorate
in 1-propanol/water mixtures

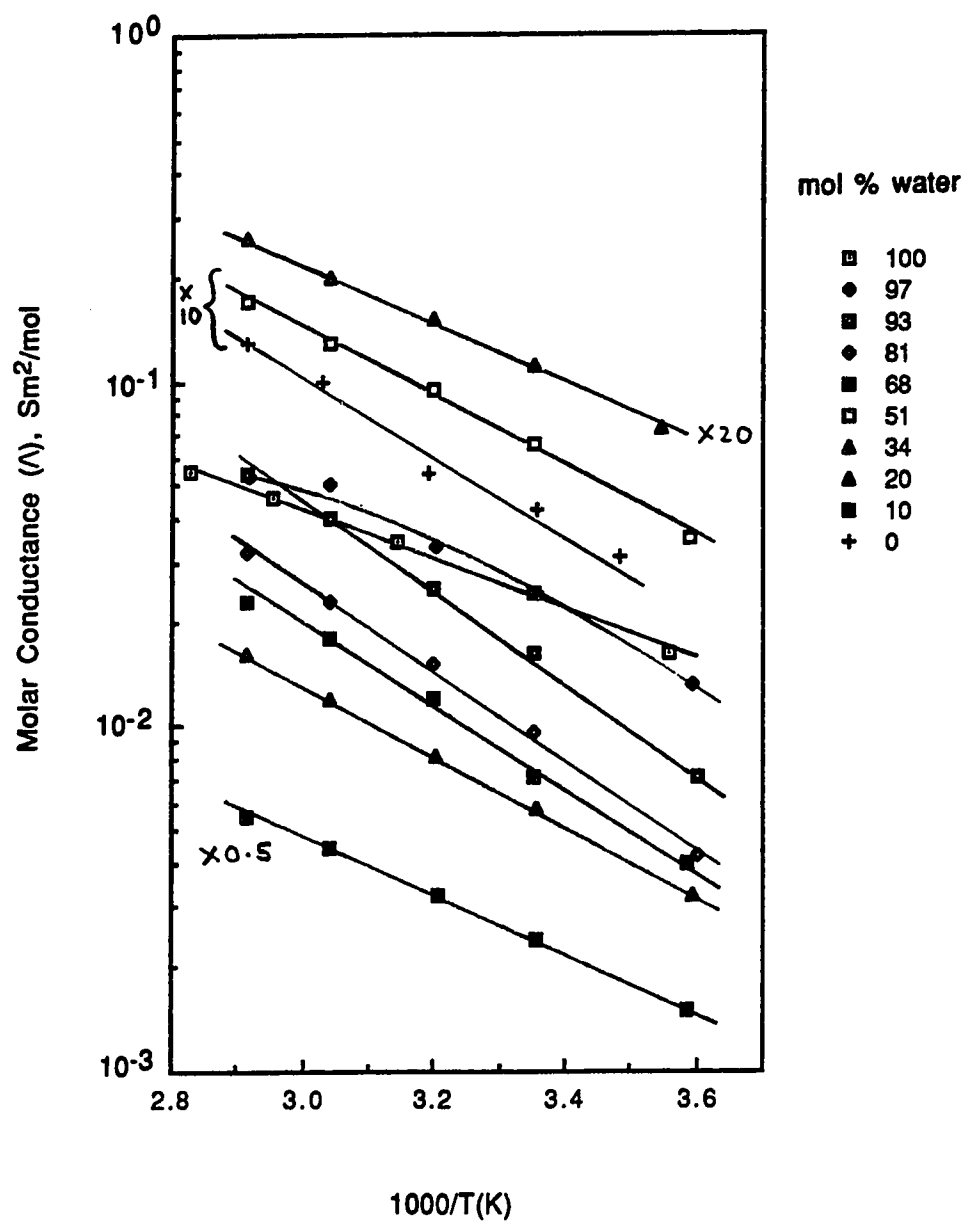


Fig. 53 Arrhenius plots of molar conductance of aluminum perchlorate
in 1-propanol/water mixtures

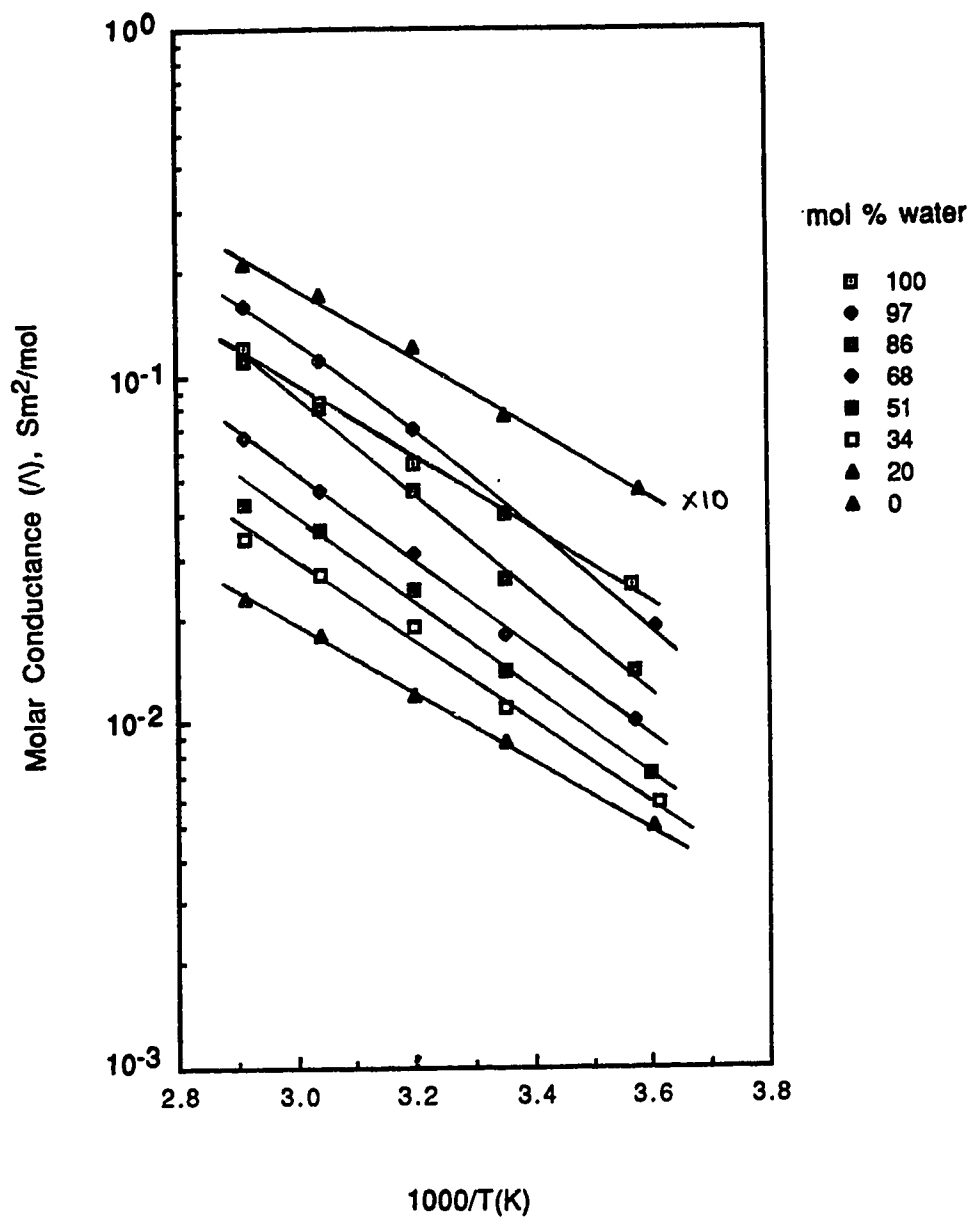


Fig. 54 Composition dependence of the activation energy of conductance
of some inorganic electrolytes in 1-propanol/water mixtures

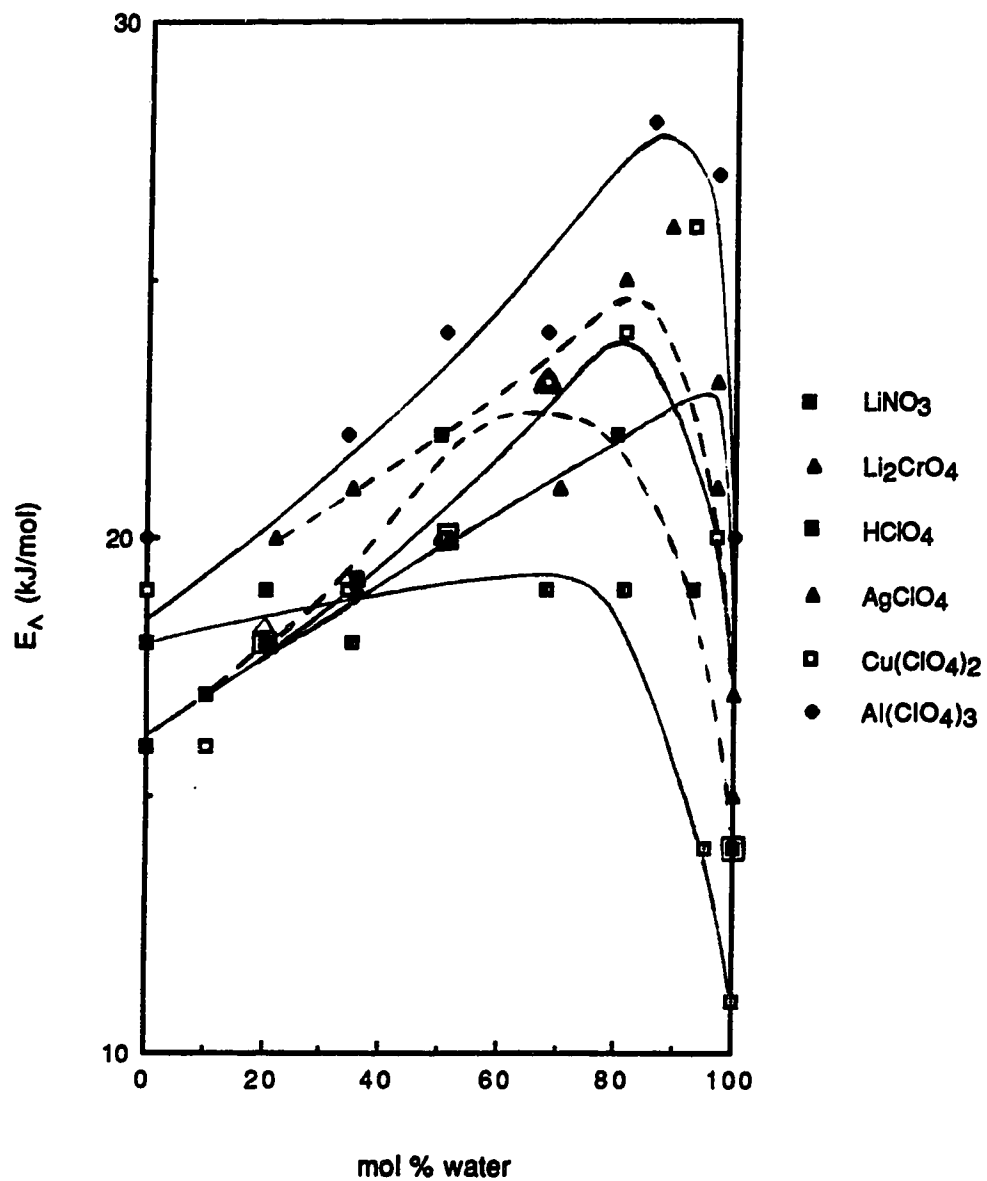


Table 35. Temperature and composition dependence of molar conductances (Λ) of lithium nitrate in 1-propanol/water mixtures.

X_w	Temp (K)	Λ_o ($10^{-3} \text{ S m}^2/\text{mol}$)	X_w	Temp (K)	Λ_o ($10^{-3} \text{ S m}^2/\text{mol}$)
1.00	277.8	7.1	0.34	277.6	1.4
	298.2	12		298.2	2.7
	319.1	16		312.4	3.6
	337.4	22		328.9	5.0
	358.4	27		343.0	6.5
E_Λ , kJ/mol		14			19
0.93	297.2	5.6	0.20	279.7	1.4
	319.1	11		298.2	2.3
	337.4	15		317.5	3.5
	353.0	18		338.4	5.0
	363.6	20		353.2	6.2
E_Λ , kJ/mol		19			18
0.80	279.7	2.1	0.10	278.3	1.2
	298.2	3.8		298.2	2.2
	317.5	6.2		312.5	3.0
	338.4	9.7		328.9	3.7
	353.2	12		343.1	4.8
E_Λ , kJ/mol		22			17
0.50	279.7	1.7	0.00 ^(a)	279.7	1.3
	296.3	2.7		298.2	2.0
	318.9	5.0		317.5	3.0
	338.5	7.4		338.4	4.5
	358.5	11		353.2	5.8
E_Λ , kJ/mol		22			16

(a) Λ_o calculated from curved specific conductance versus concentration plots.

Table 36. Temperature and composition dependence of molar conductances (Λ) of lithium chromate in 1-propanol/water mixtures.

X_w	Temp (K)	Λ_o ($10^{-3} \text{ S m}^2/\text{mol}$)	X_w	Temp (K)	Λ_o ($10^{-3} \text{ S m}^2/\text{mol}$)
1.00	279.7	14	0.68	279.7	2.7
	298.2	23		298.2	5.2
	317.4	32		317.4	8.4
	338.3	44		338.4	12
	357.7	55		353.2	16
E_Λ , kJ/mol		17			23
0.97	279.7	10	0.35 ^(a)	279.7	2.5
	298.2	18		298.2	4.4
	317.3	28		317.4	6.7
	338.2	39		338.4	11
	357.6	48		353.2	15
E_Λ , kJ/mol		21			21
0.81	279.7	4.0	0.22 ^(a)	279.7	2.5
	298.2	8.2		298.2	4.1
	317.3	14		317.4	5.9
	338.2	21		338.4	8.9
	357.6	28		353.2	11
E_Λ , kJ/mol		25			20

(a) Λ_o calculated from curved specific conductance versus concentration plots.

Table 37. Temperature and composition dependence of molar conductances (Λ) of perchloric acid in 1-propanol/water mixtures.

X_w	Temp (K)	Λ_o ($10^{-3} \text{ S m}^2/\text{mol}$)	X_w	Temp (K)	Λ_o ($10^{-3} \text{ S m}^2/\text{mol}$)
1.00	281.2	27	0.51	276.5	3.1
	298.1	35		298.2	6.2
	312.4	44		312.5	7.5
	328.9	49		329.0	13
	343.1	57		343.3	16
E_Λ , kJ/mol		11			20
0.95	278.5	19	0.35	275.9	2.7
	298.2	29		298.2	4.4
	312.5	37		312.4	6.7
	329.0	47		328.9	9.3
	343.4	54		343.2	12
E_Λ , kJ/mol		14			18
0.68	275.9	4.9	0.20	276.4	2.0
	298.1	9.5		298.2	3.8
	312.4	13		312.5	5.3
	328.9	18		328.9	7.5
	343.3	23		343.3	9.9
E_Λ , kJ/mol		19			19
0.81	275.7	7.1	0.00	275.5	2.5
	298.2	14		298.2	3.8
	312.4	20		312.4	4.9
	330.1	27		328.9	5.4
	343.1	32		343.3	7.3
E_Λ , kJ/mol		19			18

Table 38. Temperature and composition dependence of molar conductances (Λ) of silver perchlorate in 1-propanol/water mixtures.

X_w	Temp (K)	Λ_o ($10^{-3} \text{ S m}^2/\text{mol}$)	X_w	Temp (K)	Λ_o ($10^{-3} \text{ S m}^2/\text{mol}$)
1.00	277.4	8.2	0.36	279.7	2.1
	298.2	13		298.2	3.5
	312.5	17		317.5	5.7
	328.9	24		338.3	8.8
	343.0	27		353.3	12
E_Λ , kJ/mol		15			19
0.97	277.4	6.3	0.20	279.7	1.8
	298.2	14		298.2	2.8
	312.5	19		317.5	4.6
	328.9	29		338.3	7.1
	343.0	36		353.3	9.2
E_Λ , kJ/mol		23			19
0.89	277.4	3.1	0.10	279.7	1.6
	298.2	8.6		298.2	2.7
	312.5	13		312.4	3.6
	328.9	20		328.8	5.1
	343.0	24		343.0	6.5
E_Λ , kJ/mol		26			17
0.70	280.9	3.1	0.00	279.9	1.5
	298.1	5.0		298.2	2.3
	312.3	7.5		317.5	3.4
	328.8	11		338.2	5.2
	343.0	15		353.3	6.8
E_Λ , kJ/mol		21			16
0.50	279.7	2.5			
	298.2	4.0			
	317.5	7.6			
	338.3	12			
	353.3	14			
E_Λ , kJ/mol		20			

Table 39. Temperature and composition dependence of molar conductances (Λ) of copper(II) perchlorate in 1-propanol/water mixtures.

X_w	Temp (K)	Λ_o ($10^{-3} \text{ S m}^2/\text{mol}$)	X_w	Temp (K)	Λ_o ($10^{-3} \text{ S m}^2/\text{mol}$)
1.00	281.0	16	0.51	278.5	3.5
	298.2	24		298.2	6.5
	318.0	34		312.7	9.4
	338.5	46		328.8	13
	353.5	55		342.9	17
E_A , kJ/mol		14			20
0.97	278.2	13	0.34	278.2	3.2
	298.0	24		298.1	5.7
	312.4	33		312.3	8.1
	328.9	50		328.8	12
	342.5	53		343.1	16
E_A , kJ/mol		20			19
0.93	277.8	7.1	0.20	281.9	3.6
	298.2	16		298.2	5.5
	312.5	25		312.5	7.5
	328.9	40		329.0	10
	343.0	54		343.0	13
E_A , kJ/mol		26			18
0.81	277.8	4.2	0.10	279.0	3.0
	298.2	9.5		298.1	4.8
	312.5	15		312.0	6.4
	328.9	23		328.8	8.8
	343.0	32		343.0	11
E_A , kJ/mol		24			16
0.68	278.8	4.0	0.00	287.3	3.1
	298.2	7.1		298.1	4.2
	312.5	12		313.4	5.4
	328.8	18		330.2	10
	342.9	23		343.0	13
E_A , kJ/mol		23			19

Table 40. Temperature and composition dependence of molar conductances (Λ) of aluminum perchlorate in 1-propanol/water mixtures.

X_w	Temp (K)	Λ_o ($10^{-3} \text{ S m}^2/\text{mol}$)	X_w	Temp (K)	Λ_o ($10^{-3} \text{ S m}^2/\text{mol}$)
1.00	280.2	2.5	0.51	277.8	0.71
	298.2	4.0		298.2	1.4
	312.4	5.6		312.4	2.4
	328.9	8.4		328.9	3.6
	343.0	12		343.0	4.3
$E_A, \text{ kJ/mol}$		20			24
0.97	277.4	1.9	0.34	276.8	0.59
	298.2	4.0		298.2	1.1
	312.5	7.0		312.4	1.9
	328.9	11		328.9	2.7
	343.0	16		343.0	3.4
$E_A, \text{ kJ/mol}$		27			22
0.86	279.9	1.4	0.20	277.7	0.50
	298.2	2.6		298.2	0.88
	312.4	4.7		312.4	1.2
	328.9	8.1		328.9	1.8
	343.0	11		343.0	2.3
$E_A, \text{ kJ/mol}$		28			19
0.68	280.0	1.0	0.00	279.4	0.47
	298.2	1.8		298.2	0.76
	312.4	3.1		312.4	1.2
	328.9	4.7		328.9	1.7
	343.0	6.7		343.0	2.1
$E_A, \text{ kJ/mol}$		24			20

B. 2-Propanol/Water Mixtures

The specific conductance *versus* concentration plots are shown in Figure 55 (A-H) for LiNO_3 , Figure 56 (A-D) for Li_2CrO_4 , Figure 57 (A-G) for HClO_4 , Figure 58 (A-I) for AgClO_4 , Figure 59 (A-H) for $\text{Cu}(\text{ClO}_4)_2$, and Figure 60 (A-H) for $\text{Al}(\text{ClO}_4)_3$. The Arrhenius plots of molar conductance are shown in Figure 61 for LiNO_3 , Figure 62 for Li_2CrO_4 , Figure 63 for HClO_4 , Figure 64 for AgClO_4 , Figure 65 for $\text{Cu}(\text{ClO}_4)_2$, and Figure 66 for $\text{Al}(\text{ClO}_4)_3$. The results are summarized in Figure 67 and Tables 41-46.

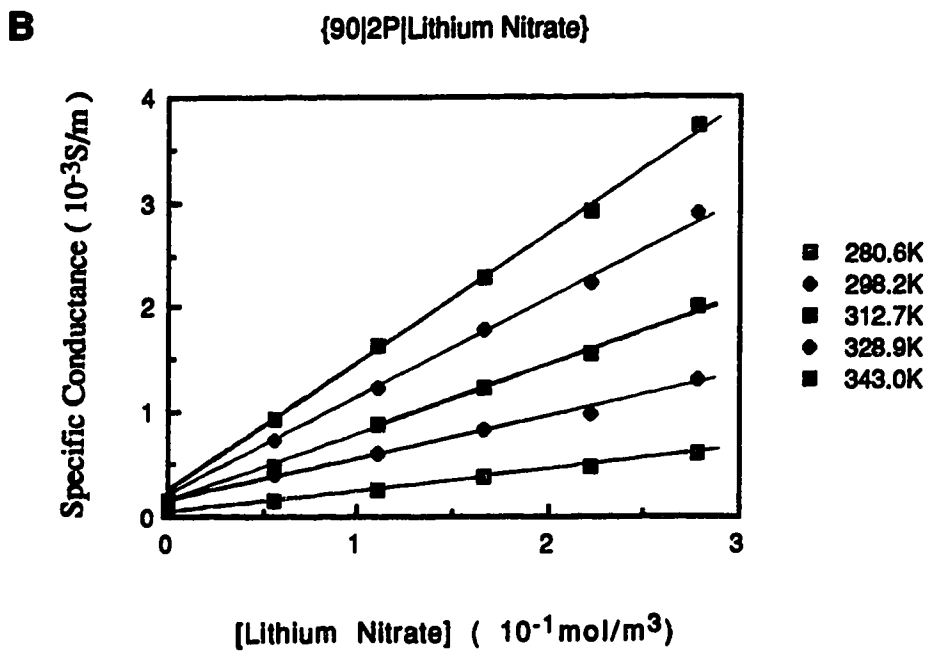
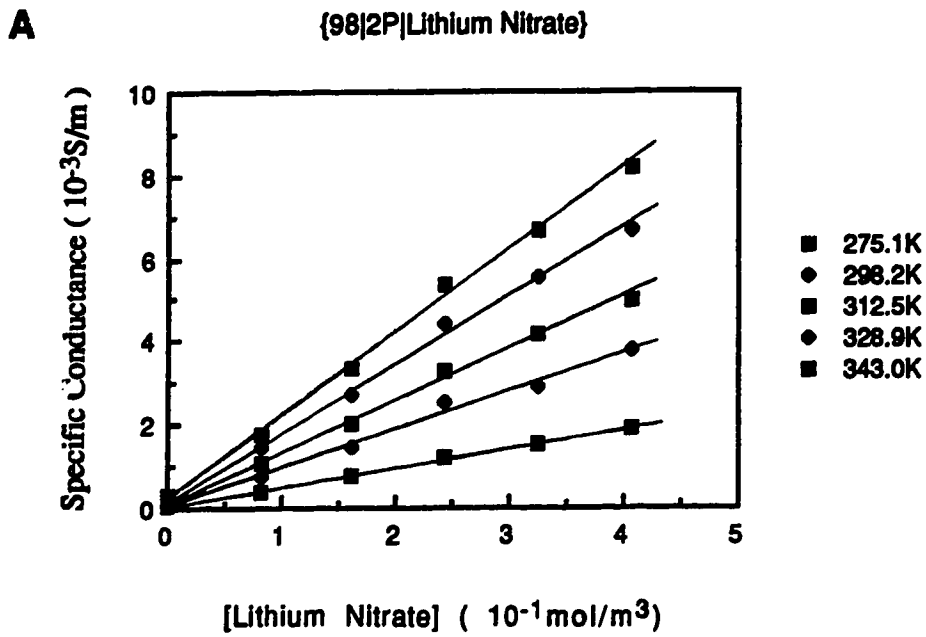
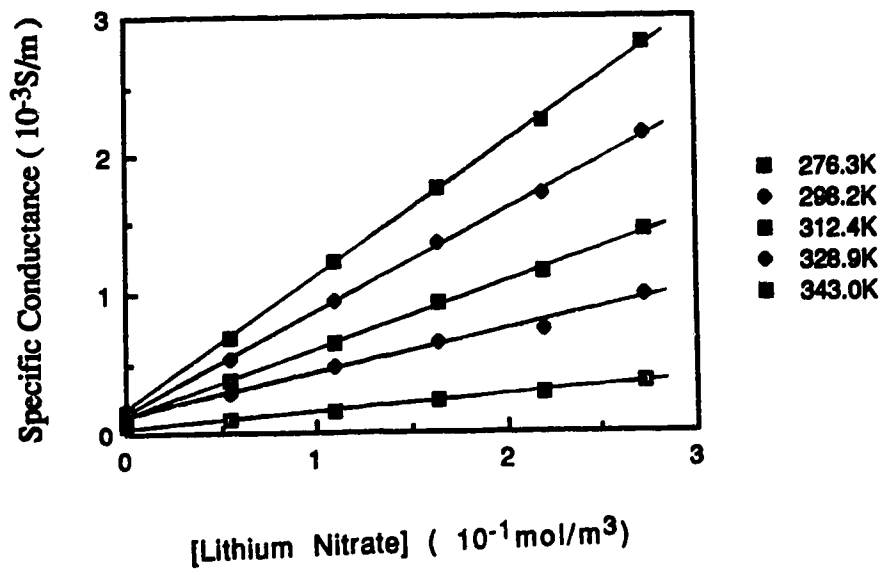
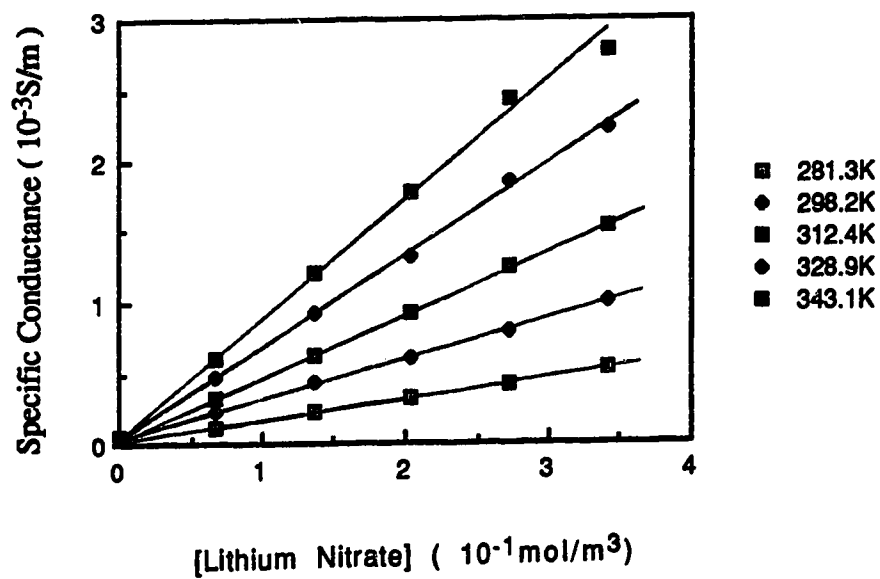
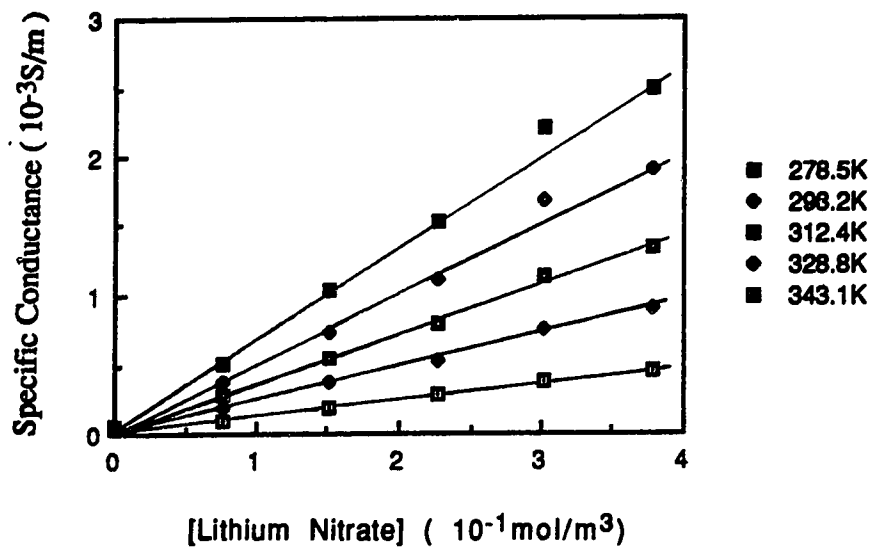
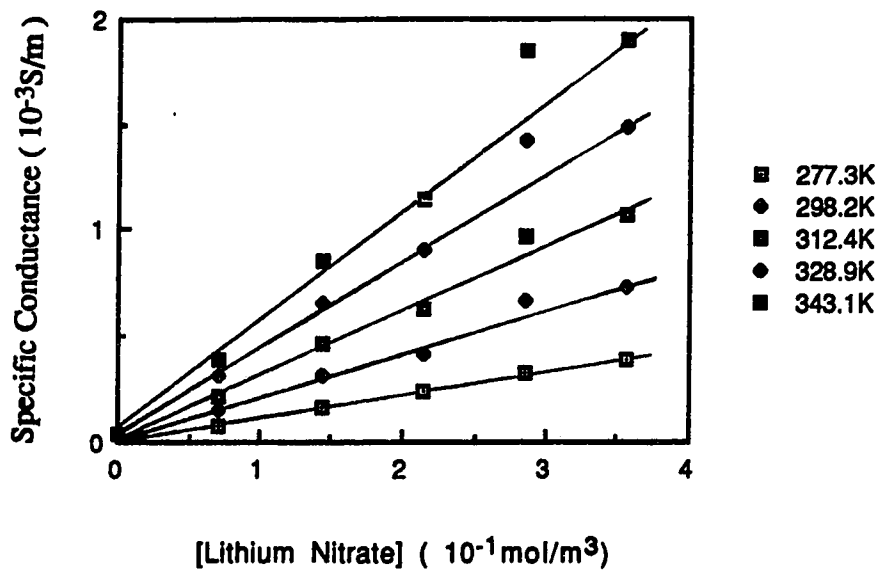
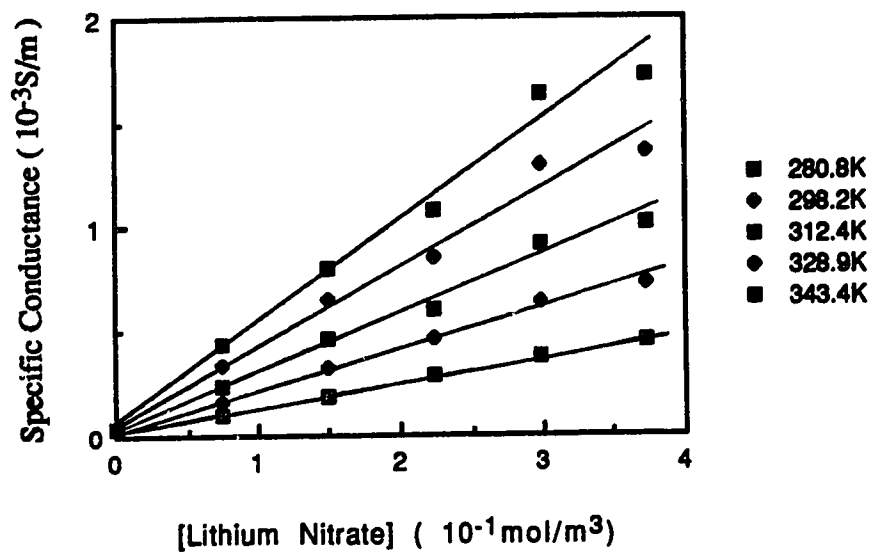
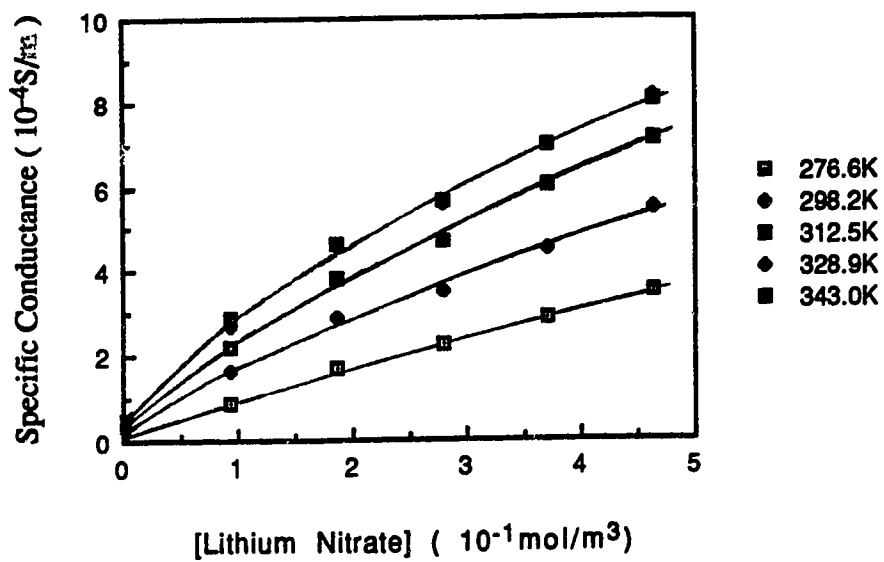


Fig. 55 Temperature and concentration dependence of the conductance of
(A-H) lithium nitrate in 2-propanol/water mixtures

C**{81|2P|Lithium Nitrate}****D****{71|2P|Lithium Nitrate}**

E**{52|2P|Lithium Nitrate}****F****{35|2P|Lithium Nitrate}**

G**{20|2P|Lithium Nitrate}****H****{0|2P|Lithium Nitrate}**

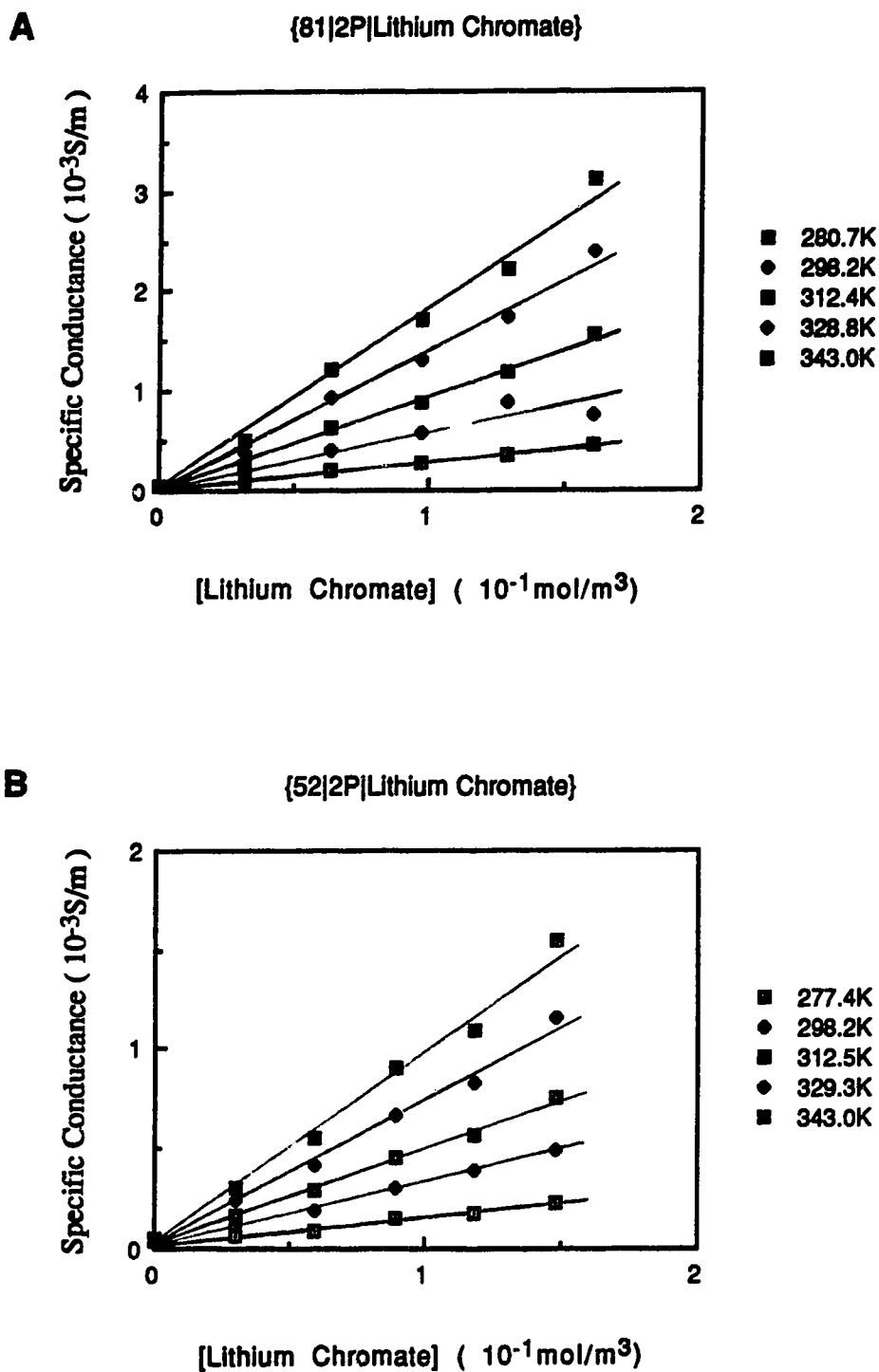
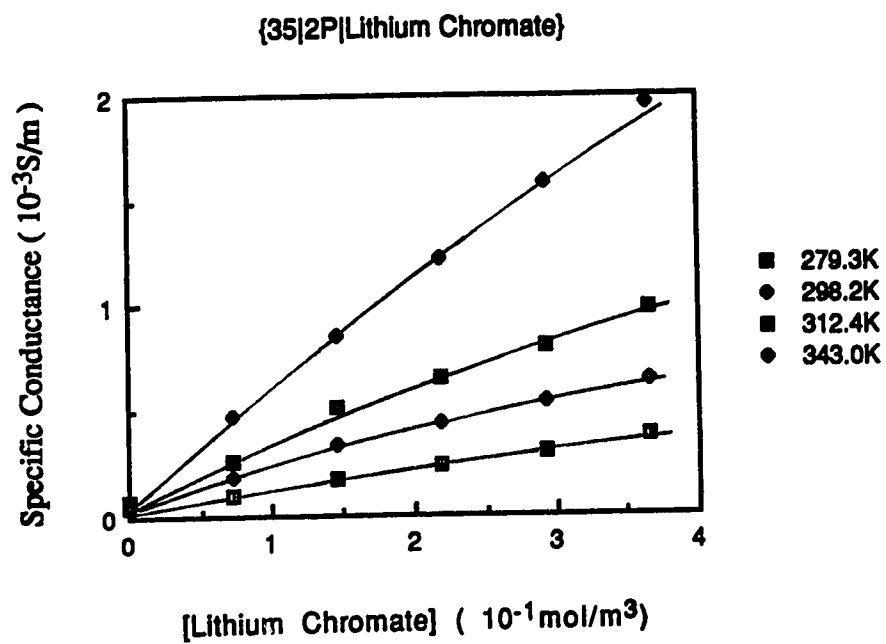


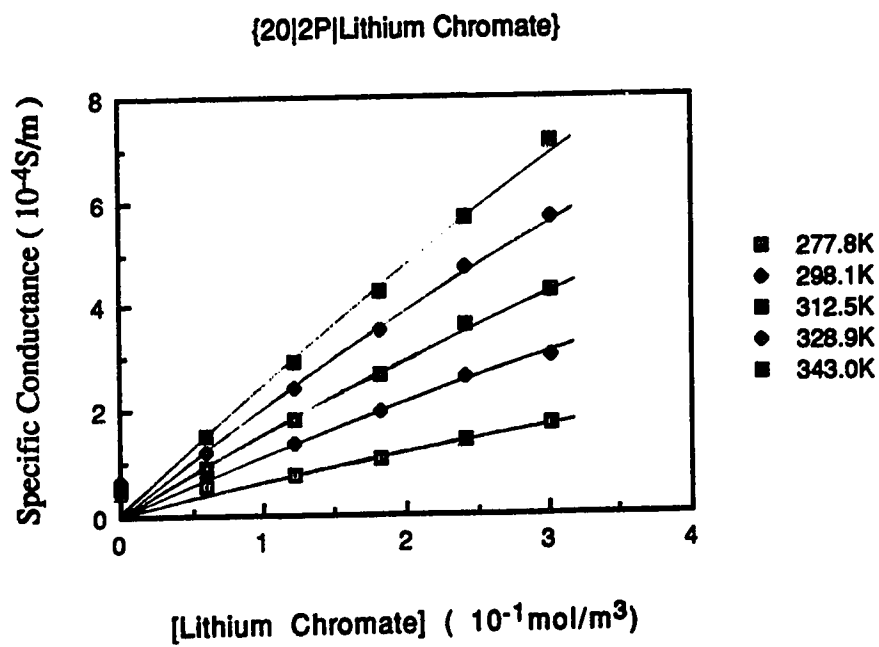
Fig. 56
(A-D)

Temperature and concentration dependence of the conductance of
lithium chromate in 2-propanol/water mixtures

C



D



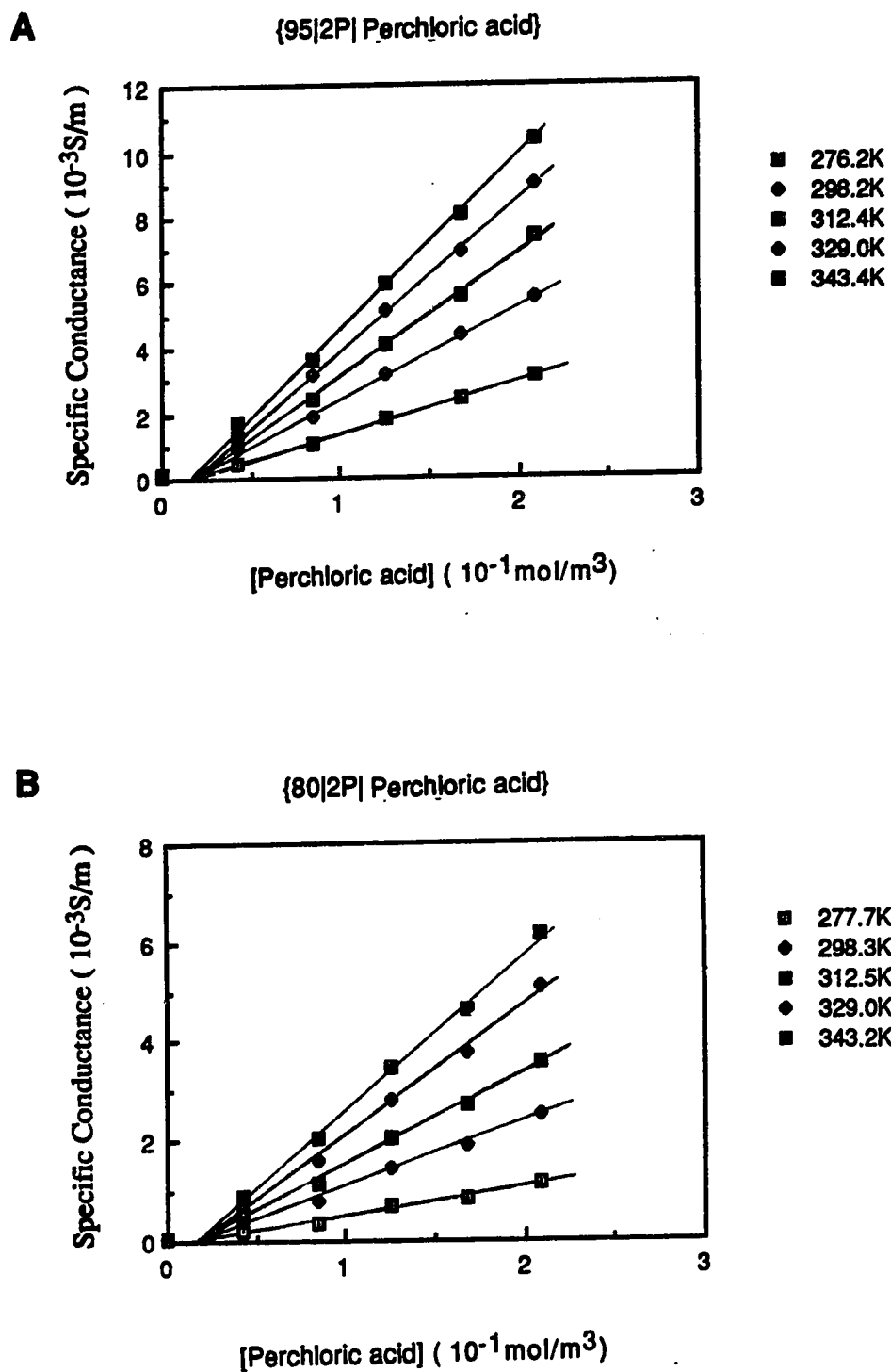
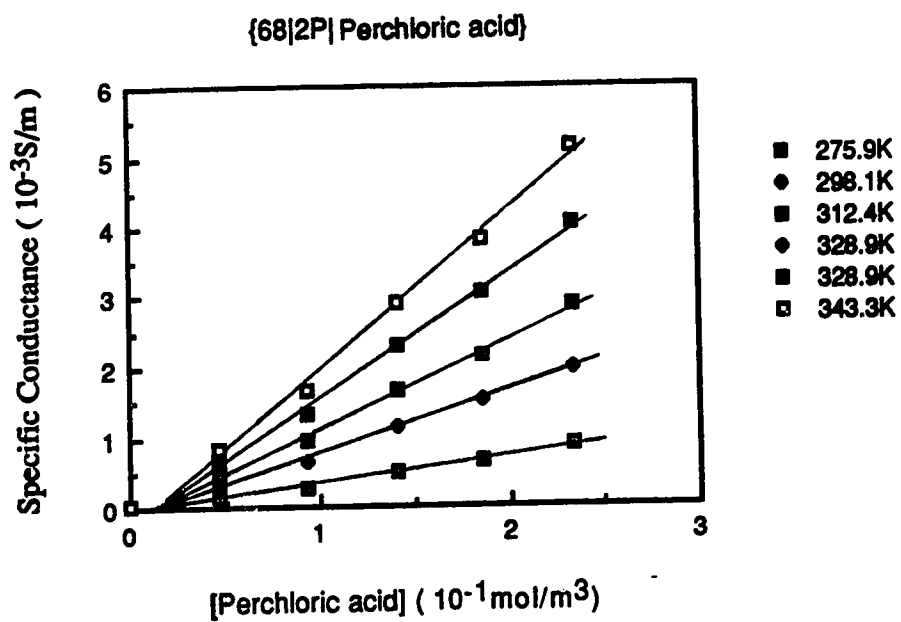
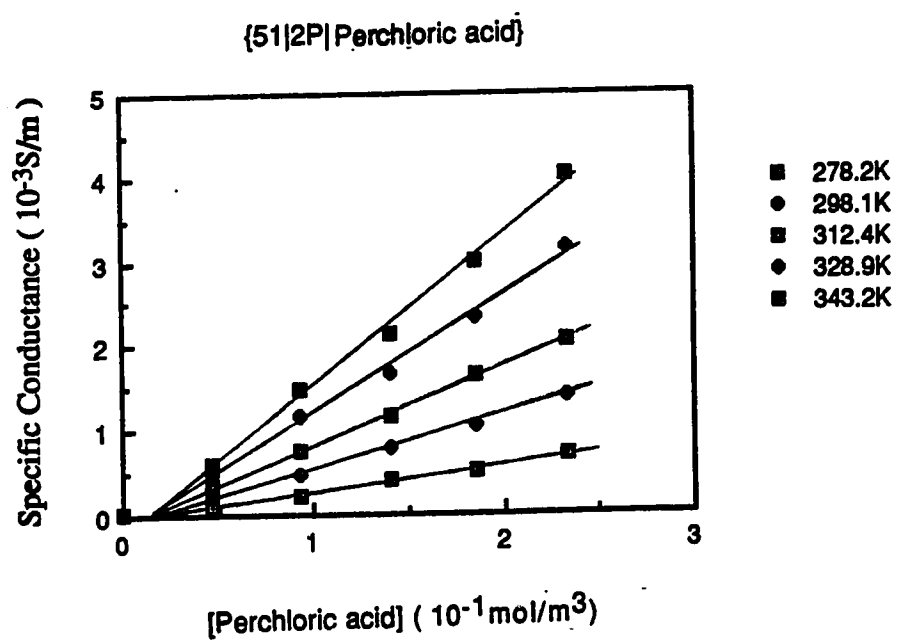
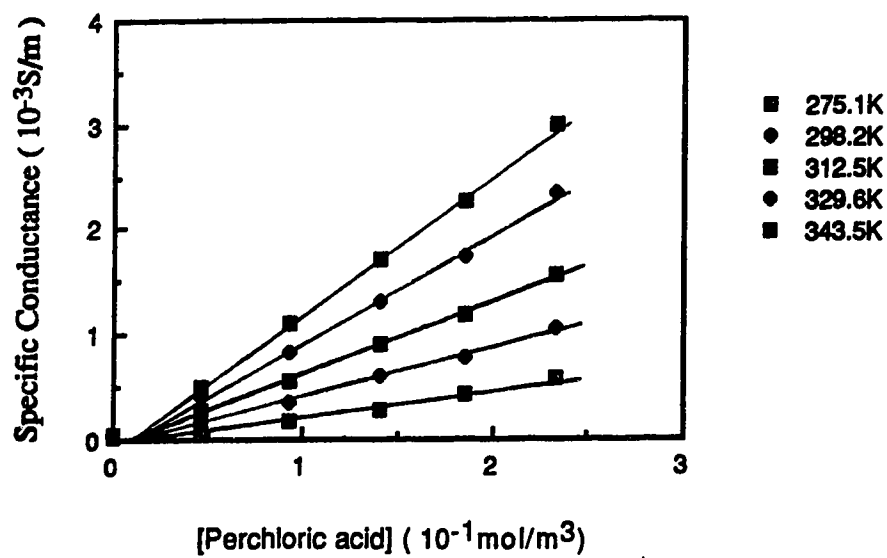


Fig.57 Temperature and concentration dependence of the conductance of
(A-G) perchloric acid in 2-propanol/water mixtures

C**D**

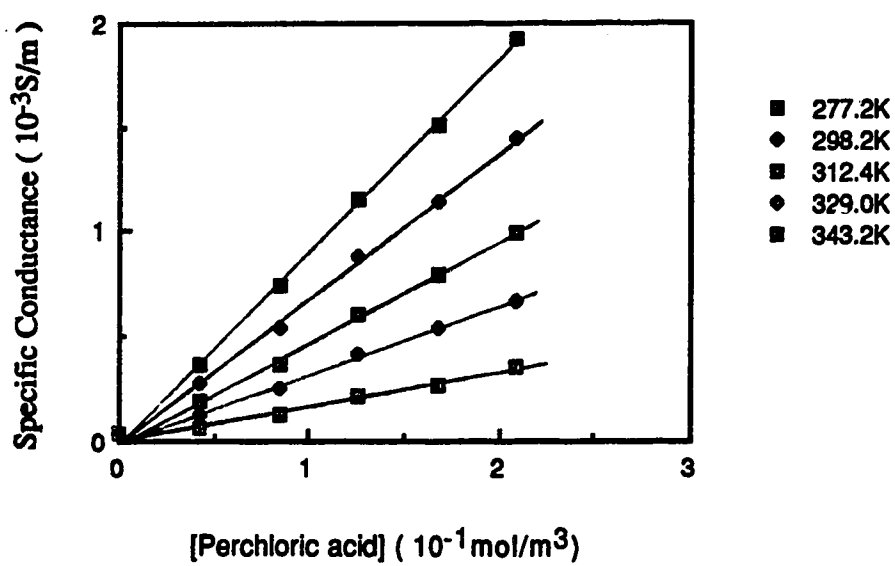
E

{35|2P| Perchloric acid}

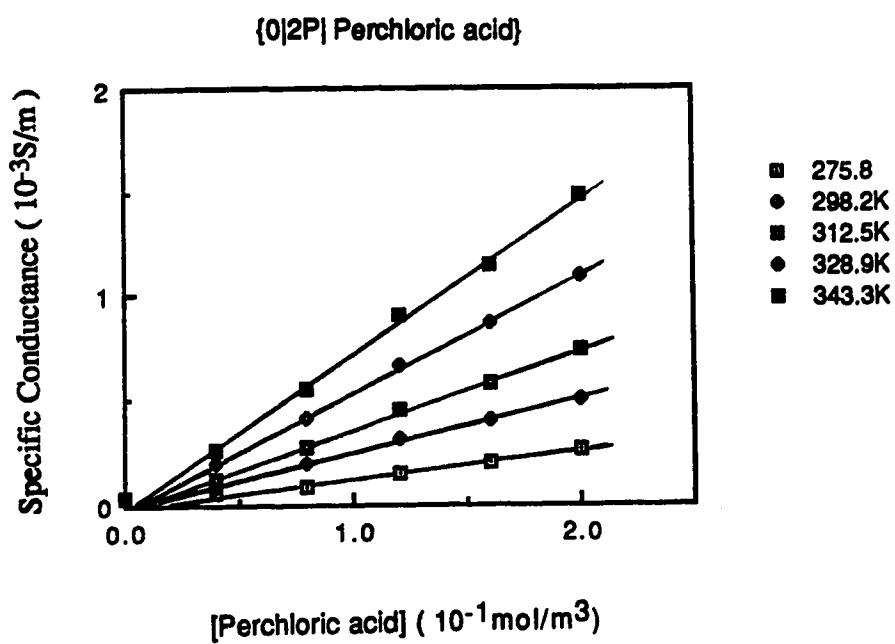


F

{20|2P| Perchloric acid}



G



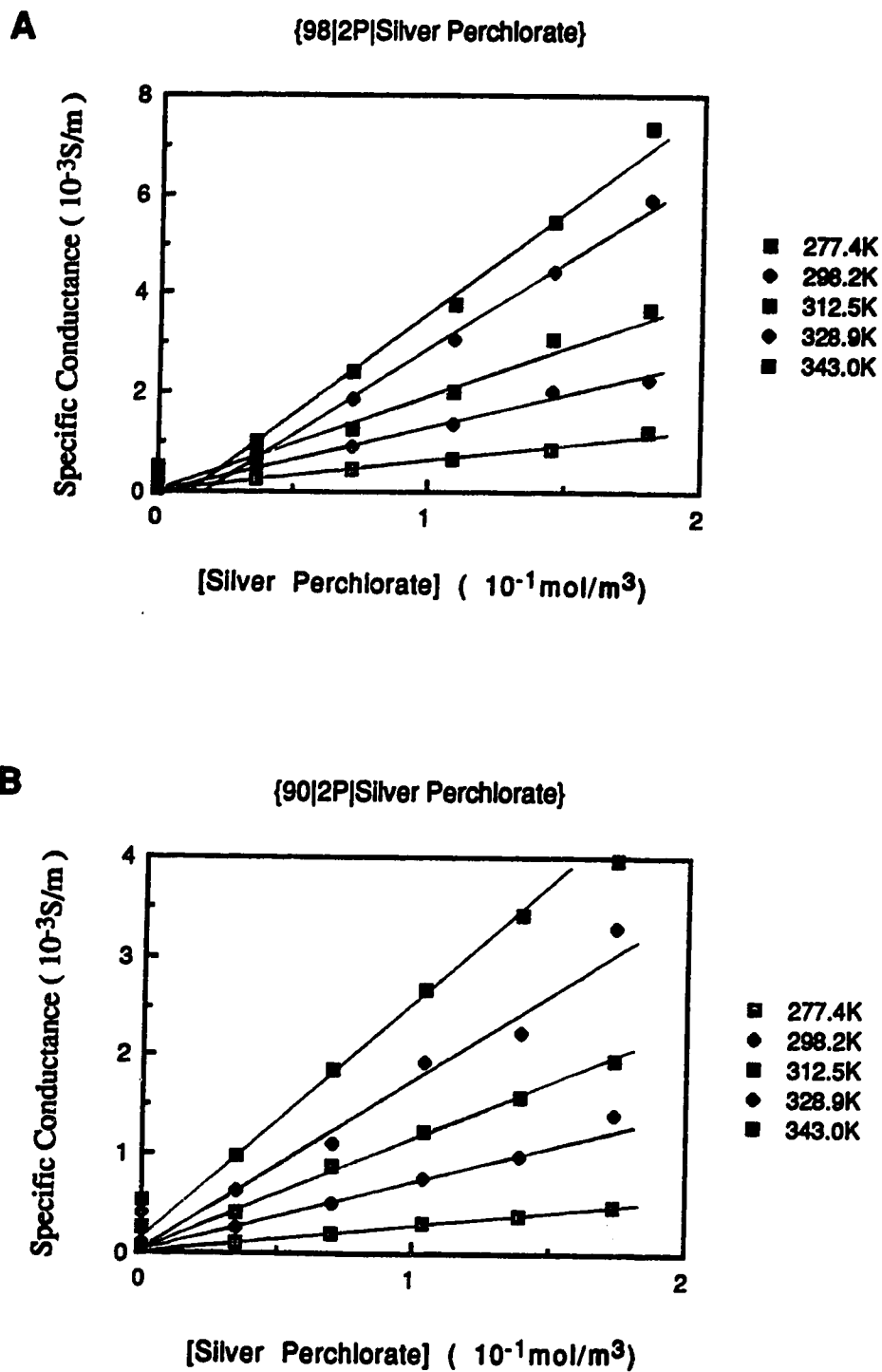
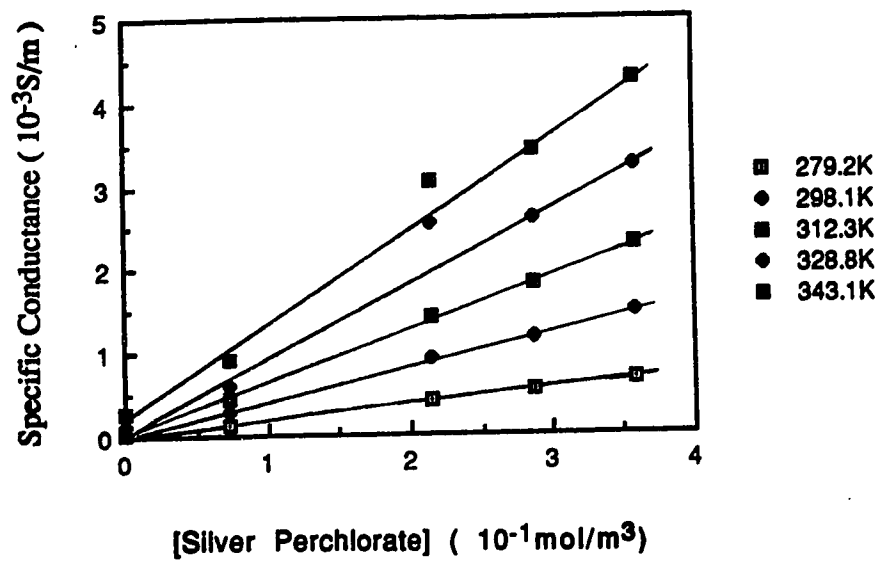
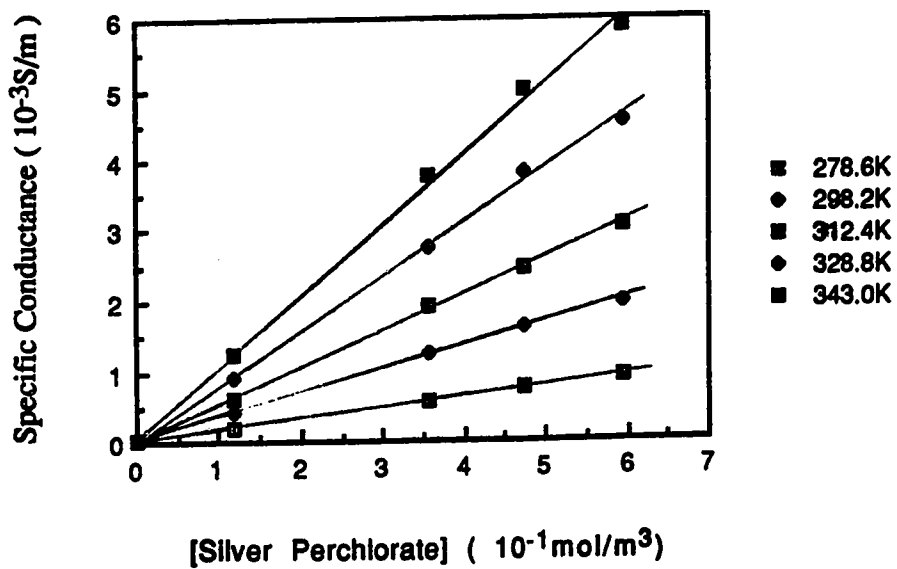
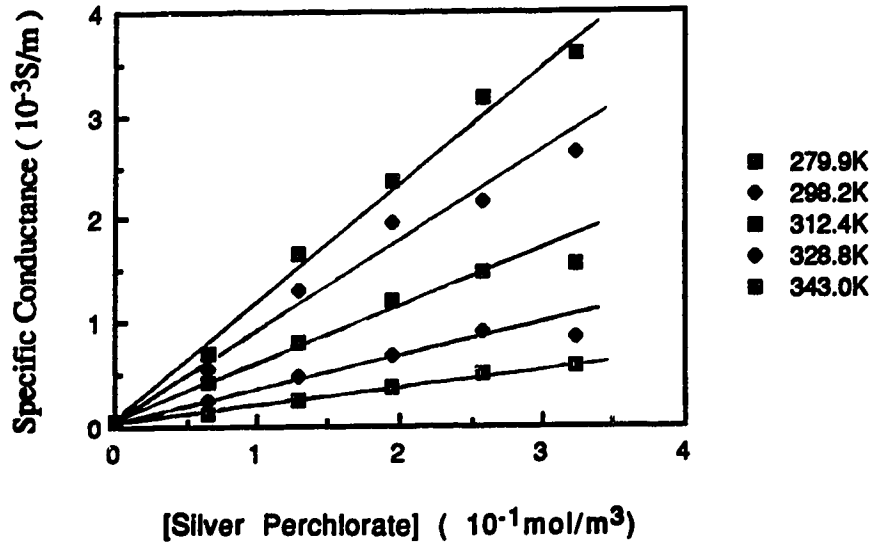
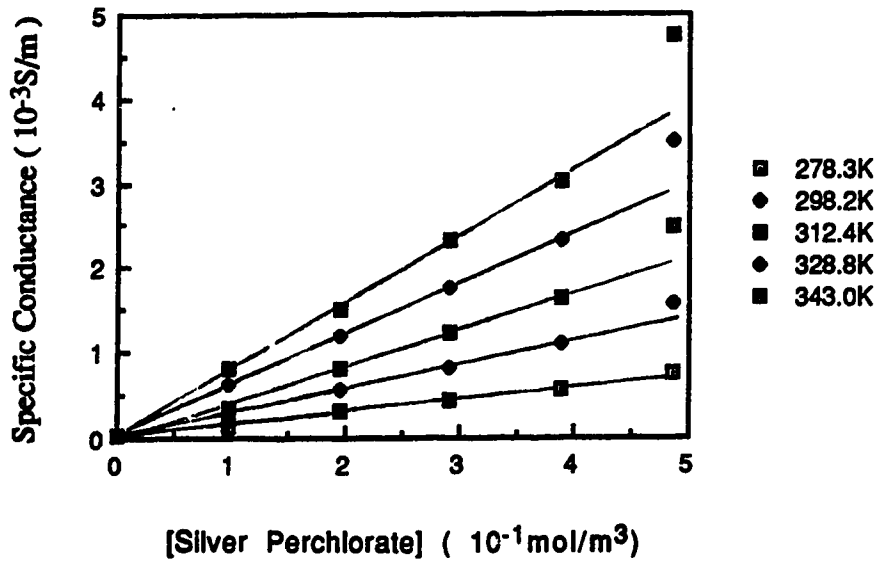


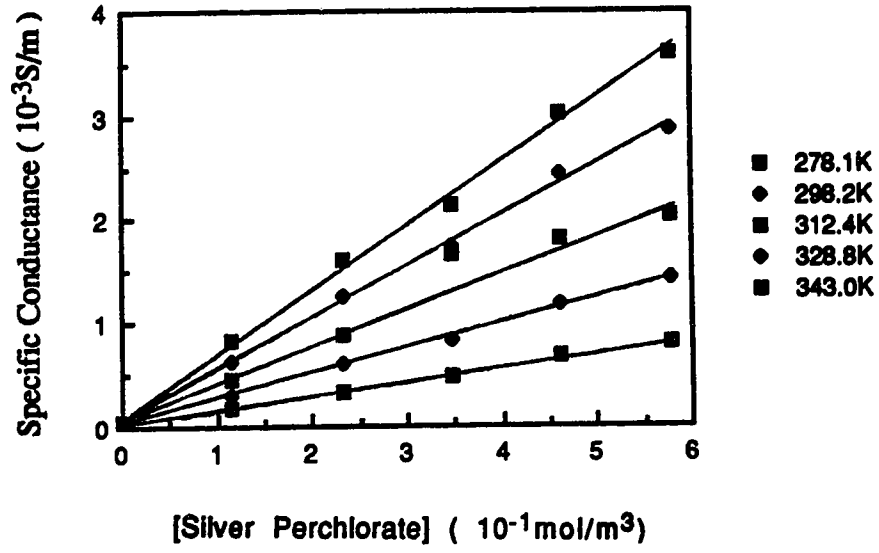
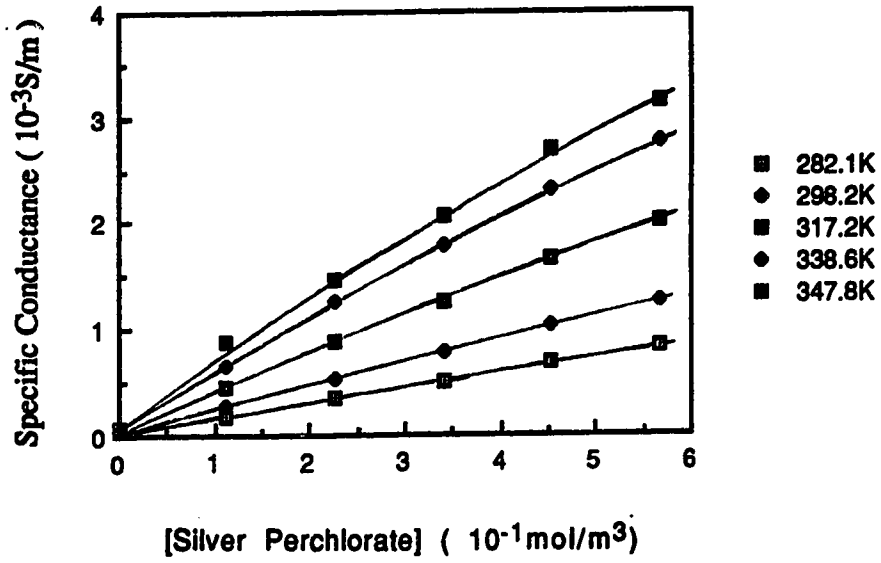
Fig.58

(A-I)

Temperature and concentration dependence of the conductance of silver perchlorate in 2-propanol/water mixtures

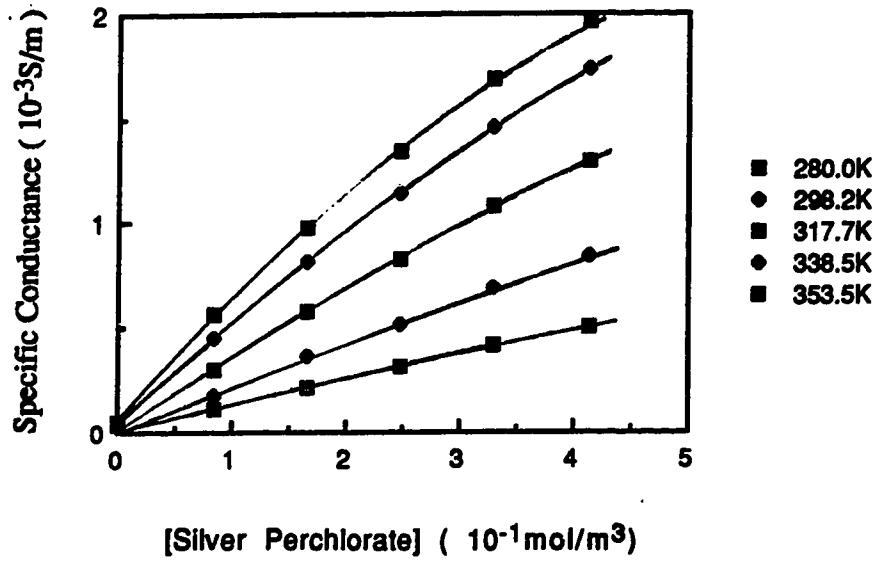
C**{81|2P|Silver Perchlorate}****D****{71|2P|Silver Perchlorate}**

E**{52|2P|Silver Perchlorate}****F****{35|2P|Silver Perchlorate}**

G**{20|2P|Silver Perchlorate}****H****{10|2P|Silver Perchlorate}**

I

{0|2P|Silver Perchlorate}



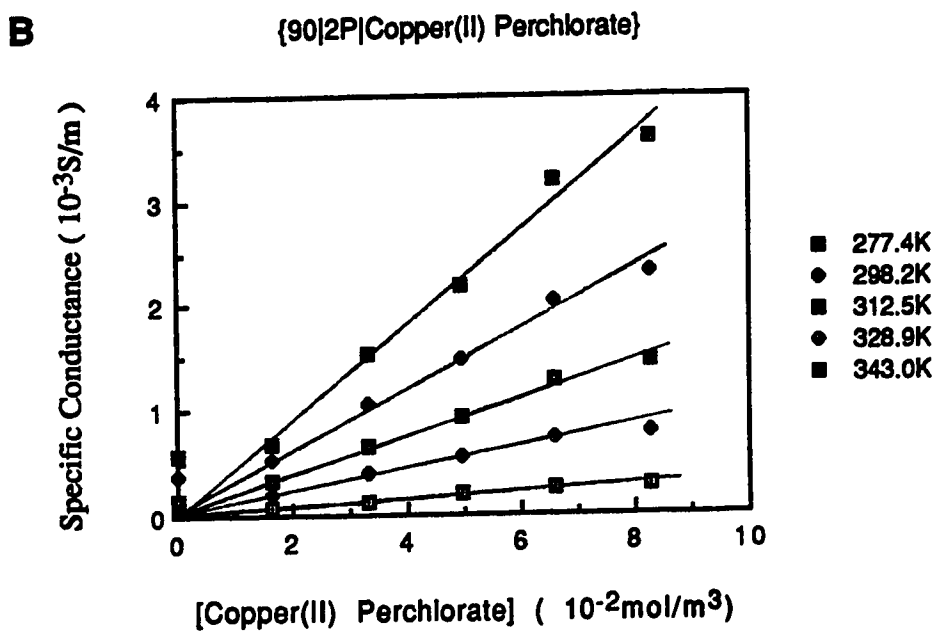
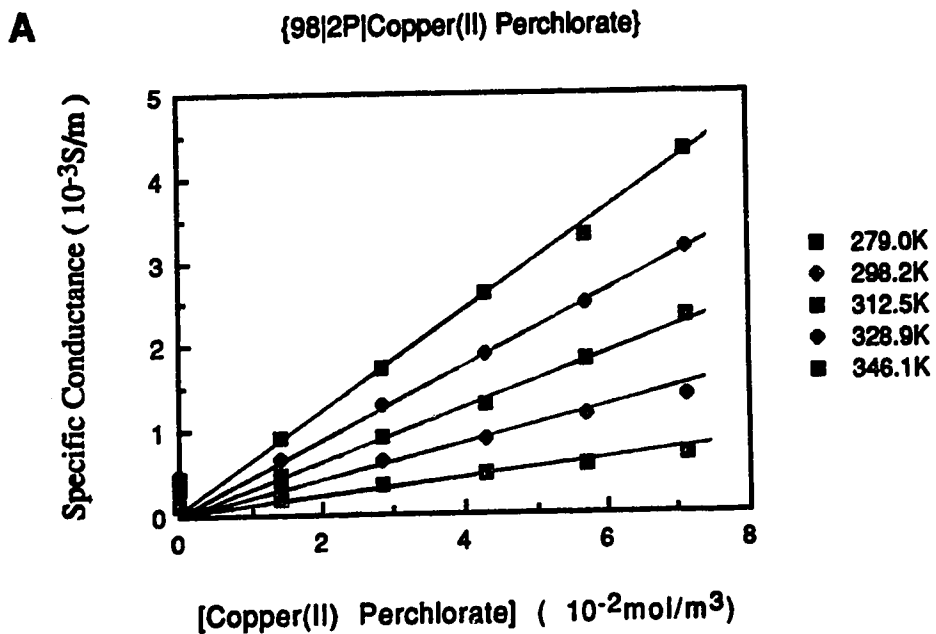
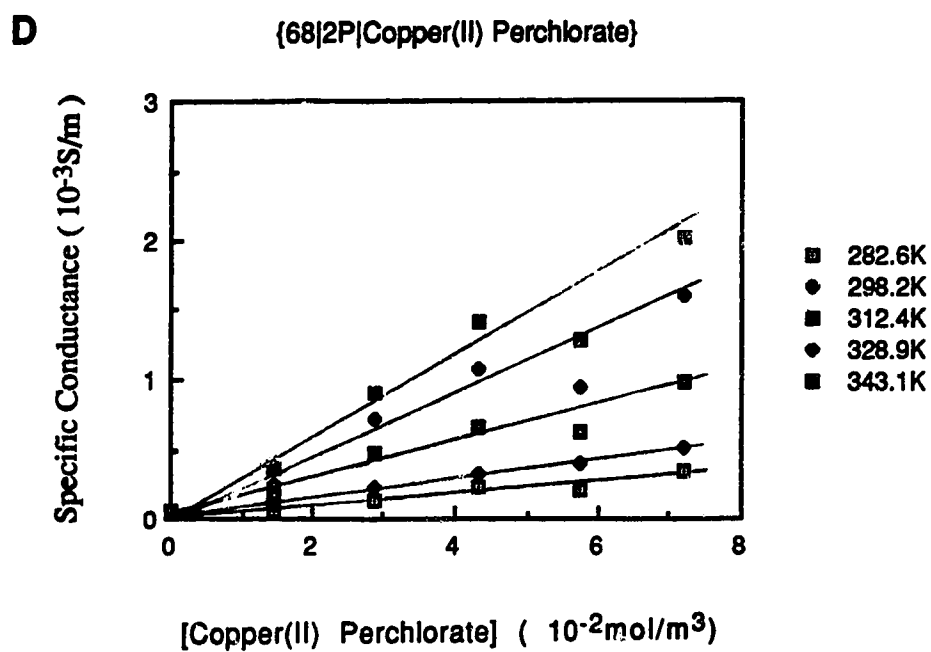
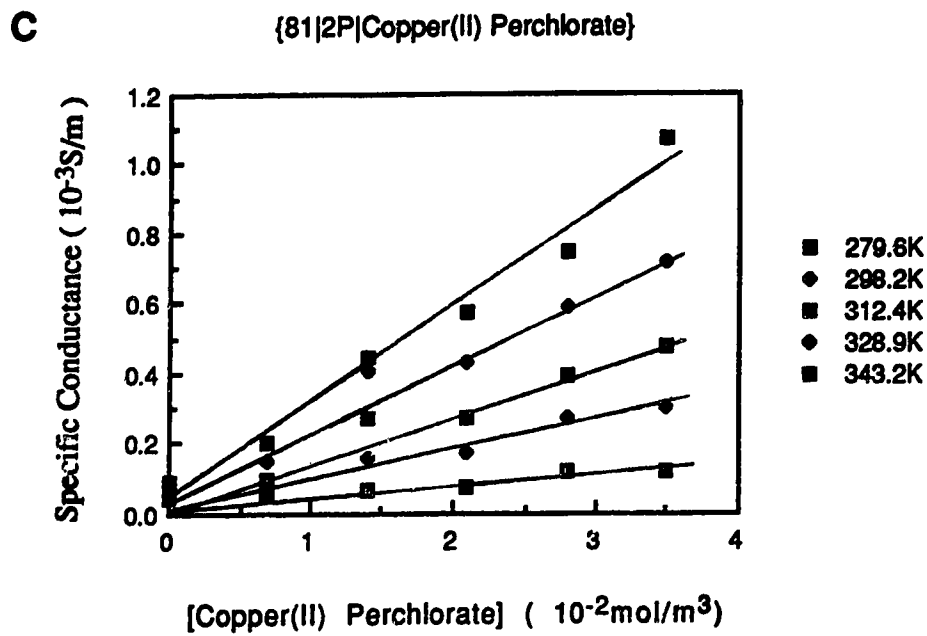
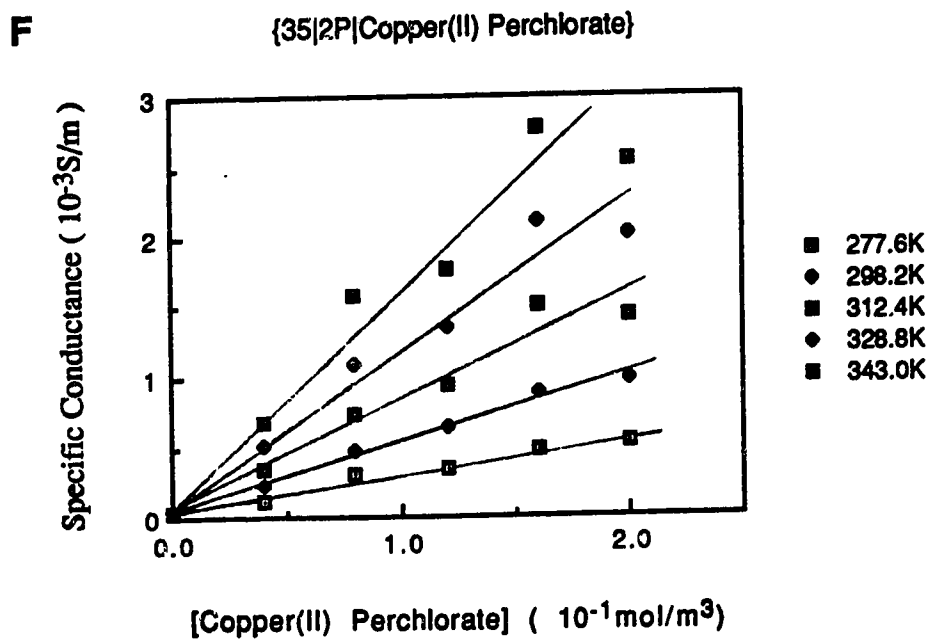
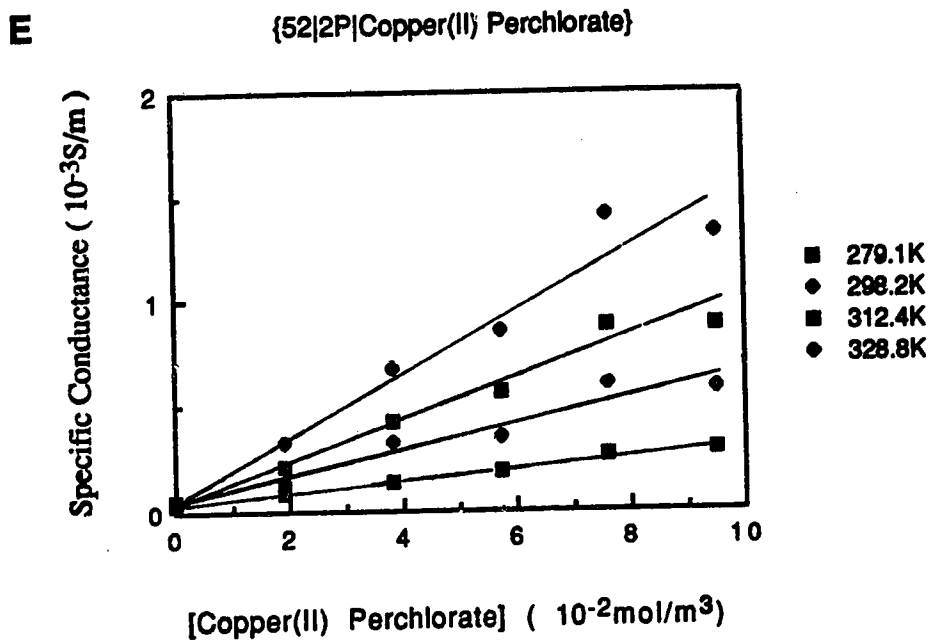
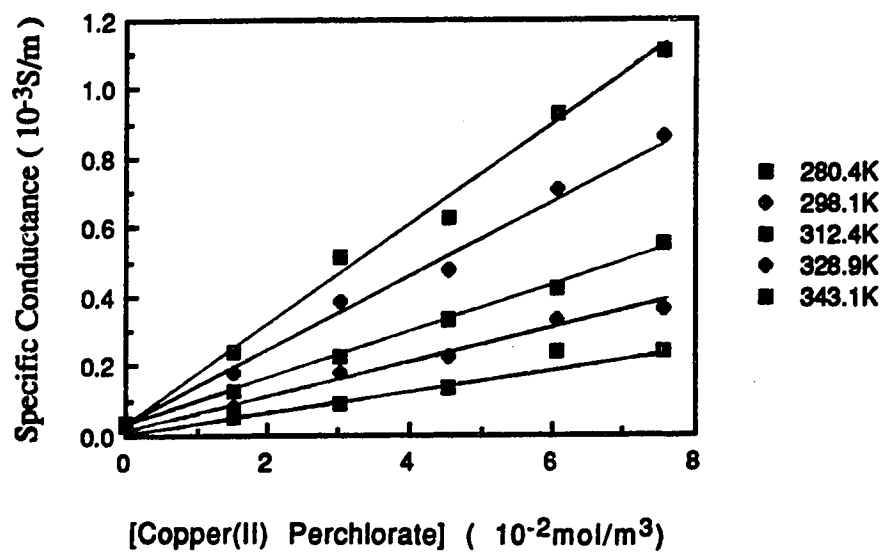
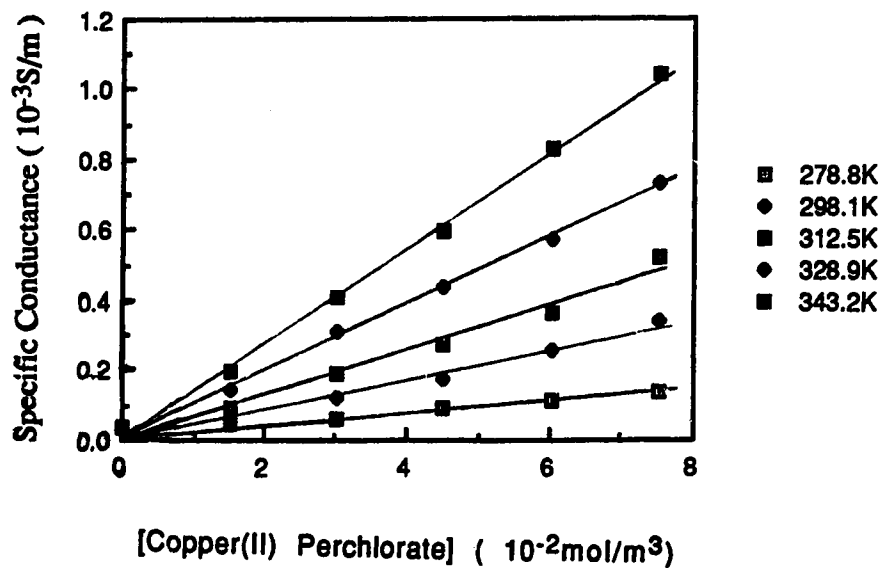


Fig. 59
(A-H)

Temperature and concentration dependence of the conductance of
copper(II) perchlorate in 2-propanol/water mixtures





G**{20}2P[Copper(II) Perchlorate]****H****{0}2P[Copper(II) Perchlorate]**

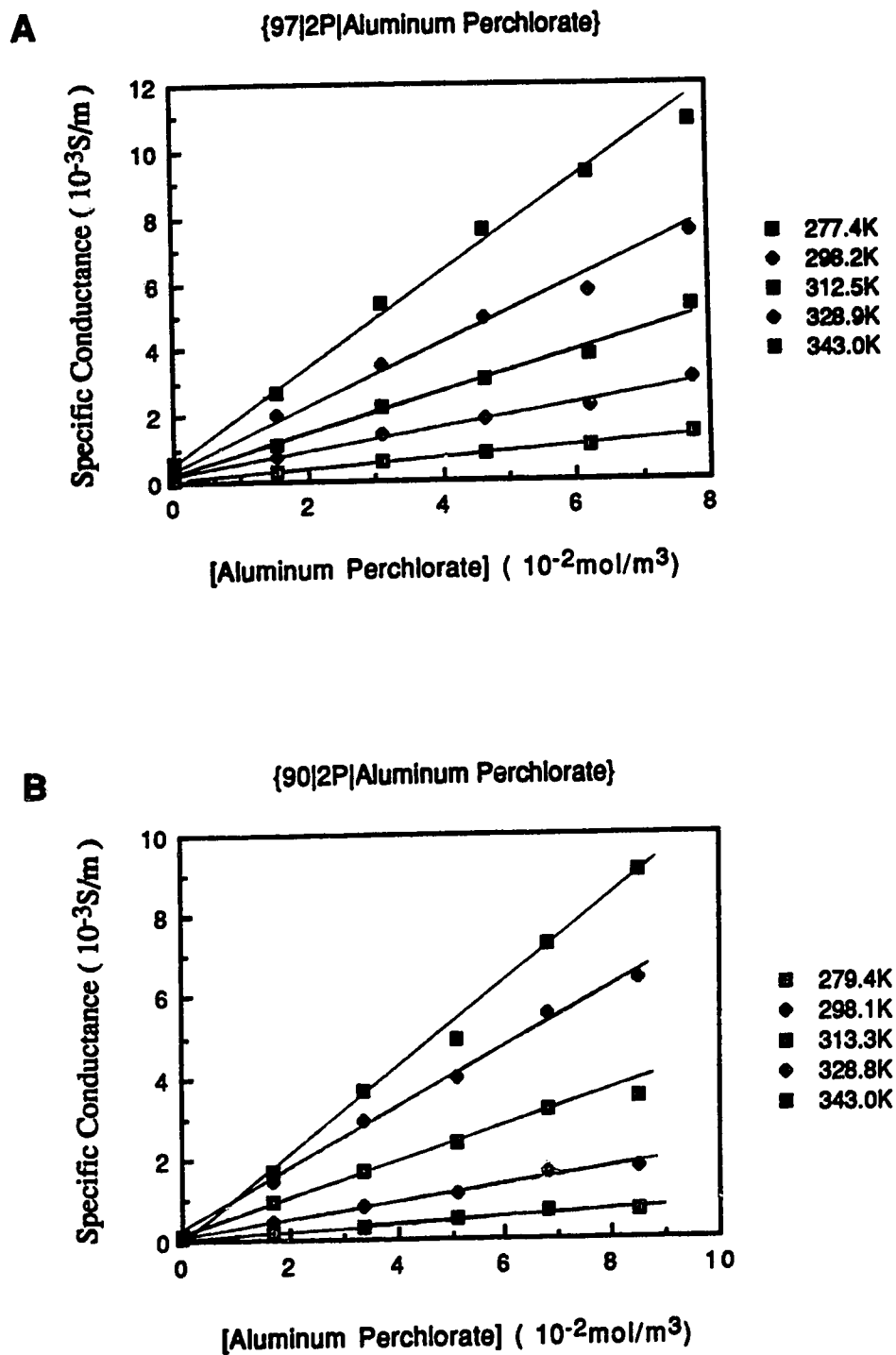
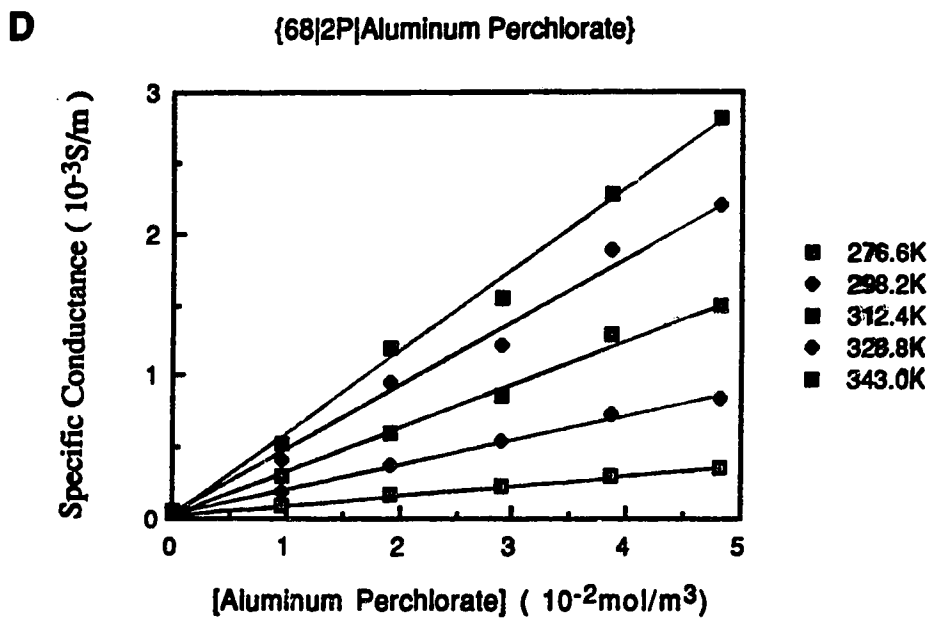
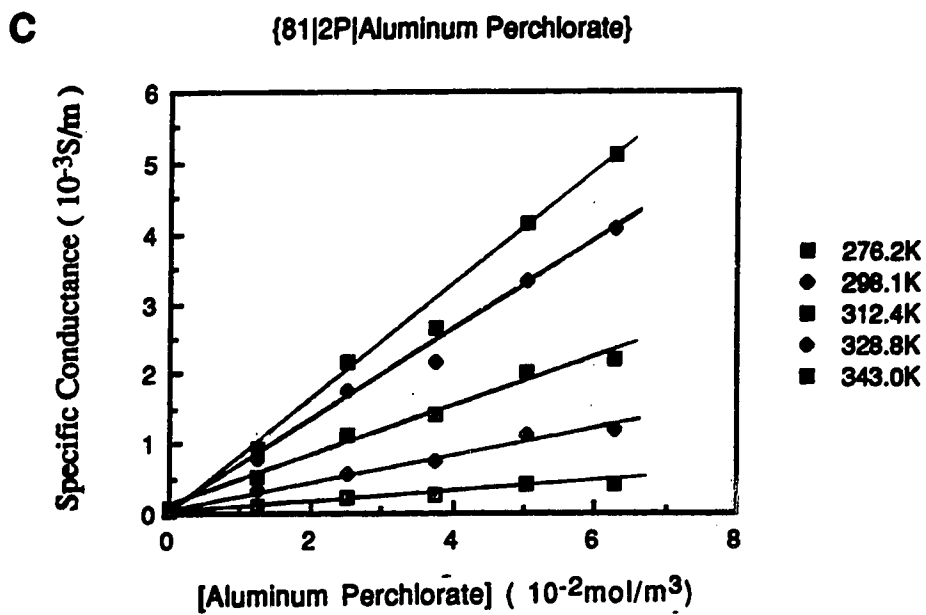
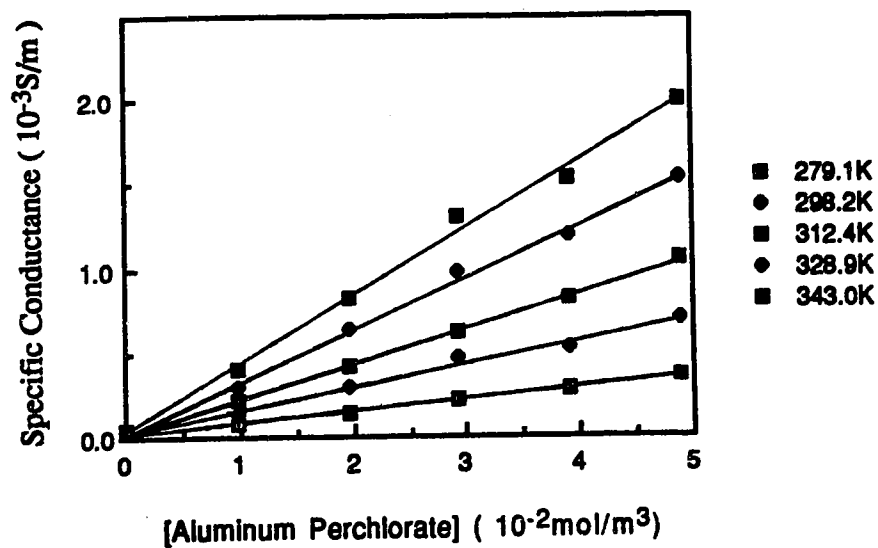
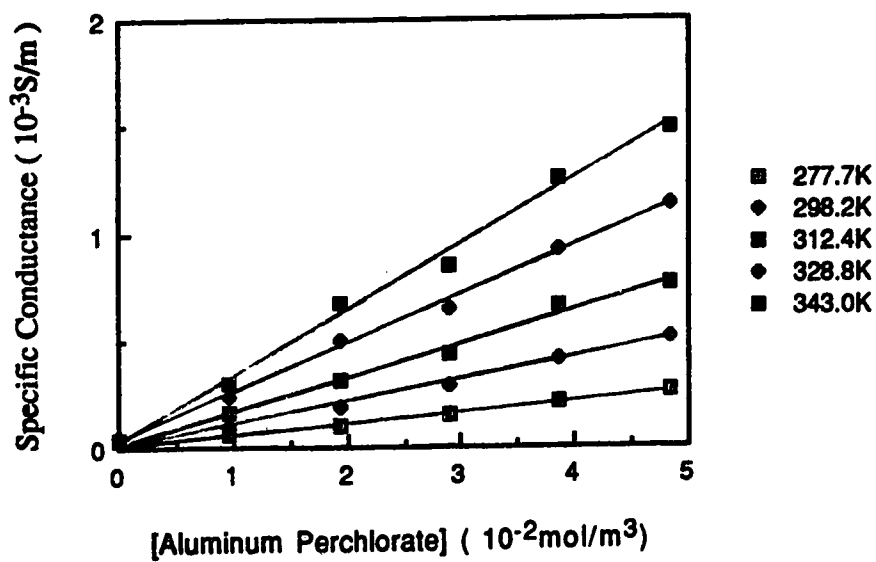


Fig. 60

Temperature and concentration dependence of the conductance of aluminum perchlorate in 2-propanol/water mixtures

(A-H)



E**{52|2P|Aluminum Perchlorate}****F****{36|2P|Aluminum Perchlorate}**

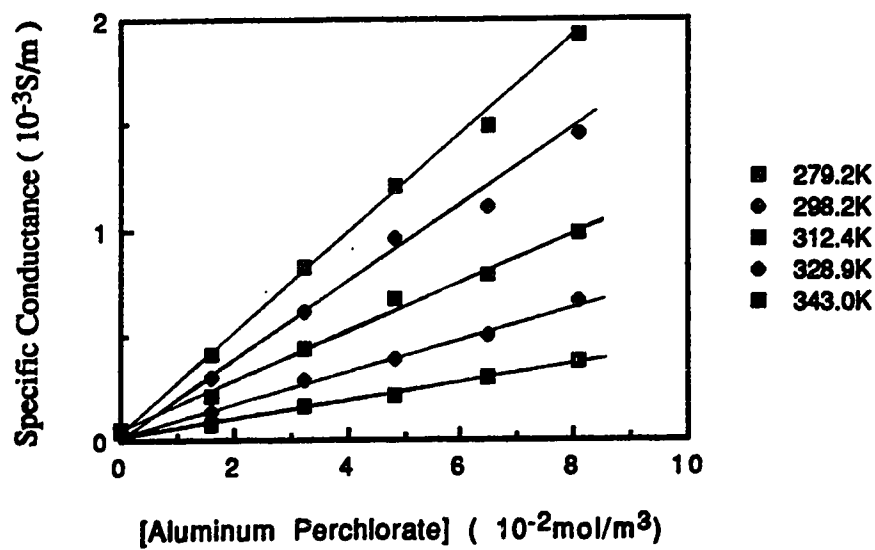
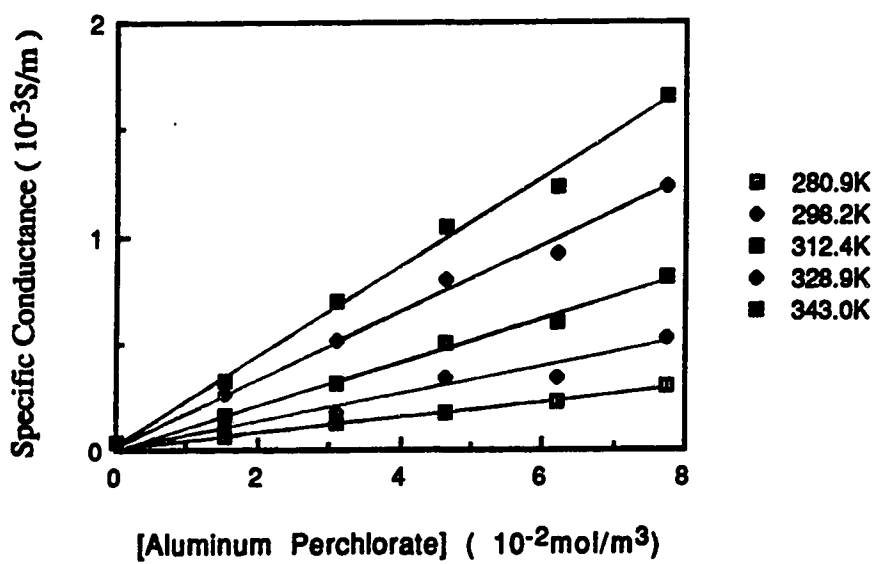
G**{20|2P|Aluminum Perchlorate}****H****{0|2P|Aluminum Perchlorate}**

Fig. 61 Arrhenius plots of molar conductance of lithium nitrate
in 2-propanol/water mixtures

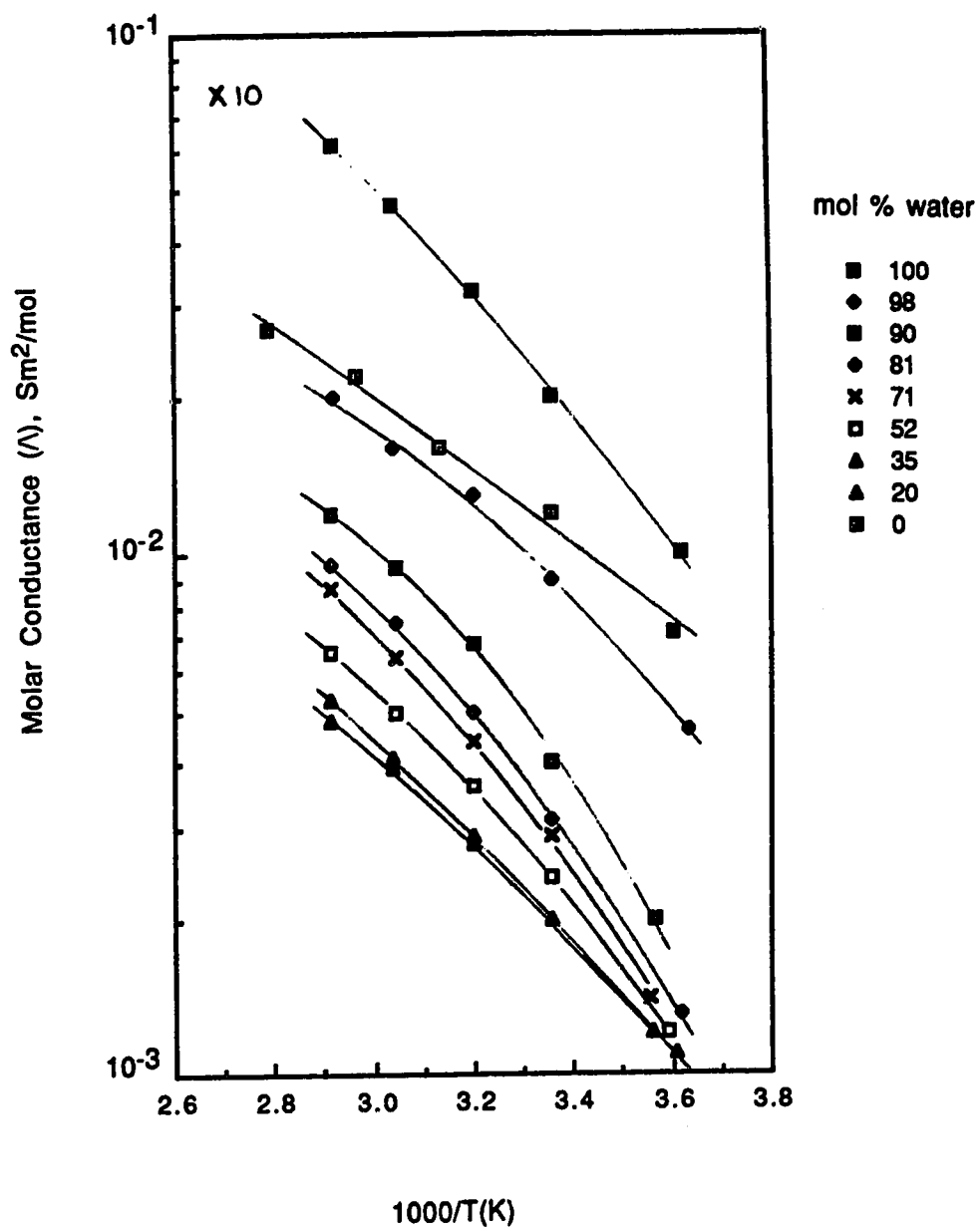


Fig. 62 Arrhenius plots of molar conductance of lithium chromate
in 2-propanol/water mixtures

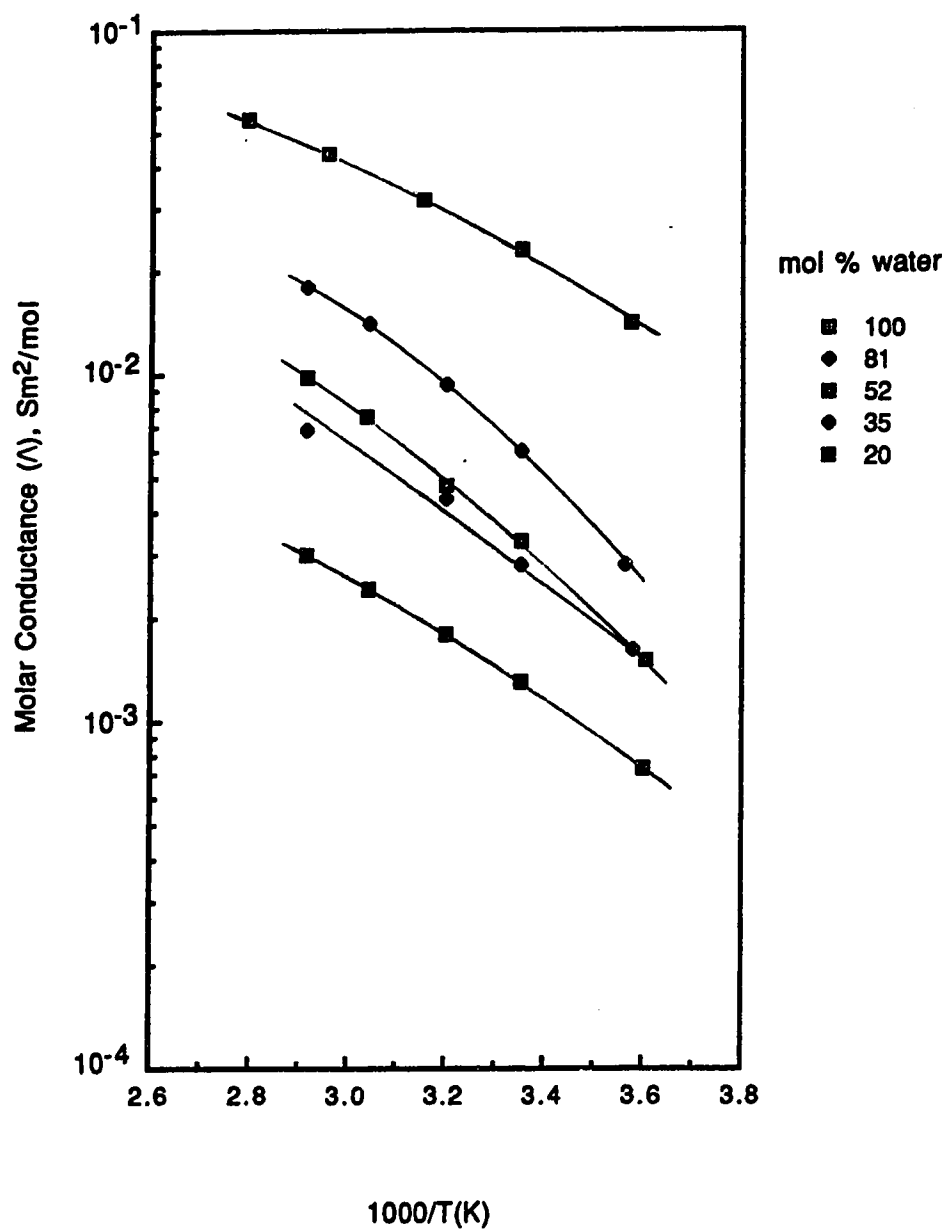


Fig. 63 Arrhenius plots of molar conductance of perchloric acid in 2-propanol/water mixtures

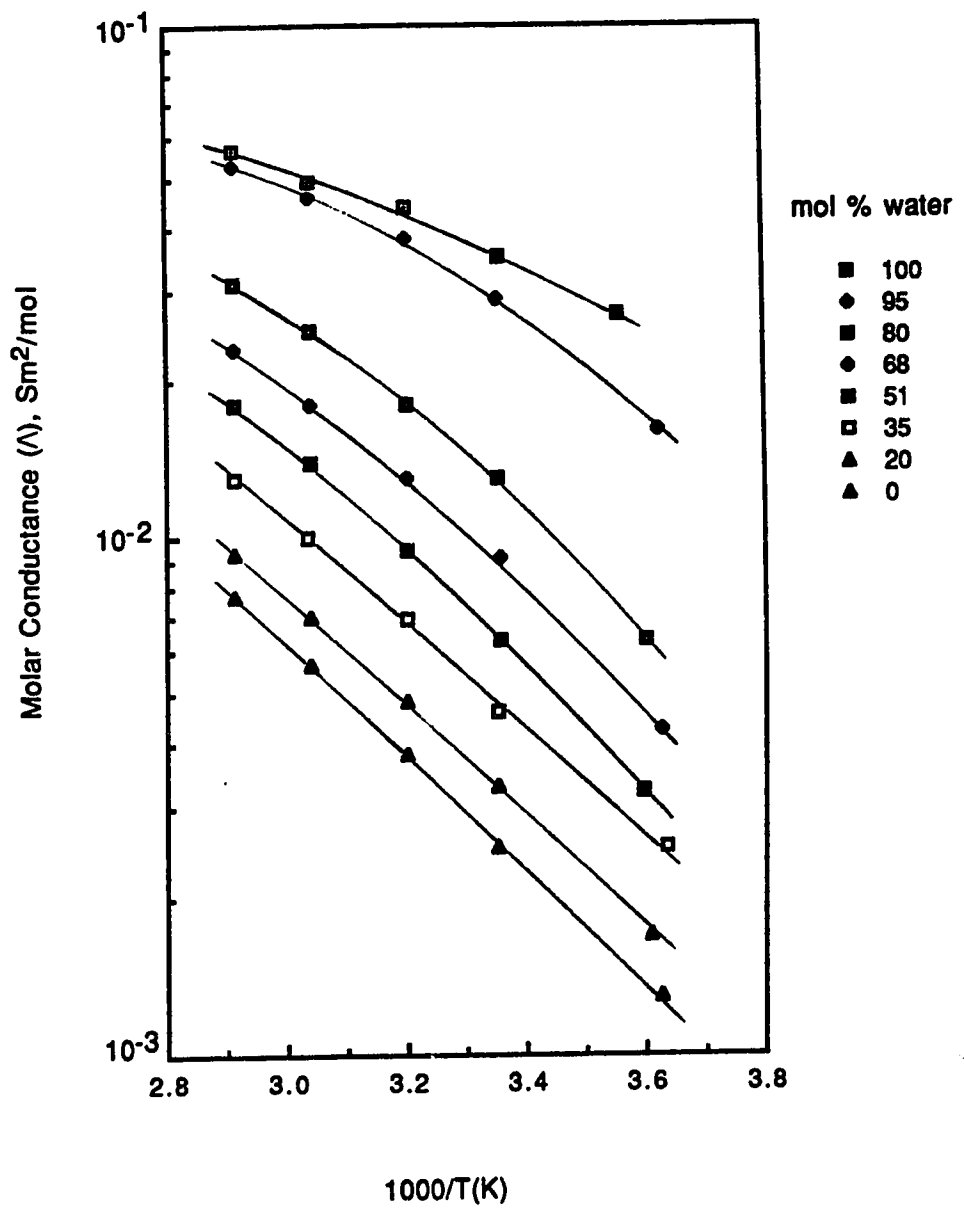


Fig. 64

Arrhenius plots of molar conductance of silver perchlorate
in 2-propanol/water mixtures

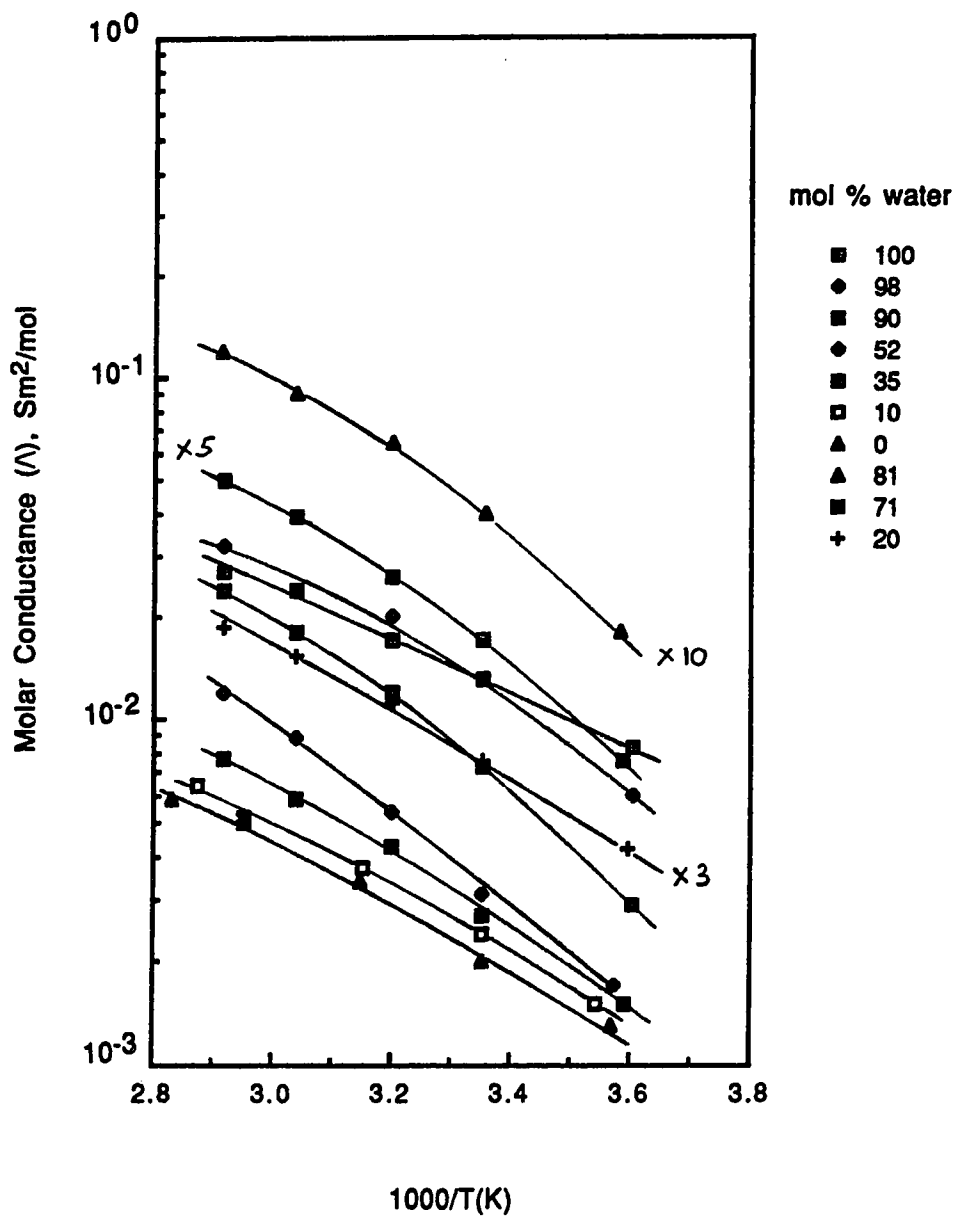


Fig. 65

Arrhenius plots of molar conductance of copper(II) perchlorate
in 2-propanol/water mixtures

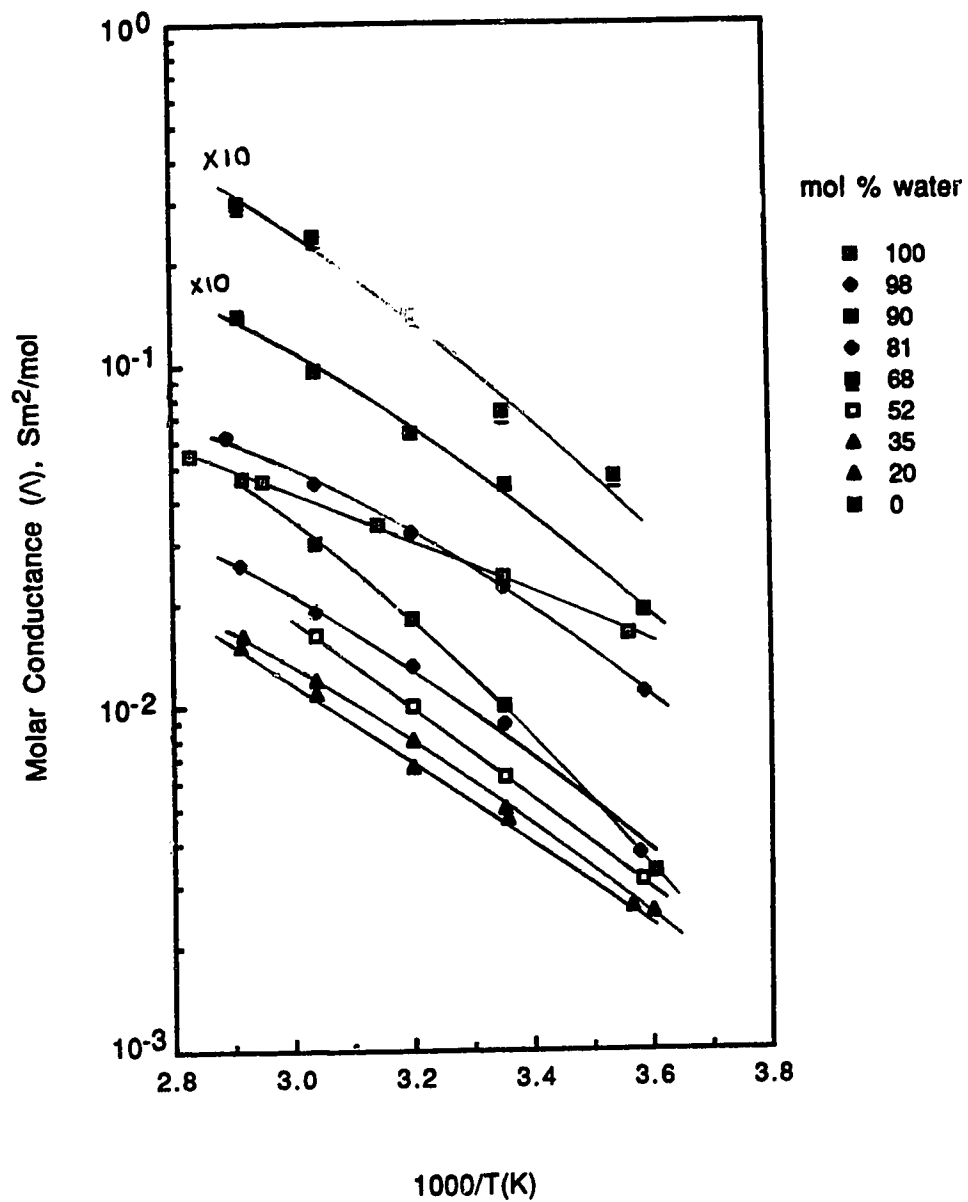


Fig. 66

Arrhenius plots of molar conductance of aluminum perchlorate
in 2-propanol/water mixtures

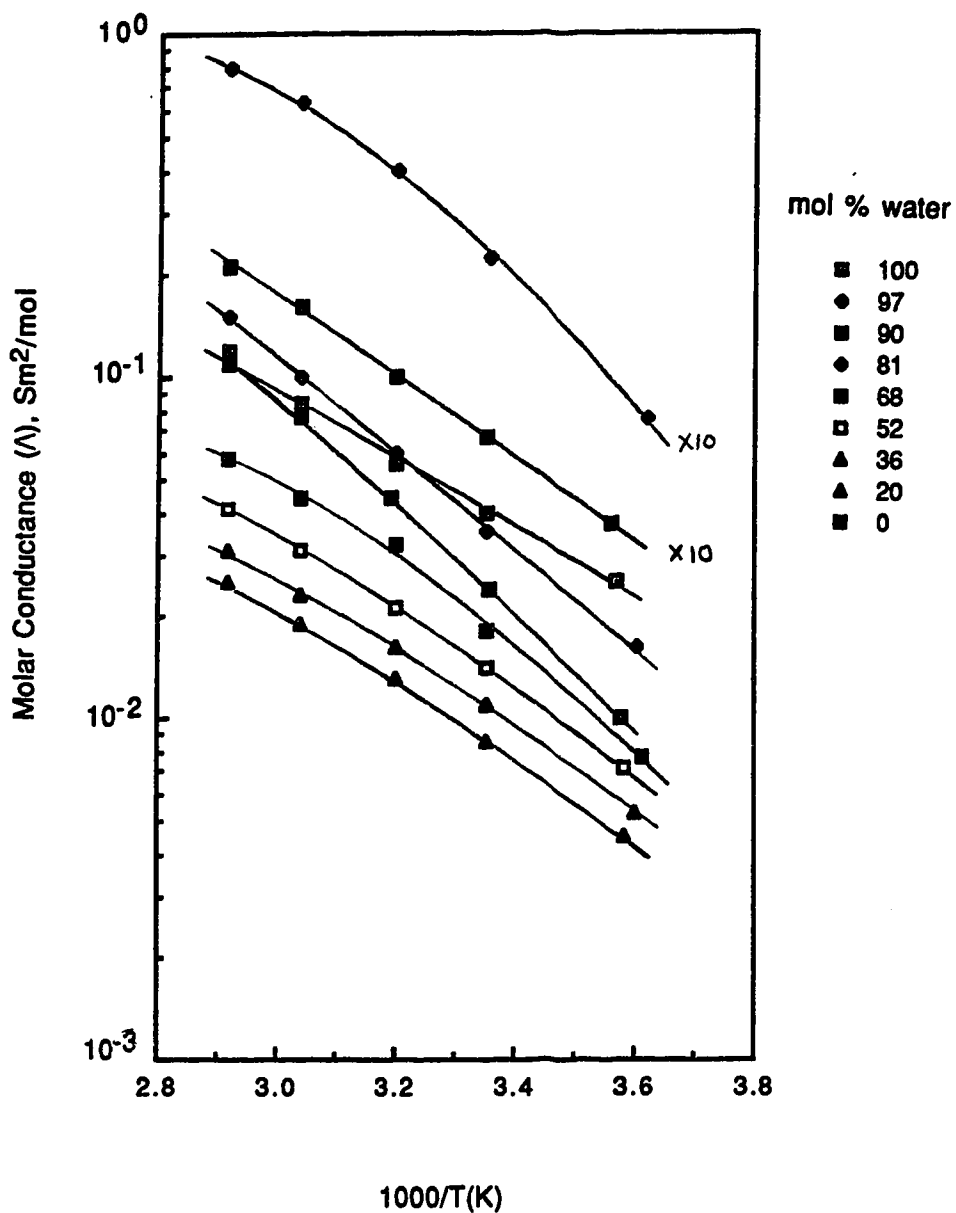


Fig. 67 A Composition dependence of the activation energy of conductance
of some inorganic electrolytes in 2-propanol/water mixtures

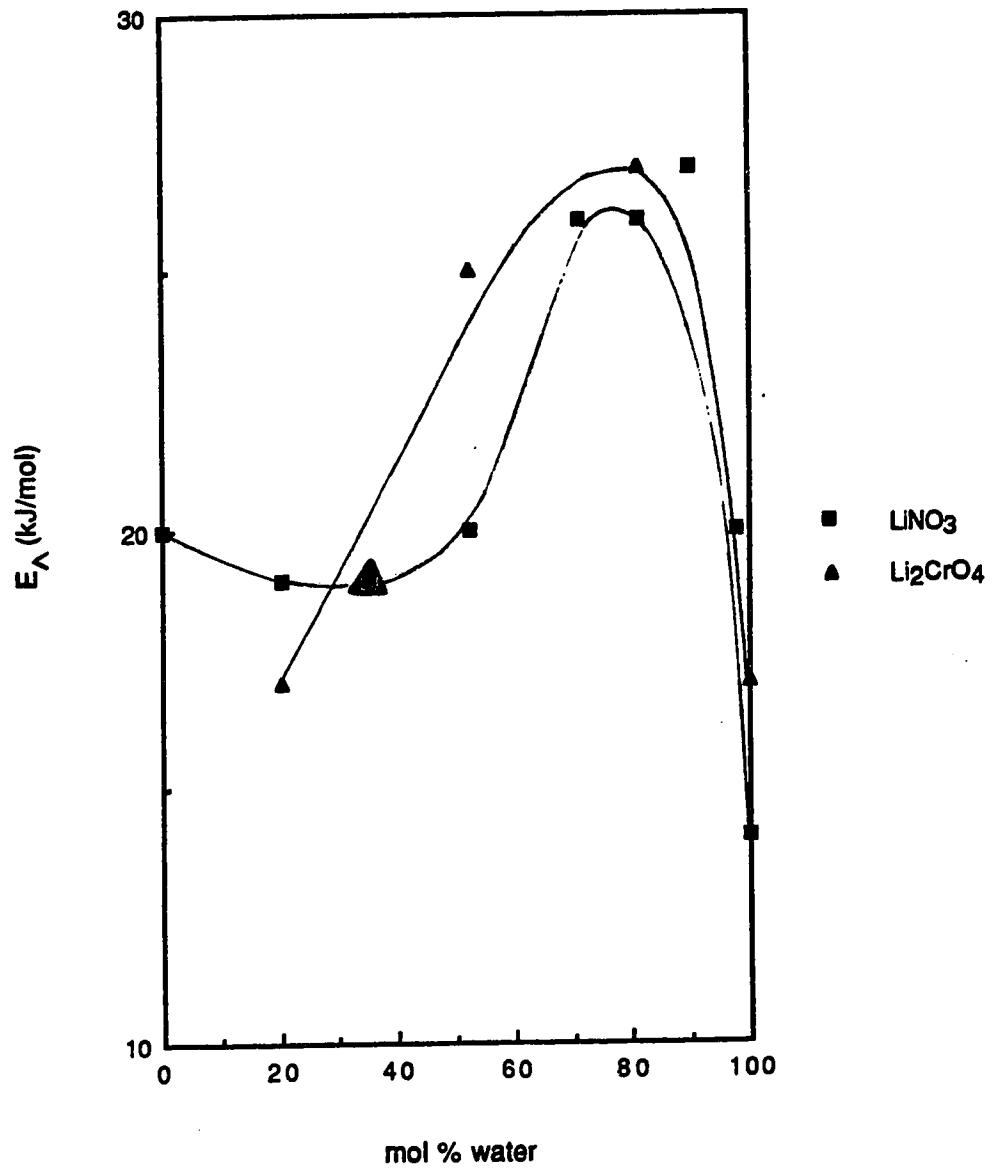


Fig. 67 B Composition dependence of the activation energy of conductance of some inorganic electrolytes in 2-propanol/water mixtures

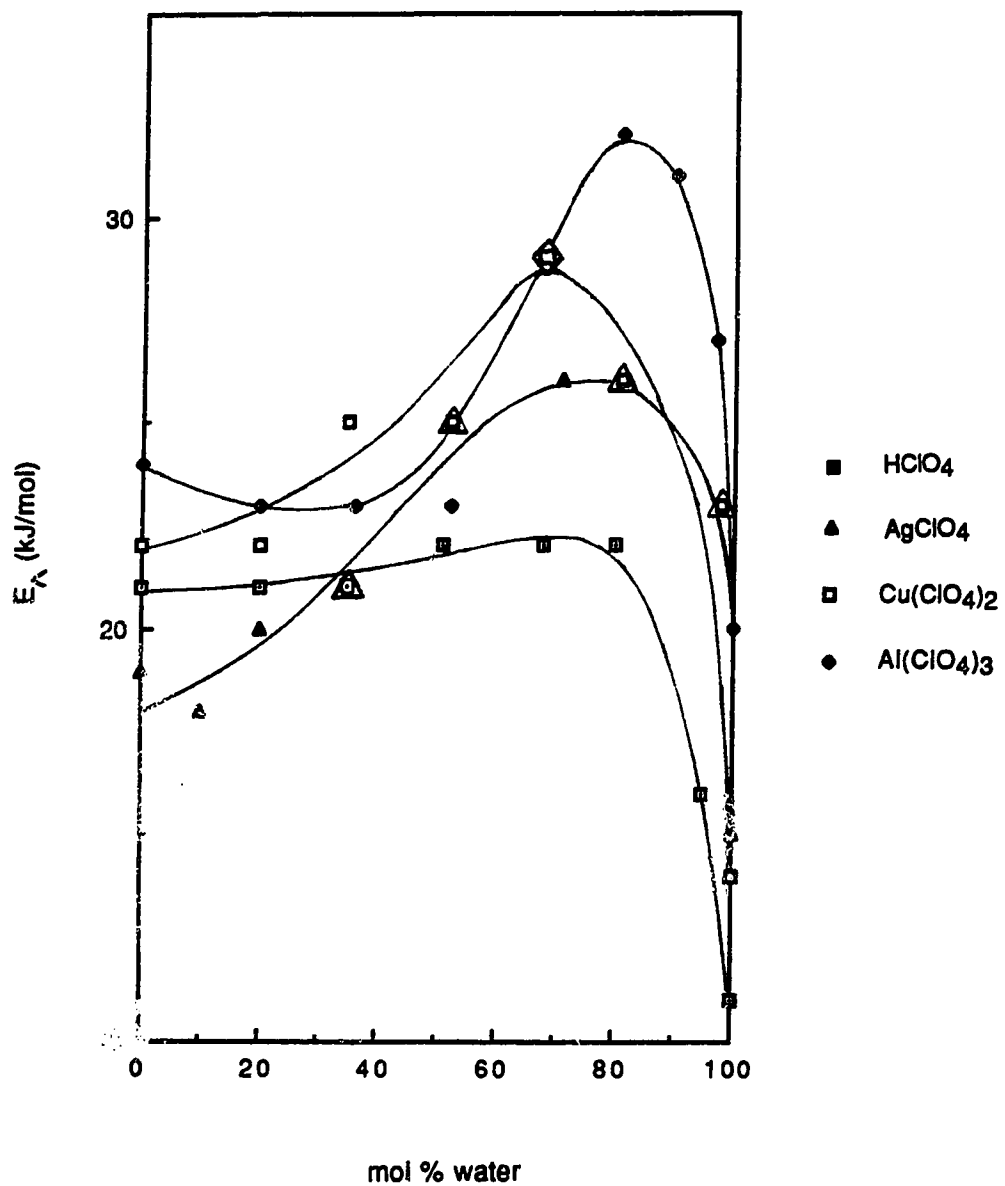


Table 41. Temperature and composition dependence of molar conductances (Λ) of lithium nitrate in 2-propanol/water mixtures.

X_w	Temp (K)	Λ_0 ($10^{-3} \text{ S m}^2/\text{mol}$)	X_w	Temp (K)	Λ_0 ($10^{-3} \text{ S m}^2/\text{mol}$)
1.00	277.7	7.1	0.52	278.5	1.2
	298.2	12		298.2	2.4
	319.	16		312.4	3.6
	377.4	22		328.8	5.0
	358.4	27		343.1	6.5
E_A , kJ/mol		14			20
0.98	275.1	4.6	0.35	277.3	1.1
	298.2	9.0		298.2	2.0
	312.5	13		312.4	2.9
	328.9	16		328.9	4.1
	343.0	20		343.1	5.3
E_A , kJ/mol		20			19
0.90	280.6	2.0	0.20	280.8	1.2
	298.2	4.0		298.2	2.0
	312.7	6.8		312.4	2.8
	328.8	9.5		328.9	3.9
	343.1	12		343.4	4.8
E_A , kJ/mol		27			19
0.81	276.3	1.3	0.00 ^(a)	276.6	1.0
	298.2	3.1		298.2	2.0
	312.4	5.0		312.5	3.2
	328.8	7.4		328.9	4.7
	343.1	9.6		343.0	6.1
E_A , kJ/mol		26			20
0.71	281.3	1.4			
	298.2	2.9			
	312.4	4.4			
	328.8	6.4			
	343.1	8.6			
E_A , kJ/mol		26			

(a) Λ_0 calculated from curved specific conductance *versus* concentration plots.

Table 42. Temperature and composition dependence of molar conductances (Λ) of lithium chromate in 2-propanol/water mixtures.

X_w	Temp (K)	Λ_o ($10^{-3} \text{ S m}^2/\text{mol}$)	X_w	Temp (K)	Λ_o ($10^{-3} \text{ S m}^2/\text{mol}$)
1.00	279.7	14	0.35(a)	279.3	1.6
	298.2	23		298.2	2.8
	317.4	32		312.4	4.4
	338.3	44		343.0	6.9
	357.7	55		342.9	17
E_Λ , kJ/mol		17			19
0.81	280.7	2.8	0.20(a)	277.8	0.73
	298.2	6.0		298.1	1.3
	312.4	9.4		312.5	1.8
	328.8	14		328.9	2.4
	343.0	18		343.0	3.0
E_Λ , kJ/mol		27			17
0.52	277.4	1.5			
	298.2	3.3			
	312.5	4.8			
	329.3	7.5			
	343.0	9.8			
E_Λ , kJ/mol		25			

(a) Λ_o calculated from curved specific conductance *versus* concentration plots.

Table 43. Temperature and composition dependence of molar conductances (Λ) of perchloric acid in 2-propanol/water mixtures.

X_w	Temp (K)	Λ_o ($10^{-3} \text{ S m}^2/\text{mol}$)	X_w	Temp (K)	Λ_o ($10^{-3} \text{ S m}^2/\text{mol}$)
1.00	281.2	27	0.51	278.2	3.2
	298.1	35		298.1	6.3
	312.4	44		312.4	9.4
	328.9	49		328.9	14
	343.1	57		343.2	18
E_Λ , kJ/mol		11			22
0.95	276.2	16	0.35	275.1	2.5
	298.2	29		298.2	4.6
	312.4	38		312.5	6.9
	329.0	46		329.6	10
	343.4	53		343.5	13
E_Λ , kJ/mol		16			21
0.80	277.7	6.3	0.20	277.2	1.7
	298.3	13		298.2	3.3
	312.5	18		312.4	4.8
	329.0	25		329.0	7.0
	343.2	31		343.2	9.3
E_Λ , kJ/mol		22			21
0.65	275.9	4.2	0.00	275.8	1.3
	298.1	9.1		298.2	2.5
	312.4	13		312.4	3.8
	328.9	18		329.0	5.7
	343.3	23		343.3	7.7
E_Λ , kJ/mol		22			21

Table 44. Temperature and composition dependence of molar conductances (Λ) of silver perchlorate in 2-propanol/water mixtures.

X_w	Temp (K)	Λ_o ($10^{-3} \text{ S m}^2/\text{mol}$)	X_w	Temp (K)	Λ_o ($10^{-3} \text{ S m}^2/\text{mol}$)
1.00	277.4	8.2	0.52	279.9	1.7
	298.2	13		298.2	3.1
	312.5	17		312.4	5.4
	328.9	24		328.8	8.8
	343.0	27		343.0	12
E_Λ , kJ/mol		15			25
0.98	277.4	6.0	0.35	278.3	1.5
	298.2	13		298.2	2.7
	312.5	20		312.4	4.3
	328.9	24		328.8	5.9
	343.0	32		343.0	7.6
E_Λ , kJ/mol		23			21
0.90	277.4	2.9	0.20	278.1	1.4
	298.2	7.3		298.2	2.5
	312.5	12		312.4	3.7
	328.9	18		328.8	5.1
	343.0	24		343.0	6.2
E_Λ , kJ/mol		28			20
0.81	279.2	1.8	0.10 ^(a)	282.1	1.5
	298.1	4.0		298.2	2.4
	312.3	6.4		317.2	3.7
	328.8	9.0		338.6	5.2
	343.1	12		347.8	6.4
E_Λ , kJ/mol		26			18
0.71	278.6	1.5	0.00 ^(a)	280.0	1.3
	298.2	3.4		298.2	2.0
	312.4	5.2		317.7	3.4
	328.8	7.8		338.5	5.0
	343.0	10		353.5	5.9
E_Λ , kJ/mol		26			19

(a) Λ_o calculated from curved specific conductance *versus* concentration plots.

Table 45. Temperature and composition dependence of molar conductances (Λ) of copper(II) perchlorate in 2-propanol/water mixtures.

X_w	Temp (K)	Λ_o ($10^{-3} \text{ S m}^2/\text{mol}$)	X_w	Temp (K)	Λ_o ($10^{-3} \text{ S m}^2/\text{mol}$)
1.00	281.0	16	0.52	279.1	3.1
	298.2	24		298.2	6.2
	318.0	34		312.4	10
	338.5	46		328.8	16
	353.5	55		342.9	17
E_A , kJ/mol		14			25
0.98	278.9	11	0.35	277.6	2.5
	298.2	22		298.2	5.0
	312.5	32		312.4	8.0
	328.9	45		328.8	12
	346.0	62		343.0	16
E_A , kJ/mol		23			25
0.90	277.4	3.3	0.20	280.4	2.6
	298.2	10		298.1	4.7
	312.5	18		312.4	6.7
	328.9	30		328.9	11
	343.0	47		343.1	15
E_A , kJ/mol		28			22
0.81	279.6	3.7	0.00	278.8	1.9
	298.2	8.9		298.1	4.4
	312.4	13		312.5	6.3
	328.9	19		328.9	9.6
	343.2	26		343.2	14
E_A , kJ/mol		26			22
0.68	282.6	4.7			
	298.2	7.3			
	312.4	14			
	328.9	24			
	343.1	30			
E_A , kJ/mol		29			

Table 46. Temperature and composition dependence of molar conductances (Λ) of aluminum perchlorate in 2-propanol/water mixtures.

X_w	Temp (K)	Λ_o ($10^{-3} \text{ S m}^2/\text{mol}$)	X_w	Temp (K)	Λ_o ($10^{-3} \text{ S m}^2/\text{mol}$)
1.00	280.2	2.5	0.52	279.1	0.71
	298.2	4.0		298.2	1.4
	312.4	5.6		312.4	2.1
	328.9	8.4		328.9	3.1
	343.0	12		343.0	4.1
E_Λ , kJ/mol		20			23
0.97	277.4	1.6	0.36	277.7	0.53
	298.2	3.5		298.2	1.1
	312.5	6.0		312.4	1.6
	328.9	10		328.8	2.3
	343.0	15		343.0	3.1
E_Λ , kJ/mol		27			23
0.90	279.4	1.0	0.20	279.2	0.45
	298.1	2.4		298.2	0.86
	313.3	4.4		312.4	1.3
	328.8	7.6		328.9	1.9
	343.0	11		343.0	2.5
E_Λ , kJ/mol		31			23
0.81	276.2	0.75	0.00	280.9	0.37
	298.1	2.2		298.2	0.67
	312.4	4.0		312.4	1.0
	328.8	6.3		328.9	1.6
	343.0	7.9		343.0	2.1
E_Λ , kJ/mol		32			24
0.68	276.6	0.77			
	298.2	1.8			
	312.4	3.2			
	328.8	4.4			
	343.0	5.8			
E_Λ , kJ/mol		29			

C. 2-Butanol/Water Mixtures

The molar conductance *versus* concentration plots are shown in Figure 68 (A-C) for LiNO_3 , Figure 69 (A-F) for HClO_4 , Figure 70 (A-G) for Tl(OAc) , Figure 71 (A-G) for $\text{Cu(ClO}_4)_2$, and Figure 72 (A-F) for $\text{Al(ClO}_4)_3$. The Arrhenius plots of molar conductance are shown in Figure 73 for LiNO_3 , Figure 74 for HClO_4 , Figure 75 for Tl(OAc) , Figure 76 for $\text{Cu(ClO}_4)_2$, and Figure 77 for $\text{Al(ClO}_4)_3$. The results are summarized in Figure 78 and Tables 47-51.

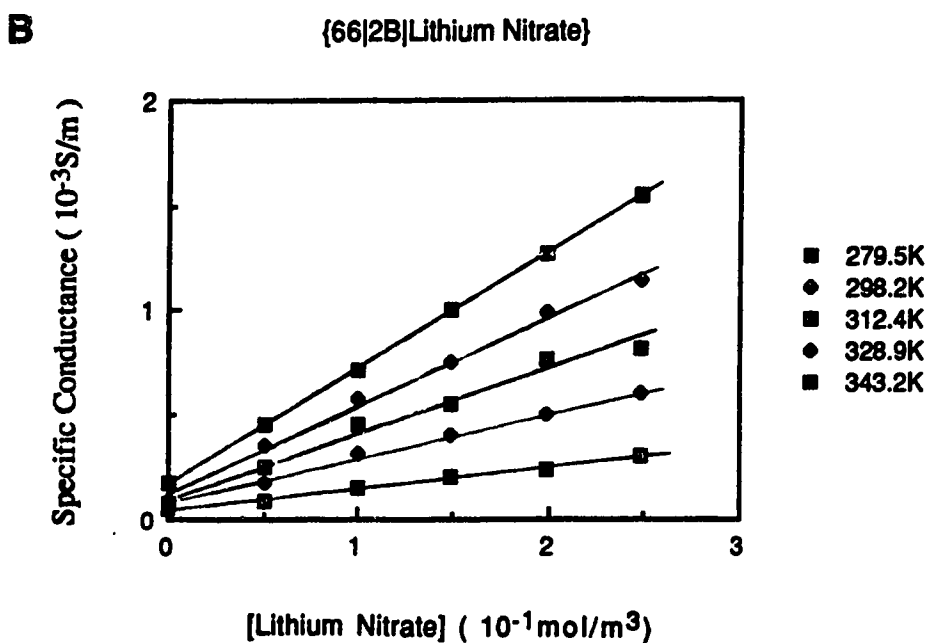
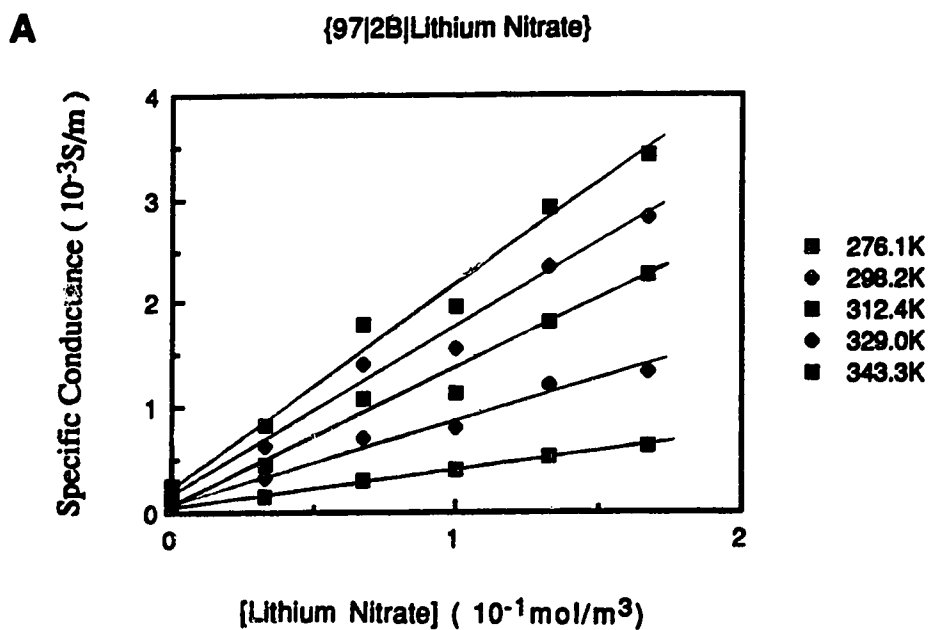
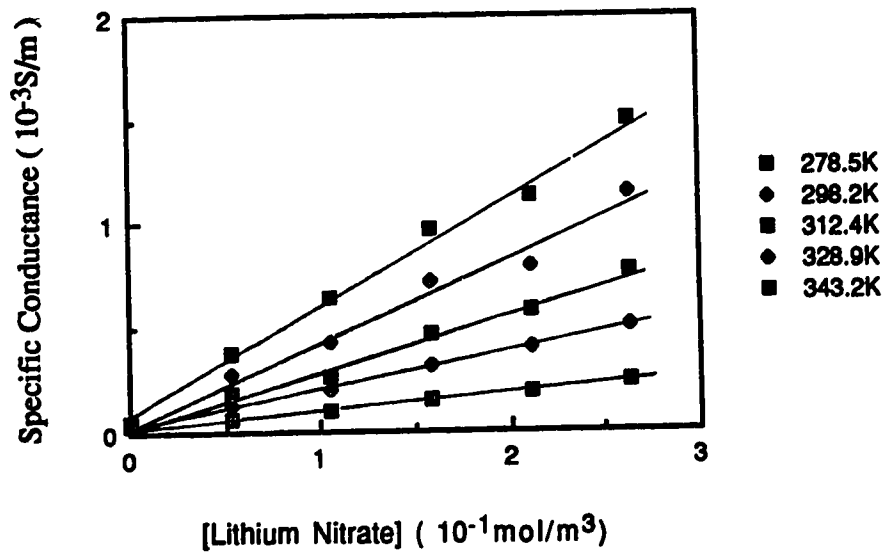
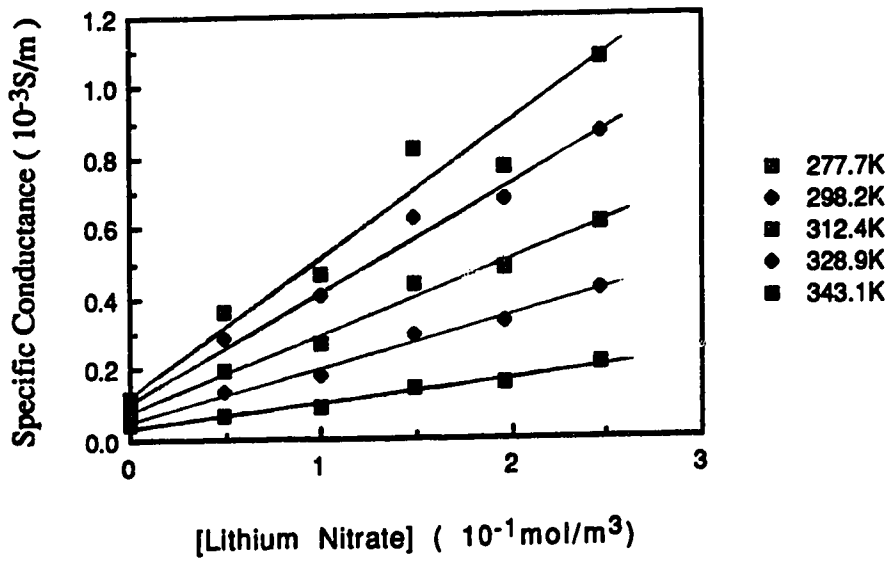
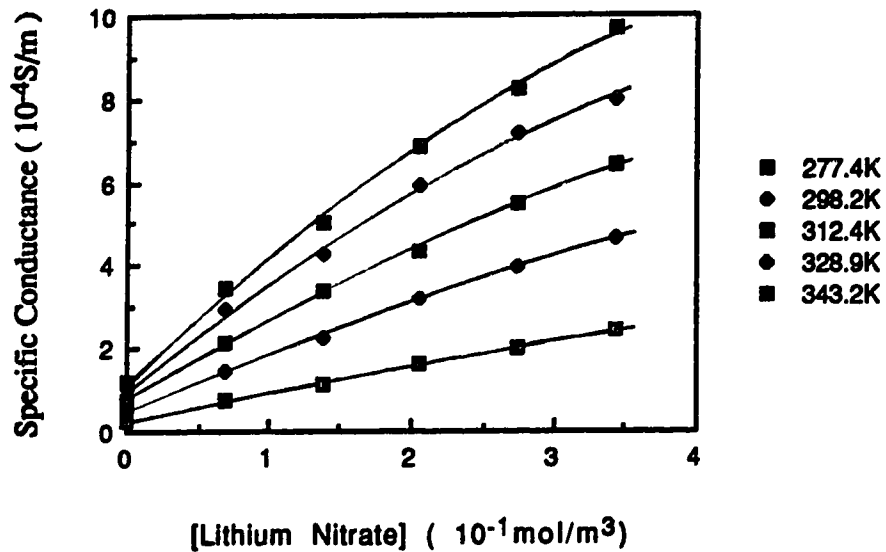


Fig.68 Temperature and concentration dependence of the conductance of lithium nitrate in 2-butanol/water mixtures (A-G)

C**{51|2B|Lithium Nitrate}****D****{34|2B|Lithium Nitrate}**

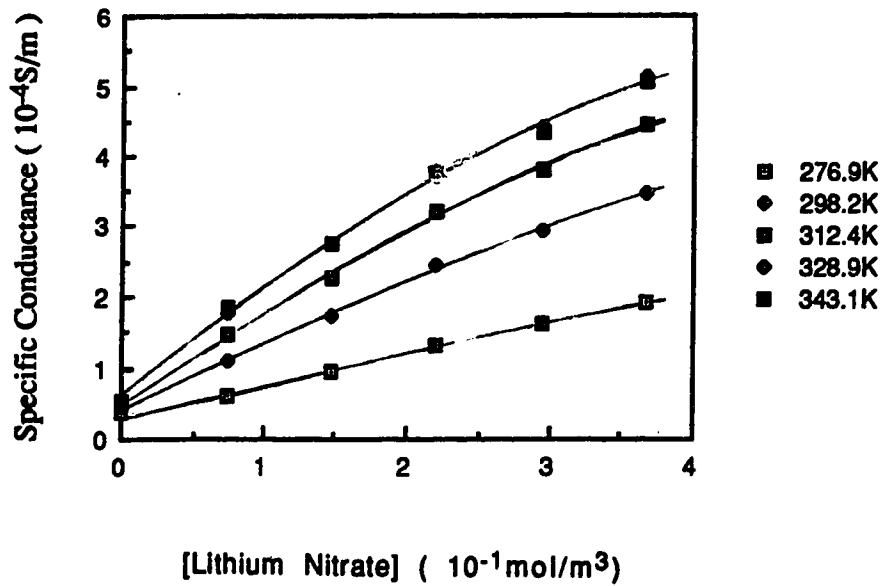
Π

{20|2B|Lithium Nitrate}



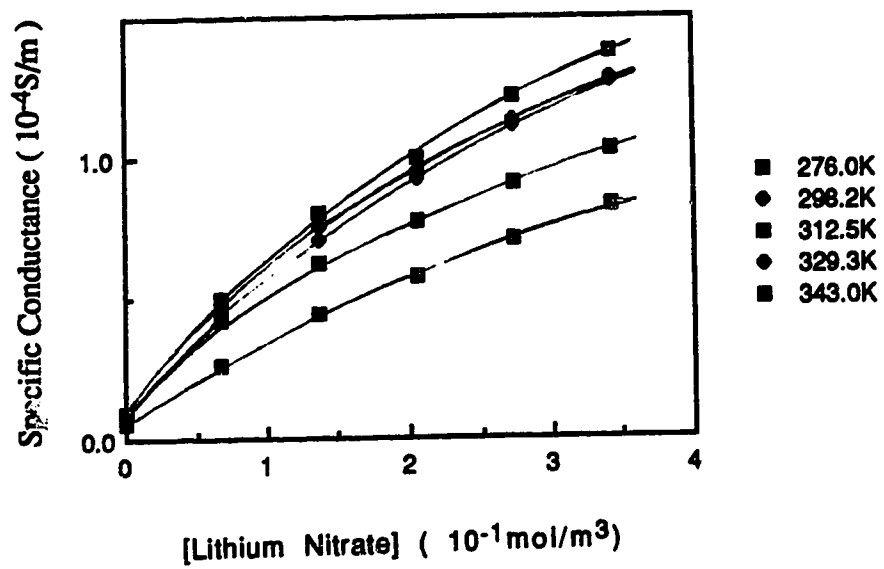
Π

{10|2B|Lithium Nitrate}



G

{0|2B|Lithium Nitrate}



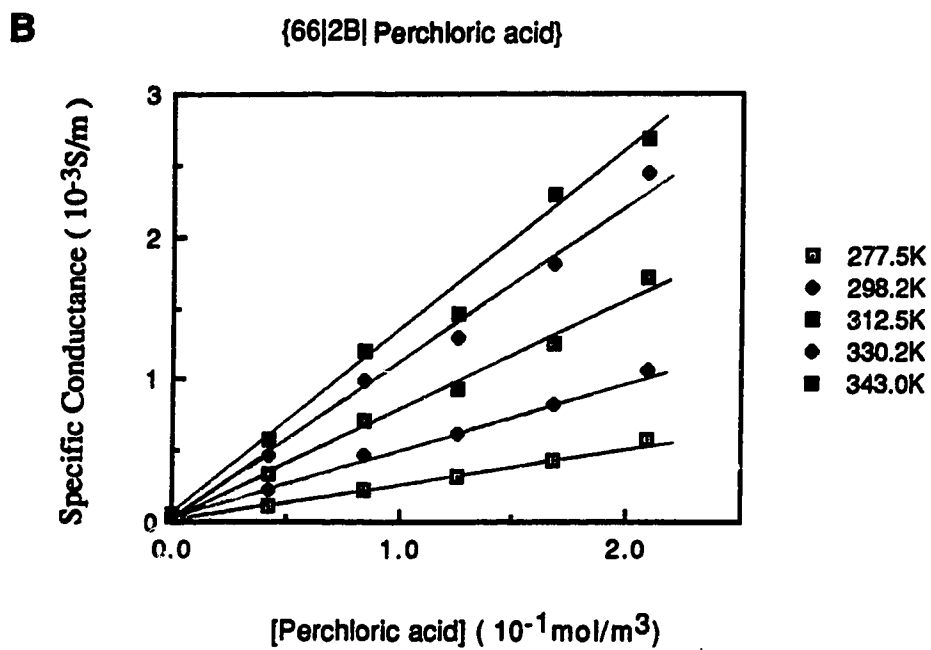
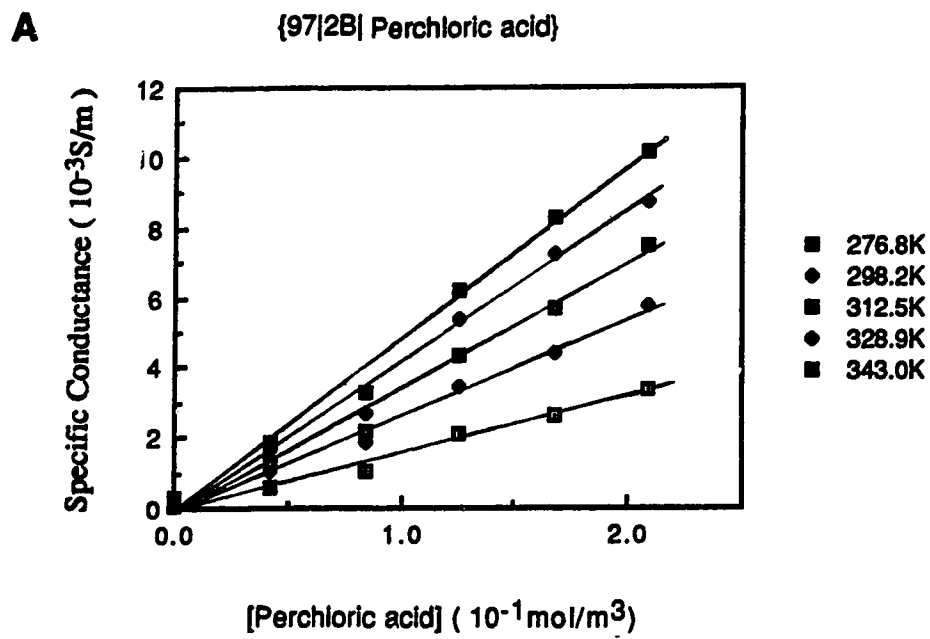
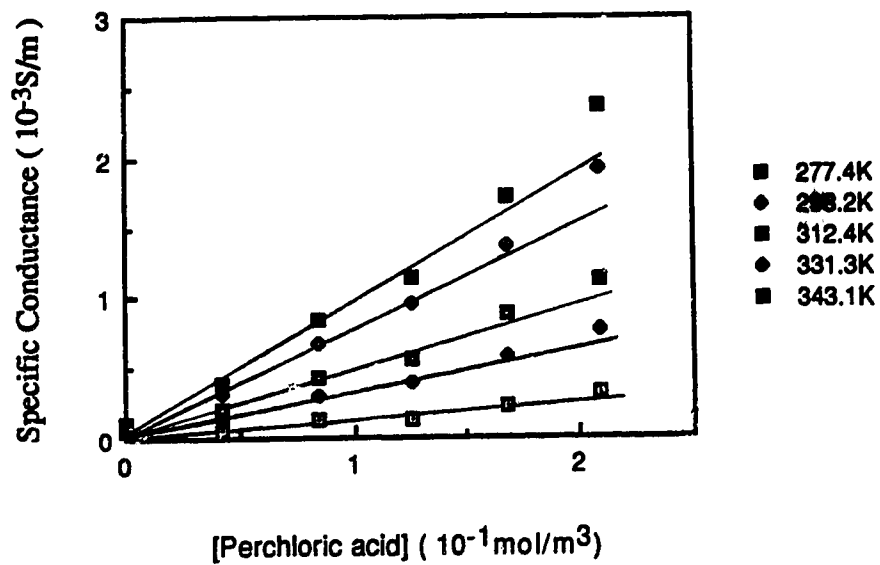
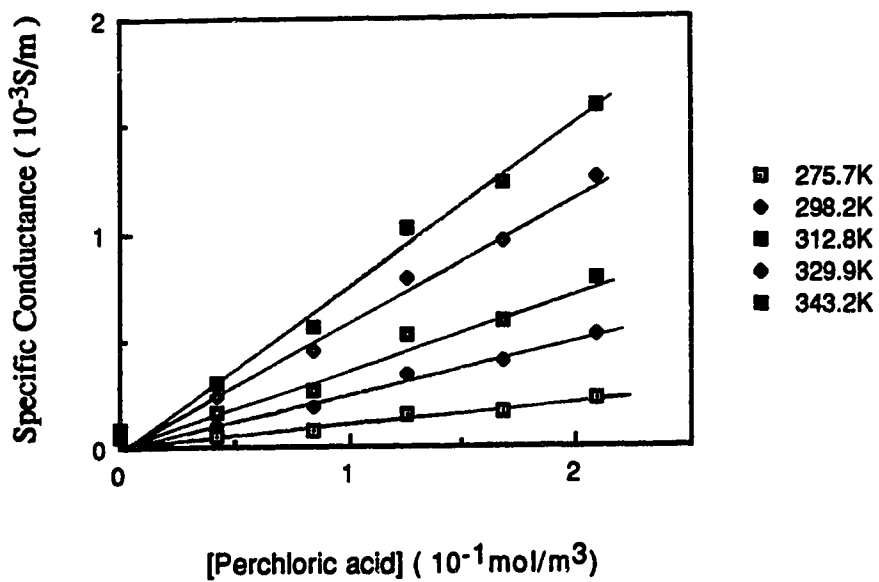
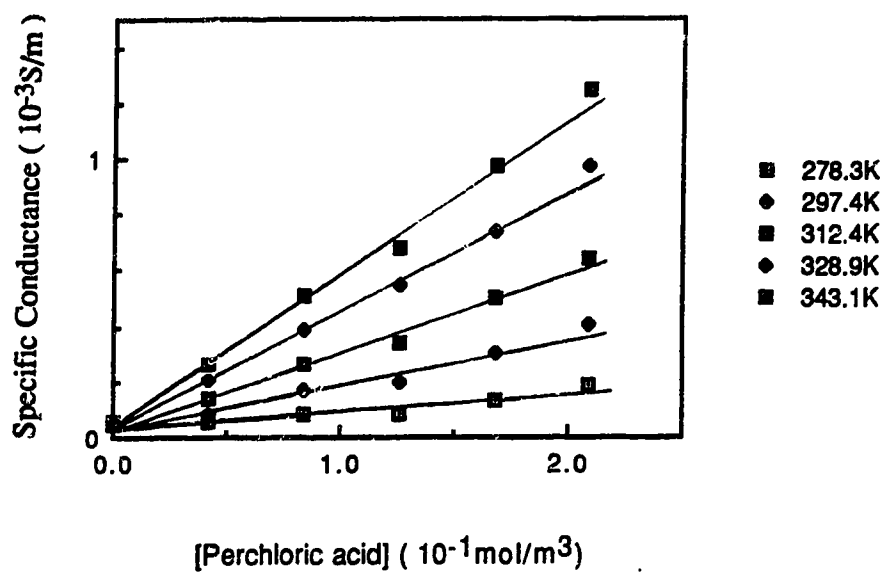


Fig.69 Temperature and concentration dependence of the conductance of perchloric acid in 2-butanol/water mixtures (A-F)

C**{51|2B| Perchloric acid}****D****{34|2B| Perchloric acid}**

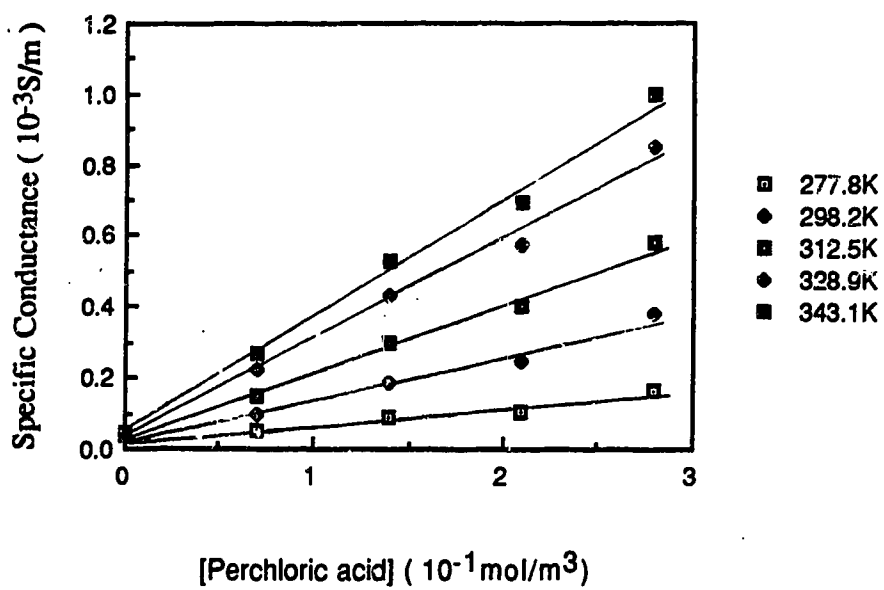
E

{20|2B|Perchloric acid}



F

{0|2B|Perchloric acid}



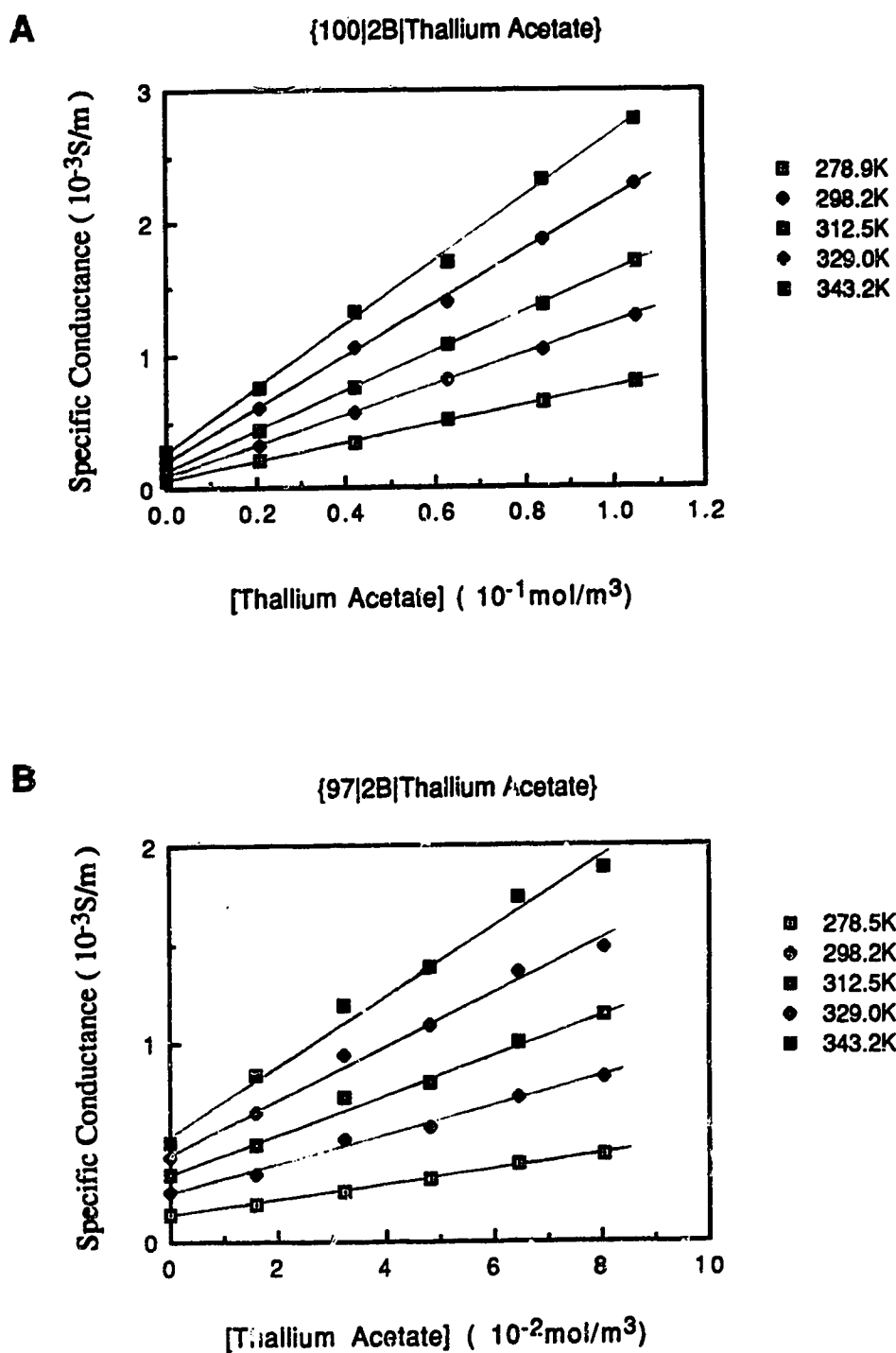
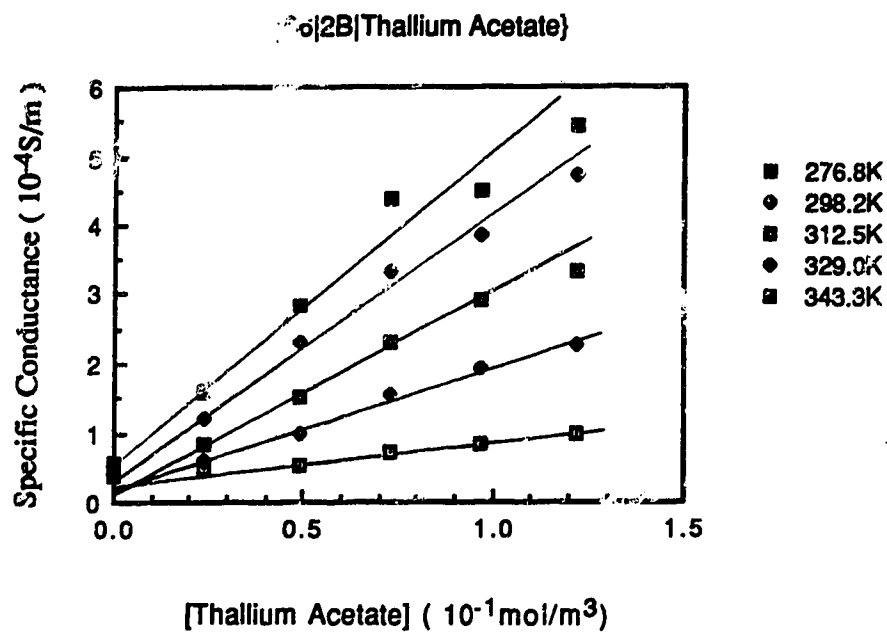
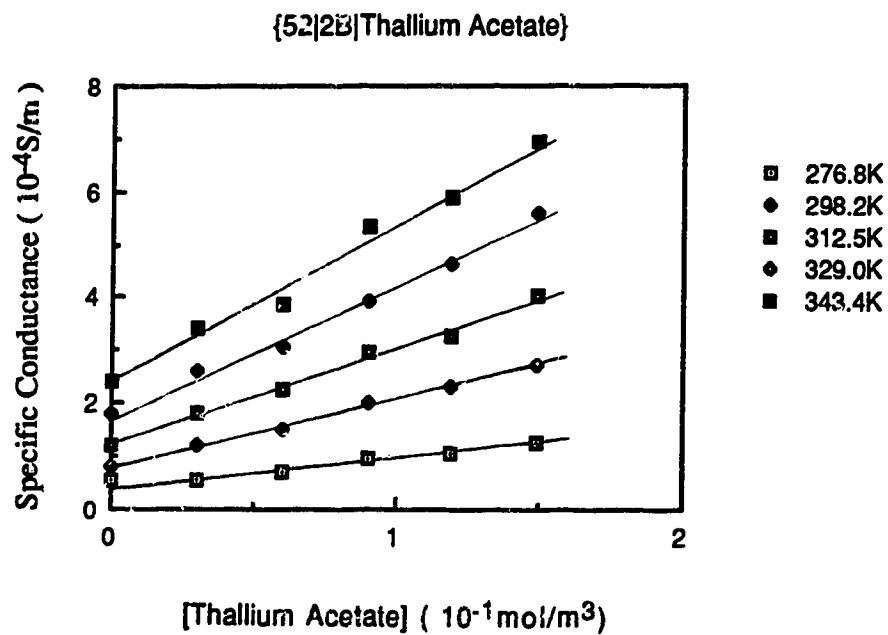


Fig.70 Temperature and concentration dependence of the conductance of
(A-G) thallium acetate in 2-butanol/water mixtures

C

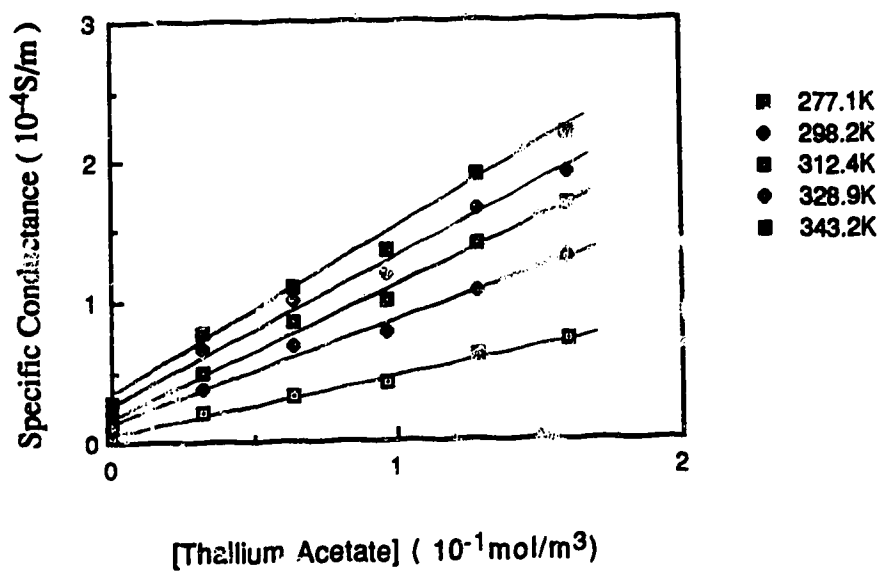


D



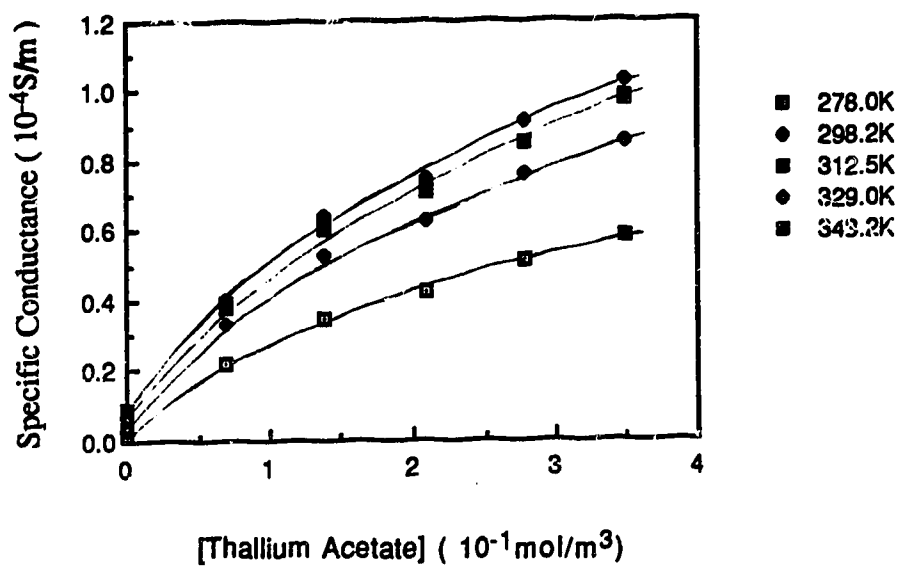
F

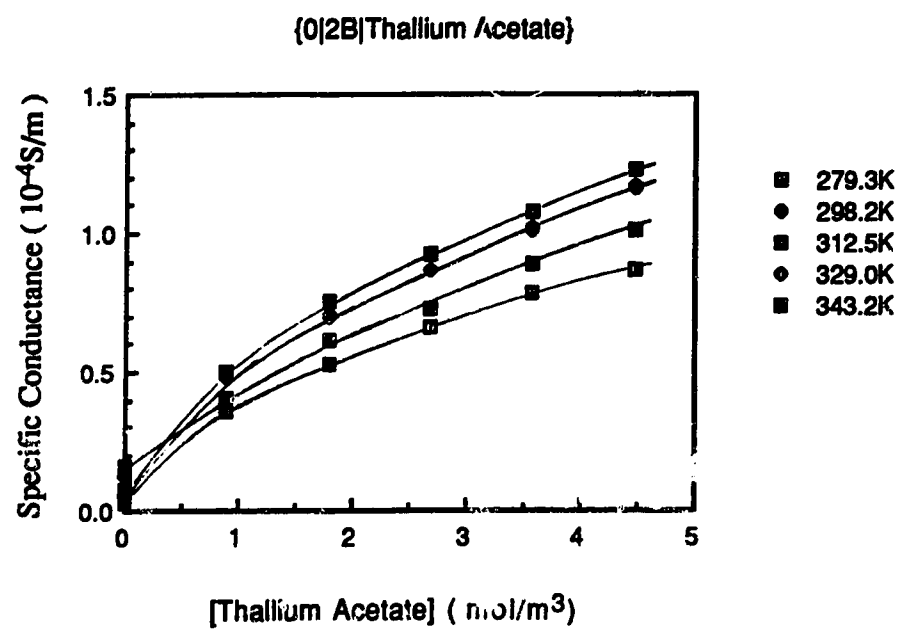
{34|2B|Thallium Acetate}



F

{20|2B|Thallium Acetate}



G

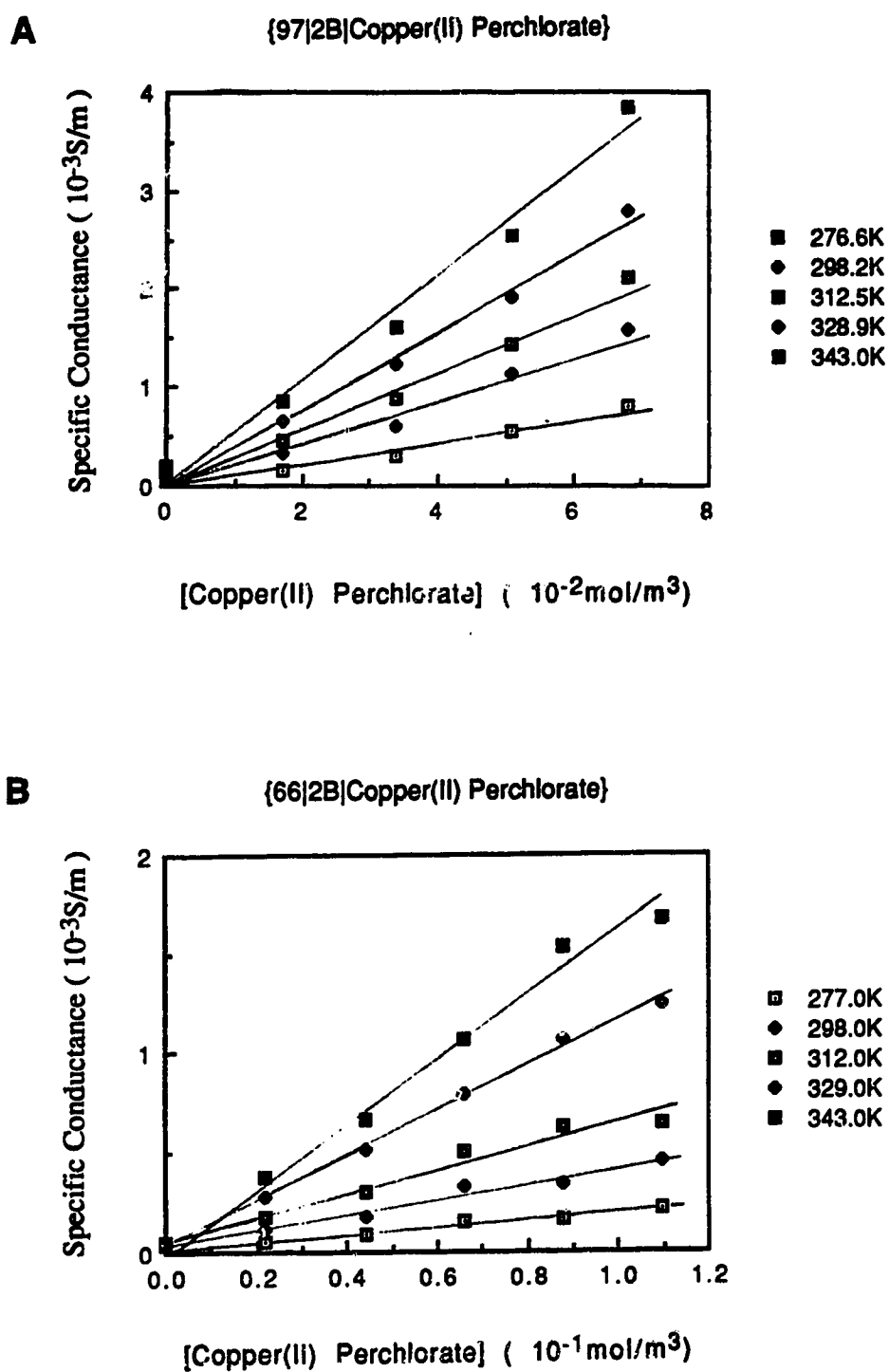
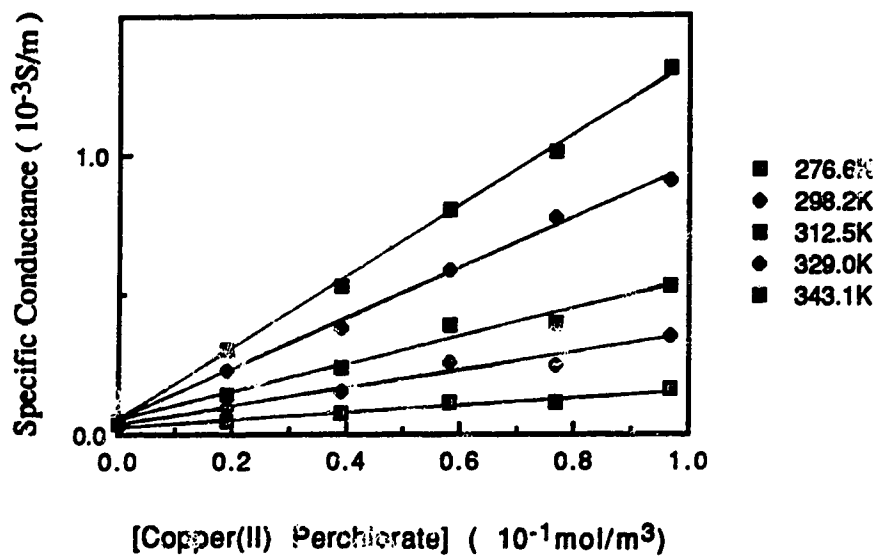


Fig. 71 Temperature and concentration dependence of the conductance of
(A-G) copper(II) perchlorate in 2-butanol/water mixtures

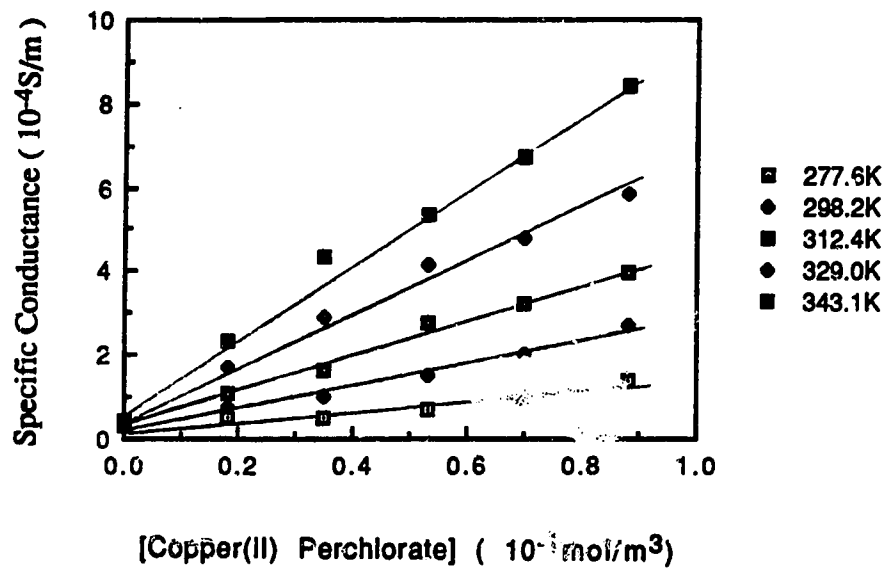
C

{52|2B|Copper(II) Perchlorate}



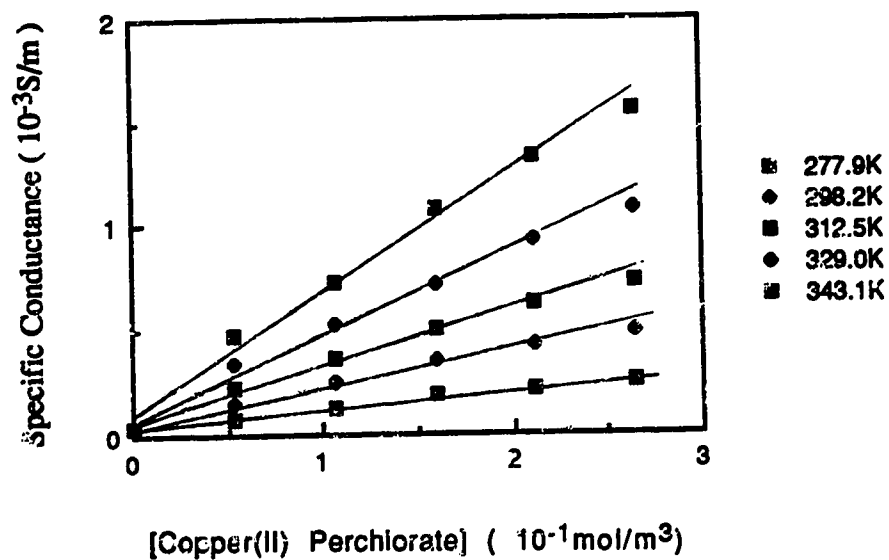
D

{34|2B|Copper(II) Perchlorate}



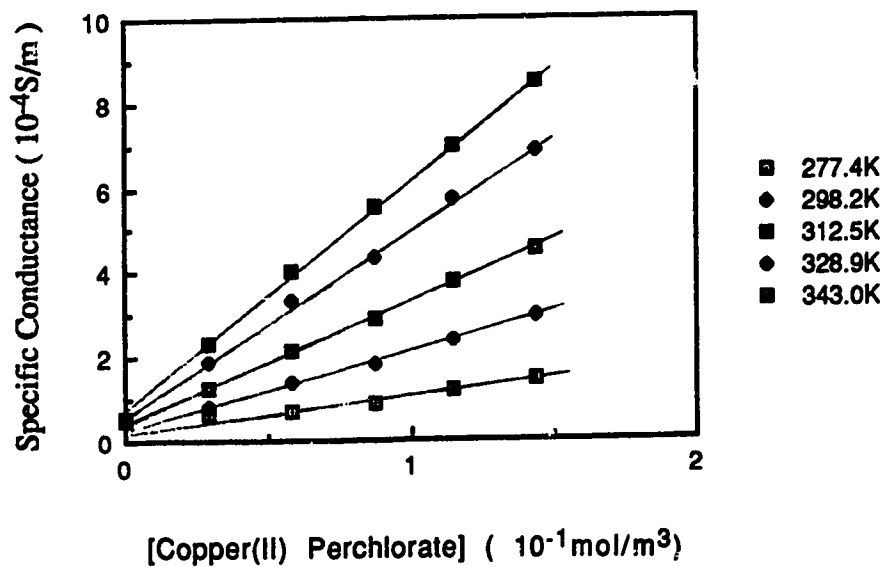
E

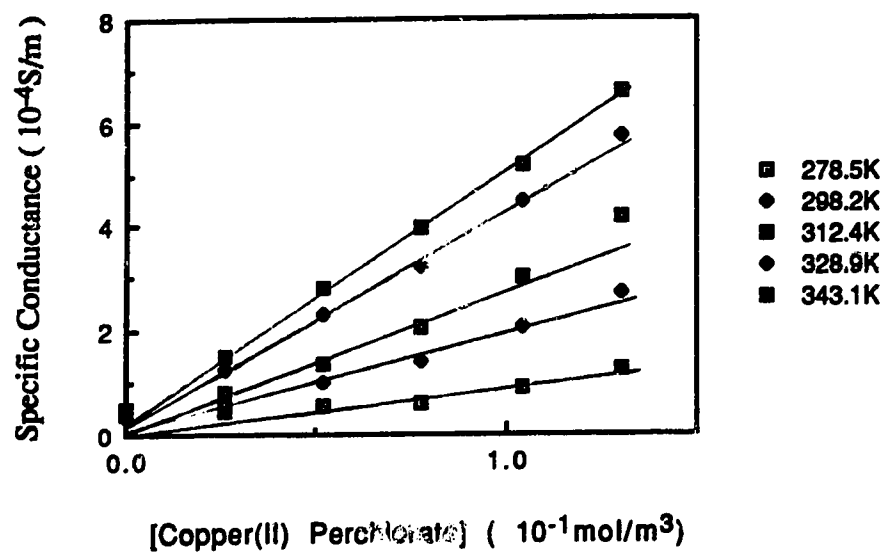
{20|2B|Copper(II) Perchlorate}



F

{10|2B|Copper(II) Perchlorate}



G**{0|2B|Copper(II) Perchlorate}**

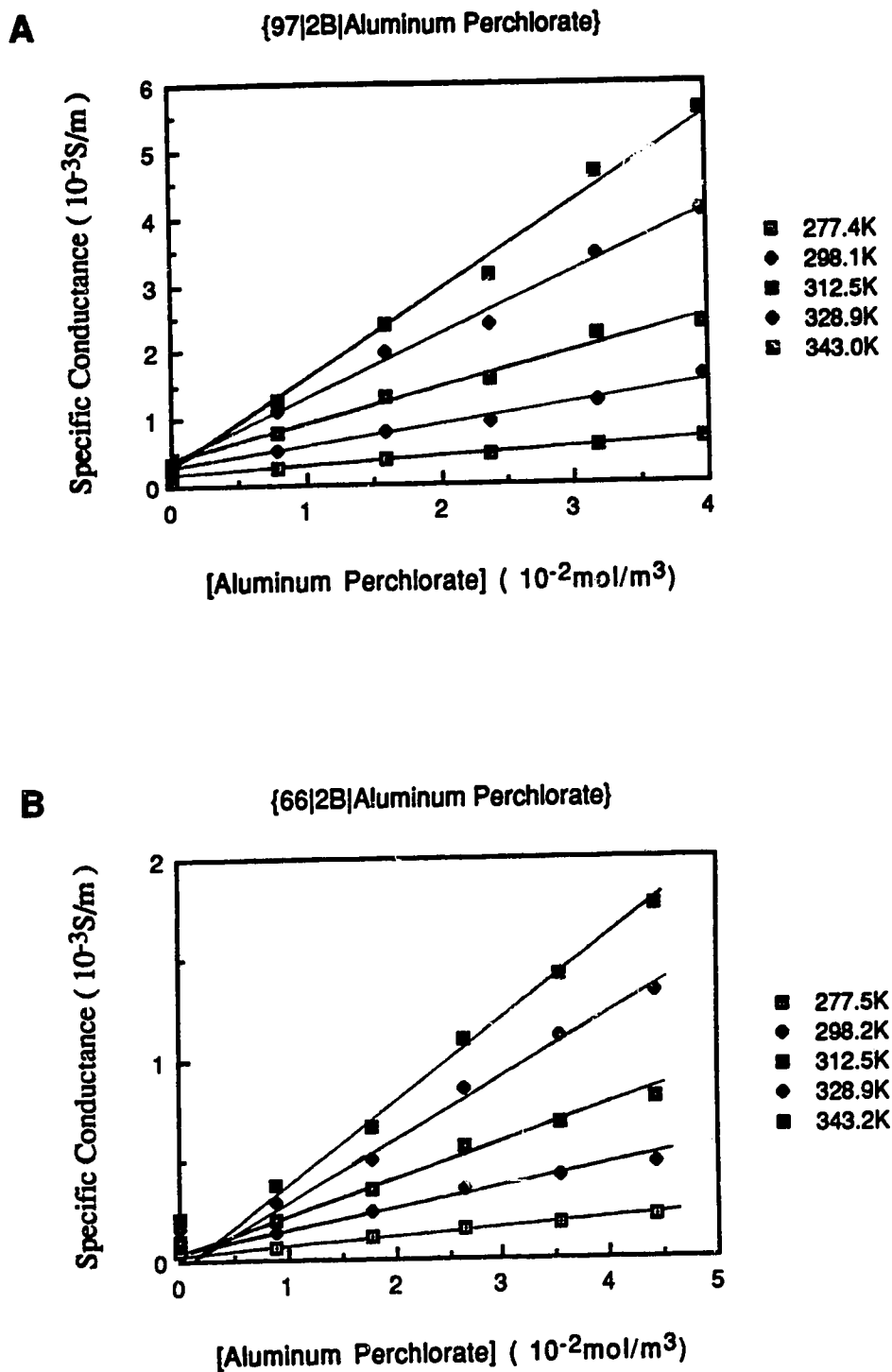
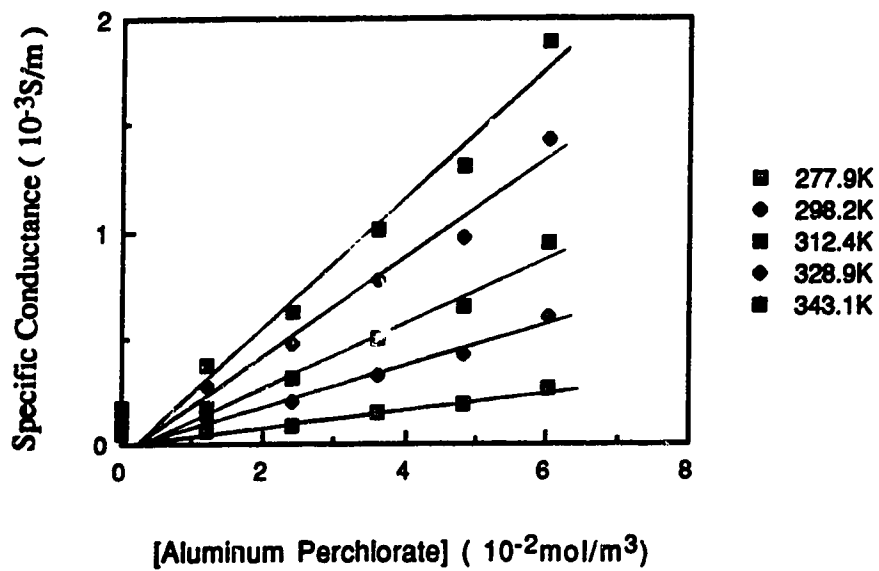


Fig.72 Temperature and concentration dependence of the conductance of
(A-F) aluminum perchlorate in 2-butanol/water mixtures

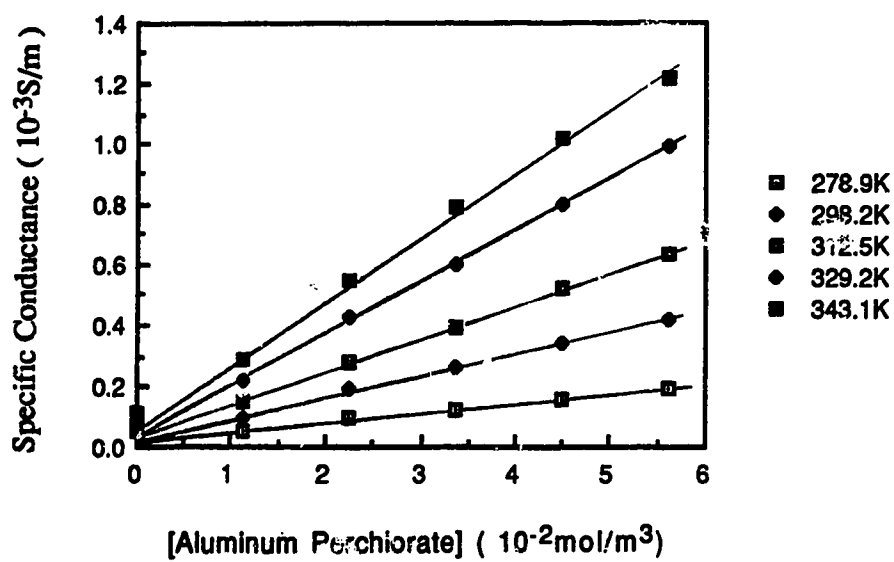
C

{51|2B|Aluminum Perchlorate}



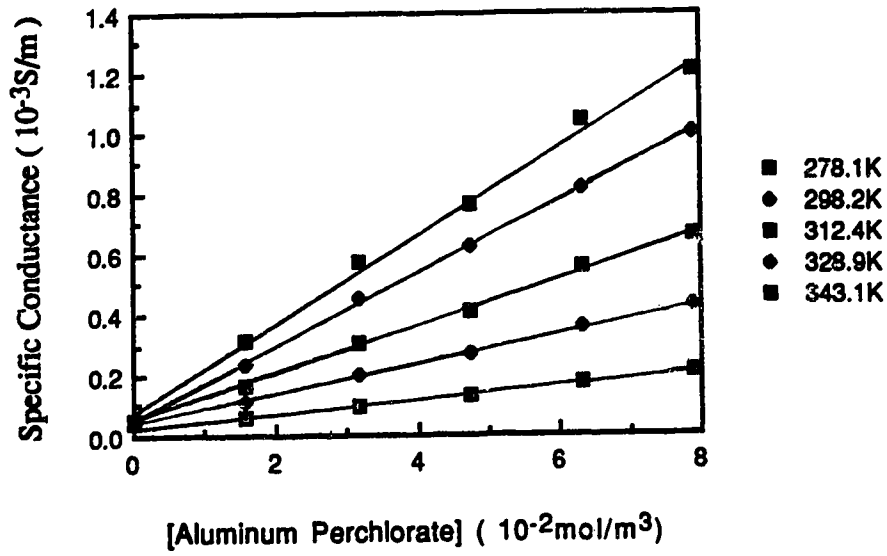
D

{34|2B|Aluminum Perchlorate}



E

{20|2B|Aluminum Perchlorate}



F

{0|2B|Aluminum Perchlorate}

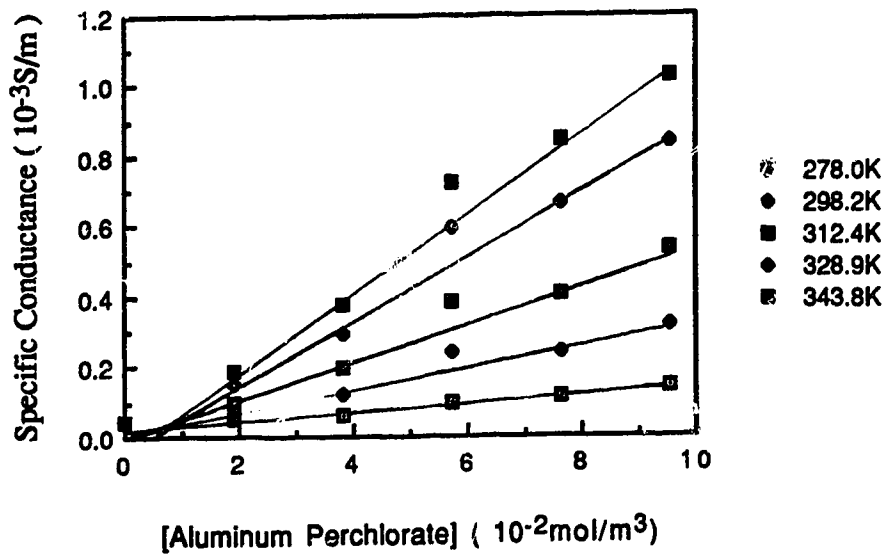


Fig. 73 Arrhenius plots of molar conductance of lithium nitrate
in 2-butanol/water mixtures

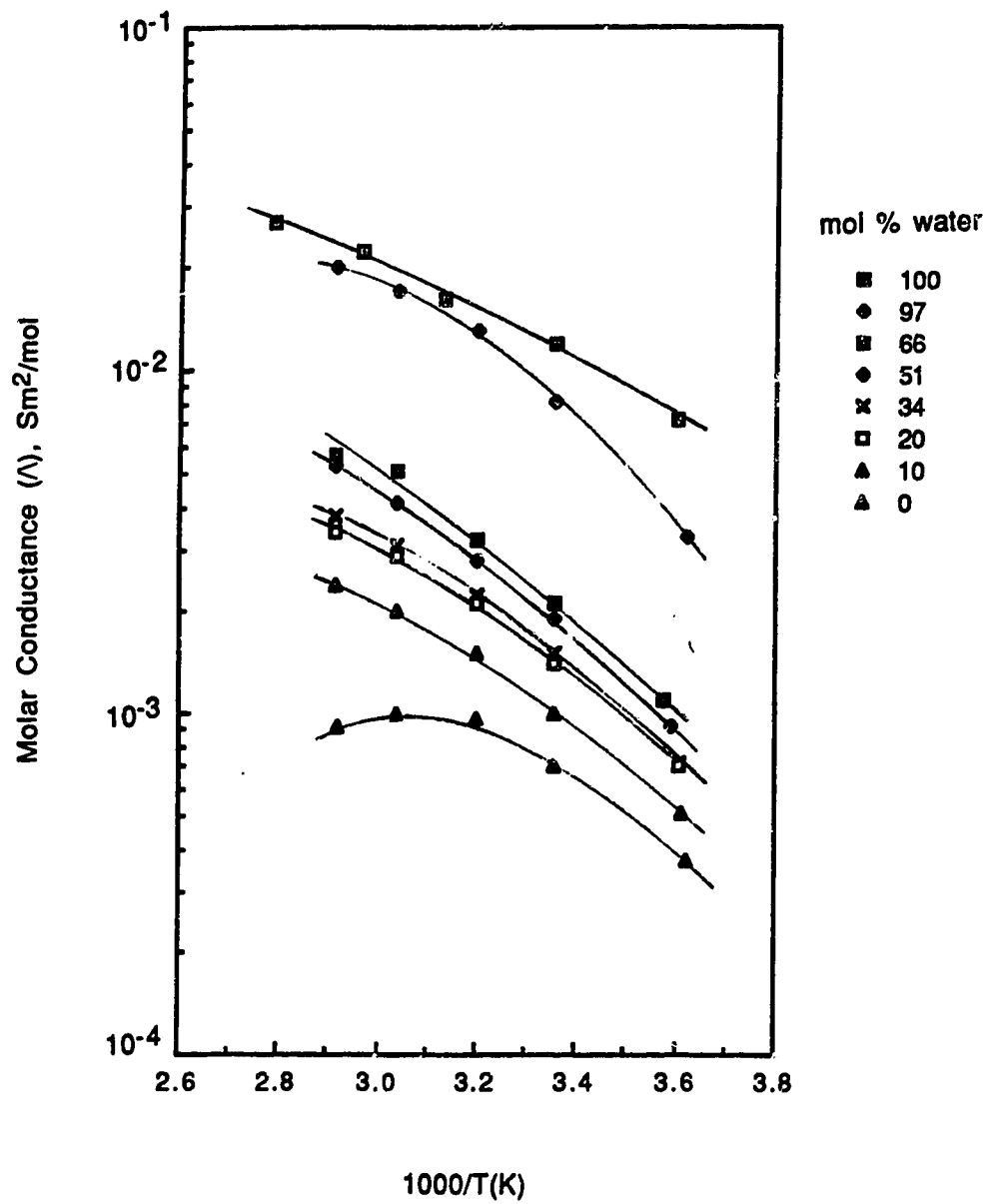


Fig. 74

Arrhenius plots of molar conductance of perchloric acid
in 2-butanol/water mixtures

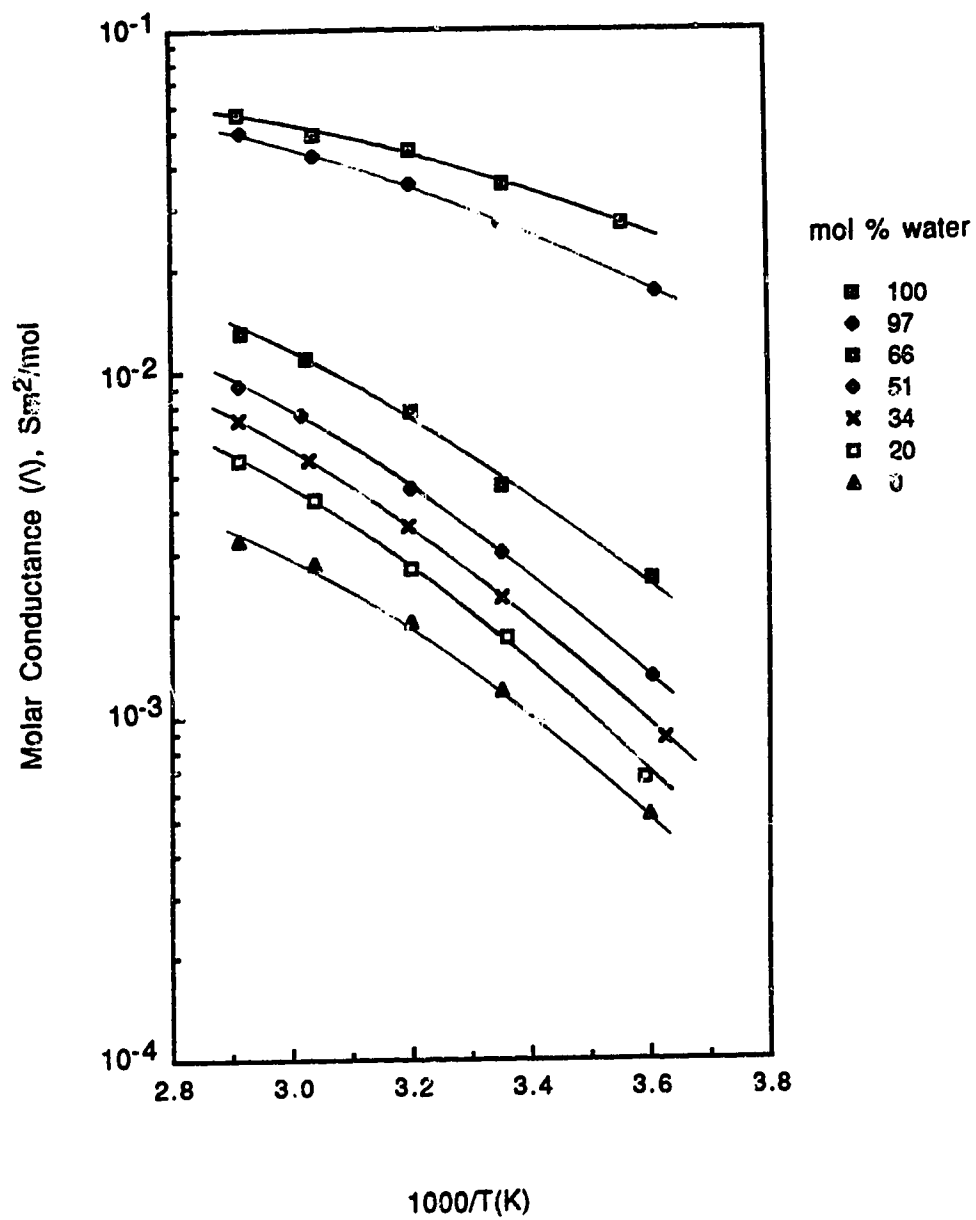


Fig. 75 Arrhenius plots of molar conductance of thallium acetate in 2-butanol/water mixtures

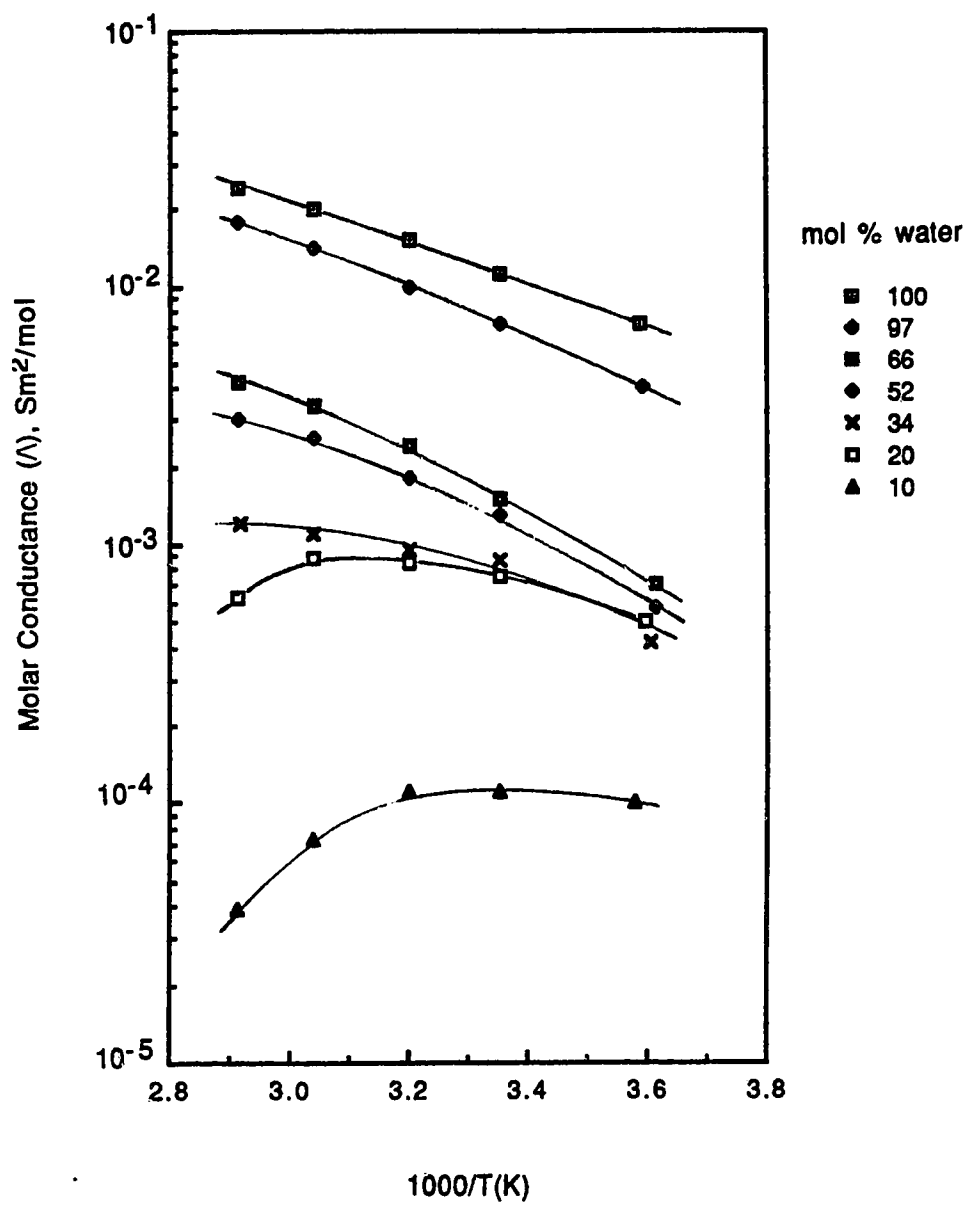


Fig. 76 Arrhenius plots of molar conductance of copper(II) perchlorate
in 2-butanol/water mixtures

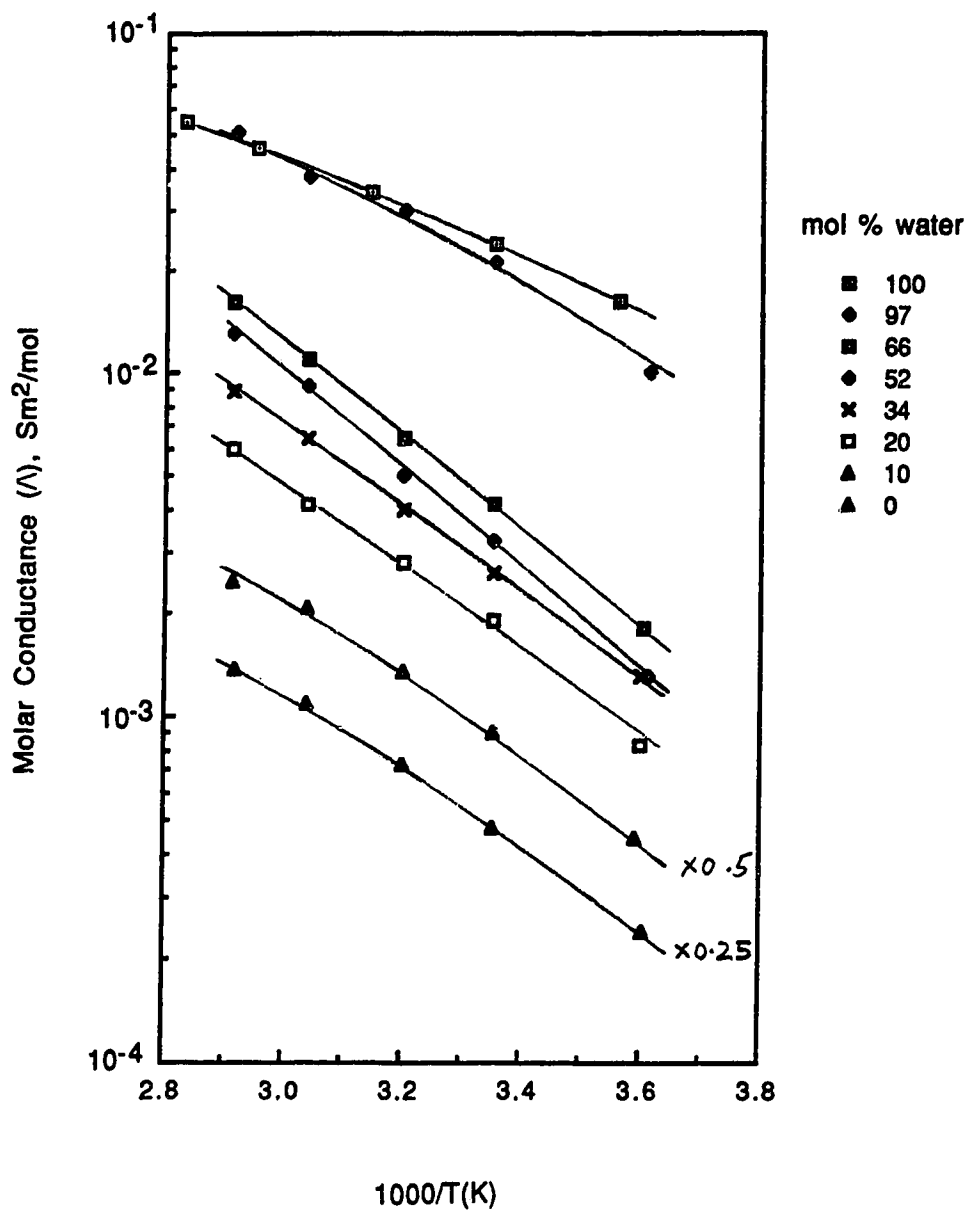


Fig. 77 Arrhenius plots of molar conductance of aluminum perchlorate
in 2-butanol/water mixtures

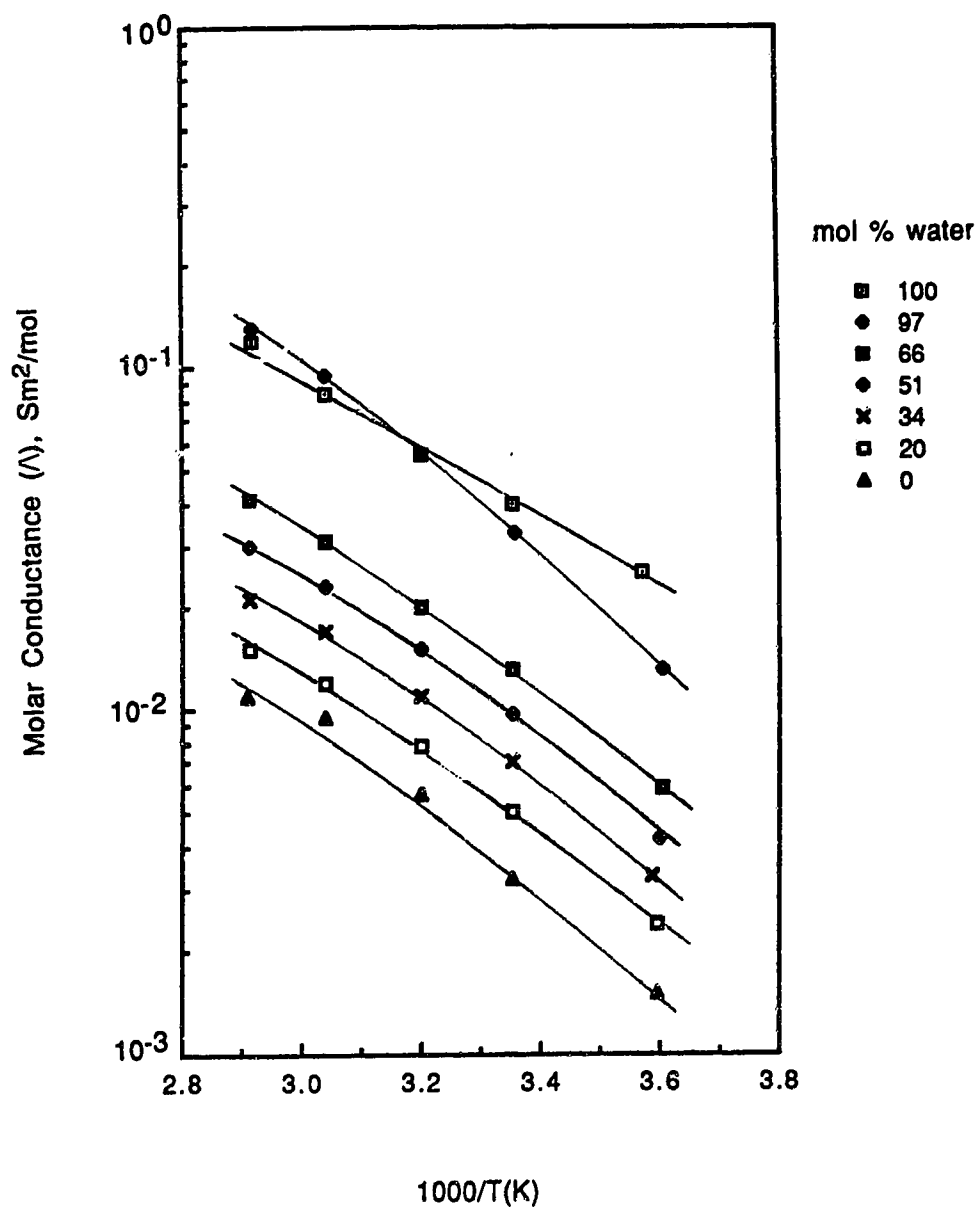


Fig. 78 Composition dependence of the activation energy of conductance of some inorganic electrolytes in 2-butanol/water mixtures

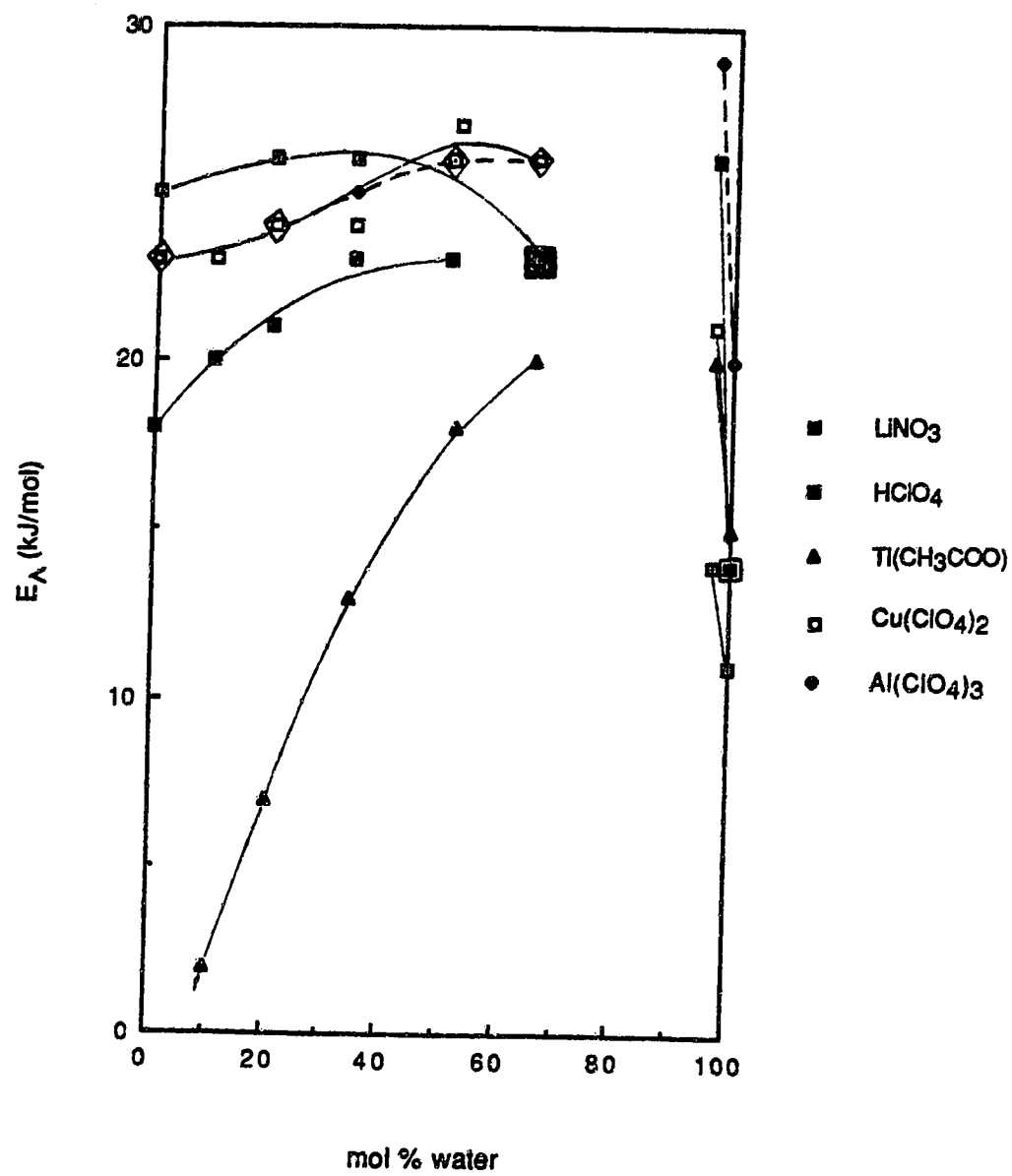


Table 47. Temperature and composition dependence of molar conductances (Λ) of lithium nitrate in 2-butanol/water mixtures.

X_w	Temp (K)	Λ_o ($10^{-3} \text{ S m}^2/\text{mol}$)	X_w	Temp (K)	Λ_o ($10^{-3} \text{ S m}^2/\text{mol}$)	
1.00	277.8	7.1	0.34	277.7	0.71	
	298.2	12		298.2	1.5	
	319.1	16		312.4	2.2	
	337.4	22		328.9	3.1	
	358.4	27		343.1	3.8	
E_Λ , kJ/mol			14			23
0.97	276.1	3.3	0.20	277.4	0.70	
	298.2	8.1		298.2	1.4	
	312.4	13		312.4	2.1	
	329.0	17		328.9	2.9	
	343.3	20		343.2	3.4	
E_Λ , kJ/mol			26			21
0.66	279.5	1.1	0.10	276.9	0.51	
	298.2	2.1		298.2	1.0	
	312.4	3.2		312.4	1.5	
	328.9	5.1		328.9	2.0	
	343.2	5.7		343.1	2.4	
E_Λ , kJ/mol			23			20
0.51	278.5	0.91	0.00	276.0	0.37	
	298.2	1.9		298.2	0.70	
	312.4	2.8		312.5	0.96	
	328.9	4.1		329.3	1.0	
	343.2	5.3		343.0	0.92	
E_Λ , kJ/mol			23			18

Table 48. Temperature and composition dependence of molar conductances (Λ) of perchloric acid in 2-butanol/water mixtures.

X_w	Temp (K)	Λ_o ($10^{-3} \text{ S m}^2/\text{mol}$)	X_w	Temp (K)	Λ_o ($10^{-3} \text{ S m}^2/\text{mol}$)
1.00	281.2	27	0.34	275.7	0.87
	298.1	35		298.2	2.2
	312.4	44		312.8	3.6
	328.9	49		329.9	5.6
	343.1	57		343.2	7.3
E_Λ , kJ/mol		11			26
0.97	276.8	17	0.20	278.3	0.67
	298.2	27		297.4	1.7
	312.5	35		312.4	2.7
	328.9	43		328.9	4.3
	343.0	50		343.1	5.6
E_Λ , kJ/mol		14			26
0.66	277.5	2.5	0.00	277.8	0.52
	298.2	4.7		298.2	1.2
	312.5	7.6		312.5	1.9
	330.2	11		328.9	2.8
	343.0	13		343.1	3.3
E_Λ , kJ/mol		23			25
0.51	277.4	1.3			
	298.2	3.0			
	312.4	4.6			
	331.3	7.5			
	343.1	9.1			
E_Λ , kJ/mol		26			

Table 50. Temperature and composition dependence of molar conductances (Λ) of copper(II) perchlorate in 2-butanol/water mixtures.

X_w	Temp (K)	Λ_o ($10^{-3} \text{ S m}^2/\text{mol}$)	X_w	Temp (K)	Λ_o ($10^{-3} \text{ S m}^2/\text{mol}$)
1.00	281.0	16	0.34	277.6	1.3
	298.2	24		298.2	2.6
	318.0	34		312.4	4.0
	338.5	46		329.0	6.4
	353.5	55		343.1	8.9
$E_A, \text{ kJ/mol}$		14			24
0.97	276.6	10	0.20	277.9	0.83
	298.2	21		298.2	1.9
	312.5	30		312.5	2.8
	328.9	38		329.0	4.1
	343.0	51		343.1	6.0
$E_A, \text{ kJ/mol}$		21			24
0.66	277.3	1.8	0.10	277.4	0.95
	298.2	4.1		298.2	1.9
	312.4	6.4		312.5	2.9
	328.9	11		328.9	4.4
	343.1	16		343.0	5.5
$E_A, \text{ kJ/mol}$		26			23
0.52	276.6	1.3	0.00	278.5	0.88
	298.2	3.2		298.2	1.8
	312.5	5.0		312.4	2.7
	329.0	9.2		328.9	4.1
	343.1	13		343.1	4.9
$E_A, \text{ kJ/mol}$		27			23

Table 51. Temperature and composition dependence of molar conductances (Λ) of aluminum perchlorate in 2-butanol/water mixtures.

X_w	Temp (K)	Λ_{∞} ($10^{-3} \text{ S m}^2/\text{mol}$)	X_w	Temp (K)	Λ_0 ($10^{-3} \text{ S m}^2/\text{mol}$)
1.00	280.2	2.5	0.34	278.9	0.33
	298.2	4.0		298.2	0.70
	312.4	5.6		312.5	1.1
	328.9	8.4		329.2	1.7
	343.0	12		343.1	2.1
$E_A, \text{ kJ/mol}$		20			25
0.97	277.4	1.3	0.20	278.1	0.24
	298.1	3.3		298.2	0.50
	312.5	5.6		312.4	0.78
	328.9	9.4		328.9	1.2
	343.0	13		343.1	1.5
$E_A, \text{ kJ/mol}$		29			24
0.66	277.5	0.59	0.00	278.0	0.15
	298.2	1.3		298.2	0.32
	312.5	2.0		312.4	0.57
	328.9	3.1		328.9	0.94
	343.2	4.1		343.8	1.1
$E_A, \text{ kJ/mol}$		26			23
0.51	277.9	0.42			
	298.2	0.96			
	312.4	1.5			
	328.9	2.3			
	343.1	3.0			
$E_A, \text{ kJ/mol}$		26			

CHAPTER FOUR

DISCUSSION

In this work, the solvent effects on solvated electron reaction rates with solutes that have different charges (positive or negative) were studied as a function of temperature in 1-propanol/water, 2-propanol/water and 2-butanol/water mixtures. The solutes used were lithium nitrate, lithium chromate, perchloric acid, silver perchlorate, thallium acetate, copper(II) perchlorate, and aluminum perchlorate. The second-order rate constants for the counter ions, perchlorate, acetate and lithium are less than $10^3 \text{ m}^3/\text{mol}\cdot\text{s}$ in water (83). Therefore, the observed rate constants are due to NO_3^- , CrO_4^{2-} , H_s^+ , Ag_s^+ , Tl_s^+ , Cu_s^{2+} , and Al_s^{3+} .

I. Solvated Electron Reactions with Negative Ions

The rate constant data were analyzed according to the modified Arrhenius equation

$$k_2/f = A_2 \exp(-E_2/RT) \quad [13]$$

where E_2 is the overall energy of activation of the reaction and A_2 is the pre-exponential factor. Values of the Debye factor f were calculated for a range of values of ϵ and T , using a value of r_f appropriate to each reactant ion (Figure 79) (NO_3^- , 1.5 nm; CrO_4^{2-} , 2.0 nm; nitrobenzene, 1.0 nm). The value of ϵ of each solvent at each T used in the experiments was obtained by interpolation of data in ref. 121. The value of k_2 was divided by the value of f at the corresponding values of ϵ , T , r_f . Arrhenius plots of $\log(k_2/f)$ against T^{-1} are shown for NO_3^- in Figures 9, 21 and 33, and for CrO_4^{2-} in Figures 11 and 23.

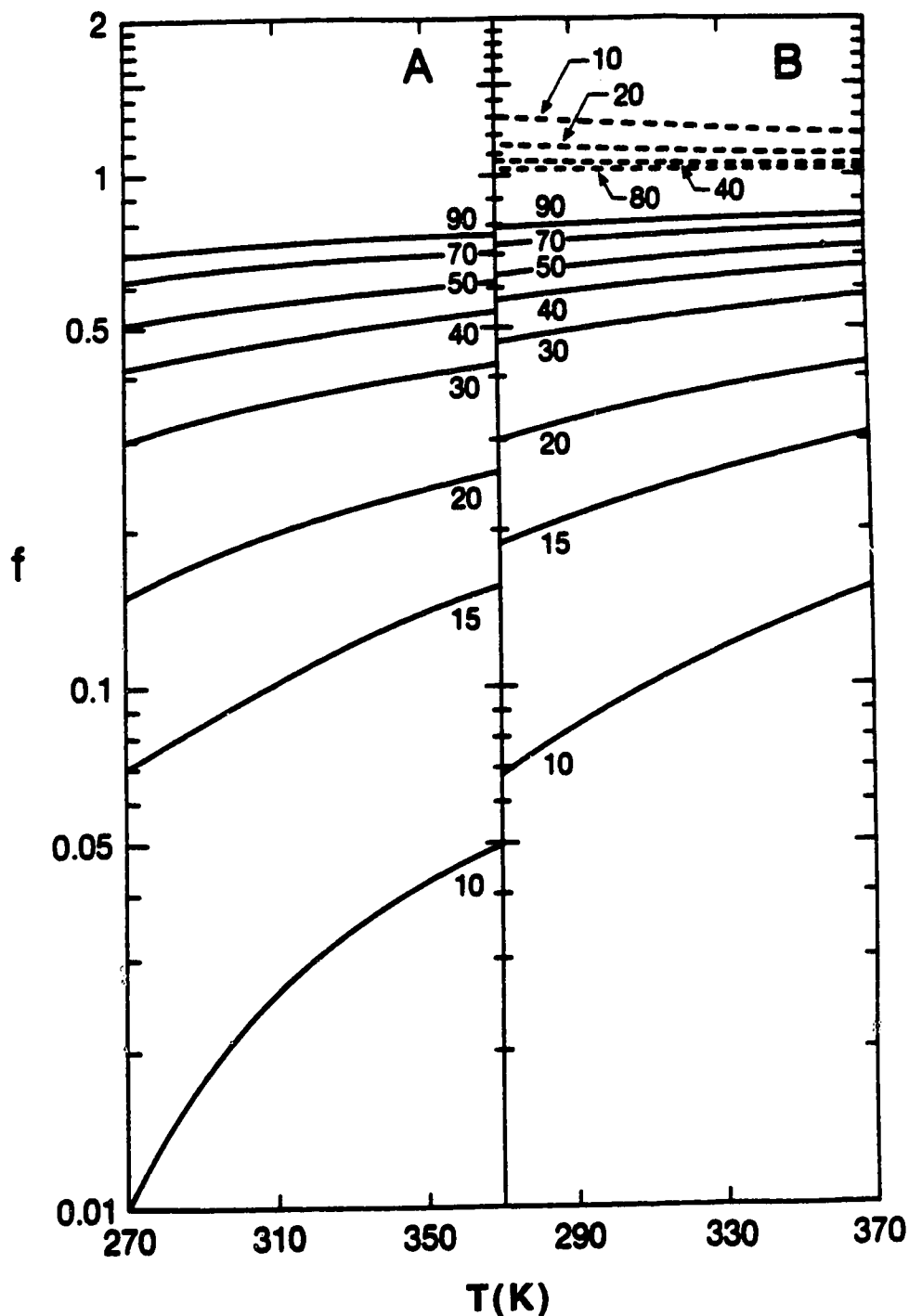


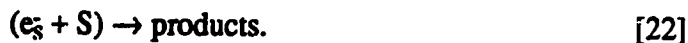
Fig. 79 Temperature dependence of the Debye factor f at different values of dielectric permittivity ϵ . A: CrO_4^{2-} , using $r_r = 2.0$ nm. B: _____, NO_3^- , using $r_r = 1.5$ nm; ---, nitrobenzene, using $r_r = 1.0$ nm, $\theta = 0$ rad, and $M = 1.4 \times 10^{-29}$ C.m in eq. [6]. Values of ϵ are indicated.

Plots of E_2 and $\log A_2$ against solvent composition are shown in Figures 80A and 81A, respectively. The plots are S curves. Addition of water to alcohol decreased E_2 and $\log A_2$ for NO_3^- . Chromates are not sufficiently soluble in pure alcohol or at <20 mol% water to measure k_2 , but the values of E_2 and $\log A_2$ at >20 mol% water decrease with increasing water content. The solvent composition effect is smaller for $(e_s^- + \text{CrO}_4^{2-})$ than for the less efficient $(e_s^- + \text{NO}_3^-)$.

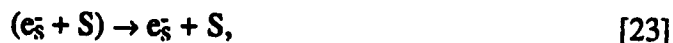
The reaction of e_s^- with nitrobenzene is nearly diffusion controlled (101, 106) and may be used as a reference. For a diffusion controlled reaction E_2 is essentially that of diffusion of e_s^- and S, which encounter each other at random,



and immediately react,



In slow reactions most encounter pairs diffuse apart again,



in which case the measured E_2 is mainly the activation energy of reaction [22].

In general, the measured rate constant k_2 is related to the rate constants of the specific reactions [21], [22] and [23] by:

$$k_2 = k_{21}k_{22}/(k_{23} + k_{22}). \quad [24]$$

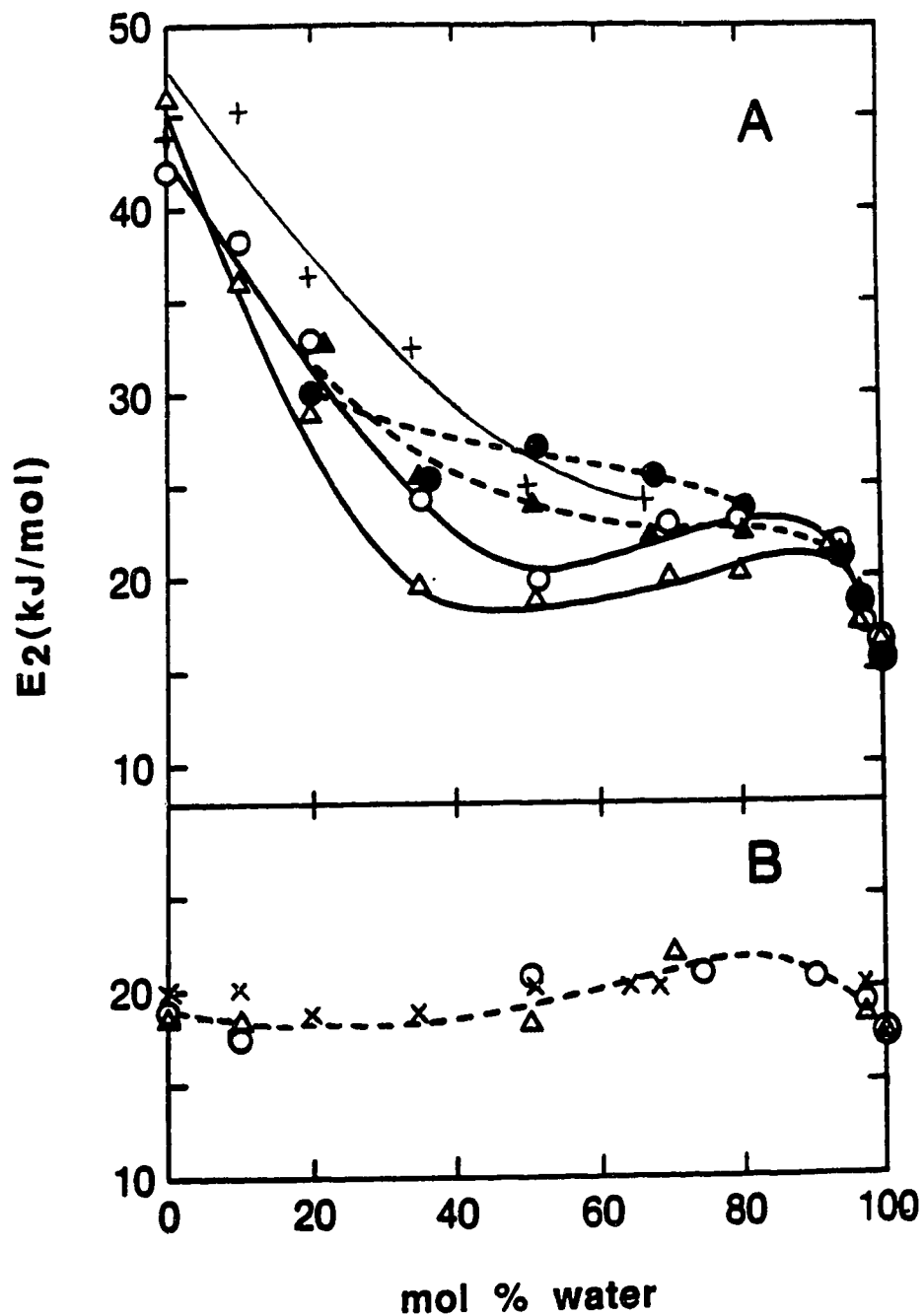


Fig. 80 Solvent composition dependence of the activation energies E_2 near 298K. A: open symbols and +, $(e_s^- + NO_3^-)$, solid symbols, $(e_s^- + CrO_4^{2-})$. B: $(e_s^- + nitrobenzene)$. Triangles, 1-propanol; circles, 2-propanol; x and +, 2-butanol.

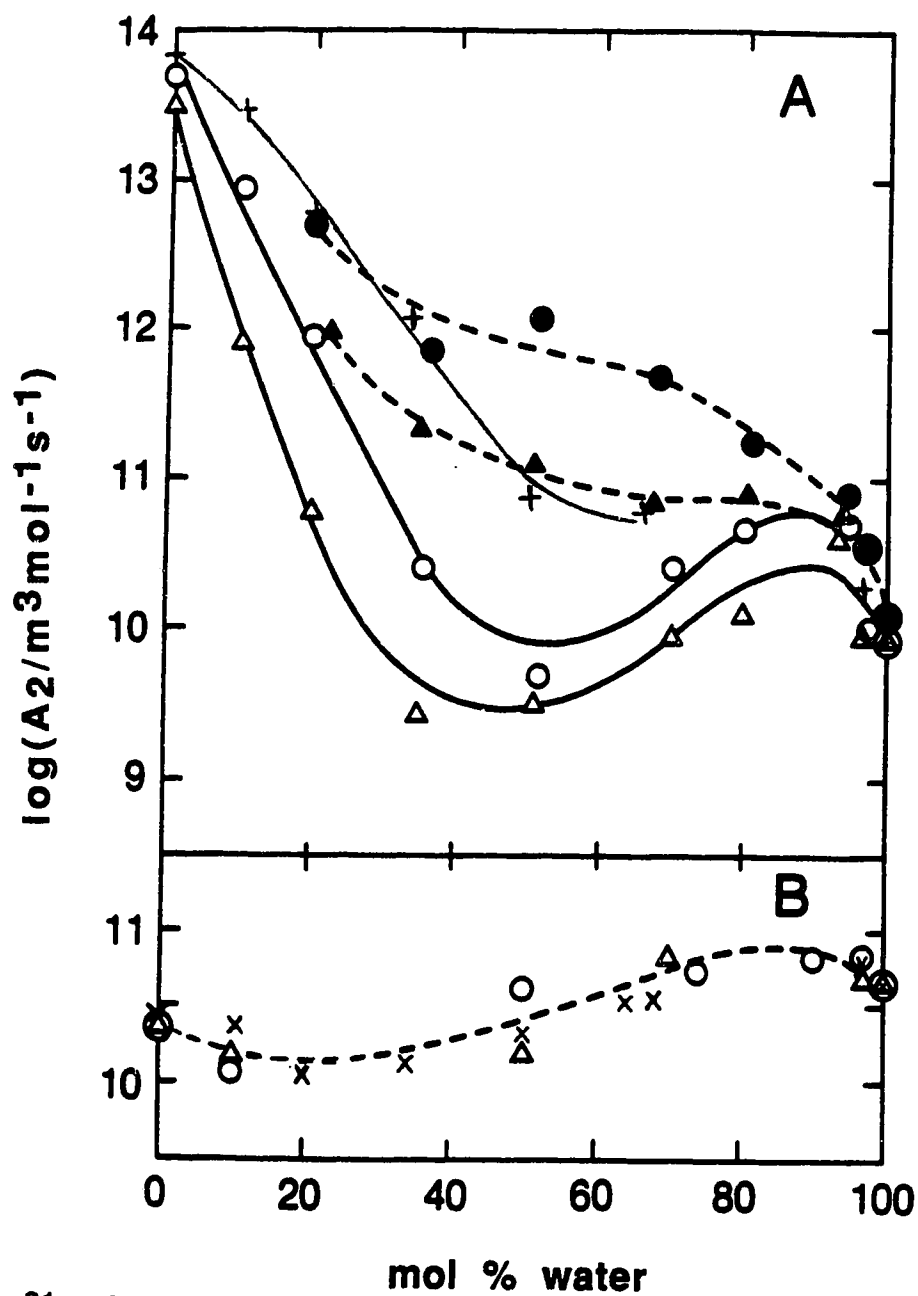


Fig. 81 Solvent composition dependence of $\log A_2$ near 298K.

A: open symbols and +, ($e^-_s + \text{NO}_3^-$), solid symbols, ($e^-_s + \text{CrO}_4^{2-}$).

B: ($e^-_s + \text{nitrobenzene}$). Triangles, 1-propanol; circles, 2-propanol; x and +, 2-butanol.

When $k_{22} \gg k_{23}$ one has $k_2 \approx k_{21}$, and when $k_{22} \ll k_{23}$ one has $k_2 \approx k_{21}k_{22}/k_{23} = K_{21,23}k_{22}$, where $K_{21,23}$ is the equilibrium constant of reactions [21] and [23]. In the former case,

$$E_2 \approx E_{21} \quad [25]$$

and in the latter,

$$\begin{aligned} E_2 &\approx \Delta H_{21} + E_{22} \\ &\approx E_{22} \end{aligned} \quad [26]$$

where $\Delta H_{21} = E_{21} - E_{23} \approx 0$ is the enthalpy change of reaction [21] excluding the coulombic energy $U(r_r)$.

The activation energy of ($e_s^- +$ nitrobenzene) has been obtained from plots of $\log(k_2/f)$ against T^{-1} (Figures 82 and 83) using k_2 values from refs. 101, 105 and 106. The values of E_2 do not vary greatly with solvent composition (Figure 80B), and are similar to E_η for viscosity (Tables 2, 14 and 26) as expected from eq. [10]. The values of f for the nitrobenzene reaction are not much different from unity, so the present values of E_2 are ≤ 1 kJ/mol greater than those obtained from k_2 alone (101,105,106).

For the reactions of e_s^- with nitrate and chromate ions the values of E_2 in the water-rich solvents are similar to those for nitrobenzene (Figure 80). However, in the alcohol-rich solvents E_2 increases with alcohol content. For ($e_s^- + NO_3^-$) the value of E_2 in each pure alcohol is nearly three times that in pure water.

The pre-exponential factor A_2 for a diffusion-controlled reaction includes the reaction radius r_r and the pre-exponential factor of D (eq. [2]) or of η (eq. [11]). The value of A_2 for ($e_s^- +$ nitrobenzene) changes little with solvent composition (Figure 81B).

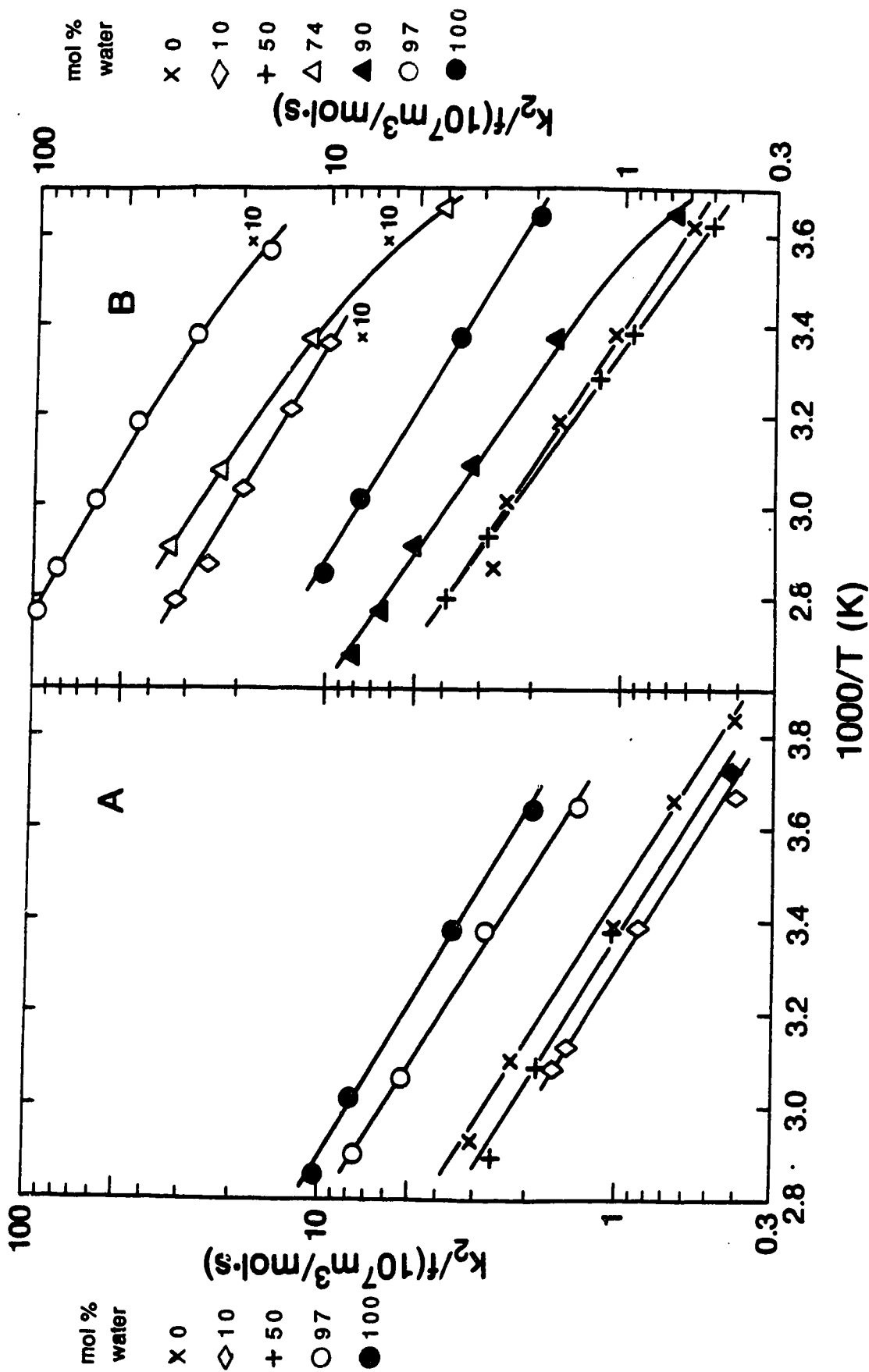


Fig. 82 Arrhenius plots of $k_2(e^-s + \text{nitrobenzene}) / f_j$ in 1-propanol/water (A) and 2-propanol/water (B) mixed solvents. Values of k_2 are from refs. 101 and 106

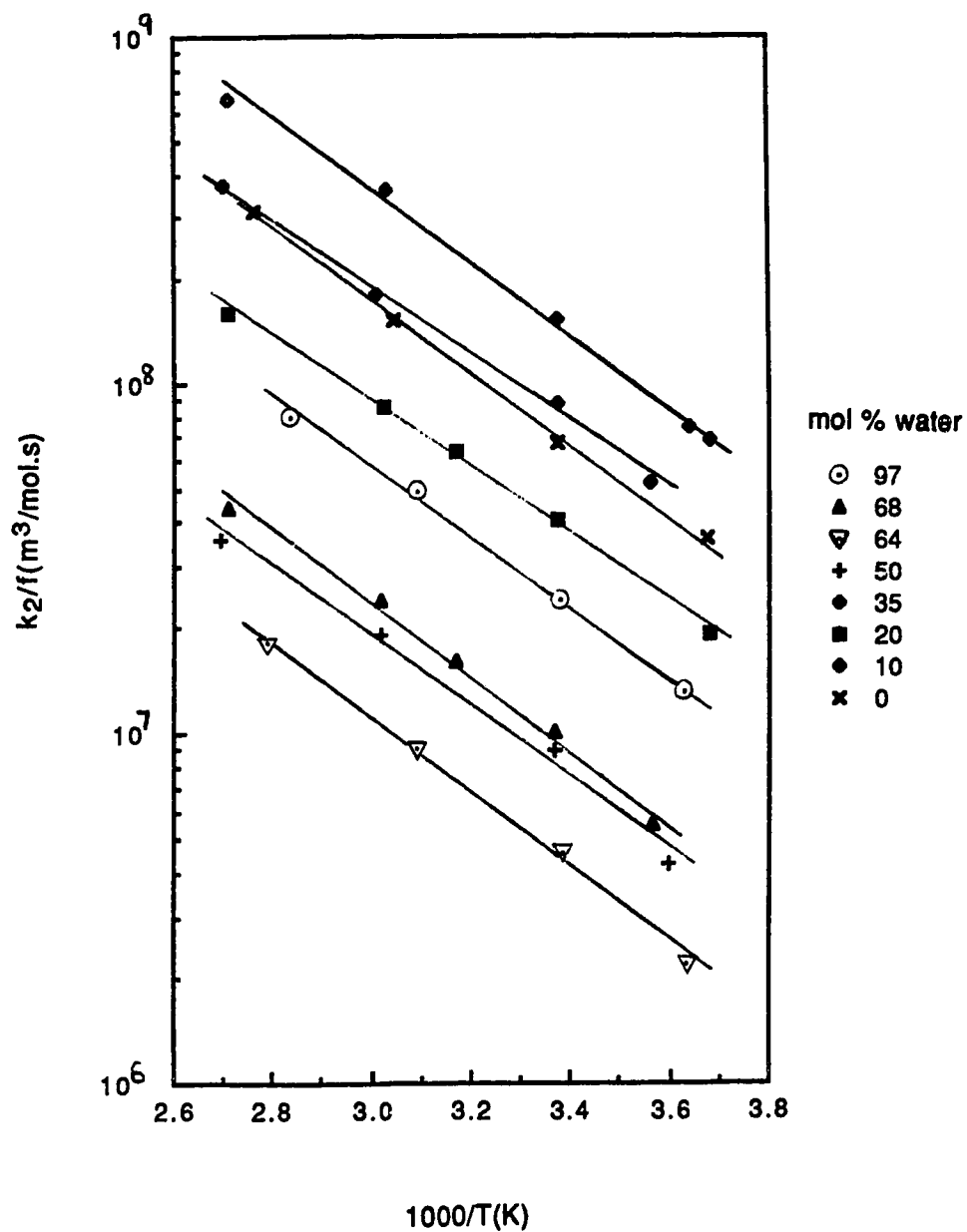


Fig. 83 Arrhenius plots of $k_2(e^- + \text{nitrobenzene}) / f$ in 2-butanol/water mixed solvents. Values of k_2 are from ref. 105.

In pure water the values of A_2 for $(e_s^- + NO_3^-)$ and $(e_s^- + CrO_4^{2-})$ were smaller than that for $(e_s^- + \text{nitrobenzene})$. The ionic reactions apparently require solvent molecular rearrangement about the reaction site, which decreases the entropy of the system and makes the random attainment of the correct configuration less probable, thereby slowing the reaction (104).

Addition of 3-5 mol% of alcohol to the water increases the value of A_2 for the ion reactions to equal that for nitrobenzene (Figure 81). The presence of the small amount of alcohol in the water alters the solvent structure (101) in such a way as to make more probable the attainment of a suitable configuration of solvent molecules about the reaction site. The change of solvent structure upon addition of 3 mol% of 1-propanol, 2-propanol or 2-butanol to water also increases the optical absorption energy (19) and free ion yield (122,123) of e_s^- .

Further increase of alcohol content of the solvent increases A_2 for $(e_s^- + CrO_4^{2-})$ in a manner similar to that of E_2 (Figures 80 and 81). The interplay of the values of A_2 and E_2 for this reaction is such that k_2/f (eq. [13]) decreases upon addition of up to 20 mol% alcohol to the water, then increases again at higher alcohol contents (Figure 84B). The value of k_2 itself (Figure 84A) decreases monotonically with increasing alcohol content of the solvent because the dielectric permittivity decreases (Table 1). This increases the coulombic repulsion between the reactants and inhibits their mutual approach to within the reaction distance r_T .

The solvent composition dependence of A_2 ($e_s^- + NO_3^-$) is more complex (Figure 81A). The coulombic repulsion between e_s^- and NO_3^- is smaller than that between e_s^- and CrO_4^{2-} , yet the reaction rate constant of the former is smaller (Figure 84A). The electron affinity of NO_3^- is evidently smaller than that of CrO_4^{2-} . Unfortunately, values of relative reduction potentials for these one electron reactions are not available for comparison (124,125). Both reactions are more rapid in 2-propanol and 2-butanol than in

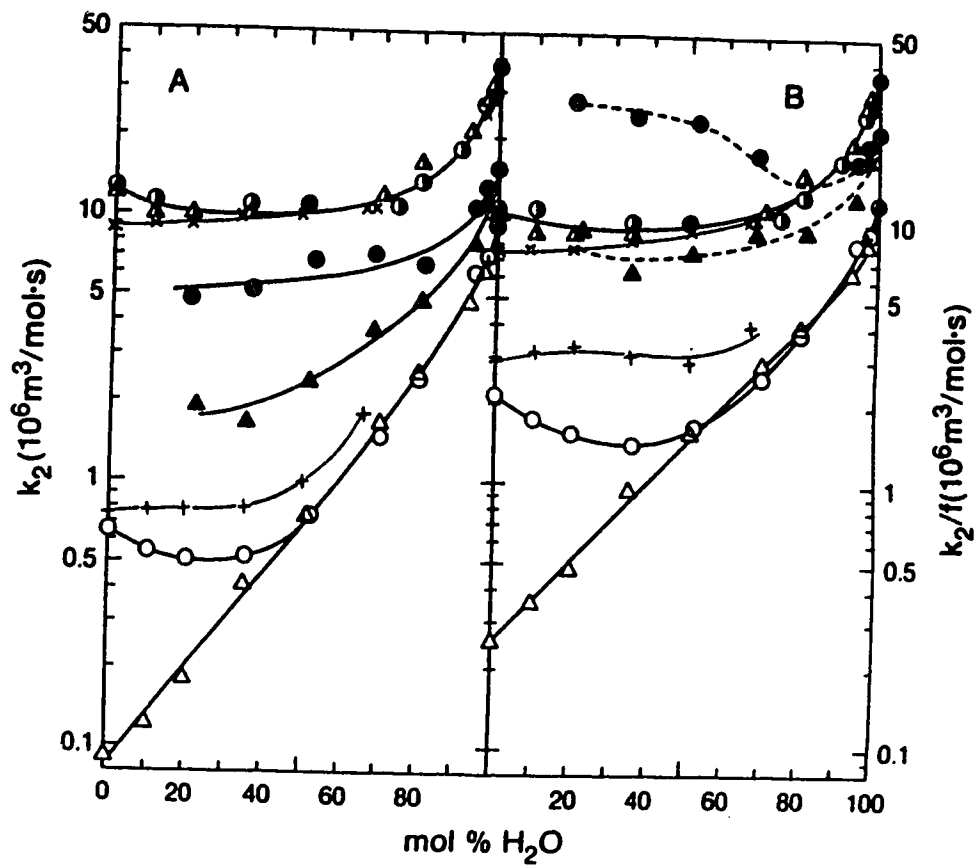


Fig. 84 Solvent composition dependence of k_2 (A) and k_2/f (B) at 298K.

Triangles, 1-propanol; circles, 2-propanol; + and x 2-butanol.

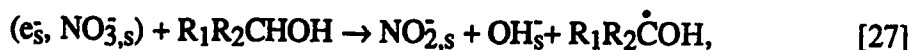
Open symbols and +, NO_3^- ; half open and x, nitrobenzene; solid,
 CrO_4^{2-} .

1-propanol (Figure 84), which indicates a more direct involvement of the 2-propanol and 2-butanol in reaction [22].

A. Effect of Solvent Viscosity

The solvent viscosity dependence of $k_2\eta/fT$ (eq. [12]) at 298K is shown in Figure 85. The values for CrO_4^{2-} are similar to those for nitrobenzene, so $(e_s + \text{CrO}_4^{2-})$ is also nearly diffusion controlled. A value of $k_2\eta/fT = 100$ with $\kappa \approx 1$ corresponds to $r_r/r_d \approx 18$. The large values of r_r/r_d found here are due mainly to the small values of r_d for e_s : 0.05 nm in water and 0.09 nm in 2-propanol (104). The small effective radius (Stokes' rigid sphere model) of e_s for diffusion is attributed to the easy deformability of e_s and its amoeba-like migration.

The values of $k_2\eta/fT$ for $(e_s + \text{NO}_3^-)$ are relatively small (Figure 85), so the reaction is far from being diffusion controlled. Reaction [22] is slow in this case. The value of $k_2\eta/fT$ in pure 2-propanol is 11-fold larger than that in 1-propanol. It is 18-fold larger in 2-butanol than that in 1-propanol. The values of $k_2(e_s + \text{NO}_3^-)$ in t-butanol/water (107) are nearly the same as those in the corresponding 1-propanol/water solutions. The molecular structure of t-butanol is $(\text{CH}_3)_3\text{COH}$. In comparing these four alcohols, 2-propanol and 2-butanol have a much more reactive C-H group than do the other two; it is the $(\text{CH}_3)_2\text{C} \begin{matrix} \text{H} \\ \diagup \\ \text{OH} \end{matrix}$ or $(\text{CH}_3)(\text{C}_2\text{H}_5)\text{C} \begin{matrix} \text{H} \\ \diagup \\ \text{OH} \end{matrix}$. This group evidently participates chemically in reaction [22], as for example,



where the dot on $\text{R}_1\text{R}_2\dot{\text{C}}\text{OH}$ indicates the unpaired electron on the "free radical".

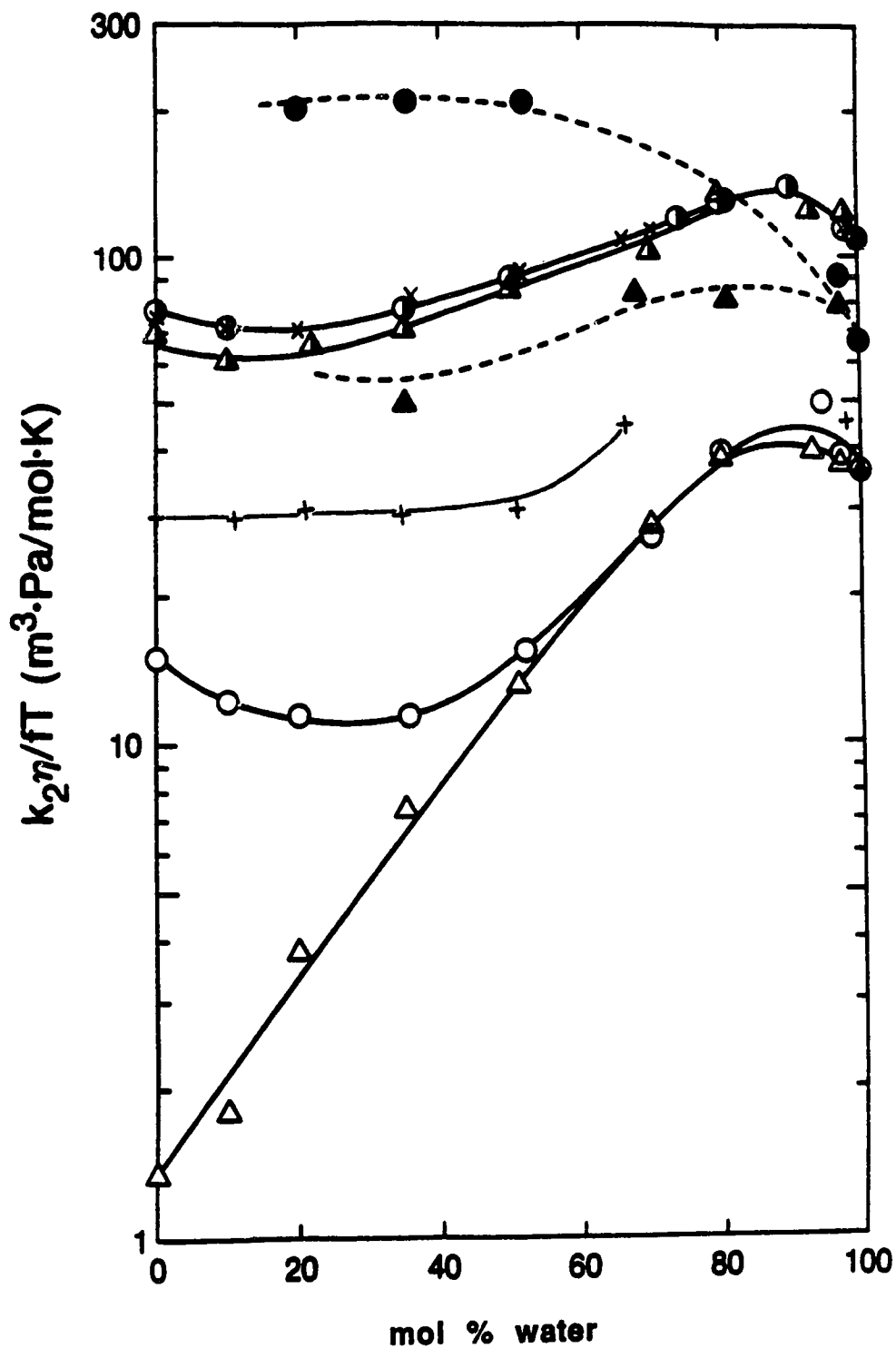
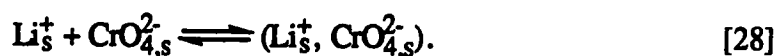


Fig. 85 Solvent composition dependence of $k_2\eta/\Gamma T$ at 298K. Triangles, 1-propanol; circles, 2-propanol; + and x, 2-butanol. Open symbols and +, NO_3^- ; half open and x, nitrobenzene; solid, CrO_4^{2-} .

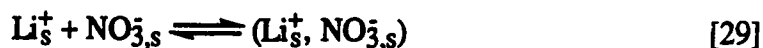
B. Comparison with Ionic Conductivities (Diffusion Coefficients)

Values of molar conductivities of NO_3^- , CrO_4^{2-} and e_s^- are not known for most of the solvents. In pure water at 298K the ratios of the λ 's of $e_s^-:\text{CrO}_4^{2-}:\text{NO}_3^-:\text{Li}_s^+$ are 4.7:4.3:1.9:1.0, so the diffusion coefficients D are in the ratios 4.7:1.1:1.9:1.0. Thus diffusion of e_s^- dominates the relative motion of each reactant pair. As an indication of the solvent composition effect on ionic diffusion the molar conductivities of the salts, $\Lambda(\text{Li}_s^+, \text{NO}_3^-)$ and $\Lambda(2\text{Li}_s^+, \text{CrO}_4^{2-})$ were measured at the concentrations used in the rate constant determinations. In water the ratio $[\lambda(e_s^-) + \lambda(\text{NO}_3^-)]/\Lambda(\text{Li}_s^+, \text{NO}_3^-) = 2.3$, which is about twice the value of $[\lambda(e_s^-) + 0.25 \lambda(\text{CrO}_4^{2-})]/\Lambda(2\text{Li}_s^+, \text{CrO}_4^{2-}) = 0.92$. Thus the solvent composition dependences of κ_r for the reactions of e_s^- with NO_3^- and CrO_4^{2-} can be approximated by the variations of the ratio $z_i k / f \Lambda T$, where z_i is the charge on the anion and Λ is the molar conductivity of the salt.

The solvent composition dependences of Λ at 298K are shown in Figure 86. In the alcohol-rich solvents the plots of chromate conductance against concentration were sublinear, which indicates ion pair formation:



The same was true of nitrate in pure 2-propanol:



Association constants of [28] and [29] were estimated from the curved plots; by comparison of various individual cation and anion mobilities in water (125) it was assumed that the ionic conductivities in these solvents were in the ratios $\lambda[\text{CrO}_4^{2-}] \approx 2\lambda[\text{NO}_3^-] \approx 4\lambda[\text{Li}_s^+] \approx 4\lambda[(\text{Li}_s^+, \text{CrO}_4^{2-})]$. The corresponding values of molar conductivities of the salts at infinite dilution, Λ_0 , are shown in Figure 86.

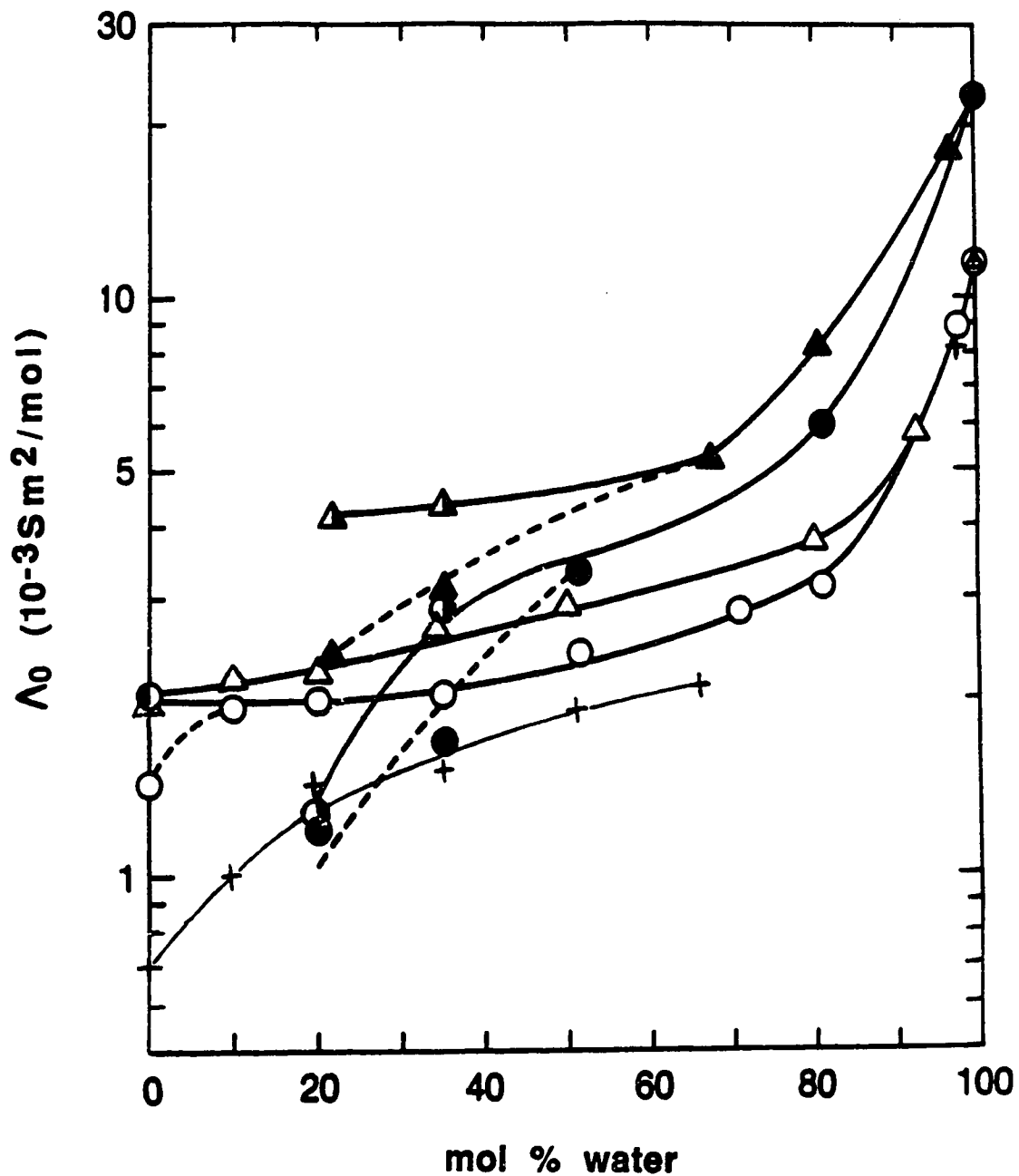


Fig. 86

Solvent composition dependence of molar conductivities of lithium nitrate and lithium chromate at 298K. S=siemens=C/V.s. Triangles, 1-propanol; circles, 2-propanol: open symbols, NO_3^- ; solid symbols, CrO_4^{2-} ; +, NO_3^- in 2-butanol, except \blacktriangle , \bullet , \bullet , values of Λ_0 calculated from sublinear plots of Λ against salt concentration.

The Arrhenius temperature coefficients E_A are listed in Tables 35, 36, 41, 42, and 47.

For LiNO_3 the equation for the association constant K is

$$K = \frac{x}{(a-x)^2} \quad [30]$$

where x is the amount of association of Li_3^+ and NO_3^- , and the total concentrations are a . Then the conductance λ of the solution is given by

$$\lambda = 3K(a-x) \quad [31]$$

where K is the molar conductivity of Li_3^+ ; $\Lambda_0 = 3Ka$ which is the value of λ at $x = 0$.

For Li_2CrO_4 the equation for the association constant K is

$$K = \frac{x}{(2a-x)(a-x)} \quad [32]$$

where x is the amount of association of Li_3^+ and CrO_4^{2-} , and the total concentrations are $2a$ for Li_3^+ and a for CrO_4^{2-} . Then the conductance λ of the solution is given by

$$\begin{aligned} \lambda &= K[(2a-x) + 4(a-x) + x] \\ &= K(6a-4x) \end{aligned} \quad [33]$$

where K is the molar conductivity of Li_3^+ ; $\Lambda_0 = 6Ka$ which is the value of λ at $x = 0$.

The Arrhenius plots of the estimated association constants are shown in Figure 87.

The solvent composition dependences of $z_1k_2/f\Lambda_0T$ at 298K are shown in Figure 88.

The shapes of the curves are similar to those in Figure 85, but the alcohol end of the

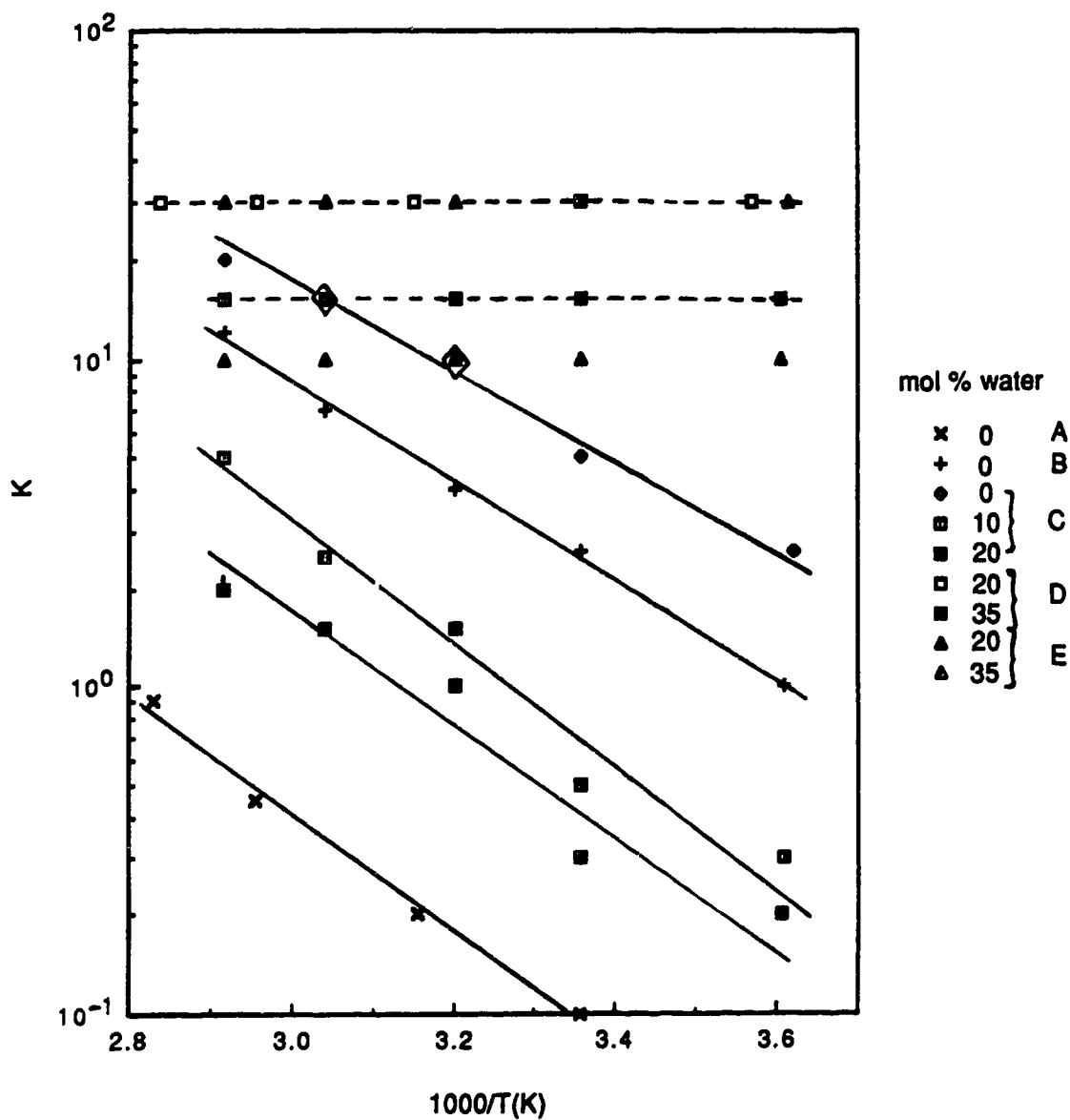


Fig. 87

Arrhenius plots of the association constants of LiNO_3 and Li_2CrO_4 in alcohol-rich solvents of 1-propanol/water, 2-propanol/water and 2-butanol/water.

LiNO_3 in 1-propanol/water, A; 2-propanol/water, B; 2-butanol/water, C;

Li_2CrO_4 in 1-propanol/water, D; 2-propanol/water, E.

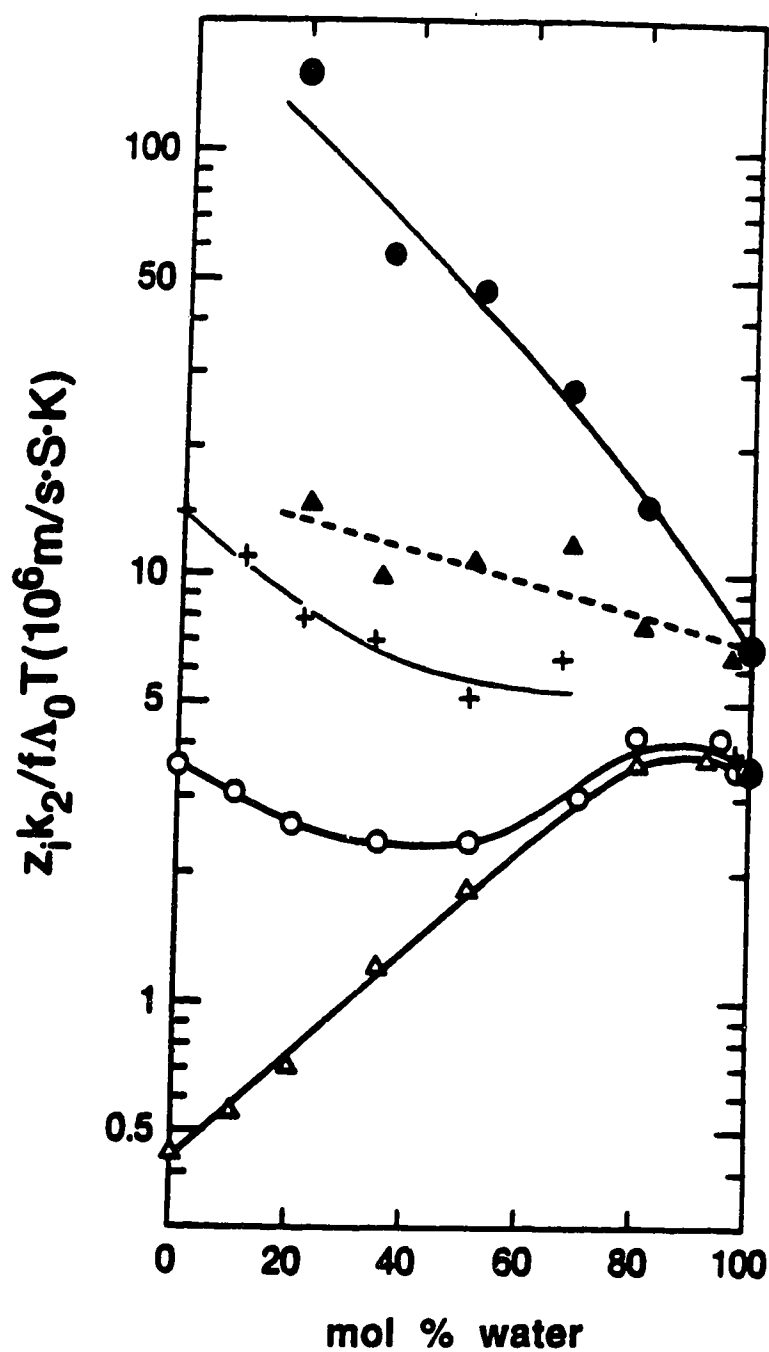


Fig. 88

Solvent composition dependence of $z_i k_2 / f \Lambda_0 T$ at 298K, where z_i is the number of charges on the anion. Triangles, 1-propanol; circles, 2-propanol: open symbols, NO_3^- ; solid symbols, CrO_4^{2-} ; +, NO_3^- in 2-butanol.

curves in Figure 88 are two to four times higher relative to the water end than those in Figure 85. In water at 298K the value of the molar conductivity of e_s^- ($18 \times 10^{-3} \text{ S}\cdot\text{m}^2/\text{mol}$) is 4.7 times larger than that for Li_s^+ ($3.9 \times 10^{-3} \text{ S}\cdot\text{m}^2/\text{mol}$). In 2-propanol the conductivity ratio e_s^-/Li_s^+ is about $4.8 \times 10^{-3}/0.6 \times 10^{-3} \approx 8$ (see e_s^- mobility compilation in ref. 11). Replacement of $\lambda_o(e_s^-)$ for $\lambda_o(\text{Li}_s^+)$ would lower the left ends of the curves in Figure 88 by a factor of 1.7 and decrease the mismatch with Figure 85.

The solvent dependence of the effective radius r_d for mutual diffusion of Li_s^+ and NO_3^- is given by the dependence of $[\Lambda_o(\text{Li}_s^+, \text{NO}_3^-)]^{-1}$; from eqs. [7] and [10], $r_d = N_A \xi^2 / 6\pi\eta \Lambda_o$. For Li_s^+ and CrO_4^{2-} the difference of charge is a complication. The required value of $[\lambda_+ + (\lambda_-/z^2)]$ may be approximated as either $\Lambda_o/z = [\lambda_+ + (\lambda_-/z)]$, or $\lambda_o/z^2 = [(\lambda_+/z) + (\lambda_-/z^2)]$. Since $\lambda(\text{CrO}_4^{2-}) \approx 4\lambda(\text{Li}_s^+)$ in water, Λ_o/z^2 was chosen. Thus,

$$\begin{aligned} r_d &\approx z^2 N_A \xi^2 / 6\pi\eta \Lambda_o & [34] \\ &\approx 8 \times 10^{-16} z^2 / \eta \Lambda_o. \end{aligned}$$

Values of r_d from eq. [28] for $\text{Li}_s^+ + \text{NO}_3^-$ and $\text{Li}_s^+ + \text{CrO}_4^{2-}$ are plotted against solvent composition in Figure 89. With the exception of 100% to 97 mol% water, the value of r_d increases steadily with alcohol content of the solvent. The larger values in alcohol are attributed to the larger sizes of the molecules that solvate (are attracted to) the ions; the ratio of molar volumes of alcohol/water at 298K are 4.2 for 1-propanol, 4.3 for 2-propanol and 5.2 for 2-butanol (126).

II. Solvated Electron Reactions with Positive Ions

Solvent effects on solvated electron reaction rates with H_s^+ , Ag_s^+ , Tl_s^+ , Cu_s^{2+} , and Al_s^{3+} were studied as a function of temperature in 1-propanol/water, 2-propanol/water and

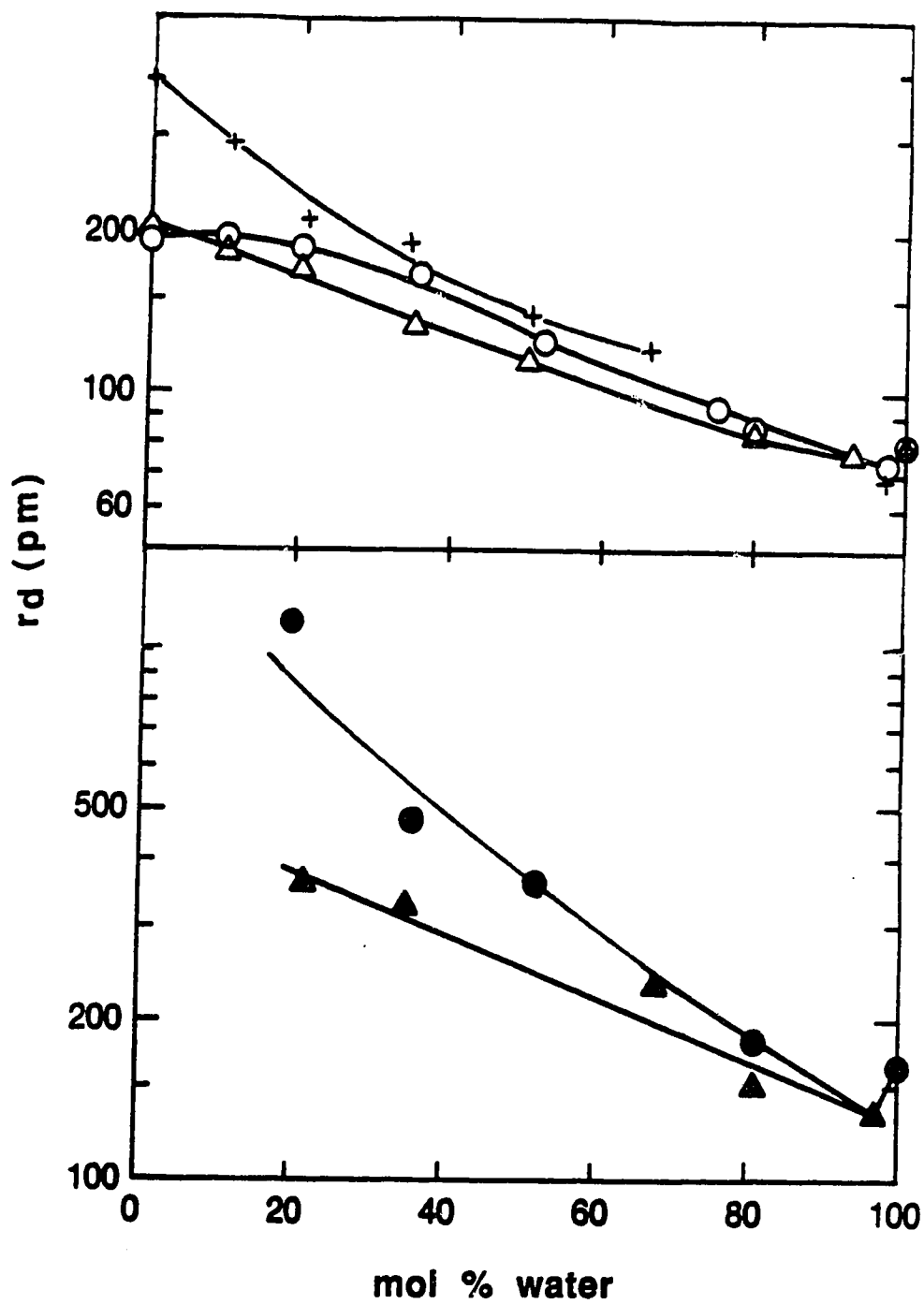


Fig. 89

Solvent composition dependence of r_d of $\text{Li}^+ + \text{NO}_3^-$ and $\text{Li}^+ + \text{CrO}_4^{2-}$ at 298K.

Triangles, 1-propanol; circles, 2-propanol: open symbols, NO_3^- ; solid symbols, CrO_4^{2-} ; +, NO_3^- in 2-butanol.

2-butanol/water mixed solvents. Values of the Debye factor f were calculated for a range of values of ϵ and T , using a value of r_f appropriate to each solute (Figure 90). The value of ϵ of each solvent at each T used in the experiments was obtained by interpolation of data in refs. 121 and 128.

Arrhenius plots of $\log(k_2/f)$ against T^{-1} were shown for H_s^+ in Figure 13, for Ag_s^+ in Figure 15, for Cu_s^{2+} in Figure 17, and for Al_s^{3+} in Figure 19 for 1-propanol/water mixtures.

Arrhenius plots of $\log(k_2/f)$ against T^{-1} in 2-propanol/water mixtures were shown for H_s^+ in Figure 25, for Ag_s^+ in Figure 27, for Cu_s^{2+} in Figure 29, and for Al_s^{3+} in Figure 31.

Figures 35, 37, 39, and 41 show the Arrhenius plots for H_s^+ , Tl_s^+ , Cu_s^{2+} , and Al_s^{3+} in 2-butanol/water mixtures, respectively.

The composition dependences of k_2/f at 298K are shown in Figures 91, 92 and 93 for 1-propanol/water, 2-propanol/water and 2-butanol/water, respectively. The variation of k_2/f with the solvent composition is more drastic than that for k_2 itself (Figures 94, 95 and 96). In general, the second-order rate constant increases with increasing charge on the positive ion. But, when the coulombic factor f is taken into account, k_2/f values for Ag_s^+ and Tl_s^+ are greater than those for Cu_s^{2+} and Al_s^{3+} . For H_s^+ , k_2/f have relatively the highest values.

Addition of a small amount of water to pure 1-propanol caused the k_2/f for Al_s^{3+} to drop, then increase again when more than 2 mol% of water was added (Figure 91). Addition of water to pure 2-propanol caused the value of k_2/f for Al_s^{3+} to increase continuously until about 80 mol% of water was added. The value of E_r (the optical absorption energy half way up the low energy (red) side of the band) is a measure of the trap depth of the solvated electron. Addition of a small amount of water causes the value of E_r to decrease for 1-propanol. (It increases for 2-propanol and 2-butanol.) This has been explained in terms of the formation of a hydrogen bonded solvent structure which consists of two alcohol tetramers joined together by a water molecule inbetween them,

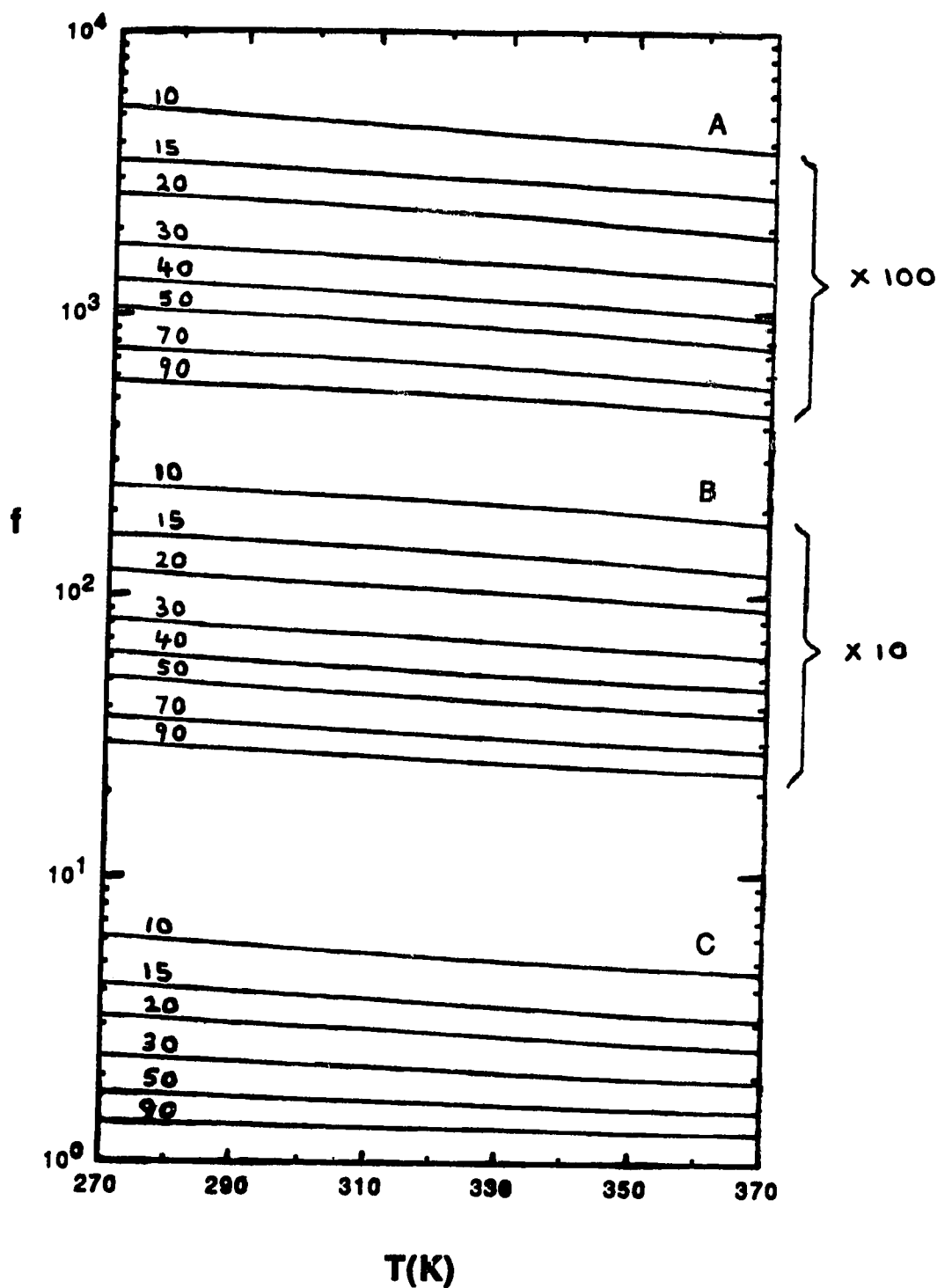


Fig. 90

Temperature dependence of the Debye factor f at different values of dielectric permittivity . A: for $z=+1$ using $r_f=1.0\text{nm}$. B: for $z=+2$ using $r_f=0.5\text{nm}$. C: for $z=+3$ using $r_f=0.35\text{nm}$. Values of ϵ are indicated.

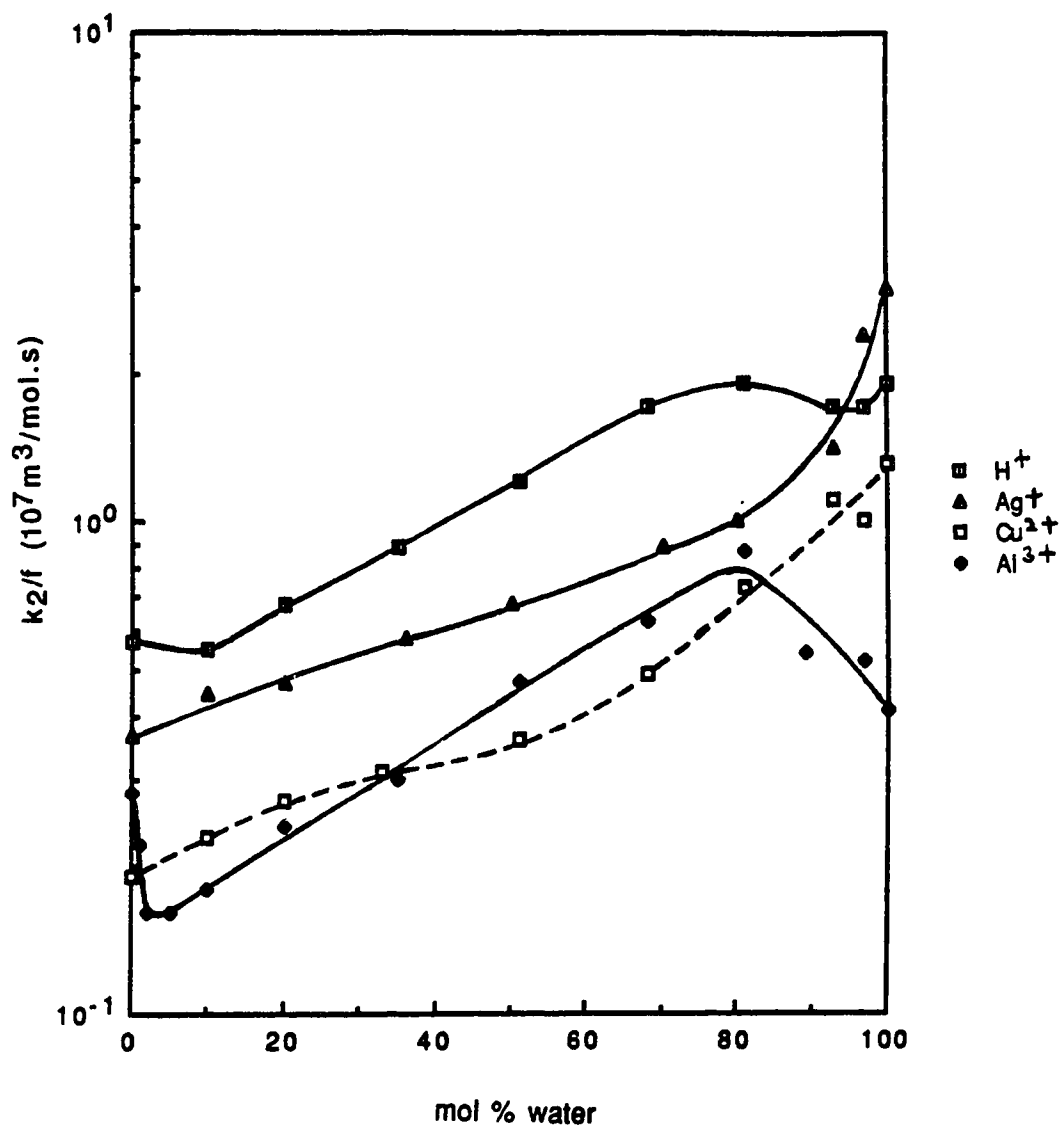


Fig. 91

The composition dependence of k_2/f for positive ions in 1-propanol/water mixtures at 298K.

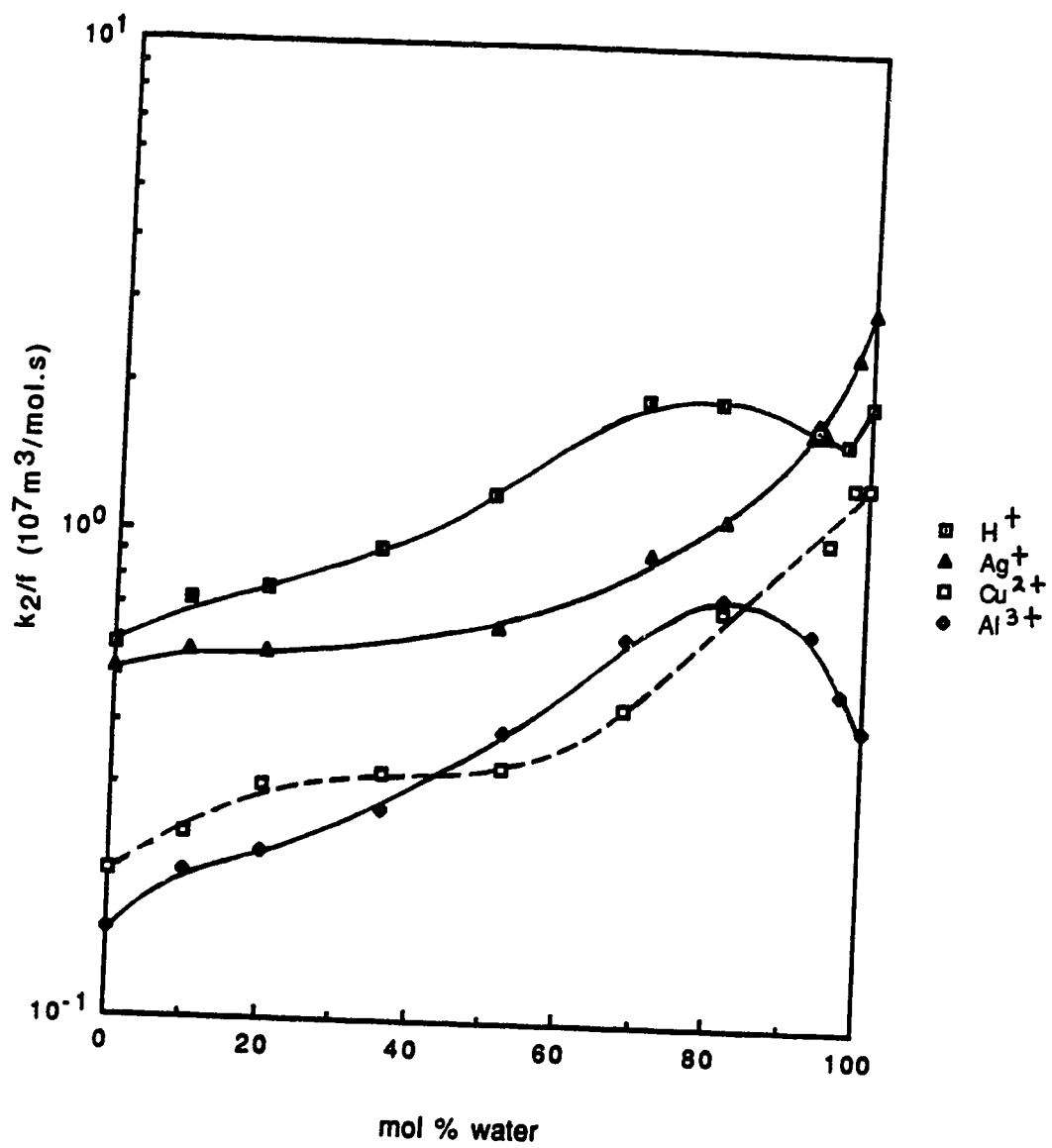


Fig. 92

The composition dependence of k_2/f for positive ions in 2-propanol/water mixtures at 298K.

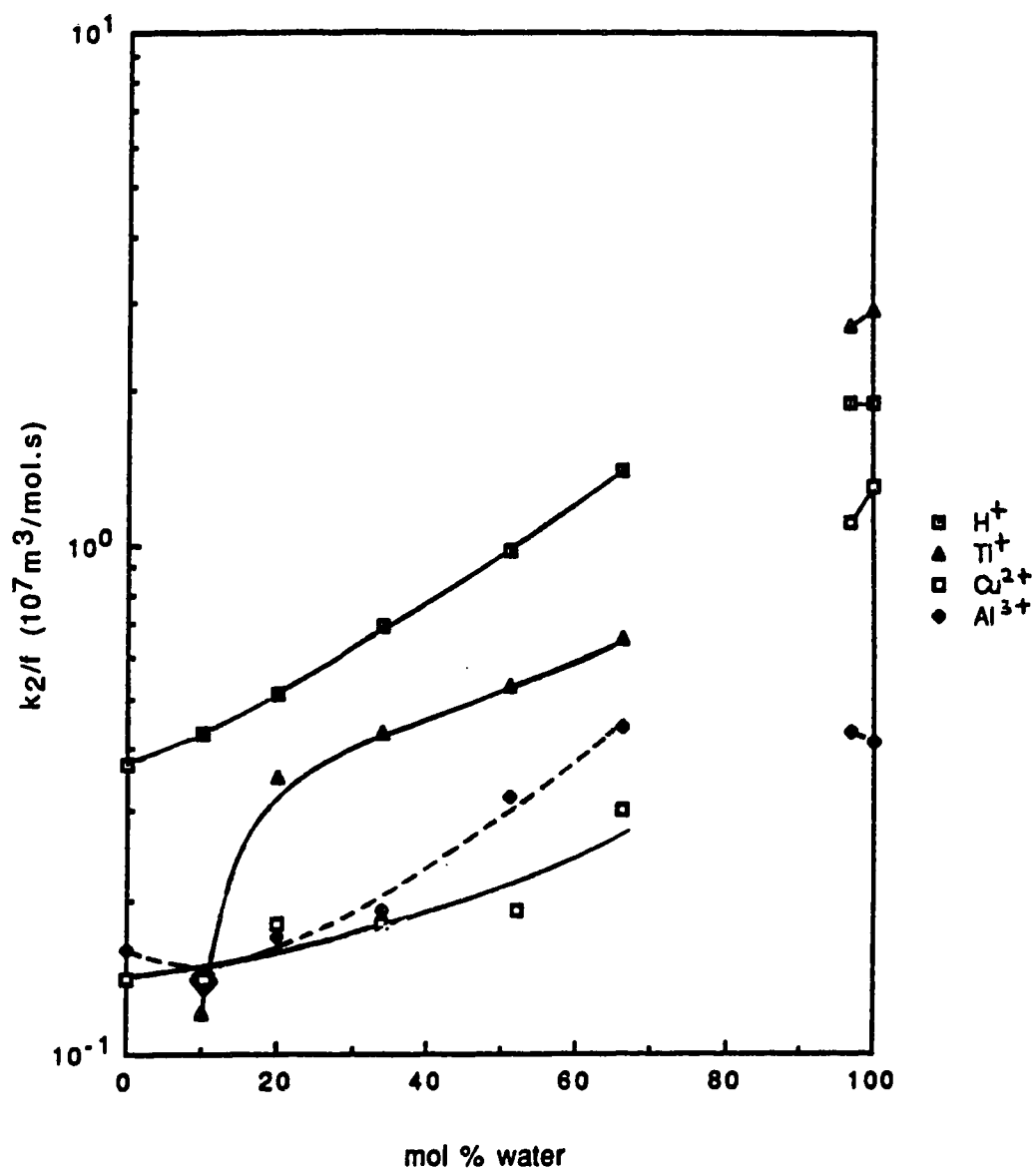


Fig. 93

The composition dependence of k_2/f for positive ions in 2-butanol/water mixtures at 298K.

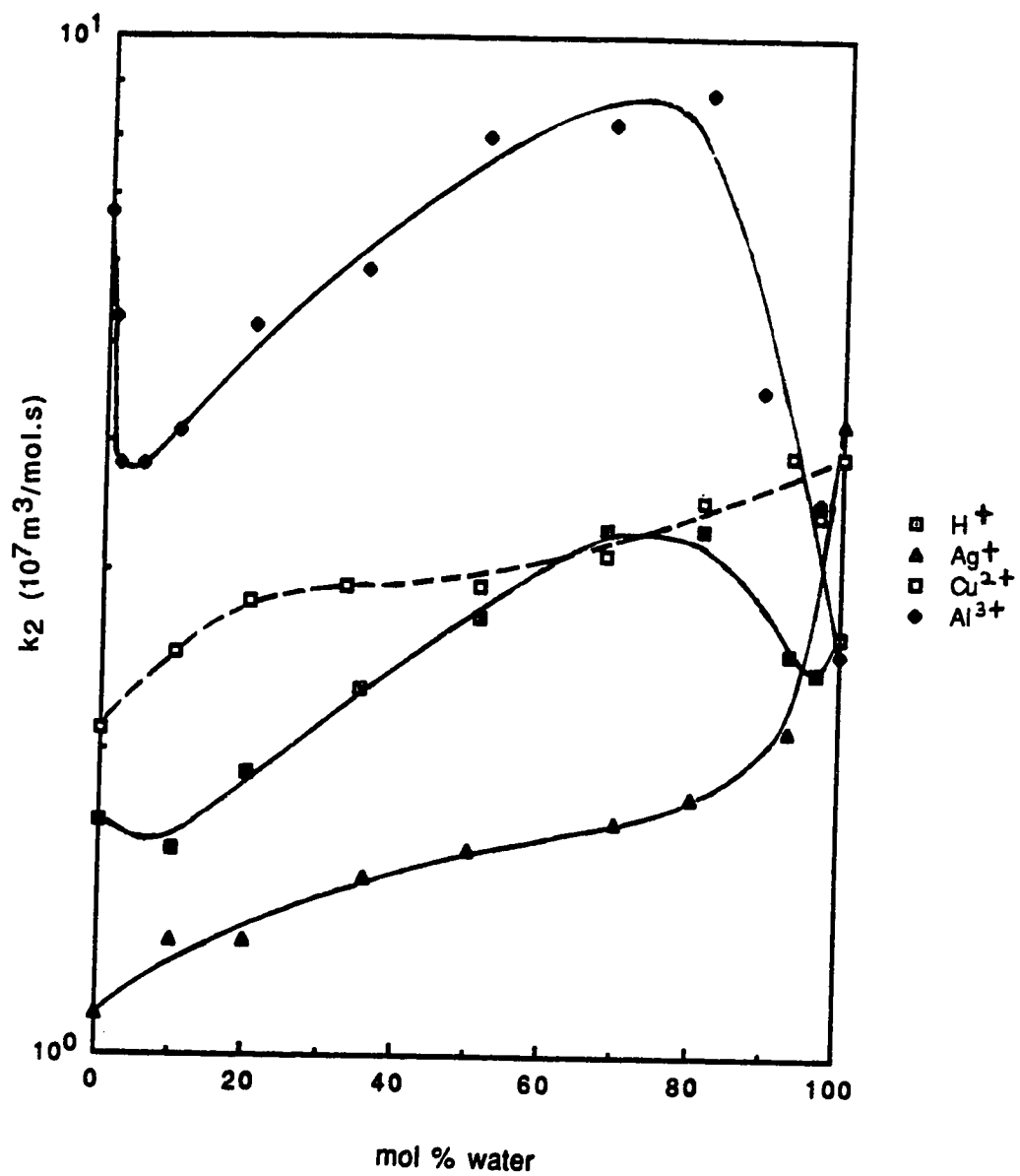


Fig.94

The composition dependence of k_2 for positive ions in 1-propanol/water mixtures at 298K.

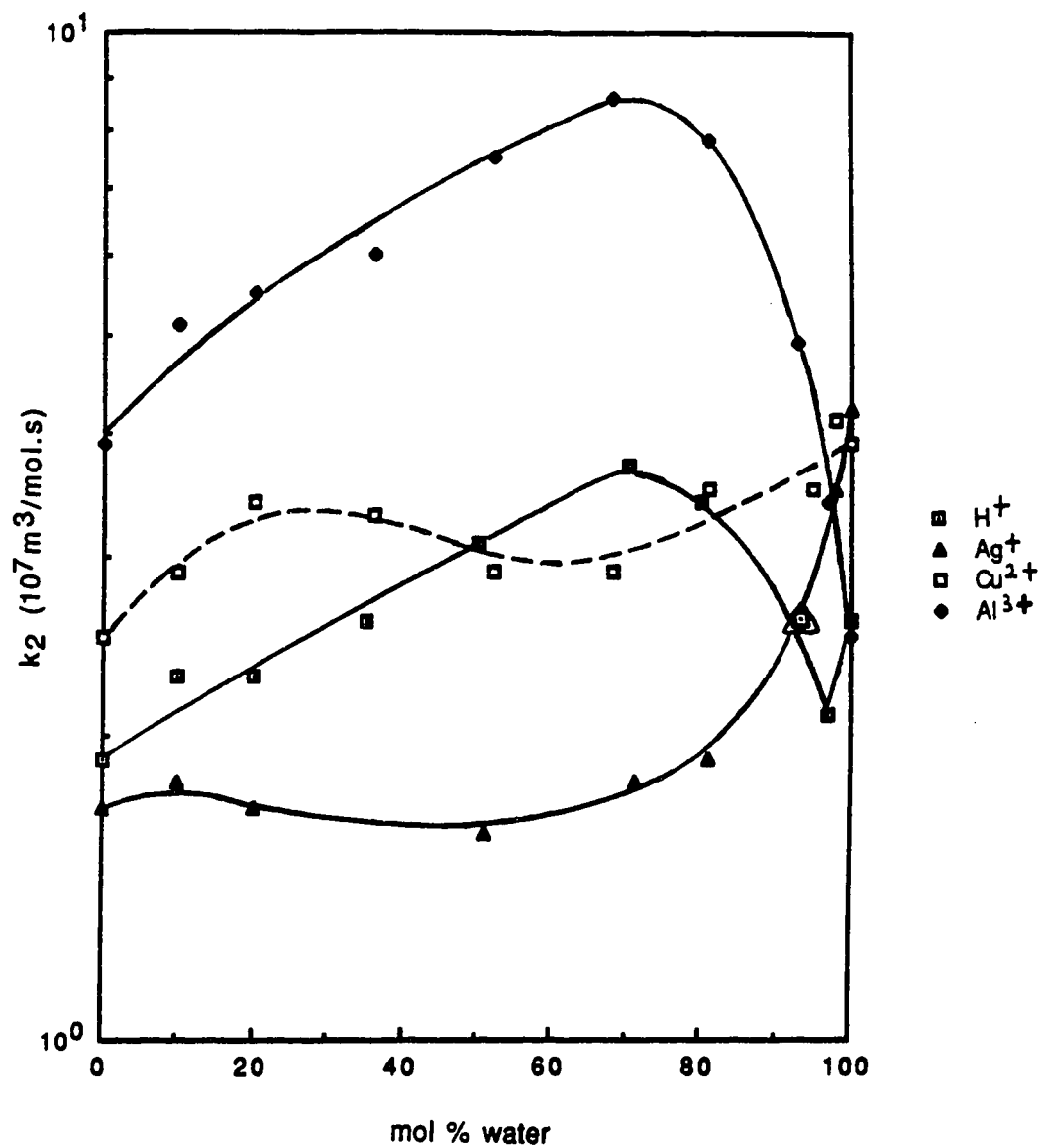


Fig.95

The composition dependence of k_2 for positive ions in 2-propanol/water mixtures at 298K.

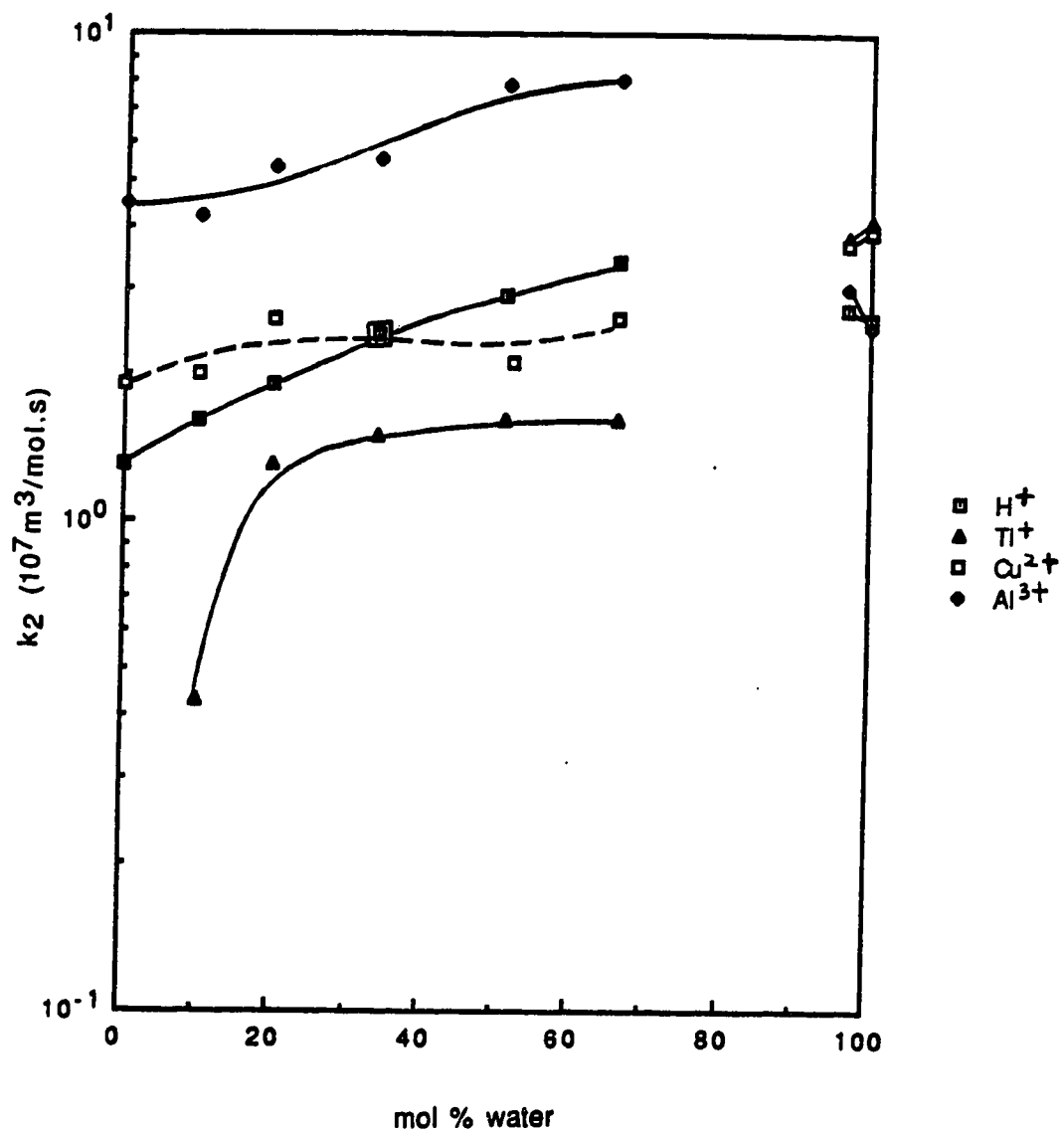


Fig. 96

The composition dependence of k_2 for positive ions in 2-butanol/water mixtures at 298K.

towards 10 mol% of water on the composition scale. This would tend to decrease the availability of OH functional groups to the electron solvation site (19). Thus addition of water to pure 1-propanol would decrease the solvation energy of the electron. This phenomenon could lead to a decrease in entropy of activation for ($e_s^- + Al_s^{3+}$) as a small amount of water is added to pure 1-propanol, which is reflected in the $\log A_2$ vs mol% H_2O plot (see later, Figure 100). This could be the reason for the decrease in k_2/f as a small amount of water is added to pure 1-propanol.

Plots of E_2 against solvent composition are shown in Figures 97, 98 and 99 for 1-propanol/water, 2-propanol/water and 2-butanol/water, respectively. The activation energies for the reaction of solvated electrons with the positive ions are generally higher than those with negative ions (119). The activation energy of a diffusion controlled reaction is the energy of diffusion for the reacting species. Therefore, the energies of diffusion for positive ions could be higher than for negative ions. The value of E_2 for H_s^+ in the water-rich solvents are relatively low because of the low activation energy of diffusion (proton hopping mechanism (127)).

Plots of $\log A_2$ against solvent composition are given in Figures 100, 101, and 102 for 1-propanol/water, 2-propanol/water and 2-butanol/water, respectively. The value of A_2 increases with the addition of alcohol except in the case of Al_s^{3+} . The presence of a small amount of alcohol in the water apparently alters the solvent structure in such a way as to make more probable the attainment of a suitable configuration of solvent molecules about the reaction site. Addition of water to pure 2-butanol causes A_2 for Tl_s^+ to increase. Addition of water to pure alcohols causes A_2 for H_s^+ to also increase.

A. Effect of Solvent Viscosity

The solvent viscosity dependences of $k_2\eta/fT$ at 298K are shown in Figures 103 and 104. The values of $k_2\eta/fT$ for all the positive ions in all the solvents vary with composition in a similar manner. The values pass through a maximum near 80 mol%

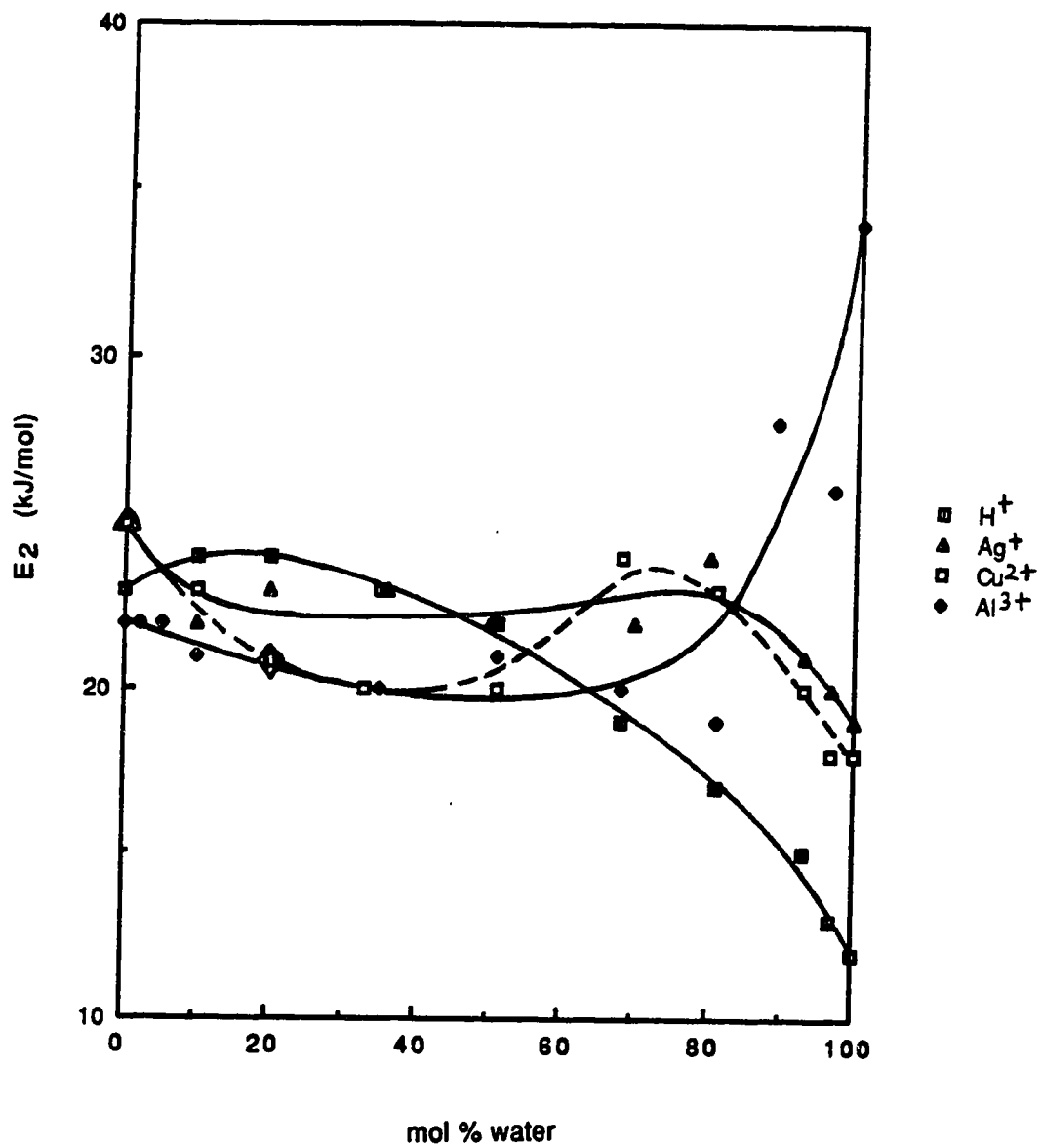


Fig. 97

The composition dependence of the activation energies for the reaction of solvated electrons with positive ions in 1-propanol/water mixtures.

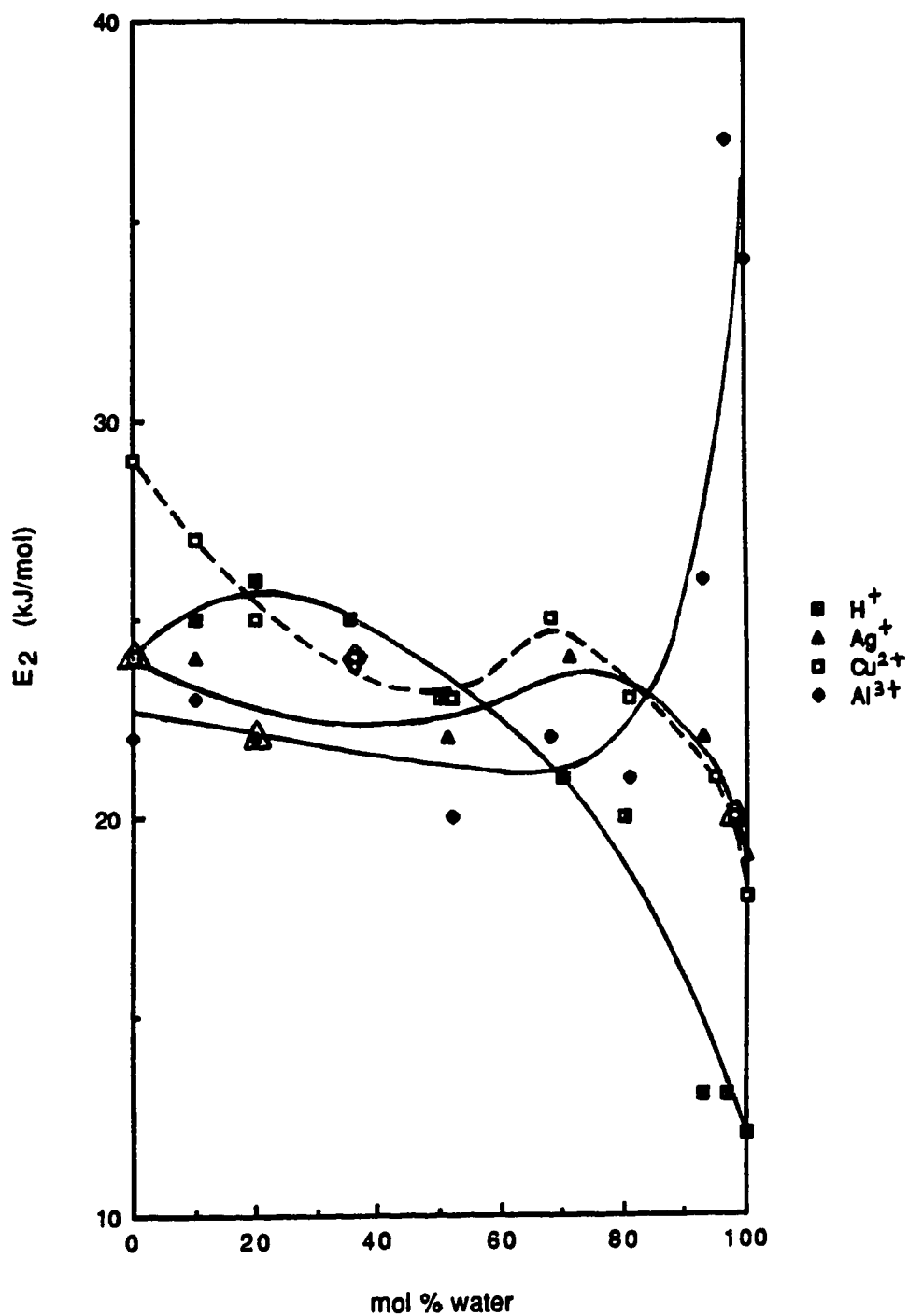


Fig. 98

The composition dependence of the activation energies for the reaction of solvated electrons with positive ions in 2-propanol/water mixtures.

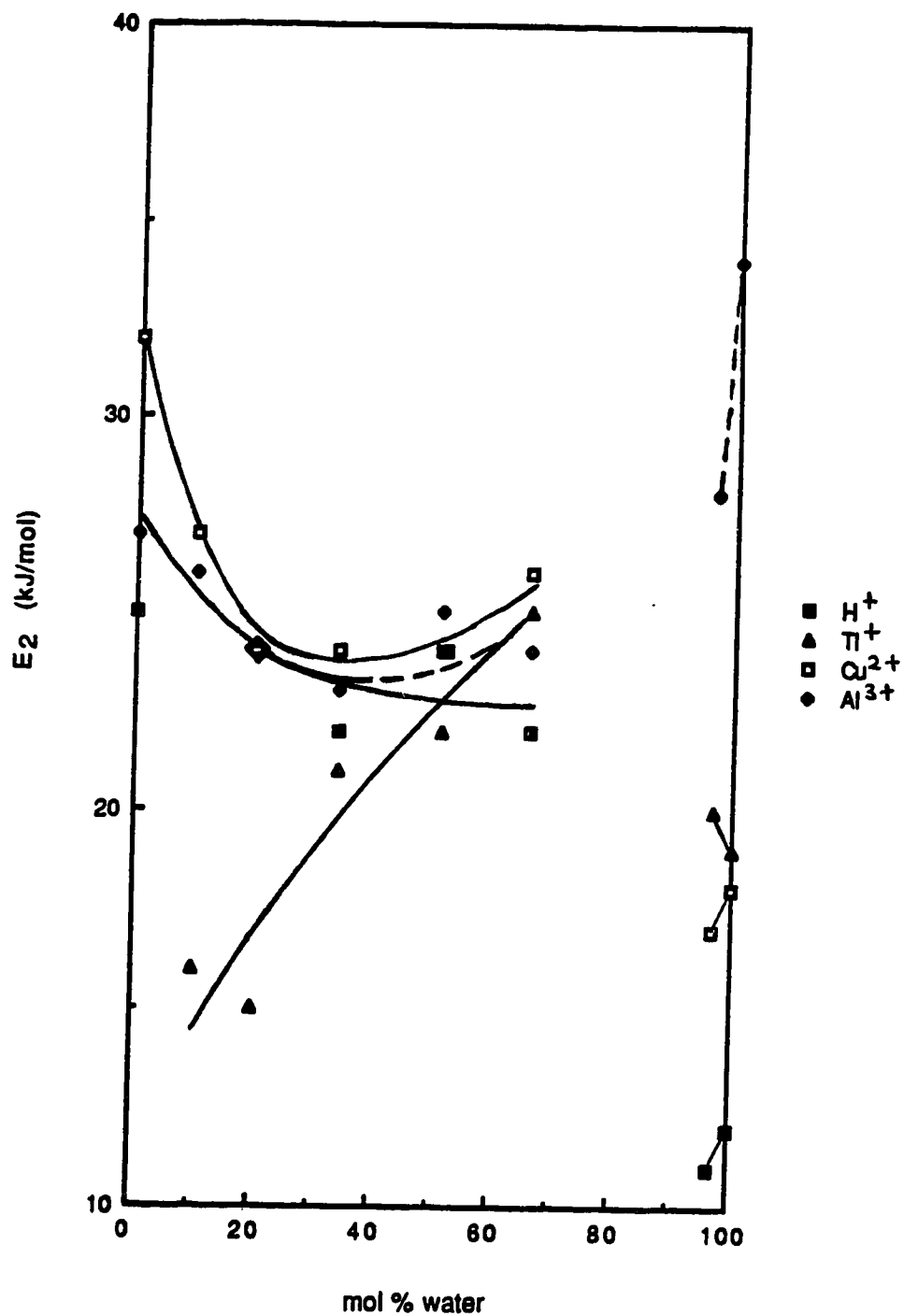


Fig. 99

The composition dependence of the activation energies for the reaction of solvated electrons with positive ions in 2-butanol/water mixtures.

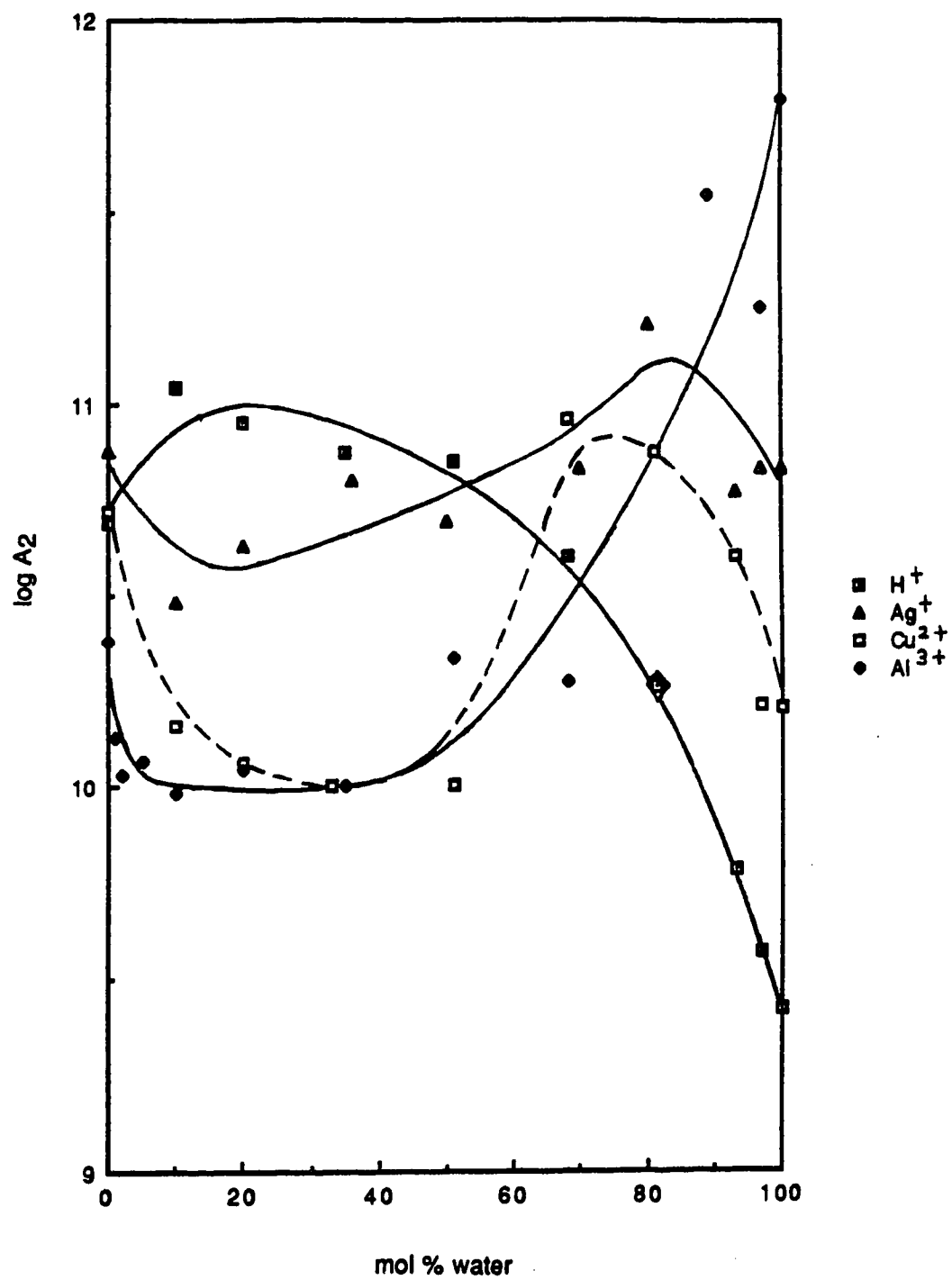


Fig. 100

The composition dependence of $\log A_2$ for the reaction of solvated electrons with positive ions in 1-propanol/water mixtures.

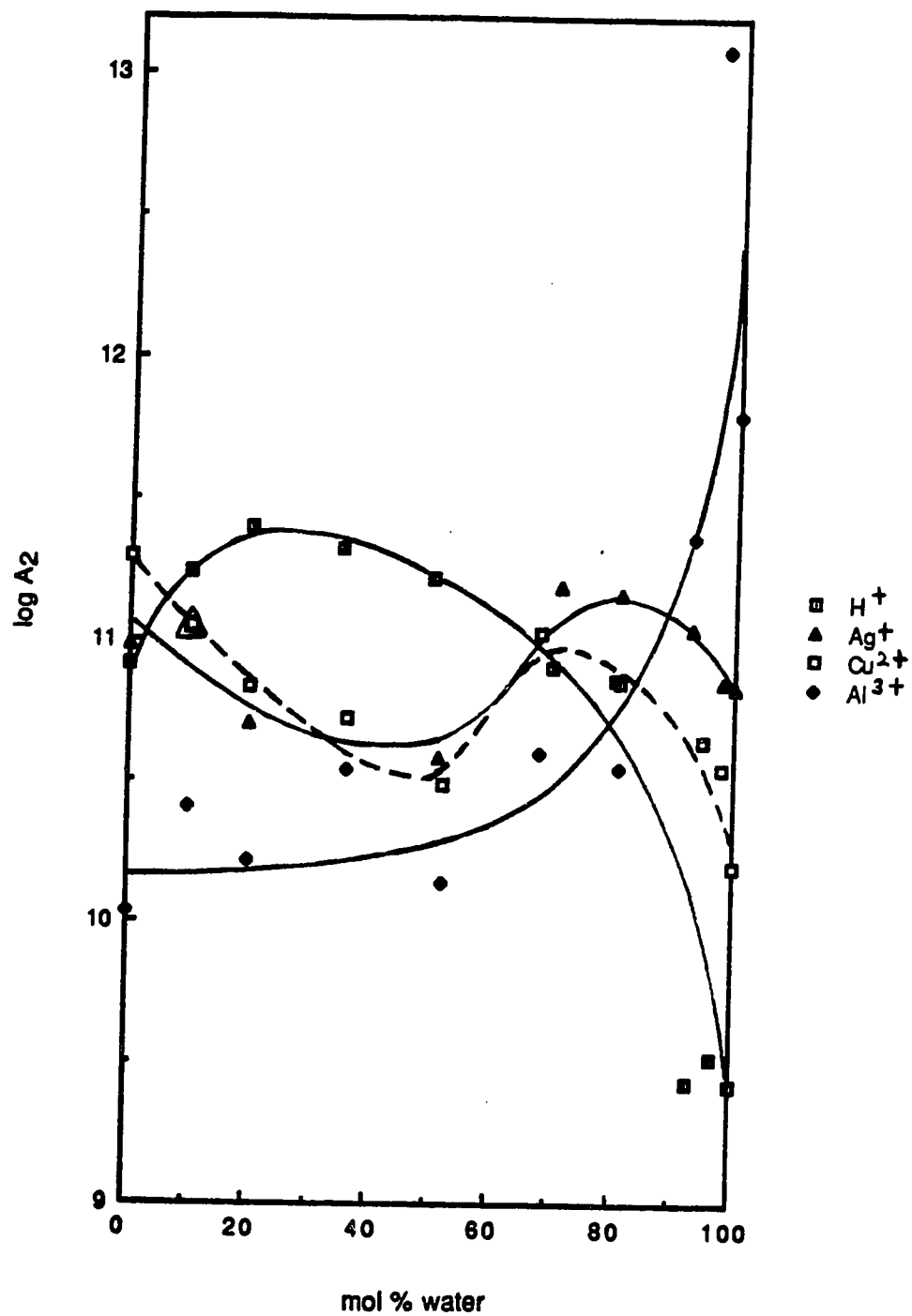


Fig. 101

The composition dependence of $\log A_2$ for the reaction of solvated electrons with positive ions in 2-propanol/water mixtures.

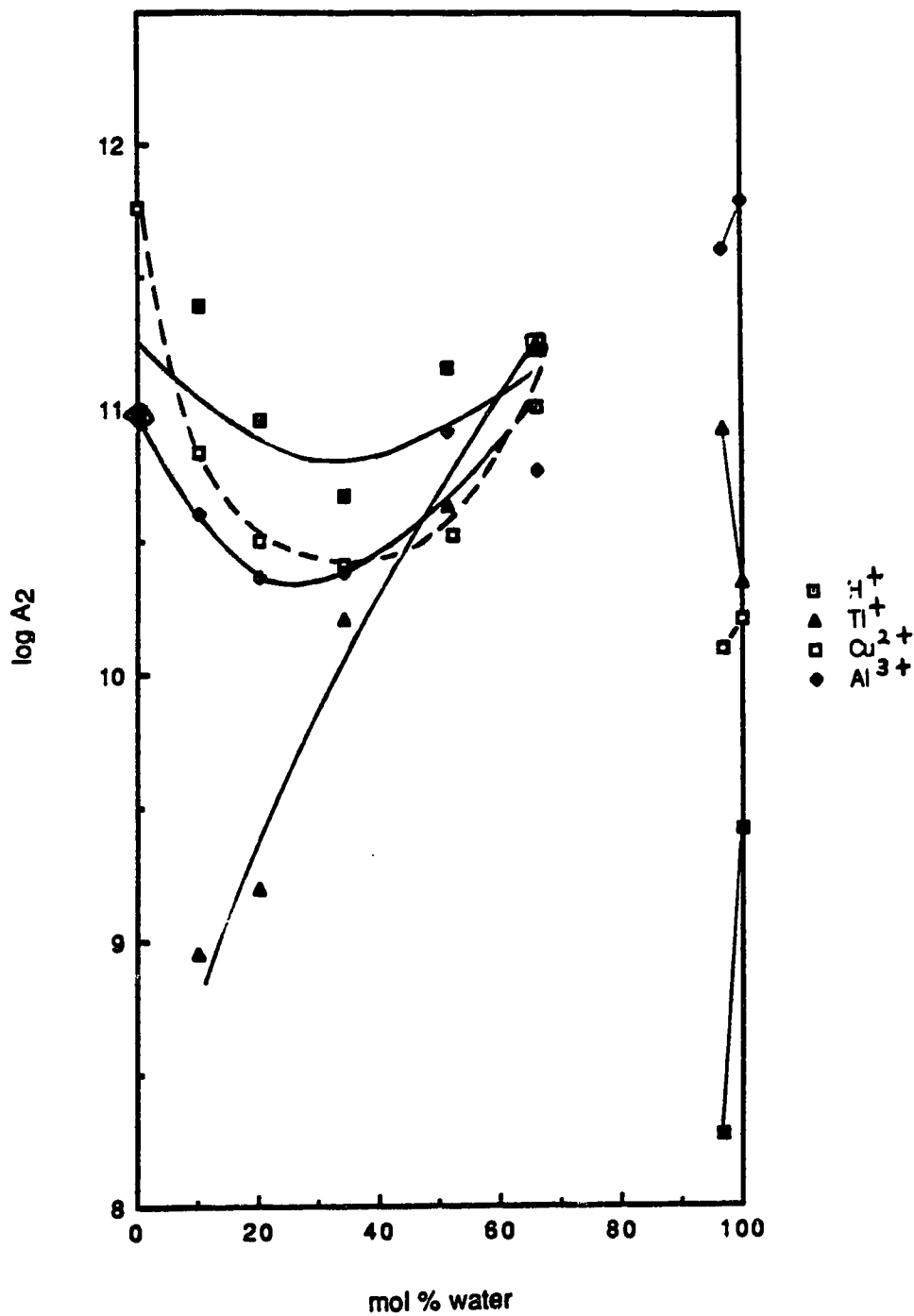


Fig. 102

The composition dependence of $\log A_2$ for the reaction of solvated electrons with positive ions in 2-butanol/water mixtures.

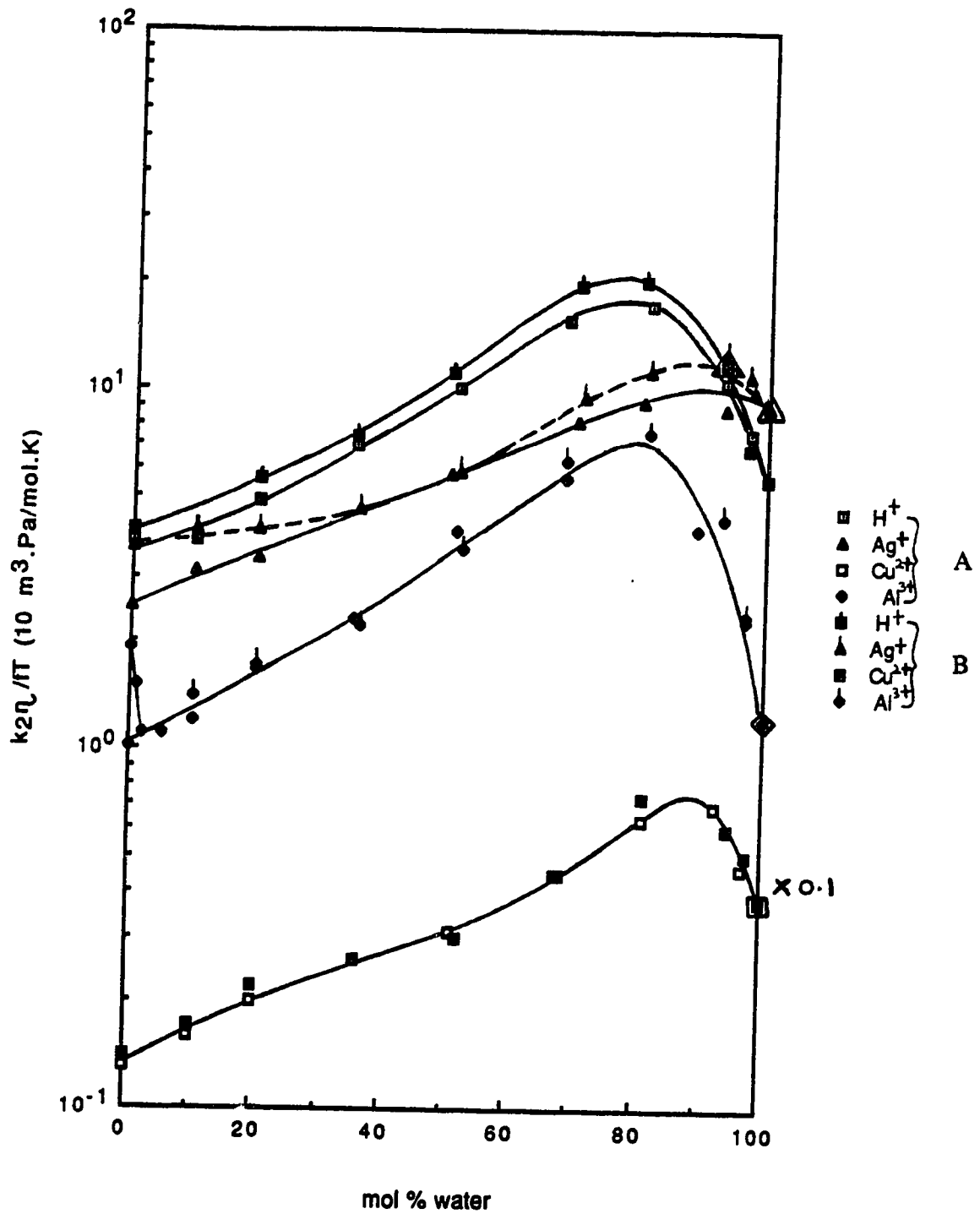


Fig. 103

The composition dependence of $k_2\eta/IT$ for positive ions in 1-propanol/water and 2-propanol/water mixtures at 298K. A: 1-propanol/water.

B: 2-propanol/water.

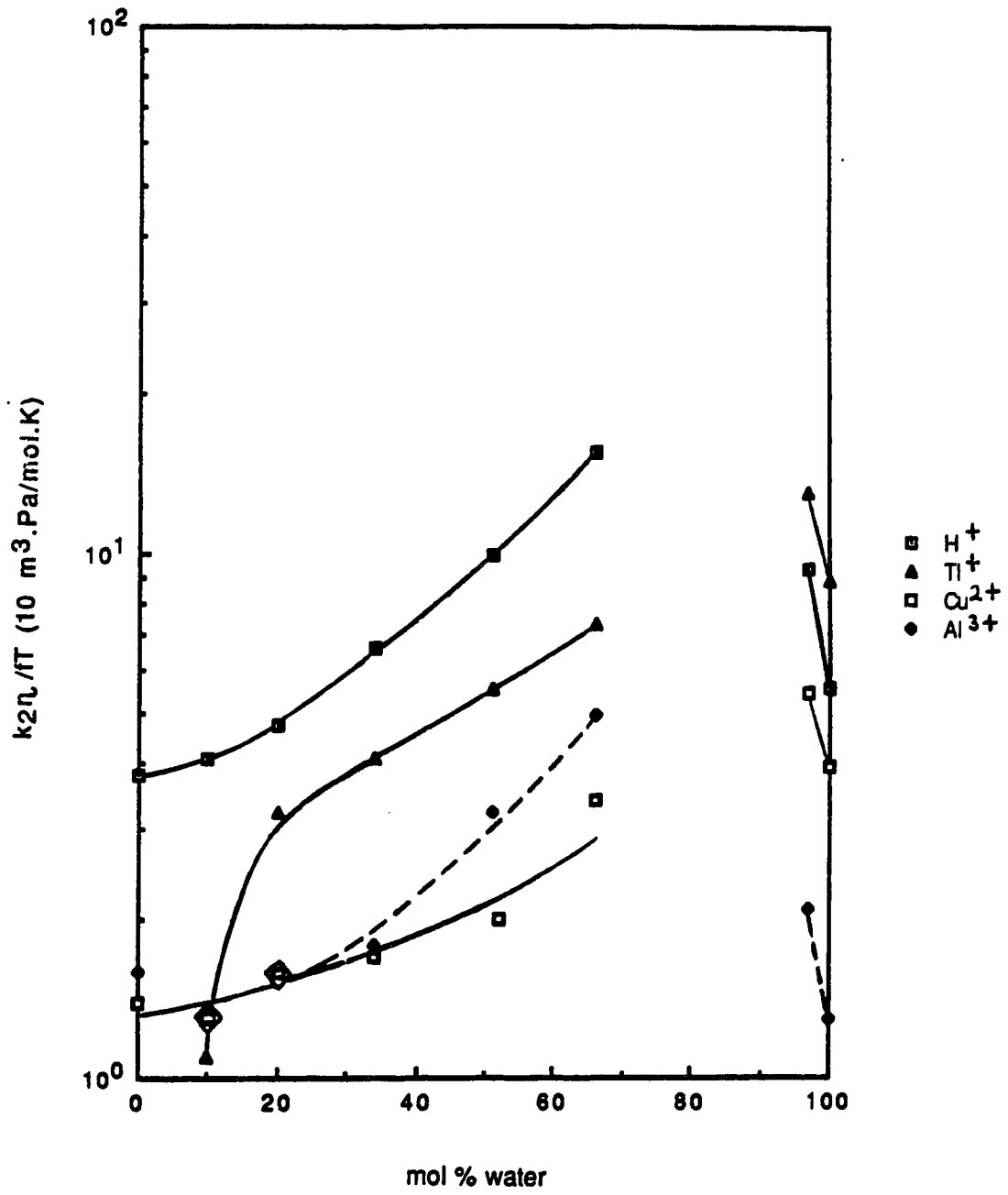


Fig. 104

The composition dependence of $k_2\eta/TT$ for positive ions in 2-butanol/water mixtures at 298K.

water. They decrease towards both pure alcohol end and pure water end. (For 2-butanol/water mixtures the composition range from 66-97 mol% water cannot be achieved because of the insolubility of 2-butanol and water in this region.)

Recall that $k_2\eta/fT = 5.5\kappa (r_r/r_d)$, and that $k_2\eta/fT = 100$ would correspond to $\kappa \approx 1$ with $r_r/r_d \approx 18$. The large values of r_r/r_d are due mainly to small values of r_d for e_s^- : 0.05 nm in water and 0.09 nm in 2-propanol (9).

The values of $k_2\eta/fT$ are relatively low in alcohol-rich solvents. The values of $k_2\eta/fT$ for $(e_s^- + Al_s^{3+})$ are also relatively low in water-rich solvents in comparison to those of other positive ions. Therefore, in these regions, the reaction is far from being diffusion controlled ($\kappa \ll 1$). Reaction [22] is slow in these cases. The values of $k_2\eta/fT$ are relatively low for $(e_s^- + Cu_s^{2+})$ and $(e_s^- + Al_s^{3+})$ compared to those of $(e_s^- + Ag_s^+)$, $(e_s^- + Tl_s^+)$ and $(e_s^- + H_s^+)$. The reason for this could be difficulty in formation of unstable Cu_s^+ or Al_s^{2+} by reaction of a solvated electron with Cu_s^{2+} or Al_s^{3+} . In aqueous solution, the Cu_s^+ ion is unstable with respect to the Cu_s^{2+} ion and neutral Cu. The equilibrium



lies far to the right (124). Compounds of Cu(I) are covalent. Compounds of Al_s^{2+} have not been observed.

B. Comparison with Ionic Conductivities

The solvent composition dependence of molar conductivities of the salts at 298K are shown in Figures 105 to 107. The Arrhenius temperature coefficients E_A are given in Tables 37-40 for 1-propanol/water, Tables 43-46 for 2-propanol/water and Tables 48-51 for 2-butanol/water mixtures.

In the alcohol rich solvents the plots of conductance against concentration for $AgClO_4$ and $TlOAc$ were sublinear, which indicates ion pair formation

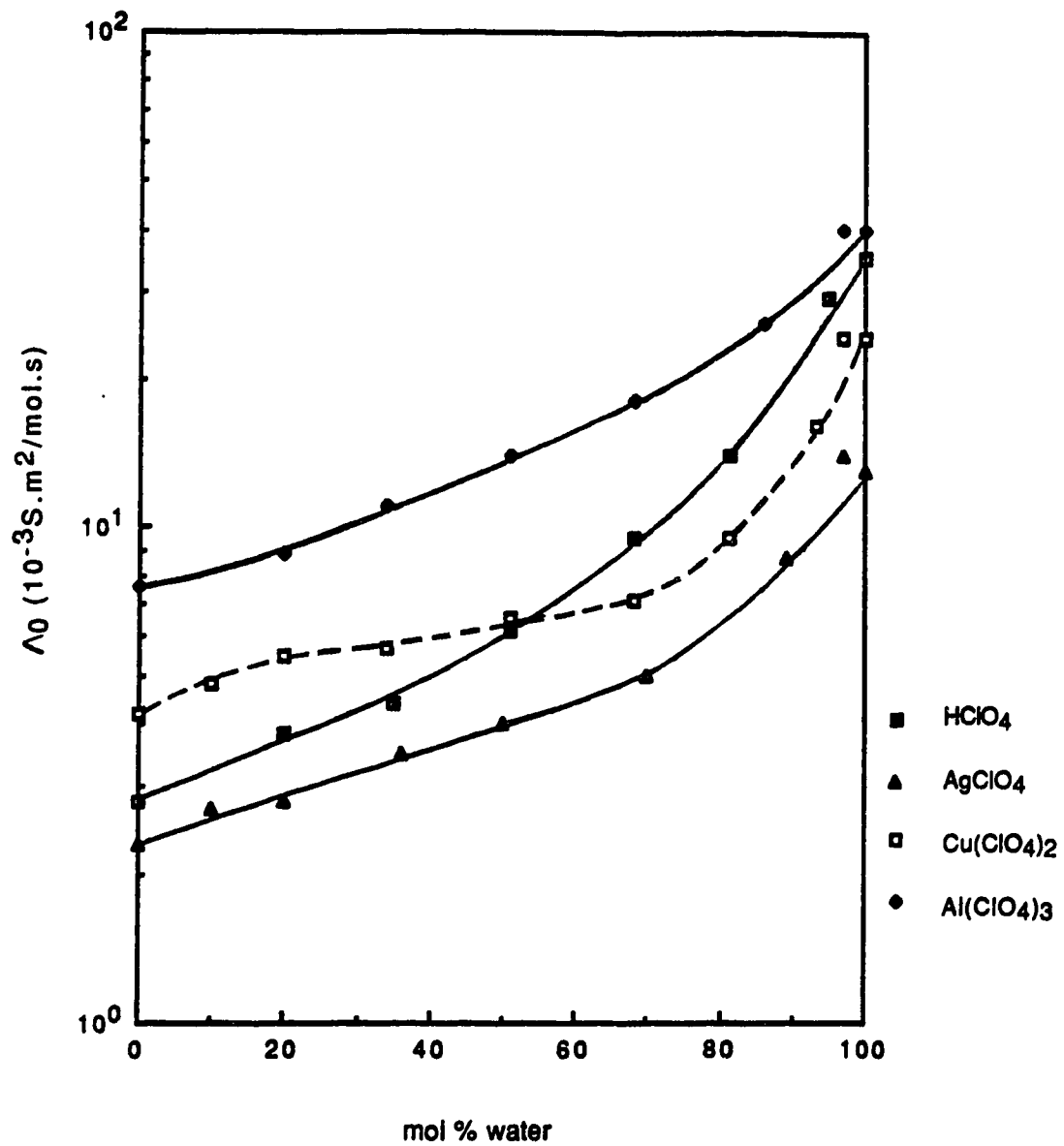


Fig. 105

The composition dependence of molar conductivity of some inorganic electrolytes in 1-propanol/water mixtures at 298K.

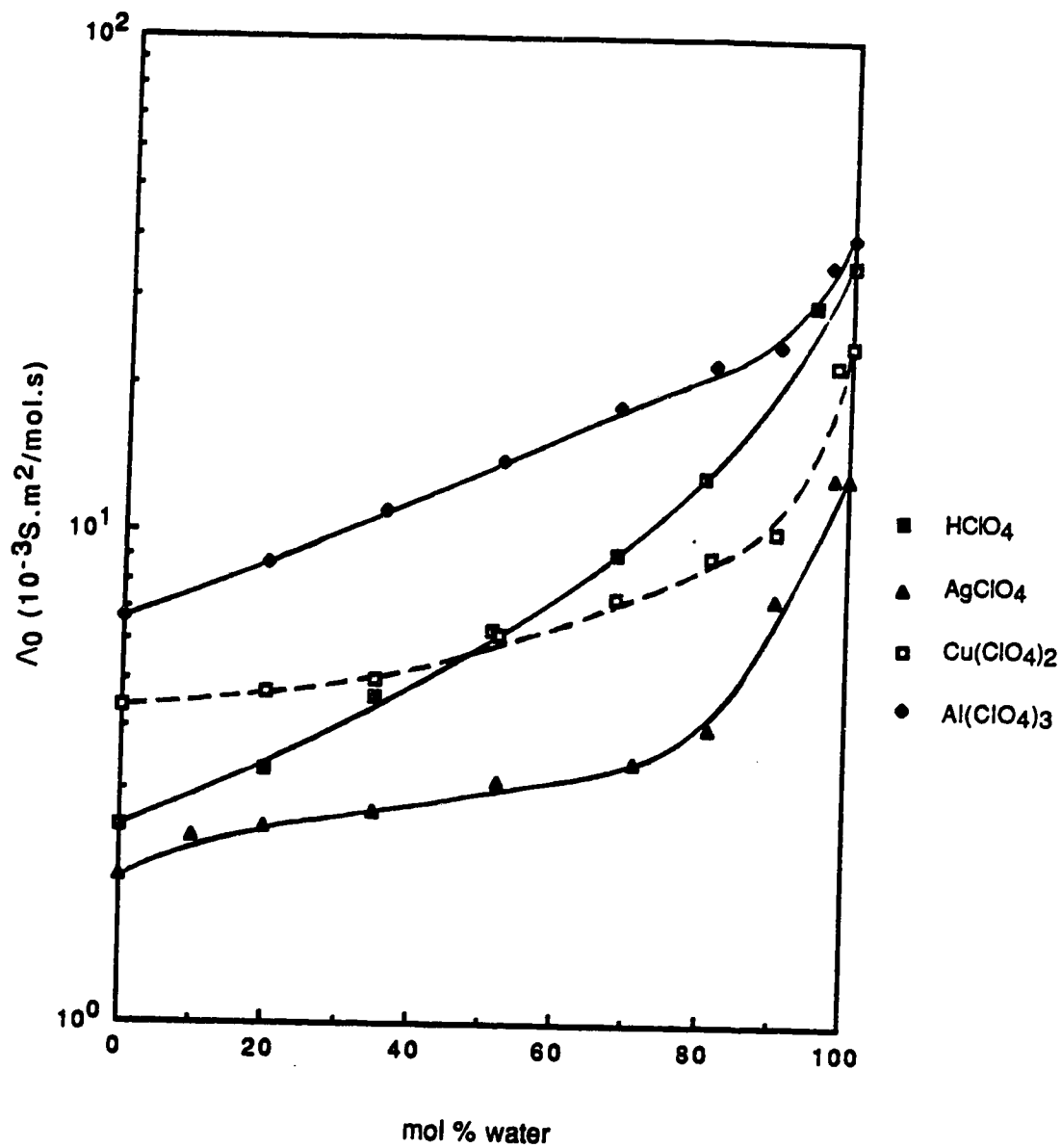


Fig. 106

The composition dependence of molar conductivity of some inorganic electrolytes in 2-propanol/water mixtures at 298K.

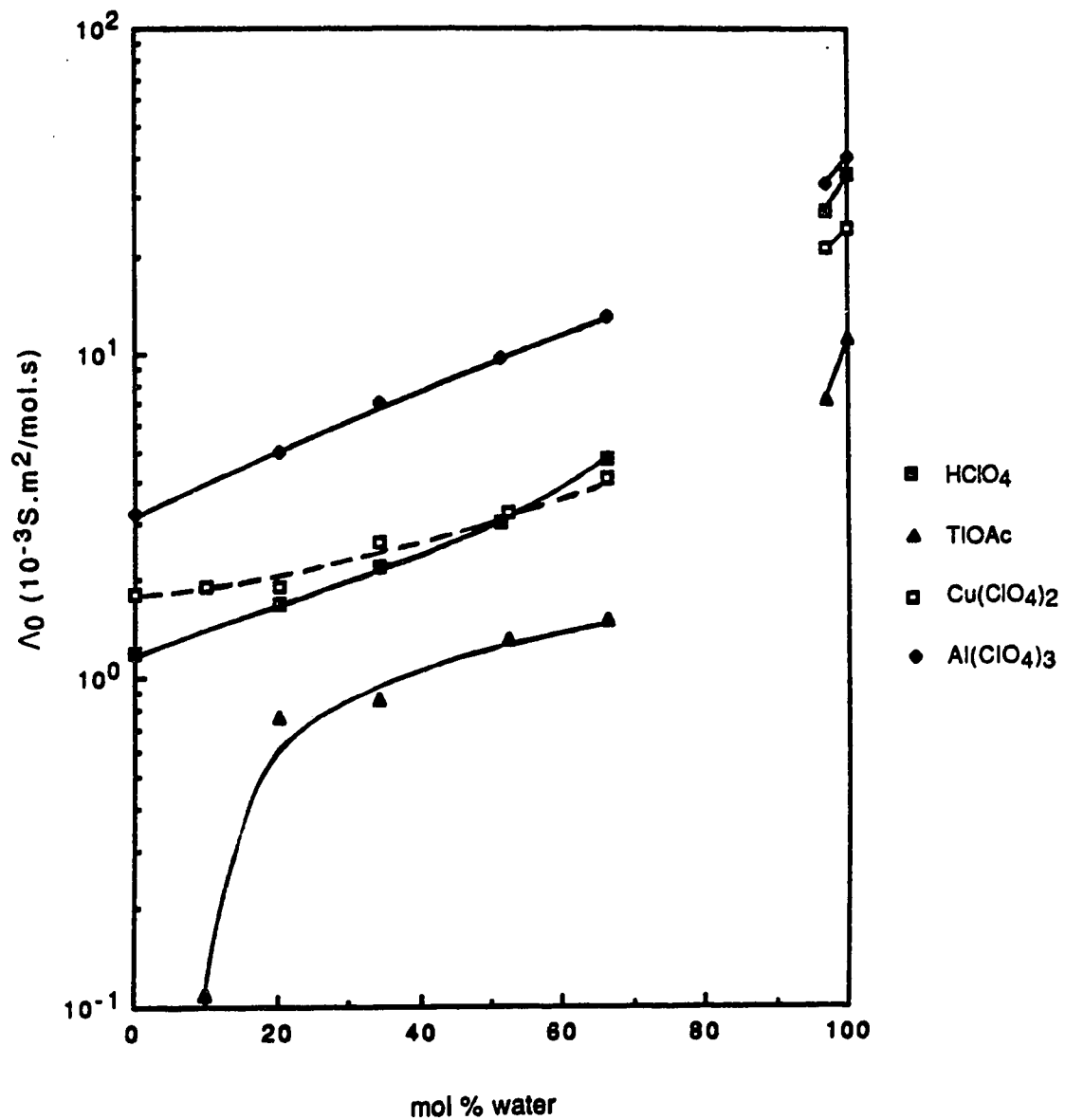
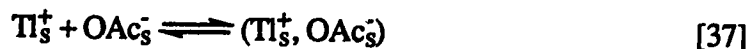


Fig. 107

The composition dependence of molar conductivity of some inorganic electrolytes in 2-butanol/water mixtures at 298K.



and



Association constants of [36] and [37] were estimated from the curved plots; by comparison of various individual cation and anion mobilities in water, the ionic conductivities in these solvents were assumed to be $\Lambda(\text{Ag}_s^+) \approx \Lambda(\text{ClO}_{4,s}^-)$ and $\lambda(\text{Tl}_s^+) \approx \lambda(\text{OAc}_s^-)$.

For AgClO_4 and TlOAc the equation for the association constant K is

$$K = \frac{x}{(a-x)^2} \quad [38]$$

where x is the amount of association of Ag_s^+ and $\text{ClO}_{4,s}^-$ or Tl_s^+ and OAc_s^- , and the total concentrations are a . Then the conductance λ of the solution is given by

$$\lambda = 2K(a-x) \quad [39]$$

where K is the molar conductivity of Ag_s^+ or Tl_s^+ ; $\Lambda_0 = 2Ka$ which is the value of λ at $x = 0$.

However, for AgClO_4 the concentrations used to measure second-order rate constants are about 20 times lower than those used to measure conductances. The percentages of AgClO_4 existing as ions Ag_s^+ and $\text{ClO}_{4,s}^-$ in pure 2-propanol, $(a-x)100/a$ are 98 and 99% even at the temperatures at which the association constants had the highest values 2 and 1, respectively.

In the solvent where 10 mol% of water is added to 2-propanol, the percentage of AgClO_4 existing as ions $(a-x)100/a$ is 98% at the highest temperature used at which the association constant had the highest value (Fig. 108).

The Arrhenius plots of the estimated association constants are shown in Figure 108.

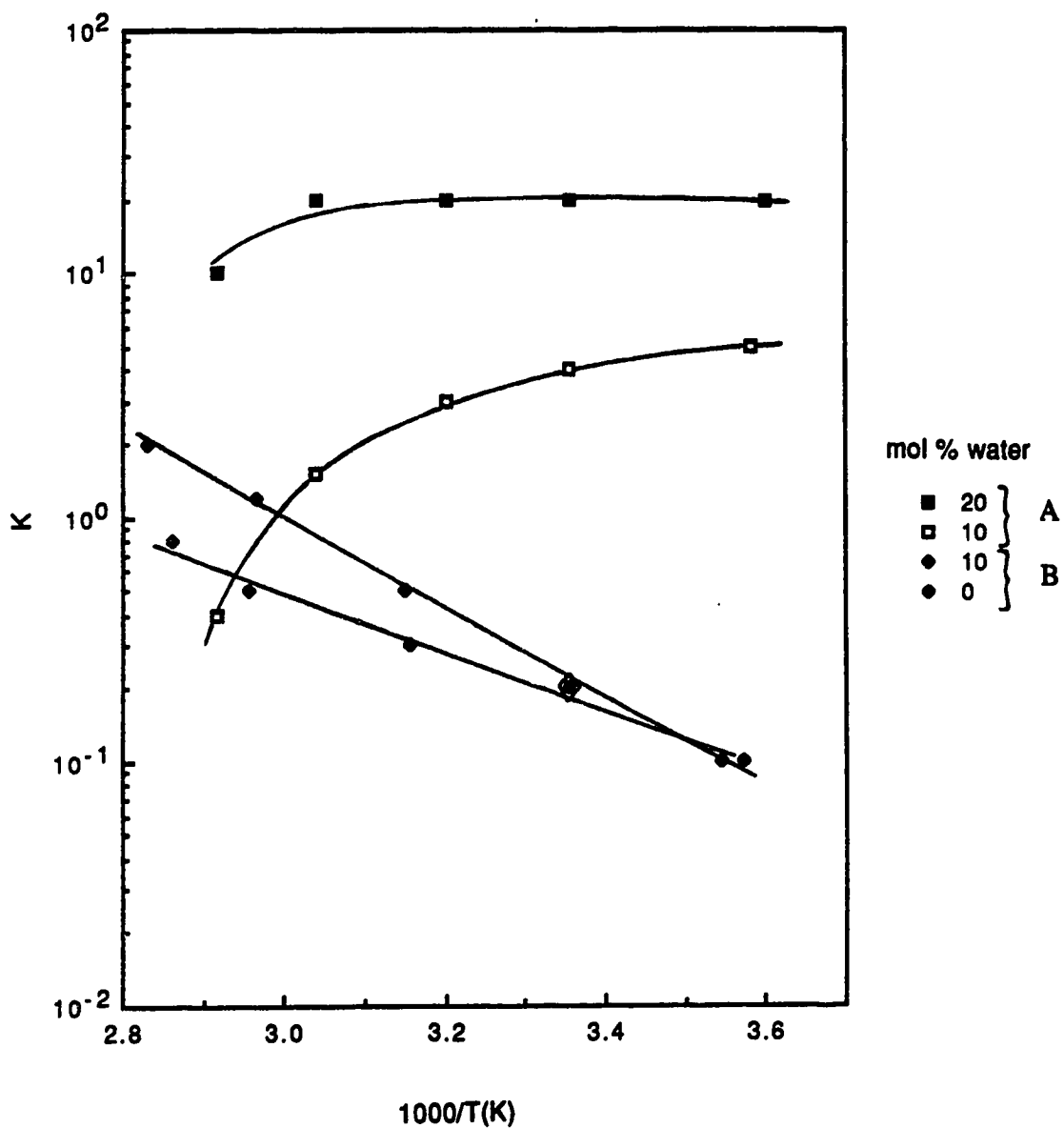


Fig. 108

Arrhenius plots of the association constants of AgClO_4 and TIOAc in alcohol-rich solvents of 2-propanol/water and 2-butanol/water. A: TIOAc in 2-butanol/water. B: AgClO_4 in 2-propanol/water.

Values of molar conductivities of Ag_s^+ , Tl_s^+ , Cu_s^{2+} , Al_s^{3+} , and e_s^- are not known for most of the solvents. In pure water at 298K the ratios of the λ 's of e_s^- : H_s^+ : Ag_s^+ : Tl_s^+ : Cu_s^{2+} : Al_s^{3+} are 4.7:9.1:1.6:2.0:3.0:4.9 so the diffusion coefficients are in the ratios 4.7:9.1:1.6:2.0:0.8:0.5. Thus diffusion of e_s^- dominates the relative motion of each reactant pair except for H_s^+ .

The molar conductivities $\Lambda(\text{H}_s^+, \text{ClO}_{4,s}^-)$, $\Lambda(\text{Tl}_s^+, \text{OAc}_s^-)$, $\Lambda(\text{Ag}_s^+, \text{ClO}_{4,s}^-)$, $\Lambda(\text{Cu}_s^{2+}, 2\text{ClO}_{4,s}^-)$, and $\Lambda(\text{Al}_s^{3+}, 3\text{ClO}_{4,s}^-)$ were measured as in the case of negatively charged solutes. In water the ratio $[\lambda(e_s^-) + \lambda(\text{H}_s^+)]/\Lambda(\text{H}_s^+, \text{ClO}_{4,s}^-) = 1.3$, $[\lambda(e_s^-) + \lambda(\text{Ag}_s^+)]/\Lambda(\text{Ag}_s^+, \text{ClO}_{4,s}^-) = 1.9$, $[\lambda(e_s^-) + \lambda(\text{Tl}_s^+)]/\Lambda(\text{Tl}_s^+, \text{OAc}_s^-) = 2.2$, $[\lambda(e_s^-) + 0.25\lambda(\text{Cu}_s^{2+})]/\Lambda(\text{Cu}_s^{2+}, 2\text{ClO}_{4,s}^-) = 0.8$, and $[\lambda(e_s^-) + 0.1\lambda(\text{Al}_s^{3+})]/\Lambda(\text{Al}_s^{3+}, 3\text{ClO}_{4,s}^-) = 0.5$. Thus the solvent dependences of κ_r for the reaction of e_s^- with H_s^+ , Ag_s^+ , Tl_s^+ , Cu_s^{2+} , and Al_s^{3+} can be approximated by the variation of the ratio $z_i k_2 / f \Lambda T$ where z_i is the charge on the ion and Λ is the molar conductivity of the salt.

The solvent composition dependences of $z_i k_2 / f \Lambda_0 T$ at 298K are shown in Figures 109 and 110. The shapes of the curves are similar to those of $k_2 \eta / f T$, but the alcohol end of the curves in Figures 109 and 110 are higher relative to the water end than those in $k_2 \eta / f T$ plots. As in the case of $\text{NO}_{3,s}^-$ and $\text{CrO}_{4,s}^{2-}$ the replacement of $\lambda(e_s^-)$ for $\lambda(\text{ClO}_{4,s}^-)$ and $\lambda(\text{OAc}_s^-)$ would lower the left ends of the curves in Figures 109 and 110, and decrease the mismatch with $k_2 \eta / f T$ curves.

The effective radius for mutual diffusion r_d is

$$r_d \approx 8 \times 10^{-16} z^2 / \eta \Lambda_0 \quad [34]$$

For Cu_s^{2+} and Al_s^{3+} , the difference of charge on the ion and its counter ion is a complication. For $\text{Cu}(\text{ClO}_4)_2$ and $\text{Al}(\text{ClO}_4)_3$ the required values of $(\lambda_+/z_+^2) + \lambda_-$ were in between $\Lambda_0(\text{salt})/z_+$ and $\Lambda_0(\text{salt})/z_+^2$. So $\Lambda_0(\text{salt})/z_+^2$ was chosen as was also chosen for negatively charged reactants.

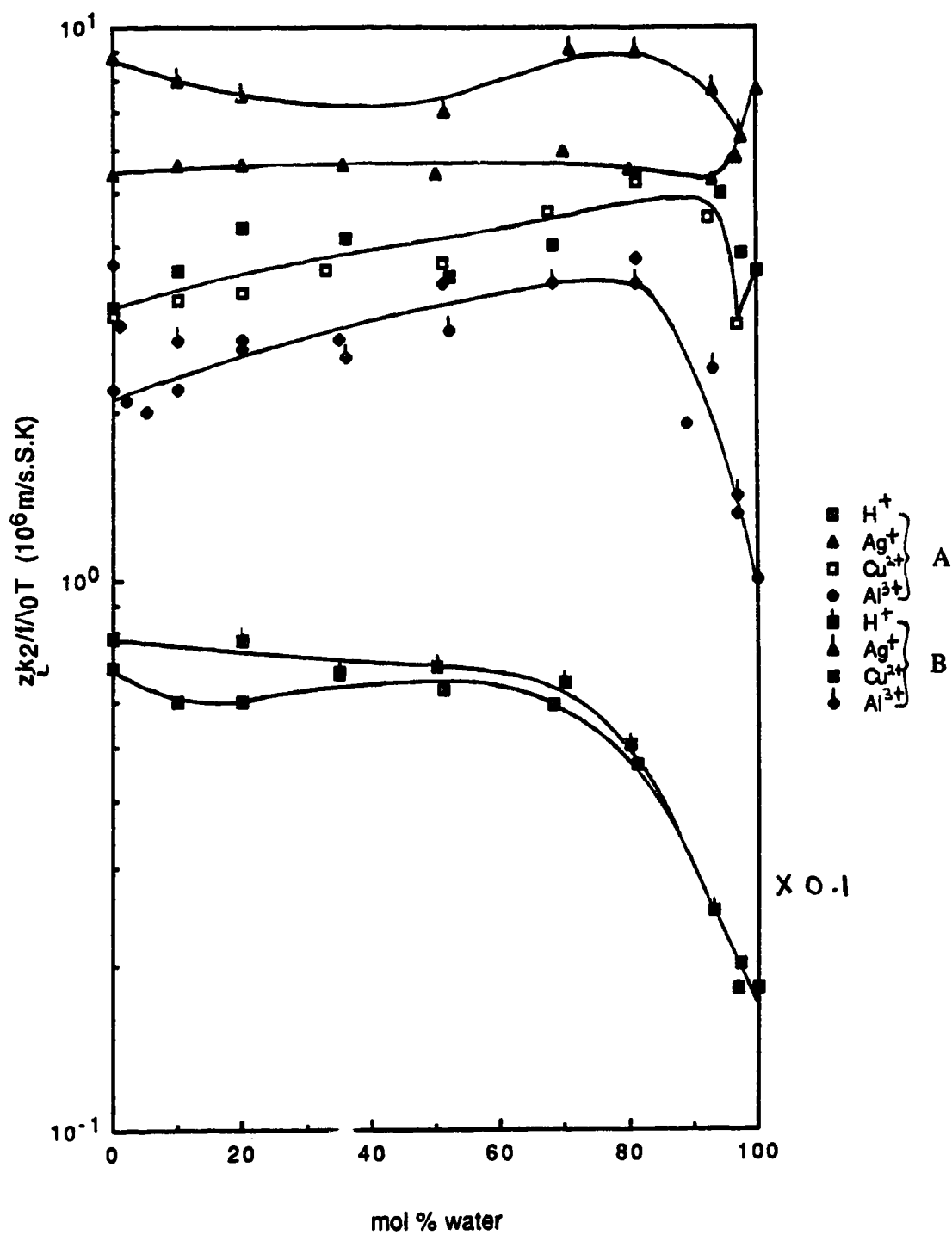


Fig.109

The composition dependence of $z_k^2 / (f \Lambda_0 T)$ for some inorganic electrolytes in 1-propanol/water and 2-propanol/water mixtures at 298K. A: 1-propanol/water. B: 2-propanol/water.

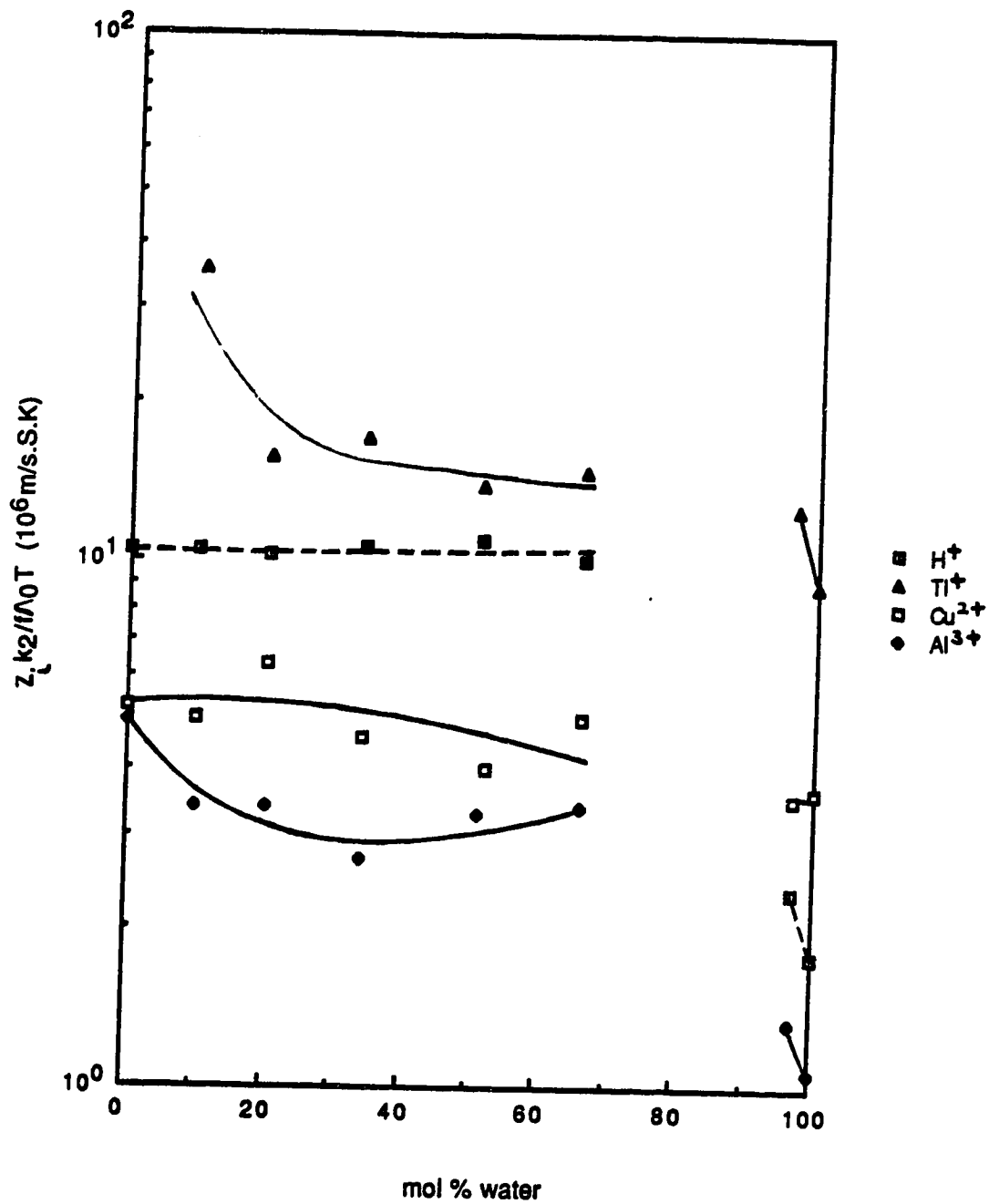


Fig.110

The composition dependence of $z_k k_2 / f \Lambda_0 T$ for some inorganic electrolytes in 2-butanol/water mixtures at 298K.

Values of r_d from equation [34] for $H_s^+ + ClO_{4,s}^-$, $Tl_s^+ + OAc_s^-$, $Ag_s^+ + ClO_{4,s}^-$, $Cu_s^{2+} + ClO_{4,s}^-$, $Al_s^{3+} + ClO_{4,s}^-$ are plotted against solvent composition in Figure 111. With the exception of 100% to 97-90 mol% water the value of r_d increases steadily with alcohol content of the solvent. The larger values in alcohol are attributed to the larger sizes of the molecules that solvate the ions. The values of r_d in the alcohol rich side for 2-butanol/water mixed solvents are relatively higher than those for 1-propanol and 2-propanol/water mixtures. The ratio of molar volumes, alcohol/water for 2-butanol at 298K is 5.2 which is higher than those for 1-propanol and 2-propanol, 4.2 and 4.3, respectively (126).

III. Conclusion

The reactivities of solvated electrons with solutes are dependent on the electron affinity of the solute, the solvent structure, the electron-solvent, and solute-solvent interactions.

The reaction of solvated electrons with nitrate ions and chromate ions are strongly dependent on properties of the solvent. The liquid structure influences both the rate of diffusion of the reactants and the reaction probability of the reactant encounter pair. The solvent participates chemically in the reaction of the reactant pair, which is evident from the increasing magnitude of the values of $k_2\eta/fT$ (e_s^- , $NO_{3,s}^-$) in the sequence pure 1-propanol, 2-propanol and 2-butanol. In comparing these three alcohols, 2-butanol and 2-propanol have much more reactive C-H groups since this H atom is attached to a secondary C atom. In 1-propanol the corresponding H atom is attached to a primary C atom and the bond is stronger.

The values of $k_2\eta/fT$ for ($e_s^- + CrO_{4,s}^{2-}$) are similar to those for ($e_s^- +$ nitrobenzene), so ($e_s^- + CrO_{4,s}^{2-}$) is also nearly diffusion controlled. The values of $k_2\eta/fT$ for ($e_s^- + NO_{3,s}^-$) are relatively small, especially in alcohol-rich solvents, so the reaction is far from being diffusion controlled.

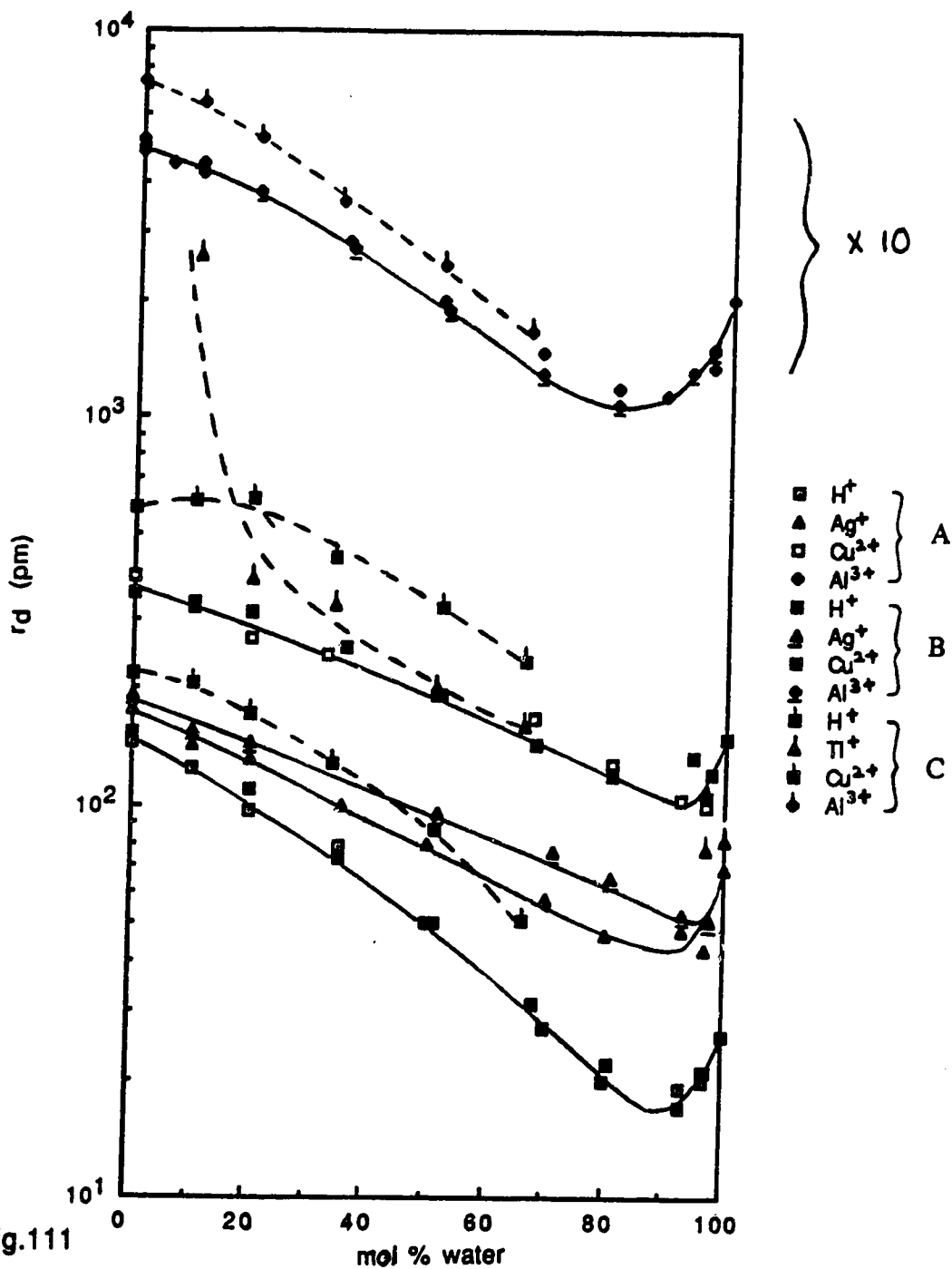


Fig.111

The composition dependence of the mutual radius for diffusion for some inorganic electrolytes in 1-propanol/water, 2-propanol/water and 2-butanol/water mixtures at 298K. A:1-propanol/water. B:2-propanol/water. C: 2-butanol/water.

The plots of E_2 and $\log A_2$ for NO_3^- and CrO_4^{2-} against solvent composition are S curves. Addition of water to alcohol-rich solvents of NO_3^- and CrO_4^{2-} decreased E_2 and $\log A_2$. The values of E_2 in water-rich solvents are similar to those for nitrobenzene, but E_2 increases with alcohol content. The values of $\log A_2$ for NO_3^- and CrO_4^{2-} are smaller than that for nitrobenzene. The ionic reactions apparently require solvent molecular rearrangement about the reaction site, which decreases the entropy of the system and makes the random attainment of the correct configuration less probable, thereby slowing the reaction.

The value of A_2 increases as 3-5 mol% alcohol is added to pure water. The presence of the small amount of alcohol in the water makes attainment of a suitable configuration easier.

The solvent composition effect is smaller for $(e_s^- + \text{CrO}_4^{2-})$ than for the less efficient $(e_s^- + \text{NO}_3^-)$.

The composition dependences of $k_2\eta/fT$ for the positive ions follow a similar pattern, having a maximum near 80 mol% water and decreasing towards both alcohol and water ends of the plots. The values of $k_2\eta/fT$ for Cu_s^{2+} and Al_s^{3+} are relatively smaller than those for H_s^+ , Ag_s^+ and Tl_s^+ , probably due to difficulty in formation of unstable Cu_s^+ and Al_s^{2+} .

In pure water the activation energy of $(e_s^- + \text{H}_s^+)$ is much lower than those of $(e_s^- + \text{Ag}_s^+)$, $(e_s^- + \text{Tl}_s^+)$, $(e_s^- + \text{Cu}_s^{2+})$, and $(e_s^- + \text{Al}_s^{3+})$, but the activation energy of $(e_s^- + \text{H}_s^+)$ increases as the alcohol content of the solvent increases. On the other hand, the activation energy of $(e_s^- + \text{Al}_s^{3+})$ in water is much higher than those of reactions of other positive ions, but the activation energy decreases as alcohol is added to water. Addition of water to alcohol-rich solvents of Tl_s^+ causes E_2 to increase.

The variations of $\log A_2$ are quite similar to those of E_2 .

In general, the values of E_2 are similar to the activation energies of conductance E_{Λ_0} except for Al_s^{3+} in pure water solvent and negative ions in alcohol-rich solvents.

The molar electrical conductivities Λ_0 of the salts are related to the diffusion coefficients of the ions. The values of the effective Stokes radius r_d for mutual diffusion of the ions increase steadily with alcohol content of the solvent for all the solutes, with the exception of the region within a few mol% of pure water.

The minimum in r_d near 90 mol% water is attributed to a decrease in microscopic viscosity of the fluid in the vicinity of the ions, relative to the shear viscosity of the bulk fluid. The ions evidently remain in the disordered water and do not associate with the more viscous structures that are nucleated by the alcohol molecules. The larger values of r_d in alcohol are attributed to the larger sizes of the molecules that solvate the ions. In pure 2-butanol r_d has the highest values in all the cases.

The composition dependence of $z_1 k_2 / f \Lambda_0 T$ was similar to that of $k_2 \eta / f T$, but the alcohol ends of the curves were two to six times higher relative to the water ends than those in $k_2 \eta / f T$ curves. Replacement of $\lambda_0(e_3^-)$ for $\lambda_0(Li_3^+)$, $\lambda_0(ClO_4^-)$ and $\lambda_0(OAc_3^-)$ would lower the alcohol end of the curves of $z_1 k_2 / f \Lambda_0 T$.

REFERENCES

1. P.P. Edwards, *Adv. Inorg. Chem. Radiochem.* **25**, 135 (1982).
2. W. Weyl, *Ann. Phys.* **121**, 601 (1864), quoted by J.C. Thompson in "Electrons In Liquid Ammonia", Clarendon Press, Oxford, 1976, p. 2.
3. C.A. Kraus, "The Properties of Electrically Conducting Systems", Chemical Catalogue Co., New York, 1922, p. 375.
4. G.W.A. Fowles, W.R. McGregor and M.C.R. Symons, *J. Chem. Soc.* 3329 (1957).
5. E.J. Hart and J.W. Boag, *J. Am. Chem. Soc.* **84**, 4090 (1962).
6. S. Arai and L.M. Dorfman, *J. Chem. Phys.* **41**, 2190 (1964).
7. G.R. Freeman, *Actions Chimiques et Biologiques des Radiations* **14**, 73 (1970).
8. F.Y. Jou and G.R. Freeman, *Can. J. Chem.* **54**, 3693 (1976).
9. A.J. Birch and G. Subba Rao, *Adv. Org. Chem.* **8**, 1 (1972).
10. L.M. Dorfman and M.S. Matheson, "Pulse Radiolysis", Reprinted from "Progress In Reaction Kinetics", Vol. 3, Ed. G. Porter, Pergamon Press, Oxford, 1965.
11. G.R. Freeman, "Kinetics of Nonhomogeneous Processes: A Practical Introduction for Chemists, Biologists, Physicists, and Materials Scientists", Wiley-Interscience, New York, 1987, Chapters 2 and 6.
12. J. Jortner and A. Garthon, *Can. J. Chem.* **55**, 1801 (1977).
13. G.R. Freeman in "Radiation Research", Ed. G. Silini, North-Holland, Amsterdam, 1966, p. 113.
14. J.E. Bennet, B. Mile and A. Thomas, *J. Chem. Soc. (A)* 1393 (1967).
15. U. Schindewolf, *Angew Chem. Int. Ed.* **7**, 190 (1968).
16. J. Jortner and R.M. Noyes, *J. Phys. Chem.* **70**, 770 (1966).
17. W.J. Moore, "Physical Chemistry", 3rd Edition, Prentice Hall, Englewood Cliffs, N.J., 1962, p. 337.
18. P.H. Tewari and G.R. Freeman, *J. Chem. Phys.* **51**, 1276 (1969).

19. A.D. Leu, K.N. Jha and G.R. Freeman, *Can. J. Chem.* **60**, 2342 (1982).
20. J.C. Thompson, "Electrons In Liquid Ammonia", Clarendon Press, Oxford, 1976, p. 99.
21. D. Huppert, P. Avouris and P.M. Rentzepis, *J. Phys. Chem.* **82**, 2282 (1978).
22. T.R. Tuttle, S. Golden, S.L. Wenje and C.M. Stupak, *J. Phys. Chem.* **88**, 3811 (1984).
23. D.C. Walker, *Can. J. Chem.* **55**, 1987 (1977).
24. J. Jortner and N.R. Kestner, *J. Phys. Chem.* **77**, 1040 (1973).
25. A. Kajiwara, K. Funabashi and Naleway, *Phys. Rev.* **A6**, 808 (1972).
26. R. Lugo and P. Delahay, *J. Chem. Phys.* **57**, 2122 (1972).
27. G.L. Hug and I. Carmicheal, *J. Phys. Chem.* **86**, 3410 (1982).
28. K. Funabashi, I. Carmicheal and W.H. Hamill, *J. Chem. Phys.* **69**, 2652 (1978).
29. J.K. Baird, L.K. Lee and E.J. Meehan, *J. Chem. Phys.* **83**, 3710 (1985).
30. T. Kimura, O. Hirao, C. Okabe and K. Fueki, *Can. J. Chem.* **62**, 64 (1984).
31. J.K. Baird and C.H. Morales, *J. Phys. Chem.* **89**, 774 (1985).
32. K.F. Baverstock and P.J. Dyne, *Can. J. Chem.* **48**, 2812 (1970).
33. T. Shida, S. Iwata and T. Watanabe, *J. Phys. Chem.* **76**, 3683 (1972).
34. K. Kato, S. Takagi and K. Fueki, *J. Phys. Chem.* **85**, 2684 (1981).
35. R.A. Ogg, *Phys. Rev.* **69**, 243 (1946).
36. J. Jortner, *J. Chem. Phys.* **30**, 839 (1959).
37. D.A. Copeland, N.R. Kestner and J. Jortner, *J. Chem. Phys.* **53**, 1189 (1970).
38. D.F. Feng, K. Fueki and L. Kevan, *J. Chem. Phys.* **58**, 3281 (1973).
39. A. Banerjee and J. Simons, *J. Chem. Phys.* **68**, 415 (1978).
40. D. Chandler, *J. Phys. Chem.* **88**, 3400 (1984).
41. P.J. Rossky and J. Schnitker, *J. Phys. Chem.* **92**, 4277 (1988).
42. M. Sprik, R.W. Impey and M.L. Klein, *J. Chem. Phys.* **83**, 5802 (1985).
43. L. Kevan, *J. Phys. Chem.* **84**, 1232 (1980).

44. G.R. Freeman, *J. Phys. Chem.* **77**, 7 (1973).
45. A.D. Leu, K.N. Jha and G.R. Freeman, *Can. J. Chem.* **61**, 1115 (1983).
46. R.R. Hentz and G.A. Kenney-Wallace, *J. Phys. Chem.* **78**, 514 (1974).
47. G.E. Hall and G.A. Kenney-Wallace, *Chem. Phys.* **32**, 313 (1978).
48. F.Y. Jou and G.R. Freeman, *Can. J. Chem.* **57**, 591 (1979).
49. F.Y. Jou and G.R. Freeman, *Can. J. Chem.* **60**, 1809 (1982).
50. J.D. Bernal and P.H. Fowler, *J. Chem. Phys.* **1**, 515 (1933).
51. A.H. Narten, *J. Chem. Phys.* **56**, 5681 (1972).
52. A.H. Narten and H.A. Levy, *J. Chem. Phys.* **55**, 2263 (1971).
53. J.A. Pople, *Proc. Royal Soc.* **A222**, 498 (1954).
54. S.A. Rice and M.G. Sceats, *J. Phys. Chem.* **85**, 1107 (1981).
55. S.A. Rice and M.G. Sceats in "Water: A Comprehensive Treatise" Vol. 7, Ed. F. Franks, Plenum, 1982.
56. F.H. Stillinger and A. Rahman, *J. Chem. Phys.* **60**, 1545 (1974).
57. H.E. Stanley and J. Teixeira, *J. Chem. Phys.* **73**, 3404 (1980).
58. H.S. Frank and Y.W. Wen, *Discuss. Faraday Soc.* **24**, 133 (1957).
59. G.J. Safford, P.S. Leung, A.W. Neumann and P.C. Schaffer, *J. Chem. Phys.* **50**, 4444 (1969).
60. G. Nemethy and H.A. Scheraga, *J. Chem. Phys.* **36**, 3382 (1962).
61. A.T. Hagler, G. Nemethy and H.A. Scheraga, *J. Chem. Phys.* **76**, 3229 (1972).
62. M.S. Jhon, H. Eyring, J. Grosh and T. Ree, *J. Chem. Phys.* **44**, 1456 (1966).
63. Y.I. Naberukhin, *J. Struct. Chem.* **25**, 223 (1984).
64. P.J. Rossky, *Pure Appl. Chem.* **57**, 1043 (1985).
65. P. Huyskens, *J. Mol. Struct.* **100**, 403 (1983).
66. "The Hydrogen Bond", Ed P. Schuster, G. Zundel and C. Sandorfy, Vol. 3, North Holland Publishing, 1976, p. 1070.

67. M.C.R. Symons and V.K. Thomas, *J. Chem. Soc. Faraday Trans. I* **77**, 1883 (1981).
68. H.H. Eysel and J.E. Bertie, *J. Mol. Struct.* **142**, 227 (1986).
69. B.M. Pettit and P.J. Rossky, *J. Chem. Phys.* **78**, 7296 (1983).
70. W.L. Jorgensen, *J. Phys. Chem.* **90**, 1276 (1986).
71. J.G.J. Kirkwood, *Chem. Phys.* **7**, 911 (1939).
72. L. Liszi, L. Meszaros and I. Ruff, *Acta Chim. Acad. Sci. Hung.* **104**, 279 (1980).
73. J.P. Hasted in "Aqueous Dielectrics", Chapman and Hall, London, 1973, p. 176.
74. A. D'Aprano, I.D. Donato, G. D'Arrigo, D. Bertollini, M. Cassetari and G. Salvetti, *Mol. Phys.* **55**, 475 (1985).
75. B. Marongin, I. Ferino, R. Monaci, V. Solinas and S. Forraza, *J. Mol. Liq.* **28**, 229 (1984).
76. A.C. Brown and D.J.G. Ives, *J. Chem. Soc.* 1608 (1962).
77. Y.I. Naberukhin and V.A. Rogov, *Russ. Chem. Rev.* **40**, 207 (1971).
78. H. Tanaka, K. Nakanish and H. Touhara, *J. Chem. Phys.* **81**, 4065 (1984).
79. T.M. Bender and R. Pecora, *J. Phys. Chem.* **90**, 1700 (1986).
80. W.L. Jorgensen, J. Gao and C. Ravimohan, *J. Phys. Chem.* **89**, 3470 (1985).
81. A.H. Hafez and H. Sadek, *Acta Chim. Acad. Sci. Hung.* **89**, 257 (1976).
82. A. D'Aprano, D. Donato, E. Caponetti and V. Agrigento, *J. Sol. Chem.* **8**, 793 (1979).
83. M. Anbar, M. Bambenek and A.B. Ross, *Natl. Stand. Ref. Data Ser., Natl. Bur. Stand.* **43** (1973).
84. I.A. Taub, M.C. Sauer, Jr. and L.M. Dorfman, *Discuss. Faraday Soc.* **36**, 206 (1963).
85. I.A. Taub, D.A. Harter, M.C. Sauer Jr. and L.M. Dorfman, *J. Chem. Phys.* **41**, 979 (1964).

86. S. Arai and L.M. Dorfman, *J. Chem. Phys.* **41**, 2190 (1964).
87. G.L. Bolton and G.R. Freeman, *J. Am. Chem. Soc.* **98**, 6825 (1976).
88. K. Okazaki and G.R. Freeman, *Can. J. Chem.* **56**, 2313 (1978).
89. A.M. Afanassiev, K. Okazaka and G.R. Freeman, *J. Phys. Chem.* **83**, 1244 (1979).
90. A.M. Afanassiev, K. Okazaki and G.R. Freeman, *Can. J. Chem.* **57**, 839 (1979).
91. M.S. Tunuli and Farhataziz, *J. Phys. Chem.* **90**, 6587 (1986).
92. S. Farhataziz, S. Kalachandra and M.S. Tunuli, *J. Phys. Chem.* **88**, 3837 (1984).
93. S. Kalachandra and S. Farhataziz, *Chem. Phys. Lett.* **73**, 465 (1980).
94. M.A. Rauf, G.H. Stewart and S. Farhataziz, *Radiat. Phys. Chem.* **26**, 433 (1985).
95. B.H. Milosovljevic and O.I. Micic, *J. Phys. Chem.* **82**, 1359 (1978).
96. O.I. Micic and B. Cercek, *J. Phys. Chem.* **81**, 833 (1977).
97. O.I. Micic and B. Cercek, *J. Phys. Chem.* **78**, 285 (1974).
98. F. Barat, L. Gilles, B. Hickel and L. Lesigne, *J. Phys. Chem.* **77**, 1711 (1973).
99. H.A. Schwarz and P.S. Gill, *J. Phys. Chem.* **81**, 22 (1977).
100. J. Cygler and G.R. Freeman, *Can. J. Chem.* **62**, 1265 (1984).
101. Y. Maham and G.R. Freeman, *J. Phys. Chem.* **89**, 4347 (1985).
102. Y. Maham and G.R. Freeman, *J. Phys. Chem.* **91**, 1561 (1987).
103. Y. Maham and G.R. Freeman, *J. Phys. Chem.* **92**, 1506 (1988).
104. P.C. Senanayake and G.R. Freeman, *J. Phys. Chem.* **91**, 2123 (1987).
105. P.C. Senanayake and G.R. Freeman, *J. Chem. Phys.* **87**, 7007 (1987).
106. Y. Maham and G.R. Freeman, *Can. J. Chem.* **66**, 1706 (1988).
107. P.C. Senanayake and G.R. Freeman, *J. Phys. Chem.* **92**, 5142 (1988).
108. C.C. Lai and G.R. Freeman, *J. Phys. Chem.* **94**, 302 (1990).
109. G. Nemethy and H.A. Scheraga, *J. Chem. Phys.* **36**, 3401 (1962).
110. M.S. Thon and H. Eyring, *J. Am. Chem. Soc.* **90**, 3071 (1968).

111. F.X. Hassion and R.H. Cole, *J. Chem. Phys.* **23**, 1756 (1955).
112. D. Bertolini, M. Cassettari and G. Salvetti, *J. Chem. Phys.* **78**, 365 (1983).
113. M.V. Smoluchowski, *Z. Phys. Chem.* **92**, 129 (1917).
114. P. Debye, *Trans. Electrochem. Soc.* **82**, 265 (1942).
115. A. Einstein in "Investigations on the Theory of Brownian Movement", Ed R. Fürth, Dover, New York, 1956, p. 75.
116. M. Anbar and E.J. Hart, *ACS Adv. in Chem.* **81**, 79 (1968).
117. J.H. Baxendale, E.M. Fielden and J.P. Keene, *Proc. Roy. Soc. A* **286**, 320 (1965).
118. P.C. Senanayake, Ph.D. Thesis, University of Alberta, 1987.
119. C.C. Lai, Ph.D. Thesis, University of Alberta, 1989.
120. K.N. Jha, G.L. Bolton and G.R. Freeman, *Can. J. Chem.* **50**, 3073 (1972).
121. J. Timmermans, "Physico-chemical Constants of Binary Mixtures", Vol. 4, Wiley-Interscience, New York, 1960.
122. A.D. Leu, K.N. Jha and G.R. Freeman, *Can. J. Chem.* **61**, 1115 (1983).
123. For the meaning of "free ion yield" see G. Ramanan, N. Gee and G.R. Freeman, *Can. J. Phys.* **68**, xxxx (1990).
124. R.S. Boikess and E. Edelson, "Chemical Principles", 3rd Ed., Harper & Row, New York, 1985, p. A-19.
125. D. Dobos, "Electrochemical Data", Elsevier, Amsterdam, 1975.
126. R.W. Gallant, "Physical Properties of Hydrocarbons", Vol. 1, Gulf Publishing Co., Houston, TX, 1968.
127. G.R. Freeman, "Radiation Chemistry", 1968, p. 125.
128. Y.Y. Akhadov, "Dielectric Properties of Binary Solutions", Pergamon Press, Oxford, 1981.